



Soil Mineralogy

Joseph W. Stucki
University of Illinois

20 Alteration, Formation, and Occurrence of Minerals in Soils <i>G. Jock Churchman and David J. Lowe</i>	20-1
Introduction • Alteration of Primary Minerals • Occurrence of Clay Minerals in Soils • Influence of Mode of Formation upon Predictions of Properties of Soils from Their Clay Mineralogy • Acknowledgments • References	
21 Phyllosilicates <i>Hideomi Kodama</i>	21-1
Introduction • General Structural Features • Occurrence of Phyllosilicates • Phyllosilicates in Soil Environments • Identification of Soil Phyllosilicates • Addendum • Appendix • References	
22 Oxide Minerals in Soils <i>Nestor Kämpf, Andreas C. Scheinost, and Darrell G. Schulze</i>	22-1
Introduction • Iron Oxides • Manganese Oxides • Aluminum Oxides • Silicon Oxides • Titanium and Zirconium Minerals • References	
23 Poorly Crystalline Aluminosilicate Clay Minerals <i>James Harsh</i>	23-1
Structure of Poorly Crystalline Materials • Identification and Synthesis of Allophane and Imogolite • Occurrence of Imogolite and Allophane in Natural Environments • Surface Charge Characteristics of Short-Range Ordered Aluminosilicates and Variable-Charge Soils • Interaction of Allophane and Imogolite with Other Soil Constituents • References	

FUNDAMENTAL TO THE EXISTENCE of soil is its inorganic mineral fraction. Indeed, of all soil constituents only this one is required. Without it, soil ceases to be soil. Organic matter, bacteria, and fertilizer chemicals greatly enhance various properties of the soil, but without the inorganic minerals, it is reduced to a soilless medium incapable of the diverse range of functions that are often taken for granted. A correct and complete understanding of the soil requires, therefore, an understanding of soil mineralogy.

A common misconception is that soil minerals are rather inert, unchanging, and nonlabile. The chapters in this part quickly dispel this view by painting a very different picture. They will show that the soil minerals are not only diverse in their origins, structures, and chemistry, but they provide the backbone for active chemical surfaces where many reactions are catalyzed and basic behaviors of the soil are born and changed. As described here and elsewhere in this book, these active surfaces

of the so-called inert fraction react with organic matter, invoking mutual alterations in the behavior of both the minerals and the organic matter. Life-sustaining liquid water is held at their surfaces and in their interstitial pores, and even retained in the liquid state at very low temperatures to preserve plant life during hard winter months. Oxidation–reduction reactions alter the chemical and physical properties of the constituent Fe- and Mn-bearing minerals, thus creating real-time transformations that are critical to many soil processes. Soil minerals come in a wide range of particle sizes and morphologies, which add texture and body to the soil, and vary in their degree of crystallinity. Their colors are also diverse, ranging from intense reddish brown to very light gray, or even green, yellow, or blue. They are dynamic in their properties, constantly changing with climate, time, and other environmental conditions. Some changes are rapid; others, slow. These attributes bring the soil to life, as it were, and create the framework within which the plant and

animal kingdoms spring forth and are sustained through every season and in every clime.

Minerals, the heart of the soil, are a dynamic and essential resource, classified according to their properties. Presented in the following chapters are descriptions of how minerals are formed and transformed. Specifics are given regarding the properties and behavior of the phyllosilicates, the plate-shaped minerals;

iron, aluminum, and other (oxyhydr)oxides, which represent the more highly weathered mineral constituents; and amorphous minerals, which display active chemical properties but lack high order in their crystals. These are among the most important of the soil minerals. As such, knowledge of their characteristics will provide the basis from which a more complete understanding of soil physical and chemical properties may be acquired.

Alteration, Formation, and Occurrence of Minerals in Soils

20.1	Introduction	20-1
20.2	Alteration of Primary Minerals.....	20-2
	Common Primary Minerals in Soils • Observations of Relative Stabilities of Primary Minerals in Soils • Thermodynamic and Structural Explanations of Relative Stabilities • Processes and Products of Alteration of the Main Types of Primary Minerals by Weathering • Peculiarities of Processes and Products of Alteration by Weathering in Soils • Processes of Mineral Alteration and Formation by Weathering: Summary	
20.3	Occurrence of Clay Minerals in Soils.....	20-31
	Occurrence of Kaolinite in Soils • Occurrence of Halloysite in Soils • Occurrence of Illite in Soils • Occurrence of Vermiculite in Soils • Occurrence of Smectite in Soils • Occurrence of Palygorskite and Sepiolite in Soils • Occurrence of Iron Oxides in Soils • Occurrence of Manganese Oxides in Soils • Occurrence of Aluminum Hydroxides, Oxyhydroxides, and Oxides in Soils • Occurrence of Phosphate, Sulfide, and Sulfate Minerals in Soils • Occurrence of Pyrophyllite, Talc, and Zeolites in Soils • Occurrence of Neogenetic Silica in Soils • Occurrence of Titanium and Zirconium Minerals in Soils • Occurrence of Highly Soluble Minerals in Soils • Occurrence of Secondary Minerals in Soils: Summary	
20.4	Influence of Mode of Formation upon Predictions of Properties of Soils from Their Clay Mineralogy	20-48
	Introduction: The Role of Mineralogy in Soil Science • Contributions of Classical Clay Mineralogy toward Explanations of Soil Properties • Potential of Classical Clay Mineralogy for Explaining Soil Properties • Nature of Soil Minerals and Relationship to Their Mode of Formation	
	Acknowledgments.....	20-54
	References.....	20-54

G. Jock Churchman
University of Adelaide

David J. Lowe
University of Waikato

20.1 Introduction

This chapter, like Churchman (2000), seeks to bring readers up to date with information and understanding about the alteration of minerals and the nature of their products in the context of the formation and development of soils. It complements the articles by Bergaya et al. (2006), and recent books by Velde and Meunier (2008) and Velde and Barré (2010). This current chapter differs from Churchman (2000) in that it discusses the manner in which minerals, and especially secondary minerals, actually occur in soils, that is, it deals (in Section 20.3) with the occurrence, as well as the alteration and formation, of minerals in soils.

Secondary minerals are the most reactive inorganic materials in soils. Furthermore, they occur commonly in association with the most reactive organic materials in soils. It has often been inferred that knowledge of the properties of these reactive materials should enable close predictions of the useful soil properties, whether for growing plants, for filtering and partitioning water flow, for

immobilizing contaminants, for supporting human-made structures, or for other purposes. However, most of the information about the formation of secondary minerals through the alteration of primary minerals derives from studies of largely inorganic processes taking place in relatively “clean” environments. The soil, by contrast, is a heterogeneous milieu that is a dynamic part of the biosphere continually changing in response to climatic variations over all scales of time and space. It is not at all surprising that the minerals in the soil can be quite different in their chemical and physical characteristics from those of the “type” minerals formed in more “geological” environments with which they may share a name and ideal crystalline structure (Churchman, 2010). Chadwick and Chorover (2001) made the point that the crisp boundaries in stability diagrams are, in the real world of natural soils, not so clear-cut. However, the effort involved in understanding the real nature of minerals in soils is worthwhile in view of the potential reward of being able to explain and predict properties across different sorts of soils from the nature of their constituents

TABLE 20.1 Definitions of Terms

Term	Definitions ^a	References	Issues with Definitions
Mineral	An element or compound that is normally crystalline and that has formed as a result of geological processes	Gaines et al. (1997)	Crystallinity implies a regularity of structure, but this is dependent on type of analysis. Some materials (e.g., volcanic glass) lack a fixed structure and are referred to as mineraloids; others such as allophane, earlier thought to be amorphous and technically thus not minerals, are now known to be nanocrystalline and hence do qualify as minerals
Primary minerals	Mineral deposited or formed at the same time as the rock containing it	Lapidus (1987)	Minerals in sedimentary and partially metamorphosed rocks may contain secondary minerals from earlier cycles
Secondary minerals	Mineral formed as a result of alteration of preexisting minerals	Adapted from Lapidus (1987)	Minerals commonly altered in several steps; hence all products of 1° mineral alteration are 2° minerals Often referred to as “clay minerals”
Weathering	Weathering is the breakdown of geological deposits by physical, chemical, and biochemical processes <ul style="list-style-type: none"> Physical weathering includes breakdown by thermal and mechanical action, generating smaller particles (comminution); chemical weathering includes breakdown by hydrolysis, carbonation, hydration, dissolution, oxidation, and reduction, changing the physical and chemical properties of the original geological deposits 	Ashman and Puri (2002) and Buol et al. (2003)	Some regard weathering as encompassing both the breakdown of primary minerals and the synthesis of new secondary minerals, but others distinguish between two phases, <i>decomposition</i> and <i>argillization</i> , the latter being the synthesis of secondary minerals (mainly clays)
Soil	The natural, 3D body (comprising pedons), typically up to ~1 to 2 m thick (thicknesses can vary markedly), of unconsolidated mineral and organic material mantling the land surface that can support rooted land plants, and which <ul style="list-style-type: none"> Is characterized by one or more soil horizons (“layers”) that have evolved through additions, losses, transfers, and transformations of energy and matter by interactions of climate, biota, relief, and parent materials through time, and which differ from the material(s) from which they derive Comprises solids (inorganic and organic matter), liquids, and gases Is essential to life through recycling of nutrients, carbon, and oxygen Is nonrenewable in human timescales 	Schaetzl and Anderson (2005)	Most definitions of soil fail to encompass and recognize its complexity as the most complex ecosystem on Earth and as a biological habitat and critically important repository for genes. Soil is also being considered increasingly in policy making, for example, as a provider of “ecosystem services” (e.g., Blum et al., 2006) and as “natural capital” (the stock of biotic and abiotic mass that contains energy and organization) (see Sparling et al., 2006, and Robinson et al., 2009)

^a Working definition for this chapter.

and that of their associations. As discussed in Section 20.4, soil mineralogy has to some extent been in decline as a subdiscipline of soil science and it may be that this is due, at least in part, to the often-unjustified assumption that soil minerals are similar in their properties to those of their well-characterized “types” formed in nonsoil environments. The implications of this erroneous or only partly true assumption, and new directions for soil clay mineralogy, are also discussed in Section 20.4.

This chapter deals with minerals, both primary and secondary, with the processes of weathering and associated clay formation, and with soils. We define each of these terms in Table 20.1, which also includes some alternative definitions, and some issues involved in these definitions.

20.2 Alteration of Primary Minerals

20.2.1 Common Primary Minerals in Soils

The most common primary minerals found in soils are listed in Table 20.2 within their chemical (compositional) types and their mineralogical groupings together with the types of (crystal) structures for these groupings. Table 20.2 also lists chemical formulae for the minerals or groups of minerals and summarizes the general sorts of soils in which they occur and often also their relative abundance in these soils. Other properties of the minerals listed are given in Churchman (2006, Table 3.1). In soils, primary minerals, as residuals of physical and chemical weathering processes, most commonly occur in coarser particles

TABLE 20.2 Structure, Composition, and Soil Occurrences of Common Primary^a Minerals in Soils

Chemical Type	Group	Structural Type	Common Soil Minerals	Chemical Formula	Related Phases	Soils of Main Occurrence
Silicates ^b	Silica	Tectosilicate	Quartz	SiO ₂	Cristobalite Tridymite Opal (biogenic)	Quartz in almost all soils, Nil/minor from basalt
			Feldspar	Tectosilicate	Orthoclase	KAlSi ₃ O ₈
	Albite	NaAlSi ₃ O ₈			Oligoclase	
	Oligoclase	Na _x Ca _y AlSi _z O ₈ (x ≫ y), (z = 2-3)			Andesine	
	Anorthite	CaAl ₂ Si ₂ O ₈				
	Labradorite	Ca _y Na _x AlSi _z O ₈ (y ≫ x), (z = 2-3)			Bytownite (all plagioclases)	
	Zeolite	Tectosilicate	Clinoptilolite	Na ₃ K ₃ (Al ₆ Si ₃₀ O ₇₂) · 24H ₂ O	Erionite Faujasite Hollandite	Rare in soils; analcime formed in high pH saline soils
			Analcime	Na ₁₆ Al ₁₆ Si ₃₂ O ₉₆ · 16H ₂ O	Laumontite Mordenite	
	Mica	Phyllosilicate (dioctahedral)	Muscovite	KAl ₂ AlSi ₃ O ₁₀ (OH) ₂	Paragonite Maragarite Glauconite	Widespread
		Phyllosilicate (trioctahedral)	Biotite	K(MgFe ^{II}) ₃ AlSi ₃ O ₁₀ (OH) ₂	Phlogopite Clintonite Lepidolite	
	Chlorite	Phyllosilicate	Chlorite	(Fe,Mg,Al) ₆ (Si,Al) ₄ O ₁₀ (OH) ₈	Cookeite Sudoite Bonbassite	Only in very slightly weathered ("raw") soils
	Serpentine	Phyllosilicate	Chrysotile	Mg ₃ Si ₂ O ₅ (OH) ₄	Antigorite Lizardite Amesite Berthierine	Rare in soils
	Amphibole	Inosilicate (double chain)	Hornblende	(Ca,Na) _{2,3} (Mg,Fe,Al) ₅ (Si,Al) ₈ O ₂₂ (OH) ₂	Tremolite Actinolite Cummingtonite Glaucophane	Quite widespread, but absent from highly weathered soils
	Pyroxene	Inosilicate (single chain)	Augite	(Ca,Na)(Mg,Al,Fe)(Si,Al) ₂ O ₆	Enstatite Hypersthene Diopside Pigeonite Jadeite Spodumene Hedenbergite	Relatively rare except in some volcanic soils (especially intermediate-basic)
	(Cyclosilicate)	Cyclosilicate	Tourmaline	(Na,Ca)(Li,Mg,Al)(Li,Fe,Mn) ₆ (BO ₃) ₃ Si ₆ O ₁₈ (OH) ₄	Beryl	Rare
	(Sorosilicate)	Sorosilicate	Epidote	Ca ₂ (Al,Fe)Al ₂ O(Si ₂ O ₇)SiO ₄ (OH) ₄	Zoisite	Uncommon
	Olivine	Nesosilicate	Forsterite	Mg ₂ SiO ₄	Fayalite Tephroite Monticellite	Rare
	Garnet	Nesosilicate	Almandine	Fe ₃ Al ₂ (SiO ₄) ₃		Rare
	Zircon	Nesosilicate	Zircon	ZrSiO ₄	Baddeleyite (ZrO ₂)	Widespread

(continued)

TABLE 20.2 (continued) Structure, Composition, and Soil Occurrences of Common Primary^a Minerals in Soils

Chemical Type	Group	Structural Type	Common Soil Minerals	Chemical Formula	Related Phases	Soils of Main Occurrence
Nonsilicates	Phosphates	Insular, hexagonal	Apatite	$\text{Ca}_5(\text{PO}_4)_3(\text{OH},\text{F},\text{Cl})$	Fluorapatite	Some in “raw” soils
					Hydroxyapatite	
					Variscite	
					Wavellite	
					Monazite	
Titanium oxide	Carbonate	Tetragonal	Rutile	TiO_2	Brookite Sphene (CaTiSi_3)	Widespread in small amounts
		Rhombohedral	Calcite	CaCO_3	Aragonite Siderite (FeCO_3)	Common in arid soils
Carbonate	Rhomboidal	Rhomboidal	Dolomite	$\text{CaMg}(\text{CO}_3)_2$	Ankerite Mg calcite	From dolomitic rocks
					Iron oxide	Cubic

^a Some are also formed in soils, hence may also be regarded as secondary minerals.

^b Volcanic glass (including obsidian) is an amorphous solid with a poorly ordered internal structure comprising loosely linked SiO_4 tetrahedra (Fisher and Schminke, 1984). Of widely varying composition, it is a common primary mineraloid in many volcanic soils and derivatives.

(of sand- and silt-size), although the phyllosilicates such as the micas, chlorite, vermiculite, and talc, and some oxides, such as those of titanium and also apatite, and volcanic glass, can also be found in reasonable proportions in the clay-size fractions of some soils.

20.2.2 Observations of Relative Stabilities of Primary Minerals in Soils

In most cases, weathering involves the reaction of minerals (or mineraloids) with water, or, at least, an aqueous solution. There are exceptions where alteration of primary minerals occurs but where liquid water is either absent or is not the primary agent effecting alteration. This is the case in cold (and polar) and also hot desert zones on Earth (Shoji et al., 2006). It is probably also the case in some extraterrestrial environments, such as the Moon, but not in others, such as Mars, where there is abundant evidence for liquid water, at least in the past (Certini and Scalenghe, 2006). In environments where liquid water does not provide the main weathering milieu, the dominant agents of alteration nonetheless involve climatic factors; hence, they constitute weathering. These include mainly physical actions such as frost wedging and successive freezing and thawing in cold desert zones on Earth (Shoji et al., 2006), processes such as wind ablation in both hot and cold terrestrial desert zones, and such processes as solar wind irradiation on Moon (Certini and Scalenghe, 2006), and perhaps also on other dry extraterrestrial bodies and regions. Other agents besides the purely climatic can also alter primary minerals, given enough time. Among these are some resulting from various human activities (Certini and Scalenghe, 2006), including agriculture (Velde and Meunier, 2008), mining (Murakami et al., 1996; Banfield and Murakami, 1998), landfills

(Batchelder et al., 1998), industrial pollution (Rampazzo and Blum, 1992; Yaron et al., 2010), and probably also global climate change (Berg and Banwart, 2000; Amundson, 2001; Leifeld, 2006). Most of these agents affect mineral alteration via aqueous solutions, although in some cases, for example, the oxidation of sulfides, particularly iron pyrite, alteration of minerals occurs when water is absent (Dent and Pons, 1995). Nevertheless, alteration by weathering most often occurs in an aqueous environment and the most important determinant of the relative stability of primary minerals to weathering is their relative solubility in water.

All minerals have some solubility in water. Only rarely, however, for example, for simple salts like halite (NaCl) found, for example, in arid and saline soils, do they dissolve congruently in water. Instead, hydrolysis commonly occurs with the more soluble components being removed selectively from the mineral. This removal may leave a solid residue, which differs in composition from the original mineral, or a solid alteration product that precipitates out of the solution. The solid precipitate will most likely have a different composition and perhaps also a different crystal structure from that of its antecedent (partly or completely) dissolved mineral. Some texts refer to the synthesis or precipitation of such products as “argillization,” meaning the formation of clay; in this case, the term “weathering” encompasses only the decompositional phase (Figure 20.1) (e.g., Buol et al., 2003). Another term widely used is neogenesis, effectively the formation or synthesis of new clays and other secondary material from the breakdown products of antecedent minerals.

A simple chemical analogy of the hydrolysis undergone by silicates, the most common type of primary mineral, in water, is realized when they are considered as salts of silicic acid H_4SiO_4 and bases of the appropriate cation (Carroll, 1970; Chamley, 1989).

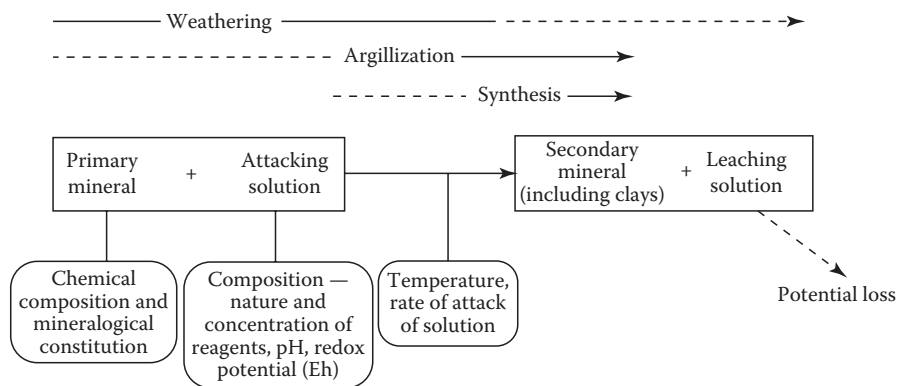
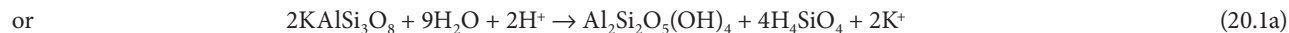


FIGURE 20.1 Weathering (and associated processes of argillization and synthesis) in relation to the factors governing the genesis of secondary minerals including clays in soils. (Modified after Percival, H.J. 1985. Soil solutions, minerals, and equilibria. New Zealand Soil Bureau Scientific Report 69. Department of Scientific and Industrial Research, Lower Hutt, New Zealand. With permission.)

Box 20.1 HYDROLYSIS OF K-FELDSPAR, INTERPRETED AS A SALT, TO FORM KAOLINITE

Silicate minerals \equiv salt of silicic acid plus base of appropriate cation

\therefore K-feldspar \equiv silicic acid + hydroxyl-Al (+K⁺)



The hydrolysis of silicates in water results in an acid, namely, silicic acid, and a base, namely, the hydroxy-Al-Si, kaolinite (see Box 20.1). Because most aqueous solutions in which weathering takes place are acidic because water is charged with dissolved CO₂, giving rise to a continuous supply of carbonic acid H₂CO₃ and hence H⁺ ions, hydrogen ions are important weathering agents. Therefore, Equation 20.1a represents the natural situation more realistically than Equation 20.1.

The relative stabilities of the principal primary minerals in soils to alteration have long been studied. More than 70 years ago, Goldich (1938) drew up a stability series for these minerals (Figure 20.2) that has generally stood the test of time and further experimentation, for example, by Franke and Teschner-Steinhardt (1994).

20.2.3 Thermodynamic and Structural Explanations of Relative Stabilities

Goldich's series (Figure 20.2) makes thermodynamic sense insofar as the minerals therein are in the identical (but reversed) order to those in Bowen's classic reaction series describing the

order in which the minerals crystallized out of a magma on cooling (Bowen, 1922). Goldich (1938) reasoned that the higher the temperature at which a mineral crystallized from magma, the greater the extent to which it was out of equilibrium with the surface temperature of Earth and, therefore, the more susceptible it would be to breakdown by weathering at the Earth's surface.

The alteration of a particular mineral or mineraloid begins with the disruption of its weakest bond. Structural explanations of the relative stabilities of minerals have followed this generalization. Bonds in all silicates are based on silica tetrahedra. Their strength depends on the following: (1) the nature of the links between tetrahedra, (2) the extent of substitution of four-valency Si within tetrahedra by three-valency Al and hence gain of negative charge (isomorphous substitution), and (3) the extent of incorporation of charge-balancing cations, and their location, in the structure. In Table 20.3, we show the nature of bonding in the different structural types of silicates (see Table 20.2 to identify the relevant minerals).

Sposito (1989) pointed to an apparent correspondence between the ordering of the molar Si:O ratios in the silicate units, namely, olivines < pyroxenes < amphiboles < micas < feldspars = quartz

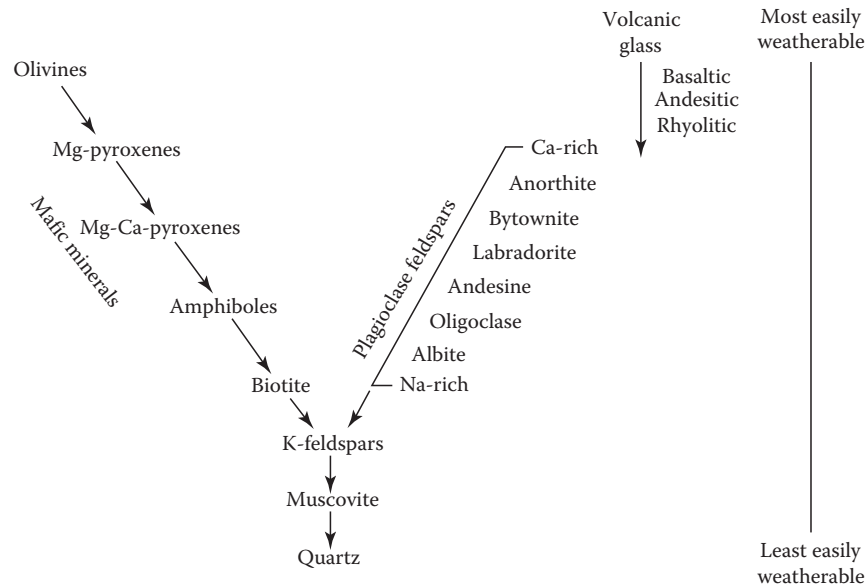


FIGURE 20.2 Stability series for the common primary minerals (after Goldich, S.S. 1938. *A study in rock weathering*. *J. Geol.* 46:17–58.) and also volcanic glass (not part of the Goldich series). Basaltic and other glasses, and olivines, are normally the first phases altered by weathering (Wolff-Boenisch, D. et al., 2004).

TABLE 20.3 The Nature of Bonding and the Weakest Bonds in Different Types of Silicates That Are Common in Soils (in Order of Decreasing Stability)^a

Structural Type	Group Name	Formula, Structure	Silicate Unit		
			Shared O per Si	Weakest Bonds	Examples
Framework	Tectosilicates	SiO ₂	4	Si–O	Quartz
	Tectosilicates	SiO ₂ , with Al substitution	4	With cations (K ⁺ , Na ⁺ , and Ca ²⁺)	Feldspars
Layer	Phyllosilicates	Si ₂ O ₅ ²⁻ , with Al substitution, as a sheet joined to Al-, Mg-, Fe-OH sheet	3	With interlayer cations, usually K ⁺	Micas
Single chains	Inosilicates	SiO ₃ ²⁻ , with Al substitution	2.5	With divalent, and other cations	Pyroxenes
Double chains	Inosilicates	Si ₄ O ₁₁ ⁶⁻ , with Al substitution	2	With divalent, and other cations	Amphiboles
Isolated tetrahedra	Nesosilicates	SiO ₄ ²⁻	0	With divalent cations	Olivines

^a Cyclosilicates (e.g., tourmaline) have two O bonds per Si and sorosilicates (e.g., epidote) have one O bond per Si, but neither is common in soils (Table 20.2).

and that in the Goldich series. Nonetheless, reference to Table 20.3 may lead to oversimplification concerning possible structural control on the relative stability of silicates to weathering, especially when other silicates besides those in the broad groups represented by both types of ordering are considered. Following Loughnan (1969), for example, we note that both zircon (ZrSiO₄) and andalusite (Al₂SiO₅) are nesosilicates like olivine and have (Si:O)_{molar} ratios of 0.25 and 0.2, respectively, which are equal or less than those of olivine and yet are both very stable (i.e., resistant) to breakdown by weathering, in contrast to olivine, which is notably unstable according to Goldich's (1938) series (Figure 20.2). Furthermore, the broad classifications shown in Table 20.3 hide the observed differences in the stabilities between individual minerals within structural types. Within the phyllosilicate mica group, biotites are generally much less stable than muscovites, whereas the tectosilicate feldspars include albites and anorthites, each with quite different stabilities.

Another danger of oversimplification arises because weathering (and argillization) is not simply a matter of dissolution of the silicate minerals in water. Instead, weathering often occurs in an acid environment and, commonly in soils, also involves a range of organic compounds, which can complex the ions in the silicate structure and can both enhance their breakdown and affect its course and the products formed (e.g., Velde and Barré, 2010).

The rate at which hydrolysis affects cations released is related to the strength of the bonds formed by the cations within the minerals, according to Pauling's electrostatic valency principle (Pauling, 1929). The ratio of the valency (the charge on the ion) to the coordination number (the number of ions of opposite charge surrounding an ion) is known as the electrostatic valency. The smaller its value, the greater the ease of hydrolysis (Paton et al., 1995). The hydrolysis, or replacement of a cation in a crystal structure by H⁺, of K is relatively easy because it is univalent (K⁺).

It is commonly found in feldspars, where its coordination number is 9, and in micas, where it has a coordination number of 12. Hence, the electrostatic valency of K in these minerals is 1:9 and 1:12, respectively (Paton et al., 1995). The hydrolysis of Al is more difficult because it is trivalent (Al^{3+}), with coordination numbers of 6 or 4, so the electrostatic valency of Al in primary minerals is either 1:2 or 3:4. These differences between cations, and also between the same cations in different minerals, are reflected in the relative responses of the four main groups of silicates to weathering pressures (Paton et al., 1995). The solubility or relative mobility of various ions such as Ca, K, and Mg relates to ionic potential, which is the ionic charge (valency) divided by the ionic radius (size), so that ions with a low ionic potential such as Na^+ , K^+ , Ca^{2+} , and Mn^{2+} are more easily leached (lost) in solution, although temperature and pH affect solubility as well (Schaetzl and Anderson, 2005).

Some components of the silicate framework can greatly influence the rate and nature of their breakdown. Chief among these is Fe. According to Millot (1970), the most important weathering reactions involve Fe, a component of many of the primary minerals involved in soil formation (Table 20.2). Along with Mn, which is less abundant in the primary soil-forming minerals (Table 20.2), Fe generally occurs in its reduced form in primary minerals. Fe occurs as Fe(II) and Mn as Mn(II). These are both easily converted to their oxidized forms—Fe(III) and Mn(IV)—when oxidation occurs, for example, when soils dry. This change in valency sets up a charge imbalance in the appropriate minerals, leading to a loss of other ions from the mineral structures, which can destabilize the minerals, enhancing their further breakdown by hydrolysis, which is assisted by the hydrogen ions produced during oxidation. The oxidized forms of Fe and Mn occur as oxides and oxyhydroxides and those of Fe, in particular, are almost ubiquitous in soils. Seasonal wetting and drying cause alternate oxidation and reduction of Mn(II) and Mn(IV) and lead to the common precipitation of the blue-black mineral pyrolusite (MnO_2)—as well as other forms of MnO_2 such as todorokite (Churchman et al., 2010)—as redox segregations (also known as redox concentrations) in the form of coatings (mangans), nodules, or concretions (Vepraskas, 1992; Birkeland, 1999). Manganese oxides in most conditions form preferably to those of Fe during wetting and drying because of the greater ease of acceptance of electrons by Mn than by Fe. The reduction of Fe(III) to Fe(II), commonly by organisms during phases in which a soil is waterlogged, and then its oxidation on drying, leads to Fe oxides being precipitated as mottles, coatings, or concretions. The persistence of reducing conditions causes soil matrix materials to have pale, low-chroma colors (described as redox depletions), and these grayish colors characterize continuously reduced soils that, therefore, have few or no redox segregations (Birkeland, 1999; Vepraskas et al., 2004; Morgan and Stolt, 2006). Brinkman (1970) characterized the clay decomposition brought about by cyclical alternation of redox conditions by the name of “ferrolysis.” Even so, a reexamination of some texture-contrast soils having coarser topsoils than subsoils by Van Ranst and De Coninck (2002) found that

such coarsening with depth could be more easily attributed to the translocation of clay than to its destruction.

Weathering and argillization, together with soil formation, generally occur in a dynamic system that is open to the wider environment. Leaching—the removal or loss of material in solution—commonly occurs. The driving force that provides the chemical potential energy for mineral alteration is the difference in composition between the “attacking” solution and the solid mineral. However, it is the rate of leaching, which governs the rate of removal of solutes, which most influences the rate of mineral alteration and any subsequent precipitation (Figure 20.1). It also influences the course that the alteration takes. Garrels and Mackenzie (1971) stated that, given sufficient leaching, almost all rocks or unconsolidated deposits will leave a residue that is largely composed of the relatively insoluble oxides of Al, Fe, and Ti.

Hence, the origin of primary minerals as given by their temperature of crystallization from magma influences their thermodynamic stability against breakdown by weathering in an aqueous environment, as does their structure and their particular chemical composition (Figure 20.1). However, such environmental factors as the particular composition of the solutions bathing the minerals, the dynamics of the redox conditions, and the rate of throughflow of water past the minerals can play a decisive role in the kinetics, course, and ultimate products of their alteration.

20.2.4 Processes and Products of Alteration of the Main Types of Primary Minerals by Weathering

Early work exploring either the fate of primary minerals or the origin of secondary minerals on weathering (e.g., Jackson et al., 1948) tended to take the stance that specific primary minerals have led to particular secondary minerals as products. A 1:1 correspondence between altered rock-forming mineral and phyllosilicate product appears justified when one dominant type of primary mineral is altered more than others in the parent material and the overlying soil, saprolite, or regolith more generally is dominated by just one type of secondary mineral (clay). Some modern studies have also concluded that each type of primary mineral generally leads to one particular type of secondary mineral. Thus, according to a generalization by Wilson (2006), the weathering of granite rocks leads most commonly to kaolin minerals (kaolinite and halloysite), largely deriving from the alteration of feldspars, and vermiculite minerals from the alteration of micas. Furthermore, many clay minerals appear to be found in close proximity to particular types of altered primary minerals, for example, halloysite tubes on altered feldspar (Figure 20.3). Clay minerals may also have a morphology that appears to mimic that of altering or altered primary minerals. The similarity in shapes between vermicular books of kaolinite and degraded micas, often occurring as some form of vermiculite (Figure 20.4), can be suggestive of a micaceous origin for the particular kaolinite. To examine whether there is always a 1:1 relationship between particular

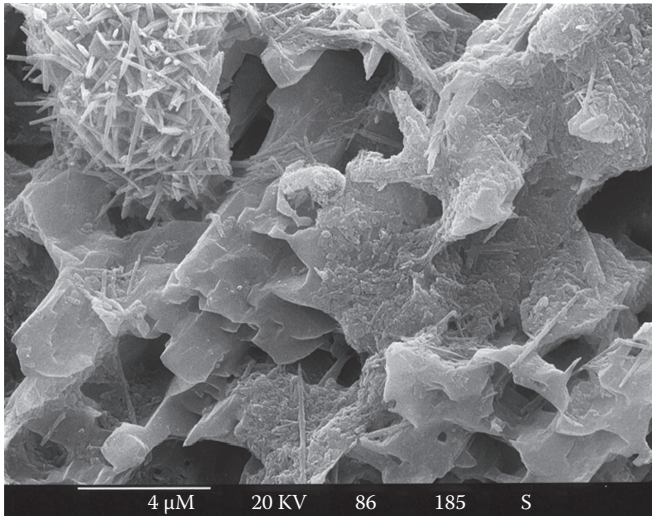


FIGURE 20.3 Scanning electron micrograph of tubular halloysite occurring in close proximity to weathered feldspar in granitic saprolite from Hong Kong. (Photo by Stuart McClure. Reproduced with the permission of the Geotechnical Engineering Office, Civil Engineering Office, Hong Kong.)

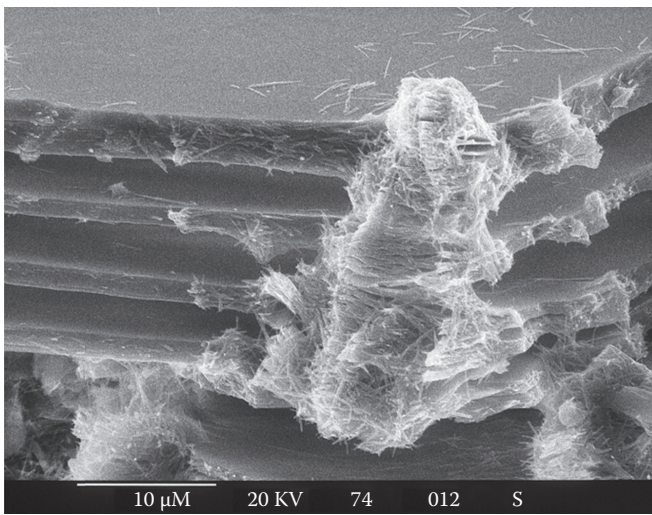


FIGURE 20.4 Scanning electron micrograph of vermicular kaolinite (with some halloysite tubes) occurring in close proximity to weathered mica in granitic saprolite in Hong Kong. (Photo by Stuart McClure. Reproduced with the permission of the Geotechnical Engineering Office, Civil Engineering Office, Hong Kong.)

primary minerals and specific secondary minerals, the following subsections summarize studies that have concentrated on the fate of individual types of primary minerals to alteration by weathering. In these subsections, the generalizations have often been drawn from studies of the weathering of rocks or other geological deposits, the minerals derived from these, and at depth within soil profiles. The influence of particular soil factors on the alterations and products of weathering is discussed in Section 20.2.5.

20.2.4.1 Processes and Products of Alteration of Olivines, Pyroxenes, and Amphiboles by Weathering

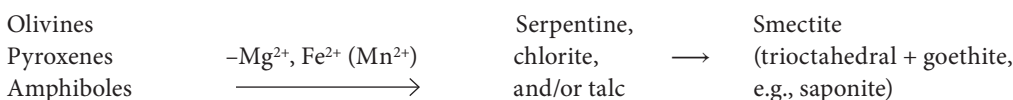
In an open environment, generally unstable olivines easily lose Mg^{2+} , and Fe^{2+} (or Mn^{2+} if manganous) to give, first serpentine, then a smectite (commonly saponite), and also goethite, which together have been characterized as “iddingsite” (Loughnan, 1969; Nahon et al., 1982; Eggleton, 1984). Both optical (Craig and Loughnan, 1964) and electron microscopy (Eggleton, 1984) have enabled identification of iddingsite as a mixture of saponite and goethite. Nahon et al. (1982) made the important observation that an aluminous dioctahedral smectite had formed from the breakdown of the Mg-olivine, forsterite (Mg_2SiO_4), which contains very little Al. They suggested that Al probably derived from the simultaneous breakdown of a pyroxene, enstatite. Secondary minerals could, therefore, derive their elemental constituents from the breakdown of more than one primary mineral. Indeed, olivines could give rise to a variety of secondary mineral products, including smectite, kaolinite, halloysite, and also various oxides, hydroxides, and oxyhydroxides of Fe, and, if present, also Mn, upon leaching (Huang, 1989).

Pyroxenes and amphiboles, although slightly more stable than olivines, tend to break down in a similar fashion to the olivines in the field, with an initial loss of their divalent cations, typically Mg, Ca, and Fe(II). Chlorite and/or smectite often result, although talc may also be formed. Calcite can also form as one of the products if Ca is released in abundance (Loughnan, 1969; Eggleton and Boland, 1982; Huang, 1989). Examination at the fine scale of the mineral grain revealed that amphibole weathering led to a dioctahedral (montmorillonite) and a trioctahedral (saponite) smectite, and also kaolinite–smectite simultaneously at the early stages of alteration, with halloysite developing with time (Proust et al., 2006). The different products were associated with different crystallographic faces of the host amphibole (see Section 20.2.5.1). As with olivines, pyroxenes and amphiboles could give rise to products with simpler structures, such as kaolinite, Fe(III) oxides, and anatase upon strong leaching (see also Wilson, 2004). The common pathway of alteration of this group of minerals by weathering is shown in Box 20.2.

Many laboratory studies have been designed to help understand the initial stages of alteration of these ferromagnesian minerals. At low pH, divalent ions are lost relative to silica, whereas the converse occurs at high pH with a preferential loss of Si (Schott and Berner, 1985). It has usually been inferred that leached layers, depleted in some of their original constituents, develop as a result on mineral surfaces (Schott and Berner, 1985; Banfield et al., 1995). Experimental studies (e.g., Velbel, 1985) have often indicated weathering rates that far exceed those observed in nature by up to 5 orders of magnitude (Banfield and Barker, 1994).

However, by following evidence from electron microscopy particularly, weathering of olivines, pyroxenes, and amphiboles has been seen to involve the formation, enlargement, and coalescence of etch pits developed on crystal dislocations

Box 20.2 INITIAL ALTERATION OF OLIVINES, PYROXENES, AND AMPHIBOLES AS COMMONLY REPORTED



(Huang, 1989; Hodder et al., 1991; Seyama et al., 1996; Wilson, 2004) rather than through an enleached layer. Velbel and Barker (2008) have acknowledged that surface tension upon air-drying samples for conventional scanning electron microscopy (SEM) may affect surface structure and have examined partially weathered pyroxenes using high-pressure cryofixation (HPF) and cryo-field emission gun SEM, both of which avoid the surface tension effects of air-drying. They were thus able to view the products formed in small-scale etch pits on the pyroxenes and have concluded that pyroxene weathers to smectite by a multi-stage process. Velbel and Barker (2008) proposed that the process includes initial dissolution, topotactic reactions, mechanical disruption from wetting and drying cycles, further dissolution and, eventually, microbial colonization of the pores, with weathering finally enhanced by microbial extracellular polymers. As for the alteration of feldspars (see Section 20.2.4.2), the findings from laboratory studies may not reflect the processes occurring in the field because of oversimplification of the factors involved in natural weathering.

Nonetheless, Mogk and Locke (1988), using Auger electron spectroscopy (AES), found that naturally weathered hornblende showed systematic cation depletion to depths of ~ 120 nm. They considered that the dissolution of minerals generally occurs from both their surfaces and their bulk. Furthermore, Welch and Banfield (2002) were able to produce microstructural channeling effects in the olivine, fayalite, from laboratory dissolution experiments with an initial pH of 2.0, which were identical to those seen in the naturally weathered mineral (e.g., Banfield et al., 1991). X-ray photoelectron spectroscopy (XPS) had shown earlier that surfaces are coated by films of Fe(III) oxides both at low and high pH (Schott and Berner, 1985; Casey et al., 1993; Seyama et al., 1996), and Welch and Banfield (2002) found that when either microbes that enzymatically oxidize iron or instead ferric iron was added to the system, the minerals degraded at a greatly reduced rate. They identified the formation of laihunite, a ferric-ferrous olivine-like mineral containing vacant atomic sites, in the region of the mineral surface. This laihunite would protect the mineral against further dissolution.

Generally, alteration of primary minerals to give secondary products involves either transformation within the solid state

or neoformation, with either partial or complete dissolution of solutes, then their reprecipitation as new secondary phases. Structural considerations appear to dictate that neither the neosilicate olivines, with independent silica tetrahedra, nor the inosilicate pyroxenes and amphiboles with tetrahedra in chains, can transform directly within the solid state to phyllosilicate clay minerals with flat sheets. Nevertheless, high-resolution transmission electron microscopy (HRTEM) observations of weathering amphiboles led Banfield and Barker (1994) to conclude that a type of transformation of amphiboles to smectites can occur within the solid state. They observed these reactions occurring in interstitial spaces within the primary amphiboles, with secondary smectites formed in a topotactic relationship to the altering amphibole. The change was described as a partial depolymerization of the amphibole structure leading to a repolymerization to that of smectite. There is no need for bulk water to bring about this change, with the water of hydration of the smectite product being able to supply the water required for the transformation reaction. Although Banfield and Barker (1994) pointed out that this type of transformation is not representative of all weathering reactions, it enables episodic alteration to take place within rocks or geological deposits, where it is limited by an intermittent supply of water and, therefore, much slower than that occurring on the surfaces of rocks or rock minerals immersed in aqueous solution. Banfield et al. (1995) found that smectites could form within weathering pyroxenoids (rhodonite and pyroxmangite, both $MnSiO_3$), which were studied by a similar type of in situ transformation. Periodic drying, which often occurs in this situation, may promote the repolymerization of phyllosilicates rather than depolymerized silica (Banfield et al., 1995). The reaction has little significance for soil formation, however, because the smectitic products are "quite ephemeral" and disappear when transported from the altered rock into the more open soil environment (Wilson, 2004).

Not all workers have considered that the primary ferromagnesian minerals are altered directly to phyllosilicates such as smectites. Nahon and Colin (1982) and Singh and Gilkes (1993) both identified amorphous or noncrystalline intermediates in the alteration of (different) pyroxenes. In comparing this observation with those of Banfield and coworkers, among others, who

observed direct formation of phyllosilicates on altering ferromagnesian minerals, Wilson (2004) cautioned that the course of formation of phyllosilicates may have been established by prior hydrothermal or deuteritic alteration in the latter cases and alteration by weathering had continued along the predisposed course.

20.2.4.2 Processes and Products of Alteration of Feldspars by Weathering

Feldspars have been thought to give rise to many different types of secondary minerals, encompassing the range of structural complexity from smectites through to gibbsite and quartz. Allen and Hajek's (1989) review referred to several studies where smectites have been identified as products of the alteration of feldspars. These authors surmised that the resultant smectites would be beidellitic because the parent feldspars lacked Mg or Fe, and Nettleton et al. (1970) characterized a smectite seen to form directly from a feldspar crystal as a beidellite–montmorillonite. Reports of the alteration of feldspars to gibbsite and quartz, at the lower end of the scale of structural complexity, were given by Allen and Hajek (1989) and Estoule-Choux et al. (1995). Otherwise, feldspars have been considered as the source minerals for micas (Carroll, 1970; Millot, 1970) and very often also for kaolinites and halloysites (Eswaran and Wong, 1978; Calvert et al., 1980; Anand et al., 1985). The micaceous minerals formed from feldspars, both K-feldspars and plagioclases, have often been described as “sericitic,” with the process of their formation being described as sericitization (Carroll, 1970; Millot, 1970). However, the term sericite has also been used to describe white mica formed from the reaction of biotite with plagioclase during metamorphism (Meunier and Velde, 1976). Furthermore, orthoclase (a K-feldspar) has been considered to hydrolyze to muscovite (Hemley, 1959). On the contrary, Meunier and Velde (1979) found that the micaceous phase, which they considered to be an illite, developed at a boundary between muscovite and orthoclase within weathering granite, and contained more Fe and Mg than either the muscovite or orthoclase. Hence, the illite formed (precipitated) out of solution. Using electron microscopy, Eggleton and Buseck (1980) detected micaceous phases forming within vacuoles within microcline. They considered these to be either illite or interstratified illite–smectite. Bétard et al. (2009) found that an illite formed within nonalkali feldspar (a plagioclase) by neof ormation in Luvisols in north-east Brazil, and, more generally, they considered this particular weathering reaction to be typical of semiarid tropical and subtropical climates.

Studies of the artificial weathering of feldspars in controlled conditions in the laboratory have largely focused on the possibility of the formation of a leached layer on feldspar surfaces during their alteration. On the one hand, different types of surface-sensitive analyses—including secondary ion mass spectrometry, SIMS (also known as ion microprobe) (Muir and Nesbitt, 1997); elastic recoil detection, ERD, and Rutherford backscattering, RBS (Casey et al., 1988, 1989); and XPS (Muir et al., 1989, 1990; Hellmann et al., 1990)—indicated the formation of a dealcalized

leached layer of up to 1 μm deep, especially at low pH. The leached product from an albite was identified as an amorphous phase with some of the characteristics of nanocrystalline allophane, which later became detached (Kawano and Tomita, 1994). The fate of the leached layer was found to be dependent upon the Si:Al ratio in the parent feldspar (Oelkers and Schott, 1995). Where this ratio was 1, as in plagioclases (anorthite was studied), the removal of Al led to completely detached silica tetrahedra, but where it was 3, as in alkali feldspars, Si tetrahedra that were still partially linked remained.

On the other hand, some measurements by XPS (Berner and Holdren, 1979) showed no leached layer forming, and when the artificial alteration was carried out at near-neutral pH values (between 5 and 8), rather than at low pH, the layer formed was only thin (Blum and Stillings, 1995). Huang (1989) concluded that, in any case, leached layers are not thick enough to inhibit transport and also that there were no continuous layers of secondary precipitates on weathered feldspars. As in the case of olivines, pyroxenes, and amphiboles, dissolution of feldspars probably occurred at sites of excess energy such as dislocations (Huang, 1989).

HRTEM studies have shown that unweathered feldspars are often turbid as a result of minute vesicles being filled with fluid (Hochella and Banfield, 1995), consistent with the observation that they can have a high microporosity (Worden et al., 1990). HRTEM has also shown that their alteration often occurs preferentially at crystal defects (Wilson and McHardy, 1980; Holdren and Speyer, 1987) and that secondary minerals form throughout the primary mineral, not just at grain boundaries (Banfield and Eggleton, 1989; Banfield et al., 1991). Application of SEM and associated energy-dispersive x-ray (EDX) analyses showed etch pits and secondary coatings (of a kaolin mineral) developing as the weathering alteration of feldspars progressed (Inskeep et al., 1993). These authors saw the formation of secondary coatings on feldspars as an integral part of their alteration. These were not observed in artificial weathering studies. Essential features of weathering in the field include those of seasonal wetting and drying, a generally high solid:solution ratio, and long residence times for water (Inskeep et al., 1993). The net effect is a weathering rate, determined for plagioclases, that is several orders of magnitude slower than the experimental dissolution rate (White et al., 1996, 2005; White and Brantley, 2003). Maher et al. (2009) have shown that other factors besides mineral dissolution rate and the rate of aqueous transport of solutes, notably the rate of secondary mineral precipitation, ensure a much slower rate of weathering of minerals, including feldspars, in the field than in the laboratory. Furthermore, fungi have been shown to contribute to the breakdown of feldspars on weathering, partly, at least, through their tunneling by organic anions exuded at the tips of the hyphae of (presumably ectomycorrhizal) fungi (Smits et al., 2005; see also Section 20.2.5.3 on podzolization). Failure to reproduce these features in necessarily hastened artificial weathering studies under closely controlled conditions almost certainly means that their results cannot be applied readily to the understanding of natural weathering.

20.2.4.3 Processes and Products of Alteration of Micas by Weathering

Changes from any of the neosilicate olivines, with independent silica tetrahedra, the inosilicate pyroxenes and amphiboles with tetrahedra in chains, and the tectosilicate feldspars with continuous frameworks of silica and alumina tetrahedral, to yield phyllosilicate clay minerals with flat layers, all involve some dissolution and recrystallization. These processes usually occur within the solution phase, when they can confidently be labeled as neogenesis, although, as we have seen from Banfield and coworkers, descriptions (see Section 20.2.4.1), neogenesis can also take place by a type of transformation within the solid phase that involves successive depolymerization and repolymerization. By contrast, phyllosilicate micas can transform easily to phyllosilicate clay minerals in the solid state.

The main changes that occur in these transformations are exchange of the interlayer cations and reduction in the charge of the layers. Potassium ions occupy the interlayer regions of the common micas, biotite and muscovite. The replacement of K^+ by hydrated cations such as Mg or Ca leads to a loss of strength of binding between adjacent layers. The interlayers expand, so that, with complete replacement by hydrated divalent cations, the basal spacing increases from 1.0 to 1.4 nm and vermiculite is formed. The concomitant reduction in layer charge has been supposed to occur by a wide variety of mechanisms. These include incorporation of protons into the layers (Raman and Jackson, 1966; Leonard and Weed, 1967), exchange of Si for Al in the tetrahedral sheet (Jackson, 1964; Sridhar and Jackson, 1974; Vicente et al., 1977), loss of hydroxyls (Stucki and Roth, 1977), and the deprotonation of hydroxyl groups and the loss of octahedral Fe, both occurring together (Farmer et al., 1971; Douglas, 1989; Fanning et al., 1989).

In soils particularly, micas rarely transform completely to vermiculite. In soil science, the term “illite” is most commonly used to describe clay-sized micaceous minerals. According to Grim et al.’s (1937) original definition of illite, it was “a general term for the mica-like clay minerals occurring in argillaceous sediments,” which also “showed substantially no expanding lattice characteristics.” It tends to be used more widely in practice. Illites commonly show a deficit of K and an excess of water in comparison with muscovite or biotite. This deficit reflects the greater ease of loss of K from micas that are fine grained rather than coarse, together with a paradoxical especially strong retention of some K in the fine-grained micas against replacement, both in nature and in the laboratory (Fanning et al., 1989).

Fine-grained micaceous minerals that include some expanding layers are sometimes also called illite (Grim, 1968; Wentworth, 1970; Norrish and Pickering, 1983; Weaver, 1989; Laird and Nater, 1993). Strictly speaking, however, these are interstratified illite (or mica)–vermiculites (or smectites). The interstratification may be either random or regular. If they are regular, with close to a 1:1 mix of the two constituent layer types, these two types alternate and the basal spacing is a sum of the

spacings of the unaltered mica layers (1.0 nm) and the hydrous vermiculite layers (1.4 nm), giving a resultant spacing of 2.4 nm.

Alternating layer types in regular 1:1 interstratifications are explained by the replacement of the K ions in one interlayer by hydrated divalent ions, leading to the expansion of this interlayer, causing, in turn, a strengthening of the bond between K^+ and the aluminosilicate layers in the two adjacent interlayers (Bassett, 1959). These bonds probably strengthen because of a shift of structural hydroxyl groups toward the opened interlayer (Norrish, 1973). Regular interstratifications of micas with vermiculite (and also with smectites, as products of further transformation of micas) tend to occur in soils in colder climates, such as the upland regions of the former Yugoslavia (Gjems, 1970), Scotland (Wilson, 1970), Scandinavia (Kapoor, 1973), and the South Island of New Zealand (Churchman, 1980). In these cold climates, the displacement of interlayer K^+ occurs more slowly and in more discrete steps, that is, via alternate interlayer regions, than in warmer climates, where the transformation occurs more rapidly and in a relatively haphazard fashion to give irregular layer stacking. The release of K^+ from micas is considered to occur by either layer weathering, as proposed by Jackson et al. (1952), or edge weathering, as proposed by Mortland (1958), or both. In the former, most, if not all, of the K^+ in a particular interlayer is released virtually simultaneously. This release commonly occurs in the alteration of clay-sized micas. In edge weathering, K ions are released by diffusion from edges and fractures. This loss by diffusion commonly occurs in the alteration of larger mica flakes and has been observed as fraying in artificially altered micas, but it can also take place alongside layer weathering in clay-size micas (Fanning et al., 1989).

Trioctahedral micas, among them biotite and phlogopite, weather more readily than dioctahedral micas, including muscovite and most illites. Plants can bring about the transformation of biotite to vermiculite through their extraction of K from the mineral (Section 20.2.5.3). Among vermiculites in soils, the dioctahedral forms are more common than their trioctahedral counterparts (Jackson, 1959). Not only are the dioctahedral vermiculites more stable, but also they can form from biotites at the expense of the trioctahedral varieties as a result of a structural rearrangement whereby some octahedral cations are lost from the structure only to be replaced by some Al cations that are lost from tetrahedral sites (Douglas, 1989).

Transformation of micas in soils to expandable phases often occurs under acidic conditions. When pHs are relatively low (ca. 5 ± 0.5) and organic matter contents are low, Al is mobile in the aqueous phase as hydroxyl cations, and, where wetting and drying frequently occur, the conditions favor the deposition of Al-hydroxy species in the interlayers of vermiculites (and also smectites; Rich, 1968). The products, which are nonexpandable or only poorly expandable, are known by a variety of names including dioctahedral chlorite, pedogenic chlorite, 2:1–2:2 intergrade, chloritized vermiculite, and hydroxyl-interlayered vermiculite (HIV), and also their smectitic counterparts, such as hydroxyl-interlayered smectite (HIS) (Barnhisel and Bertsch, 1989).

Aluminous interlayers can protect vermiculites from further breakdown (Douglas, 1989) but can be destroyed by chemicals that dissolve Al hydroxyl species, including citrates. Citrates were once used routinely prior to x-ray diffraction (XRD) analyses (Mehra and Jackson, 1960) but their use can lead to the loss of potentially useful genetic information from the occurrence of the aluminous interlayers (Churchman and Bruce, 1988).

Vermiculitization of micas/illites has been found to occur by the expansion of the interlayer region into a wedge shape, known as the “frayed edge site” (Sawnhey, 1972; Nakao et al., 2009). Through the use of a measurement known as “radiocesium interception potential” (RIP), which gives the amount of these frayed edge sites, Nakao et al. (2009) have compared minerals in soils that have formed from parent materials containing micas in various parts of Asia for their vermiculitic character in relation to the moisture regimes in which they have formed. RIP measures the selectivity of the frayed edge sites for Cs⁺ in comparison with hydrated ions. A high RIP value, indicating a high selectivity for Cs, indicates a high concentration of vermiculite per se, whereas a low value can indicate either that little transformation of illite/mica has occurred or else that hydroxyl-Al interlayering has blocked the frayed edge sites that develop with vermiculitization. Nakao et al. (2009) discovered that, in subtropical Thailand, with an ustic moisture regime in which there is a distinct dry season, illites showed little alteration and, consequently, RIP was low. However, in a strongly leaching udic moisture regime and hyperthermic temperature regime in Indonesia, an advanced degree of vermiculitization was indicated by a high RIP. By contrast, an udic and mesic moisture regime in temperate Japan, while also producing a high degree of vermiculitization, nonetheless gave a low RIP value. This result arose because hydroxyl-Al interlayers blocked frayed edges. Nakao et al. (2009) noted that an index of weathering that is based on the degree of vermiculitization showed no relationship with one based on the oxidation status of Fe, which implied that the Thai soil was highly weathered despite its mica/illite showing little or no alteration. The factors that affect the development of Fe oxides in soils and those that affect loss of K⁺ from the interlayers of micas and illites need bear no relation to one another. In particular, Nakao et al.’s (2009) results showed that the balance between the time spent by a soil in a dry season and the extent of leaching that occurs plays an important role in determining the extent of vermiculitization of its constituent micaceous phases.

Under low pH conditions, commonly where organic matter contents are high, as they often are under forests, micas may transform to smectites in soils as a result of acid leaching. These conditions typify podzolization and smectites often form through the transformation of micas in the eluviated horizons of podzols. The resulting smectites are generally Al-rich and hence beidellitic (Ross and Mortland, 1966; Churchman, 1980; Borchardt, 1989), but may also be montmorillonitic (Aragoneses and García-González, 1991). Strong weathering without podzolization can also transform micas to smectites (Stoch and Sikora, 1976; Egashira and Tsuda, 1983; Senkayi et al., 1983; Singh and Gilkes, 1991; van Wesemael et al., 1995), even in Antarctic soils,

where smectites were among the transformation products of micas (Boyer, 1975). Smectites formed this way have generally been identified as beidellites. Their genesis contrasts strongly with those of most smectites, which form at high pH under poor drainage (see also Section 20.3.5).

Under cool climates, and, with sufficient rainfall, vermiculitic layers that are interstratified with mica layers can themselves be further transformed while the adjacent mica layers remain essentially unaltered. Thus, stepwise transformations of (muscovite) mica, first to regularly interstratified mica-vermiculite, then to regularly interstratified mica-beidellite, have occurred over a climosequence on increasing rainfall on mica-chlorite schist in South Island, New Zealand (Churchman, 1978, 1980). These changes to alternate layers have occurred under a current grassland vegetation, rather than under native forest. Indeed, soils within the area that have formed under forest, but with the same precipitation regime as one of the wetter sites in the climosequence under grassland, showed advanced transformation of the mica to a discrete beidellite phase. It appears that the often more acidic exudates from trees (e.g., Courchesne, 2006) impose a stronger weathering regime than that under grassland, so that the driving force exceeds that leading to transformation of alternate layers alone.

An advantage of many cool-climate studies is that not all primary minerals alter at the same rate, and the origin of secondary minerals can, therefore, be traced to the few, if not single, primary minerals that have altered. In the bulk of Churchman’s (1978, 1980) studies, feldspars were fresh and only mica and chlorite showed signs of alteration. In warmer climates and, with sufficient throughflow of water and passage of time, micas break down further to form 1:1 minerals, both kaolinite and halloysite. Although the direct formation of kaolin minerals from micas alone cannot be concluded when other primary minerals have also altered, many workers have established that micas have altered to form kaolins mainly because of the appearance of the secondary minerals as pseudomorphs after the micas. This apparent pseudomorphic replacement applies for kaolinites formed in tropical Nigeria (Ojanuga, 1973), from tertiary weathering in Europe (Stoch and Sikora, 1976), in ferrallitic (lateritic) soils in Western Australia (Gilkes and Suddhiprakarn, 1979), and in deeply weathered soils in the continental United States (Rebertus et al., 1986), and also for both halloysite and kaolinite formed alongside each other in close association with biotite in tropical Malaysia (Eswaran and Yeow, 1976).

Mainly with the help of electron microscopy, some workers have even found that kaolin minerals can form from micas early in the weathering process including from both biotite (Ahn and Peacor, 1987; Banfield and Eggleton, 1988) and muscovite (Robertson and Eggleton, 1991). Ahn and Peacor (1987) showed that kaolinite can also form as (irregularly) intercalated layers between biotite layers, presumably by a dissolution/crystallization process whereby one biotite layer gives rise to two kaolinite layers. This change takes place within “plasmic microsystems” (Velde and Meunier, 2008) involving small differences in chemical potentials, which arise because of connections with a major

passageway for water outside a rock or geological deposit. Such an occurrence—the kaolinization of biotite—may have occurred in weathered tephra beds aged ca. 350,000 years in northern New Zealand and which contain biotite in the unweathered parent tephra (Rangitawa tephra). The kaolinized mineral occurs as a sand-sized golden platy mineral. It comprises (using SEM) nearly nine primary (6–8 μm thick), four secondary (1–1.5 μm), and five to seven tertiary (0.7 μm) lamellae units, and was characterized via XRD as a K-depleted, partially random interstratified micaceous kaolinite intergrade containing <50% of 1 M trioctahedral mica and >50% of partially disordered dioctahedral kaolinite (Shepherd, 1984; Lowe and Percival, 1993).

Conversely, some (Eswaran and Yeow, 1976; Gilkes and Suddhiprakarn, 1979) have found that vermiculite—often considered to be an unstable intermediate phase (Kittrick, 1973)—nonetheless occurred alongside kaolin minerals in soils formed under strong leaching. One of the likely reasons for the appearance of apparently early weathering products such as vermiculite alongside apparently late stage products such as kaolin minerals is that iron (oxyhydr)oxides are very common products of the weathering of micas. The secondary iron phases coat other minerals such as vermiculites and preserve them against further breakdown. They include goethite (Sousa and Eswaran, 1975; Eswaran and Yeow, 1976; Gilkes and Suddhiprakarn, 1979; Banfield and Eggleton, 1988) as well as hematite (Gilkes and Suddhiprakarn, 1979). Several studies of the products of natural weathering of micas (Rice and Williams, 1969; Aldridge and Churchman, 1991; Aoudjit et al., 1996; Seyama et al., 1996), using variously Mössbauer and XPS spectroscopy, as well as the laboratory study of Farmer et al. (1971), have shown that total Fe and Fe(II) were depleted from micas on weathering while Fe(III), Fe gels, and Fe(oxyhydr)oxides built up outside the micas. Oxides and hydroxides of other metals, including Al, as gibbsite (Gilkes and Suddhiprakarn, 1979), and also titanium dioxide (Milnes and Fitzpatrick, 1989), may also have formed, at least partially, from micas.

20.2.4.4 Processes and Products of Alteration of Chlorites by Weathering

Chlorites occur most commonly as trioctahedral minerals in parent materials for soils. They originate mainly from low-grade metamorphic rocks and as products of the early alteration of Fe- and Mg-containing primary minerals such as augite, hornblende, biotite, and serpentines (see Section 20.2.4.5). They are not common in soils mainly because of their low stability with regard to weathering. The initial stages of their alteration are similar to those of micas and involve the loss of their interlayer species, most often hydroxides of Mg (i.e., brucite structures), but also those of Fe and other cations. Products of the earliest stages of weathering of chlorites have been identified variously as a randomly interstratified hydrous phase (Churchman, 1980), swelling chlorite, which is a type of chlorite depleted of some of its interlayer hydroxides (Stephen and MacEwan, 1951; Bain and Russell, 1981), and sometimes also regular interstratifications of chlorite and swelling chlorite (Churchman, 1980), as well as a

chlorite-vermiculite intergrade (Murakami et al., 1996). There is also a strong tendency to form 1:1 regular, or “semiregular,” chlorite-vermiculite interstratifications at the next early stage of weathering. This mineral type has been observed in weathering by Johnson (1964), Herbillon and Makumbi (1975), Churchman (1980), Banfield and Murakami (1998), and Aspandiar and Eggleton (2002a, 2002b) among others. A study with atomic-resolution transmission electron microscopy (TEM) led Banfield and Murakami (1998) to propose that there was a tendency toward regular 1:1 interstratification because interlayer Mg and Fe (oxyhydr)oxides are removed from every second interlayer on account of a layer shift (of $\sim a/3$) occurring after the removal of one interlayer (oxyhydr)oxide that thereby stabilizes the adjacent interlayer (oxyhydr)oxide. The stabilization means that the (oxyhydr)oxide in the next interlayer is more labile to replacement. However, Wilson (2004) warned that observations of regular chlorite-vermiculite interstratifications should be treated with caution as products of weathering alone because some, at least, of the parent rocks may have undergone prior hydrothermal alteration. Interstratified chlorites and also vermiculite-like phases have been found to occur in some metamorphosed rocks. Nonetheless, not all sequences of alteration of chlorites are the same, with several authors (e.g., McKeague and Brydon, 1970; Bain, 1977; Churchman, 1980; Ross et al., 1982; Righi et al., 1993; Carnicelli et al., 1997) finding that the chlorite component, often of chlorite-mica schists, disappeared as a result of acid weathering in a podzolized soil, or spodosol. Chlorite dissolved, typically leaving a solid residue of iron oxides and oxyhydroxides, for example, goethite (Bain, 1977; Ross et al., 1982). Frequently, however, there is further development of the interstratifications of chlorite with vermiculite to discrete vermiculite (Loveland and Bullock, 1975; Murakami et al., 1996). Often also, smectites are considered to form from chlorite (Herbillon and Makumbi, 1975; Carnicelli et al., 1997). Although the primary chlorites are trioctahedral, the resulting vermiculites and smectites are mostly dioctahedral (Wilson, 2004). Ultimately, kaolin minerals, both kaolinite (Herbillon and Makumbi, 1975; Murakami et al., 1996) and also halloysite (Cho and Mermut, 1992), can result from the strong weathering of chlorites.

20.2.4.5 Processes and Products of Alteration of Serpentine by Weathering

Serpentine rocks, which are dominated by serpentines (mainly chrysotile, antigorite, and minor lizardite), together with iron oxides and such minerals as amphiboles, pyroxenes, and talc (e.g., Bonifacio et al., 1997), are generally unstable in soils. In central California, this rock type gave rise to virtually pure Fe-rich smectite in the fine clay (<0.2 μm) fraction (Wildman et al., 1968). These authors attributed the mineralogical change to the loss of the more mobile elements Mg and Si and relative enrichment of Fe and Al. In the Massif Central in France, alteration of serpentine in a poorly drained B horizon led to a trioctahedral chlorite, which is normally regarded as a primary mineral, and also to its alteration products: a regularly interstratified chlorite-vermiculite and a nontronitic smectite

(Ducloux et al., 1976). This change, while involving some loss of Mg and Si—as expected in an open soil system—is more typical of a closed system (Ducloux et al., 1976). The weathering products of a serpentinite in northwest Italy were found to depend strongly on drainage conditions (Bonifacio et al., 1997). Low-charge vermiculite sometimes formed but either dissolved or was transformed to smectite if drainage was poor. An aluminous chlorite could result from either the preformed vermiculite or smectite as a result of interlayering by hydroxy-Al. Lee et al. (2003) in California and Caillaud et al. (2004) in France also found that vermiculite and smectite were formed in the course of weathering of serpentinites. In general, the smectites formed from serpentinites per se are complex and heterogeneous according to Caillaud et al. (2004). Caillaud et al. (2004) focused on a microsystem in the serpentinite weathering system. The types of vermiculite and/or smectite formed varied, with both trioctahedral and dioctahedral structural types covering a range of layer charges, depending upon their originating primary minerals. For instance, a thin lizardite bastite gave rise to Al-poor trioctahedral saponite, whereas a dioctahedral Fe-rich montmorillonite appeared to derive directly from chrysotile. Using a toposequence in Taiwan on serpentinite containing chrysotile, antigorite, and lizardite, and also chlorite and talc, Hseu et al. (2007) were able to identify the products of weathering as, first, smectite that was dominantly trioctahedral, then interstratified chlorite-vermiculite, and, finally, kaolinite and quartz.

20.2.4.6 Processes and Products of Alteration of Volcanic Parent Materials by Weathering

One outstanding feature of volcanic materials as parent materials for clay-size minerals is that they usually contain glass, which is a fast-weathering source of Si and Al (and other elements) for mineral neogenesis. They can also contain other weatherable minerals, depending on their origin, nature, and composition. Broadly, volcanic materials may originate from effusive eruptions, forming lavas, or explosive eruptions that generate fragmental, unconsolidated deposits called pyroclastic materials, or tephra, which may be distributed widely by the wind. Among the latter, there are three main types, based on composition. These are (1) basaltic, which are rich in Fe and Mg, reflecting usually high contents of ferromagnesian, or mafic, minerals, namely, olivines, amphiboles, and pyroxenes, as well as feldspars and brownish-colored basaltic glass low in Si and relatively high in Al; (2) rhyolitic, which have abundant Si-rich glass comparatively low in Al, and which may contain minor amounts of mafic minerals including biotite, and also feldspars; and (3) andesitic or dacitic, which are intermediate in composition between basaltic and rhyolitic eruptives (see Section 33.3, for more details on their composition, occurrences, and properties).

20.2.4.6.1 Glass

The alteration of glass is a special case. Glass is an amorphous solid with a poorly ordered internal structure comprising loosely linked SiO₄ tetrahedra with considerable intermolecular space

(in which cations such as sodium occur) (Fisher and Schminke, 1984). The hydration and breakdown of glass results in fluxes of some elements from the glass into interstitial pore waters, and the very rapid precipitation of secondary minerals from such solutions as well as replacement of glass shards by new minerals (e.g., Daux et al., 1994). Dissolution of basaltic glass, and probably also other glass types, as determined by Oelkers and Gislason (2001) and Gislason and Oelkers (2003), proceeds in effectively three steps: (1) relatively rapid and largely complete removal of univalent and divalent cations from the near-surface glass structure via the breaking of metal–oxygen bonds and their replacement with proton–oxygen bonds, (2) Al-releasing exchange reactions between three aqueous H⁺ ions and Al in the glass structure, and (3) relatively slow detachment of partially liberated silica. The tetrahedrally coordinated Si–O bonds are the most stable bonds in the glass framework. Si tetrahedra on the glass surface may be connected to the glass framework via one to three bridging oxygens, and the rate of release of any Si atom at the surface decreases markedly as the number of bridging oxygen bonds increases (Gislason and Oelkers, 2003). The breaking of Al–O bonds does not destroy the glass framework but instead only partially liberates the silica tetrahedral chains by removing adjoining Al atoms (Gislason and Oelkers, 2003). Glass dissolution rates demonstrably increase with decreasing Si content (Wolff-Boenisch et al., 2004), and, hence, basaltic glass (low in Si) usually dissolves faster than andesitic glass (intermediate Si content) or rhyolitic glass (high in Si) under similar environmental conditions (Neall, 1977; Hodder et al., 1990; Shoji et al., 1993b; De Vleeschouwer et al., 2008; Sigfusson et al., 2008; Figure 20.2). In all cases, fragmental and vesicular glass components, such as those which occur in tephra deposits, have high surface areas and are very porous and so break down very quickly, and at rates closely proportional to geometric surface areas (e.g., Dahlgren et al., 2004; Wolff-Boenisch et al., 2004). The initial alteration of basaltic glass, described widely as “palagonitization,” is described as a special case in Section 20.2.4.6.3.

20.2.4.6.2 Formation of Allophane and Halloysite from Volcanic Parent Materials

Allophane and halloysite are the most common secondary minerals that are formed in soils developed from loose volcanic material or tephra, which may be ash, pumice, and cinders (the last also referred to as scoria).

Using ²⁷Al and ²⁹Si NMR, Hiradate and Wada (2005) have deduced a mechanism for the formation of allophane from glass as another step in the weathering-synthesis process (Figure 20.5). This mechanism involves (1) dissolution of Al mainly from volcanic glass (via Al-releasing exchange reactions with protons) and its concomitant transformation from its tetrahedral to octahedral state, from ^{IV}Al to ^{VI}Al; (2) hydrolysis of the Al released into solution to give a gibbsite-like sheet; (3) dissolution (via breaking of Si–O bonds) of Si from volcanic glass, where it occurs as a silica gel-like polymer, to give monosilicic acid in solution; and (4) reaction between the gibbsite-like sheet and monosilicic acid to generate allophane.

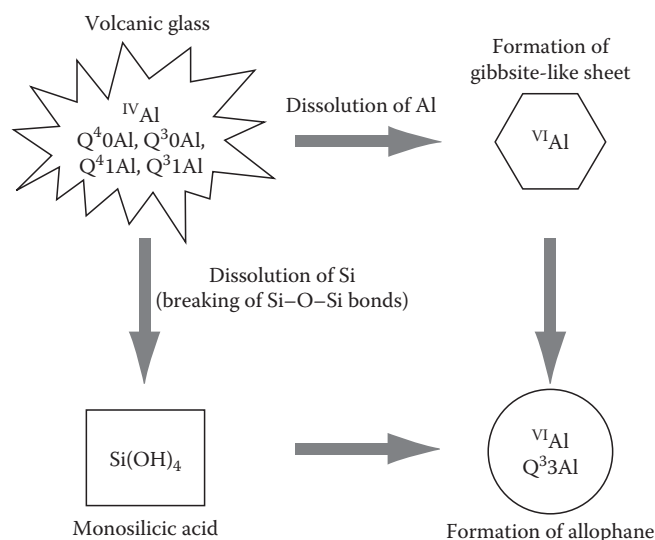


FIGURE 20.5 Model depicting the formation of allophane. Q notation describes the connectivity of a Q unit—that is, an Si atom surrounded by four oxygen atoms—to other Si atoms (Wright and Sommerdijk, 2001): Q4 indicates that the Q unit is fully interconnected with silicate groups, and Q3 indicates that the Q unit is linked in three places (referred to as branching points). (Redrawn from Hiradate, S., and S.-I. Wada. 2005. Weathering processes of volcanic glass to allophane determined by ^{27}Al and ^{29}Si solid-state NMR. *Clays Clay Miner.* 53:401–408, Fig. 4. With permission of The Clay Minerals Society.)

This process is consistent with modern understanding about the crystal structure of allophane. Its structure is regarded as being based on that of imogolite, another aluminosilicate that is sometimes found (typically in small amounts) in soils derived from tephra and in some other soils including podzols. Imogolite has an ideal chemical formula of $SiO_2 \cdot Al_2O_3 \cdot 2H_2O$ and, therefore, an Al:Si ratio of 2:1. The imogolite structure, established by Cradwick et al. (1972), consists of a defect gibbsitic Al-octahedral sheet framework. Si in each silica tetrahedron is attached to this framework by sharing three of its O atoms (hence the Q3 notation shown in Figure 20.5) with an octahedrally coordinated Al on the gibbsitic sheet while the remaining O atom on the tetrahedrally coordinated Si acquires an H atom to form a Si–OH bond pointing away from the gibbsitic sheet. Although imogolite, which comprises long, thin hollow nanotubes, always in bundles, has a definite XRD pattern (Yoshinaga and Aomine, 1962), and, hence, some long-range order, allophane gives extremely broad, low-intensity humps in XRD and is regarded as a mineral with short-range order (SRO), or a poorly ordered aluminosilicate, as well as a “structured nanomineral” (Hochella, 2008; Theng and Yuan, 2008; McDaniel et al., Section 33.3). The best term for it is “nanocrystalline,” meaning structured at the nanometer scale, that is, 1–100 nm. (Another nanocrystalline mineral that occurs commonly but usually in relatively small amounts in weathered tephtras and other materials, and which is analogous to allophane, is ferrihydrite, described later herein.) Allophane composition varies over a much greater range than that of imogolite, although morphologically all unit particles

comprise tiny hollow spherules or “nanoballs” (Parfitt, 2009). In soils, there are two main types: (1) Al-rich, with Al:Si ~ 2:1—these are imogolite-like or proto-imogolite allophanes—and (2) Si-rich, with Al:Si ~ 1:1—these are halloysite-like allophanes. The imogolite-like nanocrystalline structure applies only to Al-rich allophane, which is the most common type (Parfitt, 2009). Generally, it has an XRD pattern that is often indefinite, even if distinct peaks appear for some samples (Parfitt, 1990), but the pattern is likely to be indistinct when allophane is associated with long-range-ordered crystalline minerals. Therefore, a number of other sophisticated instrumental methods have been proposed for its identification. Earlier, these included infrared spectroscopy, differential thermal analysis, and TEM (Fieldes, 1955). More recently, electron diffraction (Wada and Yoshinaga, 1969), small-angle neutron scattering (Hall et al., 1985), ^{27}Al and ^{29}Si NMR (Goodman et al., 1985; Hiradate and Wada, 2005; Hiradate et al., 2006), and XPS (He et al., 2008) have also been used. Yet, it is a chemical method, for the extraction of Al and Si, among other metals, using acidified ammonium oxalate and developed long ago by Tamm (1922), which has become the standard (and critically important) procedure for both identifying and quantifying allophane (Parfitt and Henmi, 1980; Parfitt and Wilson, 1985; Wada, 1987, 1989).

Halloysite often also forms by the weathering of tephra. Although halloysite, as a 1:1 Si:Al mineral with the same aluminosilicate composition as kaolinite, has often been identified by a peculiar shape in electron micrographs (see Section 20.3.2), it is only the occurrence, or else evidence for prior occurrence, of interlayer water that distinguishes halloysites unequivocally from kaolinites (Churchman and Carr, 1975; Churchman, 2000). With the knowledge that allophane is a fast-forming SRO (nanocrystalline) product from the dissolution mainly of glass whereas halloysites, being crystalline with long-range order, generally give distinct peaks in XRD, there has been much debate over the question of whether allophane alters to halloysite and, if so, how this change occurs. There have been two main schools of thought regarding this question. One of these, proposed by Fieldes (1955) and which was the predominant idea until around the 1980s, held that allophane altered to halloysite with the passage of time. This mineralogical change was considered to occur by a solid-phase transformation involving dehydration and “crystallization” from an “amorphous” material.

According to the alternative view, which was formulated in Parfitt et al. (1983) and subsequent papers (e.g., Parfitt et al., 1984; Parfitt, 1990, 2009), it is the concentration of Si in soil solutions [Si], and availability of Al, which largely determine the nature of the aluminosilicate secondary minerals that form from volcanic parent materials by weathering. In particular, allophane is favored by a lower [Si], whereas halloysite tends to result when [Si] is relatively high. This theory was based on mineralogical and soil solution data from a rainfall sequence of soils formed on tephra-derived deposits in northern New Zealand. It was supported by Singleton et al. (1989) who measured in detail modern solution [Si] in soils forming a drainage sequence on tephric materials of similar composition and age.

Parfitt's theory helped to explain some anomalies concerning the application of Fieldes' (1955) hitherto pervasive theory that allophane seemed to inevitably alter or "transform" to halloysite with time. Fieldes' theory was based on the worldwide recognition that halloysite tended to occur at depth in many tephra-derived soil sequences whereas allophane predominated in surface horizons. Because such sequences become stratigraphically older with increasing depth, the assumption was made that allophane formed first and then, after ca. 10,000–15,000 years, it apparently transformed to halloysite (see review by Lowe, 1986). However, in northern New Zealand, McIntosh (1979) showed that authigenic halloysite (both spheroidal and tubular) had formed by recent processes in tephra deposits only ~1800 years old. He demonstrated that such halloysite formation was a consequence of resilication from a Si-rich soil solution—the resilication was indicated by Si:Al ratios of ~2 at depths of ≥ 2 m, in contrast to values of ≤ 1 in surface horizons, and by modern lysimeter leachate compositions (McIntosh, 1980). Other reports had previously demonstrated the seemingly "anomalous" occurrence of halloysite in young soils (Hay, 1960; Bates, 1962; Bleeker and Parfitt, 1974), and electron micrographs showed a close association of halloysite with the surfaces of parent minerals/mineraloids, both glass (Dixon and McKee, 1974) and feldspars (Tazaki, 1979; see Lowe, 1986, and also Figure 20.3 herein). Similarly, Ogura et al. (2008) showed in recent, proximal scoriaeous tephra (deposited since AD 800) near Mt. Fuji, Japan, that the coarse particle sizes and large pores facilitated rapid drying, aiding the concentration of Si and hence neoformation of tiny spherical halloysite particles. Thus, it became clear that halloysite, rather than allophane, was able to form directly from tephra materials in young soils under certain conditions where [Si] was relatively high. In reality, [Si] may vary seasonally, and kinetic considerations can lead to the formation of halloysite if the periods of high [Si] greatly exceed those when [Si] is low. The use of oxygen isotopes to trace the temperature of formation of minerals, among other techniques, led Ziegler et al. (2003) to conclude that halloysite has formed continuously from the early stages of formation from basalt in an arid zone in Hawaii as the result of prolonged extremely dry seasons following short periods of intense rainfall. The release of Al in the latter had been followed by a prolonged buildup of Si and hence halloysite formation. In addition, it had long been known that allophane was present in some very old weathered-tephra sequences (Ward, 1967; Tonkin, 1970), which had always been a puzzle in view of the Fieldes' model (although the amounts of allophane were not well quantified at that time). A key study was that by Stevens and Vucetich (1985) who used ammonium oxalate dissolution methods to quantify allophane content in a 10 m high tephra weathering sequence in northern New Zealand dating back ca. 350,000 years (the basal tephra being reidentified more recently as the Rangitawa tephra: Lowe et al., 2001). They demonstrated unequivocally that abundant allophane was present in many beds in the sequence. Moreover, through tephrochronology, Stevens and Vucetich (1985) were able to show that allophane (as well as subordinate gibbsite) was predominant during warm,

wet interglacial periods but that halloysite predominated during cool, dry glacial periods, implying that changing environmental conditions had led to changing [Si] and hence different clays. A similar finding was recorded by Bakker et al. (1996). Thus, the weathering of tephra followed separate pathways leading to the formation either of allophane or halloysite, rather than following a single pathway governed by time (Lowe, 1986).

The idea that a high [Si] favored halloysite also made sense of reports of the formation of halloysite instead of allophane when there was a thick overburden (Mejia et al., 1968; Aomine and Mizota, 1973; Wada, 1987; Cronin et al., 1996), and also where drainage was impeded or poor (Aomine and Wada, 1962; Dudas and Harward, 1975; Stevens and Vucetich, 1985; Cronin et al., 1996). Both these situations would give rise to a buildup of Si that, it was then thought, would react with preformed allophane to form halloysite (Aomine and Wada, 1962; Dudas and Harward, 1975; Saigusa et al., 1978).

Zehetner et al. (2003), in Andean Ecuador, Rasmussen et al. (2007), in the Sierra Nevada in California, and Chadwick et al. (2003), on Kohala Mountain in Hawaii, studied the mineralogy of soils formed at different altitudes but from a common volcanic source (andesitic/dacitic ash, andesitic lahar, and basaltic lava, respectively). In each case, it was found that allophane (with imogolite and ferrihydrite in Hawaii) was dominant in soils at higher altitudes and halloysite in soils at lower altitudes, confirming the trends discovered by Nizeyimana et al. (1997) in a similar study on volcanic materials in Rwanda. At higher altitudes, the precipitation is greater; hence, leaching is stronger, solution [Si] is lower, and allophane prevails in the soils formed there. Conversely, precipitation and degree of leaching are lower, and [Si] in solution is higher, at lower altitudes and so halloysite dominates in these soils. Chadwick et al. (2003) emphasized in their Hawaiian study, however, that as moisture increased along the sampling transect, different sets of secondary minerals were favored in response to conditions controlled by arid conditions, by rapid and intense cycles of wetting and drying, or by essentially continuously wet conditions. They developed a leaching index as the ratio of water balance to the integrated porosity of the top meter of soil on an annual basis. The index reached 1 (total filling of the pore space each year) where the mean annual precipitation (MAP) was ~1400 mm. Index values >1 indicated intense leaching conditions because of pore water replacement; leaching losses of soluble base cations and Si were nearly complete at such index values, whereas only 60% of Al had been lost. Where index values were <1 , leaching losses were progressively lower with the lowest rainfall sites having lost 10%–20% of the original base cations and Si, but none of the Al.

Rasmussen et al. (2007) found further that soils in intermediate zones of altitude contained both allophane and halloysite and also that soils at extremely high altitudes had neither allophane nor halloysite but instead were dominated by interlayered 2:1 Si:Al layer silicates, which they considered to be inherited from the parent material. These authors considered that climate controlled the clay minerals formed from the volcanic materials. Rainfall explained the secondary phases formed except at the

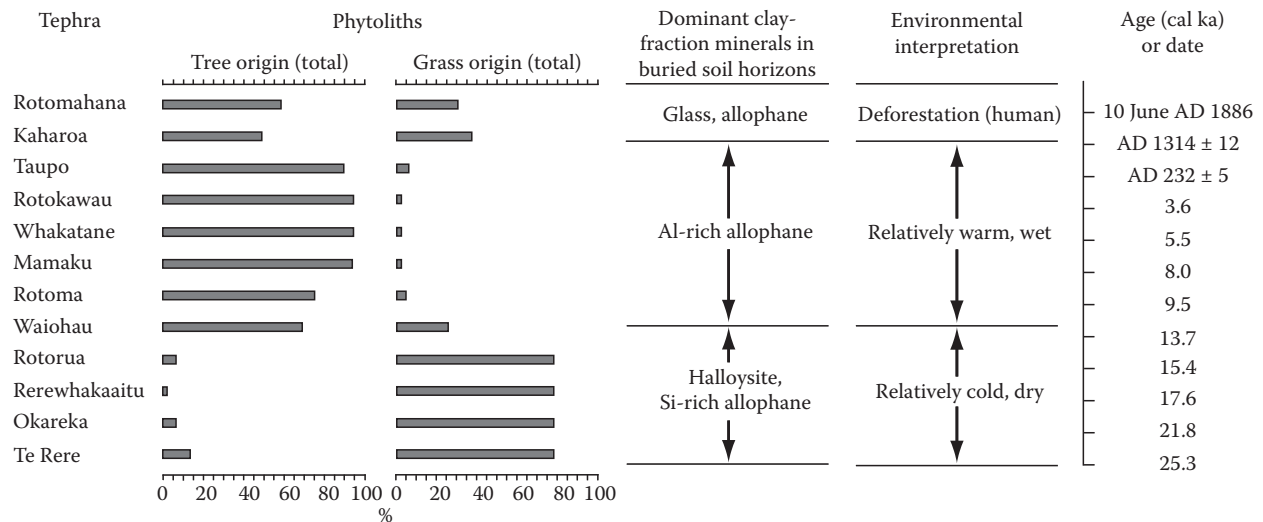


FIGURE 20.6 Dominant clay minerals and phytoliths identified in buried soil horizons in a sequence of 11 rhyolitic tephra and one basaltic tephra (Rotokawau) deposited near Rotorua, New Zealand, since ~25,000 calendar (cal) years ago showing the relationship between the clay mineral assemblages and environment (based on Green, 1987; Sase et al., 1988; Lowe and Percival, 1993; Kondo et al., 1994). ka, thousands of years before present. Dates for Kaharoa and Taupo eruptions are from Hogg et al. (2003, 2011); other ages are from Lowe et al. (2008). (Modified after Newnham, R.M., D.J. Lowe, and P.W. Williams. 1999. Quaternary environmental change in New Zealand: A review. *Prog. Phys. Geog.* 23:567–610. With permission of SAGE Publications.)

higher, colder sites, where temperature inhibited mineral alteration and the formation of new mineral phases. These altitudinal (hence rainfall) studies have further demonstrated the validity of Parfitt et al.'s (1983) model for the effect of [Si] in controlling the formation of secondary minerals from the weathering of volcanic parent materials (where Al availability effectively is unlimited). Further evidence for the validity of this model was demonstrated in a succession of buried soil horizons formed on rhyolitic tephra dating back ~25,000 years near Rotorua in New Zealand (Figure 20.6; Newnham et al., 1999). Cold and dry conditions and grassland vegetation before ~13,000 years ago resulted in halloysite (with minor Si-rich allophane) being formed because of limited Si leaching under lowered rainfall. Al-rich allophane was formed after ~13,000 years ago when Si loss increased through stronger leaching as rainfall and temperatures increased and forest replaced the grassland. In addition, halloysite formation was likely enhanced through enrichment by SiO₂ in leachates carried down the section as the tephra accumulated above, and by a concomitant reduction in permeability in the halloysitic horizons, which have a greater bulk density (Parfitt et al., 1983; Bakker et al., 1996). The paleoenvironmental interpretation was established by analyses of phytoliths (siliceous plant cell remains) at the same site together with palynological and other evidence from sites elsewhere in the region (Sase et al., 1988; Kondo et al., 1994; Newnham et al., 1999). A similar conclusion was reached in a parallel study in Mexico (Sedov et al., 2003).

The model was further supported by a study of seven pedons within the caldera of a volcano in Italy, which showed that the secondary minerals reflected the hydraulic properties, namely, drainage, of the parent materials (Vacca et al., 2003). In this case,

allophane had formed in soils developed in younger, porous, permeable ash deposits, while soils formed in older, less porous and less permeable scoria and consolidated tuffs contained crystalline minerals, especially halloysite, but no allophane.

Other aluminosilicate minerals can also form from volcanic parent materials by weathering. Possible products include 2:1 Si:Al aluminosilicates, which are most likely to occur where biotite is present as a product of the transformation of this mineral through the replacement of interlayer potassium ions, most probably by hydrated divalent cations (see Section 20.2.4.3). Various workers in the past (reviewed by Lowe, 1986) have proposed that a wide variety of 2:1 Si:Al aluminosilicates have formed in soils from volcanic parent materials, including volcanic glass, but several more recent publications (e.g., Nieuwenhuys et al., 2000; Kautz and Ryan, 2003; Mirabella et al., 2005; Rasmussen et al., 2007) have confirmed that these types of phyllosilicates, including illite, smectite, vermiculite, chlorite, kaolinite, and their interstratifications with one another, may be inherited either from the parent pyroclastic material, where they may have formed by hydrothermal processes prior to weathering, or else as a contaminant of other, nonvolcanic origin such as aeolian dust.

Nonetheless, some aluminosilicate, and also more aluminous minerals, do form from volcanic parent materials either alongside, or instead of, allophane and halloysite (Theng et al., 1982). Parfitt et al. (1983) noted that gibbsite was recognized in a 1968 report as a product of the weathering of volcanic ash that was deposited in root channels in soils from Japan while it has also been found to occur in the weathering products of volcanoclastic materials in northern California that have rhyolitic, andesitic, and basaltic inputs (Takahashi et al., 1993). In these latter soils, gibbsite occurs alongside imogolite (or imogolite-like 2:1 Al:Si

allophane) and also halloysite. This concurrence suggests that gibbsite formation may occur during the wet season (winter and early spring) of the Mediterranean (or xeric) climate in northern California, while, as soils dry out in the approach to summer (the dry season), first imogolite/allophane, and then halloysite, is formed. In humid tropical conditions in Cameroon, the occurrence of minor gibbsite in a soil developed on hydrothermally altered nephelinitic materials (Si-poor, alkali-rich lavas) was attributed to the development of a strongly developed microporosity that facilitated the elimination of silica through leaching (Etame et al., 2009).

There appears to be an annual cycle among the secondary minerals resulting from the continually dissolving volcanic parent materials, particularly glass. Fieldes (1968) had proposed that halloysite formation occurred from allophane precursors as a result of seasonal drying (a process invoked also by Chadwick et al., 2003, whereby rapid wetting and drying cycles in arid zones were said to destabilize allophane, forcing it to “dehydrate and transform into halloysite”). Liliensein et al. (2003) studied a chronosequence of quite young soils on andesitic mudflows in northern California nearby those in Takahashi et al.’s (1993) study and found that the amount of allophane increased linearly and quite rapidly in soils up to 600 years of age, although the oldest of these soils had less than half as much allophane as those studied by Takahashi et al. (1993) and hence were probably less well developed than the latter soils. Liliensein et al. (2003) did not record any gibbsite in their soils.

By contrast, Nieuwenhuysse et al. (2000), who also studied a chronosequence on andesitic parent materials (lava, in this case) but in a humid tropical climate in Costa Rica, found all of allophane, kaolin minerals—kaolinite and halloysite—and gibbsite (as well as Al- and Fe-humus complexes and ferrihydrite) in soils from all ages of the parent lavas, ranging from 2,000 to ~450,000 years. Currently, mean monthly precipitation exceeds potential evaporation every month of the year in the present climate for these soils, so there is no dry season to explain the possible formation of relatively Si-rich kaolin minerals along with Si-free gibbsite and Si-poor (i.e., Al-rich) allophane. To explain the simultaneous appearance of these different minerals, Nieuwenhuysse et al. (2000), like Newnham et al. (1999), pointed to palynological evidence of a past drier climate, which evidently occurred in this region around the last glacial maximum. This drier climate, as at Rotorua in New Zealand (Figure 20.6), would have enabled Si-rich halloysite to form at that time, and some of it, at least, has persisted into the current strong leaching regime, with an average annual precipitation of 4500 mm year⁻¹. Nieuwenhuysse et al. (2000) proposed that gibbsite is formed in the soils as a result of the disintegration of the kaolin minerals under strong leaching. This mechanism explains the dominance of gibbsite among secondary minerals after 450,000 years of soil formation. By way of contrast, Certini et al. (2006) found that soils formed from 200,000 year old trachyandesite pyroclastic materials in Italy showed only well-formed gibbsite and an “embryonic” halloysite in their clay fractions. These authors

considered that both are products of the early stages of weathering of volcanic glass. In a hot, wet (perudic) climate in Guadeloupe similar to those studied by Nieuwenhuysse et al. (2000), Ndayiragije and Delvaux (2003) found that gibbsite, allophane, kaolinite, and hydroxyl-Al-interlayered smectite/vermiculite coexisted in a soil from andesitic-dacitic ash, but there was no halloysite in this soil. This soil appears to be similar mineralogically to those studied by Nieuwenhuysse et al. (2000), which occurs in a similar climate, except for the hydroxy-Al 2:1 Si:Al aluminosilicate. This last mineral was seen by Ndayiragije and Delvaux (2003) as an inheritance from the parent tephra and its aluminous interlayers were regarded as performing an antigibbsite (Jackson, 1963) or analogous antiallophane effect by preferentially sequestering Al, at least until the available interlayers became saturated.

Although activity of Si is clearly critically important in governing the formation of halloysite, allophane, or gibbsite in soils from volcanic parent materials (especially tephra) (see, e.g., a stability diagram for these minerals in Churchman, 2000, Figure 1.11), there may also be competitors for Al, such as hydroxyl-Al-interlayered smectite/vermiculite, as discussed by Ndayiragije and Delvaux (2003) (see also Kleber et al., 2007). Quite often competition for Al also arises from organic matter (especially large quantities are derived from, e.g., pampas grass *Miscanthus sinensis* in Japan), which gives rise to fast-forming, resistant Al-humus complexes in soils with pH < 5 (Shoji et al., 1993a; Dahlgren et al., 2004; Hiradate et al., 2004; Parfitt, 2009). Carboxyl groups of humic materials and the 2:1 layer silicates effectively compete for dissolved Al, leaving little Al available for coprecipitation with Si to form allophane or imogolite (Dahlgren et al., 2004; Theng and Yuan, 2008). The preferential incorporation of Al into Al-humus complexes, as with hydroxyl-Al interlayers of 2:1 layer silicates as noted above, is another example of the “antiallophane” effect (McDaniel et al., Section 33.3). Thus, preformed allophane disintegrated and was replaced by Al-humus after only 30 years under bracken fern, consistent with a fall in pH from 5.2 to 4.6 (Johnson-Maynard et al., 1997). Furthermore, weathering of tephra from the 1980 eruption of Mt. St. Helens led to Al-humus and also hydroxy-Al interlayers in 2:1 Si:Al aluminosilicates rather than to any of allophane, imogolite, or opaline silica (Dahlgren et al., 1997). However, opaline silica can form alongside Al-humus complexes, and Fe may also become incorporated into complexes with humus (Wada, 1989). Recent studies in Ecuador (Poulenard et al., 2003) and Japan (Yagasaki et al., 2006) have shown, respectively, that Al-humus complexes form rather than allophane when the content of organic C is particularly high or that allophane is dissolved in favor of Al-humus complexes when organic C content increases. As well, Al-humus complexing predominates at sites more distal to volcanoes because such sites infrequently receive a “top up” of Al through the deposition of weatherable tephra in comparison with sites closer to volcanic sources that are more regularly dusted with tephra.

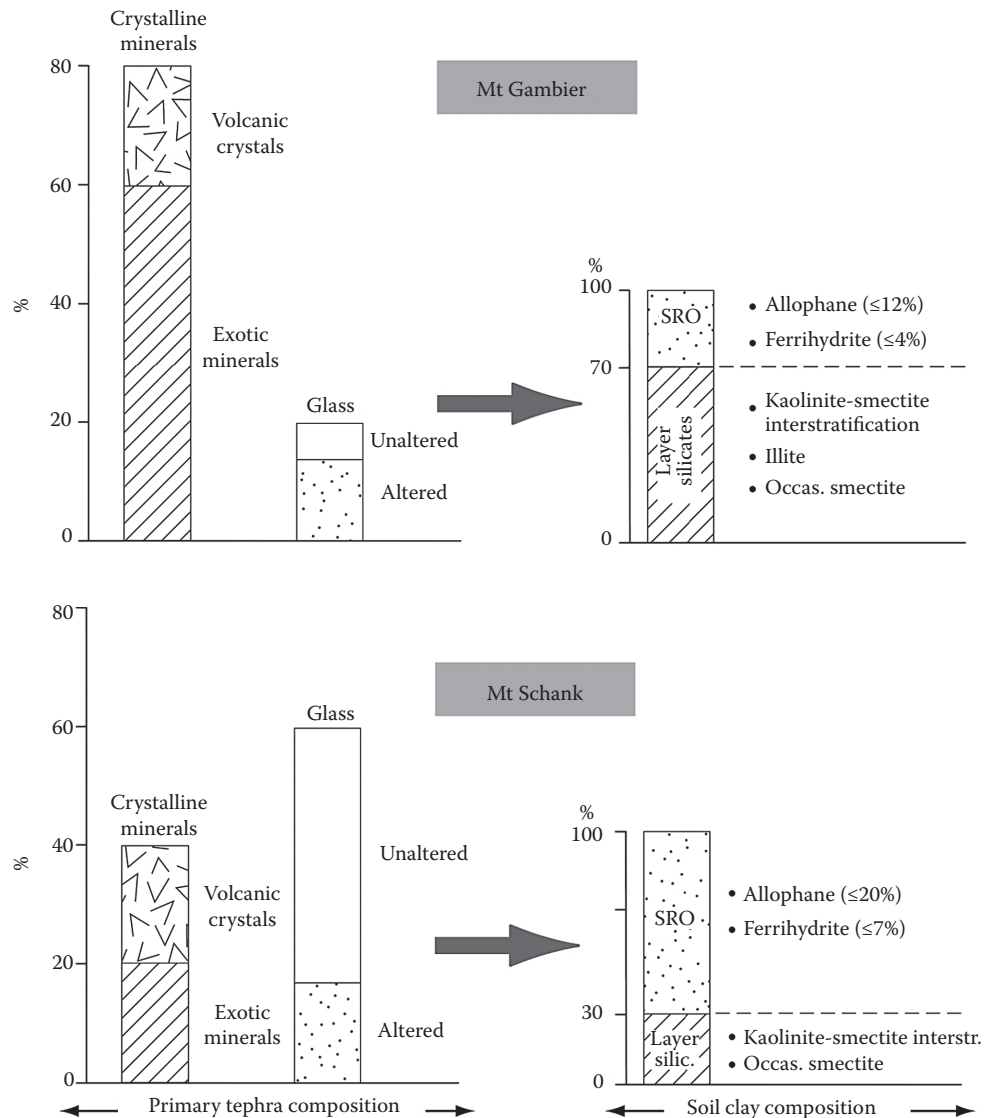


FIGURE 20.7 Contrasts in sand mineral assemblages of soils on mid-Holocene basaltic tephra erupted from Mt. Gambier and nearby Mt. Schank in South Australia have led to markedly different soil clay compositions under a xeric moisture regime. SRO, short-range order (i.e., nanocrystalline); interstr., interstratification; occas., occasional. (Modified after Lowe, D.J., and D.J. Palmer. 2005. Andisols of New Zealand and Australia. *J. Integr. Field Sci.* 2:39–65. With permission of Tohoku University.)

A variety of secondary minerals could be found in soils developed in the erupted material from the basaltic volcanoes at Mts. Gambier and Schank in southeast South Australia, which are only 10 km apart and both about 5000 years old (Lowe et al., 1996; Lowe and Palmer, 2005; Takesako et al., 2010). The main types of clay minerals formed in a xeric moisture regime with a relatively low average annual precipitation of 700 mm are shown for each location in Figure 20.7. They are compared with the categories of primary minerals in the parent materials, which comprise both volcanic and nonvolcanic “exotic” minerals incorporated into the eruptives from underlying calcareous sands and limestone. There is a contrast between the clays found at or near Mt. Gambier, on the one hand, and Mt. Schank, on the other. The

former are dominated by layer silicate minerals, including interstratifications of kaolinite and smectite, illite, and some discrete smectite. The secondary minerals in soils in the vicinity of Mt. Schank show less variety. They tend to contain more allophane and ferrihydrite than those from the Mt. Gambier area. For the soils from both sites, while both kaolinite–smectite and illite occur in many Australian soils (Norrish and Pickering, 1983; Churchman et al., 1994) and probably do not originate from the recent volcanic material, the discrete smectite found in poorly drained subsoils is probably formed by neogenesis from elements from the dissolution of the basaltic tephra (Lowe et al., 1996; Lowe and Palmer, 2005; Takesako et al., 2010). Notably, there was no halloysite formed in any of the soils at either Mt. Gambier

or Mt. Schank. Allophane showed a range of composition within profiles; its Al:Si ratio determined using acid oxalate-extractable Al (minus organically associated pyrophosphate-extractable Al) as a ratio to acid oxalate-extractable Si was Al:Si ~ 2 in upper parts of the soil profiles but dropped to Al:Si ~ 1 lower in the same profiles (Lowe et al., 1996; Lowe and Palmer, 2005). Lowe et al. (1996) suggested that there had been seasonal leaching during winter and early spring, leading to the formation of Al-rich allophane toward the surface, but weaker leaching (or even slight accumulation of Si) at depth, leaving Si-rich allophane rather than halloysite.

The volume of water draining through the upper part of the profile each year has been measured as about 280 mm, which just exceeds the threshold of about 250 mm for Al-rich allophane to form according to models derived from New Zealand data (Parfitt et al., 1984; Lowe, 1995). Jongmans et al. (1994) also found both Al-rich and Si-rich forms of allophane, respectively, in the B and C horizons, in the same profiles in soils in Guadeloupe. Alloway et al. (1992) similarly found differences in Al:Si ratios (and 15 bar water retention) in upbuilding Andisols in the Taranaki region of North Island, New Zealand, which they attributed to changing

climatic conditions from late glacial to postglacial periods; increasing rainfall and fewer prolonged dry periods resulted in higher Al:Si ratios because of increasing desilication.

Lowe (1986, 1995) and Lowe and Percival (1993) summarized data on the critical conditions for the formation of each of the main products of the weathering of volcanic ash. These are given in Figure 20.8, which also shows if Andisols are likely to have formed, and if they are of the allophanic or Al-humus (nonallophanic) type (McDaniel et al., Section 33.3).

A consideration of rates of chemical processes brings in the question of kinetics. Examples of kinetic studies dealing with the dissolution of glass in tephra and associated soils include those of Hodder et al. (1990, 1996) for rhyolitic tephra, Ruxton (1988), and Neall (1977) for dacitic and andesitic tephra, respectively, and Gislason and Oelkers (2003), Ziegler et al. (2003), Wolff-Boenisch et al. (2004), Shikazono et al. (2005), and Sigfusson et al. (2008) for basaltic tephra or lavas. Generally, basaltic and intermediate (andesitic, dacitic) tephra, with lower Si contents, tend to weather more readily than rhyolitic tephra, but in all cases glasses weather very quickly as noted earlier (Kirkman and McHardy, 1980;

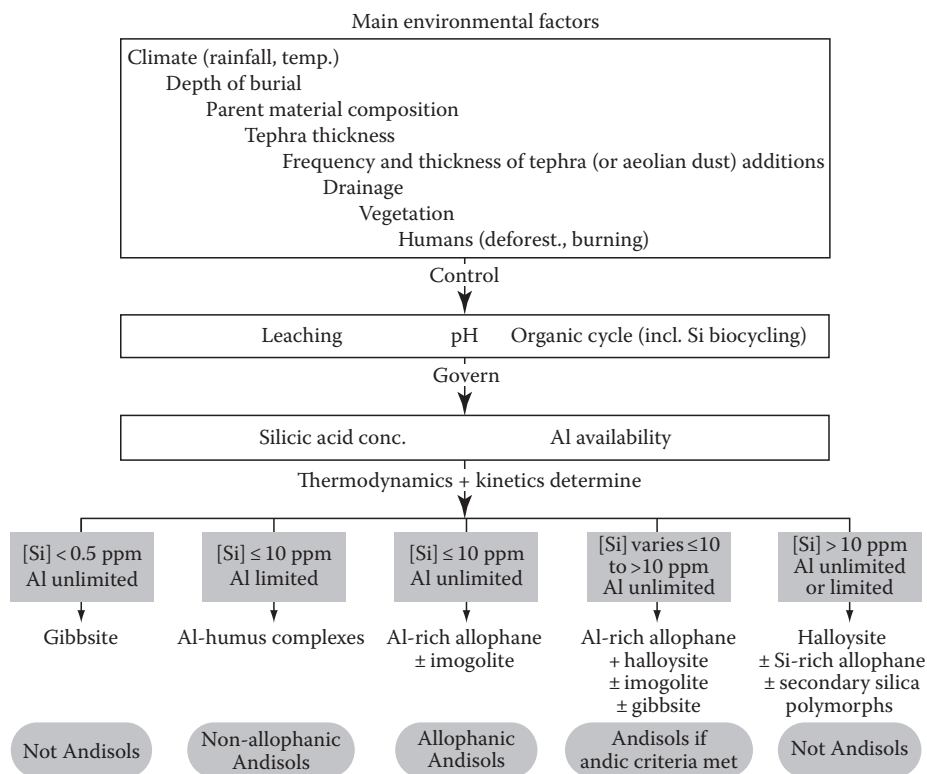


FIGURE 20.8 Environmental influences and controls that govern the critical conditions leading to the formation of different clays from the weathering of tephra, and the likely occurrence or not of Andisols as a result. ± indicates that the clay mentioned may also be present. (Modified after Lowe, D.J. 1986. Controls on the rates of weathering and clay mineral genesis in airfall tephra: A review and New Zealand case study, p. 265–330. In S.M. Colman and D.P. Dethier (eds.) Rates of chemical weathering of rocks and minerals. Academic Press, Orlando, FL; Lowe, D.J. 1995. Teaching clays: From ashes to allophane, p. 19–23. In G.J. Churchman, R.W. Fitzpatrick, and R.A. Eggleton (eds.) Clays: Controlling the environment. Proc. 10th Int. Clay Conf., 18–23 July 1993, Adelaide, Australia. CSIRO Publishing, Melbourne, Australia.)

Wolff-Boenisch et al., 2004). Compared with hard rock, the fragmental tephra components, especially vesicular glass and pumice, have a much greater surface area and high porosity and permeability, and so break down to constituent compounds very readily (Wolff-Boenisch et al., 2004).

Ziegler et al. (2003) suggested that kinetics controlled the formation of allophane and halloysite in arid soils on the basis of their work on a chronosequence of Hawaiian soils on basaltic lavas (with ash overlying lava in one case) in arid conditions (MAP 180–225 mm). Thermodynamics do not control the composition of soils unless soil solutions remain in contact with the mineral surfaces until equilibrium is reached. Where this does not occur, such as under arid conditions, kinetic factors control the soil system (Ziegler et al., 2003). Clay mineral synthesis in the Hawaiian arid-zone chronosequence was thus shown by Ziegler et al. (2003) to be controlled by the kinetics of soil drying, rather than thermodynamics, so that halloysite was the favored aluminosilicate end product with the formation of smectite inhibited by kinetic factors (and a lack of micas to “fuel” the dominant pathway for smectite formation; Chadwick et al., 2003). In Cameroon, the depth distributions of 0.7 and 1 nm halloysite in soils developed on weathered nephelinite lavas were able to be related to both kinetic and thermodynamic factors by Etame et al. (2009). That Si concentrations increased with depth in the profiles while Al remained relatively constant, and 1 nm halloysite occurred exclusively in lower horizons whereas both 0.7 and 1 nm halloysites were present in upper horizons, led Etame et al. (2009) to two suggestions. First, the 1 nm halloysite formation was controlled by direct precipitation from Si–Al-rich solutions (released from the weathering of primary minerals), and, therefore, the availability of Si was the only factor that controlled its formation at the base of the profile. Second, the presence of both forms of halloysite in the upper parts of the profiles implied that kinetics, hence time, controlled the evolution of halloysite through wet–dry seasonality, aided by the thermodynamically favorable factor of the availability of Si (Etame et al., 2009). In tropical Costa Rica, the predominance of 1.0 nm over 0.7 nm halloysite in the wetter, lower subsoil horizons of profiles studied by Kleber et al. (2007) was attributed to Si enrichment by percolating waters (i.e., mainly for kinetic reasons).

Returning to the question of whether it is time (Fieldes, 1955) or solution concentration/activity, particularly of Si (Parfitt et al., 1983, 1984), that governs whether or not allophane or halloysite persists in soils from volcanic parent materials (leaving aside Al-humus complexing), it may be said that while the evidence is very strongly in favor of solution conditions determining the nature of the minerals formed, the passage of time also appears to enhance halloysite formation at the expense of allophane via the so-called Ostwald ripening process (e.g., Chadwick and Chorover, 2001; Dahlgren et al., 2004; Rasmussen et al., 2007). This direction of change is consistent with the thermodynamic stabilities of the two mineral types (see, e.g., Figure 1.11 in Churchman, 2000). Structural considerations, however, mean

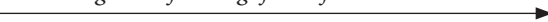
that an Al-rich allophane, with isolated tetrahedra on the inside of a spherule of coiled gibbsite-like sheets, cannot transform in the solid state into halloysite, where sheets of linked silica tetrahedra are generally coiled around alumina octahedra and hence are in the opposite conformation one to each other as in the allophane spherule. Therefore, dissolution and recrystallization must be involved in the change from allophane to halloysite. Nonetheless, it is likely that the passage of time effects other changes, which affect the environment in which mineral alteration and formation take place, so that conditions that favor the formation of allophane early in the weathering process change to those favoring halloysite formation. Most often in upbuilding terrains, this comes about through an increase in [Si], which may result from a buildup of overburden through ongoing tephra deposition, or the development of impediments to efficient drainage (e.g., Cronin et al., 1996). Another possible change may be toward a drier climate, so that there is less throughflow of water and hence a buildup of Si in solution. An alternative situation is that reported by Chadwick and Chorover (2001) for a Hawaiian chronosequence on basaltic lavas and ash deposits not subject to ongoing burial by later eruptives. There, the ongoing depletion of [Si] and increase in [H⁺] under high rainfall after ca. 400,000 years eventually led to the formation of more stable kaolin (halloysite and kaolinite) and gibbsite. Previously, conditions had apparently favored the formation of allophane. Chadwick and Chorover (2001) noted that [Al] in solution also declined over time, a result that follows from increasing crystallinity and decreasing solubility of gibbsite and kaolin in the soil. Inconsistencies between observed soil mineral composition and stability-field plots of solution chemistry data are evidence of kinetic limitations to mineral transformations according to Chadwick and Chorover (2001), who also noted that such discrepancies can be resolved through consideration of mineral transformation rates and Ostwald ripening processes but that the requisite kinetic data are often lacking.

In considering longer timescales of glacial and interglacial cycles in temperate volcanic landscapes not directly glacierized, the marine oxygen isotope records show that cooler and drier conditions associated with glaciations persisted ~80%–90% of the time whereas warmer and wetter conditions associated with interglaciations occurred for ~10% to 20% of the time. In these landscapes, where long sequences are well preserved, therefore, it might be expected that soils developed from accumulations of weathered tephra of similar composition dating back several hundreds of thousands of years to one or two millions of years should be dominated by halloysite rather than allophane (e.g., as evident in the so-called Kauroa and Hamilton ash tephra sequences in northern New Zealand that date back to ca. 2.3 Ma; Lowe and Percival, 1993; Lowe et al., 2001).

Overall, the relationship between the minerals formed from volcanic parent materials (especially tephra) and solution [Si], as it is affected by the throughflow of water and given appropriate kinetic circumstances, can be expressed by Box 20.3:

Box 20.3 RELATIONSHIP BETWEEN THROUGHFLOW OF WATER, Si CONCENTRATION, AND TYPES OF CLAYS FORMED FROM VOLCANIC PARENT MATERIALS

	Smectite	Halloysite/Si-rich Allophane	Al-rich Allophane	Gibbsite
Al:Si	0.5	1.0	2.0	∞

Increasing rate of throughflow of water
Decreasing Si concentration/activity


We note in addition that allophane can be formed in a range of nonvolcanic materials through strong leaching and acid conditions, as occur, for example, in loess in upland areas of southern New Zealand (e.g., Eger and Hewitt, 2008), and as a result of podzolization (see Section 20.2.5.3.2).

Parallel to the alteration of aluminosilicate minerals and the formation of allophane, halloysite, and perhaps also gibbsite or smectites, iron is also lost from parent Fe-bearing minerals and incorporated into secondary solid phases. Ferrihydrite forms early in the process of weathering of volcanic parent materials from the precipitation and oxidation to Fe(III) of soluble Fe(II) that had been released into solution from volcanic glass and also feldspars and mafic minerals (e.g., McDaniel et al., Section 33.3). It is the presence of other species in solution such as silicate and phosphate ions and soluble organic compounds that inhibit the formation of the more crystalline forms of iron, such as goethite and hematite (e.g., Childs, 1992; Bigham et al., 2002). However, the type of iron oxide that is formed is a function of the same environmental conditions that also affect which particular aluminosilicates are formed in volcanogenic soils. Hence, in young soils on andesitic mudflows, the buildup of ferrihydrite with time paralleled that of allophane, albeit that the amount of allophane formed was ~10 times or more than that of ferrihydrite (Lilienfein et al., 2003). In a chronosequence of soils in the humid tropics, Nieuwenhuys et al. (2000) found that Fe occurred mainly as Fe-humus in the two younger soils, especially in their A horizons, but also as ferrihydrite, especially at depth, whereas it occurred mainly as goethite throughout the oldest soil in the sequence. Further, the iron oxides in soils in a xeric moisture regime that contain all of gibbsite, imogolite and/or Al-rich allophane, and halloysite as aluminosilicates were dominantly highly crystalline—they were mainly goethite, reflecting strong seasonal drying (Takahashi et al., 1993). Soils in a toposequence on andesitic lahar deposits covering a range of climatic zones generally showed a similar pattern to that for

the aluminosilicates, with poorly crystalline forms giving a high oxalate-Fe analysis dominant in soils at higher altitudes and more crystalline forms giving a high dithionite-Fe analysis in soils at lower altitudes (Rasmussen et al., 2007). There was a further subtlety with Fe analyses, however, insofar as the proportion of oxalate-Fe to dithionite-Fe rose again at the lowest altitude, where the MAP was also lowest. In this drier zone, less leaching probably led to higher retention of Si in soil solution, which would inhibit Fe oxide crystallization (Rasmussen et al., 2007).

20.2.4.6.3 The Special Case of “Palagonite”

In the volcanic and geochemical literature especially, the term “palagonite” is widely used to describe the first stable product of basaltic volcanic glass alteration (e.g., Fisher and Schminke, 1984; Cas and Wright, 1987; Daux et al., 1994). Palagonite has also been described in the clay science literature but uncommonly (e.g., Singer and Banin, 1990; Drief and Schiffman, 2004) and it thus deserves some attention here. As reviewed by Stronck and Schmincke (2002), palagonite (named after the location Palagonia in Sicily) is a heterogeneous substance, usually with highly variable optical and structural properties ranging from a clear, transparent, isotropic, smooth, and often concentrically banded material, commonly called “gel-palagonite,” to a translucent, anisotropic, slightly to strongly birefringent material of fibrous, lath-like, or granular structure, commonly called “fibro-palagonite.” It ranges in color from yellowish to shades of brown. Since it was first defined in 1845 as a new mineral, palagonite has been interpreted in numerous studies to be a heterogeneous material composed variously of different aluminosilicate clays, zeolites, and oxides, or mixtures of these. Based on XRD, HRTEM, atomic force microscopy (AFM), and electron microprobe analyses, palagonite is now interpreted by most to be composed of a variety of smectites and very minor amounts, if any, of zeolites and oxides (Stronck and Schmincke, 2002). At more advanced stages of alteration, other secondary phases are known to form following Ostwald “ripening” processes.

Palagonite evidently comprises spherical structures 20–60 nm in diameter, which have been interpreted as “microcrystallite precursors of smectite” (Stroncik and Schmincke, 2002)—that is, palagonite would seem to be a nanocrystalline variety of smectite(s). Drief and Schiffman (2004) identified an Fe-rich montmorillonite-like composition in their study on Hawaiian basaltic deposits. The atomic structure of palagonite and, especially, its structural evolution are not yet fully understood, but both are important to glass-alteration rates and to the evolution of the whole water–rock–soil system (Stroncik and Schmincke, 2001). Because kinetic and thermodynamic modeling and mass-balance calculations necessitate exact differentiation of all the secondary products developing during alteration, the term “palagonite” should be used only for the hydrous nanocrystalline alteration product (“gel-palagonite”), not for the long-range-ordered crystalline material evolving from the palagonite itself (Stroncik and Schmincke, 2001, 2002).

The so-called palagonitization of basaltic volcanic glass is a continuous process of glass dissolution and palagonite formation and evolution, which, according to Stroncik and Schmincke (2001), can be subdivided into two different reaction stages with changing element mobilities. Stage 1 is the congruent hydration and dissolution of thermodynamically unstable glass and contemporaneous precipitation of “fresh,” gel-like, amorphous (or nanocrystalline), optically isotropic, mainly yellowish palagonite. This stage, kinetically controlled and consistent with the models of Hodder et al. (1990, 1993), is accompanied by the loss of Si, Al, Mg, Ca, Na, and K, active enrichment (gain) of H₂O, and the passive enrichment (“default” accumulation relative to other elements) of Ti and Fe. Stage 2 is an aging process during which the thermodynamically unstable palagonite reacts with the surrounding fluid and crystallizes to smectite. This stage is accompanied by uptake of Si, Al, Mg, and K from solution and the loss of Ti and H₂O. Ca and Na are still showing losses, whereas Fe reacts less consistently, remaining either unchanged or showing losses (Stroncik and Schmincke, 2001, 2002).

20.2.5 Peculiarities of Processes and Products of Alteration by Weathering in Soils

Much—although not all—of the information on the processes and products of alteration of primary minerals by weathering that is summarized in the preceding Section 20.2.4 comes from observations of rocks or geological deposits, minerals associated with these materials, and saprolites deep within soil profiles. However, soil profiles can encompass a range of conditions, from fragmented, almost abiotic, rock through to organic-rich material containing a great variety of microbial, faunal, and also plant life. The different parts of soil profiles represent different regimes for water, from abundant and mobile to scarce and largely immobile, so studies of some nonsoil situations where each of these prevail are relevant to weathering in some parts of soils but not in others. Most soils have a significant biological input, at least in their surface layers, and, therefore, the biological factor in mineral alteration and formation tends to play a larger role in

the genesis of soil minerals than in those from rocks subject to largely abiotic weathering. Furthermore, some processes, notably podzolization, occur within permeable soils but not in impermeable rocks under certain environmental conditions and deserve particular attention. In addition, soils can be further developed even following the depletion of easily weatherable rock-derived minerals. Secondary minerals can themselves be altered and new phases formed. Each of these particular aspects of mineral development in soils will be discussed in the following sections.

20.2.5.1 The Effect of Position within Soil Profiles on Hard Rock

In a recent review, Wilson (2004) showed that position in the weathering profile on indurated rock has a crucial influence on the nature of the environment for weathering and hence on the processes involved and products formed, as well as the rates at which changes occur. Note that modified models are required for soils formed on unconsolidated materials or, especially, those developed through upbuilding pedogenesis. Following Delvigne (1998), a fully developed weathering profile comprises a soil, which is delineated (in a straightforward case) into A and B horizons (solum) and usually C or CR horizons comprising saprolite/alterite, which consists of completely disaggregated rock grading to the rock base, with fabric and texture changing with depth. At the base of the whole profile is the (partly) weathered rock (R horizon), which may be hard and coherent but also incorporates fractures and fissures. Among other features, an increase in surface area characterizes the upward change from the rock to the solum (Hochella and Banfield, 1995).

There is also a trend of decreasing porosity and permeability from soil down to rock, so that water can flow quite freely within the soil, but can be either stagnant or held in capillaries in the rock. Hence, there is a much greater chance of an equilibrium being established between the minerals and the largely immobile solution within the rock than between the minerals and the highly dynamic water in the soils zone.

Following Velde and Meunier (2008), we note that alteration within the rock proceeds in microsystems. Meunier and Velde (1979) followed the alteration of granites by weathering through developments occurring at the scale of microsites. The system is highly heterogeneous at this fine scale; grains of the primary minerals, muscovite, orthoclase, and biotite each give rise to multiphase assemblages upon alteration. Alteration of the whole mineral assemblage appears to take place in three stages. In the first stage, alkalis are lost but the Si:Al ratio is preserved as illitic mica, beidellite, and vermiculite are variously formed. The second stage involves a loss of both alkalis and silica with kaolinite and oxides resulting. The authors surmised that there is a third stage where quartz is dissolved, leaving only oxides, but not silica. This last stage is seen in tropical weathering. The processes of in situ alteration of ferromagnesian minerals to smectites and of feldspars to illite that were studied by Eggleton and coworkers and Banfield and coworkers, among others, and cited in Section 20.2.4 herein, also occur within microsites where the physical constraints as well as the chemical availability of reagents limit the reactions that

can take place. In a particularly close study of microsites within one mineral type (amphibole) on weathering, Proust et al. (2006) found that montmorillonite formed on the (001) amphibole face and saponite on the (110) face, while the sawtooth (001) face fracture surface hosted a kaolinite–smectite and, with time, also halloysite and montmorillonite. The establishment of local equilibria may occur at different sites, within both a single crystal, as in the amphibole studied by Proust et al. (2006), and also within different fractures and fissures in a rock (see the diagrammatic representation for granite in Figure 4.19 of Velde and Meunier, 2008). Within microsites where secondary products remain in close proximity to host primary minerals, reactions may even occur between product and host minerals (Velde and Meunier, 2008). As a result, vermiculite may form by recrystallization in a microsite from the dissolution products of the adjacent secondary minerals, saponite or Fe–beidellite and their primary precursor, amphibole for one example (Velde and Meunier, 2008). For another example (Velde and Meunier, 2008), product smectite and host K-feldspar may react together to give rise to illite and kaolinite.

The solid:solution ratio is very high in hard rocks that remain coherent yet contain small fractures and fissures. By great contrast, the solid:solution ratio in the solum or unconsolidated geological deposits within the weathering profile is likely to be both very low and quite variable on both a daily and seasonal basis, except in special circumstances, for example, in a desert or frozen soil. The dynamic nature of soils alone ensures that the possibility of predicting the course of weathering via stability diagrams for the component clay minerals (e.g., Kittrick, 1967) cannot be realized. Minerals awash in the dynamic water phase in soils almost certainly remain well out of equilibrium with those solutions (Chadwick and Chorover, 2001; Wilson, 2004). However, those formed in microsites within weathering rocks deeper in the weathering profile may not appear in bulk analyses of soils above the weathering rock. In particular, trioctahedral smectites formed during early stages of alteration are rarely reported in soils. Either they are unstable in the soil environment (Wilson, 2004) or they are present in only vanishingly small concentrations (Proust et al., 2006), or both.

20.2.5.2 Weathering in the Absence or Shortfalls of Water

Generally on Earth, weathering occurs because there is sufficient—and usually excess—water to effect alteration of primary minerals and either transformation to related secondary phases or neogenesis of new (secondary) minerals. However, mineral alteration and formation are also observed to occur where there is little, or no, water. Studies in the normally frozen Antarctic have shown clear evidence for chemical weathering occurring there. As well as salts such as gypsum and sodium sulfate formed by recrystallization from elements leached from rocks by occasional (liquid) water, abundant iron oxides also occur (Claridge, 1965). Furthermore, clay minerals occur—most commonly transformation products of micas such as vermiculites, but also montmorillonite. This last mineral was thought to form in the arid and highly alkaline environment by similar processes to

those seen in other terrestrial environments, but occurring at a much slower rate (Claridge, 1965). Some, but not all, clay minerals in Antarctic soils could be inherited from other land masses to the north (e.g., dust blown from southern South America; Delmonte et al., 2004). Boyer (1975) collected weathering products such as rinds on rocks from part of Antarctica and identified various 2:1 minerals, including chlorite–vermiculite and also identified montmorillonite. These products all indicated that chemical weathering had taken place. In the arid Sahel in west Africa, Ducloux et al. (2002) identified beidellite, kaolinite, and mica in soils. They concluded that these minerals formed by a process called “xerolysis,” whereby desiccation in a hot climate leads to protons from dissociated water reacting with crystalline minerals to produce secondary products.

The new frontier for clay mineralogy is outer space, and especially other planets in our solar system, and there has been a particular focus on Mars from a clay mineralogical viewpoint quite recently. Earlier exploration of Mars involved fly-bys, with spectra being used to identify materials on the Martian surface by remote sensing. These data could have been interpreted to indicate the presence of some phyllosilicates (Hamilton et al., 2003), but the evidence was equivocal. The collection of samples by Exploration Rover from the planet’s surface showed that the ferric sulfate, jarosite, which is commonly associated with acid sulfate soils on Earth (see Section 20.2.5.3.4), and also possible relicts of gypsum at the Meridian Planum landing site (Madden et al., 2004). Other work on samples from a number of different locations on the planet has confirmed the widespread occurrence of secondary sulfates and also iron oxides (Hurowitz and McLennan, 2007). Hurowitz and McLennan (2007) considered that they originated from altered olivines in Martian rocks. These various localized occurrences of sulfates and iron oxides were compared with the results of a general survey of most of the surface of Mars that was carried out by an image spectrometer during an aerial survey of the planet (Poulet et al., 2005). The survey had earlier identified sulfates in localities in addition to those reported by Madden et al. (2004) and Hurowitz and McLennan (2007), but Poulet et al. (2005) also identified phyllosilicates in several localities, albeit that their distribution was quite heterogeneous. They included Fe/Mg smectites in some areas and montmorillonite in others. These occurrences suggested that there had been water in some localities on Mars, in order to alter basaltic and similar rocks to give phyllosilicates, although the sulfates derive from a different, more acidic, environment. More recent work (e.g., Bishop et al., 2008; Mustard et al., 2008; Ehlmann et al., 2009) has identified phyllosilicates in a number of localities on the surface of Mars. The discovery of phyllosilicates has aided our understanding of the climatic history of Mars (Newsom, 2005; Poulet et al., 2005). On Earth, meteorites considered to have come from Mars have been studied for their mineralogy, and iddingsite, comprising a mixture of smectites, iron oxides, and silica, has been identified on the altered surfaces and in the veins of the meteorites (Wentworth et al., 2005). These authors drew an analogy between mineral alteration and formation that has taken place on Mars with that which has occurred—and is

occurring—in the Dry Valleys of Antarctica. Examined at the submicroscopic scale, the patterns of alteration of primary silicates, for example, amphiboles and pyroxenes, were similar in an Antarctic Dry Valley (Wright Valley) and in the Mars meteorites (Wentworth et al., 2005). In addition, soils in the Dry Valleys contain evaporated salts at their surfaces, as have been seen in soils on Mars. In both of these arid situations, alteration processes and their products are distributed heterogeneously, indicating an uneven distribution of water available for the alteration and subsequent formation of minerals, both in space (in the Antarctic Dry Valleys) and in time (in the Martian past).

20.2.5.3 Biota as Important Agents in Mineral Alteration and Formation

It has long been recognized, including by the pioneers in pedology, for example, V.V. Dokuchaev and Hans Jenny, that biota play an important, sometimes dominant, role as one of the agents in the development of soils from rocks and other geological materials. Plants, animals, and microbes share an equivalent status to parent materials, climate, topography, and time as soil-forming factors. Therefore, it comes as no surprise to find that biota in their different forms demonstrably play a major role in the alteration of primary minerals and the formation of secondary clay minerals.

Even so, it is arguable that the role of biota in the formation of clay minerals has been relatively neglected in comparison with those of other soil-forming factors, such as parent materials and climate. Churchman (2000) noted that studies of the alteration and formation of minerals had largely concentrated on processes involving inorganic agents, while observing that there had been an upsurge in studies of the role played by biological and biochemical agents in the previous decade. The effect of these agents on weathering changes is now one of the more active areas of research on mineral alteration and formation in relation to soils (e.g., Dong et al., 2009).

20.2.5.3.1 Plants as Weathering Agents

Plants have been shown to be important weathering agents. Mortland et al. (1956), Hinsinger et al. (1992, 1993), and Hinsinger and Jaillard (1993) showed that trioctahedral micas in soils lost potassium from their interlayers as a result of the growth of plants in the soils. In general, this process is that of vermiculitization (or the formation of beidellitic smectites) (Section 20.2.4.3). However, it generally occurs via mixed-layer randomly interstratified species. In soils, illite–smectites are the most common form of these (Velde and Meunier, 2008). Indeed, since this type of clay mineral is not found in buried sediments or rocks, it is peculiar to the soil environment, according to these authors. Furthermore, it is found particularly in the A and B horizons of soils (the solum), confirming its origin in surface alteration processes (ibid.). Although plants, in general, are the main agents of alteration of trioctahedral micas to produce illite–smectites, Velde and Meunier (2008) summarized observations in the literature to conclude that prairie soils (Mollisols) dominated by grasses contain illite–smectite together with varying amounts of illite under different climate conditions. Even

though vermiculites are rare in prairie soils, they can occur in significant amounts in young mountain soils according to Velde and Meunier (2008). Expanded (to vermiculite or smectite) and partially expanded (to mixed-layer illite–smectite) products occur, and these often acquire Al-hydroxy interlayers (see Section 20.2.4.3) under forest (Velde and Meunier, 2008). It was the development of a method of XRD peak decomposition by Lanson (1997) that enabled the detection of some of these mineral changes attributable to plants, which can be subtle.

Acidification can be an important effect of plant growth and consequently can play an important role in alteration by weathering. Protons are released into soil solutions to balance the overall charge when roots take up more cations than anions (e.g., Hinsinger et al., 2001; Courchesne, 2006; Calvaruso et al., 2009). For some tree species, it is the uptake of NH_4^+ in preference to NO_3^- by roots that ensures acidification, specifically in the rhizosphere (Calvaruso et al., 2009). Roots (and fungal hyphae tips as noted above) also exude organic acids into soils (Courchesne, 2006). More Ca, Na, Mg, Si, and especially Fe were released from leached basalt when plants were grown in the fresh rock than when there were no plants (Hinsinger et al., 2001). When soils within the rhizosphere of a Norway spruce and an oak were compared with the bulk soil, it was found that Fe and Al, and therefore their “amorphous” (i.e., nanocrystalline) mineral phases, as well as Al-hydroxy interlayers in 2:1 Si:Al aluminosilicates, were dissolved as a result of acidification by the plant roots (Calvaruso et al., 2009). Forest soils in Taiwan showed a lack of hydroxyl interlayering of 2:1 Si:Al aluminosilicates in the surface O, A, and E horizons but there was interlayering, which was shown to involve both Al and Fe, in deeper horizons (Pai et al., 2004). It was thought that a low pH and possible chelation of Al and Fe by organic material, which was abundant in and on the surfaces of the soils, led to the clean interlayers in the expandable aluminosilicates near the surface, whereas the higher pH and lower organic contents in lower horizons were conducive to their formation in the clay minerals there (Pai et al., 2004). In a later study, Pai et al. (2007) found that acidification at the surface of forest soils elsewhere in Taiwan decreased the charge of the K-depleted aluminosilicate layers, which they characterized as vermiculite, occurring either as the discrete phase or in mixed-layers with vermiculite. In the North Island of New Zealand, Jongkind and Burman (2006) found that weathering under kauri (*Agathis australis*) trees, which produce especially low pHs (4.0 ± 0.2) left vermiculites depleted of hydroxyl interlayering and even brought about some conversion of vermiculite to smectite, as Churchman (1980) had found to occur in soils under another native (beech) tree species (*Nothofagus* sp.) in the South Island of New Zealand. By matching the rare-earth compositions of the silica particles found within the roots of ferns with those of aluminosilicate minerals in the soil surrounding the roots, Fu et al. (2002) found strong evidence for the dissolution of clay minerals to leave deposits of silica following their incorporation into plant roots.

Plants can bring about very rapid changes in soil minerals (Turpault et al., 2008). A seasonal study by these authors showed that in the rhizosphere close to tree roots, mineral dissolution,

with loss of citrate-extractable Al and Si, occurred in surface layers in spring because of enhanced biological activity. That some of the Al came from interlayers was shown in XRD by an increased ease of collapse of these upon K-saturation and also an increase in cation exchange capacity (CEC). There was a corresponding migration of Al and Si to lower layers. Perceptible changes in the XRD patterns occurred within only 3 months.

20.2.5.3.2 The Special Case of Podzolization

Organic compounds from the activities and decomposition of biota have long been thought responsible for extracting and transporting Fe and Al ions and incidentally producing new minerals from them in the process of podzolization (e.g., Russell, 1973), even if equally valid inorganic mechanisms have also been put forward for this process (e.g., Farmer et al., 1980; Wang et al., 1986), as will be discussed further.

Podzolization usually involves the intense leaching of parent materials and soils with acidic solutions. In podzolization, Al, Fe, Mg, and Si are mobilized (e.g., Farmer, 1982; Farmer and Fraser, 1982; Farmer et al., 1983; Taylor, 1988; Churchman, 2000; Giesler et al., 2000). Podzolization can be contrasted with the processes, sometimes collectively referred to as “andosolization,” involved in forming allophane and other andic soil materials mainly in tephra-derived soils (Section 20.2.4.6). Normally, allophane and other nanocrystalline clays are formed in situ during andosolization (even though the process typically requires desilication via leaching) whereas podzolization always involves the *translocation* of mobile constituents as organic or inorganic complexes, or both, from very acid horizons in the upper profile and subsequent immobilization in lower horizons through an increase in pH, via microbial action, or by adsorption, precipitation, etc. That such movement takes place has been confirmed by micromorphological studies (e.g., Farmer et al., 1980, 1983, 1985; Farmer and Lumsdon, 2001). Broadly speaking, the processes involved in podzolization are as follows: (1) enhanced mineral weathering in upper A and E (“eluvial”) horizons; (2) transport of Al, Fe, and Si and probably also organic matter from upper horizons to lower B horizons—either in metal–organic complexes (chelates) or as independent inorganic complexes including “proto-imogolite sols,” and as independent organic complexes; and (3) deposition of the Al and Fe as oxides, together usually with allophane, from (according to Farmer et al., 1985) a mixed $\text{Al}_2\text{O}_3\text{--Fe}_2\text{O}_3\text{--SiO}_2\text{--H}_2\text{O}$ sol, in so-called illuvial Bs horizons.

There have been a number of theories put forward to explain the changes that take place in soils as a result of podzolization (see Churchman, 2000, for proponents and arguments involved in earlier discussions, and elsewhere in this handbook). Briefly, these can be grouped into two main hypotheses, both of which may apply to some degree depending on site-specific soil environments (e.g., Wang et al., 1986; Lundström et al., 2000): (1) the organic or “fulvate” hypothesis and (2) the inorganic or “proto-imogolite” hypothesis. A third is the so-called rock-eating fungi hypothesis, which is associated with mycorrhizal fungi found in many soils under pines and heaths commonly in parts of Europe and Scandinavia and elsewhere (Jongmans et al., 1997; van Breemen et al., 2000a).

The fungal hyphal tips, which produce organic acids (e.g., citric or oxalic), “drill” directly into mineral grains including feldspars, thereby bypassing the external acid soil solution, and hence the E horizon is regarded as the fungal “eaten” part of the soil.

An eccentric view is that of Do Nascimento et al. (2004, p. 536) who have described podzolization as a deferralization process whereby the chemical elements that had accumulated during ferralization are “progressively exported towards the drainage network under the combined effects of waterlogging, organic matter accumulation, and lateral subsurface and surface water flows.” In a somewhat related study, Lucas (2001) compared the dynamics operating in podzols with those in ferralsols (Oxisols) regarding the rates of Si recycling (including storage as phytoliths) by plants and the rates of loss, by leaching, of Si and organometallic complexes involving Al, Fe, and organic matter. This author concluded that the main constituents of the “weathering mantle” ultimately depended on the balance between (1) the stability of the clay minerals, sustained by the plant Si cycling, and (2) the leaching of plant-induced organo-Al compounds. These findings were evident in equatorial areas where old soils are markedly affected by biological activity, and they were also seen in temperate areas (Lucas, 2001).

After reviewing the literature, Lundström et al. (2000) concluded that organic complexes were important in both the weathering and deposition (or immobilization) processes and Jansen et al. (2005) also decided, on experimental grounds, that organic matter played an important role in the transport of Al and Fe down profiles to create illuvial horizons, at least in podzols in the Netherlands and similar climatic zones, while conceding that podzols may form by slightly different mechanisms in both cooler and warmer climatic zones. Contrary views are evident in, for example, Farmer and Lumsdon (2001) who argued that “fulvic acid plays no active role in podzolization, but only recycles Al and Fe, that has been transferred by biological processes to the O horizon, back to the Bh horizon” (p. 177). Buurman and Jongmans (2005) proposed that podzolization in boreal zones, on nutrient-rich parent materials at high latitudes and high altitudes, hence cold climates, occurred with organic matter (OM) dynamics that led to little accumulation of OM (so-called “fast” OM dynamics), and, hence, illuvial B horizons were dominantly inorganic. These authors proposed an alternative route for podzolization in hydro-morphic situations on nutrient-poor parent materials, including in warmer climates, where OM dynamics were “slow,” by their nomenclature and would lead to organic-rich illuvial horizons.

Regardless of mechanism, podzolization leads to essentially two compartments of the soils according to their weathering status and the nature of the secondary phases (Ugolini et al., 1991). These are (1) the upper horizons, and especially the distinct eluvial (or “fungal eaten”) E horizon, and (2) the taxonomically diagnostic lower illuvial horizons, and especially the equally distinct Bh and Bs horizons. (Both or only one of the Bh or Bs may be present in podzol soils.) Considerable recent effort has been expended into studying the early stages of podzolization, largely in soils in the boreal zone, namely, under forests, in northern and/or alpine Europe, from a mineralogical viewpoint

(Melkerud et al., 2000; Mossin et al., 2002; Mokma et al., 2004). Mokma et al. (2004), tracing the earliest stages of podzolization in sandy soils in Finland, found visual evidence for translocation of C, Al, and Fe after 230 years of soil formation while there was evidence of allophane in a Bs horizon after 900 years. There were few differences between the crystalline minerals in the soils of different ages (up to 11,300 years). Buried podzol profiles in northern New Zealand exhibit thin E, Bh, and Bs horizons (about 20, 2, and 5 cm in thickness, respectively) formed on a pumiceous rhyolitic tephra layer deposited in ca. AD 232. The Bs horizons contain allophane. The developing podzols were subsequently buried in ca. AD 1314 by deposition of another rhyolitic tephra (Lowe, 2008). The profiles thus reflect about 1082 years of podzolization under ~1500 mm annual rainfall in a mesic temperature regime under broadleaf-podocarp forest.

In three soils on Quaternary deposits in Fennoscandia, Melkerud et al. (2000) found that the most easily weatherable primary minerals, biotite, chlorite, and hornblende, were depleted from the eluvial horizon, which had the highest concentration of quartz. Vermiculite dominated the clay mineralogy of the E horizons and was also present, but with incorporated Al-hydroxy interlayers, in the B horizon, where poorly ordered or nanocrystalline imogolite-type materials (i.e., allophane) also occurred. Mossin et al. (2002) specifically searched for imogolite in three Danish podzols. Some proto-imogolite allophane rather than imogolite per se was found, but in smaller amounts than had been found in podzols further north in Scandinavia and not at all under spruce, which was responsible for the lowest pH for the soils. They ascribed the generally relatively lower contents of allophane to a lower pH, an increase in organic matter, and a parent material with a low content of easily weatherable minerals. The pH conditions and other factors such as aluminum extractability and solubility are important in explaining the differences in composition in different parts of the podzol profile (e.g., Zysset et al., 1999; Lundström et al., 2000; Farmer and Lumsdon, 2001).

Recently, several other authors have particularly examined the effect that the podzolization, namely, acid leaching, process has had upon micaceous clay minerals. The results of some earlier studies of this kind are discussed in Section 20.2.4.3 and also earlier in this section herein and in Churchman (2000). While the general consensus from earlier studies was that beidellitic smectites are often identified as a stable phase, if not an end product, of the alterations of micaceous minerals that take place in podzol E horizons as a result of eluviation, Righi et al. (1999), Gillot et al. (2001), Mirabella and Egli (2003), and also Egli et al. (2004) have all found that the smectites that form in this way can be quite complex. They constitute a mixture of several populations with various layer charges (Gillot et al., 2001). A chronosequence of soils in Finland enabled these last authors to find that the products of mica transformation included both a relatively high-charge ferromagnesian smectite and also a vermiculite with higher charge in younger soils. They thought that the Fe-Mg smectite arose from the transformation of the ferromagnesian primary mineral biotite and from Fe-Mg-bearing chlorite present in the rocks, whereas the vermiculite, which was aluminous, was a transformation

product of dioctahedral micas (muscovite and phengite). In older soils, smectites with a lower charge resulted from both the dissolution of the higher charged trioctahedral smectites and also a progressive decrease in the charge of the dioctahedral expanded phases (Gillot et al., 2001). Righi et al. (1999) found the nature of the aluminosilicate products of podzolization in the eluvial A and E horizons differed from those in the B horizons within a different chronosequence of soils. The A and E (eluvial) horizons contained a mixed-layer mica-smectite, and, given time, also discrete smectite from the transformation of dioctahedral mica. The B (illuvial) horizons, by contrast, contained mixed-layered mica-vermiculite and smectite. These last clays were the products of the alteration by transformation of trioctahedral minerals, notably biotite and chlorite (Righi et al., 1999). These authors explained the differences between the transformational products by a difference in the nature of the acids involved as weathering agents in the two different parts (or compartments) of the soil profile. In the upper, eluvial compartment, organic acids are responsible for the mineralogical changes and these are more aggressive than the carbonic acid in the lower compartment, which includes the illuvial horizons (Righi et al., 1999). It is only in the upper compartment that dioctahedral minerals become altered, and the organic acids responsible for the alteration there dissolve the products of weathering of the trioctahedral minerals. Their dissolution leads to phases that are translocated to the illuvial Bh and Bs horizons where they accumulate as “amorphous” (i.e., probably nanocrystalline) Fe and Al oxides and as recrystallized gibbsite in these particular soils (Righi et al., 1999). Studying an altitudinal sequence of five podzolized soils in Italian alpine regions, Mirabella and Egli (2003) also found that the smectites formed in either eluvial or illuvial horizons were highly heterogeneous, mostly comprising mixtures of montmorillonite with interstratified beidellite-montmorillonite, but never consisting of beidellite alone. Some were interlayered with hydroxy-Al species, which needed to be removed by citrate treatment before the underlying phases could be distinguished, but their removal showed that the specific expandable micaceous phases with their variety of layer charges had been formed prior to interlayering (Mirabella and Egli, 2003). The most intense weathering, leading to the lowest charged smectites, occurred in podzols below the tree line but closest to it. Clearly, in many of these studies, certain trees are a major factor in the intensification of the podzolization process, if not in its occurrence, in some environments. Churchman (1980) also found that, although podzolization could occur under grasslands provided the rainfall was sufficiently high, the mineralogical changes to micaceous phases were more advanced in soils that were just a few meters away, but which were below the tree line. In the podzols under grassland on both mica-chlorite schist and graywacke lithologies, regularly interstratified mica-beidellite dominated the clay fractions and there was no discrete beidellite present, but discrete beidellite occurred in substantial amounts in podzols under native *Nothofagus* beech forest in New Zealand (Churchman, 1980).

Although beidellitic smectites appear to constitute a stable phase in podzols formed in boreal zones, there can be a sequence

of products formed at different stages during the podzolization process, as discussed by, for example, Churchman (2000), and also by Righi et al. (1999). Studying seven podzol profiles in the Tatra Mountains in Poland, Skiba (2007) has concentrated on the alteration processes of dioctahedral micas within all parts of these soils. This author found a variety of transformational products of dioctahedral micas that varied in the regularity of ordering of their interstratifications with (at first) vermiculites, in the expandability of the vermiculites formed, both as interstratified layers and also as discrete phases, and in the degree of interlayering of vermiculites with smectite, leading ultimately to a discrete smectite phase. Many of these also exhibited interlayering with hydroxy-Al species when pH was ≥ 4.4 . Skiba (2007) also claimed that kaolinite formed neogenetically in these podzols from Al and Si released by weathering.

Three podzols forming in tropical and subtropical climatic zones have been studied in Taiwan by Lin et al. (2002), among others. There was a very similar mineralogical pattern to those seen in podzols in the cooler boreal zone. Illite was altered to vermiculite, or sometimes to interstratified illite-vermiculite in eluvial horizons. There was no interlayering with hydroxy-Al species in the eluvial horizons, which exhibited very low pHs under forest but some occurred in B horizons at higher pHs, and Lin et al. (2002) also considered that translocated Fe, Al, and organic acids coated the Al-interlayered vermiculitic phases with organometallic compounds and thus stabilized them against breakdown. As in many other podzols, the system was characterized by the eluviation, translocation, and deposition of mainly Al and Fe by organic acids.

The general mineralogical pattern in podzols is summarized in Box 20.4. It is given for podzols on micaceous parent materials, which are common for many podzolized soils, although podzols can form on many parent materials or lithologies.

20.2.5.3.3 Apparent Counteraction of Weathering by Plants

Some work has indicated that plants, as well as acting as potential weathering agents, may also act to counter the course of mineral development that might otherwise be expected from the

operation of the other main weathering agents such as climate. Thus, in a chronosequence on basalt in the tropics, both the early formation of an illite and also a lower content of gibbsite in A horizons than in C horizons across much of the sequence were attributed by He et al. (2008) to the transport by plants of nutrients (K, and also Si, as siliceous phytoliths) to the surface of soils. Together the increases in these nutrients have led to the formation and retention of illite and 2:1 aluminosilicates more generally, at least until they are finally weathered out in the oldest soils. Both April and Keller (1990) and also Calvaruso et al. (2009) found that there was a buildup of the discrete mica phase (respectively muscovite and illite in the two reports) relative to its degraded counterpart in the rhizospheres of trees in comparison with the bulk soils. Barré et al. (2009) have concluded from a review of the literature that this effect of plants retarding weathering changes, which is known as “nutrient uplift,” “element translocation,” or “biological pumping,” is widespread, and that “the clay mineralogy observed in surface soils is probably largely plant mediated.” The uptake and biocycling of Si by plants has also been studied by Drees et al. (1989), Lucas et al. (1993), Derry et al. (2005), Farmer (2005), and Henriot et al. (2008). The concentration of Si by “nutrient uplift” has probably contributed, at least, to the preservation of kaolinite and halloysite, respectively, in the surfaces of forest soils in Brazil (Furian et al., 2002) and Costa Rica (Kleber et al., 2007), while strong tropical weathering has led to gibbsite dominating the mineralogy of the saprolite in the Brazilian case and the subsoil in the Costa Rican one. An examination of published data on Si concentrations in Bs horizons in several European forest soils, as well as experimental data for some of these, led Farmer et al. (2005) to postulate that plant phytoliths provide a sink, hence short-term nutrient uplift, for Si from soil solutions during the growing season that is released back to solutions during winter and spring. Such a viewpoint is supported by data derived from studies of plant-related movement in soils of Al and Fe as well as that of Si in both temperate and tropical soils that were reviewed by Lucas (2001), although differences are evident for different environments (see Figure 6 in Lucas, 2001). Nonetheless, Lucas (2001) concluded

Box 20.4 MINERALOGICAL PATTERN IN PODZOLS DEVELOPED ON MICACEOUS PARENT MATERIALS

Incr. Al, Fe, pH	Horizons	Type	Alteration	Phyllosilicates	Nanocrystalline (SRO) Minerals
↓	A, E	Eluvial	Accelerated loss of cations including Al, Fe, K, Si	Beidellitic or smectite or vermiculite; interstratified with illite, or discrete	—
	Bs, Bh	Illuvial	Normal extent of alteration, for example, for climate	Vermiculitic, <i>not</i> smectitic, i/strat. or discrete, poss. Al-interlayered	Allophane and/or imogolite, Fe oxides, especially ferrihydrite

that in most places (tropical as well as temperate), the weathering mantle can be regarded as being in a “dynamic equilibrium sustained by plants.” Derry et al. (2005) found that most of the silica released to Hawaiian stream water had passed through the biogenic silica pool rather than originating directly from mineral–water reactions in soils in this basaltic environment.

20.2.5.3.4 Humans and Other Fauna as Weathering Agents

The human being is one biological agent with a potential to affect soil mineralogy, which cannot always be ignored. Apart from such effects on soil mineralogy as those from enhanced erosion—leading to, for example, truncation of profiles and transportation of soil minerals over distances from a few meters to the diameter of an entire hemisphere (e.g., Syers et al., 1969) by water or wind—people’s activities can also either enhance or retard the influence of other organisms on mineral weathering, whether through the effects of agriculture, pollution, construction, and engineering activities and/or effects on climate and hydrology at either local or global scales (e.g., see Yaron et al., 2010). In the particular case of acid sulfate soils, which are increasing in area globally because of human activities, and which are of increasing concern as a form of both soil and environmental degradation (Dent and Pons, 1995; Ritsema et al., 2000), large-scale changes wrought by humans have led to mineralogical changes, which contribute to the properties of these soils, which have been labeled “the nastiest soils in the world” by Dent and Pons (1995). Classed often as Sulfaquents, acid sulfate soils, which are most commonly coastal, but may also occur in nontidal seepage and marsh areas affected by dryland salinity (Fitzpatrick et al., 1996), originate from the oxidation of sulfides, most commonly of Fe and most often pyrite FeS_2 , but sometimes also Fe monosulfides such as mackinawite (tetragonal FeS), pyrrhotite (hexagonal FeS), and greigite (Fe_3S_4) (Burton et al., 2009). These Fe sulfides are themselves products of earlier bacteria-mediated reduction of sulfate ions (Dent and Pons, 1995; Fitzpatrick et al., 1996). Sulfuric acid results from the oxidation of the sulfides (such as occurs after draining the soils), which occurs only slowly in an abiotic environment, but which is greatly accelerated in the presence of Fe-oxidizing bacteria (Ritsema et al., 2000). The sulfuric acid thus produced reacts with soil minerals generally to give a range of compounds. Of these, jarosite ($\text{KFe}_3(\text{OH})_6(\text{SO}_4)$), also known as “cat clay” because of its yellow, fecal-like color, is most widely recognized as a component of acid sulfate soils (Dent and Pons, 1995; Fitzpatrick et al., 1996), and schwertmannite ($\text{Fe}_8\text{O}_8(\text{OH})_{8-2x}(\text{SO}_4)_x$), has been recognized in some under very acid conditions (Fitzpatrick et al., 1996; Burton et al., 2006, 2008). The Fe oxidic phases, ferrihydrite $\text{Fe}_5\text{HO}_8 \cdot 4\text{H}_2\text{O}$ and goethite, can also form (op. cit.), but many other minerals have been found to form as a result of the processes contributing to the evolution of these soils. These minerals include hydrated sulfates of Na and Fe (sideronatrite and natrojarosite), Na and Al (tamarugite), Mg and Fe (copiapite), and Pb and Fe (plumbojarosite), as well as gypsum, halite, the Fe oxyhydroxide, akaganéite, and a poorly ordered Al oxyhydroxide (R.W. Fitzpatrick and M.S. Skwarnecki, unpublished results), as well as elemental sulfur (Burton et al., 2009). In the case of acid

sulfate soils, the effects of human intervention in certain environments have been to promote mineralogical changes that are mediated by microbes.

Agriculture brings about disequilibrium in soils (Velde and Meunier, 2008). The effect of cropping on clay mineralogy was assessed through analyses of samples taken from the long-term Morrow experimental plots at the University of Illinois for >80 years cropping of different types and with different management regimes (Velde and Peck, 2002). Continuous cropping with corn has led to a marked loss of illite in favor of illite–smectite phases. In contrast, rotation cropping over the same period has had little effect on clay mineralogy. However, 80 years of growing rice in flood-irrigated soils in China showed strong effects on clay minerals in the soils (Li et al., 2003). Micaceous phases, including interstratified phases, have largely been lost, as have Fe oxides, but a Si-poor ferromagnesian chlorite has formed. Pastures can also influence clay mineralogical development. Poldered sediments in France with up to ~850 years of development under prairie enabled Velde et al. (2003) to show that the dominantly illite–smectite clay minerals in topsoils, which were influenced the most by grass growth, hardly changed with time from those in the sediment. On the other hand, the same type of clay minerals in the subsoils became more smectitic over the same time period. The subsoils had a higher pH than the topsoils, which were more-or-less neutral in pH. The grasses appeared to stabilize the particular mixed-layer composition of the original clay minerals.

The common agricultural practice of adding fertilizers to soils can also have effects on the mineralogy of soils. Thus, Simonsson et al. (2009) found that soils subjected to the long-term use of K fertilizers had contents of illite, both as a discrete phase and also within mixed layers, which reflected the rate of addition of the fertilizers—illite was more concentrated where fertilizer additions had been higher. K release from the soil minerals appeared to be reversible except where hydroxyaluminum interlayers occurred, presumably blocking K^+ from entering or leaving the interlayers (Simonsson et al., 2009). Velde and Peck (2002) also found that additions of NPK fertilizer after >40 years of continuous cropping with corn restored the clay minerals to their original state whereas, as already noted, illite was sufficiently depleted of K over >80 years of this treatment without fertilizer additions to register a significant change to illite–smectite (I–S). These authors suggested that I–S plays the role of a K buffer that releases K when plants cannot access other sources of this essential nutrient and stores it when there is an excess of K. Pernes-Debuyser et al. (2003) found that the content of nonexpandable illite increased at the expense of expandable I–S in long-term K-addition treatments of soil without plants with either KCl or manure at Versailles in France. Fertilization with ammonium-based N-fertilizers has also been shown to affect clay mineralogy through an increase in the contents of nanocrystalline aluminosilicates and also hydroxyl–Al interlayers in 2:1 minerals (McGahan et al., 2003). On the contrary, Tye et al. (2009) noticed that the greatest mineralogical changes in the long-term plots at Rothamsted in the United Kingdom occurred when fertilization with ammonium sulfate led to pHs falling below 3.7, when

hydroxyl-Al interlayers in 2:1 minerals became solubilized, allowing entry of the interlayers to K^+ and NH_4^+ .

Fauna can also aid weathering processes by moving soil materials, especially by bringing less-weathered or unweathered subsurface materials to the soil and land surface as occurs by termites for example in building mounds, and worm ingestion and excretion (e.g., Paton et al., 1995; Johnson, 2002; Meysman et al., 2006). In maritime Antarctica, which receives more liquid water than the Antarctic continent, ornithogenic soils formed on basaltic and andesite rocks in abandoned penguin rookeries and which are organic-rich due to penguin guano show considerable development of secondary minerals, mainly as noncrystalline or nanocrystalline phases, including 1:1 (Al:Si) allophane (Simas et al., 2006).

20.2.5.3.5 *Microorganisms as Weathering Agents*

It is well recognized that microbes act as reducing agents and thereby contribute to the reassignment of Fe and Mn from primary minerals or secondary oxides, oxyhydroxides, and hydroxides into solution and ultimately into new oxidic phases upon drying, sometimes with the solubilization and release of trace metals such as Co and Ni (e.g., Quantin et al., 2001). Microbes also act commonly as oxidizing agents (such as in the formation of ferrihydrite in seepages). Their activity, when simulated by a series of oxidation-reduction cycles, transformed the short-range-ordered iron oxide “nanogoethite” to microcrystalline goethite and microcrystalline hematite (Thompson et al., 2006). They may also bring about mineral alteration through root exudates, as in the tunneling action of fungal hyphae on feldspars and other mineral grains (van Breemen et al., 2000b; Smits et al., 2005, see Section 20.2.4.2). Müller (2009) has shown that the weathering effect of bacteria can vary greatly between different genetic derivatives of a single strain. Organic acids resulting from the life and death of organisms have also been recognized as important agents in mineral alteration (e.g., Huang and Schnitzer, 1986; Robert and Chenu, 1992). In particular, dicarboxylic acids have been identified in soils (Hue et al., 1986) where they greatly enhance rates of dissolution (Amrhein and Suarez, 1988) through ring compounds as ligands for sequestering metals on mineral surfaces (Casey, 1995). One of the main effects of organic acids on weathering may come through their supply of protons (Ugolini and Sletten, 1991; Nesbitt, 1997). It has also been shown in nature and in experiments that both aluminosilicate minerals and oxides of Fe and Mn can form by nucleation on bacteria (Urrutia and Beveridge, 1994; Ferris, 1997; Tazaki, 1997, 2005; Chan et al., 2009). Magnetite formed partly by bacteria in soils has been described, for example, by Maher and Taylor (1988) and Geiss and Zanner (2006). Observations made by Ueshima and Tazaki (2001) in both deep-sea sediments and laboratory experiments showed that aluminosilicates (nontronite in this case) could be formed on extracellular polysaccharides from microbes. The role of microorganisms in the weathering of glass or volcanic materials has been described, amongst others, by Thorseth et al. (1995), Kawano and Tomita (2001, 2002), and Stroncik and Schmincke (2002). According to the last authors,

bacteria and microorganisms create a local microenvironment as a result of the fluids of their metabolic products. These fluids are either acidic or basic in pH, depending on the type of bacteria: an acidic pH essentially results in incongruent glass dissolution, whereas a basic pH results in congruent glass dissolution, leaving large pits on the glass surface (Stroncik and Schmincke, 2002). Microbial activity thus enhances the rate of dissolution of volcanic glass and microbial alteration also results in the formation of authigenic phases and is accompanied by redistribution of elements.

Hence, microorganisms may play a number of roles in mineral weathering. As summarized by Barker et al. (1997), these include the following: (1) physical disintegration of rocks; (2) production of acids and chelating ligands to accelerate chemical alteration; (3) stabilization of soils to increase their time of exposure to chemical agents; (4) production of extracellular polymers to moderate water potential, maintain diffusion channels, and themselves act as ligands for chelation and also as nuclei for mineral neof ormation; and (5) absorption of nutrients to lower solution concentrations and increase the chemical potential for weathering. All these roles may also be performed by plants, including grasses, crops, and trees (e.g., Courchesne, 2006). In addition, they may be carried out by other biological agents, including lichens (Adamo and Violante, 2000; Chen et al., 2000), fungus-growing termites (Jouquet et al., 2002), and mycorrhizal fungus (Jongmans et al., 1997; van Breemen et al., 2000a, 2000b; Certini et al., 2003). With regard to mycorrhizal fungus, the cited authors concluded that the fungal hyphae dissolved and extracted nutrients directly from mineral grains, such as feldspar and hornblende, through their intrusion into fractures and fissures in the geological deposits and by “drilling” directly into minerals, thereby bypassing the external solution phase. However, in studying the microbiological colonization of primary mineral weathering in volcanic soils in Italy, Wilson et al. (2008) found in this case that microbial activity, particularly fungal activity, was not an effective agent of mineral weathering, that the association with clay minerals was indirect, and that fungal weathering of primary minerals was probably less important than previously claimed as a source of plant nutrients. These authors concluded that preformed cleavages and microporous features in primary minerals enable the penetration of fungi for them to bring about mineral alterations and noted that these features were generally absent in the soils they studied.

20.2.5.3.6 *The Ecology of Biota and Soil Minerals*

Bennett et al. (2001), in noting that microbes bring about the alteration of minerals through their selective extraction of essential nutrients from the minerals, posed the question of whether the suite of microorganisms is partly, at least, controlled by the mineralogy and by the ability of particular microorganisms to use the nutrients contained within the minerals present. Soil minerals, both primary and secondary, may thus be viewed in the ecological context that is characterized by Young and Crawford (2004) as “the soil-microbe complex.” Building on the concept of plants as ecosystem engineers, and on published information on

the effects of particular plant species on soils, van Breemen and Finzi (1998) reviewed the evidence that such effects can provide a positive feedback to such plants. They concluded that there was strong evidence for plant-soil feedbacks in a variety of ecosystems, and they argued that these feedbacks could have played a role in the evolution of the plant species in question. Earlier, van Breemen (1992) had asked the question: “have soils merely been influenced by biota or have biota created soils as natural bodies with properties favorable for terrestrial life?” Coleman and Crossley (2003) argued for the latter by reference to the storage in soils of the life-limiting element, phosphorus. They contended that (1) the interaction of biota with primary minerals produces soluble Fe (and other cations) by weathering; (2) Fe in particular is brought into the solid phase as oxides (including oxyhydroxides) by oxidation aided by (iron oxidizing) bacteria; and (3) the Fe oxides are kept in a largely amorphous or nanocrystalline form, from which P can be extracted by plants more efficiently than from crystalline oxides, through their interaction with (biota-derived) humic substances. Recent experimental

work has shown both that (1) bacteria can effect the production of polymeric molecules within the structures of (smectitic) clay minerals, hence probably improving the environment for the survival of the bacteria (Alimova et al., 2009), and (2) the structure of bacterial communities in soil is influenced by the (primary) minerals in their microhabitat (Carson et al., 2009). Chickens and eggs come to mind in assessing whether biota or minerals are the limiting factors in the ecology of the soil, but it is clear that, while both are important, it is their interactions that are of overriding and vital importance to the sustainable functioning of soil and the life it supports.

20.2.6 Processes of Mineral Alteration and Formation by Weathering: Summary

Secondary minerals are formed as a result of the alteration of primary minerals or mineraloids by either (1) transformation in the solid state or (2) hydrolysis, dissolution, and recrystallization out of solution, namely, neogenesis. Figure 20.9 summarizes these two possible mechanisms.

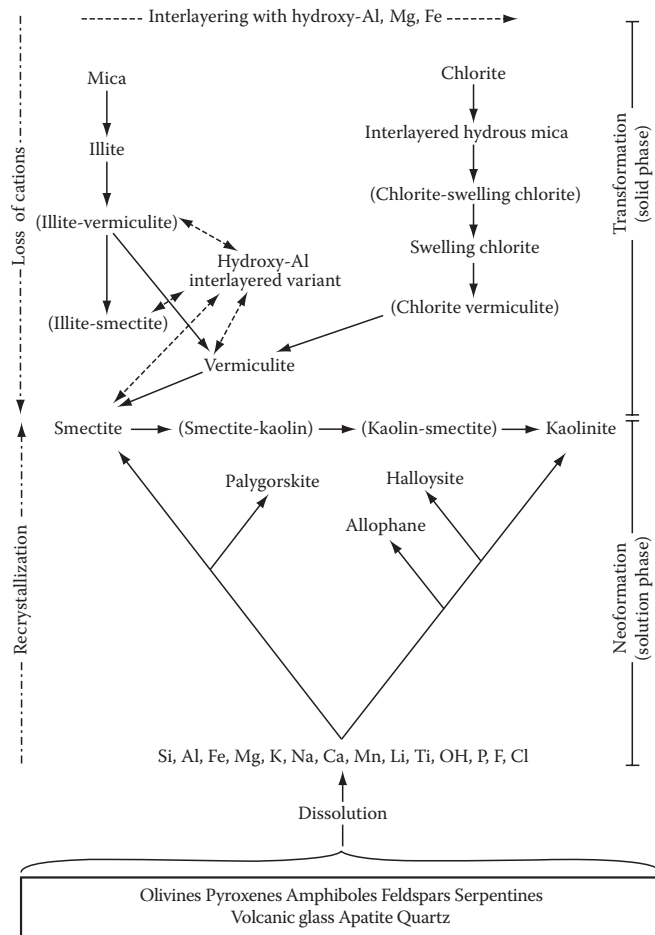


FIGURE 20.9 Main pathways for mineral alteration and formation in soils via either neof ormation (lower part of figure) or transformation (upper part). (After Churchman, G.J. 1978. Studies on a climosequence of soils in tussock grasslands. 21. Mineralogy. N.Z. J. Sci. 21:467–480; Wilson, M.J. 2004. Weathering of the primary rock-forming minerals: Processes, products and rates. Clay Miner. 39:233–266.)

20.3 Occurrence of Clay Minerals in Soils

This section concentrates on the particular forms in which clay minerals occur within soils, rather than the general groups of soils in which they occur, or even their distribution in particular environments or globally. These aspects are dealt with elsewhere in this handbook. Instead, our focus is on the sizes and shapes of mineral particles and peculiarities of their chemical compositions and crystal structures, largely in relation to those of “type” occurrences of minerals with the same names in more or less pure “geological” deposits, including those often used as standard specimens of each type. In this section, we also explore the associations of minerals within soils in relation both to other types of minerals and also to organic materials. In particular, we examine the possibility that there is a relationship between the mode of formation (and alteration) of clay minerals, on the one hand, and on the other, the forms they adopt and also their associations within soils.

20.3.1 Occurrence of Kaolinite in Soils

Kaolinite is the most ubiquitous phyllosilicate in soils (White and Dixon, 2002). Nonetheless, kaolinites are most abundant in highly weathered soils, which are formed in warm humid climates, although a high rainfall can result in their formation within soils in temperate climates (Weaver, 1989; White and Dixon, 2002). They can also be found in soils in colder climates that were nevertheless formed under an earlier, warmer climate, for example, by preglacial weathering in Scotland (Wilson et al., 1984). Generally, kaolinites in soils are highly disordered and many of the peaks in their XRD patterns are poorly resolved. As a result, the common index for assessing the degree of crystalline order by XRD, namely, the Hinckley index, is impossible

to measure and an alternative, empirical index was devised by Hughes and Brown (1979), which remains in use for soil kaolins (including halloysite). In developing this index, Hughes and Brown (1979) noted that kaolinites in the set of 26 soils they mainly studied, which were from Nigeria, invariably occurred along with other minerals in their clay fractions, as well as containing weatherable minerals in the coarser fractions. These authors suggested that the weatherable minerals present hindered the crystallization of well-ordered kaolins. Millot (1970) had come to a similar conclusion, suggesting more specifically that alkaline-earth cations had caused the inhibition of crystallization. Iron is a common impurity in the kaolinite structure, and there appears to be a relationship between structural Fe and crystalline order (Herbillon et al., 1976; Mestdagh et al., 1980). As Fe increases in amount, displacing the smaller Al atoms from the structure, crystal strain may increase, thereby limiting crystal growth, so that particle size as well as structural order is likely to be diminished by a high Fe content. Lim et al. (1980) had found that nonsoil kaolinites could also be poorly crystallized. Compared with their well-crystallized counterparts, seven examples of these poorly ordered kaolinites, from Georgia in the United States of America, showed not only much higher values for specific surface area particularly (between 78 and 114 m² g⁻¹, cf. 10–15 m² g⁻¹ for the well-crystallized kaolinites), but also some relatively high values for CEC. All were shown to comprise some montmorillonite and vermiculite as impurities, while six of them also contained mica. Kaolinites often occur in vermiform books, suggesting a micaceous precursor. White and Dixon (2002) suggested, rather, that micas, or, more commonly, their expanded transformation products with the same crystal

form, for example, vermiculite or beidellitic smectite, provide nucleation sites on their 001 surfaces for authigenic kaolinite formation, as shown in Figure 20.4.

A number of papers (Singh and Gilkes, 1992a; Melo et al., 2001; Hart et al., 2002; Kanket et al., 2005) have compiled data describing crystal form, measures of crystal order, and related properties such as Fe contents for kaolinites extracted from highly weathered soils in (Western) Australia, Brazil, Thailand, and Indonesia, although the last also included some halloysite or “tubular kaolins” (Churchman and Gilkes, 1989), so the total set is better described as kaolins. Together with information from Hughes and Brown (1979) for Nigerian soils, these properties are able to be compared in Table 20.4 (from Kanket et al., 2005, with data for the reference kaolinites from Hart et al., 2002). The various kaolins had many properties in common. Although there was a range for each value within each set of soil kaolins, their specific surface areas (overall range 34–88 m² g⁻¹) all exceeded those of any of the reference samples (all ≤25 m² g⁻¹) and their particle sizes, given by coherent scattering domains (CSDs), were generally less than half those of the reference kaolinites. Surface areas and particle sizes are expected to be inversely related to each other. Their Hughes and Brown (HB) index values were always less than those of the reference kaolinites, and, although some of the soil kaolins had quite high CECs, some were comparable to those of several, at least, of the reference kaolinites. Regardless of their other characteristics, however, all of the soil kaolins on which Fe was measured (those from Thailand, Western Australia, and Indonesia) had much higher contents of Fe than the reference kaolinites. With the most clear-cut differences between soils and reference kaolinites being in their surface areas, the HB measure

TABLE 20.4 Properties of Kaolins in Groups of Soils (with Standard Deviations, Where Given, in Brackets) and of Standard Kaolinites

Location	No. of Samples	d ₀₀₁ (Å)	CSD ^a (nm)	HB ^b Index	% Fe ₂ O ₃ (g kg ⁻¹)	CEC (cmol _c kg ⁻¹)	SSA ^c (g kg ⁻¹)
<i>Soils</i>							
Thailand (1) ^d	20	7.208 (0.042)	19.3 (8.9)	6.7 (1.6)	19.6 (1.8)	8.5 (2.9)	47.4 (8.8)
Thailand (2) ^e	18	7.19 (0.03)	15.4 (5.5)	6 (1)	25.3	15.2 (4.7)	44.9 (12.1)
Western Australia	7	7.213	22.9	5.6	25.7	5.0	50.8
Indonesia	6	7.212	10.8	5.6	25.4	9.4	72.8
Nigeria	26	—	—	8.0	—	—	—
Brazil	21	7.19	—	12.7	19.6	—	48.5
<i>Standards</i>							
Georgia #1460	1	7.148	26.6	18.9	8.9	3.2	25
Georgia #1261	1	7.160	43.4	32.6	2.5	3.9	10
Georgia #MP5	1	7.132	47.6	34.2	4.2	0.4	5
New Mexico (Wards)	1	7.148	43.1	60.5	4.3	4.6	13
Cornwall (ECC)	1	7.160	48.8	26.3	4.2	0.5	11

Source: Data for the soil kaolins from Kanket, W., A. Suddhiprakern, I. Kheoruenromne, and R.J. Gilkes. 2005. Chemical and crystallographic properties of kaolin from Ultisols in Thailand. *Clays Clay Miner.* 53:478–489, with data for the reference kaolinites from Hart, R.D., R.J. Gilkes, S. Siradz, and B. Singh. 2002. The nature of soil kaolins from Indonesia and Western Australia. *Clays Clay Miner.* 50:198–207.

^a CSD, 001 peak.

^b Hughes and Brown (1979).

^c Specific surface area from N₂-BET.

^d From Hart et al. (2003).

^e From Kanket et al. (2005);

— Not determined.

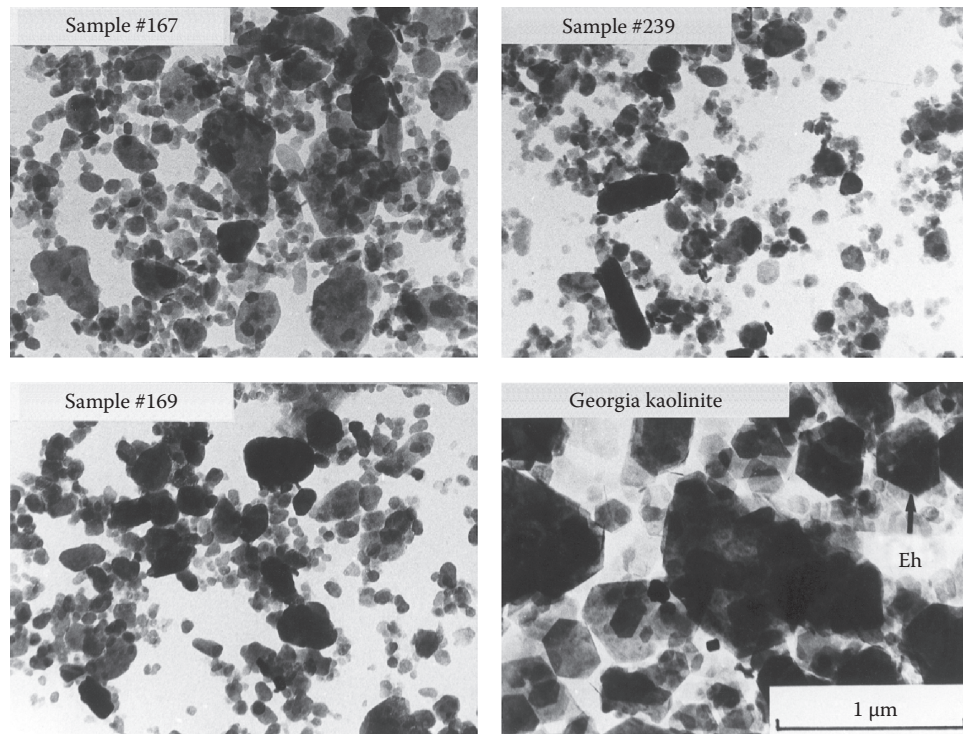


FIGURE 20.10 Transmission electron micrographs showing comparisons between some soil kaolinites from Western Australia and a reference kaolinite (from Georgia). Eh indicates a euhedral hexagonal shape for particles in the reference sample. (Micrographs copied from Singh, B., and R.J. Gilkes. 1992a. Properties of soil kaolinites from south-western Australia. *J. Soil Sci.* 43:645–667. Reproduced with permission of Wiley-Blackwell.)

of structural order, and their Fe contents, these results bear out the proposition from Herbillon et al. (1976) and Mestdagh et al. (1980) that a high Fe content leads to a low degree of structural order and small particles. Their small size, particularly, is illustrated by transmission electron micrographs showing comparisons between some soil kaolinites from Western Australia from Singh and Gilkes (1992a) and a reference kaolinite (from Georgia) (Figure 20.10). Furthermore, Singh and Gilkes (1992a) found that the kaolinites contained both K and Mg, which are largely absent from pure, well-crystallized kaolinites. Brazilian soil kaolinites were also found to contain considerable K and Mg (Melo et al., 2001). These authors suggested that there are residual micaceous layers incorporated in the kaolinites. This finding is consistent with the results of Lim et al. (1980) and also with the common observation that kaolinites appear in vermicular books by crystallization on the surfaces of micas and their transformation products (Figure 20.4). The crystal growth of the kaolinites may have been constrained by interleaved micaceous layers as well as by Fe incorporated into the kaolinite layers.

Kaolinite (and also, we shall see, halloysite) quite often occur in interstratifications with a smectite. Kaolinite–smectite interstratified phases have been found to occur worldwide, including in Scotland, Canada, throughout Africa, Australia, Central America, India, Japan, China, and the United States (see Churchman, 2000, for citations), and a more recent report (Vingiani et al., 2004) described their occurrence in Italy (Sardinia). Norrish and Pickering (1983) speculated that

kaolin–smectite interstratified phases (or “kaolin–smectites”) are likely to be a very common component of Australian soils. In Australia, and elsewhere, they have probably been often overlooked in identifications using XRD patterns. This “omission” is because the main effect of the mixed layering is to broaden and weaken XRD peaks, so that basal peaks may become invisible even though nonbasal peaks appear (Norrish and Pickering, 1983). In part, this effect is a consequence of the inherent variability of clay minerals in soils, so that the properties of the two (and sometimes more) components and their degree of order can vary from particle to particle (*ibid.*). Most kaolinite–smectites described in the literature are more kaolinitic than smectitic (Churchman et al., 1994), although Bühmann and Grubb (1991), Churchman et al. (1994), and also Ryan and Huertas (2009) each found examples where the proportion of smectite layers was >60%. In the same way that many interstratified specimens with high concentrations of kaolinite have been identified incorrectly as kaolinites (Norrish and Pickering, 1983; Churchman et al., 1994), so also some with high contents of smectite have been misidentified as smectites (Cuadros et al., 1994). Some with a high kaolinite content were probably misidentified as halloysites that have a platy morphology (Carson and Kunze, 1970; Wada et al., 1987), but each of these was later interpreted as a kaolin–smectite by Sakharov and Drits (1973) and Parfitt and Churchman (1988), respectively. The identification of phases as kaolin–smectites rather than as either of their components is important in order to fully describe the effect of clay mineralogy on soil properties

such as CEC (e.g., Seybold et al., 2005) because they give rise to higher values than can be expected from kaolinites and lower values than from smectites.

Kaolinite–smectites have been found in intermediate zones in toposequences spanning smectitic black soils at their base and kaolinitic red soils near their summits and on their steep slopes (Herbillon et al., 1981; Bühmann and Grubb, 1991; Delvaux and Herbillon, 1995; Vingiani et al., 2004). They have also been recognized within single soil profiles on basalt (Churchman et al., 1994; Vingiani et al., 2004). From the base of the profile to near its surface, their composition changed from highly smectitic to highly kaolinitic, but nonetheless with both phases being interstratified kaolinite–smectites (Churchman et al., 1994), or else more subtly, from ~35% to 40% to ~40% to 45% kaolinitic within the interstratifications (Vingiani et al., 2004). Ryan and Huertas (2009) have also located kaolinite–smectites in a set of soils within a chronosequence on mostly basaltic and andesitic parent materials. As it was within the residual soil profiles on rock (Churchman et al., 1994; Vingiani et al., 2004), the progression from youngest (found at the base of the profiles) to the oldest (at the surface in the case of the profiles) was from more smectitic (or pure smectite, in the chronosequence) to more kaolinitic. Kaolinite also occurred as a discrete phase alongside its interstratifications with smectite in the most developed (i.e., oldest) soil in the chronosequence of Ryan and Huertas (2009) and also in the soil profiles of Churchman et al. (1994) and Vingiani et al. (2004). A variety of techniques, including XRD, together with modeling of the effect of interstratifications and sometimes also peak decomposition, FTIR, HRTEM, differential thermal analysis (DTA), and permanent and variable charge analysis, have enabled various authors to seek an understanding of the origin of the process of interstratification of the 2:1 and 1:1 layers. Ryan and Huertas (2009) concluded that a layer-by-layer transformation occurs as smectite is progressively altered to kaolinite via an interstratification of the two endmember phases with each other. The transformation proceeds by localized dissolution of the 2:1 layers with initial loss of Fe and Mg from octahedral sheets and of Al from tetrahedral sheets followed by a loss of Si from tetrahedral sheets (“subtraction”) and/or a deposition of hydroxyl-Al species in interlayers, leaving 1:1 layers (“addition”) (Ryan and Huertas, 2009). These two alternative types of mechanism for the alteration had been proposed earlier by Wada and Kakuto (1983, 1989), who favored a subtraction mechanism, and by Altschuler et al. (1963) and Poncelot and Brindley (1967), who favored an addition mechanism. Albeit through studying a clay deposit rather than a soil, Watanabe et al. (1992) found support for a subtraction mechanism as a result of their discovery that opal C–T, or microcrystalline opal comprising clusters of stacking of cristobalite and tridymite over very short length scales, forms during the early stages of formation of kaolinite from smectite. Vingiani et al. (2004) discovered that the smectite in the sequence they studied consisted of a mixture of a more ferric and a more aluminous type. In the course of mineralogical evolution, there was a decrease in the proportion of the ferrous smectite layers relative to their aluminous counterparts. These

authors proposed that the (subtraction) mechanism operated through a preferential loss, by either transformation or dissolution of the ferrous smectite layers, to give kaolinite layers, with the excess Fe forming either Fe oxides (or oxyhydroxides) or becoming incorporated in kaolinite layers, or both.

Kaolinites can also form interstratifications with other types of layers besides smectites, for example, vermiculite (Jaynes et al., 1989), and can also participate in interstratified phases involving several different types of layers. The elevated CECs and also high K₂O contents of some of the soil kaolins studied by Singh and Gilkes (1992a), Melo et al. (2001), and Kanket et al. (2005), in particular, are at least partly ascribed to their interstratifications by micas and/or vermiculites. Ma and Eggleton (1999) found that some soil kaolinites in Queensland, Australia, had quite high CECs (16–34 cmol_c kg⁻¹) and HRTEM had shown that their crystals commonly comprised stacks of many kaolinite layers, which terminated in smectite layers, possibly as single layers. These stack-end smectite layers affected CEC but were usually not detectable by XRD (Ma and Eggleton, 1999).

20.3.2 Occurrence of Halloysite in Soils

As already noted (Section 20.2.4.5), halloysite is a common component of soils formed from volcanic parent materials, particularly tephra including finer components referred to as volcanic ash (e.g., Kirkman, 1981; Lowe, 1986). It has also been identified as a weathering product of a wide range of rock types including nephelinite, granite, gneissic granite and granitic gneiss, gneiss, dolorite, schist, graywacke, greenstone, granodiorite, gabbro, shale, and amphibolites (see Churchman, 2000, and also Joussein et al., 2005, for citations). Halloysite can occur in a variety of particle morphologies including tubes and microtubules, spheroids and microspheres, crumpled lamellae, crinkly films, needle-like or fiber-like forms, and prismatic forms (ibid.; see also Hong and Mi, 2006; Etame et al., 2009). Its morphology appears to relate to the content of impurity iron with substitution of the larger Fe(III) for Al in the octahedral sheet, which, without substitutions, is smaller than the tetrahedral sheet. This situation leads to partial or full correction of the misfit between the octahedral and tetrahedral sheets that, therefore, causes curling (as in tubes) in halloysites with little or no Fe. The impurity Fe also constrains crystal growth and leads to smaller particles being formed. Recently, Singer et al. (2004) have found halloysites with high contents (up to 6.5%) of Ti in their aluminosilicate structure that were plate-like, probably from the same cause: larger Ti atoms replace some Al in the octahedral sheets, hence also correcting at least some of the mismatch with the tetrahedral sheet. Even so, whereas a peculiar shape was once regarded as the distinguishing feature of halloysite in comparison with kaolinite, it is rather the occurrence, or else evidence for prior occurrence, of interlayer water that demarcates halloysites from kaolinites (see Section 20.2.4.6.2 earlier herein). Interlayer water is lost irreversibly from halloysites on drying.

However, some shapes, particularly spheroidal, appear to reflect a particular mode of formation for halloysite (Churchman,

2000). Spheroidal forms of halloysite appear often in weathering products of volcanic glass, which has a fast dissolution rate, and recrystallization from the resulting supersaturated solution appears to favor this particular shape (review by Bailey, 1990; Adamo et al., 2001; Singer et al., 2004), possibly when physically constrained, for example, within pumice cavities (Adamo et al., 2001). Nevertheless, both Churchman and Theng (1984) and Singer et al. (2004) found that spheroidal particles had higher Fe contents than even short tubes, suggesting a structural control on shape for spheroids as well as for tubes. By contrast, Johnson et al. (1990) found a spheroidal halloysite with virtually no Fe whereas Noro (1986) and also Adamo et al. (2001) found few, or only minor, differences in composition between spheroidal and tubular forms of the mineral. In any case, Soma et al. (1992), using XPS, found that Fe content varied between different layers in a halloysite, whether spheroidal or tubular. Furthermore, spheroidal- and tubular-shaped particles occur together in halloysites (Saigusa et al., 1978; Churchman and Theng, 1984), and one may alter to another in situ (Sudo and Yatsumoto, 1977), suggesting there may be no clear-cut distinction between the conditions that lead to the different particle shapes for halloysite. On the other hand, a very detailed microtextural and microanalytical study of samples taken at various depths in a weathering profile on gneiss in Greece led Papoulis et al. (2004) to deduce a sequence of mineral alteration that encompasses different morphologies for halloysite and includes two forms of kaolinite while simultaneously indicating a correlation between structural Fe and the various products in the alteration sequence. Papoulis et al. (2004) divided the alteration sequence into four successive stages. In the earliest stage, halloysite formed in very small spheres (~ 0.1 to $0.3 \mu\text{m}$ in diameter) that were located on the surfaces of plagioclase in this case. These small spheres then apparently coalesced to form tubes while new tubes also formed in the second stage. These tubes were generally quite short ($< 1 \mu\text{m}$ in length), although they could develop with time to form longer tubes with tapered ends, which, together with a relatively loose packing and subparallel orientation, suggest crystallization from solution (a conclusion supported by studies on halloysite with tapered ends by Hong and Mi, 2006). In the third stage, platy halloysite formed apparently by interconnection of the preformed tubes. This form even occurred in crude booklets, which are commonly regarded as more typical of kaolinites, albeit interleaved with a low proportion of kaolinite plates, according to Papoulis et al. (2004). These authors considered that the platy halloysite was unstable and led to the formation of plates of a poorly ordered kaolinite, with dimensions of $\sim 1 \mu\text{m}$ in length and ~ 0.1 to $0.2 \mu\text{m}$ in thickness. The change from halloysite plates to kaolinite was considered to occur within the single (third) stage by Papoulis et al. (2004). The fourth stage was one of kaolinization, with a disordered kaolinite forming first but with a well-formed book-type kaolinite as the ultimate product. Concomitant with these changes in morphology, increasing Fe in EDAX/EDS analyses of the products through the first three stages led these authors to allocate increasing proportions of Fe in octahedral sheets at the expense of Al, so that spheroidal halloysite had less substitution

of Al by Fe than tubular halloysite, whereas the platy form had the most structural Fe among the halloysites. The poorly ordered kaolinite that developed from halloysite in the third stage had a comparable degree of substitution of octahedral Al by Fe as its supposed platy halloysite precursor, and the disordered kaolinite formed first in the fourth stage had even more substitution of Fe for Al. However, the book-type kaolinite had a vanishingly small content of structural Fe. It was almost pure aluminosilicate. Overall, Papoulis et al. (2004) attributed the changes in the sequence from small spheroidal particles of halloysite through tubular and platy halloysite to poorly ordered platy, then well-ordered book-type kaolinite, largely to a changing chemistry of the ambient solutions, with a successively decreasing availability of Fe for incorporation in the aluminosilicate layers, although they conceded some role to microenvironmental conditions (e.g., time, and space available) in affecting particle morphology.

Bailey (1990) concluded that the structural difference between halloysite and kaolinite is substantial enough to make it impossible for one to give rise to the other without dissolution and recrystallization. Nonetheless, there have been many studies showing an apparent genetic relationship between halloysite and kaolinite in weathering profiles including soils and deeper regolith. There is a general trend from halloysite at depth toward kaolinite at the surface of profiles on residual rock materials (e.g., Eswaran and Wong, 1978; Calvert et al., 1980; Churchman and Gilkes, 1989; Churchman, 1990; Takahashi et al., 2001; Singer et al., 2004; Jongkind and Buurman, 2006). These studies together have covered a range of parent rock types and also climates, including tropical (Eswaran and Wong, 1978, and part of Churchman, 1990), temperate (Calvert et al., 1980; part of Churchman, 1990; Jongkind and Buurman, 2006), and Mediterranean, or xeric (Churchman and Gilkes, 1989; Takahashi et al., 2001; Singer et al., 2004). According to Papoulis et al. (2004), these trends with depth were explained in the context of their morphological and compositional development sequence of halloysite and kaolinites. They pointed out that a depth sequence in a residual weathering profile on rock is *inter alia* also a time sequence, with the earliest stages concentrated at depth and the latest (oldest) stages to be found near the surface (unlike we note the situation in upbuilding profiles where the opposite is true). Like Churchman and Gilkes (1989), these authors considered that the products of the different stages could also exist simultaneously with one another. Singer et al.'s (2004) examination of the weathering of basaltic scoria at a fine scale showed that, whereas 1.0 nm halloysite was found in vesicles in the scoria, where it was protected from dehydration, 0.7 nm halloysite and also kaolinite were found in the less scoriaceous basalt, where minerals had been exposed to seasonal drying. 1.0 nm halloysite was also found in a buried paleosol in the same region. Its burial in the paleosol had protected it from drying. In New Zealand, Lowe (1986) found that 0.7 nm halloysite predominated in the surface horizons of a soil developed on weathered tephra subject to reasonably frequent seasonal drought, whereas 1.0 nm halloysite occurred in deeper horizons that were less affected by drying. An intermediate zone of variably dehydrated

halloysite with XRD peaks between 1.0 and 0.7 nm occurred between upper and lower subsoil horizons.

These findings were corroborated by Churchman et al. (2010), who found that alteration of granite and volcanic tuff in Hong Kong had led to halloysite forming only in veins within the rocks where there was no evidence of drying, namely, no Fe or Mn oxides were present. By the same token, this study showed that kaolinite formed in these veins, either alone or in association with halloysite, where the appearance of Fe and Mn oxides indicated that drying had occurred. A weathering sequence on trachy-basaltic parent materials in Sicily was found to produce imogolite-like allophane (i.e., Al-rich allophane) in the early stages of alteration of volcanic glass and kaolinite, but no halloysite in later stages (Egli et al., 2008). This absence is probably because of the xeric moisture regime in the area. Similarly, basaltic parent materials in a xeric moisture regime in South Australia were found to produce allophane, but not halloysite (Lowe et al., 1996; Lowe and Palmer, 2005; Takesako et al., 2010; also Section 20.2.4.6). Kaolinite per se was not formed in this case, and, although kaolinite–smectite was often present in the soils, it could have been derived ultimately from limestones and calcareous dune sands underlying the basalt that were incorporated into the soil parent material during the basalt emplacement, with 1:1 Al:Si allophane the likely result of further development of initially formed 2:1 Al:Si allophane by resilication. Albeit that a drier regime tends to favor halloysite over allophane in soils from volcanic ash (see Section 20.2.4.6.2), these various observations suggest that the presence of water is a necessary condition for the formation and preservation of halloysite rather than kaolinite under similar conditions of, for example, parent material, temperature, and time.

Even so, a trend from halloysite at depth toward kaolinite at the surface in residual soil profiles does not necessarily imply that halloysite transforms to kaolinite as weathering intensifies with time. Churchman and Gilkes (1989) found rather that hydrated, tubular halloysite, which dominated the clay fraction of the saprolite deep in a lateritic profile in dolerite in Western Australia, became progressively more dehydrated and progressively more difficult to intercalate with the polar liquids—formamide, hydrazine, and a concentrated potassium acetate solution—with closer approach to the surface. As weathering intensified up the profile, kaolinite began to appear as hexagonal particles but by a different pathway from that for halloysite. As has been found elsewhere in the old, strongly leached landscapes of much of Australia (Janik and Keeling, 1993), Churchman and Gilkes (1989) observed that tubular particles with a kaolin layer structure and composition appeared even in the uppermost duricrust of the weathering profile, but they were dehydrated and completely resistant to intercalation by polar liquids.

In seeming contradiction to this trend and also to Bailey's (1990) contention that halloysite and kaolinite cannot transform from one to the other in the solid phase, both Robertson and Eggleton (1991) and also Singh and Gilkes (1992b) showed electron micrographs from within weathering profiles in Australia in which tubular particles, suggesting halloysite, are seen to

apparently form on the surface of kaolinite platy particles. Dissolution of kaolinite and recrystallization of halloysite could have occurred in both situations.

Like kaolinites, halloysites have been found to form interstratified phases with smectites. However, halloysite–smectites form under conditions different from those that result in kaolinite–smectites (Delvaux and Herbillon, 1995). Delvaux and Herbillon (1995, and earlier papers cited therein) have generally found interstratified halloysite–smectites in soils formed from volcanic ash. They form under similar (usually alkaline) conditions, which give rise to smectites but where the drainage is less restricted (i.e., more leaching occurs) than for smectite formation (Glassmann and Simonson, 1985; Smith et al., 1987).

There do not appear to be any studies of the form of halloysites and their associations in soils that are similarly detailed to those of soil kaolinites by Singh, Gilkes, and coauthors (Section 20.3.1). However, many electron micrographs, including those of the highly halloysitic Naiké and Hamilton soils in New Zealand (formed from strongly weathered tephra) that are shown in Fieldes (1968) and Churchman and Theng (1984), respectively, display mainly tubular particles that are practically all $<0.2\ \mu\text{m}$. Lowe (1986) also found tubes, some split, between ~ 0.07 and $\sim 0.3\ \mu\text{m}$ in length in similar materials. Furthermore, high values for surface areas of halloysites in soils or halloysite-rich soils from around the world have been recorded by several workers (Quantin et al., 1984; Theng, 1995; Takahashi et al., 2001; Singer et al., 2004). Specific surface areas $>100\ \text{m}^2\ \text{g}^{-1}$ were measured for soil halloysites or halloysitic soils in all of the studies cited. These area measurements point to the likelihood that halloysites, like kaolinites, commonly occur as quite small particles in soils. The fineness of their particles very likely reflects compositional or structural features that have limited crystal growth. In the case of the high surface area halloysites studied by Singer et al. (2004), it is likely that the high degree of substitution of Al by Fe and/or Ti introduced strains into the layer structure that limited the size of particles. The clay fractions of two halloysitic soils studied by Takahashi et al. (2001) were found to have high CECs and a high selectivity for K^+ in addition to high surface areas, and ^{27}Al -NMR showed that their constituent halloysites had $\sim 2\%$ tetrahedral Al and probably also some Al vacancies and impurity Fe in their octahedral sheets. They contained some Fe as oxides, which could have been present as surface coatings, and some 2:1 Si:Al minerals could also have been present in the clay fraction, even if not detected there, because of their obvious appearance in coarser fractions. While these authors could not reach unequivocal conclusions about the extent to which halloysite per se contributed to the unusual properties of these soils, the dilemma they encountered was the result of the complex mineral assemblages that could involve halloysites in soils and emphasizes how halloysites, like kaolinites, can be bound into multiphase associations in soils.

Halloysites often occur in close associations with iron oxides and oxyhydroxides in soils (Churchman and Theng, 1984; Bakker et al., 1996; Takahashi et al., 2001; Pochet et al., 2007; Etame et al., 2009). Pochet et al. (2007) showed that they can

form stable microaggregates with Fe oxides, and especially ferrihydrite that probably preserve the halloysites in spite of nearby soils being at an advanced state of weathering, which would normally drive the change toward kaolinite in a humid tropical environment.

In a study of soils formed from nephelinite (alkali- and rare-earth-rich lava) in tropical Cameroon, Etame et al. (2009) demonstrated a chemical dependence of the halloysites upon parent minerals: Ce-rich halloysite characterized alteromorphs formed from the mineral phillipsite, Fe-rich halloysite characterized alteromorphs on clinopyroxene, Ca-rich halloysite characterized alteromorphs on hauyne, and K-rich halloysite characterized alteromorphs on leucite. A Ce-rich halloysite (Ce_2O 0.1%) was also identified in saprolite derived from hydrothermally altered nephelinite (Etame et al., 2009).

20.3.3 Occurrence of Illite in Soils

Illites can form in soils by weathering as a result of transformation, in the solid phase, from micas (Section 20.2.4.3, and also, via biota, Section 20.2.5.3) and, like most of the other secondary minerals, they can also precipitate by neogenesis out of solution. There is little doubt that they most commonly form by transformation from primary micas. The degree of transformation they have undergone differs greatly, so that, in younger and less-weathered soils, especially those in arid environments (Section 20.2.5.2), the clay-sized micaceous phases may be mainly a product of comminution of primary micas by physical weathering processes (e.g., Fanning et al., 1989). In this case, the secondary phase may be better described as clay-sized mica rather than as illite. However, the term illite is used quite widely to describe mica-like clay-size minerals in soils, as already noted (Section 20.2.4.3). In all but the youngest or little-weathered soils, the micaceous phase in their clay fraction, hereafter referred to as illite, or illitic, contains some expanded layers; hence, some degree of interstratification of the K-rich illite layers with vermiculite or smectite layers that have become depleted in K through its displacement by hydrated cations. Hence, they are expandable.

Micas, especially muscovite and biotite, are particularly abundant in mica schists and some other metamorphic rocks (Fanning et al., 1989). Mica schists are especially abundant because they originate from the metamorphosis of argillaceous sediments such as shales and slates (*ibid.*). According to Fairbridge and Bourgeois (1978), shales comprise ~40% to 60% of all sedimentary rocks by volume and ~80% of crustal weathering products. As relatively soft minerals, micas in the schists are readily broken down during transport and sedimentation. Thence, they become important components of shales and slates, the types of sedimentary rocks from which they originated. Hence, illite may originate by inheritance from micas in underlying or nearby sedimentary shales or slates that may ultimately be recycled by metamorphosis into new mica schists (e.g., Garrels and Mackenzie, 1971). Illite in soils formed from these widespread sedimentary rocks is most abundant in the coarse clay (0.2–2 μm) size fraction (Fanning et al., 1989).

On the other hand, illite that has undergone considerable transformation to include expansible 2:1 layers of vermiculite and/or smectite is more likely to occur in the fine clay (<0.2 μm) size fraction (Fanning et al., 1989; Laird et al., 1991; Robert et al., 1991). Studying soil clays derived from the major sedimentary rocks, Robert et al. (1991) found that illite–smectite interstratified phases (I–S) are “the most widespread and representative soil clays,” a conclusion that was echoed by Velde and Meunier (2008; see also Section 20.2.5.3). Generally, they are randomly interstratified (Thompson and Ukrainczyk, 2002). Robert et al. (1991) distinguished two types of I–S. One, which they termed “micromicas,” may occur as large crystals and have layers with 1 nm periodicity that are separated by “swelling spaces” (Robert et al., 1991). It is a “structural” type of interstratification. The other type consists of random superpositions of elementary particles, “like monolayers,” to quote Robert et al. (1991). These authors characterized it as a “textural” type of interstratification, which is the same type as that identified by Nadeau et al. (1984) in the context of diagenetic clay minerals in sandstones.

One of the main conclusions to be drawn from Robert et al.’s (1991) work is that I–S, as common soil clays, differ significantly from reference clays. Among their defining characteristics, they are always multiphase, their smectitic phase is dominantly dioctahedral, and Al-rich, hence beidellitic (Robert et al., 1991), their particles have a very small lateral extension (often 30–50 nm) and a very small number of layers. Furthermore, their smectite component includes partially collapsed layers, and the clays have a high external surface area, particularly relative to their internal surface area (Robert et al., 1991). Laird et al. (1991) studied an I–S mineral that fully occupied fine clay fractions of a soil and found that the smectitic layers comprised a high-charge Fe-rich montmorillonite. This finding is at odds with several reports of soil smectites being more beidellitic, albeit Fe-rich (see Section 20.3.5). Laird et al. (1991) also found that the illitic layers had a low, largely tetrahedral charge, and were dioctahedral. Their layer charge was more typical of a beidellite than an illite. These authors speculated that the illitic layers in the I–S could themselves constitute a breakdown product of illite in the coarse clay fraction or else they could have formed by the collapse of preformed beidellite layers, but the evidence available to Laird et al. (1991) favored neither mechanism. Examination of a fine clay (0.02–0.06 μm) fraction by HRTEM in a later study (Laird and Nater, 1993) revealed that this was composed of (1) two-layer elementary illite particles, which were most abundant, (2) one-layer elementary smectite particles, and (3) rare discrete multilayer illite particles. The elementary illite particles could be separated from the smectitic component and were shown to comprise a rectorite-like phase with alternate swelling and nonswelling layers except that, in this case, the swelling and nonswelling layers each had a similar low charge of ~0.47 per formula unit in contrast to rectorite, with ~0.35 for the swelling and ~0.85 for the nonswelling layers (Laird and Nater, 1993). Like Robert et al. (1991), Laird and coauthors identified this I–S mineral phase as being characteristic of soils. Whereas it was identified as a component of an interstratification with smectite by Laird

et al. (1991), the ease of its separation, together with the lack of a 1 nm (10 Å) peak for illite in XRD analysis, indicated that the I-S phase in this fine clay fraction is a “textural” type of interstratification, similar to those identified by Nadeau et al. (1984), and, in soils, by Robert et al. (1991).

Illite can also form by neogenesis. Such illites include some that have formed in close proximity of feldspars, most probably out of solutions bathing the feldspars (Section 20.2.4.2). In many soils in Australia (Norrish and Pickering, 1983), and also in Iran (Mahjoory, 1975) and in some semiarid soils in North America (Nettleton et al., 1970), there is a concentration of illite toward the surface of soils, contrary to the trend in soils where micas are subject to transformation, which leads to increasing vermiculite and smectite at the expense of illite toward soil surfaces. The trend toward more illite in surface soils than at depth suggests that illite may have formed by neogenesis in these soils. Norrish and Pickering (1983) characterized a Fe-rich illite from a deposit (“Muloorina”) near a seasonally wet and dry central lake in Australia (Lake Eyre) as a product of neogenesis in the lacustrine environment (although it may not be pedogenic) (Wilson, 1999). Its neogenetic origin was suggested by the very uniform shape and size of its particles, which are almost all $\sim 0.07\ \mu\text{m}$ in diameter (see Churchman, 2000, Figure 1.8a). Similarly sized and shaped particles of illite are also found in a number of soils in various parts of Australia (e.g., Willalooka—see Norrish and Pickering, 1983). The size, shape, and uniformity of these illites are in complete contrast to those originating from micas in rocks. They are more similar in their size and shape to the lacustrine illite from Muloorina (Norrish and Pickering, 1983) than to clay-size breakdown products of rock-derived micas. Berkgaot et al. (1994) found a mineral alongside halloysite in soils formed from pyroclastic layers in a semiarid climate in Israel that comprised very thin crystallites of a randomly interstratified I-S with 70% illite layers and which they considered had formed authigenically. An authigenic origin for illite/mica in soils in Hawaii that was proposed by Swindale and Uehara (1966) was later discredited when oxygen isotope ratios for the fine quartz found alongside the mica in the soils indicated its origin as tropospheric continental dust (Rex et al., 1969) and it was concluded by Syers et al. (1969) that the mica had arrived in the soils in aerosolic dust along with the quartz. Similar findings have been made in other countries such as Japan and New Zealand (e.g., Mizota and Takahashi, 1982; Stewart et al., 1984; Inoue and Sase, 1996; Nagashima et al., 2007; Marx et al., 2009).

20.3.4 Occurrence of Vermiculite in Soils

Most vermiculites in soils have formed by the transformation of micas by weathering (Wilson, 1999), although some form by the analogous transformation of chlorites (Wilson, 1999; Velde and Meunier, 2008) (see also Sections 20.2.4.3 and 20.2.4.4). Dioctahedral vermiculite is much more common in soil clays than its trioctahedral counterpart (Wilson, 1999). This is because, although the first transformation products of trioctahedral biotite (and phlogopite) and also chlorite on weathering

may well be trioctahedral, for example, the regularly interstratified phases, hydrobiotite and chlorite-vermiculite, a variety of structural and composition changes occur within the aluminosilicate layers alongside the loss of K^+ during vermiculitization (see Section 20.2.4.3). The net result of these changes is the loss of Al from the tetrahedral sheet and its gain in the octahedral sheet at the expense of Fe^{2+} and Mg. As a consequence, the layer structure becomes more dioctahedral (Wilson, 2004). Nonetheless, in the North Island of New Zealand, the occurrence of trioctahedral vermiculite in a soil derived from a composite of weathered tephros was attributed to the presence of biotite, which was known to occur in some of the parent tephros because such tephros had been preserved unweathered in layers within sediments in lakes adjacent to the soil (Lowe, 1986).

Although dioctahedral micas are much more stable in the weathering environment than trioctahedral micas, their alteration can also lead eventually to vermiculites, sometimes via regularly interstratified mica-vermiculites, as found in soils formed on mica schists in the South Island of New Zealand (Churchman, 1980). However, where pHs are moderately acid, that is, between about 4.6 and 5.8, organic matter contents are relatively low and there is frequent wetting and drying—all conditions that are conducive to the vermiculitization of micas—Al-hydroxy species are deposited, usually as polymeric cations, in the interlayers of vermiculites (and also some smectites). As a result, vermiculites in soils most often occur with incorporated hydroxyl-Al interlayers (see Churchman, 2000; Wilson, 2004).

Only few reports have considered the possibility of a neogenetic origin for vermiculite. These include those of Smith (1962), who observed that vermiculite replaced feldspars in some Scottish soils of igneous rock origin, and also Barshad and Kishk (1969), who found dioctahedral micas in soils derived from rocks containing no mica. Ildefonse et al. (1979) found that a vermiculite formed as large (up to $150\ \mu\text{m}$) crystals by crystallization from solution, hence by neogenesis, within a weathered metagabbro-containing plagioclase and amphiboles, hence no micaceous precursor. However, this trioctahedral vermiculite proved to be unstable within the soil above the weathered rock, where it was replaced by a Fe-rich smectite.

20.3.5 Occurrence of Smectite in Soils

Smectites occur in soils either because they are inherited from parent materials, have been formed by neogenesis by crystallization from solutions of the constituents of rocks, or else they are the products of the strong, or long-term, transformation of micas and chlorites. They share the possibility of an inherited origin with most other types of clay minerals. Either (1) preformation in, or prior to, the development of parent materials, for example, sedimentary rocks; (2) a detrital origin from other eroded soils or soft sediments; and arguably also (3) preformation in the soil profile but under previous conditions that differ from those currently prevailing (Buol, 1965), have been responsible for the occurrence of at least a large part of the smectites found in skeletal soils and soils in arid zones and also in some

soils found in strongly leaching climatic regimes (Wilson, 1999). Hence, inheritance may be the main or a major source of smectites in Entisols, Aridisols, and Ultisols and could also have contributed to soils classified into almost all the other orders of *Soil Taxonomy* (Wilson, 1999).

The possible origin of smectites by the transformation of micas and chlorites by acid leaching, and particularly, podzolization, processes was discussed in Sections 20.2.4.3, 20.2.4.4, and 20.2.5.3 (and particularly Section 20.2.5.3.2). The smectites formed in this way, and hence those found in the eluvial horizons of podzols, that is, Spodosols, are beidellitic (Ross and Mortland, 1966; Churchman, 1980; Carnicelli et al., 1997; Wilson, 1999; April et al., 2004), consistent with the effect of acid leaching in selectively removing structural Mg, especially, from 2:1 Si:Al aluminosilicates, which thereby become more aluminous. As the products of changes in the solid state they may also be expected to occur, like most illites (Section 20.3.3), mainly within the coarse clay fractions of soils.

Most typically, however, smectites have been formed in soils by neogenesis from alkaline solutions that have developed under poor drainage. Their formation requires high concentrations of Si and basic cations and is therefore favored typically from basic parent materials. Concentrations of smectites comprising bentonite deposits form under similar conditions, most commonly from large bodies of water, for example, lakes or marine lagoons or shallow-marine embayments into which tephra has fallen or been deposited fluvially (e.g., Millot, 1970; Chamley, 1989; Naish et al., 1993; Velde, 1995; Gardam et al., 2008). Work in New Zealand on detrital glass deposits in shallow-marine Holocene muds showed that the early diagenetic transformation of glass to smectite occurred as a two-stage process initially with diffusion-controlled hydration and dissolution of glass followed by first-order precipitation of smectite (Hodder et al., 1993). Interstitial marine waters of slightly reduced salinity (lower Ca^{2+} , Na^{+}) and higher concentrations of dissolved silica relative to those in ocean water played a key role in the smectite formation. Rate constants for both the dissolution of glass and the precipitation of smectite were two orders of magnitude greater than those determined for the formation of clay minerals on similar tephra-derived glassy materials in soils (Hodder et al., 1993).

Some of the knowledge of the conditions for the formation of smectites by neogenesis has come from studies of the conditions for their formation in the laboratory (e.g., Harder, 1972, 1977; Siffert, 1978; Farmer, 1997). The requirements for a successful synthesis of a smectite included $\text{pH} > 7.5$ and some Mg and/or Fe in solution. In nature, smectites are often found in calcareous environments, which provide a high pH, and often also where leaching is infrequent or minimal, or where there is an impediment to drainage (e.g., Fieldes and Swindale, 1954; Lowe et al., 1996). However, smectites can form from many types of rocks or geological deposits and minerals, provided that they can provide a sustained supply of the necessary cations and silica (Churchman, 2000).

The origin of smectites occurring in soils is not always clear-cut. While smectites formed by transformation may occur in

relatively large particles, as already noted, smectites most often are especially fine-grained materials, a feature more consistent with a neogenetic origin. Somewhat confusingly, Boettinger and Southard (1995) found an aluminous dioctahedral smectite occurring in each of the sand, silt, and clay fractions of an arid zone soil. Although the soils also contained biotite, a trioctahedral vermiculite, and a hydroxyl-interlayered 2:1 Si:Al aluminosilicate, Boettinger and Southard (1995) considered that the smectite in all size fractions was neogenetic, with the coarser particles comprising aggregates of smectite cemented by opaline silica. A geomorphic and salinity gradient transect in another arid environment contained smectite in both its beidellitic and montmorillonitic varieties (Reid et al., 1996). These authors considered that there were multiple origins for the smectite in the soils. The beidellites probably originated from shales by transformation processes, and, while some montmorillonite was inherited, the groundwater chemistry was suitable for some having been neofomed. Studying a toposequence of soils surrounding an alkaline-saline lake in Brazil, Furquim et al. (2008) found smectites in both an upper zone that is largely higher than lake level and also a lower zone that is submerged seasonally by the lake. However, the smectites in the two zones were different structurally and compositionally, pointing to different origins for each of them. In the upper zone, a dioctahedral Fe- and Al-rich ferribeidellite had formed as a result of the transformation of micas whereas in the lower zone, trioctahedral Mg-rich smectites that were characterized as saponitic or stevensitic had formed, apparently by chemical precipitation from the lake, that is, by neogenesis (Furquim et al., 2008).

Most smectites in soils are dioctahedral, including the products of the alteration of Mg-rich serpentinite, where saponite might be expected to form (Wildman et al., 1968). Saponite often does form as a weathering product—for example, within the crystals of altered rocks containing ferromagnesian minerals (Section 20.2.4.1)—but it can give way to dioctahedral smectites in the upper parts of soil profiles (Section 20.2.5.1). Of these, the beidellitic and montmorillonitic varieties of smectites are most common in soils, although nontronites have been found there (Sawhney and Jackson, 1958). Even so, nontronite is thought to be particularly susceptible to attack by complexing agents from roots (Farmer, 1997). Generally, soil smectites have more tetrahedral Al and more octahedral Fe than the type of montmorillonite associated with most bentonites (Wilson, 1987; Weaver, 1989). There appears to be a tendency toward a ferribeidellite composition for smectites in soils, albeit that a given soil smectite is most probably heterogeneous in composition. Petit et al. (1992) found that the smectite in a lateritic profile in Brazil could be described as a true solid solution between nontronite and beidellite endmembers.

Smectites themselves can be subject to alteration and change within soils. As already discussed (Section 20.3.1), smectites can incorporate kaolinite layers to become interstratified kaolinite-smectites (K-S), most probably following the prior adsorption of hydroxyl-Al species into their interlayers (e.g., Ryan and Huertas, 2009). Kaolinite appears to be the ultimate product of this process (Section 20.3.1). Nevertheless, Fisher and Ryan (2006), studying

a chronosequence of soils on fluvial fill terraces in tropical Costa Rica, found that there was a transition with age from smectite-rich to kaolinite-rich soils without any K-S intermediates being formed along the way. The smectite was a beidellite and the kaolinite was disordered. These authors generalized their results and those of others who had studied this transition by suggesting that K-S forms as an intermediate phase in the transition from S to K where the MAP is between ~500 and ~2000 mm, whereas the transition occurs without a K-S intermediate when MAP is more than ~3000 mm. The changes may be more subtle, however, resulting in a change within the composition and structure of the smectite. Thus, a low-charge beidellite inherited from the parent pelitic sediment was converted to a high-charge beidellite during the formation of a Vertisol (Righi et al., 1995).

20.3.6 Occurrence of Palygorskite and Sepiolite in Soils

The fibrous 2:1 Si:Mg clay minerals, palygorskite and sepiolite—the so-called hormite minerals—undoubtedly occur in the sedimentary parent materials of many soils containing these minerals; and, until relatively recently, their inheritance from these parent materials was considered to be their source in soils (Singer, 2002). However, both have since been found to form in soils in many countries, including Israel, Syria, Egypt, Morocco, Iraq, Iran, Turkey, Spain, Portugal, China, the United States, Mexico, Australia, South Africa, and Argentina (see summaries in Zelazny and Calhoun, 1977; Singer, 1989, 2002; Churchman, 2000; and reports by Owliaie et al., 2006; Bouza et al., 2007; Kadir and Eren, 2008). Even so, they almost invariably form in calcareous environments (Singer, 2002) and often in calcretes, in particular. Verrecchia and Le Coustumer (1996) have listed many reports of their occurrence in calcretes and there are also later similar reports (e.g., Kadir and Eren, 2008). The main conditions under which they form have been summarized as (1) a fluctuating saline or alkaline groundwater, (2) strong and continuous evaporation, and (3) a sharp textural transition (Singer and Norrish, 1974; Singer, 1989, 2002). A strong textural transition means that water is likely to accumulate at the transitional boundary, hence maintaining a saturated solution from which the hormite minerals can precipitate, under even arid conditions. Calcretes (or caliches) provide such a transition and, hence, these minerals are often found in or below these secondary carbonate concretions. Albeit that palygorskite is most commonly associated with calcareous soils, gypsiferous soils appeared to contain more palygorskite than calcareous soils within the same region in Iran (Khormali and Abtahi, 2003; Owliaie et al., 2006). It appears that an increase in the concentration of Mg that occurred upon the precipitation of gypsum was particularly conducive to the neogenesis of palygorskite (Owliaie et al., 2006).

Chemically, the neogenetic formation of both palygorskite and sepiolite requires considerable magnesium and silicon in a high pH solution. Palygorskite would also require some Al and Fe (Singer, 1989). Although there had been no reproducible synthesis of palygorskite, at least up until Singer (2002), sepiolite has

been synthesized many times from alkaline solutions with high activities of Mg, and Si (see, e.g., Churchman, 2000), confirming the conditions for their formation in nature. In nature, the required Mg may originate in dolomite or Mg-containing calcite. The conversion of high-Mg calcite into low-Mg calcite has been observed to accompany palygorskite formation (Singer, 1989, 2002). The required Si may derive from the dissolution of any silicate mineral, including illite and chlorite (Galán et al., 1975; Galán and Castillo, 1984; Dias et al., 1997; Owliaie et al., 2006), smectites (see Singer, 1989; Bouza et al., 2007; Kadir and Eren, 2008), and even quartz (Singer, 1989, 2002). It is not surprising that smectites may give rise to palygorskite and/or sepiolite because the chemical conditions of high [Mg], high [Si], and a high pH are shared among these three mineral types. Bouza et al. (2007) suggested that, as Mg concentration increased with time in calcic and calcic-gypsic horizons in a weathering profile in Argentina, smectite gave way to palygorskite. Nor, therefore, is it surprising that palygorskites and sepiolites often occur together with smectites in soils and may disappear in their favor, as observed by Paquet and Millot (1972), Khormali and Abtahi (2003), Owliaie et al. (2006), and Bouza et al. (2007), for example. Paquet and Millot (1972) suggested that this dissolution and reformation occurs when rainfall rises to a MAP of merely 300 mm. Khormali and Abtahi (2003) found an inverse relationship between the occurrences of palygorskite and smectite with regard to soil available water, measured by the ratio of precipitation to plant transpiration. Smectite was favored over palygorskite at higher values of soil available water. On the other hand, in soils in an irrigated cropping area in India, smectite predominated in the rain-fed soils, but irrigation, which exacerbates salinity and sodicity (and attendant waterlogging), had led to the formation of palygorskite in just 40–50 years (Hillier and Pharande, 2008). It appears that evaporative concentration of the irrigation waters has led to solution conditions more favorable to the formation of palygorskite than smectite. It has also been observed that the highly siliceous environment in which palygorskite and sepiolite form may give rise to an excess of Si in solution, which results in deposits of secondary silica upon their formation (Singer, 1989; Verrecchia and Le Coustumer, 1996). Experiments with nonsoil palygorskite and sepiolite showed that they were unstable, giving rise to kaolinite, within the rhizospheres of common agricultural crops (Khademi and Arocena, 2008). In this situation, the high acidity of the rhizospheres and the extraction of Mg from the minerals by the crops had destabilized them (see also Section 20.2.5.3).

Palygorskite is much more common than sepiolite in soils (Singer 1989, 2002). However, Bouza et al. (2007) found that sepiolite formed chronologically after palygorskite within a mature calcrete.

20.3.7 Occurrence of Iron Oxides in Soils

Iron oxides and oxyhydroxides (generically known as “iron oxides”) occur in almost all soils (Allen and Hajek, 1989). They are usually the product of the oxidation of Fe(II) occurring

either within the structure of primary minerals or upon their breakdown by weathering, whereupon the newly formed Fe(III) hydrolyzes (e.g., Churchman, 2000). The resulting iron oxides are essentially insoluble at the pH values encountered in soils and are mainly remobilized by reduction. As we have seen for soils from volcanic materials particularly (Section 20.2.4.6), the specific Fe oxides that occur in a soil depend largely on the environmental conditions under which they were formed.

Following Schwertmann and Taylor (1989), Cornell and Schwertmann (1996), Churchman (2000), Bigham et al. (2002), and Schwertmann (2008), in the main, we can make some generalizations regarding the conditions under which goethite or hematite are formed. Goethite, which is yellow to yellowish brown in color depending partly on particle size, is found in soils almost everywhere. But it is most common in cool and temperate climates and where there are high contents of organic matter. Hematite, by contrast, is most common in aerated soils in generally warmer temperatures in the tropics and subtropics and also in arid and semiarid regions, as well as in xeric (or Mediterranean) climate zones. Hematite is characteristically red in color. High organic matter content favors the formation of goethite over hematite, and it is not uncommon to find soils with yellowish goethitic topsoil over red hematitic subsoil. Goethite also tends to be favored at low pH, hematite at higher pHs. Laboratory syntheses have shown that from ferrihydrite as a starting material, the most goethite was formed at a pH near 4, while the maximum yield of hematite occurred at pHs between 7 and 8. Synthetic work has also shown that hematite is favored over goethite by a high rate of release of Fe into solution. This finding is consistent with the observed occurrence of hematite in a soil on basalt but not in a nearby soil on shale (Kämpf and Schwertmann, 1982). Hematite is the preferred phase where the activity of water is low, as in small pores, and is also the most stable phase thermodynamically in smaller particles (Langmuir and Whittemore, 1971). These latter authors predicted that goethite would be the stable phase in particles >76 nm and hematite in smaller particles. While Al substitution for Fe is common in all Fe oxides, synthetic work has shown that goethite can accommodate more Al in its structure than hematite. Fritsch et al. (2005) explained yellowing toward the surface of a weathering profile on sediments in Brazil by upward changes in both the relative amounts of goethite and hematite and also in the extent of Al substitution of goethite. Hematite and Al-poor goethite that are remnants of prior weathering of the sediments in a different climate have dissolved, with Al-rich goethite forming in their place by recrystallization, according to Fritsch et al. (2005). In some tropical soils, the formation of hematite is at the expense of goethite when temperatures are high, the aeration good, the pH near neutrality, and organic matter is rapidly transformed (Etame et al., 2009).

Poorly crystallized or nanocrystalline ferrihydrite is also widespread in soils, particularly in those formed from tephra, and also in the illuvial or placic B horizons of podzols (see Churchman, 2000, and McDaniel et al., Section 33.3). Its formation is favored by rapid oxidation of Fe and when silicates and organic matter, particularly, but also other ions, are present

in soil solutions to inhibit crystallization of goethite and other Fe oxides, including lepidocrocite (Churchman, 2000; Bigham et al., 2002), and soil ferrihydrites can contain significant amounts of Si (Childs, 1992). Nonetheless, ferrihydrite often also occurs in association with goethite and lepidocrocite (Bigham et al., 2002). In the laboratory, it has been found that ferrihydrite is easily converted to hematite (Schwertmann and Taylor, 1989). Nonetheless, ferrihydrite and hematite are rarely found together in soils, indicating that the conversion is also rapid in nature. Even so, Adamo et al. (1997) found ferrihydrite together with both hematite and goethite in the products of weathering of a volcanic rock by lichens. They appear to occupy different microsites in the altering rock.

The formation of lepidocrocite is favored by seasonally anaerobic conditions in noncalcareous soils. It forms when there is an accumulation of Fe²⁺ together with a slow rate of oxidation (Alekseev et al., 2005). Lepidocrocite is found in ocherous mottles, root mats, and crusts (Cornell and Schwertmann, 1996; Churchman, 2000; Bigham et al., 2002). It is often found in association with goethite. Lepidocrocite was found in all three soils in a hydromorphic sequence in Ohio (Smeck et al., 2002), but in different amounts according to ease of drainage. These authors concluded that the formation of lepidocrocite was favored in horizons that were saturated for between 5% and 50% of the part of the year when the soil temperatures were >5°C. Alekseev et al. (2005) found that lepidocrocite was concentrated in the bottom of the "active" layer immediately above permafrost in Russia. The existence of the permafrost below concentrated solutes in this layer and the low temperature slow oxidation.

Maghemite occurs in soils in the tropics and subtropics, often in association with hematite, and most often in surface soils (Schwertmann and Taylor, 1989; Churchman, 2000; Bigham et al., 2002). A common mode of formation of maghemite appears to be through the heating of other Fe oxides in the presence of organic matter, as occurs in bush and forest fires. Schwertmann and Taylor (1989) suggested that a temperature of between 300°C and 425°C is conducive to the formation of maghemite. It may also form by the oxidation of precursor magnetite in parent materials, according to the authors cited herein. However, a completely different, alternative origin for this magnetic mineral was suggested by Rivers et al. (2004) to explain its occurrence in association with hematite in soils on alluvium that has in-filled low-lying areas in Tennessee. These authors suggested that there had been reduction of Fe(III), either microbial or abiotic, to form magnetite in the hydromorphic soil. Magnetite occurs in many soils but is usually found in the sand and silt fractions rather than the clay fraction and is generally considered to have been inherited from the parent rock. Nonetheless, a partially oxidized form of magnetite was found to occur along with hematite in nodules in an Oxisol in Brazil that has developed from magnetite-free parent materials, so a pedogenic origin has been invoked for the mineral in this soil (Viana et al., 2006). These authors considered that the magnetite in this soil formed under seasonal burning and also that it is becoming converted to hematite by atmospheric oxidation in air. Some

authors (Maher and Taylor, 1988; Geiss and Zanner, 2006) have considered that some magnetite in soils may have had a bacterial origin (see Section 20.2.5.3.5).

Other Fe oxides formed in soils include schwertmannite, from acid sulfate soils (see Section 20.2.5.3.4), and “green rusts,” found in a highly hydromorphic soil by Trolard et al. (1997).

Iron oxides can be extremely labile in the soil environment. They are quickly reduced or oxidized when redox conditions change in soils, as they can do intermittently over even quite short time periods (hours to days or weeks) and also seasonally. The activity of microbes can play a central role in the formation and dissolution of iron oxides. A wide variety of microorganisms are involved in these processes and much remains to be understood about their operation (Fortin and Langley, 2005). Suffice it to say here that Fe oxides are often biogenic (see also Section 20.2.5.3). Furthermore, there is widespread recognition that Fe is commonly mobilized in soils by reduction occurring through the activity of microbes in anoxic conditions (Robert and Berthelin, 1986; Schwertmann and Taylor, 1989; Robert and Chenu, 1992). The ensuing reduction occurs along with the oxidation of decomposing biomass.

It is a feature of iron oxides in soils that they are most often closely associated with the other components of soils, including particularly aluminosilicate clay minerals, which as small-charged particles attract Fe oxides and other reactive species to their surfaces and pores. Following the well-accepted convention that (citrate-) dithionite-extractable Fe represents free, or well-crystallized oxides, (acid ammonium) oxalate-extractable Fe represents poorly crystallized oxides, and pyrophosphate-Fe stands

for the metal associated with organic matter, Table 20.5 shows the relative amounts of these forms of Fe and their distribution in relation to aluminosilicate clays in a range of soils, mainly taken from papers in the most recent literature, which have presented data for both different forms of Fe and also estimates of the relative abundance of the phyllosilicates present. The data for selected horizons within one soil of each type are given in Table 20.5. The soils in Table 20.5 represent a wide range of soil orders and lithologies, and soil horizons are also given for each soil. The table shows that there were substantial proportions of iron oxides and Fe-organic complexes in their various forms in all horizons of all the soils examined. They were associated with virtually all of the types of phyllosilicates that occur in soils.

20.3.8 Occurrence of Manganese Oxides in Soils

Manganese oxides are a widespread but usually minor component of soils (McKenzie, 1989; Dixon and White, 2002). Generally, they occur in soils in small particles, leading to poor peaks in XRD. They are more abundant in soils from mafic, that is, basic, rocks than from siliceous materials (Dixon and White, 2002). Because reduced Mn (Mn(II)) is very soluble as a divalent cation and is mobile in soils, they commonly form as coatings on rocks, on ped surfaces, and on other soil particles, as well as in concretions, segregations, pans, and nodules, often with Fe oxides (McKenzie, 1989; Churchman, 2000; Dixon and White, 2002). They are characteristically black in color but give a brown streak.

TABLE 20.5 Occurrence of Iron in Oxides and Oxyhydroxides and in Organic Complexes in a Range of Soils with Different Phyllosilicate Clays

Soil Subgroup	Main Lithology	Horizon	pH	Fe ^a (g kg ⁻¹)				Phyllosilicates in Clay Fraction ^b	References
				Fe _d	Fe _o	Fe _p	Fe _t		
Gypsic	Gypsiferous	Ay	7.6	7.8	n.d.	n.d.	16.0	Paly ~ smec ~ chl > ill	Owliaie et al. (2006)
Haplustept		2By2	7.7	2.1	n.d.	n.d.	9.9	Paly > chl ~ ill > smec	
Humic Umbrisol	Granite, orthogneiss	Ah1	4.0 ^c	22.0	14.0	15.2	51.2	Verm ~ HIS ~ HIV > ill = kaol > chl	Zanelli et al. (2006)
		BC	5.0	6.6	2.2	0.5	9.3	Ill ~ HIV ~ (ill-HIV) ~ allo > verm ~ chl	
Mollic Eutrocryept	Calcschists, serpentinites	A	6.5	16.6	8.8	3.4	28.2	Chl > ill > serp > talc	Scalenghe et al. (2002)
		C	8.1	12.3	4.5	0.8	17.8	Chl > ill > serp > talc	
Typic Haplothod	Shale, sandstone	A	3.7	1.4	0.8	1.1	3.3	Ill ~ kaol ~ (ill-verm) > verm	Pai et al. (2004)
		Bs2	4.8	48.4	16.9	10.1	75.4	Ill ~ kaol ~ HIV > (ill-verm) > verm	
Ultic Haplothod	Marine sediments	E	3.7	37.6	8.4	5.5	51.4	Verm ~ (i-v) ~ ill ~ qtz > kaol ~ gibb	Lin et al. (2002)
		Bhs	4.2	59.2	17.7	19.9	86.8	Verm > HIV > ill ~ kaol ~ qtz ~ gibb	
Typic Haploxerert	Olivine basalt	Ap	6.7	26	n.d.	n.d.	53	(Kaol-smec 40:60) > (k-s 95:5) > ill	Vingiani et al. (2004)
		C	8.1	21	n.d.	n.d.	96	(K-s 40:60) > kaol ~ (k-s 95:5) > ill	
Andic Haploxeralf	Rhyolitic ash on andesite	A1	6.8	3.2	0.5	0.1	3.8	Hall ~ HIV > allo	Takahashi et al. (1993)
		2Bt3	6.2	10.1	0.5	0.1	10.7	Hall > gibb ~ allo	
Acruoxic Fulvudand	Andesitic lava	Ah1	3.9	2.8	1.7	1.5	6.0	Gibb > kaol > goe > ferr	Nieuwenhuys et al. (2000)
		BC	5.2	4.1	0.8	0.0	4.9	Allo > goe > ferr	
Orthoxic Tropohumult	Olivine basalt	Ap	5.9	9.0	n.d.	n.d.	n.d.	Kaol > goe	Gallez et al. (1976)
		B21t	5.8	10.3	n.d.	n.d.	n.d.	Kaol > goe	

^a Values of Fe extractable by dithionite (Fe_d), oxalate (Fe_o), and pyrophosphate (Fe_p), also total (Fe_t).

^b Minerals usually given by first three or four letters of their name, except for quartz (qtz) and HIV; interstratified minerals in brackets: their components often by first letters only; relative amounts of minerals as given in the appropriate reference.

^c In CaCl₂, other pH values in H₂O.

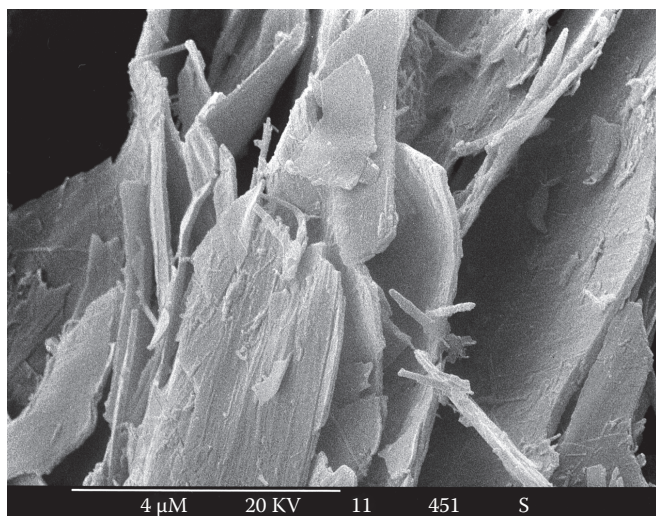


FIGURE 20.11 Scanning electron micrograph of crystals of todorokite, with some kaolin minerals, in infill formed as a result of the weathering of granitic saprolite in Hong Kong. (Photo by Stuart McClure. Reproduced with the permission of the Geotechnical Engineering Office, Civil Engineering Office, Hong Kong.)

Their distinctive appearance, especially in, for example, concretions and nodules, gives a strong indication of prior oxidation, including by seasonal drying as noted earlier in this chapter (e.g., Birkeland, 1999; Vepraskas et al., 2004). Churchman et al. (2010) used their occurrence to trace a history of dehydration, leading to the conditions for the formation of kaolinite rather than halloysite in some saprolites in Hong Kong. Manganese oxides form when conditions favor their oxidation; hence, they are often found in subsoils with a higher pH than the upper layers and are common in calcareous soils. Manganese also occurs as a Mn carbonate (rhodochrosite) in calcareous soils (Dixon and White, 2002).

Among the polymorphs of MnO_2 , birnessite, especially, and lithiophorite have most often been identified in soils. However, birnessite occurs in soils as poorly developed crystals and the crystals of birnessite produced by biological oxidation of Mn(II) in the laboratory are similarly poorly developed, as are those precipitated from solutions with a high Si content (Dixon and White, 2002), suggesting that their formation in soils occurs via micro-biological oxidation or at an early stage of soil formation, or both (McKenzie, 1989; Dixon and White, 2002). Todorokite has been identified in Texas in nodules from a Vertisol and on the surface of weathered siderite boulders (Dixon and White, 2002) and appeared in large crystals in saprolite on both granite and volcanic tuff in Hong Kong (Churchman et al., 2010), as seen in Figure 20.11, alongside both halloysite tubes and platy kaolinite particles.

20.3.9 Occurrence of Aluminum Hydroxides, Oxyhydroxides, and Oxides in Soils

Gibbsite is the most common of the various hydroxides, oxyhydroxides, and oxides of aluminum in soils (e.g., see Churchman, 2000). It occurs in soils of any age whenever Si is

in low supply. Hence, it occurs under strong leaching. Where there is a gradation in the extent of leaching, often because of an altitudinal change, gibbsite may occur in the most heavily leached soils whereas kaolinite occurs when there is a lesser degree of leaching. This tendency appeared to be the case for temperate mountain soils in South Carolina (Norfleet et al., 1993), as well as for soils in the humid tropics, where gibbsite was dominant in the highlands and kaolinite in the lowlands (Herbillon et al., 1981). In some Oxisols, gibbsite may be most abundant in upper horizons but decrease in concentration with depth (Huang et al., 2002). These authors also pointed out that, in the tropics, particularly, landscapes may be extremely old and the occurrence of gibbsite not necessarily related to the present soil environment. This polygenesis was illustrated in a study by Bhattacharyya et al. (2000), who found gibbsite occurring alongside mica-vermiculite phases containing hydroxy-Al interlayers in an acidic tropical soil in India. However, it has long been considered (Jackson, 1963) that the presence of these latter aluminous interlayers precludes the formation of gibbsite by the so-called antigibbsite effect. Bhattacharyya et al. (2000) explained the presence of gibbsite and these interlayers together by the prior formation of gibbsite, possibly mainly from sillimanite, in an earlier neutral to alkaline pH environment. The aluminous interlayers, by contrast, are products of weathering in the current acidic environment. An apparent contradiction of the “antigibbsite” effect was also seen by Jolicoeur et al. (2000) when they observed each of hydroxyl(-Al) interlayered vermiculite (HIV), kaolinite and/or halloysite, and gibbsite occurring together as pseudomorphs after biotite in scanning electron micrographs of saprolites and soils in central Virginia. They were considered to coexist because they each occupy their own particular microsites and microenvironments of weathering, especially in the vicinity of the altering rock material (Jolicoeur et al., 2000). Gibbsite in soils may also be inherited from saprolites (e.g., Huang et al., 2002; Simas et al., 2005). In these cases, its content decreases toward the surface within the soil profile. In another situation, the co-occurrence of both gibbsite and halloysite, together with kaolinite, goethite, hematite, maghemite, quartz, and cristobalite in old soils formed on strongly weathered andesite or associated alluvium in tropical Costa Rica, was studied by Kleber et al. (2007). They attributed the clay mineral depth-distribution patterns first to intense weathering, with gibbsite increasing with depth as the end product of prolonged tropical weathering, as noted earlier. However, the seemingly paradoxical enrichment of kaolin group minerals and quartz near the soil surface was attributed to ongoing dissolution of Si (quartz being unstable at the silica concentrations necessary for gibbsite formation, namely <0.5 ppm) and its vertical redistribution by a plant-based “biological resiliation mechanism” (Kleber et al., 2007, and see also Section 20.2.5.3.3).

Gibbsite may also occur as coatings or infillings of voids in weathered upper soil horizons (e.g., Huang et al., 2002). Gibbsite is also favored if parent materials are rich in Al (e.g., Lowe,

1986), as illustrated by the example of sillimanite within gneiss in Bhattacharyya et al.'s (2000) study.

Among Al oxyhydroxides, boehmite has been identified, along with some other poorly ordered, nanocrystalline, and/or amorphous phases in lateritic profiles, particularly at their surfaces, and also in tropical soils (e.g., Churchman, 2000; Huang et al., 2002). Some may have resulted from the dehydration of gibbsite. Other Al hydroxides, bayerite, nordstrandite, and doyleite, have been identified only rarely in soils (Huang et al., 2002). The Al oxyhydroxide, boehmite, and the Al oxide, corundum, have been reported at the surfaces of ferralitic (lateritic) profiles, whereas corundum has often been seen in the same soils that contain maghemite, for example, in ferralitic duricrusts in Western Australia (Anand and Gilkes, 1987), and these authors proposed that it formed from gibbsite and/or boehmite by dehydration in bushfires. A bushfire origin has also been suggested for maghemite (Section 20.3.7 herein).

20.3.10 Occurrence of Phosphate, Sulfide, and Sulfate Minerals in Soils

Phosphate minerals in soils appear to derive mainly by inheritance or by alteration through weathering of forms of apatite, namely, fluorapatite and hydroxyapatite, from rocks or other geological deposits, or else from reactions between phosphorus fertilizers and soil minerals (Lindsay et al., 1989; Churchman, 2000; Harris, 2002). The products are various forms of phosphates in which the Ca in apatite is substituted, to a greater or lesser degree, by other cations. Hence, there are forms of variscite, where the major cation is Al, strengite (Fe), also barrandite (Al, Fe), vivianite [Fe(II)], crandallite (Ca, Al), plumbogummite (Pb, Al, and other elements), gorceixite (Ba, Al), leucophosphite (K and Fe), along with many other variations (Norrish, 1968; Lindsay et al., 1989; Churchman, 2000; Harris, 2002). A hydrated Al hydroxyl phosphate, wavellite, is the most common Al phosphate in soils derived from phosphoric marine sediments, which are the most extensive phosphate-rich geological materials at the Earth's surface (Harris, 2002). Nevertheless, phosphates generally occur very sparsely in soils and have to be either concentrated or examined by electron optical methods to be identified (e.g., Norrish, 1968).

Sulfide minerals in soils originate ultimately from the bacterial reduction of sulfate in seawater (Doner and Lynn, 1989; Fanning et al., 2002). They occur in the unoxidized parent materials of soils and are very readily oxidized on exposure to air and drying. Pyrite is the most common sulfide mineral in the unoxidized parent materials. Sulfates, including sulfuric acid, are the products of their oxidation. The reaction of the sulfuric acid thus produced with silicates leads to hydroxyl Fe sulfate minerals, especially jarosite and schwertmannite. These, and their variants, occur typically in acid sulfate soils with their attendant environmental problems (see also Section 20.2.5.3.4). Gypsum occurs in soils as a result of its inheritance from gypsiferous parent materials (or from agricultural application), while barite, of unknown origin, has also been found in some soils, often as a white powder (Fanning et al., 2002).

20.3.11 Occurrence of Pyrophyllite, Talc, and Zeolites in Soils

Both pyrophyllite and talc are rare in soils (Zelazny and White, 1989; Churchman, 2000; Zelazny et al., 2002). As minerals originating at high temperatures and pressures, they are seldom inherited in soils. Pyrophyllite, particularly, is broken down into finer fractions by physical processes (Zelazny et al., 2002). As with other types of minerals, it is the dioctahedral species, pyrophyllite, that is more stable in the soil environment than its trioctahedral counterpart, talc (Zelazny et al., 2002). Generally, talc weathers quickly to nontronite or to Fe oxides. Both pyrophyllite and talc have been protected from breakdown by their encapsulation within Fe oxides in some soils (Zelazny et al., 2002).

Occurrences of zeolites have rarely been reported in soils, but some may have been overlooked because they are generally only present in trace amounts (Boettinger and Ming, 2002). Apart from their inheritance from zeolitic parent materials, such as through hydrothermal alteration (e.g., Kirkman, 1976), some zeolites have formed pedogenically (Ming and Mumpton, 1989; Churchman, 2000; Boettinger and Ming, 2002). The most common pedogenic zeolite is analcime. Along with chabazite, mordenite, natrolite, and phillipsite, analcime has been found to form in salt-affected, alkaline soils, which contain sodium carbonate and have a high pH (Churchman, 2000; Boettinger and Ming, 2002). These soils were both volcanic and nonvolcanic in origin. A number of zeolites have been found in soils in Antarctica that appear to have a secondary origin. These include stilbite, from the weathering of dolerite (Claridge and Campbell, 1968), phillipsite, from tephra dissolved in lakes (Claridge and Campbell, 2008), and chabazite, which has been identified by many workers and which Claridge and Campbell (2008) suggested is quite widespread as a product of thin saline films in intergranular spaces in soils. Other zeolites that have been inherited in soils from parent materials include clinoptilolite, heulandite, gismondine, mordenite, stilbite, and laumontite (Boettinger and Ming, 2002).

20.3.12 Occurrence of Neogenetic Silica in Soils

Because leaching in soil formation results in desilication, silica is often mobilized and then (if not combined with Al for example to form an aluminosilicate clay) can be reprecipitated deeper in the soil environment. Chemically precipitated overgrowths of quartz, particularly on carbonates, are relatively common in soils (Drees et al., 1989; Churchman, 2000). Quartz apparently formed by crystallization out of the dissolution products of microcline (Estoule-Choux et al., 1995; Section 20.2.4.2). In soils across two chronosequences on fluvial deposits in arkosic sands in southern California, Kendrick and Graham (2004) found that the amount of pedogenic, opaline silica (measured by extraction with tiron) increased with duration of soil development from 1.2% to 4.6% of the soil. The loss of Si from primary minerals approximately equaled the gain of secondary (opaline)

silica (Kendrick and Graham, 2004). A number of studies of fine quartz from soils and also shales found a systematic increase in oxygen isotopic ratios with decreasing size, suggesting that the smallest particles of quartz were authigenic (Sridhar et al., 1975; Churchman et al., 1976; Clayton et al., 1978). However, much neogenetic silica in soils occurs in other forms besides quartz (Monger and Kelly, 2002).

Silica cements are common in hardpans or duripans (Chadwick et al., 1987) and also fragipans (Harlan et al., 1977; Marsan and Torrent, 1989) in soils and have been seen to coat surfaces of primary minerals, for example, micas, and to fill gaps in altered minerals including feldspars and micas (Chadwick et al., 1987; Singh and Gilkes, 1993). In the extreme, silica forms massive silcretes in acidic environments (Thiry and Simon-Coinçon, 1996). Secondary silica is sometimes identified as a form of opal, either opal-CT, which is usually inherited from rocks (Munk and Southard, 1993), or opal-A, which is biogenic, and includes plant opals. These are common in some Andisols (Drees et al., 1989) and may be recycled through the death and regrowth of plants (Alexandre et al., 1997). Precipitation of secondary silica may be aided by plant-based processes related to Si uptake and recycling (Henriet et al., 2008) and by evaporation or freezing of soil water. Inorganic silica polymorphs are distinguishable from plant-derived forms of silica, phytoliths, because the latter have more complex shapes inherited from biological cells (Nanzyo, 2007). Farmer et al. (2005) concluded from their study on the concentration and flux of Si in European forest soils (both podzols and acid brown soils) that phytoliths must be the principal immediate sink of silica in soil solution (although weathering is the ultimate source). During the growing season, forest vegetation takes up most of the Si released through weathering of soil minerals and phytolith dissolution and converts it into (new) phytoliths, the latter then becoming the main source of Si leached from the soil during winter rains and spring snowmelt (Farmer et al., 2005). Opals may be transformed to quartz in duripans in soils and also by diagenesis in fossilized wood and sediments (Drees et al., 1989).

Elsass et al. (2000) examined hard plates in laminar horizons and gray mottles at depth in indurated volcanic soils ("tepetates") in Mexico and found strong evidence for the transformation of halloysite to cristobalite via an amorphous opal-A stage. In this case, it appears that the secondary silica phase, first opal-A and then eventually cristobalite, had formed as a result of subtraction of Al from halloysite into solution, rather than through addition of Si from solution as in other cases of the occurrence of secondary Si in soils. Other studies, however, have demonstrated that cristobalite in soils is usually of primary volcanic origin (e.g., Mizota et al., 1987; Wallace, 1991; Mizota and Itoh, 1993). In northern New Zealand, cristobalite isolated from three weathered, halloysitic volcanic soils was identified as alpha cristobalite (opal-C) and was invariably found to be accompanied by tridymite (Wallace, 1991). SEM and oxygen isotope data, along with the highly ordered crystal structure and subhedral grain morphologies, were interpreted to indicate that the cristobalite and tridymite had formed at high temperature from primary volcanic sources (cf. Lowe, 1986; Wallace, 1991).

20.3.13 Occurrence of Titanium and Zirconium Minerals in Soils

Although the major forms of titanium oxide, namely, anatase and rutile, and also their polymorph, brookite, as well as the Fe-Ti minerals, ilmenite, pseudorutile, titanomaghemite, and others, can all form by neogenesis in intensely weathered soils, only anatase and pseudorutile commonly form this way (Milnes and Fitzpatrick, 1989; Churchman, 2000; Fitzpatrick and Chittleborough, 2002). Otherwise, the titanium minerals in soils are inherited from parent materials. Fitzpatrick and Chittleborough (2002) leave open the possibility that zircon, the most common Zr-containing mineral, could also form authigenically in intensely weathered soils. Nevertheless, it is generally inherited from parent materials.

Pseudorutile, which occurs widely in soils, is primarily found there as an alteration product of ilmenite (Fitzpatrick and Chittleborough, 2002). In turn, pseudorutile can dissolve to yield either rutile (Grey and Reid, 1975) or anatase (Anand and Gilkes, 1984). The authigenic formation of titanomaghemite and also ferrian ilmenite may occur by heating Fe-Ti oxides to high temperatures as occurs in bushfires (Fitzpatrick and Chittleborough, 2002). Some Ti^{4+} can become incorporated in other minerals, notably the Fe oxides goethite and hematite, by isomorphous substitution, thereby potentially leading to a reversal of the charge of the Fe oxides (Fitzpatrick and Chittleborough, 2002). Singer et al. (2004) have also found Ti as an isomorphous substitute for Al in halloysite (Section 20.3.2).

20.3.14 Occurrence of Highly Soluble Minerals in Soils

The most common minerals that are laid down following their dissolution from the preformed solid state, whether primary or secondary in origin, and then reprecipitation after evaporation, include calcium carbonate, mainly as calcite, but also as aragonite and Mg calcite (Doner and Grossl, 2002). Magnesite and also dolomite may be formed in that fashion and gypsum probably has a similar origin in arid and semiarid environments (Kohut et al., 1995; Churchman, 2000). Bassanite (or hemihydrate) is usually found in surface soils, indicating its likely evaporative origin (Doner and Grossl, 2002). The highly soluble salts, halides, sulfates, and some carbonates often occur in saline soils and also in arid environments such as Antarctica (Section 20.2.5.2), which is where Bockheim (1997) observed niter ($NaNO_3$) in soils. It is an indication of its extreme aridity that nitrate, borate, chromate, and perchlorate salts have been found in the Atacama desert in Chile (Erickson, 1983; Doner and Grossl, 2002).

20.3.15 Occurrence of Secondary Minerals in Soils: Summary

The main properties of the common types of secondary minerals, and characteristics of their occurrence in soils, are summarized in Table 20.6.

TABLE 20.6 Properties of the Common Types of Secondary Minerals and Characteristics of Their Occurrence in Soils

Group	Common Soil Mineral	Chemical Formula	Related Phases and Names	Specific Surface (m ² g ⁻¹)	CEC (cmol _c kg ⁻¹)	Characteristics in Soils	Soils of Common Occurrence
<i>Silicates</i>							
Kaolin	Kaolinite	Al ₂ Si ₂ O ₅ (OH) ₄	Dickite, nacrite	6–40	0–8	Very small euhedral particles, associated with much Fe	Widespread, high in well-weathered soils
	Halloysite	Al ₂ Si ₂ O ₅ (OH) ₄ ·2H ₂ O	Endellite ^a , metahalloysite ^a 1.0 nm (10 Å) halloysite (= hydrated phase), 0.7 nm (7 Å) halloysite (= dehydrated phase)	20–60	5–10	Generally small tubular or spheroidal particles, associated with Fe	Where humid, especially from tephra (including volcanic ash)
Interstratified kaolin	Kaolinite–smectite	Variable, depending on proportions of K:S	Halloysite–smectite	Unknown	30–70		Moderately drained
Mica	Illite	K _{0.6} (Ca,Na) _{0.1} Si _{3.4} Al ₂ Fe ^{III} Mg _{0.2} O ₁₀ (OH) ₂		55–195	10–40		Widespread, especially weakly weathered soils
Interstratified mica	Illite–vermiculite	Variable, depending on proportions of I, V	Mica–vermiculite	Unknown	Unknown	Usually regular, mica–vermiculite	Eluvial horizons of podzols
	Illite–smectite	Variable, depending on proportions of I, S	Mica–smectite	Unknown	Unknown	Either regular, mica–beidellite, or random, poss. with single layers	Regular: eluvial horizons of podzols Random: very widespread, often in agricultural soils At very early stages of weathering
Interstratified chlorite	Chlorite–vermiculite	Variable, depending on proportions of C, V	Corrensite	Unknown	Unknown		At very early stages of weathering
	Chlorite–smectite	Variable, depending on proportions of C, S	Chlorite–swelling chlorite	Unknown	Unknown		At very early stages of weathering
Vermiculite	(dioctahedral)	K _{0.2} Ca _{0.1} Si _{3.2} Al _{0.8} (Al _{1.6} Fe _{0.2} Mg _{0.2})(Al _{1.5} [OH] ₄)O ₁₀ (OH) ₂	Pedogenic chlorite, HIV, 2:1–2:2 intergrade, chloritized vermiculite	Unknown	pH-variable		Leached, mildly acid soils
	(trioctahedral)	M _x ^{II} (Mg, Fe) ₃ (Al _x Si _{4-x})O ₁₀ (OH) ₂ ·4H ₂ O		50–150	100–210		Early stages of weathering, especially below soil zone
Interlayered	Pedogenic chlorite	Variable, depending on whether layers are vermiculite or smectite and interlayered species	HIV, 2:1–2:2 intergrade, chloritized vermiculite HIS, chloritized smectite	Unknown	Unknown		Intermediate pHs, ~4.6 to 5.8, with wetting and drying, low organic matter
Smectite	Beidellite	M _{0.25} Si _{3.5} Al _{2.5} O ₁₀ (OH) ₂	Nontronite, hisingerite ^a , saponite	15–160	45–160 (all smectites)	Often occur as ferribeidellites in soils, but heterogeneous	More beidellitic in acid-leached horizons; otherwise where drainage retarded and pH high
	Montmorillonite	M _{0.25} Si ₄ Al _{1.5} Mg _{0.5} O ₁₀ (OH) ₂	Stevensite, hectorite	~800 (all smectites)			
	(Palagonite)	Prob. variable		Unknown	Unknown	Nanocrystalline precursors of smectites	Early weathering products of basaltic volcanic glass

Hormite	Palygorskite	$\text{Si}_8\text{Mg}_5\text{O}_{20}(\text{OH})_2(\text{OH}_2)_4 \cdot 4\text{H}_2\text{O}$	Attapulgite ^a	140–190	3–30	Fibrous	In dry, usually calcareous regions, near textural transition in profile (both)
	Sepiolite	$\text{Si}_{12}\text{Mg}_8\text{O}_{30}(\text{OH})_2(\text{OH}_2)_4 \cdot 8\text{H}_2\text{O}$		Generally 260–330	20–45	Fibrous	
Al–Si	Imogolite	$\text{SiO}_2 \cdot \text{Al}_2\text{O}_3 \cdot 2\text{H}_2\text{O}$; Si tetrahedra within Al octahedral in tube		1500	pH-variable	Nanocrystalline: bundles of very thin hollow threads or tubules (nanotubes)	Limited, mainly from pumice, also podzol illuvial B horizons and related soil horizons
	Allophanes	Al:Si 2:1—1:1; variable between imogolite and allophane		700–1500	pH-variable	Nanocrystalline: very small spherules (nanospheres or nanoballs); closely associated with organic matter	From tephra (including volcanic ash) and in podzol illuvial B horizons, and in some other materials that are strongly leached
<i>Nonsilicates</i>							
Al hydroxide, oxyhydroxide, oxide	Gibbsite	$\text{Al}(\text{OH})_3$	Bayerite, nordstrandite, doyleite, α , or γ alumina trihydrate	Unknown	pH-variable	Hexagonal crystals	Where Si low, especially in strongly leached soils
	Boehmite	αAlOOH	Diaspore, α , or γ alumina monohydrate	Unknown, prob. high	pH-variable		Strongly weathered soil materials or soils, ferricrete (laterite), bauxite
Fe oxyhydroxide, oxide	Goethite	αFeOOH	Limonite ^a	14–77	pH-variable	Yellow to yellow-brown color	Widespread—most common iron “oxide”
	Lepidocrocite	γFeOOH	Akagenéite	Unknown, prob. high	pH-variable	Orange color	Noncalcareous soils that are seasonally anaerobic
	Hematite	$\alpha\text{Fe}_2\text{O}_3$		35–45	pH-variable	Bright red color	Soils of warmer climates
	Maghemite	$\gamma\text{Fe}_2\text{O}_3$	Titanomagnetite	Unknown, prob. high	pH-variable	Ferrimagnetic	Tropical and subtropical soils, from fires, poss. from bacteria
	Ferrihydrite	$\text{Fe}_5\text{HO}_8 \cdot 4\text{H}_2\text{O}$	Feroxyhite		200–500	pH-variable	Nanocrystalline: spherical nanoparticles, pinkish to yellowish-red color
Mn oxide	Birnessite	$\text{Na}_{0.7}\text{Ca}_{0.3}\text{Mn}_7\text{O}_{14} \cdot 2.8\text{H}_2\text{O}$	Todorokite, hollandite, lithiophorite, pyrolusite	Unknown, prob. high	pH-variable	(Blue-) black color	Widespread but usually minor component; in concretions, segregations, pans and nodules in subsoils
Sulfide	Pyrite	FeS_2	Mackinawite, greigite, pyrrhotite	Unknown	Unknown		Coastal regions and from some sediments when unoxidized
Sulfate	Gypsum	CaSO_4	Bassanite, anhydrite, barite (BaSO_4)	Unknown	Unknown		Often in desert soils
	Jarosite	$\text{KFe}_3(\text{OH})_6(\text{SO}_4)_2$	Natrojarosite, schwertmannite	Unknown	Unknown		Acid sulfate soils or strongly acid seepages
Phosphate	Plumbogummite	$\text{PbAl}_3(\text{PO}_4)_2(\text{OH})_5 \cdot 2\text{H}_2\text{O}$	Variscite (Al), strengite (Fe), crandallite (Ca), gorceixite (Ba)	Unknown	Unknown		Rare, from breakdown of rock phosphate
Ti oxide	Anatase	TiO_2		Unknown	Unknown		Widespread, in small amounts
Chloride	Halite	NaCl		Unknown	Unknown		Seasonally dry saline soils

^a Discredited name.

20.4 Influence of Mode of Formation upon Predictions of Properties of Soils from Their Clay Mineralogy

20.4.1 Introduction: The Role of Mineralogy in Soil Science

Broadly speaking, soils are studied and interpreted either as products of the natural environment, which reflect their environmental history, or else as useful materials in which to grow plants or for removing and cleaning wastes and pollutants or providing resources or “environmental services” such as regulating water flow. Minerals, and particularly secondary (clay) minerals, have likewise been regarded and assessed either as indicators of the origin of soils and of changes, which have occurred in them through their development, or else as the most reactive inorganic components of soils. For the latter role, it has often been considered that knowledge of the properties of clay minerals would be useful in predicting the agronomic and adsorptive capacities of soils. However, several indicators have suggested that soil mineralogy has come to be regarded as less important to practitioners of the discipline of soil science in recent years than its other main subdisciplines such as soil chemistry, soil physics, soil biology, pedology, spatial analysis, and pedometrics, let alone the major applied aspects of soil fertility and soil pollution, than once was the case. For example, an analysis of papers that were published in the first 100 volumes of *Geoderma*, spanning from 1967 to 2001, showed a sharp decline in those on soil mineralogy, but either a rise or no significant decline in those from the other main subdivisions of soil science (Hartemink et al., 2001). It appears that mineralogical studies have been able to make fewer worthwhile contributions in comparison with those of other aspects of soil science than in earlier times. Nonetheless, the survey of the literature for this chapter suggests that a great deal of research continues to be undertaken into the origin of secondary minerals in soils and also, to some extent, into their mode of occurrence within soils. This new work includes the recognition that the clay fractions of many soils and associated materials contain nanominerals (including allophanes and ferrihydrite as discussed earlier), which confer unique properties and reactivities (Theng and Yuan, 2008; Waychunas and Zhang, 2008). Nanoscale minerals are defined as having at least one dimension in the nanorange, that is, 1–100 nm (Hochella, 2008). Nanoscience is now regarded as being a critically important new offshoot of more traditional colloid or clay mineralogy, and the growth rate of articles being published on nanoparticle science (relevant to the geosciences) is around 10% per year, about triple the average growth rates of all scientific disciplines over a 5-year period (Hochella, 2008).

20.4.2 Contributions of Classical Clay Mineralogy toward Explanations of Soil Properties

Clay mineralogy is a relatively young area of study. Up until 1929, with the publication of a pioneering bulletin by Hendricks and Fry on the X-ray examination of soil clays that was quickly

followed by a journal paper (Hendricks and Fry, 1930), most had regarded clays, which were largely indistinct in optical microscopes, as being amorphous (Cady and Flach, 1997). XRD was very successful in determining that much of the clay-sized inorganic material in soils was composed of regular crystals like those that had been identified in minerals in rocks or other geological deposits. Although many other instrumental techniques have been applied to their identification and characterization over the intervening years, the search for and refinement of crystal structures has remained a major pursuit of clay mineralogists and XRD has continued to be their major workhorse. Its use, whether for structural determination or as the major instrument for the identification of clay-sized minerals in soils, has defined classical clay mineralogy.

Among the most useful roles promised for classical clay mineralogy in soil studies has been that of explaining the abundance of certain plant nutrients by soils. Probably chief among these has been potassium, with K-micas apparently providing a labile source of K⁺ (e.g., Norrish, 1973; Loveland, 1984). Loveland et al. (1999), in writing a history of clay mineralogy at the Rothamsted Experimental Station from 1934 to 1988, attempted to identify the reasons why considerable effort was put into this area of soil science at one of the world’s leading centers of soil research. At its outset in 1934, clay mineralogy was supposed to provide an understanding of the physicochemical behavior of the soil clay fraction mainly with respect to “the sorption and desorption of water and nutrients, with their practical consequence for soil workability and plant nutrient supply” (Loveland et al., 1999, p. 165). Its most important contributions are judged by these authors to have been in the identification of the phenomenon of interstratified minerals and the behavior of soil K. Even so, in spite of a large number of British studies, at Rothamsted and elsewhere in the United Kingdom, on the influence of clay mineralogy on the potassium-supplying power of soils, Loveland (1984, p. 700) stated that “none were successful in using clay mineralogy as a reasonably exact predictive tool for this property.” Loveland (1984) concluded that (classical) clay mineralogy related better to geotechnical properties of soils than to their nutrient-supplying power. In apparent contrast, the K-supplying power of soils formed from quartzo-feldspathic loess or alluvium and colluvium from sedimentary rocks in New Zealand showed a close relationship to the mica contents of their clay fractions (Surapaneni et al., 2002). Barré et al. (2008), studying two French soils and one from the United States, also found that micaceous minerals in soil clay-size fractions serve as reservoirs for potassium. However, they found that the ability of soils to supply K to plants, and also to extract K when it was in excess, through fertilizer additions, could only be fully understood when the micaceous minerals were delineated into five different types. These were a well-crystallized illite, a poorly crystallized illite, a highly smectitic interstratification of illite and smectite and its highly illitic counterpart, and a soil vermiculite. These could be separately determined quantitatively, relative to one another, by decomposition of the XRD peak profile, following Lanson’s (1997) procedure. Barré et al. (2008) claimed that the approach

could be used to predict the K release potential of soils generally and Velde and Barré (2010) provide many examples of the utility of this approach. It may offer a wider applicability than the relationships developed by Surapaneni et al. (2002) for soils, which have quite similar origins in just one country.

20.4.3 Potential of Classical Clay Mineralogy for Explaining Soil Properties

A different mineralogical approach using X-ray fluorescence (XRF) analyses of whole soils and also analyses of acid digests of soils by inductively coupled plasma mass spectroscopy (ICP-MS) was used to determine the normative mineralogies of forest soils in Finland at the early stages of weathering in order to explore the availability of reserves of the nutrients Ca and Mg (Starr and Lindroos, 2006). At the earliest stages of weathering, it is the extent of alteration of primary minerals rather than the nature of any secondary products that is the mineralogical characteristic that best relates to agronomic properties. Clay mineralogy per se is of little predictive use when clays have hardly been formed. For soils in most of the world's agricultural areas, however, the overwhelming contribution to the surface area of the soils, as well as virtually all of their charge, arises from material in their clay fraction (e.g., Gilkes, 1990; Churchman, 2006). The highly reactive clay-size material includes both organic and inorganic components, and it is the task of soil clay mineralogists to understand the source of the contribution made by the inorganic components. Gilkes (1990) noted that Norrish and coworkers recognized some time ago that secondary minerals in soils could hold and, when required, supply other important nutrients besides K for plants. These included manganese oxides, for cobalt (Adams et al., 1969), and iron oxides, for phosphorus (Norrish and Rosser, 1983). Classical clay mineralogy, using XRD, may be capable of detecting the presence of these oxides in soils provided that they are reasonably well crystallized, and that their XRD peaks are not masked by stronger peaks for other minerals. Even so, it is not simply their presence, but rather their detailed structural, chemical, and physical characteristics, as well as their associations with other soil entities that govern the reactivities—both chemical and physical—of these and other oxides, hydroxides, and oxyhydroxides, as well as of aluminosilicate phases in soils. Furthermore, much evidence points to the idea that metal oxides (used generally hereafter to include both oxyhydroxides and hydroxides) play a role in determining many of the useful properties of many soils that is out of proportion to their content in the soils. This status includes the indication from several earlier studies, van Raij and Peech (1972) and also Gallez et al. (1976), among them, that the surface charge–pH curves of many tropical soils show the characteristic features of metallic oxides, which have a pH-dependent variable charge. Similarly, nanocrystalline aluminosilicates such as allophane also make an extremely disproportionate contribution to both the surface area and reactivity of soils, including through a pH-dependent variable charge, even where only small amounts are present (e.g., Lowe, 1995; McDaniel et al., Section 33.3). In an effort to try to

reconcile studies that have found that Fe oxides play a positive role in aggregation in soils (e.g., Colombo and Torrent, 1991; Oades and Waters, 1991) with others in which Fe oxides do not appear to affect aggregate stabilities (e.g., Deshpande et al., 1968; Borggaard, 1983), Duiker et al. (2003) found that their effect depended upon their crystallinity. The most poorly crystalline Fe oxides played an important role along with organic matter in aggregate stabilization and, where organic matter contents were low, as in B horizons, their contributions to indices of aggregation were found to equal or exceed that of organic matter (Duiker et al., 2003), confirming similar trends seen by Churchman and Tate (1987) for the particular case of soils formed on volcanic ash. However, Al oxides may be more important than Fe oxides in governing both aggregate stability and also P adsorption in some soils. This relationship appeared to hold for Latosols in Brazil (Schaefer et al., 2004). In one soil, at least, an amorphous Al-hydroxy phase appeared to play an important role in both aggregation and P adsorption.

One property of soils that particularly demands explanation and, if possible, prediction, at this time is that of the capacity of soils to adsorb and retain organic carbon. The momentum for work to be done in this area comes from growing community concerns about the increased levels of carbon dioxide in the atmosphere, its links to global warming, and the role that soils may be able to play in sequestering excess carbon and isolating it from the atmosphere (Amundson, 2001; Kahle et al., 2002a). As Kahle et al. (2002a) pointed out, many workers have discovered relationships between clay content and carbon content, although it is noteworthy that not all have found such a link, for reasons we will discuss herein. Nevertheless, it has long been known (e.g., Greenland, 1965) that clays and organic matter can be strongly associated in soils. Even so, it has long been appreciated (e.g., Hamblin and Greenland, 1977) that the links between clays and organic matter can occur through Fe and Al oxides. Mikutta et al. (2005) and also Kleber et al. (2005) reported that for acid subsoils under forest and representing a wide range of parent rock types and rainfall, poorly crystalline oxides of both Fe and Al provided the strongest binding agents for organic matter. According to Mikutta et al. (2005), poorly crystalline to nanocrystalline Fe oxides such as ferrihydrite were particularly effective for stabilizing organic C in these soils. It is also significant that these authors found that none of the factors of clay content, namely, the specific surface area of the minerals as determined by nitrogen gas adsorption using the BET equation, total iron oxide content, or the nature of the phyllosilicate clays, was a good predictor of the ability of the soils to stabilize C. Their results confirmed those of Percival et al. (2000) who correlated the organic C contents of 167 New Zealand soils with several soil properties and found they showed significant linear relationships with oxalate-extractable Si and Al, which together represent allophane content, and also with pyrophosphate-extractable Al, which represents Al associated with organic matter, that is, “Al-humus complexes,” but found no relationship with total clay content. Rasmussen et al. (2005), also studying forest soils, came to similar conclusions as those of Percival et al. (2000). In a different,

tropical environment, but again studying forest soils on volcanic ash, Basile-Doelsch et al. (2005) found that organic C in buried horizons was strongly bound in abundant amounts in soils containing allophane, whereas buried horizons with large amounts of crystalline minerals, including feldspars and gibbsite, had little capacity for C storage. The studies by Mikutta et al. (2005) and also Kleber et al. (2005), which were on samples devoid of allophane, showed that it is not the particular occurrence of allophane or even of ferrihydrite that is necessary to provide strong links to organic C. Rather it is the capacity of poorly crystalline or nanocrystalline minerals of both Fe and Al to provide singly coordinated hydroxyl groups that are able to participate in ligand exchange with organic functional groups, which ensures strong associations with organic C, according to Kleber and coworkers in the two related 2005 reports. This generalization also bears out the results of experiments by Kahle et al. (2004) in which dissolved organic carbon (DOC) was added to soil clays that had been depleted of organic C and also to “type” phyllosilicates from nonsoil sources. This experiment showed that soil clays adsorbed much more DOC than the type clay minerals and that the difference appeared to be due to pedogenic oxides, mainly of Fe, which provide reactive hydroxyl groups for DOC sorption. In the case of some tropical soils, Barthès et al. (2008) found that organic C content and also aggregate stability were promoted when sesquioxides, especially goethite and hematite, in the soils included substitutions by Al, which increased their specific surface areas.

One of the common characteristics of Andisols is accumulation of relatively large quantities of organic matter, both in the allophanic (moderate pH) and in the nonallophanic Andisols (low pH). Allophanic Andisols may contain ~10% or more C, whereas nonallophanic andisols (dominated by Al- and/or Fe-humus

complexes) may contain as much as ~30% of C. However, the residence time of C in soils containing allophane, as measured by ^{14}C , is much greater than that of other soils (Figure 20.12; also see Parfitt, 2009).

Albeit that the studies by Kleber and coworkers on acid subsoils showed no relationship between stabilized organic C and the surface area of minerals in the soils, extent of surface intuitively appears likely to be able to explain the capacity of soils for organic C, and several workers have proposed such a relationship (e.g., Saggar et al., 1996; Kaiser and Guggenberger, 2000; Eusterhues et al., 2005). Indeed, to illustrate the point that different soils lead to different generalizations about the relationship between C content and surface area, and, incidentally, forms of Fe in soils, Kahle et al. (2002b) found that a combination of specific surface area and total (i.e., dithionite-extractable) Fe oxide content predicted C content almost completely, with an R^2 of 0.96, in the topsoils of a set of illitic soils with more or less neutral pHs that had been farmed since Medieval times. The surface areas were determined using the sorption of nonreactive nitrogen gas and hence gave a good measure of external surface (e.g., Churchman and Burke, 1991). Using isotopically labeled plant material, Saggar et al. (1996) found that its residence time during its initial decomposition in soils correlated well with the surface area of the soil as measured by the adsorption of *p*-nitrophenol. It is noteworthy that it was this particular (*p*-nitrophenol adsorption) method that showed a good relationship with organic C retained in this case. Like Churchman and Burke (1991), these authors also tried to explain soil properties (organic C uptake in this instance) by the sum of the surface areas from the literature for the mineral components of the soils and also largely failed. By contrast, consideration of the specific surface areas (SSAs) from N_2 sorption of different soil types in relation to those calculated

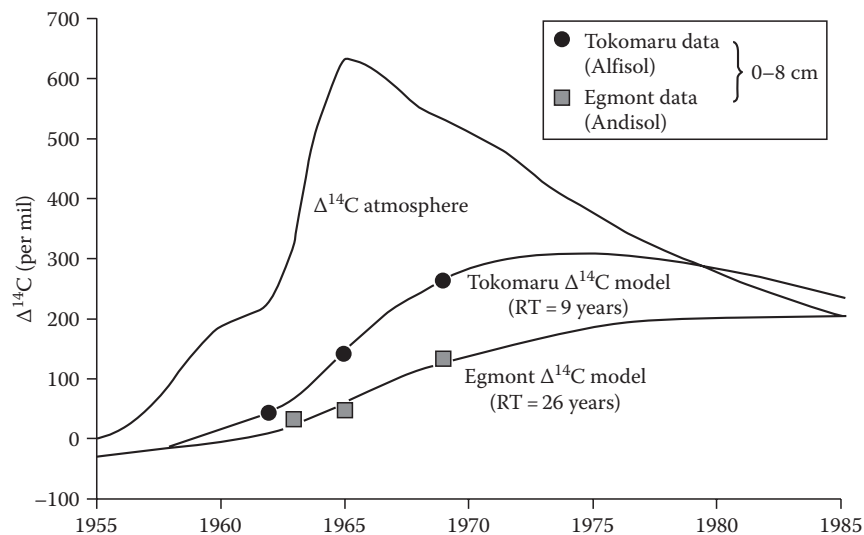


FIGURE 20.12 Model showing slower rates of incorporation and turnover of organic C using bomb-derived ^{14}C in an allophanic soil (Egmont series) compared with those of a soil without appreciable allophane (Tokomaru series) under similar climate and land use in New Zealand. (Based on Baisden, W.T., R.L. Parfitt, and C.W. Ross. 2010. Radiocarbon evidence for contrasting soil carbon dynamics in an Andisol and non-Andisol pasture soil comparison. *J. Integr. Field Sci.* 7:59–64.) RT, residence time of carbon. (Modified diagram from Parfitt, R.L. 2009. Allophane and imogolite: Role in soil biogeochemical processes. *Clay Miner.* 44:135–155. With permission of The Mineralogical Society of Great Britain and Ireland.)

for their constituent Fe oxides and allophane led Eusterhues et al. (2005) to conclude that almost all mineral-associated organic matter in soils is bound to Fe oxides. Churchman and Burke (1991) generally found that the strength of the relationship between a soil property and surface area depended upon the technique chosen to measure surface area (they compared N₂ gas sorption, with sorption of polar liquids ethylene glycol monoethyl ether [EGME] and water) and the relevance of the adsorbate to the soil property of interest. A good relationship between a particular soil property and surface area deduced from the sorption of a particular adsorbate shows that the property and the capacity of the surface for the adsorbate have similar causes but does not show that the property relates to a generic measure of surface area, which most probably does not exist.

To further complicate the nature of the relationship between minerals and organic C in soils, it is noted that a study of the energetics of organic C sorption by Mayer and Xing (2001) revealed that minerals appeared to be occluded by OM, rather than the OM being adsorbed by minerals, and that micropores were likely to be responsible for some of the associations. Kaiser and Guggenberger (2003) suggested that OM was preferentially adsorbed within, or at the mouths of, micropores <2 nm in diameter in iron oxides in soils. The results of density fractionations combined with TEM led Chenu and Plante (2006) to conclude that most OM was stabilized in soils by close associations with clays in very small microaggregates, either through adsorption or by entrapment. Wan et al. (2007) mapped organic carbon along with other elements in different soils using scanning transmission X-ray microscopy (STXM) and found that OM exists as distinct particles within microaggregates more often than as coatings on minerals. Using small-angle X-ray scattering to directly observe pores and their constituents, McCarthy et al. (2008) found that most OM was held within pores, although not necessarily very small pores, in formerly cultivated soils that had been restored to tallgrass prairie. Their main conclusion was that OM was encapsulated, rather than adsorbed, by minerals. According to Richards et al. (2009), it is the occurrence of aggregates, rather than the abundance of oxides of Fe and Al, that enabled the stabilization of OM in oxide-rich soils in the Australian subtropics. As a result, more organic C was

held in soils under rainforest and pastures than in those under pine plantations. Furthermore, Spielvogel et al. (2008), like many others (e.g., Kleber et al., 2005; Mikutta et al., 2005; Rasmussen et al., 2005), examined the causes of OM stabilization in acidic forest soils, but arrived at the conclusion that, while Fe and Al oxides, and, particularly, their poorly crystalline to nanocrystalline varieties, were responsible for stabilization, they are bound to, and stabilize, only a specific fraction of the OM. This fraction was concentrated in O/N-alkyl C and microbially derived sugars compared with the nonstabilized remainder (Spielvogel et al., 2008).

It, therefore, appears likely that the properties of the mineral fraction, which control the uptake and retention of organic C by soils, vary greatly between soils. Any generalization is likely to founder when applied to a particular case. Indeed, following Kaiser and Guggenberger (2003), Chenu and Plante (2006), Wan et al. (2007), McCarthy et al. (2008), and Richards et al. (2009), we suggest that it may be that the properties of minerals that are most important are those that enable them to form pores or aggregates for encapsulating OM, and their identification probably defies a simple summary. At the most, it can probably be concluded only that a number of possible characteristics of the mineral phases are likely to influence the capacity of soils to stabilize C and it remains for practice to show which are more important than the others in each instance. A possible list of such characteristics is given in Table 20.7. A number of studies have attempted, like Churchman and Burke (1991) and Saggart et al. (1996) with specific surface area, to explain soil properties by the sum of the contributions from their different mineral (and also, sometimes, organic) components. Properties that were proposed for explanation in this way have included CEC (Seybold et al., 2005). CECs could be largely explained within mineralogical groupings from *Soil Taxonomy* when organic C was included. Churchman and Burke (1991) also found good relationships between CECs and a measure of water retention within mineralogical groupings of soils with low carbon contents.

Together, these results suggested that the use of classical clay mineralogy to group mineralogically similar soils may be reasonably successful for predicting CECs. In addition, close comparisons of experimental and theoretical titration curves indicated

TABLE 20.7 Characteristics of Mineral Phases That Have Helped to Explain the Capacity of Various Soils for the Uptake and Retention of Organic Carbon

Most Relevant Mineral Phase and/or Property	Soil	References
Fe and Al oxides	Silty soils	Hamblin and Greenland (1977)
Allophane + pyrophosphate-Al	167 soils (from throughout New Zealand)	Percival et al. (2000)
Specific surface area + total Fe oxides	Neutral illitic topsoils	Kahle et al. (2002b)
Pedogenic oxides, mainly of Fe	Range of forest and arable soils with range of mineralogy	Kahle et al. (2004)
Fe oxides	Cambisol and podzol under forest (acid)	Eusterhues et al. (2005)
Poorly crystalline (or nanocrystalline) Fe and Al oxides, especially ferrihydrite	Acid subsoils under forest	Kleber et al. (2005) and Mikutta et al. (2005)
Allophane	Volcanic ash soils under forest	Basile-Doelsch et al. (2005)
Al-substituted Fe oxides	Tropical soils	Barthès et al. (2008)
Fe and Al oxides	Acidic forest soils	Spielvogel et al. (2008)

that surface charge densities of some soils from Argentina were apparently successfully modeled by the sum of those of their constituent mineral phases when the mineralogical compositions of the soils were determined by a Rietveld approach (Taubaso et al., 2004). This result suggests further that the charges on soils may be largely additive of those on their constituent clay-size minerals. Nonetheless, this and earlier work by a group from the same laboratory (Torres Sanchez et al., 2001) showed that there was a mismatch between the point of zero net charge (PZNC) and the isoelectric point for those soils in which Fe oxides were adsorbed on to phyllosilicate clays. Hence, the diffusion behavior of these soils, which relates to their isoelectric points (IEPs), cannot be simply regarded as additive of their component colloidal minerals but must account also for their associations with one another.

While there has been some success with the modeling of charge characteristics, both permanent (Seybold et al., 2005) and variable (Taubaso et al., 2004) from the mineral composition of soils, mineral composition patently could not describe organic matter stabilization by minerals in soils. However, in some cases, at least (Kahle et al., 2004; Kleber et al., 2005; Mikutta et al., 2005; see also Table 20.7), it appears that some functional groups, singly coordinated hydroxyl groups in particular, play a crucial role in binding natural organic compounds—albeit perhaps only a fraction of the total soil organic matter, following Spielvogel et al. (2008). Therefore, the question arises as to whether more accurate descriptions of mineral–organic associations, and of reactions of other species, for example, anions such as phosphates and arsenates with mineral surfaces, might be better made on the basis of the amount of the important functional groups present, by an approach that is analogous to that taken by modern soil organic matter studies using, for example, ^{13}C -NMR and FTIR spectral analyses (e.g., Baldock and Nelson, 2000).

Gustafsson (2001) used a “component additivity” approach in an attempt to predict, or model the adsorption of arsenate in competition with sulfate, silicic acid, and phosphate on allophane and also ferrihydrite, and tested the results against experimental data for the adsorption on the spodic horizon of a Swedish soil that contained both ferrihydrite and allophane but little organic matter. Although this approach led to results that were qualitatively realistic, Gustafsson (2001) nevertheless concluded that the approach is probably impractical, partly, at least, because it relies on the assumption that the properties of allophane and ferrihydrite in real soils can be approximated by those of gibbsite and ferrihydrite synthesized in the laboratory. Among many others, Gérard et al. (2007) have shown that this assumption is simplistic and unrealistic. In the particular case that these last authors studied, allophane formed on basalt in the Azores was found to have an especially complex genesis, leading to allophanic products with a large range of compositions. Gérard et al. (2007) claimed that not all of the allophane formed was the product of recrystallization from solution, describing some of it as “alteromorphs after lapilli or pumice,” which result from the leaching of Si and cations from these materials. The products encompassed a compositional range from pure aluminosilicates to Fe- and Ti-enriched aluminosilicates and included

varieties of both Al-rich and Si-rich allophanes, while the soils also contained many different iron phases, ferrihydrite, hematite, and also “iddingsite” (see Section 20.2.4.1), among them.

The component additivity modeling approach adopted by Gustafsson (2001) foundered because allophanes and ferrihydrite, as they are found in soils, differ in many important respects from either natural minerals from nonsoil environments such as the “stream deposit allophane” (Childs et al., 1990; Parfitt, 1990) or synthetic minerals of the same name, in the case of ferrihydrite. They are unique to soils, and they also show variations within their type. A number of other minerals are unique, or almost unique, to soil environments, and the properties and reactivities of these, also, cannot be modeled upon those of minerals found in nonsoil environments. These include fully or partially expanded 2:1 Si:Al aluminosilicates with hydroxyl-Al interlayers (see Section 20.2.4.3), which may show even seasonal changes in the soil biological system (see Section 20.2.5.3). They also include interstratified phases in their various manifestations. Velde and Meunier (2008) have characterized those of illite and smectite as being “peculiar to the soil environment” (Section 20.2.5.3.1), as well as being “the most widespread and representative soils clays.” By the same token, smectites found in soils have been characterized as being commonly ferribeidelitic in composition and, therefore, are quite different from the bentonites from which typical nonsoil montmorillonites have usually been extracted to serve as models for smectites in soils (Section 20.3.5).

However, it is not just the particular composition, structure, and arrangement of layers of the minerals in soils that often make them different from so-called typical minerals taken from nonsoil sources. They differ from the latter partly because important physical properties of secondary minerals in soils are generally different from those of nonsoil minerals. Studies of soil kaolinites from soils on three continents by Singh, Gilkes, and coworkers (Section 20.3.1), a number of studies of soil halloysites (Section 20.3.2), and a study of iron oxides by Trakoonyingcharoen et al. (2006) (Section 20.3.7), have focused specifically on the sizes and sometimes also surface areas of the particles. The studies generally concluded that those of the soil particles are almost invariably much smaller than those of their “reference” nonsoil counterparts with the same mineral names.

Soil clay minerals also differ from most, at least, of their nonsoil counterparts because of their associations with other species in soils. Apart from their ready association with organic matter that has already been discussed in this section, they are very commonly associated also with other minerals. Almost universally, they are associated with iron oxides (see Table 20.5 and Section 20.3.7) and, often, also with aluminum oxides. While the content of Fe in its various forms varies widely (Table 20.5), it is probably only in very young soils that it is nearly negligible in affecting soil properties. The youngest soil in a chronosequence on andesitic lava studied by Nieuwenhuys et al. (2000) contained only 0.4% total Fe in its lowest, CB horizon. This horizon also contained 2.2% oxalate-extractable Al and, hence, ~8% allophane, but no phyllosilicate minerals (Nieuwenhuys et al., 2000).

Table 20.5 also shows that soils are almost certainly never mono-mineralic in their secondary minerals. Only one of the soils shown there (an Orthoxic Tropohumult) is apparently monomineralic in phyllosilicates (kaolinite, in this case), but clearly also contains goethite, at least, in addition.

20.4.4 Nature of Soil Minerals and Relationship to Their Mode of Formation

Clearly, properties of soils relate to properties of clays besides those arising from their particular mineralogical characterization. Properties such as particle size and associations that minerals form with other minerals derive from their mode of formation. In general terms, minerals with a neogenetic origin from solutions in the soil occur in smaller particles than those formed by either transformation in the solid phase from primary minerals or even those that may be inherited from a source of minerals of authigenic origin from beyond the soil environment, for example, hydrothermally formed kaolinite and halloysite, or smectite in bentonite deposits of marine or lacustrine origins. A dramatic illustration of the differences that are wrought by pedogenesis in comparison with a nonsoil genesis (in this case, saprolitic) is given by the observation that the area of the 001 faces of kaolinite crystals that formed in the saprolite below 58 m depth in Brazil were more than five times larger than those that formed in the soil above it (Varajão et al., 2001). It is recalled that Kahle et al. (2002b) found that a combination of specific surface area and total (i.e., dithionite-extractable) Fe oxide content predicted C content almost completely in a set of illitic soils whereas explanations of C contents of other soils from mineral properties were more complex and usually involved poorly crystalline or nanocrystalline phases (see also Section 20.4.3). Even though the land-use history of the illitic soils and their pH may have played a role in simplifying the relationships between the inorganic (mineral) and organic components of the illitic soils (and, incidentally, in altering the course of mineral genesis), it is also most likely that the probable formation of the illite in the soils by transformation rather than neogenesis has led to mineral-organic relationships that are different from those in soils with higher proportions of neogenetic minerals, including poorly crystalline/nanocrystalline metal oxides (e.g., Kleber et al., 2005; Mikutta et al., 2005). Furthermore, it has been found that the nature of aggregation within soils dominated by kaolinites in close associations with Fe and Al oxides differs from that in soils that are more illitic. Both in a study in which aggregates were broken down mechanically (Oades and Waters, 1991) and another in which they were given the opportunity to build up through plant growth and inputs of plant residues (Denef and Six, 2005), aggregates in the kaolinitic soils were shown to comprise largely self-associations of minerals, while those in the illitic soils included close associations of minerals with organic matter.

The application of analytical techniques with higher resolution than XRD, and particularly electron microscopy, has shown that (1) “many clay particles in soils consist of complex intergrowths of different structural types rather than being the ideal

monomineralic species described in textbooks” (Gilkes, 1990, p. 72); and (2) the extent and nature (e.g., charge) of two types of kaolinites (in different Australian soils) were quite different (op. cit., p. 67). Soils are highly heterogeneous in composition and are not simply mixtures of nonassociated entities. In particular, clay minerals are commonly coated by other minerals or organic matter, or both, so that the properties of their reactive surfaces reflect the characteristics of the coating material rather than the mineral substrate. For instance, it was found that “without exception, the suspended particles in rivers and gesturing waters were negatively and quite uniformly charged” (R.J. Hunter, 1981, in Mills, 2003, p. 11). It is almost certain that these particles had a soil source. Furthermore, “Since the particles themselves varied widely as to composition, Hunter concluded that this was likely due to a coating of organic matter or metal (iron, aluminum, and/or manganese) oxide” (Mills, 2003, p. 11).

These observations all suggest that the colloidal “particles” controlling soil properties are generally heterogeneous mixtures of various types of materials, both inorganic and organic. Predictions of their properties from those of well-crystallized minerals are likely to fall short of the mark. Grouping of soils by their dominant idealized mineral types can generally give only poor, or, at best, only qualitative, predictions of their properties. A structural alternative of grouping soils by the nature of their associations of, for example, particular aluminosilicate minerals, metal oxides, and organic matter together would provide the hopeless case of too many categories; indeed, each association would be very likely unique. A better alternative is suggested by the example of research into the nature of purely organic colloids in soils.

Organic colloids in soils are alternatively known as “humic macromolecules.” Hayes et al. (1989, p. 16) have concluded, on theoretical grounds, that “it is highly unlikely that there are two humic macromolecules on earth ... which are exactly the same.” Even so, the field of the chemical and analytical study of organic colloids in soils is a very active one. It has had continuing success because instead of seeking definitive general structures of inevitably heterogeneous molecules, it has sought instead to characterize organic colloids by their “functional groups” (e.g., aromatic, carbohydrate, alkyl, carboxyl) — in other words, by their capacities to participate in reactions with other entities in soils.

Since a structural characterization of the “ultimate” particles or groupings of minerals would be similarly fraught with difficulties as that of organic colloids per se, it may be useful to classify soil minerals as contributors to soil properties (mostly via complex heterogeneous mixtures) through their characterization and appropriate grouping according to their most relevant capacities. These might include (on a weight basis) their surface area—as measured by various techniques, their charge and its variability with pH, their content of plant-available potassium, their shrink-swell capabilities, and their concentrations of reactive hydroxyl groups. Together, these properties reflect many of the most important for soil applications and may be correlated with other properties, for example, their affinity with organic matter and their capacity to adsorb phosphates or chlorides and other anions.

Nevertheless, selection of a set of useful properties by which to characterize mineral properties does not provide advances in understanding the origin of these properties. As has always been the case in mineralogical studies, this uncertainty will be reduced by advances in new instrumental techniques and in their application to soils. Undoubtedly, electron microscopy at higher resolutions, both for viewing and also for quantitative analyses, will be among these. Such techniques of surface analysis as XPS might also help. For example, Gerin et al. (2003) were able to analyze the nature of soil surface coatings, both of organic matter and also Fe and Al species, in order to better understand mineral-organic associations, and they projected more similar work with XPS. With the advent of synchrotron radiation, X-ray spectroscopic techniques, which include and enhance XPS and also XRD and XRF, but also encompass extended X-ray absorption fine structure (EXAFS), X-ray absorption near-edge structure (XANES), and other related methods have become available to determine the sites on mineral surfaces that are involved in interactions with other species (Gates, 2006).

Continuing developments in instrumental techniques undoubtedly enable better descriptions of processes involving minerals in soils, but the foregoing discussion nonetheless leads us to conclude that in order to be able to provide the best predictions or explanations of soil behavior from its clay mineralogy, the origins of the clays themselves must be thoroughly understood. The earlier parts of this chapter on the alteration, formation, and occurrence of minerals in soils thereby gains relevance to the understanding of soils both as useful materials and providers of essential ecological and human services.

Acknowledgments

We thank Max Oulton (University of Waikato) for preparing the diagrams, Stuart McClure (formerly of CSIRO Land and Water) for the scanning electron micrographs, Balwant Singh (Sydney University) for the prints of the transmission electron micrographs, Greg Rinder (Adelaide) for their preparation, and Bruce Velde (Ecole Normale Supérieure, France) for providing us with galley proofs of parts of his recent book (with A. Meunier) prior to its publication. We appreciated very much the comments, encouragement, and patience of section editor Joseph W. Stucki, and very useful comments from Aaron Thompson (University of Georgia) as a reviewer. Graham Shepherd, Brent Green, Hiroshi Takesako, Rob Fitzpatrick, and M.S. Skwarnecki are especially thanked for allowing us to cite unpublished data.

References

Adamo, P., C. Colombo, and P. Violante. 1997. Iron oxides and hydroxides in the weathering interface between *Stereocaulon vesuvianum* and volcanic rock. *Clay Miner.* 32:453–461.

Adamo, P., and P. Violante. 2000. Weathering of rocks and neogenesis of minerals associated with lichen activity. *Appl. Clay Sci.* 16:229–256.

Adamo, P., P. Violante, and M.J. Wilson. 2001. Tubular and spheroidal halloysite in pyroclastic deposits of the Roccamonfina volcano (Southern Italy). *Geoderma* 99:295–316.

Adams, S.N., J.L. Honeysett, K.G. Tiller, and K. Norrish. 1969. Factors controlling the increase of cobalt in plants following the addition of a cobalt fertilizer. *Aust. J. Soil Res.* 7:29–42.

Ahn, J.-H., and D.R. Peacor. 1987. Kaolinization of biotite—TEM data and implications for an alteration mechanism. *Am. Mineral.* 72:353–356.

Aldridge, L.P., and G.J. Churchman. 1991. The role of iron in the weathering of a climosequence of soils derived from schist. *Aust. J. Soil Res.* 29:387–398.

Alekseev, A., T. Alekseeva, V. Ostroumov, C. Siegert, and B. Gradusov. 2005. Mineral transformations in permafrost-affected soils, North Kolyma lowland, Russia. *Soil Sci. Soc. Am. J.* 67:596–605.

Alexandre, A., J.-D. Meunier, F. Colin, and J.-M. Koud. 1997. Plant impact on the biogeochemical cycle of silicon and related weathering processes. *Geochim. Cosmochim. Acta* 61:677–682.

Alimova, A., A. Katz, N. Steiner, E. Rudolph, H. Wei, J.C. Steiner, and P. Gottlieb. 2009. Bacteria-clay interaction: Structural changes in smectite induced during biofilm formation. *Clays Clay Miner.* 57:205–212.

Allen, B.L., and B.F. Hajek. 1989. Mineral occurrence in soil environments, p. 199–278. *In* J.B. Dixon and S.B. Weed (eds.) *Minerals in soil environments*. 2nd edn. SSSA, Madison, WI.

Alloway, B.V., M.S. McGlone, V.E. Neall, and C.G. Vucetich. 1992. The role of Egmont-sourced tephra in evaluating the paleoclimatic correspondence between the bio- and soil-stratigraphic records of central Taranaki, New Zealand. *Quat. Int.* 13–14:187–194.

Altschuler, Z.S., E.J. Dwornik, and H. Kramer. 1963. Transformation of montmorillonite to kaolinite during weathering. *Science* 141:148–152.

Amrhein, C., and D.L. Suarez. 1988. The use of a surface complexation model to describe the kinetics of ligand-promoted dissolution of anorthite. *Geochim. Cosmochim. Acta* 52:2785–2793.

Amundson, R. 2001. The carbon budget in soils. *Annu. Rev. Earth Planet Sci.* 29:535–562.

Anand, R.R., and R.J. Gilkes. 1984. Weathering of ilmenite in a lateritic pallid zone. *Clays Clay Miner.* 32:363–374.

Anand, R.R., and R.J. Gilkes. 1987. The association of maghemite and corundum in Darling Range laterites, Western Australia. *Aust. J. Soil Res.* 25:303–311.

Anand, R.R., R.J. Gilkes, T.M. Armitage, and J.W. Hillyer. 1985. Feldspar weathering in lateritic saprolite. *Clays Clay Miner.* 33:31–43.

Aomine, S., and C. Mizota. 1973. Distribution and genesis of imogolite in volcanic ash soils of northern Kanto, Japan, p. 207–213. *In* J.M. Serratosa (ed.) *Proc. Int. Clay Conf.* June 25–30, 1972. Madrid, Spain.

Aomine, S., and K. Wada. 1962. Differential weathering of volcanic ash and pumice resulting in formation of hydrated halloysite. *Am. Mineral.* 47:1024–1048.

- Aoudjit, H., F. Elsass, D. Righi, and M. Robert. 1996. Mica weathering in acidic soils by analytical electron microscopy. *Clay Miner.* 31:319–332.
- April, R., and D. Keller. 1990. Mineralogy of the rhizosphere in forest soils of the eastern United States. *Biogeochemistry* 9:1–18.
- April, R.H., D. Keller, and C.T. Driscoll. 2004. Smectite in Spodosols from the Adirondack mountains of New York. *Clay Miner.* 39:99–113.
- Aragoneses, F.J., and M.T. García-González. 1991. High-charge smectite in Spanish “Raña” soils. *Clay Miner.* 39:211–218.
- Ashman, M.R., and G. Puri. 2002. *Essential soil science*. Blackwell, Oxford, U.K.
- Aspandiar, M.F., and R.A. Eggleton. 2002a. Weathering of chlorite I: Reactions and products in microsystems controlled by primary minerals. *Clays Clay Miner.* 50:685–698.
- Aspandiar, M.F., and R.A. Eggleton. 2002b. Weathering of chlorite II: Reactions and products in microsystems controlled by solution avenues. *Clays Clay Miner.* 50:699–709.
- Bailey, S.W. 1990. Halloysite—A critical assessment. In V.C. Farmer and Y. Tardy (eds.) *Proc. 9th Int. Clay Conf.*, 28 August–2 September 1989, Strasbourg, Germany, Vol. 2. *Sci. Géologiq.* 86:89–98.
- Bain, D.C. 1977. The weathering of ferruginous chlorite in a podzol from Argyllshire, Scotland. *Geoderma* 17:193–208.
- Bain, D.C., and J.D. Russell. 1981. Swelling minerals in a basalt and its weathering products from Morven, Scotland: II. Swelling chlorite. *Clay Miner.* 16:203–212.
- Baisden, W.T., R.L. Parfitt, and C.W. Ross. 2010. Radiocarbon evidence for contrasting soil carbon dynamics in an Andisol and non-Andisol pasture soil comparison. *J. Integr. Field Sci.* 7:59–64.
- Bakker, L., D.J. Lowe, and A.G. Jongmans. 1996. A micromorphological study of pedogenic processes in an evolutionary soil sequence formed on late Quaternary rhyolitic tephra deposits, North Island, New Zealand. *Quat. Int.* 34–36:249–261.
- Baldock, J.A., and P.N. Nelson. 2000. Soil organic matter, p. B25–B84. In M.E. Sumner (ed.) *Handbook of soil science*. CRC Press, Boca Raton, FL.
- Banfield, J.F., and W.W. Barker. 1994. Direct observation of reactant–product interface formed in natural weathering of exsolved, defective amphibole to smectite: Evidence of episodic, isovolumetric reactions involving structural inheritance. *Geochim. Cosmochim. Acta* 58:1419–1429.
- Banfield, J.F., and R.A. Eggleton. 1988. A transmission electron microscope study of biotite weathering. *Clays Clay Miner.* 36:46–70.
- Banfield, J.F., and R.A. Eggleton. 1989. Apatite replacement and rare earth mobilization, fractionation and fixation during weathering. *Clays Clay Miner.* 37:113–127.
- Banfield, J.F., G.G. Ferruzzi, W.H. Casey, and H.R. Westrich. 1995. HRTEM study comparing naturally and experimentally weathered pyroxenoids. *Geochim. Cosmochim. Acta* 59:19–31.
- Banfield, J.F., B.J. Jones, and D.R. Veblen. 1991. An AEM-TEM study of weathering and diagenesis, Albert Lake, Oregon. Parts I and II. *Geochim. Cosmochim. Acta* 55:2781–2810.
- Banfield, J.F., and T. Murakami. 1998. Atomic-resolution transmission electron microscope evidence for the mechanism by which chlorite weathers to 1:1 semi-regular chlorite-vermiculite. *Am. Mineral.* 83:348–357.
- Barker, W.W., S.A. Welch, and J.F. Banfield. 1997. Biogeochemical weathering of silicate minerals. *Rev. Miner. Geochem.* 35:391–428.
- Barnhisel, R.I., and P.M. Bertsch. 1989. Chlorites and hydroxy-interlayered vermiculite and smectite, p. 729–788. In J.B. Dixon and S.B. Weed (eds.) *Minerals in soil environments*. 2nd edn. SSSA, Madison, WI.
- Barré, P., G. Berger, and B. Velde. 2009. How element translocation by plants may stabilize illitic clays in the surface of temperate soils. *Geoderma* 151:22–30.
- Barré, P., B. Velde, C. Fontaine, N. Catel, and L. Abbadie. 2008. Which 2:1 clay minerals are involved in the soil potassium reservoir? Insights from potassium addition or removal experiments on three temperate grassland soil clay assemblages. *Geoderma* 146:216–223.
- Barshad, I., and F.M. Kishk. 1969. Chemical composition of soil vermiculite clays as related to their genesis. *Contrib. Miner. Petrol.* 24:136–155.
- Barthès, B.G., E. Kouakoua, M.-C. Larré-Larrouy, T.M. Razafimbelo, E.F. de Luca, A. Azontonde, C.S.V.J. Neves, P.L. de Freitas, and C.L. Feller. 2008. Texture and sesquioxide effects on water-stable aggregates and organic matter in some tropical soils. *Geoderma* 143:14–25.
- Basile-Doelsch, I., R. Amundson, W.E.E. Stone, C.A. Masiello, J.Y. Bottero, F. Colin, D. Borschneck, and J.D. Meunier. 2005. Mineralogical control of organic carbon dynamics in a volcanic ash soil on La Réunion. *Eur. J. Soil Sci.* 56:689–703.
- Bassett, W.A. 1959. The origin of the vermiculite deposit at Libby, Montana. *Am. Mineral.* 44:282–299.
- Batchelder, M., J.D. Mather, and J.B. Joseph. 1998. The stability of the Oxford clay as a mineral liner for landfill. *Water Environ. J.* 12:92–97.
- Bates, T.E. 1962. Halloysite and gibbsite formation in Hawaii. *Clays Clay Miner.* 9:315–328.
- Bennett, P.C., J.R. Rogers, W.J. Choi, and F.K. Hiebert. 2001. Silicates, silicate weathering, and microbial ecology. *Geomicrobiol. J.* 18:3–19.
- Berg, A., and S. Banwart. 2000. Carbon dioxide mediated dissolution of Ca-feldspar: Implications for silicate weathering. *Chem. Geol.* 163:25–52.
- Bergaya, F., B.K.G. Theng, and G. Lagaly (eds.). 2006. *Handbook of clay science*. Vol. 1. Developments in clay science. Elsevier, Amsterdam, the Netherlands.
- Berkgaut, V., A. Singer, and K. Stahr. 1994. Palagonite reconsidered: Paracrystalline illite–smectites from regoliths on basic pyroclastics. *Clays Clay Miner.* 42:582–592.

- Berner, R.A., and G.R. Holdren, Jr. 1979. Mechanism of feldspar weathering. II. Observations of feldspars from soils. *Geochim. Cosmochim. Acta* 43:1173–1186.
- Bétard, F., L. Caner, and Y. Gunnell. 2009. Illite neoformation in plagioclase during weathering: Evidence from semi-arid northeast Brazil. *Geoderma* 152:53–62.
- Bhattacharyya, T., D.K. Pal, and P. Srivastava. 2000. Formation of gibbsite in the presence of 2:1 minerals: An example from Ultisols of northeast India. *Clay Miner.* 35:827–840.
- Bigham, J.M., R.W. Fitzpatrick, and D.G. Schulze. 2002. Iron oxides, p. 323–366. *In* J.B. Dixon and D.G. Schulze (eds.) *Soil mineralogy with environmental applications*. SSSA Book Series 7. SSSA, Madison, WI.
- Birkeland, P.W. 1999. *Soils and geomorphology*. 3rd edn. Oxford University Press, New York.
- Bishop, J.L., E.Z. Noe Dobrea, N.K. McKeown, M. Parente, B.L. Ehlmann, J.R. Michalski, R.E. Milliken, F. Poulet, G.A. Swayze, J.F. Mustard, S.L. Murchie, and J.-P. Bibring. 2008. Phyllosilicate diversity and past aqueous activity revealed at Mawrth Vallis, Mars. *Science* 321:830–833.
- Bleeker, P., and R.L. Parfitt. 1974. Volcanic ash and its clay mineralogy at Cape Hoskins, New Britain, Papua New Guinea. *Geoderma* 11:123–135.
- Blum, A.E., and L.L. Stillings. 1995. Feldspar dissolution kinetics. *Rev. Miner. Geochem.* 31:291–351.
- Blum, W.E.H., B.R. Warkentin, and E.E. Frossard. 2006. Soil, human society and the environment, p. 1–8. *In* E. Frossard, W.E.H. Blum, and B.P. Warkentin (eds.) *Function of soils for human societies*. Special Publication No. 266. Geological Society, London, U.K.
- Bockheim, J.G. 1997. Properties and classification of cold desert soils from Antarctica. *Soil Sci. Soc. Am. J.* 61:224–231.
- Boettinger, J.L., and D.W. Ming. 2002. Zeolites, p. 585–610. *In* J.B. Dixon and D.G. Schulze (eds.) *Soil mineralogy with environmental applications*. SSSA, Madison, WI.
- Boettinger, J.L., and R.J. Southard. 1995. Phyllosilicate distribution and origin in Aridisols on a granitic pediment, western Mojave desert. *Soil Sci. Soc. Am. J.* 59:1189–1198.
- Bonifacio, E., E. Zanini, V. Boero, and M. Franchini-Angela. 1997. Pedogenesis in a soil catena on serpentinite in north-western Italy. *Geoderma* 75:33–51.
- Borchardt, G. 1989. Smectites, p. 675–727. *In* J.B. Dixon and S.B. Weed (eds.) *Minerals in soil environments*. 2nd edn. SSSA, Madison, WI.
- Borggaard, O.K. 1983. Iron oxides in relation to aggregation of soil particles. *Acta Agric. Scand.* 33:257–260.
- Bouza, P.J., M. Simón, J. Aguilar, K. Del Valle, and M. Rostagno. 2007. Fibrous-clay mineral formation and soil evolution in Aridisols of northeastern Patagonia, Argentina. *Geoderma* 139:38–50.
- Bowen, N.L. 1922. The reaction principle in petrogenesis. *J. Geol.* 30:177–198.
- Boyer, S.J. 1975. Chemical weathering of rocks on the Lassiter Coast, Antarctic Peninsula, Antarctica. *N.Z. J. Geol. Geophys.* 18:623–628.
- Brinkman, R. 1970. Ferrollysis, a hydromorphic soil forming process. *Geoderma* 3:199–206.
- Bühmann, C., and P.L.C. Grubb. 1991. A kaolin–smectite interstratification sequence from a red and black complex. *Clay Miner.* 26:343–358.
- Buol, S.W. 1965. Present soil-forming factors and processes in arid and semiarid regions. *Soil Sci.* 99:45–49.
- Buol, S.W., R.J. Southard, R.C. Graham, and P.A. McDaniel. 2003. *Soil genesis and classification*. 5th edn. Iowa State Press, Ames, IA.
- Burton, E.D., R.T. Bush, and L.A. Sullivan. 2006. Sedimentary iron geochemistry in acidic waterways associated with coastal lowland acid sulfate soils. *Geochim. Cosmochim. Acta* 70:5455–5468.
- Burton, E.D., R.T. Bush, L.A. Sullivan, R.K. Hocking, D.R.G. Mitchell, S.G. Johnston, R.W. Fitzpatrick, M. Raven, S. McClure, and L.Y. Yang. 2009. Iron-monosulfide oxidation in natural sediments: Resolving microbially mediated S transformations using XANES, electron microscopy, and selective extractions. *Environ. Sci. Technol.* 43:3128–3134.
- Burton, E.D., R.T. Bush, L.A. Sullivan, and D.R.G. Mitchell. 2008. Schwertmannite transformation to goethite via the Fe(II) pathway: Reaction rates and implications for iron-sulfide formation. *Geochim. Cosmochim. Acta* 72:4551–4564.
- Buurman, P., and A.G. Jongmans. 2005. Podzolisation and soil organic matter dynamics. *Geoderma* 125:71–83.
- Cady, J.G., and K.W. Flach. 1997. History of soil mineralogy in the United States Department of Agriculture. *Adv. Geocol.* 29:211–240.
- Caillaud, J., D. Proust, D. Righi, and F. Martin. 2004. Fe-rich clays in a weathering profile developed from serpentinite. *Clays Clay Miner.* 52:779–791.
- Calvaruso, C., L. Mareschal, M.-P. Turpault, and E. Leclerc. 2009. Rapid clay weathering in the rhizosphere of Norway spruce and oak in an acid forest ecosystem. *Soil Sci. Soc. Am. J.* 73:331–338.
- Calvert, C.S., S.W. Buol, and S.B. Weed. 1980. Mineralogical transformations of a vertical rock–saprolite–soil sequence in the North Carolina Piedmont. *Soil Sci. Soc. Am. J.* 44:1096–1112.
- Carnicelli, S., A. Mirabella, G. Cecchini, and G. Sanesi. 1997. Weathering of chlorite to a low-charge expandable mineral in a Spodosol on the Apennine Mountains, Italy. *Clays Clay Miner.* 45:28–41.
- Carroll, D. 1970. *Rock weathering*. Monographs in geoscience. Plenum Press, New York.
- Carson, J.K., L. Campbell, D. Rooney, N. Clipson, and D.B. Gleeson. 2009. Minerals in soil select distinct bacterial communities in their microhabitats. *FEMS Microbiol. Ecol.* 67:381–388.
- Carson, C.D., and G.W. Kunze. 1970. New occurrence of tabular halloysite. *Soil Sci. Soc. Am. Proc.* 34:538–540.
- Cas, R.A.F., and J.V. Wright. 1987. *Volcanic successions—Modern and ancient*. Allen and Unwin, London, U.K.
- Casey, W.H. 1995. Surface chemistry during the dissolution of oxides and silicate minerals, p. 185–217. *In* D.J. Vaughan and R.A.D. Patnick (eds.) *Mineral surfaces*. Chapman and Hall, London, U.K.

- Casey, W.H., M.F. Hochella, and H.R. Westrich. 1993. The surface chemistry of manganiferous silicate minerals as inferred from experiments on tephroite (Mn_2SiO_4). *Geochim. Cosmochim. Acta* 57:785–793.
- Casey, W.H., H.R. Westrich, and G.W. Arnold. 1988. Surface chemistry of labradorite feldspar reacted with aqueous solutions at pH = 2, 3 and 12. *Geochim. Cosmochim. Acta* 52:821–832.
- Casey, W.H., H.R. Westrich, G.W. Arnold, and J.F. Banfield. 1989. The surface chemistry of dissolving labradorite feldspar. *Geochim. Cosmochim. Acta* 53:2795–2807.
- Certini, G., S. Hillier, E. McMurray, and A.C. Edwards. 2003. Weathering of sandstone clasts in a forest soil in Tuscany (Italy). *Geoderma* 116:357–372.
- Certini, G., and R. Scalenghe. 2006. Soil formation on Earth and beyond: The role of additional soil-forming factors, p. 193–210. *In* G. Certini and R. Scalenghe (eds.) *Soils: Basic concepts and future challenges*. Cambridge University Press, Cambridge, U.K.
- Certini, G., M.J. Wilson, S.J. Hillier, A.R. Fraser, and E. Delbos. 2006. Mineral weathering in trachydacitic-derived soils and saprolites involving formation of embryonic halloysite and gibbsite at Mt. Amiata, central Italy. *Geoderma* 133:173–190.
- Chadwick, O.A., and J. Chorover. 2001. The chemistry of pedogenic thresholds. *Geoderma* 100:321–353.
- Chadwick, O.A., R.T. Gavenda, E.F. Kelly, K. Ziegler, C.G. Olson, W.C. Elliott, and D.M. Hendricks. 2003. The impact of climate on the biogeochemical functioning of volcanic soils. *Chem. Geol.* 202:195–223.
- Chadwick, O.A., D.M. Hendricks, and W.D. Nettleton. 1987. Silica in duric soils: I. A depositional model. *Soil Sci. Soc. Am. J.* 51:975–982.
- Chamley, H. 1989. *Clay sedimentology*. Springer-Verlag, Berlin, Germany.
- Chan, C.S., S.C. Fakra, D.C. Edwards, D. Emerson, and J.F. Banfield. 2009. Iron oxyhydroxide mineralization on microbial extracellular polysaccharides. *Geochim. Cosmochim. Acta* 73:3807–3818.
- Chen, J., H.-P. Blume, and L. Beyer. 2000. Weathering of rocks induced by lichen colonization—A review. *Catena* 39:121–146.
- Chenu, C., and A.F. Plante. 2006. Clay-sized organo-mineral complexes in a cultivation chronosequence: Revisiting the concept of the 'primary organo-mineral complex.' *Eur. J. Soil Sci.* 57:596–607.
- Childs, C.W. 1992. Ferrihydrite: A review of structure, properties and occurrence in relation to soils. *Z. Pflanzenernähr. Bodenkd.* 155:41–448.
- Childs, C.W., R.L. Parfitt, and R.H. Newman. 1990. Structural studies of Silica Springs allophane. *Clay Miner.* 25:329–341.
- Cho, H.D., and A.R. Mermut. 1992. Evidence for halloysite formation from weathering of ferruginous chlorite. *Clays Clay Miner.* 40:608–619.
- Churchman, G.J. 1978. Studies on a climosequence of soils in tussock grasslands. 21. Mineralogy. *N.Z. J. Sci.* 21:467–480.
- Churchman, G.J. 1980. Clay minerals formed from micas and chlorites in some New Zealand soils. *Clay Miner.* 15:59–76.
- Churchman, G.J. 1990. Relevance of different intercalation tests for distinguishing halloysite from kaolinite in soils. *Clays Clay Miner.* 38:591–599.
- Churchman, G.J. 2000. The alteration and formation of soil minerals by weathering, p. F3–F76. *In* M.E. Sumner (ed.) *Handbook of soil science*. CRC Press, Boca Raton, FL.
- Churchman, G.J. 2006. Soil phases: The inorganic solid phase, p. 23–44. *In* G. Certini and R. Scalenghe (eds.) *Soils: Basic concepts and future challenges*. Cambridge University Press, Cambridge, U.K.
- Churchman, G.J. 2010. Is the geological concept of clay minerals appropriate for soil science? *Phys. Chem. Earth.* 35:922–940.
- Churchman, G.J., and J.G. Bruce. 1988. Relationships between loess deposition and mineral weathering in some soils in Southland, New Zealand, p. 11–31. *In* D.N. Eden and R.J. Furkert (eds.) *Loess: Its distribution, geology and soils*. A.A. Balkema, Rotterdam, the Netherlands.
- Churchman, G.J., and C.M. Burke. 1991. Properties of subsoils in relation to various measures of surface area and moisture contents. *J. Soil Sci.* 42:463–478.
- Churchman, G.J., and R.M. Carr. 1975. The definition and nomenclature of halloysites. *Clays Clay Miner.* 23:382–388.
- Churchman, G.J., R.N. Clayton, K. Sridhar, and M.L. Jackson. 1976. Oxygen isotopic composition of aerosol-sized quartz in shales. *J. Geophys. Res.* 81:381–386.
- Churchman, G.J., and R.J. Gilkes. 1989. Recognition of intermediates in the possible transformation of halloysite to kaolinite. *Clay Miner.* 24:579–590.
- Churchman, G.J., I.R. Pontifex, and S.G. McClure. 2010. Factors influencing the formation and characteristics of halloysites or kaolinites in granitic and tuffaceous saprolites in Hong Kong. *Clays Clay Miner.* 58:122–139.
- Churchman, G.J., P.G. Slade, P.G. Self, and L.J. Janik. 1994. Nature of interstratified kaolin-smectites in some Australian soils. *Aust. J. Soil Res.* 32:805–822.
- Churchman, G.J., and K.R. Tate. 1987. Stability of aggregates of different size grades in allophanic soils from volcanic ash in New Zealand. *J. Soil Sci.* 38:19–27.
- Churchman, G.J., and B.K.G. Theng. 1984. Interactions of halloysites with amides: Mineralogical factors affecting complex formation. *Clay Miner.* 19:161–175.
- Claridge, G.G.C. 1965. The clay mineralogy and chemistry of some soils from Ross dependency, Antarctica. *N.Z. J. Sci.* 8:186–220.
- Claridge, G.G.C., and I.B. Campbell. 1968. Soils of the Shackleton Glacier, Queen Maud Range, Antarctica. *N.Z. J. Sci.* 11:171–218.
- Claridge, G.G.C., and I.B. Campbell. 2008. Zeolites in Antarctic soils: Examples from Coombs Hills and Marble Point. *Geoderma* 144:66–72.
- Clayton, R.N., M.L. Jackson, and K. Sridhar. 1978. Resistance of quartz silt to isotopic exchange under burial and intense weathering conditions. *Geochim. Cosmochim. Acta* 42:1517–1522.

- Coleman, D.C., and D.A. Crossley, Jr. 2003. *Fundamental of soil ecology*. Academic Press, Amsterdam, the Netherlands.
- Colombo, C., and J. Torrent. 1991. Relationships between aggregation and iron oxides in Terra Rossa soils from southern Italy. *Catena* 18:51–59.
- Cornell, R.M., and U. Schwertmann. 1996. *The iron oxides*. VCH, Weinheim, Germany.
- Courchesne, F. 2006. Factors of soil formation: Biota. As exemplified by case studies on the direct imprint of trees on trace metal concentrations, p. 165–179. *In* G. Certini and R. Scalenghe (eds.) *Soils: Basic concepts and future challenges*. Cambridge University Press, Cambridge, U.K.
- Cradwick, P.D.G., V.C. Farmer, J.D. Russell, C.R. Masson, K. Wada, and N. Yoshinaga. 1972. Imogolite, a hydrated aluminium silicate of tubular structure. *Nat. Phys. Sci.* 240:187–189.
- Craig, D.C., and F.C. Loughnan. 1964. Chemical and mineralogical transformations accompanying the weathering of basic volcanic rocks from New South Wales. *Aust. J. Soil Res.* 2:218–234.
- Cronin, S.J., V.E. Neall, and A.S. Palmer. 1996. Investigation of an aggrading paleosol developed into andesitic ring-plain deposits, Ruapehu volcano, New Zealand. *Geoderma* 69:119–135.
- Cuadros, J., A. Delgado, A. Cardenete, E. Reyes, and J. Linares. 1994. Kaolinite/montmorillonite resembles beidellite. *Clays Clay Miner.* 42:643–651.
- Dahlgren, R.A., J.P. Drago, and F.C. Ugolini. 1997. Weathering of Mt. St. Helens tephra under a cryic–udic climatic regime. *Soil Sci. Soc. Am. J.* 61:1519–1525.
- Dahlgren, R.A., M. Saigusa, and F.C. Ugolini. 2004. The nature, properties, and management of volcanic soils. *Adv. Agron.* 82:113–182.
- Daux, V., J.L. Crovisier, C. Hemond, and J.C. Petit. 1994. Geochemical evolution of basaltic rocks subjected to weathering: Fate of the major elements, rare earth elements, and thorium. *Geochim. Cosmochim. Acta* 58:4941–4954.
- De Vleeschouwer, F., B. Van Vliët Lanoé, and N. Fagel. 2008. Long term mobilisation of chemical elements in tephra-rich peat (NE Iceland). *Appl. Geochem.* 23:3819–3839.
- Delmonte, B., I. Basile-Doelsch, J.-R. Petit, V. Maggi, M. Revel-Rolland, A. Michard, E. Jagoutz, and F. Grousset. 2004. Comparing the Epica and Vostok dust records during the last 220,000 years: Stratigraphical correlation and provenance in glacial periods. *Earth Sci. Rev.* 66:63–87.
- Delvaux, B., and A.J. Herbillon. 1995. Pathways of mixed-layer kaolin–smectite formation in soils, p. 457–461. *In* G.J. Churchman, R.W. Fitzpatrick, and R.A. Eggleton (eds.) *Clays: Controlling the environment*. Proc. 10th Int. Clay Conf., 18–23 July 1993. Adelaide, Australia. CSIRO Publishing, Melbourne, Australia.
- Delvigne, J. 1998. Atlas of micromorphology of mineral alteration and weathering. *The Canadian Mineralogist*. Special Publication No. 3. Mineralogical Association of Canada, Ottawa, Canada.
- Denef, K., and J. Six. 2005. Clay mineralogy determines the importance of biological versus abiotic processes for macroaggregate formation and stabilization. *Eur. J. Soil Sci.* 56:469–479.
- Dent, D.L., and L.J. Pons. 1995. A world perspective on acid sulphate soils. *Geoderma* 67:263–276.
- Derry, L.A., A.C. Kurtz, K. Ziegler, and O.A. Chadwick. 2005. Biological control of terrestrial silica cycling and export fluxes to watershed. *Nature* 433:728–731.
- Deshpande, T.L., D.J. Greenland, and J.P. Quirk. 1968. Changes in soil properties associated with the removal of iron and aluminium oxides. *J. Soil Sci.* 19:108–122.
- Dias, I., I. Gonzalez, S. Prates, and E. Galán. 1997. Palygorskite occurrences in the Portuguese sector of the Tagus basin: A preliminary report. *Clay Miner.* 32:323–328.
- Dixon, J.B., and T.R. McKee. 1974. Internal and external morphology of tubular and spheroidal halloysite particles. *Clays Clay Miner.* 22:127–137.
- Dixon, J.B., and G.N. White. 2002. Manganese oxides, p. 367–388. *In* J.B. Dixon and D.G. Schulze (eds.) *Soil mineralogy with environmental applications*. SSSA, Madison, WI.
- Do Nascimento, N.R., G.T. Bueno, E. Fritsch, A.J. Herbillon, T. Allard, A.J. Melfi, R. Astolfo, and Y. Li. 2004. Podzolization as a deferralization process: A study of an Acrisol–Podzol sequence derived from palaeozoic sandstones in the northern Amazon basin. *Eur. J. Soil Sci.* 55:523–538.
- Doner, H.E., and P.R. Grossl. 2002. Carbonates and evaporates, p. 199–228. *In* J.B. Dixon and D.G. Schulze (eds.) *Soil mineralogy with environmental applications*. SSSA, Madison, WI.
- Doner, H.E., and W.C. Lynn. 1989. Carbonate, halide, sulfate, and sulfide minerals, p. 279–330. *In* J.B. Dixon and S.B. Weed (eds.) *Minerals in soil environments*. 2nd edn. SSSA, Madison, WI.
- Dong, H., D.P. Jaisi, J. Kim, and G. Zhang. 2009. Microbe–clay mineral interactions. *Am. Mineral.* 94:1505–1519.
- Douglas, L.A. 1989. Vermiculites, p. 635–674. *In* J.B. Dixon and S.B. Weed (eds.) *Minerals in soil environments*. 2nd edn. SSSA, Madison, WI.
- Drees, L.R., L.P. Wilding, N.E. Smeck, and A.L. Senkayi. 1989. Silica in soils: Quartz and disordered silica polymorphs, p. 913–974. *In* J.B. Dixon and S.B. Weed (eds.) *Minerals in soil environments*. 2nd edn. SSSA Book Series 1. SSSA, Madison, WI.
- Drief, A., and P. Schiffman. 2004. Very low-temperature alteration of sideromelane in hyaloclastites and hyalotuffs from Kilauea and Mauna Kea volcanoes: Implications for the mechanism of palagonite formation. *Clays Clay Miner.* 52:622–634.
- Ducloux, J., Y. Guero, P. Sardini, and A. Decarreau. 2002. Xerolysis: A hypothetical process of clay particles weathering under Sahelian climate. *Geoderma* 105:83–110.
- Ducloux, J., A. Meunier, and B. Velde. 1976. Smectite, chlorite and a regular interlayered chlorite–vermiculite in soils developed on a small serpentinite body, Massif Central, France. *Clay Miner.* 11:121–135.

- Dudas, M.J., and M.E. Harward. 1975. Weathering and authigenic halloysite in soil developed in Mazama ash. *Soil Sci. Soc. Am. Proc.* 39:561–566.
- Duiker, S.W., F.E. Rhoton, J. Torrent, N.E. Smeck, and R. Lal. 2003. Iron (hydr)oxide crystallinity effects on soil aggregation. *Soil Sci. Soc. Am. J.* 67:606–611.
- Egashira, K., and S. Tsuda. 1983. High-charge smectite found in weathered granitic rocks of Kyushu. *Clay Sci.* 6:67–81.
- Eger, A., and A.E. Hewitt. 2008. Soils and their relationship to aspect and vegetation history in the eastern Southern Alps, Canterbury High Country, New Zealand. *Catena* 75:297–307.
- Eggleton, R.A. 1984. Formation of iddingsite rims on olivine: A transmission electron microscopy study. *Clays Clay Miner.* 32:1–11.
- Eggleton, R.A., and J.N. Boland. 1982. Weathering of enstatite to talc through a sequence of transitional phases. *Clays Clay Miner.* 30:11–20.
- Eggleton, R.A., and P.R. Buseck. 1980. High resolution electron microscopy of feldspar weathering. *Clays Clay Miner.* 28:173–178.
- Egli, M., A. Mirabella, A. Mancabelli, and G. Sartori. 2004. Weathering of soils in alpine areas as influenced by climate and parent material. *Clays Clay Miner.* 52:287–303.
- Egli, M., M. Nater, M.A. Mirabella, S. Raimondi, M. Plötze, and L. Alioth. 2008. Clay minerals, oxyhydroxide formation, element leaching and humus development in volcanic soils. *Geoderma* 143:101–114.
- Ehlmann, B.L., J.F. Mustard, G.A. Swayze, R.N. Clark, J.L. Bishop, F. Poulet, D.J.D. Marais, L.H. Roach, R.E. Milliken, J.J. Wray, O. Barnouin-Jha, and S.L. Murchie. 2009. Identification of hydrated silicate minerals on Mars using MRO-CRISM: Geologic context near Nili Fossae and implications for aqueous alteration. *J. Geophys. Res.* 114:E00D08. doi:10.1029/2009JE003339.
- Elsass, F., D. Dubreoucq, and M. Thiry. 2000. Diagenesis of silica minerals from clay minerals in volcanic soils of Mexico. *Clay Miner.* 35:477–489.
- Erickson, G.E. 1983. The Chilean nitrate deposit. *Am. Sci.* 71:366–374.
- Estoule-Choux, J., J. Estoule, and D. Hallalouche. 1995. Congruent dissolution of microcline and epitaxial growth of “skeletal” quartz during weathering of a granite from the central Hoggar (Algeria), p. 373–377. *In* G.J. Churchman, R.W. Fitzpatrick, and R.A. Eggleton (eds.) *Clays controlling the environment*. Proc. 10th Int. Clay Conf. CSIRO Publishing, Melbourne, Australia.
- Eswaran, H., and C.B. Wong. 1978. A study of a deep weathering profile on granite in Peninsular Malaysia. Parts I, II, and III. *Soil Sci. Soc. Am. J.* 42:144–158.
- Eswaran, H., and Y.H. Yeow. 1976. The weathering of biotite in a profile on gneiss in Malaysia. *Geoderma* 16:9–20.
- Etame, J., M. Gerard, C.E. Suh, and P. Bilong. 2009. Halloysite neoformation during the weathering of nephelinitic rocks under humid tropical conditions at Mt Etinde, Cameroon. *Geoderma* 154:59–68.
- Eusterhues, K., C. Rumpel, and I. Kögel-Knabner. 2005. Organo-mineral associations in sandy acid forest soils: Importance of specific surface area, iron oxides and micropores. *Eur. J. Soil Sci.* 56:753–763.
- Fairbridge, R.W., and J. Bourgeois. 1978. *The encyclopedia of sedimentology*. Dowden, Hutchinson and Ross, Inc., Stroudsburg, PA.
- Fanning, D.S., V.Z. Keramidas, and M.A. El-Desoky. 1989. Micas, p. 551–634. *In* J.B. Dixon and S.B. Weed (eds.) *Minerals in soil environments*. 2nd edn. SSSA, Madison, WI.
- Fanning, D.S., M.C. Rabenhorst, S.N. Burch, K.R. Islam, and S.A. Tangren. 2002. Sulfides and sulfates, p. 229–260. *In* J.B. Dixon and D.G. Schulze (eds.) *Soil mineralogy with environmental applications*. SSSA, Madison, WI.
- Farmer, V.C. 1982. Significance of the presence of allophane and imogolite in podzol Bs horizons for podzolization mechanisms: A review. *Soil Sci. Plant Nutr.* 28:571–578.
- Farmer, V.C. 1997. Conversion of ferruginous allophanes to ferruginous beidellites at 95°C under alkaline conditions with alternating oxidation and reduction. *Clays Clay Miner.* 45:591–597.
- Farmer, V.C. 2005. Forest vegetation does recycle substantial amounts of silicon from and back to the soil solution with phytoliths as an intermediate phase, contrary to recent reports. *Eur. J. Soil Sci.* 56:271–272.
- Farmer, V.C., E. Delbos, and J.D. Miller. 2005. The role of phytolith formation and dissolution in controlling concentrations of silica in soil solutions and streams. *Geoderma* 127:71–79.
- Farmer, V.C., and A.R. Fraser. 1982. Chemical and colloidal stability of sols in the Al_2O_3 - Fe_2O_3 - SiO_2 - H_2O system: Their role in podzolization. *J. Soil Sci.* 33:737–742.
- Farmer, V.C., and D.G. Lumsdon. 2001. Interactions of fulvic acid with aluminium and a proto-imogolite sol: The contribution of E-horizon eluates to podzolization. *Eur. J. Soil Sci.* 52:177–188.
- Farmer, V.C., W.J. McHardy, L. Robertson, A. Walker, and M.J. Wilson. 1985. Micromorphology and sub-microscopy of allophane and imogolite in a podzol Bs horizon: Evidence for translocation and origin. *J. Soil Sci.* 36:87–95.
- Farmer, V.C., J.D. Russell, and M.L. Berrow. 1980. Imogolite and proto-imogolite allophane in spodic horizons: Evidence for a mobile aluminium silicate complex in podzol formation. *J. Soil Sci.* 31:673–684.
- Farmer, V.C., J.D. Russell, W.J. McHardy, A.C.D. Newman, J.L. Ahlrichs, and J.Y.H. Rimsaite. 1971. Evidence for loss of protons and octahedral iron from oxidised biotites and vermiculites. *Mineral Mag.* 38:121–137.
- Farmer, V.C., J.D. Russell, and B.F.L. Smith. 1983. Extraction of inorganic forms of translocated Al, Fe and Si from a podzol Bs horizon. *J. Soil Sci.* 34:571–576.
- Ferris, F.G. 1997. Formation of authigenic minerals by bacteria, p. 187–208. *In* J.M. McIntosh and L.A. Groat (eds.) *Biological-mineralogical interactions*. Mineralogical Association of Canada. Short Course. Vol. 25. Mineralogical Association of Canada, Ottawa, Canada.

- Fieldes, M. 1955. Clay mineralogy of New Zealand soils. Part II: Allophane and related mineral colloids. *N.Z. J. Sci. Technol.* 37:336–350.
- Fieldes, M. 1968. Clay mineralogy, In *Soils of New Zealand, Part 2*. N.Z. Soil Bur. Bull. 26:22–39.
- Fieldes, M., and L.D. Swindale. 1954. Chemical weathering of silicates in soil formation. *N.Z. J. Sci. Technol.* B36:140–154.
- Fisher, C.B., and P.C. Ryan. 2006. The smectite-to-disordered kaolinite transition in a tropical soil chronosequence, Pacific coast, Costa Rica. *Clays Clay Miner.* 54:571–586.
- Fisher, R.V., and H.-U. Schminke. 1984. *Pyroclastic rocks*. Springer-Verlag, Berlin, Germany.
- Fitzpatrick, R.W., and D.J. Chittleborough. 2002. Titanium and zirconium minerals, p. 667–690. In J.B. Dixon and D.G. Schulze (eds.) *Soil mineralogy with environmental applications*. SSSA, Madison, WI.
- Fitzpatrick, R.W., E. Fritsch, and P.G. Self. 1996. Interpretation of soil features produced by ancient and modern processes in degraded landscapes. V. Development of saline sulfidic features in non-tidal seepage areas. *Geoderma* 69:1–29.
- Fortin, D., and S. Langley. 2005. Formation and occurrence of biogenic iron-rich minerals. *Earth Sci. Rev.* 72:1–19.
- Franke, W.A., and R. Teschner-Steinhardt. 1994. An experimental approach to the sequence of the stability of rock-forming minerals towards chemical weathering. *Catena* 21:279–290.
- Fritsch, E., G. Morin, A. Bedidi, D. Bonnin, E. Balan, S. Caquineau, and G. Calas. 2005. Transformation of haematite and Al-poor goethite to Al-rich goethite and associated yellowing in a ferralitic clay soil profile of the middle Amazon Basin (Manaus, Brazil). *Eur. J. Soil Sci.* 56:575–588.
- Fu, F.F., T. Akagi, and S. Yabuki. 2002. Origin of silica particles found in the cortex of *Matteuccia* roots. *Soil Sci. Soc. Am. J.* 66:1265–1271.
- Furian, S., L. Barbiéro, R. Boulet, P. Curmi, M. Grimaldi, and C. Grimaldi. 2002. Distribution and dynamics of gibbsite and kaolinite in an Oxisol of Serra do Mar, southeastern Brazil. *Geoderma* 106:83–100.
- Furquim, S.A.C., R.C. Graham, L. Barbiero, J.P. de Queiroz Neto, and V. Valles. 2008. Mineralogy and genesis of smectites in an alkaline–saline environment of Pantanal wetland, Brazil. *Clays Clay Miner.* 56:579–595.
- Gaines, R.V., H.W. Skinner, E.F. Foord, B. Mason, and A. Rosenzweig. 1997. *Dana's new mineralogy*. John Wiley & Sons, New York.
- Galán, E., J.M. Brell, A. La Iglesia, and H.S. Robertson. 1975. The Cáceras palygorskite deposit, Spain, p. 81–94. In S.W. Bailey (ed.) *Proc. Int. Clay Conf.*, Mexico. Applied Publishing, Wilmette, IL.
- Galán, E., and A. Castillo. 1984. Sepiolite–palygorskite in Spanish tertiary basins: Genetical patterns in continental environments. *Dev. Sedimentol.* 37:87–124.
- Gallez, A., A.S.R. Juo, and A.J. Herbillon. 1976. Surface and charge characteristics of selected soils in the tropics. *Soil Sci. Soc. Am. J.* 40:601–608.
- Gardam, M., A.J. Mason, A.F. Reid, G.J. Churchman, and M. Raven. 2008. Arumpo bentonite deposits: Distinctive indicators of past volcanic events in the Murray Basin, southeastern Australia. *Aust. J. Earth Sci.* 55:183–194.
- Garrels, R.M., and F.T. Mackenzie. 1971. *Evolution of sedimentary rocks*. W.W. Norton and Co, New York.
- Gates, W.P. 2006. X-ray absorption spectroscopy, p. 789–864. In F. Bergaya, B.K.G. Theng, and G. Lagaly (eds.) *Handbook of clay science. Developments in clay science 1*. Elsevier, Amsterdam, the Netherlands.
- Geiss, C.E., and C.W. Zanner. 2006. How abundant is pedogenic magnetite? Abundance and grain size estimates for loessic soils based on rock magnetic analyses. *J. Geophys. Res.* 111:B12S21. doi:10.1029/2006JB004564.
- Gérard, M., S. Caquineau, J. Pinheiro, and G. Stoops. 2007. Weathering and allophane neof ormation in soils developed on volcanic ash in the Azores. *Eur. J. Soil Sci.* 58:496–515.
- Gerin, P.A., M.J. Genet, A.J. Herbillon, and B. Delvaux. 2003. Surface analysis of soil material by x-ray photoelectron spectroscopy. *Eur. J. Soil Sci.* 54:589–603.
- Giesler, R., H. Ilvesniemi, L. Nyberg, P. van Hees, M. Starr, K. Bishop, T. Kareinen, and U.S. Lundström. 2000. Distribution and mobilization of Al, Fe and Si in three podzolic soil profiles in relation to the humus layer. *Geoderma* 94:249–263.
- Gilkes, R.J. 1990. Mineralogical insights into soil productivity: An anatomical perspective, p. 63–73. In *Transactions, 14th Int. Cong. Soil Sci.*, 12–18 August 1990, Kyoto, Japan.
- Gilkes, R.J., and A. Suddhiprakarn. 1979. Biotite alteration in deeply weathered granite. I. Morphological, mineralogical, and chemical properties. *Clays Clay Miner.* 27:249–360.
- Gillot, F., D. Righi, and M.L. Räsänen. 2001. Layer-charge evaluation of expandable clays from a chronosequence of podzols in Finland using an alkylammonium method. *Clay Miner.* 36:571–584.
- Gislason, S.R., and E.H. Oelkers. 2003. Mechanism, rates, and consequences of basaltic glass dissolution: II. An experimental study of the dissolution rates of basaltic glass as a function of pH and temperature. *Geochim. Cosmochim. Acta* 67:3817–3832.
- Gjems, O. 1970. Mineralogical composition and pedogenic weathering of the clay fraction in podzol weathering profiles in Zalesine, Yugoslavia. *Soil Sci.* 110:237–243.
- Glassmann, J.R., and G.M. Simonson. 1985. Alteration of basalt in soils of western Oregon. *Soil Sci. Soc. Am. J.* 49:262–273.
- Goldich, S.S. 1938. A study in rock weathering. *J. Geol.* 46:17–58.
- Goodman, B.A., J.D. Russell, B. Montez, E. Oldfield, and R.J. Kirkpatrick. 1985. Structural studies of imogolite and allophanes by aluminum-27 and silicon-29 nuclear magnetic resonance spectroscopy. *Phys. Chem. Miner.* 12:342–346.
- Green, B.E. 1987. Weathering of buried paleosols on late Quaternary rhyolitic tephra, Rotorua region, New Zealand. Unpublished M.Sc. thesis. University of Waikato. Hamilton, New Zealand.

- Greenland, D.J. 1965. Interactions between clays and organic compounds in soils. Part 1. Mechanisms of interaction between clays and defined organic compounds. *Soils Fertil.* 28:415–425.
- Grey, I.E., and A.F. Reid. 1975. The structure of pseudorutile and its role in the natural alteration of ilmenite. *Am. Mineral.* 60:898–906.
- Grim, R.E. 1968. *Clay mineralogy*. McGraw-Hill, New York.
- Grim, R.E., R.H. Bray, and W.F. Bradley. 1937. The mica in argillaceous sediments. *Am. Mineral.* 22:813–829.
- Gustafsson, J.P. 2001. Modelling competitive anion adsorption on oxide minerals and an allophane-containing soil. *Eur. J. Soil Sci.* 52:639–653.
- Hall, P.L., G.J. Churchman, and B.K.G. Theng. 1985. Size distribution of allophane unit particles in aqueous suspensions. *Clays Clay Miner.* 33:345–349.
- Hamblin, A.P., and D.J. Greenland. 1977. Effect of organic constituents and complexed metal ions on aggregate stability of some East Anglian soils. *J. Soil Sci.* 28:410–416.
- Hamilton, V.E., P.R. Christensen, and J.L. Bandfield. 2003. Volcanism or aqueous alteration on Mars? *Nature* 421:711–712.
- Harder, H. 1972. The role of magnesium in the formation of smectite minerals. *Chem. Geol.* 10:31–39.
- Harder, H. 1977. Clay mineral formation under lateritic weathering conditions. *Clay Miner.* 12:281–288.
- Harlan, P.W., D.P. Franzmeier, and C.B. Roth. 1977. Soil formation on loess in southwestern Indiana. II. Distribution of clay and free iron oxides and fragipan formation. *Soil Sci. Soc. Am. J.* 42:99–103.
- Harris, W.G. 2002. Phosphate minerals, p. 637–665. *In* J.B. Dixon and D.G. Schulze (eds.) *Soil mineralogy with environmental applications*. SSSA, Madison, WI.
- Hart, R.D., R.J. Gilkes, S. Siradz, and B. Singh. 2002. The nature of soil kaolins from Indonesia and Western Australia. *Clays Clay Miner.* 50:198–207.
- Hart, R.D., W. Wiriyakitnateekul, and R.J. Gilkes. 2003. Properties of soil kaolins from Thailand. *Clay Miner.* 38:71–94.
- Hartemink, A.E., A.B. McBratney, and J.A. Cattle. 2001. Developments and trends in soil science: 100 volumes of *Geoderma* (1967–2001). *Geoderma* 100:217–268.
- Hay, R.L. 1960. Rate of clay formation and mineral alteration in a 4000-year-old volcanic ash soil on St. Vincent, B.W.I. *Am. J. Sci.* 258:354–368.
- Hayes, M.H.B., P. MacCarthy, R.L. Malcolm, and R.S. Swift. 1989. The search for structure: Setting the scene, p. 3–31. *In* M.H.B. Hayes, P. MacCarthy, R.L. Malcolm, and R.S. Swift (eds.) *Humic substances*. II. John Wiley & Sons, Chichester, U.K.
- He, Y., D.C. Li, B. Velde, Y.F. Yang, C.M. Huang, Z.T. Gong, and G.I. Zhang. 2008. Clay minerals in a soil chronosequence derived from basalt on Hainan Island, China and its implication for pedogenesis. *Geoderma* 148:206–212.
- Hellmann, R., C.H. Egglestone, M.F. Hochella, Jr., and D.A. Crerar. 1990. The formation of leached layers on albite surfaces during dissolution under hydrothermal conditions. *Geochim. Cosmochim. Acta* 54:1267–1282.
- Hemley, J.J. 1959. Some mineralogical equilibria in the system $K_2O-Al_2O_3-SiO_2-H_2O$. *Am. J. Sci.* 257:241–270.
- Hendricks, S.B., and W.H. Fry. 1930. The results of X-ray and microscopical examinations of soil colloids. *Soil Sci.* 29:457–479.
- Henriet, C., N. De Jaeger, M. Dore, S. Opfergelt, and B. Delvaux. 2008. The reserve of weatherable primary silicates impacts the accumulation of biogenic silicon in volcanic ash soils. *Biogeochemistry* 90:209–223.
- Herbillon, A.J., R. Frankart, and L. Vielvoye. 1981. An occurrence of interstratified kaolinite–smectite minerals in a red-black soil toposequence. *Clay Miner.* 16:195–201.
- Herbillon, A.J., and M.N. Makumbi. 1975. Weathering of chlorite in a soil derived from a chlorite-schist under humid tropical conditions. *Geoderma* 13:89–104.
- Herbillon, A.J., M.M. Mestdagh, L. Vielvoye, and E. Derouane. 1976. Iron in kaolinite with special reference to kaolinite from tropical soils. *Clay Miner.* 11:201–220.
- Hillier, S., and A.L. Pharande. 2008. Contemporary pedogenic formation of palygorskite in irrigation-induced saline-sodic, shrink–swell soils of Maharashtra, India. *Clays Clay Miner.* 56:531–548.
- Hinsinger, P., O.N.F. Barros, M.F. Benedetti, Y. Noack, and G. Callot. 2001. Plant-induced weathering of a basaltic rock. *Geochim. Cosmochim. Acta* 65:137–152.
- Hinsinger, P., F. Elsass, B. Jaillard, and M. Robert. 1993. Root-induced irreversible transformation of a trioctahedral mica in the rhizosphere of rape. *J. Soil Sci.* 44:535–545.
- Hinsinger, P., and B. Jaillard. 1993. Root-induced release of inter-layer potassium and vermiculitization of phlogopite as related to potassium depletion in the rhizosphere of ryegrass. *J. Soil Sci.* 44:525–534.
- Hinsinger, P., B. Jaillard, and J.E. Dufey. 1992. Rapid weathering of a trioctahedral mica by the roots of ryegrass. *Soil Sci. Soc. Am. J.* 56:977–982.
- Hiradate, S., H. Hirai, and H. Hashimoto. 2006. Characterisation of allophanic Andisols by solid-state ^{13}C , ^{27}Al , and ^{29}Si NMR and by C stable isotopic ratio, $\delta^{13}C$. *Geoderma* 136:696–707.
- Hiradate, S., T. Nakadai, H. Shindo, and T. Yoneyama. 2004. Carbon source of humic substances in some Japanese volcanic ash soils determined by carbon stable isotopic ratio, $\delta^{13}C$. *Geoderma* 119:133–141.
- Hiradate, S., and S.-I. Wada. 2005. Weathering processes of volcanic glass to allophane determined by ^{27}Al and ^{29}Si solid-state NMR. *Clays Clay Miner.* 53:401–408.
- Hochella, M.F., Jr. 2008. Nanogeoscience: From origins to cutting-edge applications. *Elements* 4:373–379.
- Hochella, M.F., Jr., and J.F. Banfield. 1995. Chemical weathering of silicates in nature: A microscopic perspective with theoretical considerations, p. 353–406. *In* A.F. White and S.L. Brantley (eds.) *Chemical weathering rates of silicate minerals*. Reviews in mineralogy. Vol. 31. Mineralogical Society of America, Washington, DC.

- Hodder, A.P.W., P.J. de Lange, and D.J. Lowe. 1991. Dissolution and depletion of ferromagnesian minerals from Holocene tephra in an acid bog, New Zealand, and implications for tephra correlation. *J. Quat. Sci.* 6:195–208.
- Hodder, A.P.W., B.E. Green, and D.J. Lowe. 1990. A two-stage model for the formation of clay minerals from tephra-derived volcanic glass. *Clay Miner.* 25:313–327.
- Hodder, A.P.W., T.R. Naish, and D.J. Lowe. 1996. Towards an understanding of thermodynamic and kinetic controls on the formation of clay minerals from volcanic glass under various environmental conditions, p. 1–11. *In* S.G. Pandalai (ed.) *Recent research developments in chemical geology*. Research Signpost, Trivandrum, India.
- Hodder, A.P.W., T.R. Naish, and C.S. Nelson. 1993. A two-stage model for the formation of smectite from detrital volcanic glass under shallow-marine conditions. *Mar. Geol.* 109:279–285.
- Hogg, A.G., T.F.G. Higham, D.J. Lowe, J.G. Palmer, P. Reimer, and R.M. Newnham. 2003. A wiggle-match date for Polynesian settlement of New Zealand. *Antiquity* 77:116–125.
- Hogg, A.G., D.J. Lowe, J.G. Palmer, G. Boswijk, C. Bronk Ramsey, and R. Sparks. 2011. Definitive high-precision calendar date for the Taupo eruption derived by ^{14}C Wiggle-match dating using a New Zealand kauri-derived ^{14}C calibration curve. *The Holocene* (in review).
- Holdren, G.R., Jr., and P.M. Speyer. 1987. Reaction rate-surface area relationships during the early stages of weathering: II Data on eight additional feldspars. *Geochim. Cosmochim. Acta* 51:2311–2318.
- Hong, H.-L., and J.-X. Mi. 2006. Characteristics of halloysite associated with rectorite from Hubei, China. *Mineral. Mag.* 70:257–264.
- Hseu, Z.Y., H. Tsai, H.C. Hsi, and Y.C. Chen. 2007. Weathering sequences of clay minerals in soils along a serpentinitic toposequence. *Clays Clay Miner.* 55:389–401.
- Huang, P.M. 1989. Feldspars, olivines, pyroxenes, and amphiboles, p. 975–1050. *In* J.B. Dixon and S.B. Weed (eds.) *Minerals in soil environments*. 2nd edn. SSSA, Madison, WI.
- Huang, P.M., and M. Schnitzer (eds.). 1986. *Interactions of soil minerals with natural organics and microbes*. SSSA Special Publication No. 17. SSSA, Madison, WI.
- Huang, P.M., M.K. Wang, N. Kämpf, and D.G. Schulze. 2002. Aluminum hydroxides, p. 261–290. *In* J.B. Dixon and D.G. Schulze (eds.) *Soil mineralogy with environmental applications*. SSSA, Madison, WI.
- Hue, N.V., G.R. Craddock, and F. Adams. 1986. Effect of organic acids on aluminum toxicity in subsoils. *Soil Sci. Soc. Am. J.* 50:28–34.
- Hughes, J.C., and G. Brown. 1979. A crystallinity index for soil kaolins and its relation to parent rock, climate and soil maturity. *J. Soil Sci.* 30:557–563.
- Hunter, R.J. 1981. *The zeta potential in colloid science*. Academic Press, London, U.K.
- Hurowitz, J.A., and S.M. McLennan. 2007. A ~3.5 Ga record of water-limited, acidic weathering conditions on Mars. *Earth Planet Sci. Lett.* 260:432–443.
- Ildefonse, P., E. Copin, and B. Velde. 1979. A soil vermiculite formed from a meta-gabbro, Liore-Atlantique, France. *Clay Miner.* 14:201–210.
- Inoue, K., and T. Sase. 1996. Paleoenvironmental history of post-Toya Ash tephric deposits and paleosols at Iwate Volcano, Japan, using aeolian dust content and phytolith composition. *Quat. Int.* 34–36:127–137.
- Inskeep, W.P., J.L. Clayton, and D.W. Mogk. 1993. Naturally weathered plagioclase grains from the Idaho Batholith: Observations using scanning electron microscopy. *Soil Sci. Soc. Am. J.* 57:851–860.
- Jackson, M.L. 1959. Frequency distribution of clay minerals in major great soil groups as related to the factors of soil formation. *Clays Clay Miner.* 6:133–143.
- Jackson, M.L. 1963. Aluminum bonding in soils: A unifying principle in soil science. *Soil Sci. Soc. Am. Proc.* 27:1–10.
- Jackson, M.L. 1964. Chemical composition of soils, p. 71–141. *In* F.E. Bear (ed.) *Chemistry of the soil*. Reinhold Publishing Corporation, New York.
- Jackson, M.L., Y. Hseung, R.B. Corey, E.J. Evans, and R.C. Van den Heuval. 1952. Weathering of clay-size minerals in soils and sediments II. Chemical weathering of layer silicates. *Soil Sci. Soc. Am. Proc.* 16:3–6.
- Jackson, M.L., S.A. Tyler, A.L. Willis, G.A. Bourbeau, and R.P. Pennington. 1948. Weathering sequence of clay-size minerals in soils and sediments. I. Fundamental generalizations. *J. Phys. Colloid Chem.* 52:1237–1260.
- Janik, L.J., and J.L. Keeling. 1993. FT-IR partial least-squares analysis of tubular halloysite in kaolin samples from the Mount Hope kaolin deposit. *Clay Miner.* 28:265–378.
- Jansen, B., G.J. Nierop, and J.M. Verstraten. 2005. Mechanisms controlling the mobility of dissolved organic matter, aluminium and iron in podzol B horizons. *Eur. J. Soil Sci.* 56:537–550.
- Jaynes, W.F., J.M. Bigham, N.E. Smeck, and M.J. Shipitalo. 1989. Interstratified 1:1–2:1 mineral formation in a polygenetic soil from southern Ohio. *Soil Sci. Soc. Am. J.* 53:1888–1894.
- Johnson, L.J. 1964. Occurrence of regularly interstratified chlorite-vermiculite as a weathering product of chlorite in a soil. *Am. Mineral.* 49:556–572.
- Johnson, D.L. 2002. Darwin would be proud: Bioturbation, dynamic denudation, and the power of theory in science. *Geoarchaeology* 17:7–40.
- Johnson, S.L., S. Guggenheim, and A.F. Koster van Groos. 1990. Thermal stability of halloysite by high pressure differential thermal analysis. *Clays Clay Miner.* 38:477–484.
- Johnson-Maynard, J.L., P.A. McDaniel, D.E. Ferguson, and A.L. Falen. 1997. Chemical and mineralogical conversion of Andisols following invasion by bracken fern. *Soil Sci. Soc. Am. J.* 61:549–555.
- Jolicoeur, S., P. Ildefonse, and M. Bouchard. 2000. Kaolinite and gibbsite weathering of biotite within saprolites and soils of central Virginia. *Soil Sci. Soc. Am. J.* 64:1118–1119.

- Jongkind, A.G., and P. Buurman. 2006. The effect of kauri (*Agathis australis*) on grain size distribution and clay mineralogy of andesitic soils in the Waitakere Ranges, New Zealand. *Geoderma* 134:171–186.
- Jongmans, A.G., N. Van Breeman, U. Lundström, P.A.W. van Hees, R.D. Finlay, M. Srinivasan, T. Unestam, R. Giesler, P.-A. Melkerud, and M. Olsson. 1997. Rock-eating fungi. *Nature* 389:682–683.
- Jongmans, A.G., F. Van Oort, P. Buurman, A.M. Jaunet, and J.D.J. van Doesburg. 1994. Morphology, chemistry and mineralogy of isotropic aluminosilicate coatings in a Guadeloupe Andisol. *Soil Sci. Soc. Am. J.* 58:501–507.
- Jouquet, P., L. Mamou, M. Lepage, and B. Velde. 2002. Effect of termites on clay minerals in tropical soils: Fungus-growing termites as weathering agents. *Eur. J. Soil Sci.* 53:521–528.
- Joussein, E., S. Petit, G.J. Churchman, B. Theng, D. Righi, and B. Delvaux. 2005. Halloysite clay minerals—A review. *Clay Miner.* 40:383–426.
- Kadir, S., and M. Eren. 2008. The occurrence and genesis of clay minerals associated with Quaternary caliches in the Mersin area, southern Turkey. *Clays Clay Miner.* 56:244–258.
- Kahle, M., M. Kleber, and R. Jahn. 2002a. Review of XRD-based quantitative analyses of clay minerals in soils: The suitability of mineral intensity factors. *Geoderma* 109:191–205.
- Kahle, M., M. Kleber, and R. Jahn. 2002b. Predicting carbon content in illitic clay fractions from surface area, cation exchange capacity and dithionite-extractable iron. *Eur. J. Soil Sci.* 53:639–644.
- Kahle, M., M. Kleber, and R. Jahn. 2004. Retention of dissolved organic matter by phyllosilicate and soil clay fractions in relation to mineral properties. *Org. Geochem.* 35:269–276.
- Kaiser, K., and G. Guggenberger. 2000. The role of DOM sorption to mineral surfaces in the preservation of organic matter in soils. *Org. Geochem.* 31:711–724.
- Kaiser, K., and G. Guggenberger. 2003. Mineral surfaces and organic matter. *Eur. J. Soil Sci.* 54:219–236.
- Kämpf, N., and U. Schwertmann. 1982. Goethite and hematite in a climosequence in southern Brazil and their application in classification of kaolinitic soils. *Geoderma* 29:27–39.
- Kanket, W., A. Suddhiprakarn, I. Kheoruenromne, and R.J. Gilkes. 2005. Chemical and crystallographic properties of kaolin from ultisols in Thailand. *Clays Clay Miner.* 53:478–489.
- Kapoor, B.S. 1973. The formation of 2:1–2:2 intergrade clays in some Norwegian podzols. *Clay Miner.* 10:79–86.
- Kautz, C.Q., and P.C. Ryan. 2003. The 10 Å to 7 Å halloysite transition in a tropical soil sequence, Costa Rica. *Clays Clay Miner.* 51:252–263.
- Kawano, M., and K. Tomita. 1994. Growth of smectite from leached layer during experimental alteration of albite. *Clays Clay Miner.* 42:7–17.
- Kawano, M., and K. Tomita. 2001. Microbial biomineralization in weathered volcanic ash deposit and formation of biogenic minerals by experimental incubation. *Am. Mineral.* 86:400–410.
- Kawano, M., and K. Tomita. 2002. Microbial formation of silicate minerals in the weathering environment of a pyroclastic deposit. *Clays Clay Miner.* 50:99–110.
- Kendrick, K.J., and R.C. Graham. 2004. Pedogenic silica accumulation in chronosequence soils, southern California. *Soil Sci. Soc. Am. J.* 68:1295–1303.
- Khademi, H., and J.M. Arocena. 2008. Kaolinite formation from palygorskite and sepiolite in rhizosphere soils. *Clays Clay Miner.* 56:429–436.
- Khormali, F., and A. Abtahi. 2003. Origin and distribution of clay minerals in calcareous arid and semi-arid soils of Fars province, southern Iran. *Clay Miner.* 38:511–527.
- Kirkman, J.H. 1976. Clay mineralogy of Rotomahana sandy loam soil, North Island, New Zealand. *N.Z. J. Geol. Geophys.* 19:35–41.
- Kirkman, J.H. 1981. Morphology and structure of halloysite in New Zealand tephros. *Clays Clay Miner.* 29:1–9.
- Kirkman, J.H., and W.J. McHardy. 1980. A comparative study of the morphology, chemical composition and weathering of rhyolitic and andesitic glass. *Clay Miner.* 15:165–173.
- Kittrick, J.A. 1967. Gibbsite–kaolinite equilibria. *Soil Sci. Soc. Am. Proc.* 31:314–316.
- Kittrick, J.A. 1973. Mica-derived vermiculites as unstable intermediates. *Clays Clay Miner.* 21:479–488.
- Kleber, M., R. Mikutta, M.S. Torn, and R. Jahn. 2005. Poorly crystalline mineral phases protect organic matter in acid subsoil horizons. *Eur. J. Soil Sci.* 56:717–725.
- Kleber, M., L. Schwendenmann, E. Veldkamp, J. Röhnert, and R. Jahn. 2007. Halloysite versus gibbsite: Silicon cycling as a pedogenetic process in two lowland rain forest soils of La Selva, Costa Rica. *Geoderma* 138:1–11.
- Kohut, C., K. Muehlenbachs, and M.J. Dudas. 1995. Authigenic dolomite in a saline soil in Alberta, Canada. *Soil Sci. Soc. Am. J.* 59:1499–1504.
- Kondo, R., C.W. Childs, and I. Atkinson. 1994. Opal phytoliths in New Zealand. Manaaki Whenua Press, Lincoln, New Zealand.
- Laird, D.A., P. Barak, E.A. Nater, and R.H. Dowdy. 1991. Chemistry of smectitic and illitic phases in interstratified soil smectite. *Soil Sci. Soc. Am. J.* 55:1499–1504.
- Laird, D.A., and E.A. Nater. 1993. Nature of the illitic phase associated with randomly interstratified smectite/illite in soils. *Clays Clay Miner.* 41:280–287.
- Langmuir, D., and D.O. Whittemore. 1971. Variations in the stability of precipitated ferric oxyhydroxides, p. 209–234. *In* R.F. Gould (ed.) *Nonequilibrium systems in natural water chemistry*. Advances in Chemistry Series No. 106. American Chemical Society, Washington, DC.
- Lanson, B. 1997. Decomposition of experimental X-ray diffraction patterns (profile fitting): A convenient way to study clays. *Clays Clay Miner.* 45:132–146.
- Lapidus, D.F. 1987. *Collins dictionary of geology*. Collins, London, U.K.
- Lee, B.D., S.K. Sears, R.C. Graham, C. Amrhein, and H. Vali. 2003. Secondary mineral genesis from chlorite and serpentine in an ultramafic soil toposequence. *Soil Sci. Soc. Am. J.* 65:1183–1196.

- Leifeld, J. 2006. Soils as sources and sinks of greenhouse gases, p. 23–44. Geological Society of London Special Publication No. 266.
- Leonard, R.A., and S.B. Weed. 1967. Influence of exchange ions on the b-dimension of dioctahedral vermiculite. *Clays Clay Miner.* 15:149–161.
- Li, Z., B. Velde, and D. Li. 2003. Loss of K-bearing clay minerals in flood-irrigated, rice-growing soils in Jiangxi province, China. *Clays Clay Miner.* 51:75–82.
- Lilienfein, J., R.G. Qualls, S.M. Uselman, and S.D. Bridgham. 2003. Soil formation and organic matter accretion in a young andesitic chronosequence at Mt. Shasta, California. *Geoderma* 116:249–264.
- Lim, C.H., M.L. Jackson, R.D. Koons, and P.A. Helmke. 1980. Kaolins: Sources of differences in cation-exchange capacities and cesium retention. *Clays Clay Miner.* 28:223–229.
- Lin, C.-W., Z.-Y. Hseu, and Z.-S. Chen. 2002. Clay mineralogy of Spodosols with high clay contents in the subalpine forests of Taiwan. *Clays Clay Miner.* 50:726–735.
- Lindsay, W.L., P.L.G. Vlek, and S.H. Chien. 1989. Phosphate minerals, p. 1089–1130. *In* J.B. Dixon and S.B. Weed (eds.) *Minerals in soil environments*. 2nd edn. SSSA, Madison, WI.
- Loughnan, F.C. 1969. *Chemical weathering of the silicate minerals*. Elsevier, New York.
- Loveland, P.J. 1984. The soil clays of Great Britain: 1. England and Wales. *Clay Miner.* 19:681–707.
- Loveland, P.J., and P. Bullock. 1975. Crystalline and amorphous components of the clay fractions in brown podzolic soils. *Clay Miner.* 10:451–469.
- Loveland, P.J., I.G. Wood, and A.H. Weir. 1999. Clay mineralogy at Rothamsted: 1934–1988. *Clay Miner.* 34:165–183.
- Lowe, D.J. 1986. Controls on the rates of weathering and clay mineral genesis in airfall tephra: A review and New Zealand case study, p. 265–330. *In* S.M. Colman and D.P. Dethier (eds.) *Rates of chemical weathering of rocks and minerals*. Academic Press, Orlando, FL.
- Lowe, D.J. 1995. Teaching clays: From ashes to allophane, p. 19–23. *In* G.J. Churchman, R.W. Fitzpatrick, and R.A. Eggleton (eds.) *Clays: Controlling the environment*. Proc. 10th Int. Clay Conf., 18–23 July 1993, Adelaide, Australia. CSIRO Publishing, Melbourne, Australia.
- Lowe, D.J. (ed.). 2008. Guidebook for pre-conference North Island field trip A1 “ashes and issues.” Australian and New Zealand 4th Joint Soils Conf., Massey University, Palmerston North, p. 1–194. New Zealand Society of Soil Science, Christchurch, New Zealand (ISBN 978-0-473-14476-0).
- Lowe, D.J., G.J. Churchman, R.H. Merry, R.W. Fitzpatrick, M.J. Sheard, and W.H. Hudnall. 1996. Holocene basaltic volcanogenic soils of the Mt. Gambier area, South Australia, are unusual globally: What do they tell us? p. 153–154. Australian and New Zealand National Soils Conf. 1996. Vol. 2. Oral papers. Australian Society of Soil Science, University of Melbourne, Australia.
- Lowe, D.J., and D.J. Palmer. 2005. Andisols of New Zealand and Australia. *J. Integr. Field Sci.* 2:39–65.
- Lowe, D.J., and H.J. Percival. 1993. Clay mineralogy of tephra and associated paleosols and soils, and hydrothermal deposits, North Island. Guidebook for New Zealand pre-conference field trip F1, p. 1–110. 10th Int. Clay Conf., 18–23 July 1993, Adelaide, Australia.
- Lowe, D.J., P.A.R. Shane, B.V. Alloway, and R.M. Newnham. 2008. Fingerprints and age models for widespread New Zealand tephra marker beds erupted since 30,000 years ago: A framework for NZ-INTIMATE. *Quat. Sci. Rev.* 27:95–126.
- Lowe, D.J., J.M. Tippet, P.J.J. Kamp, I.J. Liddell, R.M. Briggs, and J.L. Horrocks. 2001. Ages on weathered Plio-Pleistocene tephra sequences, western North Island, New Zealand. *Les Dossiers de l'Archeo-Logis* 1:45–60.
- Lucas, Y. 2001. The role of plant in controlling rates and products of weathering: Importance of biological pumping. *Annu. Rev. Earth Planet. Sci.* 29:135–163.
- Lucas, Y., F.J. Luizao, A. Chauvel, J. Rouiller, and D. Nahon. 1993. The relation between biological activity of the rain forest and mineral composition of soils. *Science* 260:521–523.
- Lundström, U.S., N. Van Breeman, and D. Bain. 2000. The podzolisation process. A review. *Geoderma* 94:91–107.
- Ma, C., and R.A. Eggleton. 1999. Surface layer types of kaolinite: A high-resolution transmission electron microscope study. *Clays Clay Miner.* 47:181–191.
- Madden, M.E.M., R.J. Bodnar, and J.D. Rimstidt. 2004. Jarosite as an indicator of water-limited chemical weathering on Mars. *Nature* 431:821–823.
- Maher, K., C.I. Steefel, A.F. White, and D.A. Stonestrom. 2009. The role of reaction affinity and secondary minerals in regulating chemical weathering rates at the Santa Cruz Soil Chronosequence, California. *Geochim. Cosmochim. Acta* 73:2804–2831.
- Maher, B.A., and R.M. Taylor. 1988. Formation of ultrafine-grained magnetite in soils. *Nature* 336:368–370.
- Mahjoory, R.A. 1975. Clay mineralogy, physical, and chemical properties of some soils in arid regions of Iran. *Soil Sci. Soc. Am. Proc.* 39:1157–1164.
- Marsan, F.A., and J. Torrent. 1989. Fragipan bonding by silica and iron oxides in a soil from northwestern Italy. *Soil Sci. Soc. Am. J.* 53:1140–1145.
- Marx, S.K., H.A. McGowan, and B.S. Kamber. 2009. Long-range dust transport from eastern Australia: A proxy for Holocene aridity and ENSO-type climate variability. *Earth Planet. Sci. Lett.* 282:167–177.
- Mayer, L.M., and B. Xing. 2001. Organic matter-surface area relationships in acid soils. *Soil Sci. Soc. Am. J.* 65:250–258.
- McCarthy, J.F., J. Ilavsky, J.D. Jastrow, L.M. Mayer, E. Perfect, and J. Zhuang. 2008. Protection of organic matter in soil microaggregates via restructuring of aggregate porosity and filling of pores with accumulating organic matter. *Geochim. Cosmochim. Acta* 72:4725–4744.
- McDaniel, P.A., D.J. Lowe, O. Arnalds, and C.-L. Ping. 2012. Andisols. *In* Li, Y. and Sumner, M.E. (eds.) *Handbook of soil science*. 2nd edn. CRC Press (Taylor & Francis), London, U.K.

- McGahan, D.G., R.J. Southard, and R.J. Zasoki. 2003. Mineralogical comparison of agriculturally acidified and naturally acidic soils. *Geoderma* 114:355–368.
- McIntosh, P.D. 1979. Halloysite in a New Zealand tephra and paleosol less than 2500 years old. *N.Z. J. Sci.* 22:49–54.
- McIntosh, P.D. 1980. Weathering products in Vitrandept profiles under pine and manuka, New Zealand. *Geoderma* 24:225–239.
- McKeague, J.A., and J.E. Brydon. 1970. Mineralogical properties of ten reddish brown soils from the Atlantic provinces in relation to parent materials and pedogenesis. *Can. J. Soil Sci.* 50:47–55.
- McKenzie, R.M. 1989. Manganese oxides and hydroxides, p. 439–465. *In* J.B. Dixon and S.B. Weed (eds.) *Minerals in soil environments*. 2nd edn. SSSA, Madison, WI.
- Mehra, O.P., and M.L. Jackson. 1960. Iron oxide removal from soils and clays by a dithionite-citrate system buffered with sodium bicarbonate. *Clays Clay Miner.* 7:317–327.
- Mejia, G., H. Kohnke, and J.L. White. 1968. Clay mineralogy of certain soils of Columbia. *Soil Sci. Soc. Am. Proc.* 32:665–670.
- Melkerud, P.-A., D.C. Bain, A.G. Jongmans, and T. Tarvainen. 2000. Chemical, mineralogical and morphological characterization of three podzols developed on glacial deposits in northern Europe. *Geoderma* 94:125–148.
- Melo, V.F., B. Singh, C.E.G.R. Schaefer, R.F. Novais, and M.P.F. Fontes. 2001. Chemical and mineralogical properties of kaolinite-rich Brazilian soils. *Soil Sci. Soc. Am. J.* 65:1324–1333.
- Mestdagh, M.M., L. Vielvoye, and A.J. Herbillon. 1980. Iron in kaolinite: II. The relationship between kaolinite crystallinity and iron content. *Clay Miner.* 15:1–13.
- Meunier, A., and B. Velde. 1976. Mineral reactions at grain contacts in early stages of granite weathering. *Clay Miner.* 11:235–240.
- Meunier, A., and B. Velde. 1979. Weathering mineral facies in altered granites: The importance of local small-scale equilibria. *Mineral Mag.* 43:261–268.
- Meysman, F.J.R., J.J. Middelburg, and C.H.R. Heip. 2006. Bioturbation: A fresh look at Darwin's last idea. *Trends Ecol. Evol.* 21:688–695.
- Mikutta, R., M. Kleber, and R. Jahn. 2005. Poorly crystalline minerals protect organic carbon in clay subfractions from acid subsoil horizons. *Geoderma* 128:106–115.
- Millot, G. 1970. *Geology of clays*. Springer-Verlag, New York.
- Mills, A.L. 2003. Keeping in touch: Microbial life on soil particle surfaces. *Adv. Agron.* 78:1–43.
- Milnes, A.R., and R.W. Fitzpatrick. 1989. Titanium and zirconium minerals, p. 1131–1205. *In* J.B. Dixon and S.B. Weed (eds.) *Minerals in soil environments*. 2nd edn. SSSA, Madison, WI.
- Ming, D.W., and F.A. Mumpton. 1989. Zeolites in soils, p. 873–911. *In* J.B. Dixon and S.B. Weed (eds.) *Minerals in soil environments*. 2nd edn. SSSA, Madison, WI.
- Mirabella, A., and M. Egli. 2003. Structural transformations of clay minerals in soils of a climosequence in an Italian alpine environment. *Clays Clay Miner.* 51:264–278.
- Mirabella, A., M. Egli, S. Raimondi, and D. Giaccari. 2005. Origin of clay minerals in soils on pyroclastic deposits in the island of Lipari (Italy). *Clays Clay Miner.* 53:409–421.
- Mizota, C., and M. Itoh. 1993. Volcanic origin of a cristobalite in the Te Ngae tephric loess from North Island, New Zealand. *Clays Clay Miner.* 41:755–756.
- Mizota, C., and Y. Takahashi. 1982. Eolian origin of quartz and mica in soils developed on basalts in northwestern Kyushu and Sanoin, Japan. *Soil Sci. Plant Nutr. (Tokyo)* 28:369–378.
- Mizota, C., N. Toh, and Y. Matsuhisa. 1987. Origin of cristobalite in soils derived from volcanic ash in temperate and tropical regions. *Geoderma* 39:323–330.
- Mogk, D.W., and W.W. Locke, III. 1988. Application of Auger electron spectroscopy (AES) to naturally weathered hornblende. *Geochim. Cosmochim. Acta* 52:2537–2542.
- Mokma, D.L., M. Yli-Halla, and K. Lindqvist. 2004. Podzol formation in sandy soils of Finland. *Geoderma* 120:259–272.
- Monger, H.C., and E.F. Kelly. 2002. Silica minerals, p. 611–636. *In* J.B. Dixon and D.G. Schulze (eds.) *Soil mineralogy with environmental applications*. SSSA, Madison, WI.
- Morgan, C.P., and M.H. Stolt. 2006. Soil morphology—water table cumulative duration relationships in southern New England. *Soil Sci. Soc. Am. J.* 70:816–824.
- Mortland, M.M. 1958. Kinetics of potassium release from biotite. *Soil Sci. Soc. Am. Proc.* 22:503–508.
- Mortland, M.M., K. Lawton, and G. Uehara. 1956. Alteration of biotite to vermiculite by plant growth. *Soil Sci.* 82:477–481.
- Mossin, L., M. Mortensen, and P. Nørnberg. 2002. Imogolite related to podzolization processes in Danish podzols. *Geoderma* 109:103–116.
- Muir, I.J., G.M. Bancroft, and H.W. Nesbitt. 1989. Characteristics of altered labradorite surfaces by SIMS and XPS. *Geochim. Cosmochim. Acta* 53:1235–1241.
- Muir, I.J., G.M. Bancroft, W. Shotyky, and H.W. Nesbitt. 1990. A SIMS and XPS study of dissolving plagioclase. *Geochim. Cosmochim. Acta* 54:2247–2256.
- Muir, I.J., and H.W. Nesbitt. 1997. Reactions of aqueous anions and cations at the labradorite–water interface: Coupled effects of surface processes and diffusion. *Geochim. Cosmochim. Acta* 61:265–274.
- Müller, B. 2009. Impact of the bacterium *Pseudomonas fluorescens* and its genetic derivatives on vermiculite: Effects on trace metals contents and clay mineralogical properties. *Geoderma* 153:94–103.
- Munk, L.P., and R.J. Southard. 1993. Pedogenic implications of opaline pendants in some California late-Pleistocene Palaeoxeralfs. *Soil Sci. Soc. Am. J.* 57:149–154.
- Murakami, T., H. Isobe, T. Sato, and T. Ohnuki. 1996. Weathering of chlorite in a quartz–chlorite schist: I. Mineralogical and chemical changes. *Clays Clay Miner.* 44:244–256.
- Mustard, J.F., S.L. Murchie, S.M. Pelkey, B.L. Ehlmann, R.E. Milliken, J.A. Grant, J.-P. Bibring, et al. 2008. Hydrated silicate minerals on Mars observed by the Mars reconnaissance orbiter CRISM instrument. *Nature* 454:305–309.

- Nadeau, P.H., M.J. Wilson, W.J. McHardy, and J.M. Tait. 1984. Interparticle diffraction: A new concept for interstratification of clay minerals. *Clay Miner.* 19:757-769.
- Nagashima, K., R. Tada, A. Tani, S. Toyoda, Y. Sun, and Y. Isozaki. 2007. Contribution of aeolian dust in Japan sea sediments estimated from ESR signal intensity and crystallinity of quartz. *Geochem. Geophys. Geosyst.* 8:Q02Q04. doi:10.1029/2006GC001364.
- Nahon, D., and F. Colin. 1982. Chemical weathering of orthopyroxenes under lateritic conditions. *Am. J. Sci.* 282:1232-1243.
- Nahon, D., F. Colin, and Y. Tardy. 1982. Formation and distribution of Mg, Fe, Mn-smectites in the first stages of the lateritic weathering of forsterite and tephroite. *Clay Miner.* 17:339-348.
- Naish, T.R., C.S. Nelson, and A.P.W. Hodder. 1993. Evolution of Holocene sedimentary bentonite in a shallow-marine embayment, Firth of Thames, New Zealand. *Mar. Geol.* 109:267-278.
- Nakao, A., S. Funakawa, T. Watanebe, and T. Kosaki. 2009. Pedogenic alterations of illitic minerals represented by Radiocaesium Interception Potential in soils with different soil moisture regimes in humid Asia. *Eur. J. Soil Sci.* 60:139-152.
- Nanzyo, M. 2007. Introduction to studies on volcanic ash soils in Japan and international collaboration. *J. Integr. Field Sci.* 4:71-77.
- Ndayiragije, S., and B. Delvaux. 2003. Coexistence of allophane, gibbsite, kaolinite and hydroxyl-Al-interlayered 2:1 clay minerals in a perudic Andosol. *Geoderma* 117:203-214.
- Neall, V.E. 1977. Genesis and weathering of Andosols in Taranaki, New Zealand. *Soil Sci.* 123:400-408.
- Nesbitt, H.W. 1997. Bacterial and inorganic weathering processes and weathering of crystalline rocks, p. 113-142. *In* J.M. McIntosh and L.A. Groat (eds.) *Biological-mineralogical interactions*. Mineralogical Association of Canada. Short Course. Vol. 25. Mineralogical Association of Canada, Ottawa, Canada.
- Nettleton, W.D., K.W. Flach, and R.E. Nelson. 1970. Pedogenic weathering of tonalite in southern California. *Geoderma* 4:387-402.
- Newnham, R.M., D.J. Lowe, and P.W. Williams. 1999. Quaternary environmental change in New Zealand: A review. *Prog. Phys. Geog.* 23:567-610.
- Newsom, H. 2005. Clays in the history of Mars. *Nature* 438:570-571.
- Nieuwenhuys, A., P.S.J. Verburg, and A.G. Jongmans. 2000. Mineralogy of a soil chronosequence on andesitic lava in humid tropical Costa Rica. *Geoderma* 98:61-82.
- Nizeyimana, E., T.J. Bicki, and P.A. Agbu. 1997. An assessment of colloidal constituents and clay mineralogy of soils derived from volcanic materials along a toposequence in Rwanda. *Soil Sci.* 162:361-371.
- Norfleet, M.L., A.D. Karathanasis, and B.R. Smith. 1993. Soil solution composition relative to mineral distribution in Blue Ridge mountain soils. *Soil Sci. Soc. Am. J.* 57:1375-1380.
- Noro, H. 1986. Hexagonal platy halloysite in an altered tuff bed, Komaki City, Aichi prefecture, Central Japan. *Clay Miner.* 21:401-415.
- Norrish, K. 1968. Some phosphate minerals of soils, p. 713-723. *Trans. 9th Int. Congr. Soil Sci.*, 6-16 August 1968, Adelaide, Australia.
- Norrish, K. 1973. Factors in the weathering of mica to vermiculite, p. 417-432. *In* J.M. Serratos (ed.) *Proc. 1972 Int. Clay Conf.*, Div. de Ciencias., 25-30 June 1972, Madrid, Spain.
- Norrish, K., and J.G. Pickering. 1983. Clay minerals, p. 281-308. *In* *Soils: An Australian viewpoint*. CSIRO, Melbourne, Australia.
- Norrish, K., and H. Rosser. 1983. Mineral phosphate, p. 335-361. *In* *Soils: An Australian viewpoint*. CSIRO, Melbourne, Australia.
- Oades, J.M., and A.G. Waters. 1991. Aggregate hierarchy in soils. *Aust. J. Soil Res.* 29:815-828.
- Oelkers, E.H., and S.R. Gislason. 2001. The mechanism, rates and consequences of basaltic glass dissolution: I. An experimental study of the dissolution rates of basaltic glass as a function of aqueous Al, Si and oxalic acid concentration at 25°C and pH = 3 and 11. *Geochim. Cosmochim. Acta* 65:3671-3681.
- Oelkers, E.H., and J. Schott. 1995. Experimental study of anorthite dissolution and the relative mechanism of feldspar hydrolysis. *Geochim. Cosmochim. Acta* 59:5039-5053.
- Ogura, Y., R. Tanaka, and H. Takesako. 2008. Unique clay mineral formation in Andisols derived from Holocene tephra of Mt Fuji, Japan, p. 105. Abstracts, Joint Conf. Australia and New Zealand Soc. Soil Sci., 1-5 December 2008, Palmerston North, New Zealand.
- Ojanuga, A.G. 1973. Weathering of biotite in soils of a humid tropical climate. *Soil Sci. Soc. Am. Proc.* 37:644-646.
- Owliaie, H.R., A. Abtahi, and R.J. Heck. 2006. Pedogenesis and clay mineralogical investigation of soils formed on gypsiferous and calcareous materials, on a transect, southwestern Iran. *Geoderma* 134:62-81.
- Pai, C.W., M.K. Wang, and C.Y. Chiu. 2007. Clay mineralogical characterization of a toposequence of perhumid subalpine forest soils in northeastern Taiwan. *Geoderma* 138:177-184.
- Pai, C.W., M.K. Wang, H.B. King, C.Y. Chiu, and J.-L. Hwang. 2004. Hydroxy-interlayered mineral of forest soils. *Geoderma* 123:245-255.
- Papoulis, D., P. Tsolis-Katagas, and C. Katagas. 2004. Progressive stages in the formation of kaolin minerals of different morphologies in the weathering of plagioclase. *Clays Clay Miner.* 52:275-286.
- Paquet, H., and G. Millot. 1972. Geochemical evolution of clay minerals in the weathered products in soils of Mediterranean climate, p. 199-206. *In* J.M. Serratos (ed.) *Proc. Int. Clay Conf.*, 25-30 June 1972, Madrid, Spain.
- Parfitt, R.L. 1990. Allophane in New Zealand—A review. *Aust. J. Soil Res.* 28:343-360.
- Parfitt, R.L. 2009. Allophane and imogolite: Role in soil biogeochemical processes. *Clay Miner.* 44:135-155.

- Parfitt, R.L., and G.J. Churchman. 1988. Clay minerals and humus complexes in five Kenyan soils derived from volcanic ash—A discussion. *Geoderma* 42:365–367.
- Parfitt, R.L., and T. Henmi. 1980. Structure of some allophanes from New Zealand. *Clays Clay Miner.* 28:285–294.
- Parfitt, R.L., M. Russell, and G.E. Orbell. 1983. Weathering sequence of soils from volcanic ash involving allophane and halloysite, New Zealand. *Geoderma* 29:41–57.
- Parfitt, R.L., M. Saigusa, and J.D. Cowie. 1984. Allophane and halloysite formation in a volcanic ash bed under differing moisture conditions. *Soil Sci.* 138:360–364.
- Parfitt, R.L., and A.D. Wilson. 1985. Estimation of allophane and halloysite in three sequences of volcanic soils, New Zealand. *Catena Suppl.* 7:1–8.
- Paton, T.R., G.S. Humphreys, and P.B. Mitchell. 1995. *Soils: A new global view*. UCL Press, London, U.K.
- Pauling, L. 1929. The principles determining the structure of complex ionic crystals. *J. Am. Chem. Soc.* 51:1010–1026.
- Percival, H.J. 1985. Soil solutions, minerals, and equilibria. New Zealand Soil Bureau Scientific Report 69. Department of Scientific and Industrial Research, Lower Hutt, New Zealand.
- Percival, H.J., R.L. Parfitt, and N.A. Scott. 2000. Factors controlling soil carbon levels in New Zealand grasslands: Is clay content important? *Soil Sci. Soc. Am. J.* 64:1623–1630.
- Pernes-Debuyser, A., M. Pernes, B. Velde, and D. Tessier. 2003. Soil mineralogy evolution in the INRA 42 plots experiment. *Clays Clay Miner.* 51:577–584.
- Petit, S., T. Prot, A. Decarreau, C. Mosser, and M.C. Toledo-Groke. 1992. Crystallochemical study of a population of particles in smectites from a lateritic weathering profile. *Clays Clay Miner.* 40:436–445.
- Pochet, G., M. Van der Velde, M. Vanclooster, and B. Delvaux. 2007. Hydric properties of high charge, halloysite clay soils from the tropical South Pacific region. *Geoderma* 138:96–109.
- Poncelot, G.M., and G.W. Brindley. 1967. Experimental formation of kaolinite from montmorillonite at low temperatures. *Am. Mineral.* 52:1161–1173.
- Poulenard, J., P. Podwojewski, and A.J. Herbillon. 2003. Characteristics of non-allophanic Andisols with hydric properties from the Ecuadorian páramos. *Geoderma* 117:267–281.
- Poulet, F., J.-P. Bibring, J.F. Mustard, A. Gendrin, N. Mangold, Y. Langevin, R.E. Arvidson, B. Gondet, and C. Gomez. 2005. Phyllosilicates on Mars and implications for the early Mars history. *Nature* 438:632–627.
- Proust, D., J. Caillaud, and C. Fontaine. 2006. Clay minerals in early amphibole weathering: Tri- to dioctahedral sequence as a function of crystallization sites in the amphibole. *Clays Clay Miner.* 54:351–362.
- Quantin, P., T. Becquer, J.H. Rouiller, and J. Berthelin. 2001. Oxide weathering and trace metal release by bacterial reduction in a New Caledonia Ferralsol. *Biogeochemistry* 53:323–340.
- Quantin, P., A.J. Herbillon, C. Janot, and G. Siefferman. 1984. L' "halloysite" blanche riche en fer de Vate (Vanuatu); hypothese d'un edifice interstratifié halloysite-hisingerite. *Clay Miner.* 19:629–643.
- Raman, K.V., and M.L. Jackson. 1966. Layer charge reduction in clay minerals of micaceous soils and sediments. *Clays Clay Miner.* 14:53–68.
- Rampazzo, N., and W.E.H. Blum. 1992. Changes in chemistry and mineralogy of forest soils by acid rain. *Water Air Soil Pollut.* 61:209–220.
- Rasmussen, C., N. Matsuyama, R.A. Dahlgren, R.J. Southard, and N. Brauer. 2007. Soil genesis and mineral transformation across an environmental gradient on andesitic lahar. *Soil Sci. Soc. Am. J.* 71:225–237.
- Rasmussen, C., R.J. Southard, and W.R. Horwath. 2005. Soil mineralogy affects conifer forest soil carbon source utilization and microbial priming. *Soil Sci. Soc. Am. J.* 71:1141–1150.
- Rebertus, R.A., S.B. Weed, and S.W. Buol. 1986. Transformations of biotite to kaolinite during saprolite-soil weathering. *Soil Sci. Soc. Am. J.* 50:810–819.
- Reid, D.A., R.C. Graham, L.A. Douglas, and C. Amrhein. 1996. Smectite mineralogy and charge characteristics along an arid geomorphic transect. *Soil Sci. Soc. Am. J.* 60:1602–1611.
- Rex, R.W., J.K. Syers, M.L. Jackson, and R.N. Clayton. 1969. Eolian origin of quartz in soils of Hawaiian islands and in Pacific pelagic sediments. *Science* 163:277–279.
- Rice, C.M., and J.M. Williams. 1969. A Mössbauer study of biotite weathering. *Miner. Mag.* 37:210–215.
- Rich, C.I. 1968. Hydroxy interlayers in expansible layer silicates. *Clays Clay Miner.* 16:15–30.
- Richards, A.E., R.C. Dalal, and S. Schmidt. 2009. Carbon storage in a Ferrasol under subtropical rainforest, tea plantations, and pasture is linked to soil aggregation. *Aust. J. Soil Res.* 47:341–350.
- Righi, D., K. Huber, and C. Keller. 1999. Clay formation and podzol development from postglacial moraines in Switzerland. *Clay Miner.* 34:319–332.
- Righi, D., S. Petit, and A. Bouchet. 1993. Characterization of hydroxy-interlayered vermiculite and illite/smectite interstratified minerals from the weathering of a chlorite in a Cryorthod. *Clays Clay Miner.* 41:484–495.
- Righi, D., F. Terribile, and S. Petit. 1995. Low-charge to high-charge beidellite conversion in a Vertisol from south Italy. *Clays Clay Miner.* 43:495–502.
- Ritsema, C.J., M.E.F. van Mensvoort, D.L. Dent, Y. Tan, H. van den Bosch, and A.L.M. van Wijk. 2000. Acid sulfate soils, p. G121–G154. *In* M.E. Sumner (ed.) *Handbook of soil science*. CRC Press, Boca Raton, FL.
- Rivers, J.M., J.E. Nyquist, Y. Roh, D.O. Terry, Jr., and W.E. Doll. 2004. Investigation into the origin of magnetic soils on the Oak Ridge reservation, Tennessee. *Soil Sci. Soc. Am. J.* 68:1772–1779.
- Robert, M., and J. Berthelin. 1986. Role of biological and biochemical factors in soil mineral weathering, p. 453–495. *In* P.M. Huang and M. Schnitzer (eds.) *Interactions of soil minerals with natural organics and microbes*. SSSA Special Publication No. 17. SSSA, Madison, WI.
- Robert, M., and C. Chenu. 1992. Interactions between soil minerals and microorganisms, p. 307–404. *In* G. Stotsky and J.-M. Bollag (eds.) *Soil biochemistry*. Marcel Dekker, New York.

- Robert, M., M. Hardy, and F. Elsass. 1991. Crystallochemistry, properties and organization of soil clays derived from major sedimentary rocks in France. *Clay Miner.* 26:409–420.
- Robertson, I.D.M., and R.A. Eggleton. 1991. Weathering of granitic muscovite to kaolinite and halloysite and of plagioclase-derived kaolinite to halloysite. *Clays Clay Miner.* 39:113–126.
- Robinson, D.A., I. Lebro, and H. Vereecken. 2009. On the definition of the natural capital of soils: A framework for description, evaluation, and monitoring. *Soil Sci. Soc. Am. J.* 73:1904–1911.
- Ross, G.J., and M.M. Mortland. 1966. A soil beidellite. *Soil Sci. Soc. Am. Proc.* 39:337–343.
- Ross, G.J., C. Wang, A.I. Ozkan, and H.W. Rees. 1982. Weathering of chlorite and mica in New Brunswick podzol developed on till derived from chlorite–mica schist. *Geoderma* 27:255–267.
- Russell, E.W. 1973. *Soil conditions and plant growth*. 10th edn. Longman, London, U.K.
- Ruxton, B.P. 1988. Towards a weathering model of Mount Lamington Ash, New Guinea. *Earth Sci. Rev.* 25:387–397.
- Ryan, P.C., and F.J. Huertas. 2009. The temporal evolution of pedogenic Fe–smectite to Fe–kaolin via interstratified kaolin–smectite in a moist tropical soil chronosequence. *Geoderma* 151:1–15.
- Saggar, S., A. Parshotam, G.P. Sparling, C.W. Feltham, and P.B.S. Hart. 1996. ¹⁴C-labelled ryegrass turnover and residence times in soils varying in clay content and mineralogy. *Soil Biol. Biochem.* 28:1677–1686.
- Saigusa, M., S. Shoji, and T. Kato. 1978. Origin and nature of halloysite in Ando soils from Towada tephra. *Geoderma* 20:115–129.
- Sakharov, B.A., and V. Drits. 1973. Mixed-layer kaolinite–montmorillonite: A comparison of observed and calculated diffraction patterns. *Clays Clay Miner.* 21:15–17.
- Sase, T., M. Hosono, T. Utsugawa, and K. Aoki. 1988. Opal phylolith analysis of present and buried volcanic ash soils at Te Ngae Road tephra section, Rotorua Basin, North Island, New Zealand. *Quat. Res. (Japan)* 27:153–163.
- Sawhney, B.L. 1972. Selective sorption and fixation of cations by clay minerals: a review. *Clays Clay Miner.* 20:93–100.
- Sawhney, B.L., and M.L. Jackson. 1958. Soil montmorillonite formulas. *Soil Sci. Soc. Am. Proc.* 22:115–118.
- Scalenghe, R., E. Bonifacio, L. Celi, F.C. Ugolini, and E. Zanini. 2002. Pedogenesis in disturbed alpine soils (NW Italy). *Geoderma* 109:207–224.
- Schaefer, C.E.G.R., R.J. Gilkes, and R.B.A. Fernandes. 2004. EDS/SEM study on microaggregates of Brazilian Latosols, in relation to P adsorption and clay fraction attributes. *Geoderma* 123:69–81.
- Schaetzl, R.J., and S. Anderson. 2005. *Soils—Genesis and geomorphology*. Cambridge University Press, Cambridge, U.K.
- Schott, J., and R.A. Berner. 1985. Dissolution mechanisms of pyroxenes and olivines during weathering, p. 35–53. *In* J.I. Drever (ed.) *The chemistry of weathering*. Reidel, New York.
- Schwertmann, U. 2008. Iron oxides, p. 363–369. *In* W. Chesworth (ed.) *Encyclopaedia of soil science*. Springer, Dordrecht, the Netherlands.
- Schwertmann, U., and R.M. Taylor. 1989. Iron oxides, p. 379–438. *In* J.B. Dixon and S.B. Weed (eds.) *Minerals in soil environments*. 2nd edn. SSSA, Madison, WI.
- Sedov, S., E. Solleiro-Rebolledo, P. Morales-Puente, A. Arias-Herrie, E. Vallejo-Gómez, and C. Jasso-Castañeda. 2003. Mineral and organic components of the buried paleosols of the Nevado de Toluca, central Mexico as indicators of paleoenvironments and soil evolution. *Quat. Int.* 106–107:169–184.
- Senkayi, A.L., J.B. Dixon, L.R. Hossner, and B.E. Viani. 1983. Mineralogical transformations during weathering of lignite overburden in east Texas. *Clays Clay Miner.* 31:49–56.
- Seyama, H., M. Soma, and A. Tanaka. 1996. Surface characterization of acid-leached olivines by X-ray photoelectron spectroscopy. *Chem. Geol.* 129:209–216.
- Seybold, C.A., R.B. Grossman, and T.G. Reinsch. 2005. Predicting cation exchange capacity for soil survey using linear methods. *Soil Sci. Soc. Am. Proc.* 69:856–863.
- Shepherd, T.G. 1984. A pedological study of the Hamilton Ash Group at Welches Road, Mangawara, north Waikato. Unpublished M.Sc. thesis. University of Waikato, Hamilton, New Zealand.
- Shikazono, N., A. Takino, and H. Ohtani. 2005. An estimate of dissolution rate constant of volcanic glass in volcanic ash soil from the Mt. Fuji area, central Japan. *Geochem. J.* 39:185–196.
- Shoji, S., M. Nanzyo, and R.A. Dahlgren. 1993a. Volcanic ash soils: Genesis, properties and utilization. *Developments in soil science*. Vol. 21. Elsevier, Amsterdam, the Netherlands.
- Shoji, S., M. Nanzyo, Y. Shirato, and T. Ito. 1993b. Chemical kinetics of weathering in young Andisols from northeastern Japan using soil age normalized to 10°C. *Soil Sci.* 155:53–60.
- Shoji, S., M. Nanzyo, and T. Takahashi. 2006. Factors of soil formation: Climate. As exemplified by volcanic ash soils, p. 131–149. *In* G. Certini and R. Scalenghe (eds.) *Soils: Basic concepts and future challenges*. Cambridge University Press, Cambridge, U.K.
- Siffert, B. 1978. Genesis and synthesis of clays and clay minerals: Recent developments and future prospects, p. 337–347. *In* M.M. Mortland and V.C. Farmer (eds.) *Developments in sedimentology*. Vol. 27. Int. Clay Conf. 1978. Elsevier, Amsterdam, the Netherlands.
- Sigfusson, B., S.R. Gislason, and G.I. Paton. 2008. Pedogenesis and weathering rates of a Histic Andosol in Iceland: Field and experimental soil solution study. *Geoderma* 144:572–592.
- Simas, F.N.B., C.E.G.R. Schaefer, E.I.F. Filho, A.C. Chagas, and P.C. Brandão. 2005. Chemistry, mineralogy and micropedology of highland soils on crystalline rocks of Serra da Mantiqueira, southeastern Brazil. *Geoderma* 125:187–201.
- Simas, F.N.B., C.E.G.R. Schaefer, V.F. Melo, M.B.B. Guerra, M. Saunders, and R.J. Gilkes. 2006. Clay-sized minerals in permafrost-affected soils (Cryosols) from King George Island, Antarctica. *Clays Clay Miner.* 54:721–736.

- Simonsson, M., S. Hillier, and I. Öborn. 2009. Changes in clay minerals and potassium fixation capacity as a result of release and fixation of potassium in long-term field experiments. *Geoderma* 151:109–120.
- Singer, A. 1989. Palygorskite and sepiolite group minerals, p. 829–872. In J.B. Dixon and S.B. Weed (eds.) *Minerals in soil environments*. 2nd edn. SSSA, Madison, WI.
- Singer, A. 2002. Palygorskite and sepiolite, p. 555–584. In J.B. Dixon and D.G. Schulze (eds.) *Soil mineralogy with environmental applications*. SSSA, Madison, WI.
- Singer, A., and A. Banin. 1990. Characteristics and mode of formation of palagonite: A review, p. 173–181. In V.C. Farmer and Y. Tardy (eds.) *Proc. 9th Int. Clay Conf.*, 28 August–2 September 1989, Strasbourg, France.
- Singer, A., and K. Norrish. 1974. Pedogenic palygorskite occurrences in Australia. *Am. Mineral.* 59:508–517.
- Singer, A., M. Zarei, F.M. Lange, and K. Stahr. 2004. Halloysite characteristics and formation in the northern Golan Heights. *Geoderma* 123:279–295.
- Singh, B., and R.J. Gilkes. 1991. A potassium-rich beidellite from a lateritic pallid zone in Western Australia. *Clay Miner.* 26:233–244.
- Singh, B., and R.J. Gilkes. 1992a. Properties of soil kaolinites from south-western Australia. *J. Soil Sci.* 43:645–667.
- Singh, B., and R.J. Gilkes. 1992b. The electron-optical investigation of the alteration of kaolinite to halloysite. *Clays Clay Miner.* 40:212–229.
- Singh, B., and R.J. Gilkes. 1993. The recognition of amorphous silica in indurated soil profiles. *Clay Miner.* 28:461–474.
- Singleton, P.L., M. Mcleod, and H.J. Percival. 1989. Allophane and halloysite content and soil solution silicon in soils from rhyolitic volcanic material, New Zealand. *Aust. J. Soil Res.* 27:67–77.
- Skiba, M. 2007. Clay mineral formation during podzolization in an alpine environment of the Tatra Mountains, Poland. *Clays Clay Miner.* 55:618–637.
- Smeck, N.E., J.M. Bigham, W.F. Guertal, and G.F. Hall. 2002. Spatial distribution of lepidocrocite in a soil hydrosequence. *Clay Miner.* 37:687–697.
- Smith, W.W. 1962. Weathering of some Scottish basic igneous rocks with reference to soil formation. *J. Soil Sci.* 13:202–215.
- Smith, K.L., A.R. Milnes, and R.A. Eggleton. 1987. Weathering of basalt: Formation of iddingsite. *Clays Clay Miner.* 35:418–428.
- Smits, M.M., E. Hoffland, A.G. Jongmans, and N. Van Breeman. 2005. Contribution of mineral tunnelling to total feldspar weathering. *Geoderma* 125:59–69.
- Soma, M., G.J. Churchman, and B.K.G. Theng. 1992. X-ray photoelectron spectroscopic analysis of halloysites with different composition and particle morphology. *Clay Miner.* 27:413–421.
- Sousa, E.C., and H. Eswaran. 1975. Alteration of micas in the saprolite of a profile from Angola. A morphological study. *Pedologie* 25:71–79.
- Sparling, G.P., D. Wheeler, E.-T. Vesely, and L.A. Schipper. 2006. What is soil organic matter worth? *J. Environ. Qual.* 35:548–557.
- Spielvogel, S., J. Preitzel, and I. Kögel-Knabner. 2008. Soil organic matter stabilization in acidic forest soils is preferential and soil type-specific. *Eur. J. Soil Sci.* 59:674–692.
- Sposito, G. 1989. *The chemistry of soils*. Oxford University Press, New York.
- Sridhar, K., and M.L. Jackson. 1974. Layer charge decrease by tetrahedral cation removal and silicon incorporation during natural weathering of phlogopite to saponite. *Soil Sci. Soc. Am. Proc.* 38:847–851.
- Sridhar, K., M.L. Jackson, and R.N. Clayton. 1975. Quartz oxygen isotopic stability in relation to isolation from sediments and diversity of source. *Soil Sci. Soc. Am. Proc.* 42:1209–1213.
- Starr, M., and A.-J. Lindroos. 2006. Changes in the rate of release of Ca and Mg and normative mineralogy due to weathering along a 5300-year chronosequence of boreal forest soils. *Geoderma* 133:269–280.
- Stephen, I., and D.M.C. MacEwan. 1951. Some chlorite minerals of unusual type. *Clay Miner. Bull.* 1:157–161.
- Stevens, K.F., and C.G. Vucetich. 1985. Weathering of Upper Quaternary tephros in New Zealand. 2. Clay minerals and their climatic interpretation. *Chem. Geol.* 53:237–247.
- Stewart, R.B., V.E. Neall, and J.K. Syers. 1984. Occurrence and source of quartz in six basaltic soils from Northland, New Zealand. *Aust. J. Soil Res.* 22:365–377.
- Stoch, L., and W. Sikora. 1976. Transformation of micas in the process of kaolinitization of granites and gneisses. *Clays Clay Miner.* 24:156–162.
- Stroncik, N.A., and H.-U. Schmincke. 2001. Evolution of palagonite: Crystallization, chemical changes, and element budget. *Geochem. Geophys. Geosyst.* 2:1017. doi:10.1029/2000GC000102.
- Stroncik, N.A., and H.-U. Schmincke. 2002. Palagonite—A review. *Int. J. Earth Sci.* 91:680–697.
- Stucki, J.W., and C.B. Roth. 1977. Oxidation reduction mechanism for structural iron in nontronite. *Soil Sci. Soc. Am. J.* 41:808–814.
- Sudo, T., and H. Yatsumoto. 1977. The formation of halloysite tubes from spherulitic halloysite. *Clays Clay Miner.* 25:155–159.
- Surapaneni, A., A.S. Palmer, R.W. Tillman, J.H. Kirkman, and P.E.H. Gregg. 2002. The mineralogy and potassium supplying power of some loessial and related soils of New Zealand. *Geoderma* 110:191–204.
- Swindale, L.D., and G. Uehara. 1966. Ionic relationships in the pedogenesis of Hawaiian soils. *Soil Sci. Soc. Am. Proc.* 30:726–730.
- Syers, J.K., V.E. Berkheiser, M.L. Jackson, R.N. Clayton, and R.W. Rex. 1969. Eolian sediment influence on pedogenesis during the Quaternary. *Soil Sci.* 107:421–427.
- Takahashi, T., R.A. Dahlgren, B.K.G. Theng, J.S. Whitton, and M. Soma. 2001. Potassium-selective, halloysite-rich soils formed in volcanic materials from northern California. *Soil Sci. Soc. Am. J.* 65:516–526.

- Takahashi, T., R. Dahlgren, and P. van Susteren. 1993. Clay mineralogy and chemistry of soils formed in volcanic materials in the xeric moisture regime of northern California. *Geoderma* 59:131–150.
- Takesako, H., D.J. Lowe, G.J. Churchman, and D.J. Chittleborough. 2010. Holocene volcanic soils in the Mt Gambier region, South Australia, p. 47–50. Proceedings published on DVD and at <http://www.iuss.org>, IUSS 19th World Soil Cong., Brisbane (August 1–6, 2010), Symposium 1.3.1 Pedogenesis: Ratio and range of influence.
- Tamm, O. 1922. Eine methode Zur Bestimmung de anorganischen Komponente des Gelcomplexes im Boden. *Meddelanden fran Statens skogsforsokanstalt Stockholm* 19:387–404.
- Taubaso, C., M. Dos Santos Afonso, and R.M. Torres Sánchez. 2004. Modelling soil surface charge density using mineral composition. *Geoderma* 121:123–133.
- Taylor, R.M. 1988. Proposed mechanism for the formation of soluble Si–Al and Fe(III)–Al hydroxyl complexes in soils. *Geoderma* 42:65–77.
- Tazaki, K. 1979. Micromorphology of halloysite produced by weathering of plagioclase in volcanic ash. *Dev. Sedimentol.* 27:415–422.
- Tazaki, K. 1997. Biomineralization of layer silicates and hydrated Fe/Mn oxides in microbial mats: An electron microscopical study. *Clays Clay Miner.* 45:203–212.
- Tazaki, K. 2005. Microbial formation of a halloysite-like mineral. *Clays Clay Miner.* 53:224–233.
- Theng, B.K.G. 1995. On measuring the specific surface area of clays and soils by adsorption of para-nitrophenol: Use and limitations, p. 304–310. *In* G.J. Churchman, R.W. Fitzpatrick, and R.A. Eggleton (eds.) *Clays: Controlling the environment*. Proc. 10th Int. Clay Conf. Adelaide, Australia. CSIRO Publishing, Melbourne, Australia.
- Theng, B.K.G., M. Russell, G.J. Churchman, and R.L. Parfitt. 1982. Surface properties of allophane, halloysite, and imogolite. *Clays Clay Miner.* 30:143–149.
- Theng, B.K.G., and G. Yuan. 2008. Nanoparticles in the soil environment. *Elements* 4:395–399.
- Thiry, M., and R. Simon-Coinçon. 1996. Tertiary paleoweatherings and silcretes in the southern Paris Basin. *Catena* 26:1–26.
- Thompson, A., O.A. Chadwick, D.G. Rancourt, and J. Chorover. 2006. Iron-oxide crystallinity increases during soil redox oscillations. *Geochim. Cosmochim. Acta* 70:1710–1727.
- Thompson, M.L., and L. Ukrainczyk. 2002. Micas, p. 431–466. *In* J.B. Dixon and D.G. Schulze (eds.) *Soil mineralogy with environmental applications*. SSSA, Madison, WI.
- Thorseth, I.H., H. Furnes, and O. Tumor. 1995. Textural and chemical effects of bacterial-activity on basaltic glass—An experimental approach. *Chem. Geol.* 119:139–160.
- Tonkin, P.J. 1970. Contorted stratification with clay lobes in volcanic ash beds, Raglan-Hamilton region, New Zealand. *Earth Sci. J.* 4:129–140.
- Torres, S.R.M., M. Okamura, and R.C. Mercader. 2001. Charge properties of red Argentine soils as an indicator of iron oxide/clay associations. *Aust. J. Soil Res.* 39:423–434.
- Trakoonyingcharoen, P., I. Kheoruenromne, A. Suddhiprakarn, and R.J. Gilkes. 2006. Properties of iron oxides in red Ultisols as affected by rainfall and soil parent material. *Aust. J. Soil Res.* 44:63–70.
- Trolard, F., J.-M. Génin, M. Abdelmoula, G. Bourrié, B. Humbert, and A. Herbillon. 1997. Identification of a green rust mineral in a reductomorphic soil by Mössbauer and Raman spectroscopies. *Geochim. Cosmochim. Acta* 61:1107–1111.
- Turpault, M.-P., D. Righi, and C. Utérano. 2008. Clay minerals: Precise markers of the spatial and temporal variability of the biogeochemical soil environment. *Geoderma* 147:108–115.
- Tye, A.M., S.J. Kemp, and P.R. Poulton. 2009. Responses of soil clay mineralogy in the Rothamsted classical experiments to management practice and changing land use. *Geoderma* 153:136–146.
- Ueshima, M., and Tazaki, K. 2001. Possible role of microbial polysaccharides in nontronite formation. *Clays Clay Miner.* 49:292–299.
- Ugolini, F.C., R. Dahlgren, J. LaManna, W. Nuhn, and J. Zachara. 1991. Mineralogy and weathering processes in recent and Holocene tephra deposits of the Pacific Northwest, USA. *Geoderma* 51:277–299.
- Ugolini, F.C., and R.S. Sletten. 1991. The role of proton donors in pedogenesis as revealed by soil solution studies. *Soil Sci.* 151:59–75.
- Urrutia, M.M., and T.J. Beveridge. 1994. Formation of fine-grained silicate minerals and metal precipitates by a bacterial surface (*Bacillus subtilis*). *Chem. Geol.* 116:261–280.
- Vacca, A., P. Adamo, M. Pigna, and P. Violante. 2003. Genesis of tephra-derived soils from the Roccamonfina volcano, south central Italy. *Soil Sci. Soc. Am. J.* 67:198–207.
- van Breeman, N. 1992. Soil: Biotic construction in a Gaian sense, p. 189–207. *In* A. Teller, P. Muthy, and J.N.R. Jeffers (eds.) *Responses of forest ecosystems to environmental change*. Elsevier, Amsterdam, the Netherlands.
- van Breemen, N., R.D. Findlay, U.S. Lundström, A.G. Jongmans, R. Giesler, and M. Olsson. 2000a. Mycorrhizal weathering: A true case of mineral nutrition? *Biogeochemistry* 49:53–67.
- van Breemen, N., and A.C. Finzi. 1998. Plant-soil interactions: Ecological aspects and evolutionary implications. *Biogeochemistry* 42:1–19.
- van Breemen, N., U.S. Lundström, and A.G. Jongmans. 2000b. Do plants drive podzolisation via rock-eating mycorrhizal fungi? *Geoderma* 94:163–171.
- van Raij, B., and M. Peech. 1972. Electrochemical properties of some Oxisols and Alfisols of the tropics. *Proc. Soil Sci. Soc. Am.* 36:587–593.
- Van Ranst, E., and F. De Coninck. 2002. Evaluation of ferrollysis in soil formation. *Eur. J. Soil Sci.* 53:513–519.
- van Wesemael, B., J.M. Verstraten, and J. Sevink. 1995. Pedogenesis by clay dissolution on acid, low-grade metamorphic rocks under Mediterranean forests in southern Tuscany (Italy). *Catena* 24:105–125.

- Varajão, A.F.D.C., R.J. Gilkes, and R.D. Hart. 2001. The relationships between kaolinite crystal properties and the origin of materials for a Brazilian kaolin deposit. *Clays Clay Miner.* 49:44–59.
- Velbel, M.A. 1985. Geochemical mass balances and weathering rates in forested watersheds of the southern Blue Ridge. *Am. J. Sci.* 285:904–930.
- Velbel, M.A., and W.W. Barker. 2008. Pyroxene weathering to smectite: Conventional and cryo-field emission scanning microscopy, Koua Bocca ultramafic complex, Ivory Coast. *Clays Clay Miner.* 56:112–127.
- Velde, B. (ed.). 1995. *Origin and mineralogy of clays*. Springer-Verlag, New York.
- Velde, B., and P. Barré. 2010. *Soils, plants and clay minerals: Mineral and biologic interactions*. Springer-Verlag, Berlin, Germany.
- Velde, B., B. Goffé, and A. Hoellard. 2003. Evolution of clay minerals in a chronosequence of poldered sediments under the influence of a natural pasture development. *Clays Clay Miner.* 51:205–217.
- Velde, B., and A. Meunier. 2008. *The origin of clay minerals in soils and weathered rocks*. Springer-Verlag, Berlin, Germany.
- Velde, B., and T. Peck. 2002. Clay mineral changes in the Morrow experimental plots, University of Illinois. *Clays Clay Miner.* 50:364–370.
- Vepraskas, M.J. 1992. Redoximorphic features for identifying aquic conditions. North Carolina Agricultural Research Service Technical Bulletin No. 301. North Carolina State University, Raleigh, NC.
- Vepraskas, M.J., X. He, D.L. Lindbo, and R.W. Skaggs. 2004. Calibrating hydric soil field indicators to long-term wetland hydrology. *Soil Sci. Soc. Am. J.* 68:146–1469.
- Verrecchia, E.P., and M.-N. Le Coustumer. 1996. Occurrence and genesis of palygorskite and associated clay minerals in a Pleistocene calcrete complex, Sde Boqer, Negev Desert, Israel. *Clay Miner.* 31:183–202.
- Viana, J.H.M., P.R.C. Couceiro, M.C. Pereira, J.D. Fabris, E.I. Fernandes Filho, C.E.G.R. Schaefer, H.R. Rechenberg, W.A.P. Abrahão, and E.C. Mantovani. 2006. Occurrence of magnetite in the sand fraction of an oxisol in the Brazilian savanna ecosystem, developed from a magnetite-free lithology. *Aust. J. Soil Res.* 44:71–83.
- Vicente, M.A., M. Razzaghe, and M. Robert. 1977. Formation of aluminium hydroxy vermiculite (intergrade) and smectite from mica under acidic conditions. *Clay Miner.* 12:101–112.
- Vingiani, S., D. Righi, S. Petit, and F. Terribile. 2004. Mixed-layer kaolinite–smectite minerals in a red-black soil sequence from basalt in Sardinia (Italy). *Clays Clay Miner.* 52:473–483.
- Wada, K. 1987. Minerals formed and mineral formation from volcanic ash by weathering. *Chem. Geol.* 60:17–28.
- Wada, K. 1989. Allophane and imogolite, p. 1051–1087. *In* J.B. Dixon and S.B. Weed (eds.) *Minerals in soil environments*. 2nd edn. SSSA Book Series No. 1. SSSA, Madison, WI.
- Wada, K., and Y. Kakuto. 1983. Intergradient vermiculite-kaolin mineral in a Korean Ultisol. *Clays Clay Miner.* 31:183–190.
- Wada, K., and Y. Kakuto. 1989. “Chloritized” vermiculite in a Korean Ultisol studied by ultramicrotomy and transmission electron microscopy. *Clays Clay Miner.* 37:263–268.
- Wada, K., Y. Kakuto, and F.N. Muchena. 1987. Clay minerals and humus complexes in five Kenyan soils derived from volcanic ash. *Geoderma* 39:307–321.
- Wada, K., and N. Yoshinaga. 1969. The structure of imogolite. *Am. Mineral.* 54:50–71.
- Wallace, R.C. 1991. *New Zealand theses in earth sciences. The mineralogy of the Tokomaru silt loam and the occurrence of cristobalite and tridymite in selected North Island soils*. *N.Z. J. Geol. Geophys.* 34:113.
- Wan, J., T. Tyliczszak, and T.K. Tokunga. 2007. Organic carbon distribution, speciation, and elemental correlations within soil microaggregates: Applications of STXM and NEXAFS spectroscopy. *Geochim. Cosmochim. Acta* 71:5439–5449.
- Wang, C., J.A. McKeague, and H. Kodama. 1986. Pedogenic imogolite and soil environments: Case study of spodosols in Quebec, Canada. *Soil Sci. Soc. Am. J.* 50:711–718.
- Ward, W.T. 1967. Volcanic ash beds of the lower Waikato Basin, North Island, New Zealand. *N.Z. J. Geol. Geophys.* 10:1109–1135.
- Watanabe, T., Y. Sawada, J.D. Russell, W.J. McHardy, and M.J. Wilson. 1992. The conversion of montmorillonite to interstratified halloysite–smectite by weathering in the Omi acid clay deposit. *Clay Miner.* 27:159–173.
- Waychunas, G.A., and H. Zhang. 2008. Structure, chemistry, and properties of mineral nanoparticles. *Elements* 4:381–387.
- Weaver, C.E. 1989. *Clays, muds and shales. Developments in sedimentology*. Vol. 44. Elsevier, Amsterdam, the Netherlands.
- Welch, S.A., and J.F. Banfield. 2002. Modification of olivine surface morphology and reactivity by microbial activity during chemical weathering. *Geochim. Cosmochim. Acta* 66:213–221.
- Wentworth, S.A. 1970. Illite. *Clay Sci.* 3:140–155.
- Wentworth, S.J., E.K. Gibson, M.A. Velbel, and D.S. McKay. 2005. Antarctic dry valleys and indigenous weathering in Mars meteorites: Implications for water and life on Mars. *Icarus* 174:383–395.
- White, A.F., A.E. Blum, M.S. Schulz, T.D. Bullen, J.W. Harden, and M.L. Peterson. 1996. Chemical weathering rates of a soil chronosequence on granitic alluvium: 1. Quantification of mineralogical and surface area changes and calculation of primary silicate reaction rates. *Geochim. Cosmochim. Acta* 60:2553–2550.
- White, A.F., and S.L. Brantley. 2003. The effect of time on the weathering of silicate minerals: Why do weathering rates differ in the laboratory and field? *Chem. Geol.* 202:479–506.
- White, G.N., and J.B. Dixon. 2002. Kaolin–serpentine minerals, p. 389–414. *In* J.B. Dixon and D.G. Schulze (eds.) *Soil mineralogy with environmental applications*. SSSA Book Series No. 7. SSSA, Madison, WI.

- White, A.F., M.S. Schulz, D.V. Vivit, A.E. Blum, D.A. Stonestrom, and J.W. Harden. 2005. Chemical weathering rates of a soil chronosequence on granitic alluvium: III. Hydrochemical evolution and contemporary solute fluxes and rates. *Geochim. Cosmochim. Acta* 69:1975–1996.
- Wildman, W.E., M.L. Jackson, and L.D. Whittig. 1968. Serpentinite rock dissolution as a function of carbon dioxide pressure in aqueous solution. *Am. Mineral.* 53:1252–1263.
- Wilson, M.J. 1970. A study of weathering in a soil derived from a biotite–hornblende rock. I. Weathering of biotite. *Clay Miner.* 8:291–303.
- Wilson, M.J. 1987. Soil smectites and related interstratified minerals: Recent developments, p. 167–173. *In* L.G. Schultz, H. van Olphen, and F.A. Mumpton (eds.) *Proc. Int. Clay Conf.* Denver, 1995. The Clay Minerals Society, Bloomington, IN.
- Wilson, M.J. 1999. The origin and formation of clay minerals in soils: Past, present and future perspectives. *Clay Miner.* 34:7–25.
- Wilson, M.J. 2004. Weathering of the primary rock-forming minerals: Processes, products and rates. *Clay Miner.* 39:233–266.
- Wilson, M.J. 2006. Factors of soil formation: Parent material. As exemplified by a comparison of granitic and basaltic soils, p. 113–129. *In* G. Certini and R. Scalenghe (eds.) *Soils: Basic concepts and future challenges.* Cambridge University Press, Cambridge, U.K.
- Wilson, M.J., D.C. Bain, and D.M.L. Duthie. 1984. The soil clays of Great Britain. II. Scotland. *Clay Miner.* 19:709–735.
- Wilson, M.J., G. Certini, C.D. Campbell, I.C. Anderson, and S. Hillier. 2008. Does the preferential microbial colonisation of ferromagnesian minerals affect mineral weathering in soil? *Naturwissenschaften* 95:851–858.
- Wilson, M.J., and W.J. McHardy. 1980. Experimental etching of a microcline perthite and implications regarding natural weathering. *J. Microsc.* 120:291–302.
- Wolff-Boenisch, D., S.R. Gislason, E.H. Oelkers, and C.V. Putnis. 2004. The dissolution rates of natural glasses as a function of their composition at pH 4 and 10.6, and temperatures from 25 to 74°C. *Geochim. Cosmochim. Acta* 68:4843–4858.
- Worden, R.H., F.D.L. Walker, I. Parsons, and W.L. Brown. 1990. Development of microporosity, diffusion channels and deuteric coarsening in perthitic alkali feldspars. *Contrib. Mineral. Petrol.* 104:507–515.
- Wright, J.D., and N.A.J.M. Sommerdijk. 2001. Soil-gel materials, chemistry and applications. *Advanced chemistry texts.* CRC Press, Boca Raton, FL.
- Yagasaki, Y., J. Mulder, and M. Okazaki. 2006. The role of soil organic matter and short-range ordered aluminosilicates in controlling the activity of aluminum in soil solutions of volcanic ash soils. *Geoderma* 137:40–57.
- Yaron, B., I. Dror, and B. Berkowitz. 2010. Contaminant geochemistry—A new perspective. *Naturwissenschaften* 97:1–17.
- Yoshinaga, N., and S. Aomine. 1962. Imogolite in some Ando soils. *Soil Sci. Plant Nutr.* 8:22–29.
- Young, I.M., and J.W. Crawford. 2004. Interactions and self-organization in the soil-microbe complex. *Science* 304:1634–1637.
- Zanelli, R., M. Egli, A. Mirabella, M. Abdelmoula, M. Plötze, and M. Nötzli. 2006. “Black” soils in the southern Alps: Clay mineral formation and transformation, X-ray amorphous Al phases and Fe forms. *Clays Clay Miner.* 54:703–720.
- Zehetner, F., W.P. Miller, and L.T. West. 2003. Pedogenesis of volcanic ash soils in Andean Ecuador. *Soil Sci. Soc. Am. J.* 67:1797–1809.
- Zelazny, L.W., and F.G. Calhoun. 1977. Palygorskite (attapulgitite), sepiolite, talc, pyrophyllite and zeolites, p. 435–470. *In* J.B. Dixon and S.B. Weed (eds.) *Minerals in soil environments.* SSSA, Madison, WI.
- Zelazny, L.W., P.J. Thomas, and C.L. Lawrence. 2002. Pyrophyllite-talc minerals, p. 415–430. *In* J.B. Dixon and D.G. Schulze (eds.) *Soil mineralogy with environmental applications.* SSSA Book Series No. 7. SSSA, Madison, WI.
- Zelazny, L.W., and G.N. White. 1989. The pyrophyllite-talc group, p. 527–550. *In* J.B. Dixon and S.B. Weed (eds.) *Minerals in soil environments.* 2nd edn. SSSA, Madison, WI.
- Ziegler, K., J.C.C. Hsieh, O.A. Chadwick, E.F. Kelly, D.M. Hendricks, and S.M. Savin. 2003. Halloysite as a kinetically controlled end product of arid-zone basalt weathering. *Chem. Geol.* 202:461–478.
- Zysset, M., P. Blaser, J. Luster, and A.U. Gehring. 1999. Aluminum solubility control in different horizons of a podzol. *Soil Sci. Soc. Am. J.* 63:1106–1115.

21

Phyllosilicates

21.1	Introduction	21-1
21.2	General Structural Features.....	21-1
	Ionic Sizes and Coordination Number • Polytypes • 1:1 Layer Type (T-O Type) • 2:1 Layer Type (T-O-T Type) • 2:1:1 Layer Type (T-O-T-O Type) • Interstratified Layer Silicate Group (Mixed-Layer Type) • Modulated Layer Silicate Group	
21.3	Occurrence of Phyllosilicates.....	21-21
	As Rock-Forming Minerals • Hydrothermal Origin and the Term “Clay Minerals” • Diagenesis and Low-Grade Metamorphism • In Soils, Sediments, and Weathering Products	
21.4	Phyllosilicates in Soil Environments	21-24
	Introduction • Physical Properties • Chemical Properties • Uses of Clays	
21.5	Identification of Soil Phyllosilicates.....	21-30
	Introduction • X-Ray Diffraction Methods • Other Instrumental Methods • Quantification	
	Addendum.....	21-41
	Appendix	21-41
	References.....	21-44

Hideomi Kodama

Agriculture and Agri-Food Canada

21.1 Introduction

Phyllosilicates, in other words, layer silicates, occupy one of six subclasses under the silicates class (Table 21.1). Phyllo- is after the Greek word describing the state of leaves, like a bed or heap of leaves. Thus in science, often the word is used as a prefix to express thin layer or paper sheet like in a book. This reflects general crystal habits and morphological features of the phyllosilicates. The silicates are abundant on the earth and of greater importance than any other minerals, which is easily understood from the fact that oxygen and silicon constitute nearly 75% of the elements in the earth's crust (Figure 21.1). The fundamental unit in all silicate structures is the silicon-oxygen tetrahedron (Figure 21.2). As Bragg (1950) stated, the bonds between silicon and oxygen are so strong that the four oxygen atoms are always found at the corners of a tetrahedron of nearly constant dimensions and regular shape whatever the rest of the structure may be like. The Si-O distance is about 0.16 nm, and the O-O distance 0.26 nm. Besides the crustal abundance of these two elements, the ionic radius of Si^{4+} , 0.042 nm, is conveniently accommodated in surroundings with four oxygens to form the fundamental structural unit of all silicates, the tetrahedron having the chemical formula $(\text{SiO}_4)^{4-}$. This unit can occur independently with compensating cations like Mg^{2+} and Fe^{2+} . And also these SiO_4 tetrahedra may be linked together by having one or more oxygen atoms shared in common by neighboring tetrahedra to form indefinitely extended and more complicated structural units to cover the existing silicate minerals. This mechanism of

linking together is known as polymerization, and the classified structural units with their compositions are given in Table 21.2.

21.2 General Structural Features

The crystal structure of phyllosilicates has been determined largely by x-ray diffraction (XRD) methods that were well established within two to three decades of Roentgen's discovery of x-rays in 1895. The essential features of the mineral, typified by mica-like minerals, are the continuous 2D tetrahedral sheets of composition, $\text{Si}_2\text{O}_5^{2-}$, in which SiO_4 tetrahedra (Figure 21.3) are linked by sharing three corners of each tetrahedron to form a hexagonal mesh pattern (Figure 21.4a). Frequently Si atoms of the tetrahedra are partially substituted by Al and, to a lesser extent, by Fe^{3+} . The apical oxygen at the fourth corner of the tetrahedra, which is usually directed normal to the sheet, forms part of an adjacent octahedral sheet in which octahedra are linked by sharing edges (Figure 21.5). The junction plane between tetrahedral and octahedral sheets consists of the shared apical oxygens of the tetrahedra and unshared hydroxyls that lie at the center of each hexagonal ring of tetrahedra and at the same level as the shared apical oxygen atoms (Figure 21.6). Further details of octahedral configurations will be seen in Section 21.2.2, where the explanation of polytypes is given using the phlogopite structure as the example. Common cations that coordinate the octahedral sheets are Al, Mg, Fe^{3+} , and Fe^{2+} ; but occasionally, Li, V, Cr, Mn, Ni, Cu, and Zn substitute in considerable amounts

TABLE 21.1 Six Subclasses under the Silicate Mineral Class

Subclass (Commonly Used)	Subclass (in Other Name)
Nesosilicates	Orthosilicates
Sorosilicates	Disilicates
Cyclosilicates	Ring silicates
Inosilicates	Chain silicates—Single chain and double chain
Phyllosilicates	Layer silicates
Tectosilicates	Framework silicates

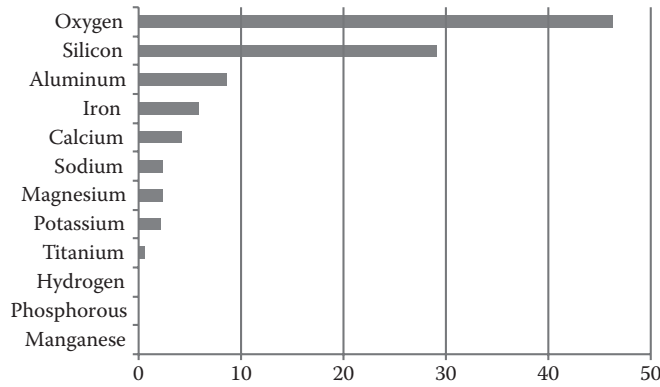


FIGURE 21.1 The 12 most abundant elements in the earth's crust. (Modified graph from Vanders, I., and P. Kerr. 1967. Mineral recognition. John Wiley & Sons, Inc., New York.)

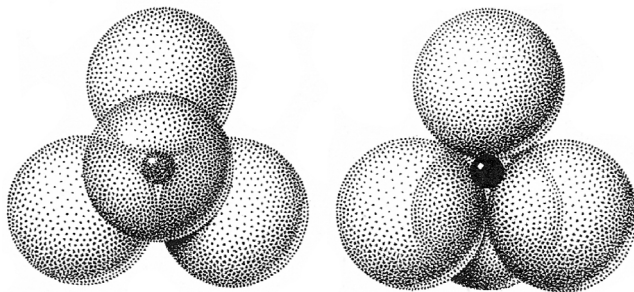


FIGURE 21.2 Close-packing representation of the SiO₄ tetrahedron. (From Klein, C., and C.S. Hurlbut, Jr., 1985. Manual of mineralogy. John Wiley & Sons, Inc., New York.)

TABLE 21.2 Unit Compositions of Six Subclasses, Mineral Group, and Species Examples

Subclass	Unit Composition	Mineral Group Example	Mineral Species Example
Nesosilicates	(SiO ₄) ⁴⁻	Olivin	Forsterite
Sorosilicates	(Si ₂ O ₇) ⁶⁻	Epidote	Zoisite
Cyclosilicates	(Si ₆ O ₁₈) ¹²⁻	Tourmaline	Elbaite
Inosilicates			
Single chain	(SiO ₃) ²⁻	Pyroxene	Diopside
Double chain	(Si ₄ O ₁₁) ⁶⁻	Amphibole	Actinolite
Phyllosilicates	(Si ₂ O ₅) ²⁻	Mica	Muscovite
Tectosilicates	(SiO ₂) ⁰	Feldspar	Albite

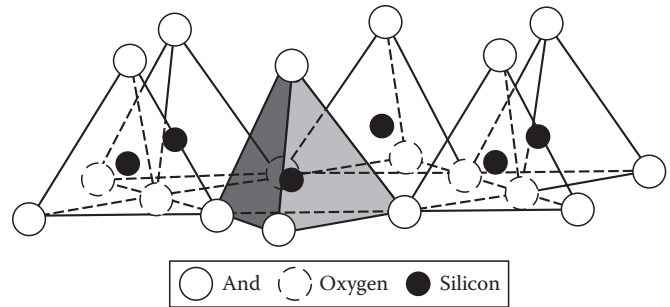


FIGURE 21.3 SiO₄ tetrahedra linking to form a hexagonal network. Single tetrahedron is shaded. (From Grim, R.E. 1968. Clay mineralogy. McGraw-Hill Book Co. Inc., New York. With permission.)

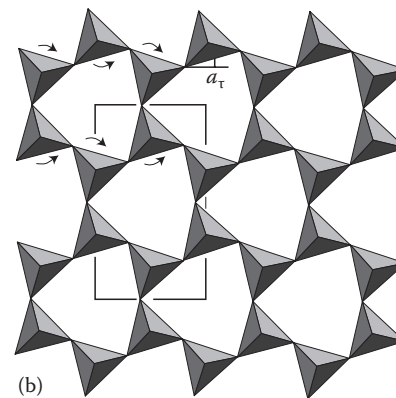
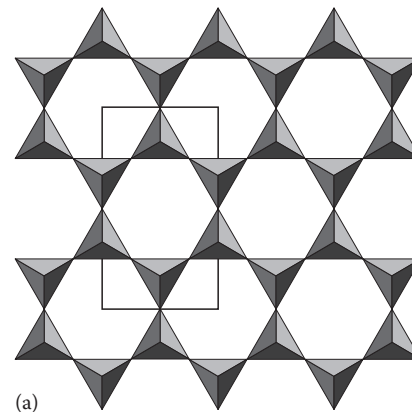


FIGURE 21.4 (a) Ideal hexagonal tetrahedral sheet. (b) Contracted sheet of ditrigonal symmetry by rotation of the tetrahedra due to a dimension misfit between tetrahedral and octahedral sheets. (With kind permission from Liebau, F. 1985. Structural chemistry of silicates: Structure, bonding, and classification. Springer-Verlag, New York.)

into the sheets. If divalent cations (M²⁺) are in the octahedral sheets, the composition is M₃²⁺(OH)₂O₄ and all the octahedra are occupied; if trivalent cations (M³⁺), the composition is M₂³⁺(OH)₂O₄ and two-thirds of the octahedra are occupied, with the absence of the third octahedron. The former type of octahedral sheet is called trioctahedral (Figure 21.7a) and the latter dioctahedral (Figure 21.7b). This distinction may occasionally be used as a subgrouping for certain mineral groups

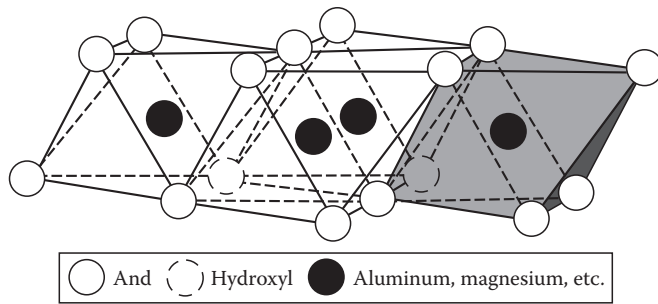


FIGURE 21.5 Single octahedron (shaded) and the sheet structure of octahedral units. (From Grim, R.E. 1968. *Clay mineralogy*. McGraw-Hill Book Co. Inc., New York. With permission.)

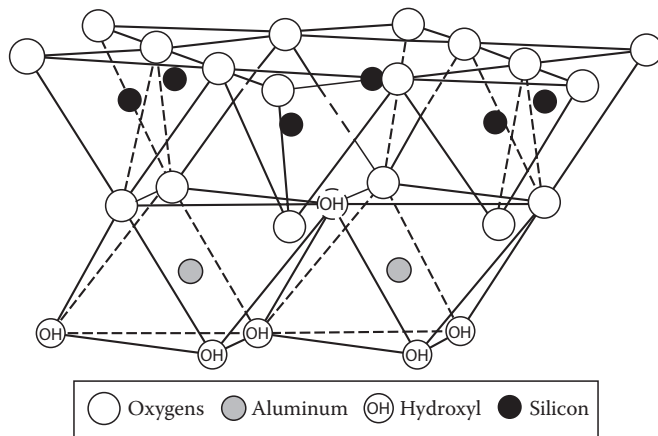


FIGURE 21.6 Structure of 1:1 layer silicate (kaolinite) illustrating the junction between tetrahedral and octahedral sheets. (From Grim, R.E. 1968. *Clay mineralogy*. McGraw-Hill Book Co. Inc., New York. With permission.)

(e.g., mica). If all the anion groups are OH in the compositions of octahedral sheets, the resulting sheets may be expressed by $M^{2+}(\text{OH})_2$ and $M^{3+}(\text{OH})_3$, respectively. Such sheets called hydroxide sheets occur singly, alternating with silicate layers in some phyllosilicates, for example, in chlorite minerals. Brucite, $\text{Mg}(\text{OH})_2$, and gibbsite, $\text{Al}(\text{OH})_3$, are typical examples of minerals having similar structures.

There are two major types for structural “backbones” of phyllosilicates called silicate layers. The unit silicate layer formed by aligning one octahedral sheet to one tetrahedral sheet is referred to as a 1:1 silicate layer (Figure 21.8a), and the exposed surface of the octahedral sheet consists of hydroxyls. In another type, the unit silicate layer comprises one octahedral sheet sandwiched by two tetrahedral sheets, which are oriented in opposite directions and is termed a 2:1 silicate layer (Figure 21.8b). If hydroxide sheets in the chlorite structure are treated as a proxy for the octahedral sheet of the silicate layer and denoted as T for the tetrahedral sheet and O for the octahedral sheet, a majority of the phyllosilicates may be grouped by T-O type, T-O-T type, and T-O-T-O type, which correspond to 1:1, 2:1, and 2:2 (2:1:1 in some occasions) silicate layers, respectively.

Real structures of phyllosilicates, however, contain substantial crystal strains and distortions, which produce irregularities such as deformed octahedra and tetrahedra rather than polyhedra

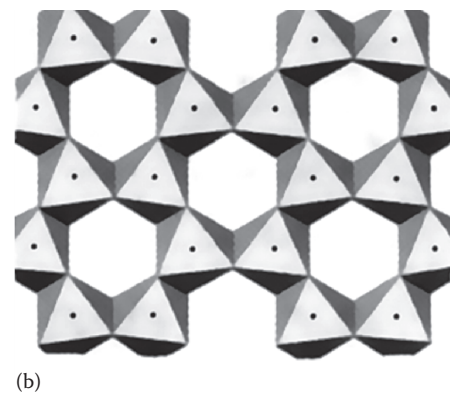
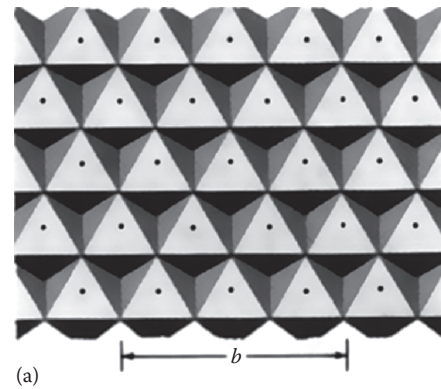


FIGURE 21.7 Difference in the octahedral sheets of clay minerals: (a) trioctahedral, with dots of M^{2+} ; (b) dioctahedral, with dots of M^{3+} . (With kind permission of Liebau, F. 1985. *Structural chemistry of silicates: Structure, bonding, and classification*. Springer-Verlag, New York.)

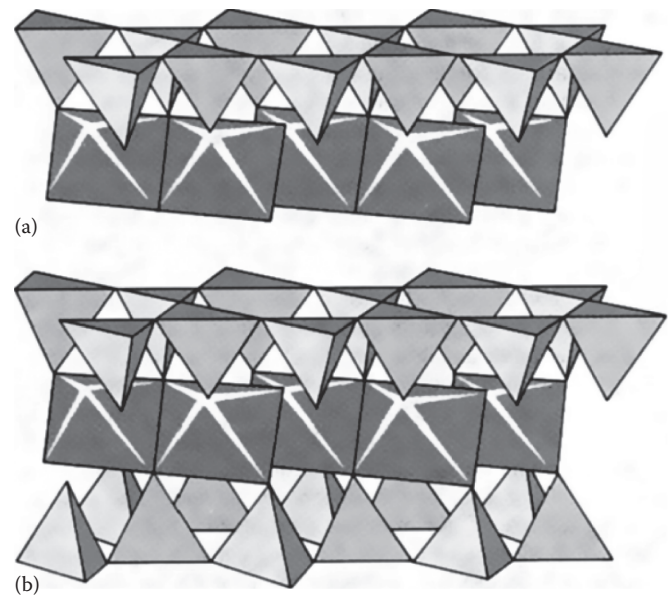


FIGURE 21.8 Two basic silicate layer types of phyllosilicates: (a) 1:1 or T-O type silicate layer structure, (b) 2:1 or T-O-T type silicate layer structure. (With kind permission of Springer Science + Business media: Liebau, F. 1985. *Structural chemistry of silicates: Structure, bonding, and classification*. Springer-Verlag, New York.)

with equilateral hexagonal faces, ditrigonal symmetry modified from the ideal hexagonal surface symmetry, and puckered surface instead of the flat plane made up by the basal oxygen atoms of the tetrahedral sheet. One of the major causes of such distortions is dimensional “misfits” between the tetrahedral and octahedral sheets. If the tetrahedral sheet contains only silicon in the cationic site and has an ideal hexagonal symmetry, the longer unit dimension within the basal dimension is 0.915 nm, which lies between the corresponding dimensions 0.86 nm of gibbsite and 0.94 nm of brucite. To fit the tetrahedral sheet into the dimension of the octahedral sheet, alternate SiO_4 tetrahedra rotate (up to a theoretical maximum of 30°) in opposite directions to distort the ideal hexagonal array into a doubly triangular (ditrigonal) array (Figure 21.4b). By this distortion mechanism, tetrahedral and octahedral sheets of a wide range of composition due to ionic substitutions can link together and maintain silicate layers. Among ionic substitutions, those between ions of distinctly different sizes most significantly affect geometric configurations of silicate layers.

21.2.1 Ionic Sizes and Coordination Number

The arrangement of anions around a cation (as normally anions are larger than cations), defined as the coordination number, would be expected to be the most symmetrical in the three dimensions, that is, 3, 4, 6, 8, and 12 ions would be arranged at the apices of an equilateral triangle, regular tetrahedron, octahedron, cube, and closest packing in order to minimize its overall potential energy. Pauling (1929) first elucidated that most minerals follow the principles that are now commonly known as Pauling’s first rule to distinguish from his second rule regarding structure stabilization by the sum of the electrostatic strengths between an anion and adjacent cations. Thus, as far as geometry is concerned, the ionic radius ratio, $R_{\text{cation}}/R_{\text{anion}}$, is the key factor for determining a polyhedron suitable for an arrangement of anions around a cation for a specific ionic combination. Assuming that ions act as rigid spheres of fixed radii, the stable arrangements of cations and

TABLE 21.3 Relationship between Radius Ratio ($R_{\text{cation}}/R_{\text{O}^{2-}}$) and Coordination Number

Radius Ratio ($R_{\text{cation}}/R_{\text{anion}}$)	Arrangement of Anions around a Cation	Coordination Number of Cation	Crystal Models Shown in Figure 21.9
0.15–0.22	Corners of an equilateral triangle	3	a
0.22–0.41	Corners of a tetrahedron	4	b
0.41–0.73	Corners of an octahedron	6	c
0.73–1	Corners of a cube	8	d
1	Closest packing	12	e

anions for particular radius ratios can be calculated from purely geometric considerations (Table 21.3) and the corresponding 3D coordination models are shown in Figure 21.9. Anions in phyllosilicate structures are mostly oxygen ions, O^{2-} , with radius of 0.132 nm. Although to a lesser extent the structures may contain F^- and $(\text{OH})^-$, radii of these anions are similar to that of oxygen. Therefore, for phyllosilicates, it is practical to compare the relationship of coordination number with the size of cation in terms of $R_{\text{cation}}/R_{\text{O}^{2-}}$ (Table 21.4). The table allows making prediction for the coordination number of a cation in phyllosilicates and for a possible ionic substitution at a specific structural site.

21.2.2 Polytypes

Because phyllosilicates maintain hexagonal or near-hexagonal symmetry, the structures allow various ways to stack up atomic planes, sheets, and layers, which may be explained by crystallographic operations such as translation or shifting and rotation, thereby distinguishing them from polymorphs (e.g., diamond–graphite; calcite–aragonite). The former involves 1D variations but the latter generally 3D ones. With a fixed chemical composition, structural varieties that are resulted from different stacking sequences are

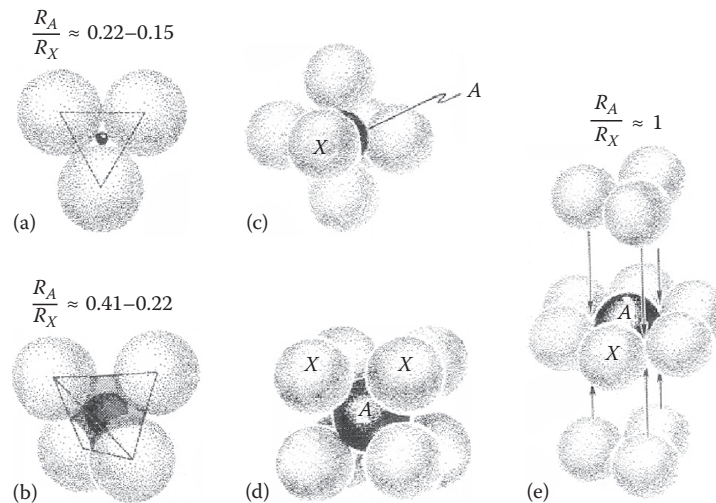


FIGURE 21.9 Coordination number (ligancy) See Table 21.3 for further details of each crystal model. (Modified after Bloss, F.D. 1971. Crystallography and crystal chemistry. Holt, Rinehart and Winston, Inc., New York.)

TABLE 21.4 Radius of Cations Commonly Present in Phyllosilicates, Radius Ratio ($R_{cation}/R_{O^{2-}}$), and Predicted and Observed Coordination Numbers

Cation	Radius (nm)	$R_{cation}/R_{O^{2-}}$	Predicted Coordination Number	Observed Coordination Number
Cs ⁺	0.167	1.26	12	12
Rb ⁺	0.147	1.11	12	8, 12
NH ⁴⁺	0.143	1.08	12	8, 12
Ba ²⁺	0.134	1.02	8	8, 12
K ⁺	0.133	1	8	8, 12
Sr ²⁺	0.112	0.84	8	8
Ca ²⁺	0.099	0.75	6	6, 8
Na ⁺	0.097	0.73	6	6, 8
Mn ²⁺	0.08	0.6	6	6
Fe ²⁺	0.074	0.56	6	6
V ³⁺	0.074	0.56	6	6
Zn ²⁺	0.074	0.56	6	6
Cu ²⁺	0.072	0.54	6	6
Co ²⁺	0.072	0.54	6	6
Ni ²⁺	0.069	0.52	6	6
Li ⁺	0.068	0.51	6	6
Ti ⁴⁺	0.068	0.51	6	6
Mg ²⁺	0.066	0.5	6	6
Fe ³⁺	0.064	0.48	6	6
Cr ³⁺	0.063	0.47	4	6
Al ³⁺	0.051	0.38	4	4, 6
Si ⁴⁺	0.042	0.31	4	4
P ⁵⁺	0.035	0.26	4	4
B ³⁺	0.023	0.17	3	3

termed polytypes. If such a variety is caused by ionic substitutions, which are minor but consistent, they are called polytypoids.

To understand this specific feature of phyllosilicates, consider the magnesium mica, phlogopite, as an example. Its silicate layer in terms of a sequence of atom planes is given in Figure 21.10. In the figure, T_L represents the atom plane at the level of apical oxygen atoms (\bullet , solid circles) of the lower tetrahedral sheet and at the same level and hydroxyl (double circles with O and \bullet) fills the center of a hexagonal array made up by six apical oxygen atoms. In addition, the projection to the plane of basal oxygen atoms (\circ , open circles) of the tetrahedral sheet is also included. O_T is the octahedral cation plane where magnesium atoms are represented by small solid circles (\bullet). T_U corresponds to the atom plane of the upper tetrahedral sheet. Unlike T_L , the direction of apical oxygen atoms is opposite to that of T_L . In T_U , the apical oxygen atoms, hydroxyls, and the projections of the basal oxygen atoms are expressed by an open circle with shaded circle, double circles, and solid circles, respectively. The lower tetrahedral sheet and the upper tetrahedral sheet having opposing vertices to each other are held together by magnesium ions. Each magnesium ion is linked to two oxygen anions and one hydroxyl from the lower tetrahedral sheet and two oxygen anions and one hydroxyl from the upper sheet to make a six coordination packing. This packing mechanism requires that the upper tetrahedral sheet be staggered by $-a/3$, where a is the unit cell dimension along the a -axis, relative to the lower tetrahedral sheet. The staggering between the two sheets, therefore, gives a monoclinic nature to the silicate layer, and this nature is common to all the basic silicate layers of phyllosilicates. The interlayer atom plane is denoted as I, in which solid circles represent potassium atoms. At the interlayer position, for example, between two silicate layers, each interlayer potassium ion keys the two layers without shift by coordinating 12 basal oxygens, 6 each from lower and upper tetrahedral sheets. Although due to the presence of interlayer potassium ions there is no shift between the two silicate layers, the orientation of the upper one

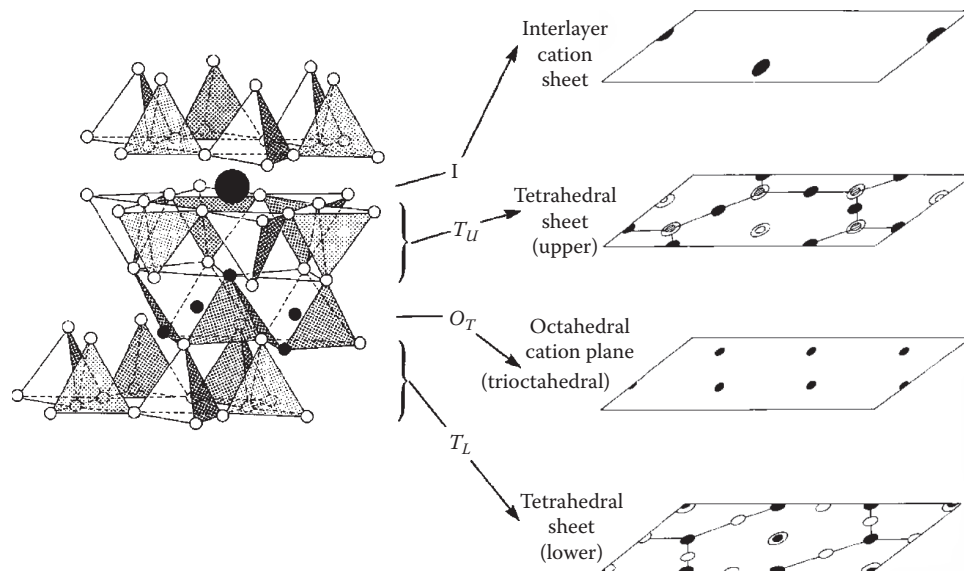


FIGURE 21.10 Idealized sketches of mica structure (phlogopite) and its structural segments (atomic planes) at four levels. (After Kodama, H. 1990. Use of color-coded transparencies for visualizing layer silicate structures, p. 169–175. In V.C. Farmer and Y. Tardy (eds.) Proc. 9th Int. Clay Conf. 1989. Strasbourg. Sci. Géol., Mém. Strasbourg, France.)

can be changed with respect to the lower one. Because these basal oxygen planes have a hexagonal or a pseudohexagonal symmetry, there are six or three possible orientations, which are related by $n \times 60^\circ$ rotations, at maximum six angles: 0° , 60° , 120° , 180° , 240° , and 300° . Among them, angles 60° and 300° are equivalent, as also are angles 120° and 240° , because the silicate layer itself has the plane of symmetry, which is parallel to the layer stagger. Thus, 0° , 60° , 120° , and 180° rotation operations lead theoretically to six simple-ordered-stacking mica layers, and they were depicted by vectors from one potassium atom to a potassium atom in the next layer in the direction of increasing height of the mica layers (Smith and Yoder, 1956). Resulting layer structures having different layer-stacking sequences are called polytypes. Mica polytypes derived by them are $1M$ (0° rotation), $2M_1$ (a continuous alternation of $\pm 120^\circ$ rotation), $2M_2$ (a continuous alternation of $\pm 60^\circ$ rotation), $3T$ ($\pm 120^\circ$ rotation), $2Or$ ($\pm 180^\circ$ rotation), and $6H$ ($\pm 60^\circ$ rotation), as expressed in an adapted simple nomenclature. The first symbol gives the number of layers in the repeat unit (subcell) and the second in italics gives the symmetry. In case of the same symmetry, the subscripts 1 and 2 are used for further distinction. Therefore, $1M$, $2M$, $3T$, $2Or$, and $6H$ indicate one-layer monoclinic, two-layer monoclinic, three-layer trigonal, two-layer orthorhombic, and six-layer hexagonal, respectively. Similar consideration can be applied to other types of layer silicates such as T-O and T-O-T-O. If polytypes are reported in nature, in the glossary of phyllosilicates given at the end of this chapter (compiled from Blackburn and Dennen, 1997, and Lalonde, 2003) a specific mineral name is given, for example, Phlogopite- $1M$, Kaolinite- $1Tc$, where the letter Tc represents triclinic. The descriptions stated above are based on the ideal or nearly ideal structure. In practice, however, there are many factors that affect the formation of polytypes, that is, ionic substitutions in the octahedral sheets, ionic substitutions for silicon atoms in the tetrahedral sheets, the degree of ordering of these substitutions, the vacancy distributions in the octahedral sheets, which normally exist in the dioctahedral layer silicates or may be caused by the oxidation of Fe^{2+} to Fe^{3+} in the sheets. These variations add more complexities to the form of polytypes.

21.2.3 1:1 Layer Type (T-O Type)

21.2.3.1 General

The structure of this type is shown in Figure 21.6 (also Figure 21.8), which was used for explaining the junction between tetrahedral and octahedral sheets. A 2D tetrahedral sheet, made up by sharing three corners of each SiO_4 tetrahedron, are attached to an octahedral sheet, thereby each cation in the octahedral sheet associates with two apical oxygen atoms and four hydroxyls to make up six coordination binding. Thus, the structure of this type of layer silicate consists of tetrahedral and octahedral sheets in which the anions at the exposed surface of the octahedral sheet are hydroxyls. General structural formula may be expressed by $Y_{2-3}Si_2O_5(OH)_4$, where Y are cations in the octahedral sheet such as Al^{3+} or Fe^{3+} for dioctahedral species and Mg^{2+} , Fe^{2+} , Mn^{2+} , or Ni^{2+} for trioctahedral species.

21.2.3.2 Serpentine-Kaolin Group

This group contains two subgroups, trioctahedral and dioctahedral. Serpentine minerals with the ideal formula of

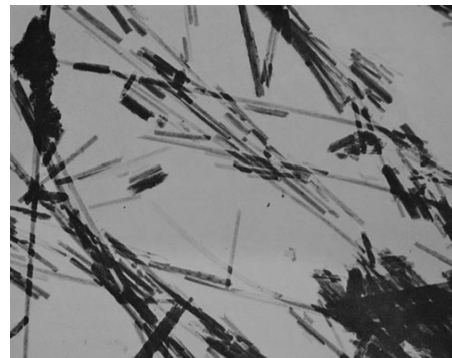


FIGURE 21.11 Electron micrograph of chrysotile. Most of the fibrils appear “solid,” but a few show the appearance of hollow tubes, and a few show “open ends.” (From Gard, J.A. (ed.). 1971. The electron-optical investigation of clays. Monograph No 3. Mineralogical Society, London, U.K. Reproduced with permission of The Mineralogical Society of Great Britain and Ireland.)

$Mg_3Si_2O_5(OH)_4$ represent the former, and kaolin minerals with $Al_2Si_2O_5(OH)_4$ represent the latter. Among trioctahedral magnesium species, chrysotile, antigorite, and lizardite are commonly known and their morphology and structure are uniquely different. (Wicks and Whittaker, 1975; Wicks and Zussman, 1975) Electron microscopic observations show that chrysotile crystals have a fibril appearance (Figure 21.11), but its cross sections clearly show cylindrical roll morphology (Figure 21.12a and b); whereas, antigorite crystals exhibit lath-shape morphology (Figure 21.13a), but the electron-diffraction photograph indicates an alternating wave structure as shown by the presence of segmental groups of superlattice spots (Figure 21.13b). The structure deduced by Kunze (1956) consists of curved layers elongated along the a -axis, but the layers change alternately their polarity (or the direction of apical oxygens in the tetrahedral sheets) at half a period of the wave to make up a full periodicity of 4.35 nm, which is the dimension of a of antigorite (Figure 21.14). These alternating wave structural characteristics may be attributed to the degree of fit between the lateral dimensions of the tetrahedral and octahedral sheets. On the other hand, lizardite crystals are platy (Figure 21.15) and have often a small amount of substitution of Al or Fe^{3+} for both Si and Mg. This substitution appears to be the main reason for the platy nature of lizardite. Obviously, morphology is one of the key characteristics to distinguish among serpentine minerals. A few selected chemical compositions of serpentine minerals are given in Table 21.5 for reference. Other than Mg, Fe^{2+} , Ni, and Mn can occupy the octahedral sites and form species such as berthierine, brindleyite, and kellyite. Chemical compositions of some such varieties are given in Table 21.6. Planar polytypes of the trioctahedral species are far more complicated than those of the dioctahedral ones, owing to the fact that the trioctahedral silicate layer has a higher symmetry because all octahedral cationic sites are occupied. Polytype structures, such as one-layer trigonal ($1T$), one-layer monoclinic ($1M$), two-layer hexagonal ($2H_1$, $2H_2$), two-layer trigonal ($2T$), two-layer orthorhombic ($2Or$), two-layer monoclinic ($2M_1$, $2M_2$), three-layer rhombohedral ($3R$),

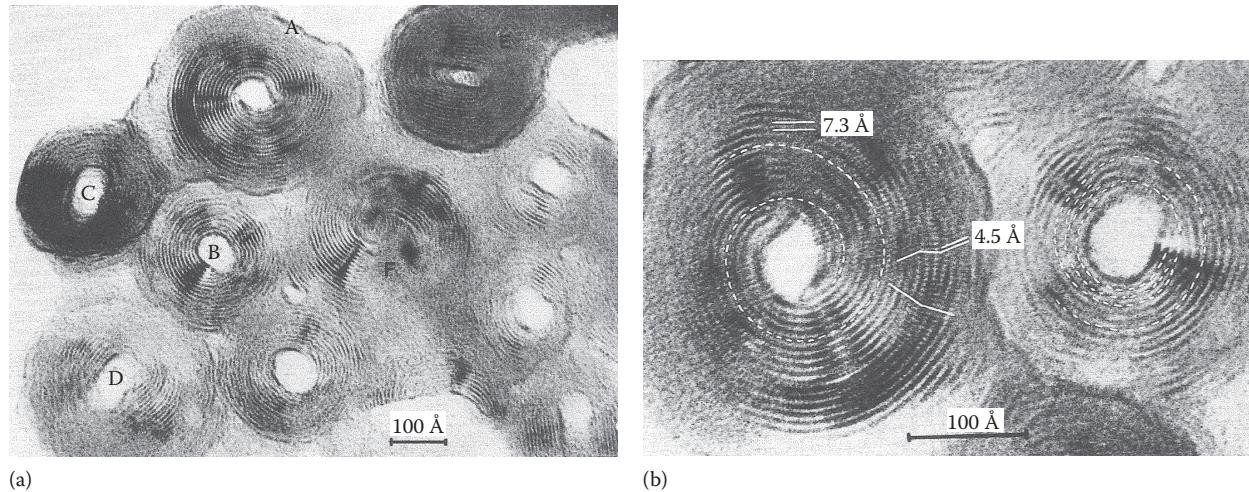


FIGURE 21.12 Electron micrographs of cross-sectioned chrysotile crystals: (a) The lattice image observed from the direction parallel to the fiber axis. (From Gard, J.A. (ed.). 1971. *The electron-optical investigation of clays*. Monograph No 3. Mineralogical Society, London, U.K.) (b) Enlarged image on crystallites A and B in micrograph (a) showing two kinds of fringe patterns, which correspond to d_{001} -spacing (0.73 nm) and d_{020} -spacing (0.45 nm). (From Gard, J.A. (ed.). 1971. *The electron-optical investigation of clays*. Monograph No 3. Mineralogical Society, London, U.K. Reproduced with permission of The Mineralogical Society of Great Britain and Ireland.)

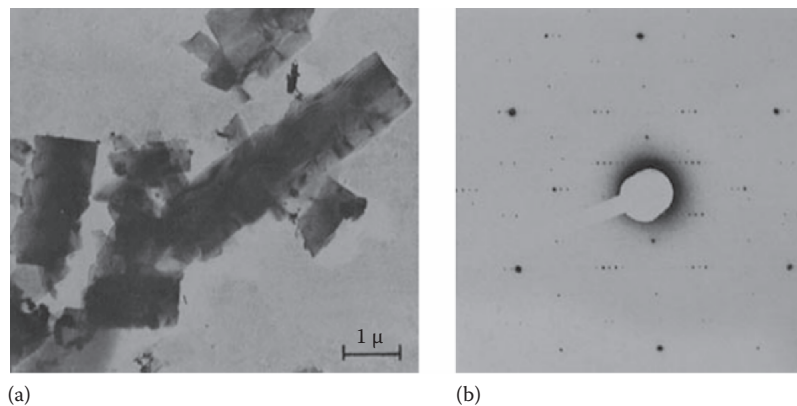


FIGURE 21.13 (a) Electron micrograph of antigorite (platy crystals), from Antigorio, Italy. (b) Electron-diffraction pattern from a single crystal of antigorite, showing the presence of a superlattice structure along the a -axis, with $a \approx 3.85$ nm. (From Gard, J.A. (ed.). 1971. *The electron-optical investigation of clays*. Monograph No 3. Mineralogical Society, London, U.K. Reproduced with kind permission of The Mineralogical Society of Great Britain and Ireland.)

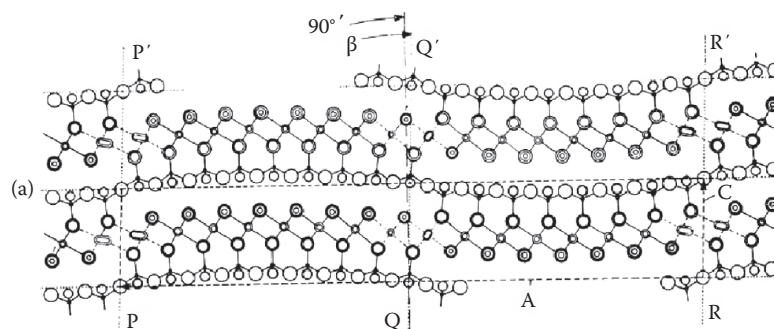


FIGURE 21.14 Structure of antigorite as viewed along the y -axis. The curved layers (radius of curvature 7.5 nm) reverse polarity at PP' , RR' , and near QQ' . (From Gard, J.A. (ed.). 1971. *The electron-optical investigation of clays*. Monograph No 3. Mineralogical Society, London, U.K. Reproduced with kind permission of The Mineralogical Society of Great Britain and Ireland.)

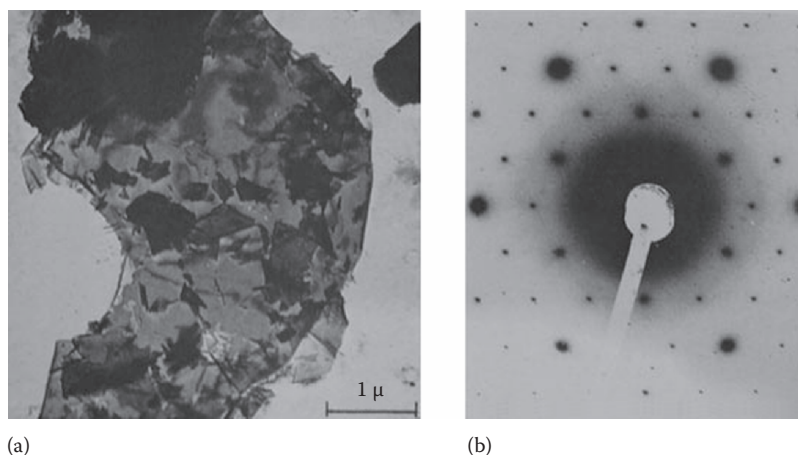


FIGURE 21.15 (a) Electron micrograph and (b) electron-diffraction pattern of lizardite, from Kennack, Cornwall (platy). (From Gard, J.A. (ed.). 1971. The electron-optical investigation of clays. Monograph No 3. Mineralogical Society, London, U.K. Reproduced with kind permission of The Mineralogical Society of Great Britain and Ireland.)

TABLE 21.5 Serpentine Mineral Analyses (1)

	1	2	3	4	5	6
SiO ₂	43.37	41.25	41.65	42.02	42.44	43.45
Al ₂ O ₃	0	0.54	0.1	0.52	0.64	0.81
TiO ₂	0	0.02	nr	None	None	0.02
Fe ₂ O ₃	0	1.32	2.88	0.19	0.19	0.88
FeO	0	0.09	0.16	0.11	0.03	0.69
MnO	0	0.07	0.05	0.03	0.03	None
MgO	43.64	41.84	41.06	41.44	42.76	41.9
CaO	0	0.02	nr	None	nr	nr
K ₂ O	0	nr	nr	0.49	0.08	0.02
Na ₂ O	0	nr	nr	0.36	0.06	0.05
H ₂ O ⁺	12.99	13.68	13.1	14.04	13.58	12.29
H ₂ O ⁻	0	0.97	nr	1.64	0.5	nr
Total	100	99.8	100.12	99.99	100.31	100.19
Numbers of cations on basis of O ₁₀ (OH) ₈						
Si	4	3.92	3.94	4	3.96	3.99
Al	0	0.06	0.01		0.04	0.01
Fe ³⁺	0	0.02	0.05			
Σ _{tet}	4	4	4	4	4	4
Al	0			0.06	0.03	0.08
Fe ³⁺	0	0.07	0.15	0.01	0.01	0.06
Fe ²⁺	0	0.01	0.01	0.01		0.05
Mg	6	5.92	5.79	5.88	5.98	5.92
Σ _{oct}	6	6.01	5.95	5.96	5.98	5.92
Ca	0					
Na	0				0.01	
K	0				0.01	

1, Ideal composition based on the structural formula, Mg₃Si₂O₅(OH)₄; 2, lizardite, Transvaal, South Africa (Deer et al., 1962); 3, lizardite, Shetland Islands, United Kingdom (Brindley and von Knorring, 1954); 4, chrysotile, Gila County, Arizona (Faust and Fahey, 1962); 5, chrysotile, Montville, New Jersey (Faust and Fahey, 1962); 6, antigorite, Mikonui, New Zealand (Zussman, 1954). Total includes 0.04% NiO; 0.04% H₂O (—).

Analyses 2–6 are taken from Newman (1987) in which original data for those analyses were referred from respective papers cited above. See Newman (1987) for original source of each analysis.

TABLE 21.6 Serpentine Mineral Analyses (2)

	1	2	3	4
SiO ₂	19.08	22.03	27.45	17.6
Al ₂ O ₃	26.66	22.91	24.09	28.55
TiO ₂	nr	3.63	0.99	<0.05
Fe ₂ O ₃	4.29	0.46	nr	2.18
Cr ₂ O ₃	nr	0.05	0.17	nr
FeO	34.52	36.68	1.15	
MnO	nr	0.04	nr	38.84
MgO	1.55	1.91	3.18	2.97
NiO	nr	nr	30.18	nr
CaO	nr	0.07	0.07	nr
K ₂ O	nr	0.03	nr	nr
Na ₂ O	nr	0.08	nr	nr
H ₂ O total	11.18			
H ₂ O ⁺	nr	10.65	nr	nr
H ₂ O ⁻	nr	0.63	nr	nr
Total	99.25	100.05	87.28	90.14
Numbers of cations on basis of O ₁₀ (OH) ₈				
Si	2.2	3.23	3.01	1.96
Al	1.8	0.77	0.99	2.04
Fe ³⁺				
Σ _{tet}	4	4	4	4
Al	1.84	1.95	2.12	1.72
Fe ³⁺	0.37	0.03		0.18
Cr ³⁺			0.01	
Fe ²⁺	3.32	3.09	0.11	
Mn				3.67
Mg	0.27	0.29	0.52	0.49
Ni			2.66	
Σ _{oct}	5.8	5.36	5.42	6.06

1, Berthierine (Brindley, 1982); 2, berthierine (Brindley, 1982); 3, brindleyite, Marmara karstic bauxite deposits, Greece (Bish, 1978); 4, kellyite, Bald Knob, North Carolina (Peacor et al., 1974).

See Newman (1987) for original source of each analysis.

TABLE 21.7 Kaolin Mineral Analyses

	1	2	3	4	5	6
SiO ₂	46.55	46.9	46.77	45.2	46.43	46.22
Al ₂ O ₃	39.49	37.4	37.79	37.02	39.54	39.92
TiO ₂	0	0.18	nr	1.26	Nil	0
Fe ₂ O ₃	0	0.65	0.45	0.27	0.15	0
FeO	0	nr	0.11	0.06	nr	0
MgO	0	0.27	0.24	0.47	0.17	0
CaO	0	0.29	0.13	0.52	Nil	0
K ₂ O	0	0.84	1.49	0.49	0.02	0
Na ₂ O	0	0.44	0.05	0.36	0.03	0
H ₂ O ⁺	13.96	12.95	12.18	13.27	14.2	13.86
H ₂ O ⁻	0	nr	0.61	1.56	nr	0
Total	100	99.92	99.82	100.47	100.54	100
Numbers of cations on basis of O ₁₀ (OH) ₈						
Si	4				3.982	3.969
Al	0				0.018	0.031
Σ _{tet}	4				4	4
Al	4				3.979	4.01
Fe ³⁺	0				0.01	
Fe ²⁺	0					
Mg	0				0.022	
Σ _{oct}	4				4.011	4.01

1, Ideal composition based on the structural formula, Al₂Si₂O₅(OH)₄; 2, kaolinite, Zettlitz, Czechoslovakia; 3, kaolinite, St. Austell, England; 4, kaolinite, Macon, Georgia; 5, dickite, Barkly East, Cape Province, South Africa; 6, nacrite, Eureka Tunnel, St. Peter's Dome, Colorado.

Analyses 1, 5, and 6 are taken from Newman (1987) in which original data for analyses 5 and 6 (recalculated after subtracting impurity) were referred from Schmidt and Heckrodt (1959) and Blount et al. (1969), respectively. Analyses 2, 3, and 4 are taken from Grim (1968) in which original data for the analysis 2 is referred from Ross and Kerr (1931) and analyses 3 and 4 from Kerr et al. (1950). For these references, see Grim (1968).

three-layer trigonal (3T), six-layer hexagonal (6H), and six-layer rhombohedral (6R) are reported (Bailey, 1969, 1980, 1988).

For the dioctahedral subgroup, kaolin minerals include kaolinite (one-layer triclinic, 1Tc), dickite (two-layer monoclinic, 2M), and nacrite (two-layer monoclinic, 2M), which are in polytypic relation. Examples of the chemical composition of kaolin minerals are given in Table 21.7. Kaolinite has triclinic symmetry. Oxygen atoms and hydroxyl ions between the layers are paired with hydrogen bonding. Because of this weak bonding, random displacements between the layers are quite common and result in a poor symmetry rather than distinctive triclinic kaolinite. Dickite and nacrite are polytypic varieties of kaolinite. Both of them consist of a double 1:1 layer and have monoclinic symmetry but distinguish themselves by different stacking sequences of the two 1:1 silicate layers.

21.2.3.3 Halloysite—Hydrated Halloysite Group

Halloysite has a composition close to that of kaolinite (Table 21.8) and is characterized by its tubular nature (see Figure 21.27) in contrast to the platy nature of kaolinite particles. Although tubular forms are the most common, other morphological varieties are also known: prismatic, rolled, pseudospherical (Figure 21.16), and platy forms. The structure of halloysite is believed to be

TABLE 21.8 Halloysite Mineral Analyses

	1	2	3
SiO ₂	40.09	46.2	44.7
Al ₂ O ₃	35.38	39.84	28.1
TiO ₂	nr	0.02	
Fe ₂ O ₃	tr	0.17	12.8
FeO	nr	nr	nr
MgO	tr	0.02	0.1
CaO	0.77	0.34	tr
K ₂ O	tr	0.02	tr
Na ₂ O	0.1	0.01	1.7
H ₂ O total			
H ₂ O ⁺	15	14	13.7
H ₂ O ⁻	8.61		
Total	100.51	100.62	100.7
Numbers of cations on basis of O ₁₀ (OH) ₈			
Si	3.907	3.957	4.029
Al	0.093	0.043	
Fe ³⁺			
Σ _{tet}	4	4	4.029
Al	3.971	3.978	2.985
Ti		0.001	
Fe ³⁺		0.011	0.868
Mg		0.003	0.013
Σ _{oct}	3.971	3.993	3.866
Ca	0.08	0.031	0
K	0	0.002	0
Na	0.019	0.002	0.297

1, Hydrated halloysite (halloysite—1 nm), Wagon Wheel Gap, Colorado (Larsen and Wherry, 1917); 2, halloysite (halloysite—0.7 nm), Djebel Debar, Morocco (Garrett and Walker, 1959); 3, iron-rich hydrated halloysite, Hokkaido, Japan (Wada and Mizota, 1982).

See Newman (1987) for original data.

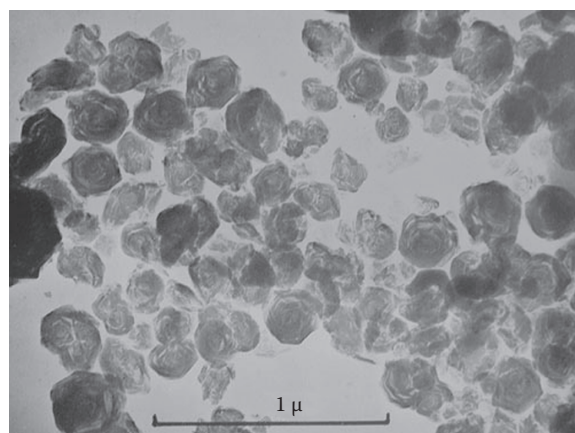


FIGURE 21.16 Electron micrograph of halloysite (with spherical structure), altered from glassy tuff. (From Sudo, T. 1959. Mineralogical study on clays of Japan. Maruzen Co. Ltd., Tokyo, Japan.)

similar to that of kaolinite, but no precise structure has been revealed yet. Halloysite has a hydrated form with composition of $\text{Al}_2\text{Si}_2\text{O}_5(\text{OH})_4 \cdot 2\text{H}_2\text{O}$. This hydrated form irreversibly changes to a dehydrated variety at relatively low temperatures (60°C) or upon being exposed to conditions of low relative humidity. The dehydrated form has a basal spacing about the thickness of a kaolinite layer (approximately 0.72 nm), and the hydrated form has a basal spacing of about 1.01 nm, the difference of 0.29 nm is approximately the thickness of one molecular layer of water. Consequently, in the hydrated form of halloysite, its silicate layers are separated by monomolecular water layers that are lost during dehydration.

21.2.4 2:1 Layer Type (T–O–T Type)

21.2.4.1 General

As seen in Figure 21.8b, the unit silicate layer of T–O–T type comprises one octahedral sheet sandwiched by two tetrahedral sheets, which are oriented in opposite directions and may be termed a 2:1 layer type. A majority of phyllosilicates hold a backbone of this type for their structures. This type includes talc, pyrophyllite, micas, brittle micas, vermiculite, and smectite.

21.2.4.2 Talc–Pyrophyllite Group

Minerals of this group have the simplest form of 2:1 layer with its unit thickness of approximately 0.92–0.96 nm—that is, the structure consists of an octahedral sheet sandwiched by two tetrahedral sheets. Talc and pyrophyllite represent the trioctahedral and dioctahedral members, respectively, of the group. In the ideal case, the structural formula of talc is expressed by $\text{Mg}_3\text{Si}_4\text{O}_{10}(\text{OH})_2$ and pyrophyllite by $\text{Al}_2\text{Si}_4\text{O}_{10}(\text{OH})_2$. Selected analyses are given in Table 21.9. Figure 21.17 shows these two structures as an extended crystal model, where the staggering between tetrahedral sheets above and below and the difference in octahedral sheets between talc and pyrophyllite is clearly seen. Each 2:1 layer of these minerals is electrostatically neutral; therefore, van der Waals forces hold the silicate layers together. One-layer triclinic and two-layer monoclinic forms are known for polytypes of pyrophyllite and talc. The ferric iron analog of pyrophyllite is called ferripyrophyllite.

21.2.4.3 True Mica Group

Mica has a basic structural unit of 2:1 layer type, like pyrophyllite or talc, but some of the silicon atoms (ideally one-fourth) are always replaced by aluminum atoms. This results in a charge deficiency that is balanced by potassium ions between the unit layers (Figure 21.18). The sheet thickness (basal spacing or dimension along the direction normal to the basal plane) is fixed at about 1 nm. Typical examples are muscovite, $\text{KAl}_2(\text{Si}_3\text{Al})\text{O}_{10}(\text{OH})_2$ for dioctahedral species and phlogopite, $\text{KMg}_3(\text{Si}_3\text{Al})\text{O}_{10}(\text{OH})_2$, and biotite, $\text{K}(\text{Mg},\text{Fe})_3(\text{Si}_3\text{Al})\text{O}_{10}(\text{OH})_2$, for trioctahedral species. Formulas rendered may vary slightly due to possible substitution within certain structural sites. The interlayer cation can be sodium instead of potassium, notably paragonite

TABLE 21.9 Talc and Pyrophyllite Analyses

	1	2	3	4	5	6
SiO ₂	63.37	62.67	63.9	63.57	66.04	66.7
Al ₂ O ₃		tr	0.03	29.25	28.15	28.3
TiO ₂		nr	0.1	0.04	nr	
Fe ₂ O ₃		nr	0.21	0.1	0.64	
FeO		2.46	nr	0.12	nr	
MnO		0.01	nr	None	nr	
MgO	31.88	30.22	31.49	0.37	0.04	
CaO		nr	0.08	0.38	0.01	
K ₂ O		nr	0.01	0.02	nr	
Na ₂ O		nr	0.02	tr	0.04	
H ₂ O ⁺	4.75	4.72	4.86	5.66	5.27	5
H ₂ O ⁻				0.66		
Total	100	100.02	100.7	100.17	100.19	100
Numbers of cations on basis of O ₁₀ (OH) ₂						
Si	4	3.99	4.01	3.89	3.975	4
Al	0			0.11	0.025	
Fe ³⁺	0					
Σ _{tet}	4	3.99	4.01	4	4	4
Al	0			1.99	1.975	2
Fe ³⁺	0		0.01	0.005	0.03	
Fe ²⁺	0	0.13		0.005		
Mg	3	2.87	2.94	0.035	0.005	
Σ _{oct}	3	3	2.95	2.036	2.01	2
Ca	0		0.005	0.025		
Na	0				0.005	
K	0					

1, Ideal composition, $\text{Mg}_3\text{Si}_4\text{O}_{10}(\text{OH})_2$; 2, talc, Muruhatten, Northern Sweden (Du Rietz, 1935); 3, talc, Manchuria (Brindley et al., 1977); 4, pyrophyllite, pale blue, Honami mine, Nagano Prefecture, Japan (Iwao and Udagawa, 1969); 5, pyrophyllite, Ibitiara Bahia, Brazil (Lee and Guggenheim, 1981); 6, ideal composition, $\text{Al}_2\text{Si}_4\text{O}_{10}(\text{OH})_2$.

Analysis 2 is referred from Deer et al. (1962). Analyses 3, 4, and 5 are taken from Newman (1987). See Newman (1987) for original source of each analysis except analyses 1 and 2.

in this case, which has an ideal formula of $\text{NaAl}_2(\text{Si}_3\text{Al})\text{O}_{10}(\text{OH})_2$. Various polytypes of the micas are known to occur. Among them one-layer monoclinic (1M), two-layer monoclinic (2M including 2M₁ and 2M₂), and three-layer trigonal (3T) polytypes are the most common. The majority of clay-size micas are dioctahedral aluminous species; those similar to muscovite are called illite (Bailey et al., 1984). The illites are different from muscovite in that the amount of substitution of aluminum for silicon is less, sometimes only one-sixth of the silicon ions are replaced. This reduces a net unbalanced charge deficiency from 1 to about 0.65 per chemical formula unit. As a result, the illites have a higher silica-to-alumina molecular ratio and lower potassium content than the muscovites (Graf von Reichenbach and Rich, 1975; Fanning et al., 1989). To some extent, octahedral aluminum ions are replaced by magnesium (Mg²⁺) and iron ions (Fe²⁺, Fe³⁺). In the illites, stacking disorders of the layers are common, but their polytypes are often unidentifiable. Celadonite and glauconite are ferric ion-rich species of dioctahedral micas. The ideal

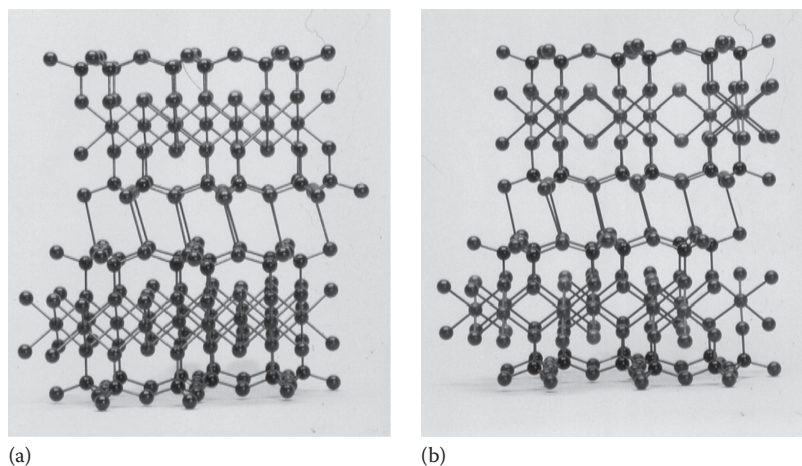


FIGURE 21.17 Extended crystal structure models of (a) talc and (b) pyrophyllite.

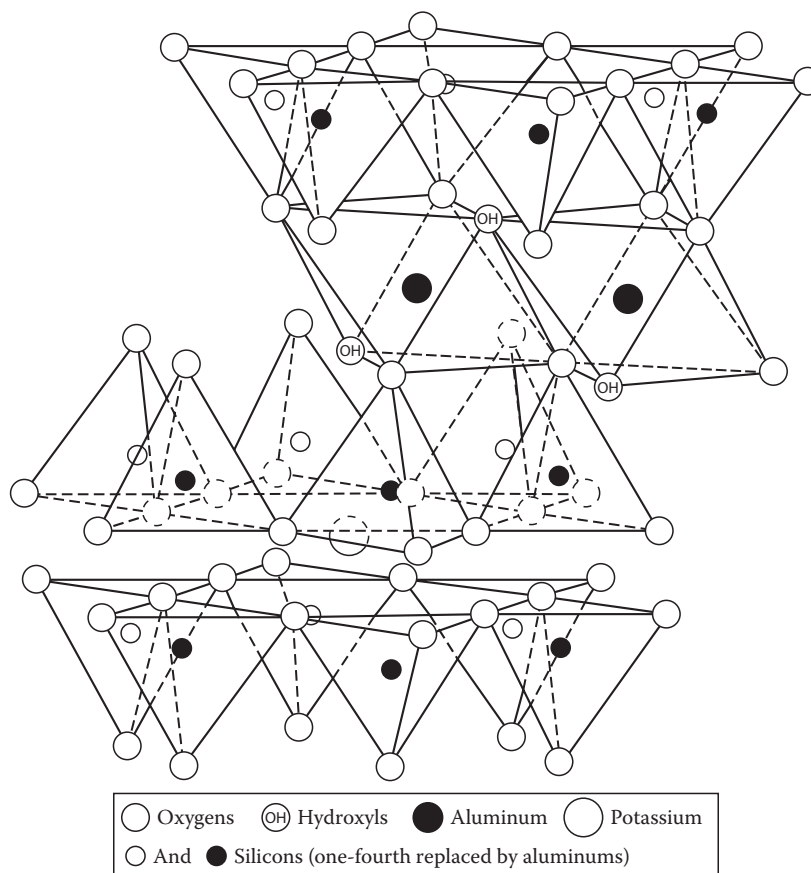


FIGURE 21.18 The structure of muscovite. (From Grim, R.E. 1968. Clay mineralogy. McGraw-Hill Book Co. Inc., New York. With permission.)

composition of celadonite may be expressed by $K(\text{Mg}, \text{Fe}^{3+}) (\text{Si}_{4-x}\text{Al}_x)\text{O}_{10}(\text{OH})_2$, where $x = 0-0.2$. Glauconite is a dioctahedral mica species with tetrahedral Al substitution greater than 0.2 and octahedral Fe^{3+} or R^{3+} (total trivalent cations) greater than 1.2. Unlike illite, a layer charge deficiency of celadonite and glauconite arises largely from the unbalanced charge due to ionic substitution in the octahedral sheets. Some chemical analyses of dioctahedral micas (Tables 21.10 and 21.11) and of trioctahedral

micas (Table 21.12) are given for reference. Comprehensive reviews on true micas are available (Bailey, 1984; Fleet, 2003).

21.2.4.4 Brittle Mica Group

Brittle micas are distinguished from true micas in having a layer charge of ~ -2.0 per formula unit, which arises entirely within the tetrahedral sheet or partly within the tetrahedral sheet and partly octahedral sheet. The tetrahedral composition varies

TABLE 21.10 Dioctahedral Mica Analyses (1)

	1	2	3	4	5	6	7	8
SiO ₂	45.26	45.87	45.24	42.63	44.94	48.42	51.19	55.61
Al ₂ O ₃	38.4	38.69	36.85	20.87	27.56	27.16	9.23	0.79
TiO ₂			0.01	0.45	0.98	0.87	0.13	
Cr ₂ O ₃				0.24	4.75			
V ₂ O ₃				13.72				
Fe ₂ O ₃			0.09			6.57	18.15	17.19
FeO		0	0.02	3.76	1.07	0.81	1.78	4.02
MnO		0	0.12	0.23	0		0.01	0.09
MgO		0.1	0.08	2.34	2.34	0	3.34	7.26
CaO			0	0.01	0	0	0.58	0.21
BaO				0.95	6.42	0.07		
K ₂ O	11.82	10.08	10.08	10.16	7.44	11.23	7.98	10.03
Na ₂ O		0.64	0.64	0.06	0.27	0.35	0.02	0.19
Cs ₂ O			0.2					
Rb ₂ O			0.93			0.19		
Li ₂ O			0.49					
F			0.91					
Cl								
H ₂ O ⁺	4.52	4.67	4.12			4.31	5.21	4.88
H ₂ O ⁻		0.7	0.09			0.19	1.95	
O≡F,Cl	100	100.05	100.24	95.21	95.77	100.17	99.67	100.27
			-0.38					
Total	100	100.05	99.86	95.21	95.77	100.17	99.67	100.27
Numbers of cations on basis of O ₁₀ (OH) ₂								
Si	3	3.009	3.024	3.061	3.136	3.297	3.71	3.995
Al	1	0.991	0.976	0.939	0.864	0.703	0.29	0.005
Fe ³⁺	0							
Σ _{tet}	4	4	4	4	4	4	4	4
Al	2	2.001	1.927	0.827	1.403	1.477	0.505	0.065
Cr					0.262	0.045		
Fe ³⁺	0		0.005	0.005		0.337	0.99	0.93
Fe ²⁺	0	0	0.001	0.226	0.062	0.046		0.24
Mg	0	0.01	0.008	0.25	0.243		0.36	0.775
Li			0.132					1.06
Other M			0.008		0.051			
Σ _{oct}	2	2.011	2.081	2.132	2.021	1.905	1.965	2.015
Ca	0		0.005	0.001			0.045	0.015
Ba				0.027	0.176	0.002		
Na	0	0.081		0.008	0.037	0.046	0.005	0.025
Rb						0.008		
K	1	0.844		0.931	0.662	0.976	0.735	0.92
Σ _{int}		0.925			0.875	1.032	0.785	0.965

1, Ideal muscovite composition, KAl₂(Si₃Al)O₁₀(OH)₂; 2, muscovite, Methuen Township, Ontario (Hurlbut, 1956); 3, muscovite (rose), Rociada, New Mexico (Heinrich and Levinson, 1953); 4, muscovite (vanadian), Hemlo gold deposit, Ontario (Pan and Fleet, 1992); 5, muscovite (barian-chromian), Hemlo-Heron Bay (Pan and Fleet, 1991); 6, phengite (high-silica muscovite), Morar, Inverness-shire (Lambert, 1959); 7, glauconite, Praha-Prosek (Cimbalnikova, 1971); 8, celadonite, Reno, Nevada (Hendricks and Ross, 1941).

Analyses 2–6 are taken from Fleet (2003). Analyses 7 and 8 are from Newman 1987 and recalculated. See Fleet (2003) or Newman (1987) for original source of each analysis.

TABLE 21.11 Dioctahedral Mica Analyses (2)

	1	2	3
SiO ₂	48.34	41.79	38.54
Al ₂ O ₃	37.87	18.98	25.61
TiO ₂	0.3	0.21	0
Cr ₂ O ₃		0.29	
V ₂ O ₃		17.55	
Fe ₂ O ₃	1.02		
FeO		1.15	2.44
MnO		0.08	0.07
MgO	0.11	2.18	1.78
CaO	0	0	0.01
BaO		3.29	
K ₂ O	3.25	9.76	0.53
Na ₂ O	0	0.16	
Cs ₂ O			25.29
Rb ₂ O			0.25
Li ₂ O			0.44
NH ₄	3.85		
F			1
H ₂ O ⁺	4.96		3.27
H ₂ O ⁻	0.31		
O≡F,Cl	100.01	95.44	99.23
	0	0	-0.42
Total	100.01	95.44	98.81
Numbers of cations on basis of O ₁₀ (OH) ₂			
Si	3.078	3.047	3.161
Al	0.922	0.953	0.839
Fe ³⁺			
Σ _{tet}	4	4	4
Al	1.92	0.679	1.637
Ti	0.014	0.012	
Cr		0.017	
V		1.026	
Fe ³⁺	0.049		
Fe ²⁺		0.07	0.167
Mn		0.005	0.005
Mg	0.01	0.237	0.218
Li			0.145
Other M			
Σ _{oct}	1.993	2.046	2.172
Ca			0.001
Na		0.081	
K	0.264	0.844	0.055
Rb			0.013
Cs			0.885
NH ₄	0.566		
Σ _{int}	0.83	0.925	0.954

1, Tobelite, Horo deposit, Toyosaka Hiroshima Prefecture, Japan (Higashi, 1982); 2, roscoelite, Hemlo gold deposit, Ontario, Canada (Pan and Fleet, 1992); 3, nanpingite, Nanping pegmatite field, Fujian, China (Yang et al., 1988).

Analyses 1, 2, and 3 are taken from Fleet (2003). See Fleet (2003) for original source of data.

from SiAl₃ to nearly Si₃Al and this is supplemented by octahedral sheet charges that range from +1.0 to 0 to nearly -1.0. As the layer charge is higher than that of true micas, divalent interlayer cations are required for compensation, instead of monovalent.

Clintonite is a trioctahedral species of ideal composition, Ca(Mg₂Al)(SiAl₃)O₁₀(OH)₂. Because high Al content in the tetrahedral sheet and Al atomic radius size is larger than Si, the hexagonal symmetry of the tetrahedral sheet is modified to ditrigonal (Figure 21.4b) by a tetrahedral rotation of 23° to match the lateral dimensions of the octahedral sheet. The reported polytypes are 1M, 2M₁, and 3T. Margarite is a known sole dioctahedral species in the brittle mica group, having ideal composition CaAl₂(Si₂Al₂)O₁₀(OH)₂, and with a 2M₁ structure. Other species belonging to the group include kinoshitalite (1M and 2M₁), with ideal formula BaMg₃(Si₂Al₂)O₁₀(OH)₂; anandite (2Or), with Ba(Fe,Mg)₃(Si₃Fe³⁺)O₁₀(OH)₂S; and bityite (2M₁), with BaLiAl₂(Si₂AlBe)O₁₀(OH)₂. Polytypes in brackets are only of high abundance. Analyses of representative brittle micas are given in Table 21.13.

21.2.4.5 Vermiculite Group

The vermiculite unit structure consists of talc-like 2:1 silicate layers separated by two molecular layers of water (approximately 0.48 nm thick). Substitutions of aluminum (Al³⁺) for silicon (Si⁴⁺) in tetrahedral sheets constitute the chief charge imbalance, but the net-charge deficiency may be partially balanced by other substitutions within the 2:1 silicate layer; but a residual net-charge deficiency always exists, commonly in the range 0.6–0.8 per O₁₀(OH)₂. This charge deficiency is satisfied with interlayer cations, which are closely associated with the water molecules between the silicate layers (Figure 21.19); Mathieson and Walker, 1954. As the net-charge deficiency is higher than smectites, in vermiculites interlayer water molecules are better coordinated with interlayer cations. In macroscopic vermiculites of hydrothermal origin, unlike those in soils, the balancing cation is mostly magnesium (Mg²⁺), sometimes associated with a small amount of calcium (Ca²⁺). The interlayer cation, however, is readily replaced by other inorganic and organic cations. A number of water molecules are related to the hydration state of cations located at the interlayer sites. Therefore, the basal spacing of vermiculite changes from about 1.05 to 1.57 nm, depending upon its crystal size, relative humidity, and the kind of interlayer cation. If potassium or ammonium ions are not present in the interlayer sites, in some extreme cases, heating vermiculite to temperatures as high as 500°C drives the water out from between the silicate layers, but the mineral quickly rehydrates at room temperature to maintain its normal basal spacing of approximately 1.4–1.5 nm. Special care would, therefore, be required to examine the dehydration–rehydration temperature of a vermiculite mineral in question.

If complete and irreversible dehydration occurs, the basal spacing becomes 0.902 nm. Figure 21.20 illustrates various hydration states of vermiculite. Note, however, that these states are affected by crystal size of the sample. Some dioctahedral analogs of vermiculite have also been reported to occur in soils (Brown, 1953).

TABLE 21.12 Trioctahedral Mica Analyses

	1	2	3	4	5	6	7	8
SiO ₂	43.21	42.98	39.17	36.05	33.96	35.21	50.31	45.51
Al ₂ O ₃	12.2	12.9	11.24	14.2	13.1	9.96	19.95	20.59
TiO ₂		0.33	2.23	4.38	3.55	0.87	0.22	0.24
Fe ₂ O ₃		0.91	1.86	6.24	3.06	6.57	0.49	1.51
FeO		2.7	16.58	13.35	32.04	42.11	2.55	9.2
MnO		0.08	0.89	0.23	0.65		2.63	0.53
MgO	28.99	25.93	13.51	12.23	0.97		0.02	0.3
CaO		0.06	0.2		0.42		0	0.27
BaO			0.05					
K ₂ O	11.29	10.63	9.29	9.36	8.47	9.2	10.14	9.68
Na ₂ O		0.25	0.62	0.14	0.27		0.49	0.6
Cs ₂ O							0.06	
Rb ₂ O							0.97	
Li ₂ O			0.18	0.02			5.39	3.66
F		6.04	3.46		0.82		7.65	7.45
Cl				0.41	0.34			
H ₂ O ⁺	4.31	1.7	1.64	3.21	2.5	3.52	0.88	1.9
H ₂ O ⁻		0.7	0.09				0.66	1.21
OΞF ₃ Cl	100	105.21	101.28	100	100.37	100	102.41	102.65
	0	-2.54	-1.48	-0.09	-0.43		-3.22	-3.14
Total	100	100.67	99.8	99.91	99.95	100	99.19	99.51
Numbers of cations on basis of O ₁₀ (OH) ₂								
Si	3	2.985	3.024	2.742	2.812	3.297	3.71	3.285
Al	1	1.015	0.976	1.258	1.188	0.703	0.29	0.715
Fe ³⁺	0							
Σ _{tet}	4	4	4	4	4	4	4	4
Al	2	0.04	1.927	0.015	0.091	1.477	0.505	1.035
Cr						0.045		
Fe ³⁺	0	0.05	0.005	0.357	0.191	0.337	0.99	0.08
Fe ²⁺	0	0.155	0.001	0.861	2.219	0.046		0.555
Mg	0	2.685	0.008	1.387	0.12		0.36	0.03
Li			0.132	0.006				1.06
Other M		0.02	0.008		0.051			
Σ _{oct}	2	2.95	2.081	2.892	2.888	1.905	1.965	2.81
Ca	0	0.005	0.005		0.037		0.045	0.02
Ba				0.027		0.002		
Na	0	0.035		0.021	0.079	0.046	0.005	0.085
Rb						0.008		
K	1	0.94		0.908	0.895	0.976	0.735	0.89
Σ _{int}		0.98		0.929	1.011	1.032	0.785	0.995

1, Ideal phlogopite composition, KMg₃(Si₃Al)O₁₀(OH)₂; 2, phlogopite, Ontario (Newman, 1987); 3, biotite, North Burgers, Ontario (Rausell Colom et al., 1965): Total includes 0.12% Cl and 0.05% Rb₂O; 4, biotite, Valle Vercelli, Northwestern Italy (Brigatti and Davoli, 1990); 5, annite, Pikes Peak granite, Colorado (Hazen and Burnham, 1973); 6, ideal annite composition KFe₃²⁺(Si₃Al)O₁₀(OH)₂; 7, lepidolite, Wakefield, Quebec, Canada (Steven, 1938; Backhaus, 1983); 8, zinnwaldite, Cinovec, Czechoslovakia (Rieder, 1970).

Analyses 2, 3, and 8 are taken from Newman 1987. Analyses 4, 5, and 7 are from Fleet (2003). See Newman (1987) or Fleet (2003) for original source of each analysis.

TABLE 21.13 Brittle Mica Analyses

	1	2	3	4	5	6
SiO ₂	15.84	24.58	30.34	29.9	24.59	33.37
Al ₂ O ₃	44	20.06	49.8	25.9	0.8	36.51
TiO ₂	nr	0.16	0.12		0.08	
V ₂ O ₄				5.4		
V ₂ O ₃				18.3		
Fe ₂ O ₃	2.04	0.71	0.35	0.4	21.15	
FeO	nr	0.04	0.51		22.7	
BeO						7.3
Mn ₂ O ₃		3.24				
MnO	nr	7.38	0.01		0.92	
MgO	20.33	16.6	0.59	1.6	2.89	0.04
CaO	13.01	0.05	11.43		0.01	14.42
BaO		17.85		9.35	23.05	
Li ₂ O			0.28			2.39
K ₂ O	0.19	3.3	0.27	0.7	0.24	0.04
Na ₂ O	0.26	0.68	1.95	1.32	0.06	0.29
F		0.21				
H ₂ O ⁺	4.56	2.9	4.65	6	5.27	5.72
H ₂ O ⁻		0.2		1.1		
OEF		-0.09				
Total	100.23	99.87	100.3	99.97	99.38	99.98
Numbers of cations on basis of O ₁₀ (OH) ₂						
Si	1.108	2.052	2.012	2.192	2.507	
Al	2.892	1.948	1.988	1.808	0.096	
Fe ³⁺	0				1.397	
Σ _{tet}	4	4	4	4	4	
Al	0.734	0.222	1.903	0.431		
Ti		0.01	0.006		0.006	
V ⁴⁺				0.287		
V ³⁺				1.076		
Fe ³⁺	0.107	0.045	0.017	0.022	0.225	
Fe ²⁺	0	0.003	0.028		1.935	
Mn ³⁺		0.206			0.037	
Mn ²⁺		0.522	0.001		0.042	
Mg	2.119	2.066	0.058	0.175	0.439	
Li			0.075			
Σ _{oct}	2.96	3.074	2.088	1.991	2.684	
Ca	0.975	0.004	0.812			
Ba		0.584		0.269	0.921	
Na	0.035	0.11	0.251	0.188	0.012	
K	0.017	0.351	0.023	0.065	0.031	
Σ _{int}	1.027	1.029	1.086	0.522	0.964	

1, Clintonite, Zlatoust, Shishim Mts., Ural, Russia (Forman et al., 1967); 2, kinoshitalite, Nodatamagawa mine, Japan (Yoshii et al., 1973); 3, margarite, Chester, Massachusetts (Storre and Nitsch, 1974); 4, chernykhite, Karatau Mts., Kazakhstan (Ankinovich et al., 1972); 5, anandite, Wilagedera, Sri Lanka (Filut et al., 1985); 6, bityite, Londonderry, Australia (Anthony et al., 1995).

Bityite: ideally CaLiAl₂(AlBeSi₂)O₁₀(OH)₂. Analyses 1–5 are taken from Fleet (2003). See Fleet (2003) for original source of each analysis.

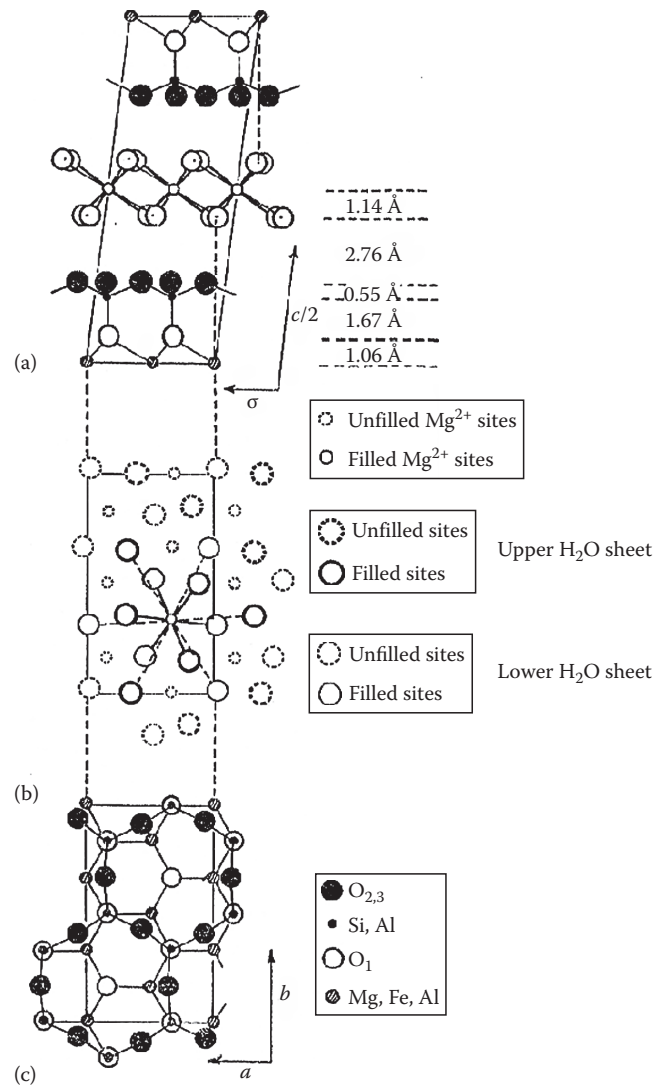


FIGURE 21.19 The crystal structure of Mg-vermiculite; (a) projection normal to ac plane, (b) projection normal to ab plane, showing inter-layer region, and (c) projection normal to ab plane, showing one-half of a silicate layer ($z = 0$ to $c/8$). (From Brown, G. (ed.). 1961. The X-ray identification and crystal structures of clay minerals. Mineralogical Society, London, U.K. Reproduced with kind permission of The Mineralogical Society of Great Britain and Ireland.)

21.2.4.6 Smectite Group

The structural units of smectite (Figure 21.21) can be derived from the structures of pyrophyllite and talc. Unlike pyrophyllite and talc, the 2:1 silicate layers of smectite have a slight negative charge owing to ionic substitutions in the octahedral and tetrahedral sheets. The net-charge deficiency is normally smaller than that of vermiculite from ~ 0.2 to 0.6 per O₁₀(OH)₂ and balanced by the interlayer cations as in vermiculite (Table 21.14). This weak bond offers an excellent cleavage between the layers. The distinguishing feature of the smectite structure from the other types is that water and other

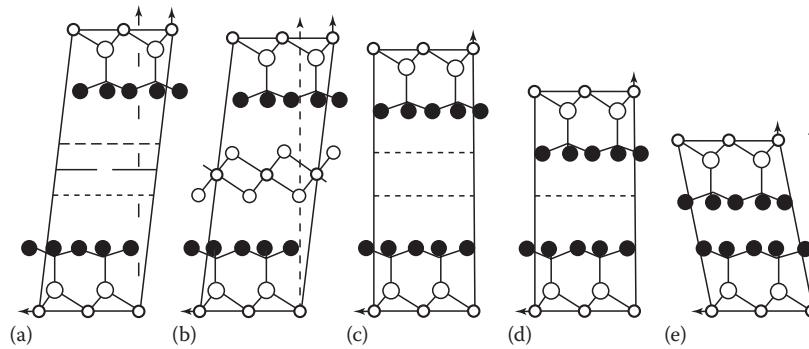


FIGURE 21.20 Various hydration states of Mg-vermiculite. Projections normal to the ac plane in the mineral at the various stages of hydration, showing the silicate layer relationships: (a) 1.481 nm phase, (b) 1.436 nm phase, (c) 1.382 nm phase, (d) 1.159 nm phase, and (e) 0.902 nm phase (key as for Figure 21.19). (From Brown, G. (ed.). 1961. *The X-ray identification and crystal structures of clay minerals*. Mineralogical Society, London, U.K. Reproduced with kind permission of The Mineralogical Society of Great Britain and Ireland.)

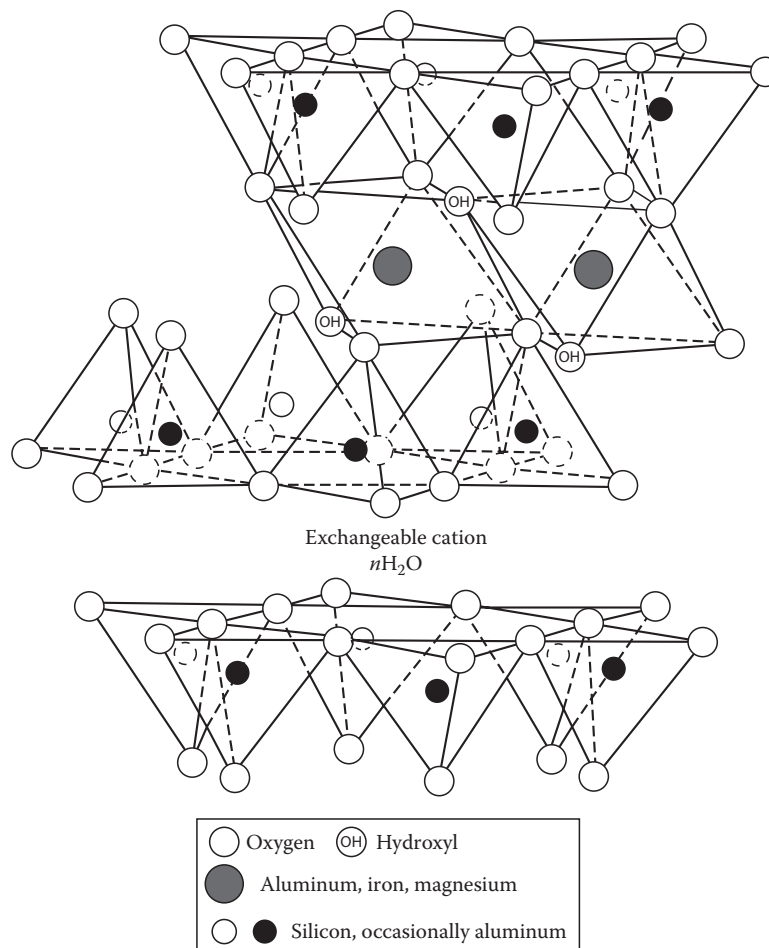


FIGURE 21.21 The structure of smectite. (From Grim, R.E. 1968. *Clay mineralogy*. McGraw-Hill Book Co. Inc., New York. With permission.)

polar molecules (in the form of certain organic substances) can, by entering between the unit layers, cause the structure to expand in the direction normal to the basal plane. Thus, this dimension may vary from about 0.96 nm, when no polar molecules are between the unit layers, to nearly complete separation of the individual layers.

The structural formula of dioctahedral aluminous smectites may be represented by $M_{x+y}^+(Al_{2-y}Mg_y^{2+})(Si_{4-x}Al_x)O_{10}$

$(OH)_2 \cdot nH_2O$, with $0.2 \leq x + y \leq 0.6$, where M^+ is the interlayer exchangeable cation expressed as a monovalent cation and x and y are the amounts of tetrahedral and octahedral substitutions, respectively. The smectites with $y > x$ are called montmorillonite and those with $x > y$ are known as beidellite. In the latter type of smectites, those in which ferric iron is a dominant cation in the octahedral sheet instead of aluminum and magnesium are called

TABLE 21.14 Smectite and Vermiculite Analyses

	1	2	3	4	5	6	7	8
SiO ₂	59.6	66.32	59.3	42.4	53.88	51.4	45.56	43.07
Al ₂ O ₃	22.17	22.42	36.11	5.6	4.47	9	15.82	16.92
TiO ₂	0.09				0.25		0.38	0.68
Fe ₂ O ₃	4.32	3.3	0.5	32.53	0.6	5.4	1.4	11.75
FeO						4.8		0.95
MnO	Tr						0.13	0.36
MgO	2.73	4.07	0.1	0.32	31.61	26.1	29.66	22.63
CaO	0.14	0.03	0.02	0.38	0.01	3.2	6.86	4.66
K ₂ O	0.03	0.06	0.11	5.14	0.05	0.12	0.17	0.03
Na ₂ O	3.18	3.68	3.98		0.01	0.04		0.06
H ₂ O ⁺	6.02				9.28			
Total H ₂ O				14.03				
Total	100.17	99.88	100.12	100.02	100.15	100	99.98	101.11
Numbers of cations on basis of O ₂₀ (OH) ₄								
Si	7.68	7.86	6.97	6.91	7.23	6.6	5.79	5.57
Al	0.32	0.14	1.03	0.77	0.71	1.36	2.21	2.43
Fe ³⁺	0			0.32	0.06	0.04		
Σ _{tet}	8	8	8	8	8	8	8	8
Al	3.05	2.99	3.98	0.29			0.16	0.14
Ti							0.04	0.07
Fe ³⁺	0.42		0.04	3.67	0.03	0.48	0.13	1.14
Fe ²⁺	0	0.29				0.52		0.1
Mn							0.01	0.04
Mg	0.52	0.72	0.02	0.04	5.97	5	5.62	4.36
Σ _{oct}	4	4	4.04	4	6	6	5.96	5.85
Ca	0.02			0.025		0.44	0.93	0.65
Mg					0.35			
Na	0.8	0.85	0.91		0	0.01		
K	0	0.01	0.02	1.13	0.01	0.02	0.03	0.02
Σ _{Inter. charge}	0.84	0.86	0.93	1.13	0.71	0.91	1.89	1.32

1, Montmorillonite, Clay Spur, Wyoming; Total includes 0.02% P₂O₅; 2, montmorillonite, Camp Berteau, France, ignited weight basis (Weir, 1965); 3, beidellite, Black Jack Mine, Owyhee County, Idaho (Weir, 1965); 4, nontronite, Garfield, Washington (Besson et al., 1983); 5, saponite, Krugersdorp, Transvaal, South Africa (Schmidt and Heystek, 1953); 6, saponite, Kozakov, Czechoslovakia (Suquet et al., 1975); 7, vermiculite, Llano County, Texas; 8, vermiculite, Ypung River, Western Australia.

See Newman (1987) for original source of each analysis.

nontronite or ferruginous smectite. Although less frequent, chromium (Cr³⁺) and vanadium (V³⁺) also are found as dominant cations in the octahedral sheets of the beidellite structure; in the case of chromium, the mineral is named volkonskoite.

The ideal structural formula of trioctahedral ferromagnesian smectites, the series saponite through iron-saponite, is given by M_x⁺(Mg, Fe²⁺)₃(Si_{4-x}Al_x)O₁₀(OH)₂·nH₂O. Tetrahedral substitution is responsible for the net-charge deficiency in the smectite minerals of this series. Besides magnesium and ferrous iron, zinc, cobalt, and manganese are known to be dominant cations in the octahedral sheet. Zinc-dominant species are called sauconite. In other types of trioctahedral smectites, the net-charge deficiency arises largely from ionic substitution or a small number of cation vacancies in the octahedral sheets, or from both. Ideally *x* is 0, but most often it is less than 0.15. Thus, the octahedral composition varies to maintain

similar amounts of net-charge deficiency as those of other smectites. Typical examples are (Mg_{3-y}□_y) for stevensite and (Mg_{3-y}Li_y) for hectorite, respectively, where □ denotes a vacancy site in the structure. In stevensite, therefore, *y* sites out of three are vacant.

The structure of smectites described above is based on their ideal model. Their actual structures are more or less distorted and show different physical appearances due to various circumstances. Electron optical diffraction examinations are most effective for their characterization. According to the accounts of Méring and his colleagues (Méring and Brindley, 1967; Méring and Oberlin, 1967, 1971; Méring, 1975), three types of layer-stacking arrangement have been observed and classified. Particles of smectites are composed of a stacking of elementary layers, in which on the average 10–20 elementary layers are stacked together, and their arrangements are ordered, semioordered, or turbostratic.

The ordered arrangement should give a clear hexagonal net (spots) pattern by the electron microdiffraction diagram. In semiordered arrangement, the mutual orientation of the elementary layers is defined by arbitrary multiples of 60° . Therefore, the stacking is no longer a triperiodic crystal but maintains “hexagonal” symmetry. If disorientation is defined by rotations about the c^* -axis (normal to the basal plane of smectites), layer stacking is called turbostratic. With the disorientation, diffraction spots of hk become diffuse and elongated, and the extent of those effects are related to the degree of disorientation. Turbostratic arrangements are unique to smectite minerals and no other phyllosilicates with such structure are known. Typically montmorillonite, hectorite, and nontronite show turbostratic structure. Beidellite and saponite are, on the other hand, known to possess relatively ordered structures.

21.2.5 2:1:1 Layer Type (T–O–T–O Type)

21.2.5.1 Chlorite Group

The structure of the chlorite minerals consists of alternate mica-like layers and brucite-like hydroxide sheets about 1.4 nm thick (Figure 21.22). Structural formulas of most trioctahedral chlorites may be expressed by four end-member compositions:

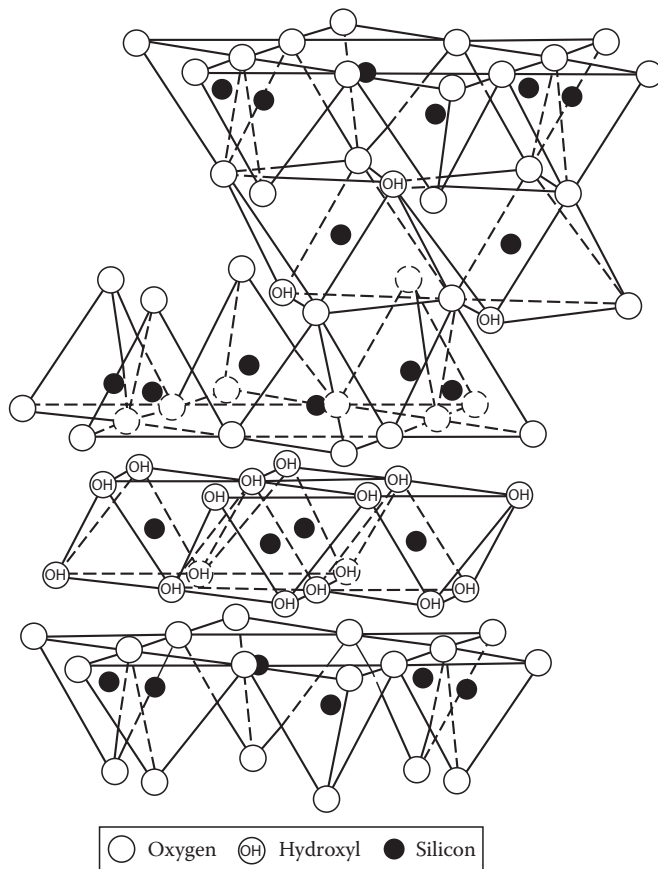
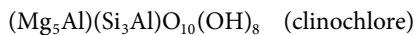
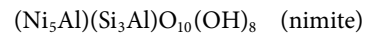
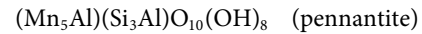
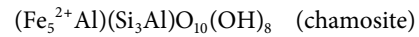


FIGURE 21.22 The structure of chlorite. (From Grim, R.E. 1968. Clay mineralogy. McGraw-Hill Book Co. Inc., New York. With permission.)



The unbalanced charge of the silicate layer is compensated by an excess charge on the hydroxide sheet caused by the substitution of trivalent cations (Al^{3+} , Fe^{3+} , etc.) for divalent cations (Mg^{2+} , Fe^{2+} , etc.). Chlorites, with an aluminous dioctahedral silicate layer and an aluminum hydroxide sheet are called donbassite and have the ideal formula of $\text{Al}_{4.33}(\text{Si}_3\text{Al})\text{O}_{10}(\text{OH})_8$ as an end-member for the dioctahedral chlorite. However, in many cases, the octahedral Al ions are partially replaced by magnesium, as in magnesium-rich aluminum dioctahedral chlorites, which are called sudoite. Cookeite is another type of dioctahedral chlorite, in which lithium (Li) substitutes for aluminum in the octahedral sheets. Selected chemical analyses are listed in Table 21.15. The symmetry of chlorite structures is variable due to the kind and amount of substitutions within the hydroxide sheet and within the tetrahedral and octahedral sites of the 2:1 silicate layer, the orientation of successive octahedral and tetrahedral sheets, and the way of the stacking of successive chlorite units. Specifically, as the chlorite unit contains hydroxide layers, the way of stacking between the basal oxygen atoms of the tetrahedral sheet and the hydroxyls in the first atomic plane of the hydroxide sheet is unique for chlorite. According to Shirozu and Bailey (1965), among six possible polytypes four are known to naturally occur and they are denoted as *Ia*, *Ib* ($\beta = 97^\circ$), *Ib* ($\beta = 90^\circ$), and *IIb*, respectively. Type I and Type II are distinguished by a difference in the shifting direction of the silicate layer with respect to that of the successive hydroxide sheet. Designation *a* indicates the case in which two-thirds of cations in the hydroxide sheet locate above tetrahedral cations and the remaining octahedral cations occupy at the center of the hexagonal rings, whereas designation *b* is the case in which cations of the hydroxide sheet distribute symmetrically upon projecting them onto the hexagonal ring. An overwhelmingly common polytype in nature is the single-layer monoclinic structure designated as *IIb*. A majority of trioctahedral chlorites including sudoite takes this polytype, while *Ib* ($\beta = 97^\circ$) and *Ib* ($\beta = 90^\circ$) polytypes are abundant in iron-rich chlorites. The *Ia* polytype is often realized in cookeite and donbassite. Chlorite structures are relatively thermally stable compared to kaolinite, vermiculite, and smectite minerals. Due to this, the presence of the XRD peak at 1.4 nm after heat treatment at 500°C – 700°C is widely used for the identification of chlorite minerals.

21.2.6 Interstratified Layer Silicate Group (Mixed-Layer Type)

As seen from the foregoing discussion, structures of phyllosilicates are strikingly similar except for sheet sequence such as T–O and T–O–T and layer thickness. Because of similarity as such, nature finds that a layer silicate of one kind interstratifies with that of another kind to make up a new structure that differs from either component layer.

TABLE 21.15 Chlorite Analyses

	1	2	3	4	5	6	7	8
SiO ₂	33.83	26.65	21.29	27.27	33	33.31	35.36	34.4
Al ₂ O ₃	12.95	16.14	19.07	15.21	35.69	44.16	47.35	51.85
TiO ₂						tr		
Fe ₂ O ₃	2.25	6.69	6.67		2.74	1.72	0.52	
FeO	3.02	34.43		2.78	0.24	1.69	0.07	
MnO	0	0.07	39.82	0.06	0.28	0.18		
ZnO			0.97					
NiO				29.49				
CoO				0.38				
MgO	34.94	4.47	41.06	10.13	14.07	0.37	0.67	
Li ₂ O						3.4		
CaO				0.38		0	0.45	
K ₂ O					0	0.67		
Na ₂ O						0.7		
H ₂ O ⁺	13.11	11.42	12.11	10.48	13.83	13.19	14.28	13.75
H ₂ O ⁻	0	0.08		0.27		0.46		
Total	100.1	99.88	100.12	100.8	100.03	99.85	99.1	100
Numbers of cations on basis of O ₁₀ (OH) ₈								
Si	3.21	3.05	2.59	3.01	3.01	2.975	3.155	3
Al	0.79	0.95	1.41	0.99	0.99	1.025	0.845	1
Fe ³⁺								
Σ _{tet}	4	4	4	4	4	4	4	4
Al	0.65	1.23	1.31	0.98	2.84	3.625	4.13	4.33
Fe ³⁺	0.16		0.6	0.36	0.19	0.115	0.035	
Fe ²⁺	0.24	3.87		0.26	0.02	0.125		
Mn			4		0.02	0.015		
Ni				2.62				
Co				0.04				
Zn			0.09					
Mg	4.94	0.76		1.68	1.91	0.05	0.09	
Li						1.22		
Σ _{oct}	5.99	5.86	6	5.96	4.98	5.15	4.26	4.33

1, Clinocllore, Zillertal, Austria; 2, chamosite, Schmiedefeld, Germany: Total Fe as Fe²⁺ in numbers of cation; 3, pennantite, Ushkatyn deposit, Kazakhstan; 4, nimate, Barberton, South Africa: Total octahedral cation number includes 0.04 Ca; 5, sudoite, (di, trioctahedral chlorite) Venn-Stavelot Massif, Ardennes, Belgium (Fransolet and Bourguignon, 1978); 6, cookeite, Northwestern USSR (Cerny, 1970); 7, donbassite, Novaya Zemlya, Russia (Drits and Lazarenko, 1967); 8, ideal donbassite composition, Al_{4.33}(Si₃Al)O₁₀(OH)₈.

Analyses 1–4 and 8 are taken from Anthony et al. (1995). Analyses 5–7 are taken from Newman (1987) and modified to fit with the table. For original data source, see Anthony et al. (1995) or Newman (1987).

The most striking examples of interstratified structures are those having a regular *AB AB ...* type structure, where *A* and *B* represent two different component layers. The interstratified minerals of this type show a long periodicity along the *c**-axis (normal to the basal plane) of the structure, which is the sum of the two individual periodicities of the component layers *A* and *B*. Several minerals are known to have structures of this type, that is, rectorite (dioctahedral mica/montmorillonite), tosudite (dioctahedral chlorite/smectite), corrensite (trioctahedral vermiculite/chlorite) in two types with high- and low-layer charge vermiculite,

hydrobiotite (trioctahedral mica/vermiculite), alietite (talcl/saponite), and kulkeite (talcl/chlorite). Analyses of selected samples of those regular interstratifications are shown in Table 21.16.

Other than the *AB AB ...* type with equal numbers of the two-component layers in a structure, a variety of modes of the layer-stacking sequence is possible from nearly regular to completely random. The following interstratifications of two components are reported in these modes in addition to those given above: Illite-smectite, glauconite-smectite, dioctahedral mica-chlorite, dioctahedral mica-vermiculite, and kaolinite-smectite. As the mixing

TABLE 21.16 Interstratified Layer Silicates (Two Components with 1:1 Ratio and Regular Sequence)

	1	2	3	4	5	6	7
SiO ₂	46.21	53.15	36.77	35.2	36.96	41.25	54.11
Al ₂ O ₃	14.44	3.48	11.6	14	32.09	36.48	40.38
TiO ₂				tr	0.34	0.07	0.01
Fe ₂ O ₃		3.48	8.19	3.48	1.57	0.67	0.15
FeO			0.98	2.9	tr		
MnO		0.03	0.08	tr			0
MgO	37.85	27.4	20.04	28.5	8.2	1.27	0.78
CaO	0.07	1.1	1.94	0.93	2.21	3.97	0.52
K ₂ O	0.06		3.84	tr	0.23		3.87
Na ₂ O		1.18	0.12	tr	0.16		0.29
H ₂ O total		10.18					
H ₂ O ⁺			6.69	10.6	12.71	7.19	
H ₂ O ⁻			7.8	4.28	6.12	6.99	
Total	100.1	100	99.93	99.89	100.59	99.72	100.24
Anion basis	A	B	C	D	E	F	G
Si	13.14	14.66	5.77	6.062	12.5	5.85	12.84
Al	2.86	1.13	2.14	1.938	3.5	2.15	3.16
Fe ³⁺		0.21	0.09				
Σ _{tet}	16	16	8	8	16	8	16
Al	1.98			0.897	9.29	3.92	8.12
Ti					0.09	0.01	0
Fe ³⁺		0.51	0.88	0.45	0.4	0.07	0.03
Fe ²⁺			0.13	0.416			
Mn		0.01	0.01				0
Mg	16.05	11.26	4.68	7.362	4.13	0.15	0.09
Σ _{oct}	18.03	11.78	5.82	9.125	13.91	4.15	8.24
Total Ca	0.02	0.33	0.34 ^a	0.172	0.8	0.59	0.14
Total K	0.02		0.77		0.1	0.15	0.09
Total Na	0.76	0.63	0.04		0.11	0.27	1.78
Σ	0.8	0.96	1.15	0.172	1.01		2.01
Exch. Ca							0.29
Exch. K							0.01
Exch. Na							0.13
Exch. Mg						0.16	
Σ _{charge}						0.32	0.72

Anion basis: A = E [O₄₀(OH)₂₀]; B = G [O₄₀(OH)₈]; C = F [O₂₀(OH)₄]; and D [O₂₀(OH)₁₀].

1, Kulkeite, chlorite-talc, Derrag, Tell Atlas, Algeria (Schreyer et al., 1982); 2, alietite, talc-saponite, Nure Valley, Piacenza Province, Italy (Alietti and Mejsner, 1980); 3, hydrobiotite, biotite-vermiculite, Rainy Creek, near Libby, Montana (Boettcher, 1966): Total includes 0.27% Cr₂O₃, 0.01% NiO, 0.01% SrO, 0.19% BaO, 0.0158% Rb₂O, 0.0005% Cs₂O and 0.06% P₂O₅; 4, corrensite, trioctahedral chlorite-vermiculite (or smectite) Sharbot Lake, Ontario, Canada (De Kimpe et al., 1987); 5, tosudite, chlorite-smectite, Niida, Akita Prefecture, Japan (Sudo and Shimoda, 1978); 6, rectorite, dioctahedral mica (Ca)-smectite, Sano mine, Nagano Prefecture, Japan (Matsuda et al., 1997); 7, rectorite, dioctahedral mica (Na)-smectite, Fort Sandeman, Baluchistan, Pakistan (Kodama, 1966): Total includes exchangeable Ca, Mg, and Sr.

See Newman (1987) for original data source of each analysis.

^a Ba is included.

ratio (proportion of the component layers) of the two-component layers varies, the number of possible layer-stacking modes increases greatly. Theoretically, any number of the kinds of component layers can form interstratified structures. In practice, however, a maximum of three-component layers have been positively identified. Interstratified structures consisting of illite-chlorite-smectite and illite-vermiculite-smectite have been reported so far. Because certain interstratified structures are known to be stable under relatively limited conditions, their occurrence may be used as a geothermometer or other geoinicator. On the other hand, Nadeau (1985) and Nadeau et al. (1984a, 1984b) proposed the fundamental particle theory, which argues that interstratified structures may be considered as artifacts of sample preparation. Extra caution is required to describe interstratified layer silicates correctly.

21.2.7 Modulated Layer Silicate Group

21.2.7.1 General

Guggenheim and Eggleton (1988) defined modulated layer silicates as those minerals that contain a periodic perturbation to the basic layer silicate structure. The basic structure involves 1:1 or 2:1 layer configurations. Thus, as the severity of the modulations increases, 2D continuous layer-like qualities diminish. The octahedral sheet of a modulated layer silicate is invariably a brucite-like (trioctahedral) sheet. Palygorskite, sepiolite, greenalite, minnesotaite, caryopilite, zussmanite, stilpnomelane, ganophyllite, bementite, etc. are known to be mineral species belonging to this group. Strictly speaking, antigorite may also be treated as one of the modulated 1:1 layer silicates. In this chapter the “phylosilicate” antigorite is thought to be represented in comparison with its other counterparts.

21.2.7.2 Sepiolite-Palygorskite Group

Sepiolite and palygorskite are papyraceous or fibrous hydrated magnesium silicate minerals (Figure 21.23) and are included in



FIGURE 21.23 Electron micrograph of palygorskite from Nawton, near Thirsk, Yorkshire. (From Gard, J.A. (ed.). 1971. The electron-optical investigation of clays. Monograph No 3. Mineralogical Society, London, U.K. Reproduced with kind permission of The Mineralogical Society of Great Britain and Ireland.)

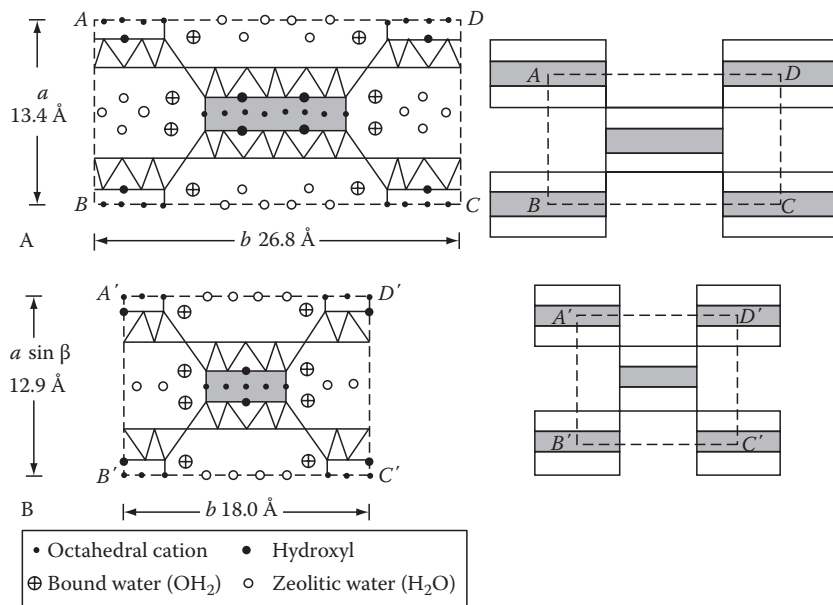


FIGURE 21.24 Structural sketches of palygorskite and sepiolite. (Reprinted from Sudo, T., S. Shimoda, H. Yotsumoto, and S. Aita. 1981. Electron micrographs of clay minerals. Developments in sedimentology. Vol. 31. Elsevier Scientific Publishing Co., New York. With permission from Elsevier.)

the phyllosilicates because they contain a continuous 2D tetrahedral sheet of composition Si_2O_5 . They differ, however, from the other layer silicates because they lack continuous octahedral sheets. The structures of sepiolite and palygorskite are alike and can be regarded as consisting of narrow strips or ribbons of 2:1 layers that are linked stepwise at the corners (Figure 21.24). One ribbon is linked to the next by inversion of the direction of the apical oxygens of SiO_4 tetrahedra, in other words, an elongated rectangular box consisting of a continuous 2:1 layer is attached by the nearest boxes at their elongated corner edges. Therefore, channels or tunnels due to the absence of the silicate layers occur on the elongated sides of the boxes. The elongation of the structural element is related to the fibrous morphology of the minerals and parallel to the a -axis. Since the octahedral sheet is discontinuous, some octahedral magnesium ions are exposed at the edges and hold bound water molecules (OH_2). In addition to the bound water, variable amounts of zeolitic (i.e., free) water (H_2O) are contained in the rectangular channels. The major difference between the structures of sepiolite and palygorskite is the width of the ribbons, which is greater in sepiolite than in palygorskite. The width determines the number of octahedral cation positions per formula unit. Thus, sepiolite and palygorskite have the ideal compositions $\text{Mg}_8\text{Si}_{12}\text{O}_{30}(\text{OH})_4(\text{OH}_2)_4(\text{H}_2\text{O})_8$ and $(\text{Mg},\text{Al},\square)_5\text{Si}_8\text{O}_{20}(\text{OH})_2(\text{OH}_2)_4(\text{H}_2\text{O})_4$, respectively. Some of Mg in sepiolite may be replaced by Al, Fe^{3+} , or Fe^{2+} . Selected analyses of this mineral group are given in Table 21.17.

21.2.7.3 Greenalite, Minnesotaitite, and Caryopilite

Greenalite was once expected to be a near iron end-member of serpentine. Guggenheim et al. (1982) showed that its structure is composed of coherent intergrowths of a trigonal polytype and a monoclinic polytype, with volume wise the former being

larger than the latter and having a domain size of about 2 nm. Minnesotaitite has a continuous octahedral sheet (Guggenheim and Bailey, 1982). Adjacent tetrahedral are present on either side of this sheet to form an approximate 2:1 layer. However, in contrast to talc, strips of linked hexagonal rings of tetrahedra are formed only parallel to γ (Figure 21.25; Guggenheim and Eggleton, 1986). Some analyses of greenalite and minnesotaitite are listed in Table 21.18, in which an analysis of caryopilite, as a manganese species of serpentine-like mineral, is included for comparison.

21.3 Occurrence of Phyllosilicates

21.3.1 As Rock-Forming Minerals

Known established species of phyllosilicates are no more than 100 (see Appendix). Although this is a rather small portion of the total mineral kingdom of some 3700 species, the occurrence of phyllosilicates is spread to a wide variety of geological environments. Among those described in the previous sections, perhaps biotite is the most; it is found in igneous rocks varying from granitic pegmatites, to granites, to syenites, to diorites, and to gabbros and peridotites. It also occurs in felsic volcanic rocks such as dacites, rhyolites, trachyte, and phonolites. In metamorphic rocks, including contact-metamorphosed rocks, biotite is formed under a wide range of temperature and pressure conditions. Muscovite is also a widespread and common rock-forming mineral, especially in pegmatites and granitic rocks. It is often found in metamorphic rocks as mica schists and as green schists with chlorite. Phlogopite occurs in metamorphosed magnesium limestones, dolomites, and ultrabasic rocks. Lepidolite is an uncommon mineral, found in lithium-rich pegmatites. Some brittle micas occur in regional contact-metamorphosed rocks.

TABLE 21.17 Palygorskite and Sepiolite Analyses

	1	2	3	4
SiO ₂	55.03	53.75	52.5	52.36
Al ₂ O ₃	10.24	10.23	0.6	0.23
Fe ₂ O ₃	3.53	1.83	2.99	0.4
FeO		0.26	0.7	
MnO				0.01
MgO	10.49	9.39	21.31	22.6
CaO		2.29	0.47	0.83
K ₂ O	0.47	0.02		
Na ₂ O		tr		
H ₂ O ⁺	10.13	12.04	9.21	9.34
H ₂ O ⁻	9.73	10.16	12.06	13.85
Total	99.62	99.97	99.84	99.62
Numbers of cations on basis of				
	A	B		
Si	7.8	7.82	11.81	11.95
Al	0.2	0.18	0.16	0.05
Fe ³⁺			0.03	
Σ _{tet}	8	8	12	12
Al	1.51	1.57		0.01
Fe ³⁺	0.38	0.2	0.47	0.07
Fe ²⁺		0.03	0.13	
Mg	2.22	2.04	7.14	7.69
Ni				
Σ _{oct}	4.11	3.84	7.74	7.77
Ca		0.36	0.11	0.2
K	0.09			
Na				
Σ charge	0.09	0.72	0.22	0.4

A: O₂₀(OH)₄(OH₂)₂ for anion basis of palygorskite;
 B: O₃₀(OH)₄(OH₂)₄ for anion basis of sepiolite.

1, Palygorskite, Attapulgis, Georgia (Bradley, 1940);
 2, palygorskite, Kuzu District, Tochigi Prefecture, Japan
 (Imai et al., 1969); 3, sepiolite, Ampandrandava,
 Maaagascar (Caillère and Hénin, 1961); 4, sepiolite, Kuzu
 District, Tochigi Prefecture, Japan (Takahashi, 1966).

Analyses are taken from Newman (1987).

21.3.2 Hydrothermal Origin and the Term "Clay Minerals"

In hydrothermal deposits or wall-rock alteration zones, many of phyllosilicates except palygorskite and sepiolite have been found as alteration products associated with hot springs and geysers and as aureoles around metalliferous deposits. Frequently a zonal arrangement of phyllosilicates, normally as very fine-grained clayey materials, is observed around the source of the alteration. The zonal arrangement varies with the type of parent rocks and the nature of hydrothermal solution. Extensive clay zones formed in close association with "kuroko" deposits contain mica (illite), chlorite, tosudite, smectite, and mica-smectite interstratifications. Pottery stones that consist of kaolinite, illite, and pyrophyllite occur as alteration products of acidic volcanic

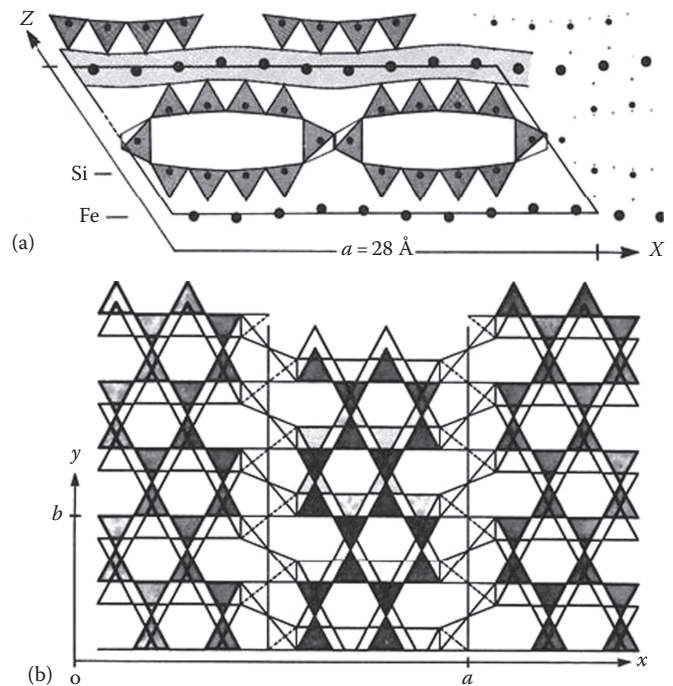


FIGURE 21.25 Structural sketches of minnesotaite: (a) Perspective view of the idealized structure in which the interlayer tetrahedra share corners to form a chain parallel to Y and (b) in the (001) plane drawing. (From Guggenheim, S., and S.W. Bailey. 1982. The superlattice of minnesotaite. *Can. Mineral.* 20:579–584.)

rocks, shales, and mudstone, while talc is formed from magnesium silicates, such as olivines, pyroxenes, and amphiboles. Generally speaking, near-neutral hydrothermal solutions generate rock alteration, including the formation of illite, chlorite, and smectite, whereas acid hydrothermal solutions generate the formation of kaolinite.

Most phyllosilicates of hydrothermal origin hold properties defined by the term "clay." The term "clay" is generally applied to the following: (1) a natural material with plastic properties, (2) an essential composition of particles found in a very fine-size fraction, which is customarily defined as particles smaller than 2 μm, and (3) a composition of very fine mineral fragments or particles that are mostly hydrous layer silicates of aluminum or occasionally containing magnesium and iron (Grim and Kodama, 1997). Although, in a broader sense, clay minerals can include virtually any minerals in the clay-size fraction, the definition adopted here is restricted to the hydrous layer silicates, which are conveniently used to distinguish themselves from macroscopic phyllosilicates. In other words, the term "clay minerals" is a synonym of microcrystalline phyllosilicates.

21.3.3 Diagenesis and Low-Grade Metamorphism

Analyses of many ancient sediments in many parts of the world indicate that very old argillaceous (clay-rich) sediments (physi-lites) are largely composed of illite and chlorite. These clay minerals are also found in carbonate rocks (calcretes). Smectite is a

TABLE 21.18 Modulated Layer Silicate Analyses

	1	2	3	4
SiO ₂	33.58	36.5	35.4	51.29
Al ₂ O ₃		0.16	2.38	0.61
TiO ₂				0.04
Fe ₂ O ₃	11.16	nr	nr	2
FeO	45.19			33.66
Total Fe as FeO ^a		46.7	0.95	nr
MnO		1.5	49.2	0.12
MgO		4.53	1.23	6.26
CaO		0.02	0.16	0
K ₂ O			0.03	0.03
Na ₂ O			0.16	0.08
H ₂ O total	10.07			
H ₂ O ⁺				5.54
H ₂ O ⁻				0.24
Total	[100]	89.41	89.4	99.87
Anion basis	O ₅ (OH) _{3.28}	O ₁₀ (OH) ₈	O ₁₀ (OH) ₈	
Si	2.18	4	4	3.95
Al				0.05
Fe ³⁺				
Σ _{tet}	2.18	4	4	4
Al		0.02	0.32	
Fe ³⁺	0.45			
Fe ²⁺	2.34	4.28	0.09	2.28
Mn		0.14	4.7	0.01
Mg		0.74	0.21	0.72
Σ _{oct}	2.79	5.18	5.32	3.01

1: Greenalite, Mesabi Range, Minnesota. Recalculated to 100% after reduction of SiO₂ and other impurities. Anion basis: O₅(OH)_{3.28}; 2: greenalite, Sokoman iron formation, Knob Lake, Labrador, Canada; 3: caryopilite, Hurricane Claim, Olympic Peninsula, Washington; 4: Minnesotaite, Mesabi district, Minnesota.

Analyses 1 and 4 are taken from Anthony et al. (1995). Analyses 2 and 3 are taken from Newman (1987).

For original data source of each analysis, see Anthony et al. (1995) or Newman (1987).

common component of many shales of Mesozoic and younger ages. As temperature and pressure increase with the progression of diagenesis, clay minerals in sediments under these circumstances change to those stable under given conditions. Therefore, certain sensitive minerals may serve as indicators for various stages of diagenesis. Typical examples are the crystallinity of illite (Kubler, 1966), illite and chlorite polytypes, and the conversion of smectite to illite. The data reported indicate that smectite was transformed into illite through interstratified illite–smectite mineral phases as diagenetic processes advanced. Much detailed work has been devoted to the conversion of smectite to illite in the lower Cenozoic–Mesozoic sediments because such a conversion appears to be closely related to oil-producing processes (Burst, 1969). In the very low-grade metamorphic zone, which is considered to be an intermediate zone between diagenetic and metamorphic zones, the occurrence of rectorite, kulkeite, pyrophyllite, and talc has been reported. Well-crystallized micas and

chlorites are often major components in metamorphic rocks. Smectites are known to occur in sediments of pyroclastic materials as the result of devitrification of volcanic ash in situ. Much discussion appears to favor marine origin for glauconite and nonmarine origin for celadonite (Dunoyer de Sagonzac, 1970; Weaver, 1989; Viede, 1992).

21.3.4 In Soils, Sediments, and Weathering Products

The formation of the clay minerals by weathering processes is determined by the nature of the parent rock, climate, topography, vegetation, and the time period during which these factors have operated. Climate, topography, and vegetation influence weathering processes by their control of the character and direction of movement of water through the weathering zone. When the dominant movement of water is downward through the alteration zone, any alkaline or alkaline-earth elements tend to be leached and primary minerals containing these components are first degraded and then broken down. If the leaching is intense, then after the removal of the alkalis and alkaline earths, the aluminum or silica may be removed from the alteration zone. This will depend on the pH of the downward-seeping waters. The pH of such water is determined, in turn, by the climate and cover of vegetation. Under warm and humid conditions, with long wet and dry periods, the surface organic material tends to be completely oxidized. The downward-seeping waters, therefore, are neutral or perhaps slightly alkaline and silica will be removed, whereas aluminum and iron will be left behind and concentrated. The result is a lateritic type of soil. Under more temperate conditions, the surface organic material is not completely oxidized and the downward-seeping water contains organic acids. In this case, aluminum and iron oxides are leached and the silicon is left behind; podzolic types of soils will develop. Under these conditions, mica and chlorite tend to be transformed into expandable clay minerals such as vermiculite and smectite or their intergrades as interstratifications. Allophane and imogolite may be present as newly formed clay minerals. In andosols, which are the soils developed on volcanic ash, allophane and imogolite as well as hydrated halloysite and halloysite are dominant components. (Wada and Greenland, 1970) Smectite is usually the sole dominant component in vertisols, which are clayey soils. Smectite and illite, with occasional small amounts of kaolinite, occur in mollisols and prairie chernozemic soils. Illite, vermiculite, smectite, chlorite, and interstratified clay minerals occur in podzolic soils. The alkaline and alkaline-earth elements remain close to the surface and the dry grassland soils (chernozem) containing illite, chlorite, and smectite, will develop. In dry areas, the dominant movement of water is not downward and leaching does not take place. In extreme dry desert areas (desert soils, some aridsols), where the concentration of magnesium is particularly high, the formation of palygorskite–sepiolite minerals has been reported. Kaolinite is the dominant component in laterite soils (oxisols). Clay minerals other than those mentioned above usually occur in various soils as minor components inherited from the parent materials of those soils (cf. Kittrick, 1985).

In general, the process of transportation and sedimentation little affects the weathering products. However, in lagoon–estuary areas, some mineral transformations are possible because environments change from nonmarine to marine and vice versa. As burial sedimentation and compaction continues, temperature and pressure increase. Weathering products in sediments change accordingly. The weathering products are transformed into other clay minerals or decomposed completely to provide constituents required for the neof ormation of clay minerals, depending on the chemical environments of the sedimentation and the types of clay minerals present in sediments prior to diagenesis.

In soils, we observe the alteration of phyllosilicates by weathering action, as in a notable case like the transformation of micas into vermiculite, smectite, or randomly interstratified layer silicates (mica–vermiculite, mica–smectite, mica–vermiculite–smectite). On the other hand, we also notice the formation of chloritic minerals from vermiculite or montmorillonite by precipitating hydroxide sheets between the silicate layers, is also noticed as a results of accretion. Other observations have supported some systematic weathering patterns: Kaolinite is formed from aluminum silicates, particularly feldspar. Chlorite is found in igneous rocks as an alteration product from Mg–Fe silicates such as olivines, pyroxenes, amphiboles, and biotite micas, and serpentine is also found in the manner similar to chlorite. In meteorites, the occurrence of iron-rich serpentines in carbonaceous chondrites is reported.

Weathering and subsequent transportation result in the accumulation of sediments at the bottom of lakes, rivers, and oceans. In the Mississippi River system, for example, smectite, illite, and kaolinite are the major components in the upper Mississippi and Arkansas Rivers, whereas chlorite, kaolinite, and illite are the major components in the Ohio and Tennessee Rivers. This is the case for nonmarine conditions. Under marine conditions, at the Gulf of Mexico, for example, smectite, illite, and kaolinite are found to be the major clay mineral composition and their compositions vary from place to place. In some limited regions, it is noteworthy that these compositions are significantly altered by other factors such as airborne effects. The high-kaolinite concentration off the west coast of Africa near the equator reflects this effect.

In a supergene enrichment process, the formation of nickel deposits at New Caledonia is well known, where Ni–serpentine minerals occur in serpentine and peridotite rocks.

21.4 Phyllosilicates in Soil Environments

21.4.1 Introduction

In the foregoing section in which phyllosilicates of hydrothermal origin were discussed, the term “clay minerals” was introduced and the term can be the synonym of phyllosilicates of clay size. The number of phyllosilicate species that occur either in clay size or in a wide range of particle sizes from macroscopic to microscopic is rather limited. Although the numbers of species are small, their quantities are huge. Hence, clay components have great impact on soil environments. The phyllosilicates commonly found in

soils and which belong to the category above include hydrated halloysite, halloysite, kaolinite, micas, chlorites, vermiculites, smectites, and their interstratified minerals. Allophane and imogolite are often associated. The occurrence of clay minerals other than these in soils is either uncommon or rare. Because of fine particles, until relatively recently no appropriate analytical techniques were available by which to determine the precise nature, composition, and structure of clays. Therefore, clays had long been believed to be noncrystalline “colloidal” substances before XRD techniques developed in the 1920s, followed a few years later by improved microscopic and thermal procedures, which established that clays are composed of a few groups of crystalline minerals (Bradley and Grim, 1948). The introduction of electron microscopic methods was very useful to determine characteristic shape and size of clay minerals. Relatively modern analytical techniques such as infrared absorption, neutron diffraction, Mössbauer spectroscopy, and nuclear magnetic resonance have been applied to advance our knowledge of crystal chemistry of clay minerals (Greenland and Hayes, 1978; Wilson, 1992).

21.4.2 Physical Properties

21.4.2.1 Optical Index, Specific Density, and Particle Shape and Size

Clay mineral particles are commonly too small for the measurement of optical properties. Oriented aggregates that are large enough for optical measurements can, however, be prepared by allowing the flake-shaped clay mineral particles to settle from a clay water suspension on a horizontal surface. The particles settle with one flake on top of another so that their basal plane surfaces are essentially parallel. Refractive indices of clay minerals generally fall within a relatively narrow range from 1.47 to 1.68. This range may be subdivided into several groups represented by major mineral species: 1.47–1.52 (allophane, hydrated halloysite); 1.53–1.58 (kaolinite minerals, vermiculite); 1.58–1.65 (nontronite, glauconite, celadonite); and 1.57–1.68 (trioctahedral chlorites). All remaining clay minerals have refractive indices ranging from 1.54 to 1.63, except that smectite minerals have a range from 1.48 to 1.61. In general, iron-rich species show high refractive indices, whereas water-rich porous mineral species have lower refractive indices. Specific densities are as follows: 2.5–2.7 g·cm⁻³ (kaolinite-group minerals); 2.5–2.9 (pyrophyllite, talc, clay micas); 2.6–3.3 (chlorite minerals); 2.6–3.0 (vermiculite); 2.5–2.8 (smectite); ~2 (palygorskite–sepiolite group); 1.7–2.4 (bulk); and 2.6–2.8 (particle) for imogolite and allophane. Table 21.19 lists density, crystallographic units, and optical data of major clay minerals.

The size and shape of clay minerals have been determined by electron micrographs. Well-crystallized kaolinite occurs as well-formed six-sided flakes (Figure 21.26), frequently with a prominent elongation in one direction. Particles with maximum surface dimensions of 0.3 to about 4 μm and thickness of 0.05–2 μm are common. The flakes of disordered kaolinite have poorly developed hexagonal outlines. Halloysite commonly occurs as tubular units with an outside diameter ranging from 0.04 to 0.15 μm (Figure 21.27). Electron micrographs of smectite frequently show

TABLE 21.19 Crystallographic, Specific Gravity, and Optical Data of Some Selected Phyllosilicates

	D (g mL ⁻³)	Crystallographic Data							Optical Data				
		<i>a</i>	<i>b</i>	<i>c</i>	α	β	γ	<i>Z</i>	α	β	γ	2 <i>V</i>	
Halloysite	2.55–2.265	0.514	0.89	1.49		101.9°		[4]					nd
Kaolinite	2.61–2.68	0.515	0.895	0.739	91.8°	104.5°–105°	90°	[2]	Biaxial (–)	1.553–1.566	1.559–1.569	1.560–1.570	23°–50°
Dickite	2.6	0.515	0.894	1.4424		96°44′		4	Biaxial (+)	1.560–1.561	1.561–1.563	1.566–1.567	52°–80°
Nacrite	2.5–2.7	0.8909	0.5146	1.5697		113°42′		4	Biaxial (–)	1.557–1.560	1.562–1.563	1.563–1.566	40°–90°
Lizardite	2.55	0.5325		0.7259				2	Uniaxial (–)	1.538–1.554	1.546–1.560	1.546–1.560	Small
Chrysotile	≈2.55	0.535	0.925	0.733		94.2°				1.532–1.544		1.545–1.553	Small
Antigorite	2.65	4.353	0.9259	0.7263		91°8.4′		16	Biaxial (–)	1.558–1.567	1.565	1.562–1.574	37°–61°
Talc	2.58–2.83	0.5287	0.9158	1.895		99.30°		4	Biaxial (–)	1.539–1.55	1.589–1.594	1.589–1.60	0°–30°
Pyrophyllite	2.65–2.9	0.516	0.8966	0.9347	91.18°	100.46°	89.64°	2	Biaxial (–)	1.534–1.556	1.586–1.589	1.596–1.601	53–62°
Muscovite	2.77–2.88	0.519	0.904	2.008		95°30′		4	Biaxial (–)	1.552–1.576	1.582–1.615	1.587–1.618	30°–47°
Glauconite	2.4–2.95	[0.527]	[0.914]	[1.009]		≈100°		2	Biaxial (–)	1.592–1.610	1.614–1.641	1.614–1.641	0°–20°
Celadonite	2.95–3.05	0.523	0.906	1.013		100°55′		2	Biaxial (–)	1.606–1.625	nd	1.579–1.661	5°–8°
Phlogopite	2.78–2.85	0.53078	0.91901	1.01547		100.08°		2	Biaxial (–)	1.530–1.590	1.557–1.637	1.558–1.637	0°–15°
Biotite	2.7–3.3	0.53	0.92	1.02		100°		2	Biaxial (–)	1.565–1.625	1.605–1.696	1.605–1.696	0°–25°
Clinochlore	2.60–3.02	0.535	0.9267	1.427		96.35°		2	Biaxial (±)	1.571–1.588	1.571–1.588	1.576–1.597	0°–50°
Chamosite	3.0–3.4	0.5373	0.9306	1.4222		97°53′		2	Biaxial (–)	1.595–1.671	1.599–1.684	1.599–1.685	0°–30°
Donbassite	2.63	0.5174	0.8956	1.426		97.83°		[2]	Biaxial (+)	1.728	1.729	1.735	52°
Vermiculite	2.2–2.6	0.524	0.917	2.86		94°36′		4	Biaxial (–)	1.520–1.564	1.530–1.583	1.530–1.583	0°–15°
Montmorillonite	2–3	0.517	0.894	0.995		nd		1	Biaxial (–)	1.492–1.503	1.513–1.534	1.513–1.534	10°–25°
Beidellite	2–3	0.5179	0.897	1.757		≈90°		nd	Biaxial (–)	1.494	1.536	1.536	
Nontronite	2.2–2.3	[0.525]	[0.91]	[1.53]		≈90°		nd	Biaxial (–)	1.567–1.600	1.604–1.632	1.605–1.643	25°–68°
Saponite	2.24–2.30	0.53	0.914	1.69		≈97°		nd	Biaxial (–)	1.48–1.54	1.50–1.58	1.50–1.58	0°–40°
Greenalite	2.85–3.15	0.554	0.955	0.744		104°20′		2					
Minnesotaitite	3.01	0.5623	0.9419	0.9624	85.21°	95.64°	90.00°	4	Biaxial	1.580–1.592	nd	1.615–1.632	Small
Palygorskite	>1.0–2.6	1.278	1.786	0.524		95.78°		4	Biaxial (–)	1.522–1.528	1.530–1.546	1.553–1.548	30°–61°
Sepiolite	>2	0.521	2.673	1.35				4	Biaxial (–)	1.515–1.520	nd	1.525–1.529	0°–50°

Source: Adapted from Yong, R.N., and B.P. Warkentin. 1975. Soil properties and behaviour. Developments in geotechnical engineering 5. Elsevier Scientific Publishing Co., Amsterdam, the Netherlands.

Unit cell: *a*, *b*, and *c* are in nanometers. *Z* is the number of formula units per unit cell and [*Z*] is estimated one. Compilation by Kodama.

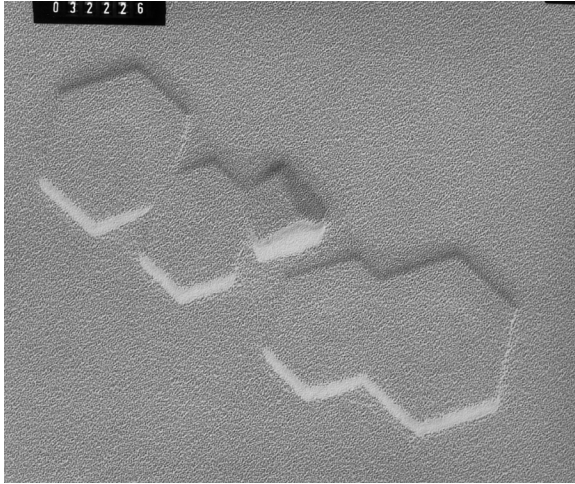


FIGURE 21.26 Electron micrograph of kaolinite, from Mont Megantic, Quebec. Quick freeze–dry and Pt shadowing. The longer side edge of the photograph equals about 2 μm .

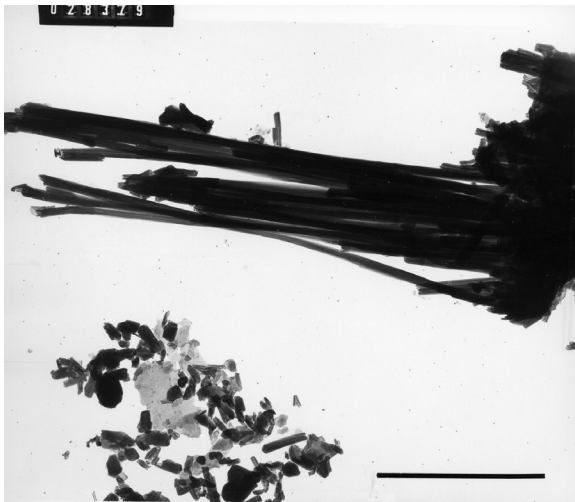


FIGURE 21.27 Electron micrograph of halloysite, in a paleosol from Gaspé, Quebec. Pt shadowing. The scale indicates 1 μm . (From Ross, G.J., H. Kodama, C. Wang, J.T. Gray, and L.B. Lafreniere. 1983. Halloysite from a strongly weathered soil at Mont Jacques Cartier, Quebec. *Soil Sci. Soc. Am. J.* 47:327–332.)

broad undulating mosaic sheets. In some cases, the flake-shaped units are discernible but frequently they are too small or thin to be seen individually without special attention (Oberlin and Méring, 1962). Illite occurs in poorly defined flakes commonly grouped together in irregular aggregates (Figure 21.28). Many of the flakes have a diameter 0.1–0.5 μm and the thinnest flakes are approximately 3 nm thick. Although sizes vary more widely, vermiculite, chlorite, pyrophyllite, talc, and serpentine minerals except for chrysotile are similar in character to the illites. As shown in Figure 21.11, chrysotile occurs in slender tube-shaped fibers with an outer diameter of 10–30 nm. Their lengths commonly reach several microns. Electron micrographs show that palygorskite occurs as elongated laths, singly or in bundles.

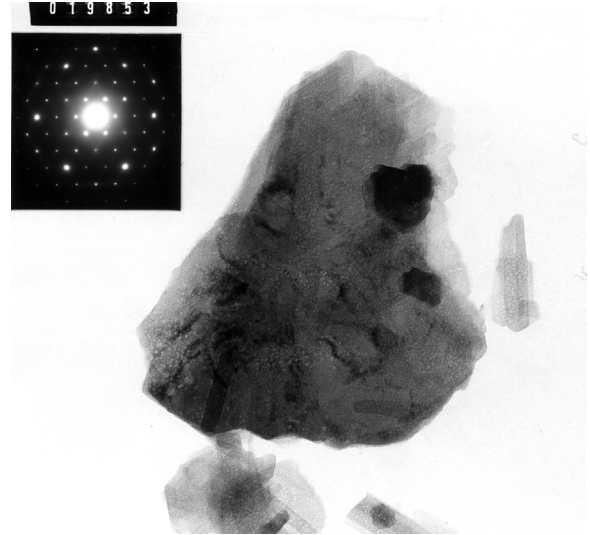


FIGURE 21.28 Electron micrograph of illite, from Eldorado, Saskatchewan. Although outline is irregular, it appears as a single crystal (about 1–1.5 μm across). (From Kodama, H., and R.S. Dean. 1980. Illite from Eldorado, Saskatchewan. *Can. Mineral.* 18:109–118.)

Frequently, the individual laths are many microns in length and 5–10 nm in width. Sepiolite occurs in similar lath-shaped units, but the laths are somewhat thicker and shorter than the palygorskite. As mentioned earlier in the structures, allophane occurs in very small spherical particles (3–5 nm in diameter), individually or in aggregated forms, whereas imogolite occurs in long thread-like tubes of several microns in length. One of the interesting features of layer silicate minerals is their modes of particle association. When a clay suspension of flaky particles flocculates, three different modes of particle association may occur: face-to-face, edge-to-face, and edge-to-edge. These modes are determined by the electrostatical interaction energy between particles, which is influenced by the kind of salt and salt concentration in the medium as well as the surface conditions of the particles.

21.4.2.2 Clay–Water Relations

Clay minerals contain water in several forms. The water may be held in pores and may be removed by drying under ambient conditions. Water also may be adsorbed on the surface of clay mineral structures and in smectites, vermiculites, hydrated halloysite, sepiolite, and palygorskite; this water may occur in interlayer positions or within structural channels. Finally, the clay mineral structures contain hydroxyls that are lost as water at elevated temperatures. The water adsorbed between layers or in structural channels may further be divided into zeolitic (free) and bound waters. The latter is bound to exchangeable cations or directly to the clay mineral surfaces. Zeolitic and bound waters may be removed by heating to temperatures on the order of 100°C–200°C and in most cases, except for hydrated halloysite, is regained readily at ordinary temperatures. Exceptions include those minerals like K-saturated vermiculite in which the interlayer K atoms do not associate with zeolitic water. The bound water is generally agreed to have a structure that is different from bulk water, being more ice-like in its

TABLE 21.20 Cation-Exchange Capacity and Specific Surface Area Data of Representative Clay Minerals, Including Imogolite and Allophane

	Cation-Exchange Capacity at pH 7 (cmol _c kg ⁻¹)	Specific Surface Area (m ² g ⁻¹)
Kaolinite	3–5	5–40
Hydrated halloysite	40–50	~1100
Illite	10–40	10–100
Chlorite	10–40	10–55
Vermiculite	100–150	~760
Smectite	80–120	40–800
Palygorskite–sepiolite	3–20	40–180
Imogolite	20–30	≈1540
Allophane	30–135	~2200

structure, even though still liquid. As the thickness of the adsorbed water increases outward from the surface, the nature of the bound liquid water changes abruptly or gradually from ice-like to that of bulk water. Ions and molecules adsorbed on the clay mineral surface exert a major influence on the thickness of the adsorbed water layers and on the nature of this water. The bound liquid water with ice-like characteristics may extend out from the clay mineral surfaces as much as 6–10 nm. Hydroxyl ions are driven off by heating clay minerals to temperatures of 400°C–700°C. The rate of loss of the hydroxyls and the energy required for their removal are specific properties characteristic of the various clay minerals. The reaction for dioctahedral minerals such as kaolinite is abrupt, whereas the loss takes place rather gradually in trioctahedral minerals. This dehydroxylation process results in the oxidation of Fe²⁺ to Fe³⁺ in ferrous-iron-bearing clay minerals. The amount of the adsorbed water is closely related to the surface area of clay minerals that is, of course, determined by their particle size and shape as well as the type of clay minerals. The range of measured surface areas of some clay minerals is given along with that of cation-exchange capacities in Table 21.20. The capacity of water retention of clay minerals is generally proportional to the extent of their surface area (e.g., Ross, 1978). As the water content increases, clays become plastic and then change to a near-liquid state. The amounts of water required for the two states are defined by the plastic and liquid limits. These limits vary with the kind of exchangeable cations and the salt concentration in the adsorbed water. The plastic and liquid limits for different clay minerals are given in Table 21.21. The plasticity index (PI), the difference between the two limits, gives a measure for the rheological (flow) properties of clays. A good example is a comparison of the PI of montmorillonite with that of allophane or palygorskite. The former is considerably greater than the latter, indicating that montmorillonite has a prominent plastic nature. Such rheological properties of clay minerals have great impacts on building foundations, highway construction, chemical engineering, and soil structure in agricultural practice.

21.4.2.3 High-Temperature Reactions

When heated at temperatures beyond dehydroxylation, the clay mineral structure may be destroyed or simply modified,

TABLE 21.21 Consistency Data of Representative Clay Minerals Including Allophane

	Plastic Limit	Liquid Limit	Plastic Index (PI)
Kaolinite–Na	26	52	26
Kaolinite–Ca	26	73	37
Illite–Na	34	61	27
Illite–Ca	40	90	50
Montmorillonite–Na	97	700	603
Montmorillonite–Ca	63	177	114
Palygorskite–sepiolite	145	171	26
Allophane (undried)	136	231	95
Allophane (dried)	78	85	7

Source: Adapted from Yong, R.N., and B.P. Warkentin. 1975. Soil properties and behaviour. Developments in geotechnical engineering 5. Elsevier Scientific Publishing Co., Amsterdam, the Netherlands.

PI = liquid limit – plastic limit. Numerical figures are expressed in dag kg⁻¹.

depending on the composition and structure of the clay minerals. In the presence of fluxes, such as iron or potassium, fusion may follow dehydroxylation very quickly. In the absence of such components, particularly for aluminous dioctahedral minerals, a succession of new phases may be formed at increasing temperatures prior to fusion. Thus, in the case of kaolinite, the first high-temperature phase formed is a silica–alumina spinel or γ -alumina plus amorphous silica that is followed at a higher temperature by the development of mullite and cristobalite prior to fusion. In general terms, the first high-temperature phases are a consequence of the original structure of the clay mineral, whereas the later phases are more in accord with the chemical composition. Information on high-temperature-phase change of the clay minerals has been obtained by the use of an x-ray diffractometer to which a small high-temperature furnace is attached. This unit provides x-ray data, while the sample is at an elevated temperature. Information concerning high-temperature reactions is important for ceramic science and industry.

21.4.3 Chemical Properties

21.4.3.1 Layer Charge and Ion Exchange

Depending upon deficiency in the positive or negative charge balance (locally or overall) of mineral structures, clay minerals are able to adsorb certain cations and anions and retain them around the outside of the structural unit in an exchangeable state, generally without affecting its basic silicate structure. These adsorbed ions are easily exchanged by other ions. The exchange reaction differs from simple sorption because it has a quantitative relationship between reacting ions. The range of the cation exchange capacities of the clay minerals is given in Table 21.20 along with specific surface areas. Exchange capacities vary with particle size, perfection of crystallinity, and nature of the adsorbed ion; hence, a range of values exists for a given mineral rather than a single specific capacity. With certain clay minerals—such as imogolite, allophane, and to some extent kaolinite—that have hydroxyls at the surfaces of their structures, exchange capacities also vary

with the pH of the medium, which greatly affects dissociation of the hydroxyls. The ion-exchange charge created as such is called pH-dependent charge or variable charge to distinguish it from the permanent layer charge originating by the ionic substitution in the structure that is independent from pH. The rate of ion exchange varies with clay mineral type and the nature and concentration of the ions. In general, the reaction for kaolinite is most rapid, being almost instantaneous. It is slower for smectites and for sepiolite and palygorskite and requires even long time, perhaps hours or days, to reach completion for illites. Under a given set of conditions, the various cations are not equally replaceable and do not have the same replacing power. Calcium, for example, will replace sodium more easily than sodium will replace calcium. Sizes of potassium and ammonium ions are similar, and the ions are fitted in the hexagonal cavities of the silicate layer. Vermiculite and vermiculitic minerals preferably and irreversibly adsorb these cations and fix them between the layers. Such a preference of one exchangeable cation over another, so-called ion selectivity, may be a tool to exploit layer-charge characteristics of clay minerals in question. Heavy metal ions such as copper, zinc, and lead are strongly attracted to the negatively charged sites on the surfaces of 1:1 layer minerals, allophane and imogolite, which is caused by the dissociation of surface hydroxyls of these minerals.

The ion exchange properties of the clay minerals are extremely important because these properties determine their physical characteristics and economic use. The availability and retention of fertilizer in soils, the adsorption and release of toxic elements in soil and aquatic environments, plasticity, and other clay properties depend to a great extent on ion exchange in general and on the identity of the exchange cation.

21.4.3.2 Solubility

The solubility of the clay minerals in acids varies with the nature of the acid, the acid concentration, the acid to clay ratio, the temperature, the duration of treatment, and the chemical composition of the clay mineral to be attacked. It also varies as a function of heating of the clay minerals and the firing temperatures prior to the acid attack. In general, ferromagnesian clay minerals are more soluble in acids than the aluminum counterparts. Basset (1960) considered that hydroxyl orientation may be an important factor for mica alteration, because in trioctahedral micas hydrogen atoms are oriented directly toward the interlayer K atoms, but in dioctahedral micas, they are tilted away from the interlayer cation. Incongruent dissolutions may result from reactions in a low acid concentration medium where the acid first attacks the adsorbed or interlayer cations and then the components of the octahedral sheet of the clay mineral structure. Frequently with aluminous clay minerals in particular, the tetrahedral silica sheets are not attacked and the morphology of the clay minerals may be retained after solution of all components except silica. In the case of higher acid concentration, such stepwise reactions may not be recognizable and the dissolution appears to be congruent. One of the important factors controlling the rate of dissolution is the concentration in the aquatic medium of the elements extracted from the clay mineral—the greater the concentration of an element

in the solution, the more hindered the extraction of the element. In alkaline solutions, a cation exchange reaction first takes place and then the silica part of the structure is attacked. The reaction depends upon the same variables as those stated for acid reactions.

21.4.3.3 Interactions with Inorganic and Organic Compounds

Smectites, vermiculites, and other expansible clay minerals can accommodate relatively large and multivalent inorganic cations between the layers. Because of this multivalency, the interlayer space is only partially occupied by such inorganic cations, which are distributed in the space-like islands. Hydroxy polymers of aluminum, iron, chromium, zinc, and titanium are known examples of such interlayering materials. Most of these are thermally stable and stand as pillars to allow a porous structure in the interlayer space. The resulting complexes, often called pillared clays, exhibit attractive properties as catalysts—namely, large surface area, high porosity, regulated pore size, high solid acidity. Cationic organic molecules, such as certain aliphatic and aromatic amines, pyridines, and methylene blue, may replace inorganic exchangeable cations present in the interlayer of expansible minerals. These organic compounds contain nitrogen atoms, which are able to be positively charged. Polar organic molecules may replace adsorbed water on external surfaces and interlayer positions. Ethylene glycol and glycerol are known to form stable specific complexes with smectites and vermiculites. The formation of such complexes is frequently utilized for the identification of these minerals. On the other hand, potassium acetate can penetrate between kaolin-type silicate layers, which are neutral and held together by hydrogen bonds, and the d_{001} of the mineral expands to 1.42 nm (Wada, 1959, 1961); if dimethyl sulfoxide, DMSO, is used, the expansion is to 1.12 nm (Camazano and Garcia, 1966); if formamide, to 1.0 nm (Weiss et al., 1963). These intercalations with organic compounds are often utilized for the characterization of kaolin minerals. However, experimental results are not always consistent. Caution is required for firm conclusions.

As organic molecules coat the clay mineral surfaces, the nature of clay particle surfaces changes from hydrophilic to hydrophobic, thereby losing its tendency to bind water. Consequently, the affinity of the material for oil increases, so that it can react with additional organic molecules. As a result, the surface of such clay minerals can accumulate organic materials. Some of the clay minerals can serve as catalysts, promoting reactions in which one organic substance is transformed to another on the mineral's surface. Some of these organic reactions develop particular colors, which may be of diagnostic value in identifying specific clay minerals. Organically clad clay minerals are used extensively in paints, inks, and plastics.

21.4.4 Uses of Clays

Clays are perhaps the oldest materials of which man has manufactured various artifacts. The making of fired bricks possibly started some 5000 years ago and was probably the second earliest industry of mankind next to agriculture. The use of clays (probably smectite) as soaps and absorbents was reported in *Natural History* by a Roman author, Pliny the Elder (AD 77). Clays composed of kaolinite are

required for the manufacture of porcelain, whiteware, and refractories. The absence of iron in this clay mineral gives it a white burning color, and the absence of alkalis and alkaline earths gives it a very high fusion temperature that makes it refractory. Whiteware bodies frequently contain talc, pyrophyllite, feldspar, and quartz in addition to the kaolinite clay, in order to develop desirable shrinkage and burning properties. If the kaolinite is poorly crystalline, the clay will have higher plastic and bonding properties.

Clays composed of a mixture of clay minerals, in which illite is most abundant, are used in the manufacture of brick, tile, stoneware, and glazed products. Small proportions of smectite in such clays provide good plastic properties, but in large amounts, smectite is undesirable because it causes too great a degree of shrinkage. Besides the ceramic industry, kaolinite is used as an extender in aqueous-based paints and as filler in natural and synthetic polymers. Smectitic clays (bentonite) are used primarily in the preparation of muds for drilling oil wells. This type of clay, which swells to several times its original volume in water, provides desirable colloidal and wall-building properties. Palygorskite and sepiolite clays also are used because of their resistance to flocculation (grouping or clustering of individual grains or flakes) under high salinity conditions. Certain clay minerals, notably palygorskite, sepiolite, and some smectites, possess substantial ability to remove color bodies from oil. These so-called Fuller's earths are used in processing many mineral and vegetable oils. Because of their large absorbing capacity, Fuller's earths are also commercially used for preparing animal litter trays and oil and grease absorbents. Acid treatment of some smectite clays increases their decolorizing ability. Much gasoline is manufactured by using catalysts prepared from either smectite-type or kaolinite-halloysite-type clay minerals. The preparation may be by acid treatment to modify the structure or by the use of kaolinite and halloysite as a source of alumina and silica for the synthesis of new zeolite-type structures. Large tonnages of kaolinite clays are used as a paper filler and a paper coating to give sheen and carry pigments. The coating clays are washed to free them from grit and then are processed by physical and chemical techniques to improve their whiteness and viscosity. In general, well-crystallized kaolinite that cleaves easily into thin flakes is desired. Palygorskite-sepiolite minerals and acid-treated smectites are used in the preparation of carbonless carbon paper because of the color they develop during reactions with certain colorless organic compounds. Large tonnages of bentonite are used as bonding agents in foundry sands for casting metals. Some poorly crystallized illites and kaolinites are also used for this purpose. Bentonite is combined with lime and coke to pelletize finely ground iron ore, which renders it suitable for use in blast furnaces. Because many clay minerals have aluminum oxide contents on the order of 30%–40%, they are potential ores for aluminum. A variety of processes have been developed to extract this element from clays but clays are not yet competitive with bauxite as a source of aluminum. Extremely large tonnages of reasonably pure clays, preferably of the kaolinite type, would be required for this purpose. Clays have a tremendous number of miscellaneous uses and for each use a particular type of clay with particular properties is important. For example,

palygorskite-sepiolite and smectite clays are used as carriers for insecticides and herbicides. Smectite clays are used as plasticizing agents and kaolinite clays are used as extenders and fillers in a large number of organic and inorganic bodies. Kaolinite and smectite clays also are used in a variety of pharmaceutical and medical preparations. For cosmetic products, kaolinite, talc, mica, and smectite clays are used. Smectite and kaolinite clays can be coated with organic molecules for use in many organic systems. Often such organic-clad clays are tailor-made to fit a particular organic system, and thus become an integral part of the system rather than simple diluents. Typical examples are their application to printing inks, oil paints, and lubrication greases. Table 21.22 gives a glimpse of industrial uses of kaolinite, smectite, and palygorskite-sepiolite minerals.

TABLE 21.22 Industrial Uses of Clay Minerals

Kaolinite	Smectite	Palygorskite–Sepiolite
Paper coating	Drilling mud	Drilling fluids
Paper filling	Foundry bond clay	Paint
Extender in paint	Pelletizing iron ores	Paper
Ceramic raw material	Sealants	Ceramics
Filler in rubber	Animal feed bonds	Asphalt emulsions
Filler in plastics	Bleaching clay	Cosmetics
Extender in ink	Industrial oil absorbents	Sealants
Cracking catalysts	Agricultural carriers	Adhesives
Fiberglass	Cat box absorbents	Pharmaceuticals
Foundries	Beer and wine clarification	Catalyst supports
Desiccants	Medical formulations	Animal feed
Cement	Polishing and cleaning agents	Petroleum refining
Pencil leads	Detergents	Anticracking agent
Adhesives	Aerosols	Reinforcing fillers
Tanning leather	Adhesives	Cat box absorbents
Pharmaceuticals	Pharmaceuticals	Suspension fertilizer
Enamels	Food additives	Agricultural carriers
Pastes and glues	Deinking of paper	Industrial floor absorbents
Insecticide carriers	Tape-joining compounds	Mineral and vegetable oil
Medicines	Emulsion stabilizer	Refining
Sizing	Crayons	Tape-joint compounds
Textiles	Cement	Environmental absorbents
Food additives	Desiccants	
Bleaching	Cosmetics	
Fertilizers	Paints	
Plaster	Paper	
Filter aids	Fillers	
Cosmetics	Ceramics	
Crayons	Catalysts	
Detergents	Pencil leads	
Roofing granules		
Linoleum		
Polishing compounds		

21.5 Identification of Soil Phyllosilicates

21.5.1 Introduction

Clay mineralogical analysis is a very important first step to elucidate soil behavior, because the clay fraction of soil is most active and influential to the physical, chemical, and biological reactions of soil. X-ray diffraction is a universally accepted method for identifying crystalline mineral components (Brindley, 1951; Brown, 1961; Brindley and Brown, 1980). Unlike the case where only pure crystalline substances are dealt with, soils are complex mixtures of various minerals with a wide range of crystallinity and compositions. Because of these complexities, we often have to compromise with identification and quantification of mineral group rather than mineral species, and the estimation of relative amounts of minerals may often be the best for a given circumstance. Nevertheless, such data provide useful information about mineral translocations and transformations that might have taken place in the soil profiles in question.

21.5.2 X-Ray Diffraction Methods

21.5.2.1 Basics

X-ray diffraction techniques provide a set of reflections from crystalline substances with various diffraction intensities as a function of diffraction angle. The simplest is, therefore, to take standard diffraction diagrams of the principal clay minerals and of the most commonly occurring impurities and to make direct comparison with the diffraction diagrams of unknown clays. For this purpose, *Mineral Powder Diffraction File Data Book* published by JCPDS (Joint Committee on Powder Diffraction Standards) is handy and useful. X-ray reflection takes place from lattice planes with indices, hkl , according to the Bragg law,

$$n\lambda = 2d_{hkl} \sin \theta \quad (21.1)$$

where

d_{hkl} is lattice spacing for planes hkl

λ is the wavelength

θ is the glancing angle of reflection

n is the order of the reflection

The latter two are often called Bragg's angle and the order of Bragg's reflection, respectively. Thus, diffraction experiments measure the quantity from

$$\frac{d_{hkl}}{n} = \frac{\lambda}{2\sin \theta} \quad (21.2)$$

and this is the lattice spacing for n th-order reflection, which is readily understood by introduction of the reciprocal space concept. The Bragg equation gives no intensity information. Diffraction intensities are generally expressed by the relation

$$I = \text{const.}(Lp) |FI|^2 G \quad (21.3)$$

where

the constant factor includes all the basic electronic terms, which arises from the fundamental x-ray scattering process

Lp is the Lorentz-polarization factor

F is the structure factor that is related to number, kind, and array fashion of the atoms on a lattice plane and the factor can be a positive or negative number

G is the Laue function that determines diffraction peak profile (Kodama et al., 1971) and, therefore, provides information about the distribution of crystallite sizes and shapes and their crystal imperfections

Figure 21.29 illustrates XRD patterns from oriented samples of muscovite and phlogopite for comparison. They show a series of basal reflections, which can be traced down to at least fifth order. The two minerals have a similar structure except for their octahedral cations, aluminum in muscovite and magnesium in phlogopite. This difference affects the $|FI|^2$ value and reflects on the diffraction pattern. Thus, the ratio $(I_{001}/I_{002})_{\text{phlogopite}} : (I_{001}/I_{002})_{\text{muscovite}}$ may be used as one of the criteria for identification. Similarly, this approach is also useful for the determination of chlorite species (Petruk, 1964; Bailey, 1972). If mineralogical data accumulation is the main purpose, more reflections should be observed. Figure 21.30 illustrates differences in diffraction patterns from random and oriented powder specimens of a muscovite. To determine polytypes, not only are the basal reflections required, but the b unit cell dimension from the d_{060} reflection and impurities must also be known.

21.5.2.2 Distinguishing among Soil Phyllosilicates

As mentioned earlier, the types of phyllosilicates occurring in soils (and particularly in its clay fraction) are limited to only several layer silicate structures (Figure 21.31), and interstratified layer silicates can also be considered as a combination of two or three basic structures. Obviously from Figure 21.31, the identification of those basic layer structures is due to determination of respective layer thickness (distance normal to the basal plane), which is obtained by XRD as d_{001} -spacing. By choosing effective and critical conditions under which basic layer units are clearly distinguished, criteria for the identification of clay minerals by XRD can be set up (Bradley, 1945). For example, the distinction between smectite and vermiculite is made as follows: Mg-saturation and treated with glycerol expand the d_{001} -spacing of smectite to 1.7–1.8 nm but do not change the d_{001} -spacing at 1.4 nm of vermiculite (Walker, 1949). With the same treatment, chlorite, mica, and kaolinite do not change their d_{001} -spacings at 1.4, 1.0, and 0.72 nm, respectively. On heating at 550°C, however, the structure of kaolinite is destroyed. The d_{001} -spacing at about 1.0 nm of hydrated halloysite contracts to 0.72 nm on heating at 100°C, therefore easily distinguishable from mica. The distinction between vermiculite and chlorite is based on the heat treatment at 550°C or saturation with K^+ , either of which causes the reduction of the d_{001} -spacing at 1.4–1.0 nm in vermiculite but no change in chlorite. These diagnostic criteria are based on

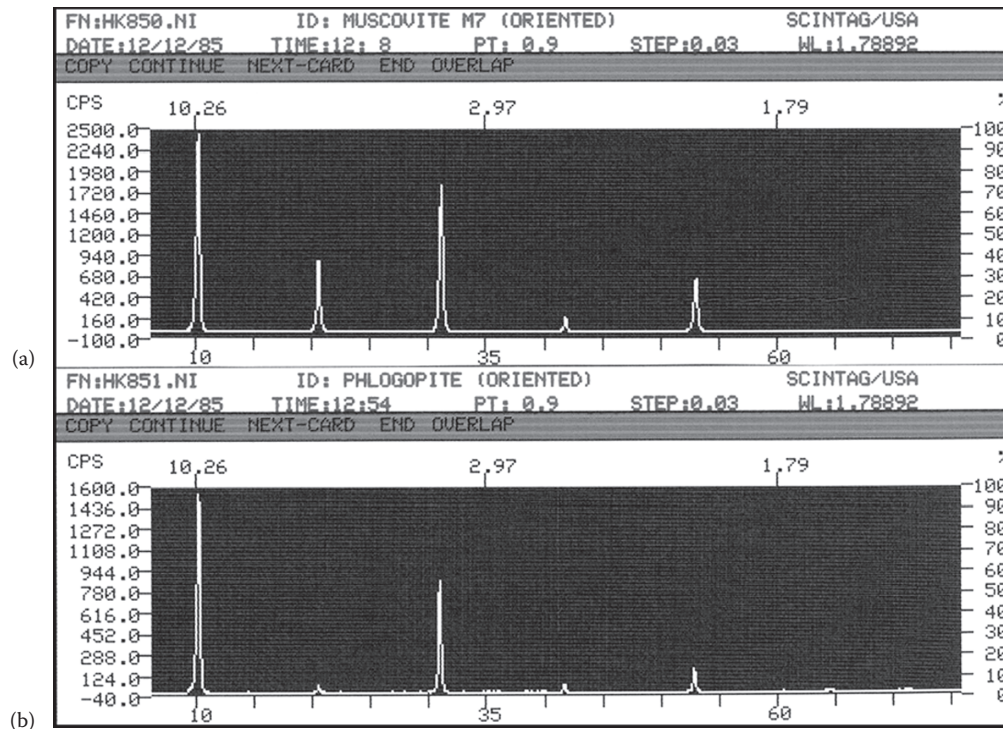


FIGURE 21.29 XRD patterns of preferred oriented samples: (a) muscovite and (b) phlogopite.

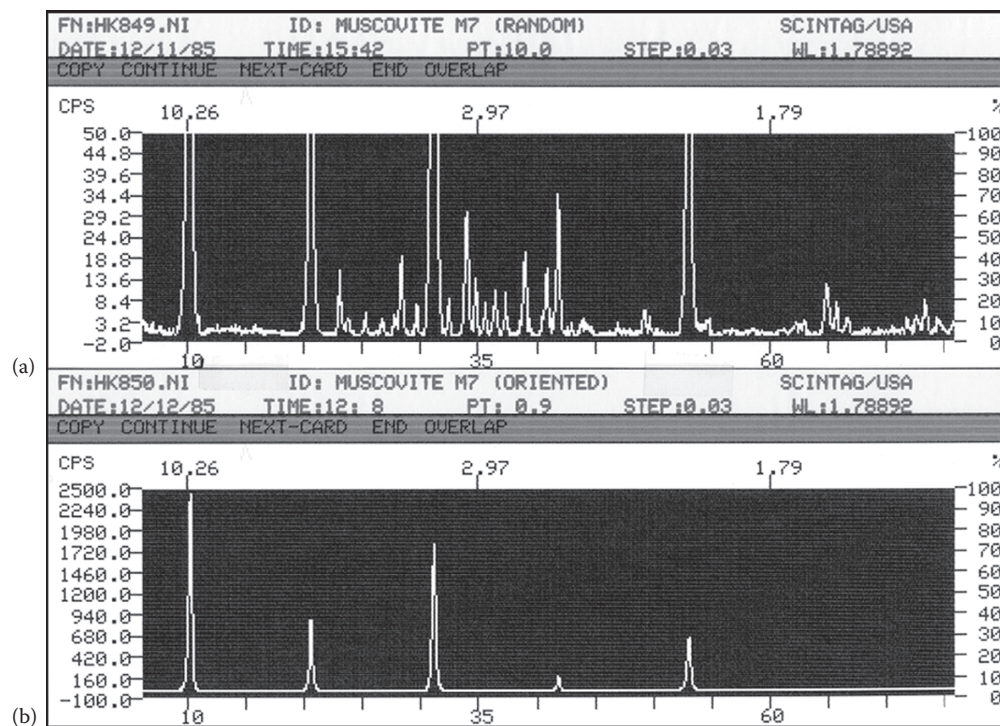


FIGURE 21.30 XRD patterns of muscovite: (a) random sample and (b) oriented sample.

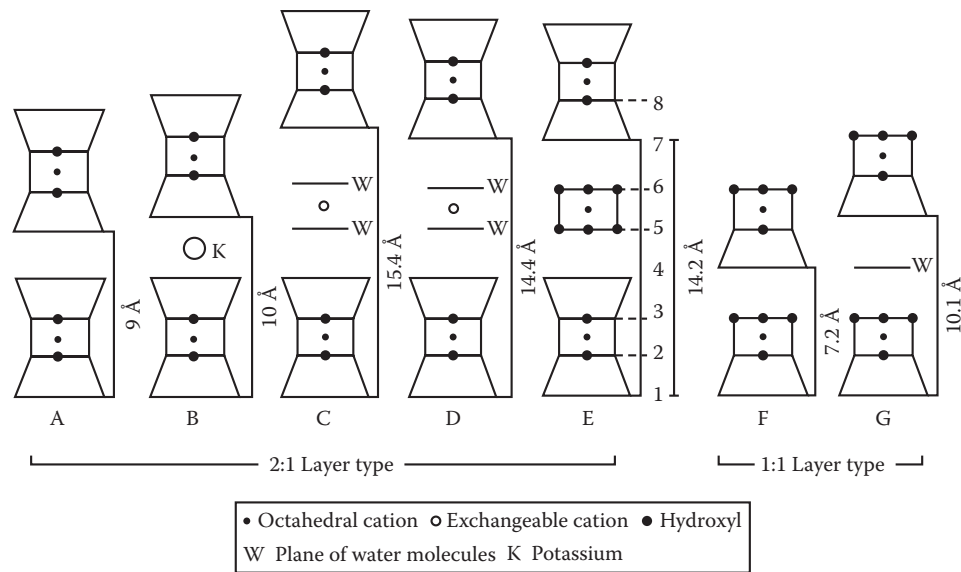


FIGURE 21.31 Diagrammatic representation of principal clay mineral structures, comparing the relative layer thickness of the unit structures. A, Talc-pyrophyllite; B, mica; C, smectite; D, vermiculite; E, chlorite; F, serpentine-kaolinite; and G, hydrated halloysite (halloysite—1.0 nm). In this presentation, tetrahedral and octahedral anions and tetrahedral cations are omitted. (From Sudo, T., S. Shimoda, H. Yotsumoto, and S. Aita. 1981. *Electron micrographs of clay minerals. Developments in sedimentology. Vol. 31.* Elsevier Scientific Publishing Co., New York.)

generally accepted specific properties of each mineral group for its definition, which may be categorized as follows:

- *Mica*. A 1.0 nm basal spacing and integral series of higher order reflections do not shift upon either hydration or glycerol solvation or heating at 550°C and 700°C.
- *Kaolinite*. Characterized by a series of basal reflections at 0.72, 0.36 nm, and so forth, which do not shift upon either hydration or solvation with glycerol but disappear upon heating at 550°C.
- *Chlorite*. An integral series of basal reflections associated with the largest spacing of 1.4 nm; does not expand by glycerol sorption and does not shift upon heating at 550°C. On heating at 700°C, the intensity of the 1.4 nm peak is enhanced in comparison with those of other peaks. One should bear in mind that the basal intensity ratio varies with chemical composition. The higher order reflections such as third- and fourth-order reflections at 0.473 and 0.355 nm, respectively, may also be used for the distinction of chlorite from kaolinite.
- *Vermiculite*. According to the conventional definition, its Mg form maintains the 1.44 nm basal spacing upon solvation with glycerol and hydration, but the spacing collapses to 1.0 nm upon heating to 550°C, whereas the K form gives the contracted spacing of 1.0 nm without heating. Although its Ca form also shows symptoms similar to those of the Mg form, in some cases, the symptoms become less definite, that is, some of the Ca forms expand beyond 1.44 nm on glycerol solvation depending upon their layer-charge characteristics.
- *Smectite*. Under intermediate humidity (about 50%), the Na form of smectite shows an expansion of its basal spacing to 1.24 nm, and the Ca (also Mg) form to 1.54 nm

(Mooney et al., 1952). These forms expand to 1.8 nm upon solvation with glycerol. Heating to 550°C causes a reduction of the basal spacing to 1.0 nm. It collapses further to 0.96 nm at 700°C, accompanied by its third-order peak at 0.32 nm. This behavior is also a characteristic of vermiculite, but nonexpandable clay minerals like mica retain their third-order peak at 0.333 nm.

After clay mineral components are distinguished at a level of the mineral group category, and if circumstances allow, the procedure of identification continues to determination at the level of mineral subgroup and finally mineral species. To reach the final stage of identification, most likely further tests are needed. For the distinction between montmorillonite and beidellite, for example, the so-called Greene-Kelly test (Greene-Kelly, 1953, 1955) based on the Hofmann-Klemen effect (Hofmann and Klemen, 1950) is often applied. For apparently chloritic minerals derived from vermiculite by acquiring hydroxide sheets between vermiculite silicate sheets, the interlayered vermiculite can be distinguished from chlorite by complexing with sodium citrate to remove the interlayer material. Further information may be obtained from XRD data if complexities due to the combination of clay mineral components themselves and associated impurity are relatively limited.

Ideally, any pretreatment would be avoided to obtain information about mineral components of soil as they are. However, cases are often unavoidable. An extreme example is given in Figure 21.32, where only a pretreatment of the clay fraction by Tiron improves XRD patterns because masking substances are mainly amorphous silica. Many soils cannot disperse without treatment for fractionation. Organic matter, carbonate, and iron oxide removal are often prerequisite. Another example

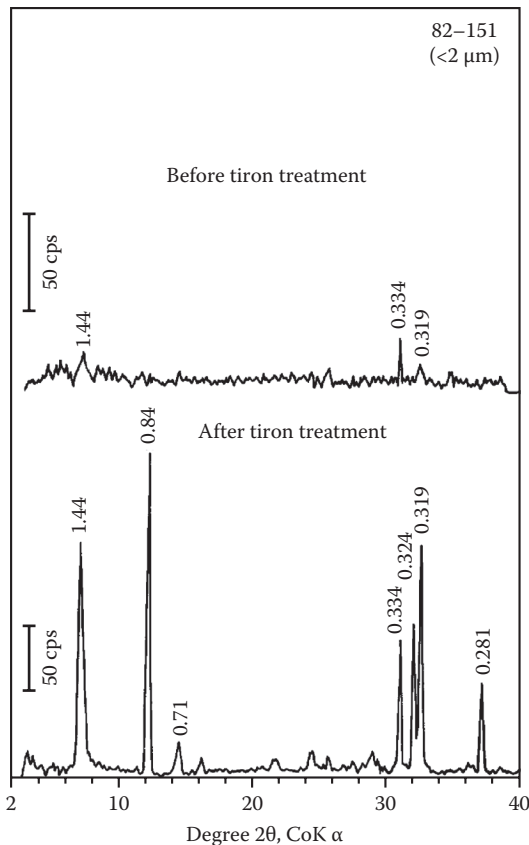


FIGURE 21.32 XRD patterns (in nm) of a soil clay before and after tiron treatment, exemplifying any suitable chemical pretreatments are often required to obtain decent XRD patterns of soil clays for identification. (From Kodama, H., and G.J. Ross. 1991. Tiron dissolution method to remove and characterize inorganic components in soils. *Soil Sci. Soc. Am. J.* 55:1180–1187.)

represents effects of various treatments on XRD patterns (Figure 21.33). After fractionation, subsamples (from a clay fraction of podzolic B horizon) were subjected to various treatments. After destruction of organic matter, the <2mm size fraction was dispersed in water by shaking overnight on an end-over-end shaker, and the clay fraction was collected by sedimentation, saturated with Mg^{2+} , and freeze-dried. This illustrates the necessity of pretreatments for amorphous substances, which mask crystalline components. A quick reference to major chemical dissolution methods is given in Table 21.23. Details of pretreatments may be consulted with appropriate manuals (Bear, 1964; Jackson, 1967; Thorez, 1975; McKeague, 1976; Klute, 1986; Dixon and Weed, 1989; Carter, 1993).

21.5.2.3 Soil Phyllosilicates of Intermediate Nature

In soil environments, especially of the temperate climate region, a majority of the weathering actions on phyllosilicates includes hydration, ion exchange, selective depletion, and partial decomposition of the minerals. As a whole, the actions are considered to be gentle ones. Under these circumstances, micas partially lose their interlayer cations to become hydrated

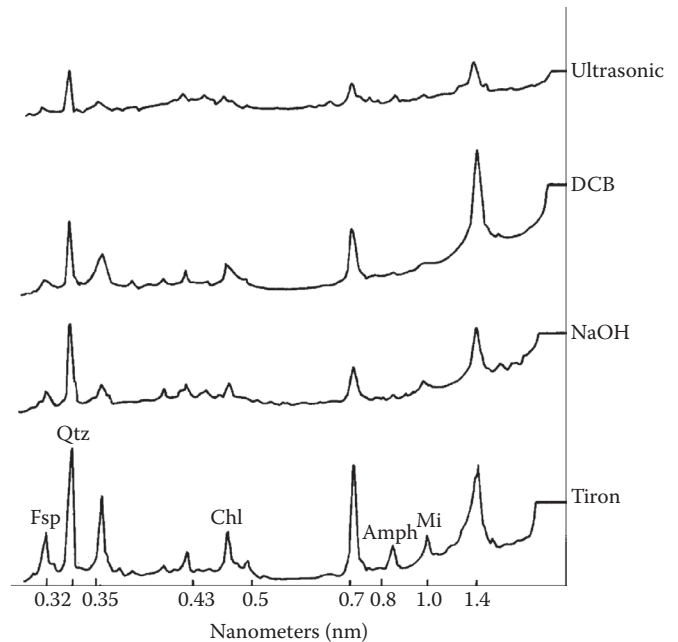


FIGURE 21.33 XRD patterns of a Mg-saturated and glycerol-solvated clay sample after four separate pretreatments. After organic matter removal, <2mm fraction was collected from the Whatcom Bf horizon and dispersed by an end-to-end shaker and then the clay fraction was obtained by sedimentation. (From Wang, C., H. Kodama, and N.M. Miles. 1981. Effect of various pretreatments on X-ray diffraction patterns of clay fractions of podzolic B horizons. *Can. J. Soil Sci.* 61:311–316.)

and expandable. Chlorites gradually experience a mild attack on their hydroxide sheets to alter toward vermiculite-like minerals. Vermiculites may undergo further ion exchange and hydration with their interlayer cations to alter toward smectites. On the contrary, in a lower horizon of the soil profile, an accretion process such as acquiring interlayer substances may take place. By this process, the following transformation routes are also possible: smectites through vermiculites to chlorites, vermiculites to chlorites, micas to chlorites, smectites through vermiculites to micas, vermiculites to micas, and so on. As these actions constantly work on minerals in soil, encountering a phyllosilicate mineral that cannot be correctly identified with a definitive soil phyllosilicate is no surprise. For example, although a soil phyllosilicate indicates a nature similar to vermiculite or smectite, positive identity as either entity may be impossible. This is due to the fact that the soil phyllosilicates possess an intermediate nature. We have observed such cases in the series mica-vermiculite, vermiculite-chlorite, smectite-chlorite, etc. One of the notable accretion processes in soils is the reaction of hydroxyl-Al ions with 2:1 phyllosilicates. Aluminum ions solubilized from minerals hydrolyze readily and are polymerized to form precipitates between expandable silicate layers like vermiculite or smectite to form a chlorite-like mineral. They can be referred to as hydroxyl-Al interlayered vermiculite or hydroxyl-Al interlayered smectite, respectively. These names have been shortened to the acronyms HIV and HIS for which Barnhisel and Bertsch (1989) proposed to standardize the terminology.

TABLE 21.23 Major Chemical Dissolution Methods

Category	Chemical Reagents Used for Dissolution	Selected References
(a) Alkaline	NaOH	Foster (1953), Hashimoto and Jackson (1960)
	Na ₂ CO ₃	Mitchell and Farmer (1962), Follett et al. (1965)
(b) Acid	HCl	Deb (1950)
(a) + (b) alkaline + acid	NaOH/HCl	Segalen (1968)
(c) Complexing	H ₄ C ₂ O ₄ , acetic acid method	Chester and Hughes (1967)
	H ₂ C ₂ O ₄ , oxalic acid method	Ball and Beaumont (1972)
	(NH ₄) ₂ C ₂ O ₄ /H ₂ C ₂ O ₄ , acid NH ₄ -oxalate method	Tamm (1922), Schwertmann (1959)
	Na ₂ C ₂ O ₄ /H ₂ C ₂ O ₄ , acid Na-oxalate method	Henmi and Wada (1976)
	C ₆ H ₄ Na ₂ O ₈ S ₂ , alkaline tiron method	Biermans and Baert (1977)
	Na ₄ P ₂ O ₇ , Na-pyrophosphate method	McKeague (1967)
	K ₄ P ₂ O ₇ , K-pyrophosphate method	Ball and Beaumont (1972)
(d) Reducing	NH ₂ OH · HCl/HCl, hydroxylamine method	Chao and Zhou (1983), Ross et al. (1985)
(c) + (d) Reducing + complexing	Na ₂ C ₆ H ₅ O ₇ /NaHCO ₃ /Na ₂ S ₂ O ₄ sodium-dithionite method	Mehra and Jackson (1960)
	K ₂ C ₂ O ₄ /H ₂ C ₂ O ₄ /Mg, Jeffries' method	Jeffries (1946)
	(NH ₄) ₂ C ₂ O ₄ /H ₂ C ₂ O ₄ /Na ₂ S ₂ O ₄ , combined oxalate method	Duchaufour and Souchier (1966)

21.5.2.4 Interstratified Layer Silicates

As mentioned earlier in the structure of interstratified layer silicates, due to the structural similarities of the clay minerals, interstratified minerals can exist in which individual crystallites are composed of elementary layers of two or more types. Such mixed structures, in some cases, do not show characteristic features of each of the component layers but possess their own identity. They show more or less intermediate nature of the component layers, they are thus called intergrades. Therefore, this intermediate nature may be useful to identify component layers. Table 21.24 gives an example of diagnostic criteria. Interstratified, or mixed layer, clay minerals represent a special case of intergrowths, in relation to a genetic relationship between components. Neglecting all questions regarding interlayer cations, ionic substitution, and layer charge, montmorillonites and vermiculites, for instance, are essentially hydrated varieties of mica having interlamellar water molecules. Instead of water, introduction of hydroxide

sheets between silicate layers of these minerals results in chlorite. Therefore, interstratifications among those minerals are expected to be common, as in fact they are. Figure 21.34 gives a graphic presentation for each of the clay minerals as an elementary component, which is known to be composed of an interstratified structure with another elementary component.

The most striking interstratifications occurs when two-component layers *A* and *B* alternate regularly to make an interstratified structure, *AB AB ...* type, having a long d_{001} -spacing = d_{001} -spacing (layer *A*) + d_{001} -spacing (layer *B*). Let P_{AB} be the probability that *B* succeeds *A* given that the first layer is *A*, perfect regularity must satisfy the conditions $P_{AB} = 1$ and $P_{AA} = 0$. As the evaluation of such conditions is not always possible, a practical measure is recommended by the Clay Minerals Society Nomenclature Committee (Bailey et al., 1982). This is based on a statistical test on a well-defined series of at least 10 00-summation spacings ($d_{AB} = d_A + d_B$), for which the suborders are integral. The coefficient of variation

TABLE 21.24 Diagnostic Criteria for Interstratified Minerals in Soils

Type of Interstratification ^a	Glycerol	Humid, >95% RH	Air-Dry, 45% RH	Very Dry, <3% RH	110°C	550°C
Mica-vermiculite	b	b	1.0–1.4	1.0–1.15	1.0–1.15	1
Mica-chlorite	b	b	1.0–1.4	b	b	1.0–1.4
Mica-smectite	0.9–1.0 or ≈1.8	Expansion	1.0–1.55	1.0–1.15	1.0–1.15	1
Vermiculite-chlorite	b	b	1.4	1.15–1.4	1.15–1.4	1.0–1.4
Vermiculite-smectite	1.4–1.8	Expansion	1.4–1.54	1.15	1.15	1
Chlorite-vermiculite	1.4–1.8	Expansion	1.4–1.54	1.15–1.4	1.15–1.4	1.0–1.4
Mica-vermiculite-chlorite	b	b	1.0–1.4	Contraction	Contraction	1.0–1.4
Mica-vermiculite-smectite	Expansion	Expansion	1.0–1.54	Contraction	Contraction	1
Vermiculite-chlorite-smectite	Expansion	Expansion	1.4–1.54	Contraction	Contraction	1.0–1.4

Source: Modified after Kodama, H., and J.E. Brydon. 1968a. A study of clay minerals in podzol soils in New Brunswick, eastern Canada. *Clay Miner.* 7:295–309.

Expansion and contraction mean shift of the original first-order reflection (air-dry) toward large and small spacing sides, respectively.

^a As Ca-saturated specimens.

^b Indicates that the basal spacing is unchanged from air-dry.

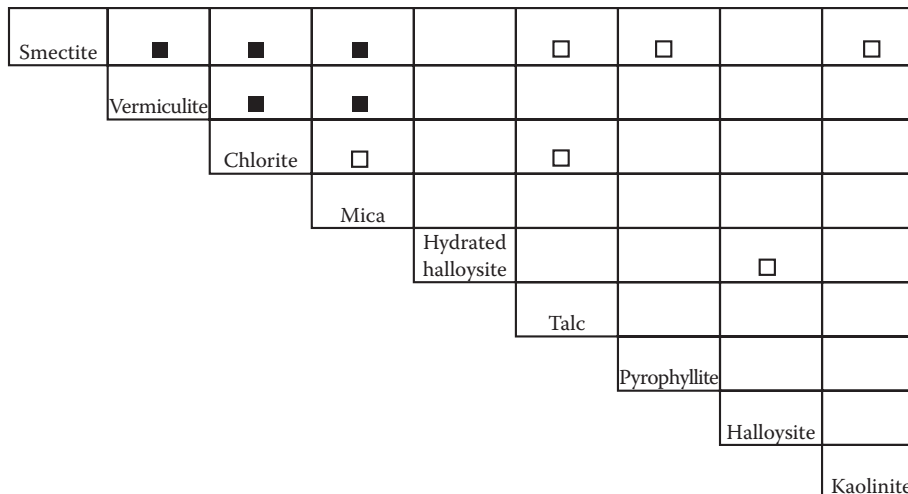


FIGURE 21.34 Diagrammatic representation of layer silicate type combination found in nature as interstratified clay minerals. ■ = frequent occurrence; □ = less-frequent occurrence. (Modified after Sudo, T., S. Shimoda, H. Yotsumoto, and S. Aita. 1981. Electron micrographs of clay minerals. Developments in sedimentology. Vol. 31. Elsevier Scientific Publishing Co., New York.)

(CV) of the d_{000} -values should be less than 0.75 to demonstrate adequate regularity of alternation. The CV is defined as $CV = 100s/X$, where the standard deviation for a small sample is $s = [\sum(X_i - X)^2 / (n - 1)]^{1/2}$, X_i is an individual observed $-x d_{000}$ -value, X is the mean

of the X_i values, and n is the number of observed X_i values. In Table 21.25, an example is shown using the case of rectorite–Ca, which is a regularly interstratified mineral, smectite–Ca mica. The observed long d_{001} -spacing is 2.8 nm on glycolation. This agrees with the summation of 1.8 nm for smectite and 1.0 nm for mica when they are glycolated. The XRD data of the rectorite show observable basal reflections up to the 20th in that recording range. The $d \times \ell$ values in the table correspond to observed $-x d_{000}$ -values (X_i). Calculations for this rectorite result in 2.751 nm for the average (X) and 0.463 for the CV value that is much smaller than the recommended value of 0.75. The majority of interstratified layer silicates is not well ordered, so they do not show basal reflection of a long spacing ($d_{AB} = d_A + d_B$) nor a rational integral series of basal reflections.

Characterization requires:

1. Determination of component layers A and B (or, and C)
2. Evaluation of the mixing ratio for the component layers A and B, that is, $A:B = m:(1 - m)$, where $0 < m < 1$
3. Probability for layer-stacking sequence as expressed by P_{AA}, P_{AB} , etc

The determination of component layers can be done by choosing appropriate diagnostic tests for them. A relatively simple method is available to evaluate the mixing ratio of two components in an irregularly interstratified structure. The principle of the method is based on the peak migration due to the interference phenomenon of x-rays (Méring, 1949). According to Méring’s idea, Figure 21.35 is constructed to explain the principle, using

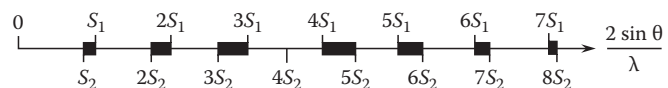


FIGURE 21.35 Demonstration of Méring’s method, in which peak migration is used for evaluating the mixing ratio of two-component layers in an interstratified clay mineral. S_1 : Na-saturated rectorite, S_2 : Ca-saturated rectorite.

TABLE 21.25 Example of the CV Test for Evaluating Regularity of Interstratifications

Rectorite–Ca, Sample # 1820			
00ℓ	d (Å)	I	d (Å) $\times \ell$
1	28.09	847	28.09 ^a
2	14.01	174	28.02 ^a
3	9.267	84	27.8
4	6.923	40	27.69
5	5.495	7	27.47
6	4.588	31	27.53
7	3.933	23	27.53
8	3.442	33	27.54
9	3.065	42	27.58
10	2.723	4	27.23
11	2.503	7	27.53
12	—	—	—
13	—	—	—
14	1.963	6	27.48
15	1.832	5	27.48
16	—	—	—
17	1.615	3	27.46
18	1.527	3	27.49
19	1.443	2	27.42
20	1.372	3	27.4
Average			27.51
CV			0.463

Source: After Matsuda, T., H. Kodama, and A.-F. Yang. 1997. Ca-rectorite from Sano mine, Nagano prefecture, Japan. *Clays Clay Miner.* 45:773–780.

^a Excluded from CV calculations.

modified rectorite samples. Sodium (Na)-saturated rectorite (S_1) and Ca-saturated rectorite (S_2) were prepared separately. Because the hydration state of Na-saturated smectite differs from that of Ca-saturated smectite under relative humidity at 50%, S_1 gives d_{001} at 2.24 nm and S_2 at 2.54 nm. In this figure, the 00ℓ reciprocal lattice rows of reciprocal spacing $S_1 = 1/d_1$ and $S_2 = 1/d_2$ are given and the heavy lines, such as between S_2 and S_1 , indicate the regions in reciprocal space where reflections are predicted to appear as two-component peaks merging together when the two are mixed coherently (in respect with x-rays) without physical segregation and do not constitute a regularly interstratified structure. The assumption is that the peaks move linearly from the position for one pure component toward the nearest position of the other component as the proportions of the components alter. This may not be rigorously correct, but information obtained this way is quite useful. This estimation should be performed by inspecting the peak migrations in as many regions as possible.

As the next step, it is desirable to determine the probability of layer-stacking sequence. A direct Fourier transform method developed by MacEwan and Wilson (1980) and MacEwan et al. (1961) has been applied widely. With mathematical approximation, MacEwan formulates the equation as

$$W_R = \left(\frac{a}{\pi} \right) \sum i(s) \cos(\mu_s R) \quad (21.4)$$

with

$$i(s) = \frac{I_s}{\Theta_s IF_s I^2}$$

where

W_R is the distribution function defined as the probability of finding another layer at the distance R measured perpendicularly from any layer

μ_s , I_s , Θ_s , and $IF_s I^2$ are values at the position of the intensity maximum

$\mu_s = 2 \sin \theta / \lambda$

I_s is the integrated intensity

Θ_s is the operational function

$IF_s I^2$ is the layer structure factor

Therefore, a Fourier transform on a series of basal reflections of unknown mixed-layer mineral gives the probability of finding layer B succeeding layer A (P_{AB}) and so on. An application to soil minerals is shown in Figure 21.36. This case happened to be a tertiary system, smectite-vermiculite-mica. The first three peaks (h_A , h_B , h_C) correspond to the probabilities of occurrence of the fundamental component layers, A (smectite), B (vermiculite), and C (mica), respectively. Obviously $P_A + P_B + P_C = 1$, therefore, $P_A = 0.53$, $P_B = 0.27$, and $P_C = 0.20$ were obtained from the observed heights for sample SMJ 1. Knowing the relation between peak heights and occurrence frequencies (for instance, $h_{AA} = P_A P_{AA}$, $h_{AB} = P_A P_{AB} + P_B P_{BA}$, etc.), calculating heights for all possible layer sequences and comparing the calculated with

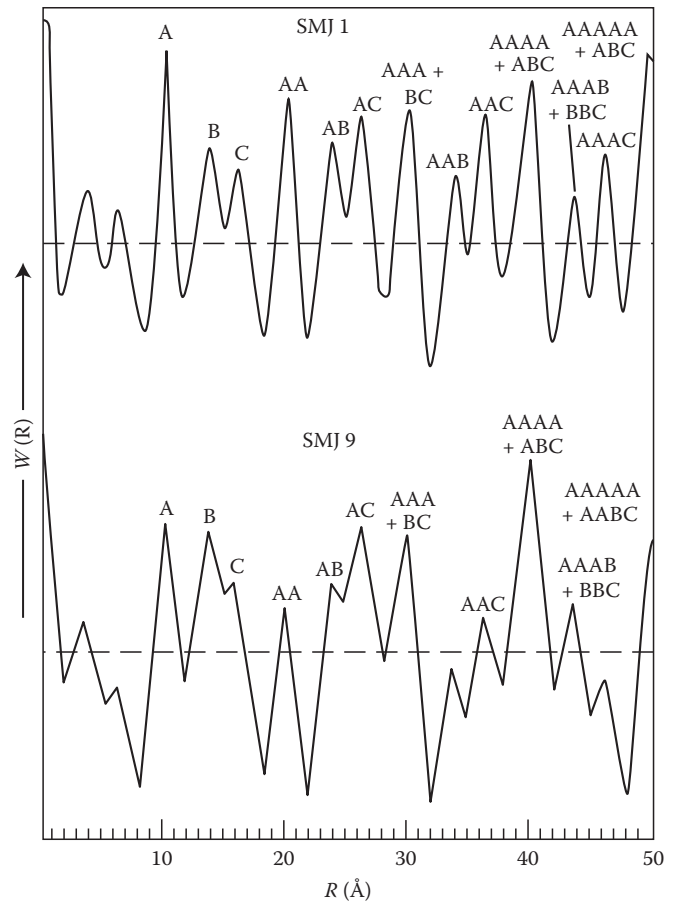


FIGURE 21.36 Example of direct Fourier transform method by MacEwan on soil clays. (From Kodama, H., and J.E. Brydon. 1968a. A study of clay minerals in podzol soils in New Brunswick, eastern Canada. *Clay Miner.* 7:295–309.)

the observed allow the probability coefficients to be estimated from the results of the Fourier transform. The direct method is applicable to any interstratifications but caution should be paid to the precision of the results obtained by the Fourier method, which may be affected by premature termination of basal reflection series and assessing the baseline for the obtained occurrence probability curve. Thus, preliminary information concerning the mixing ratio and layer-stacking sequence is acquired and diffraction patterns can be simulated by computer calculations. Several simulation approaches are available (Kakinoki and Komura, 1952, 1954; Sato, 1965, 1973; Reynolds, 1980; Moore and Reynolds, 1989; Yuan and Bish, 2010) for further refinement of the structure of interstratified layer silicates, if cases allow.

21.5.3 Other Instrumental Methods

21.5.3.1 X-Ray Diffraction Photograph Methods

Undoubtedly x-ray diffractometer methods are dominating to collect diffraction data nowadays. However, in the case where only a limited quantity of sample is available, classical photographic methods by the Debye-Scherrer camera is still useful

to obtain maximum information on a mineral in a fraction of milligram. This camera method can avoid preferred orientation to which phyllosilicates have a strong tendency. The determination of polytypes requires details of nonbasal reflections. Therefore, the use of camera techniques is beneficial. Gandolfi camera is one type of a modified Debye-Scherrer x-ray powder diffraction camera. In this camera (Figure 21.37a), the mounted sample rotates around two axes, that is, the sample stage arm rotating around the center of the camera and the sample on a

goniometer head itself rotating around an axis tilted 45° to the central rotating axis. With this camera, a single-mineral crystal, or grain, or aggregate, in a fraction of millimeter size, is sufficient to provide adequate powder diffraction patterns without grinding. Examples are presented in Figure 21.38b. Wilson and Clark (1978) developed a method for identifying minerals on thin sections by a combination of optical observations and XRD analysis. This is an interesting area to be explored further for routine application.

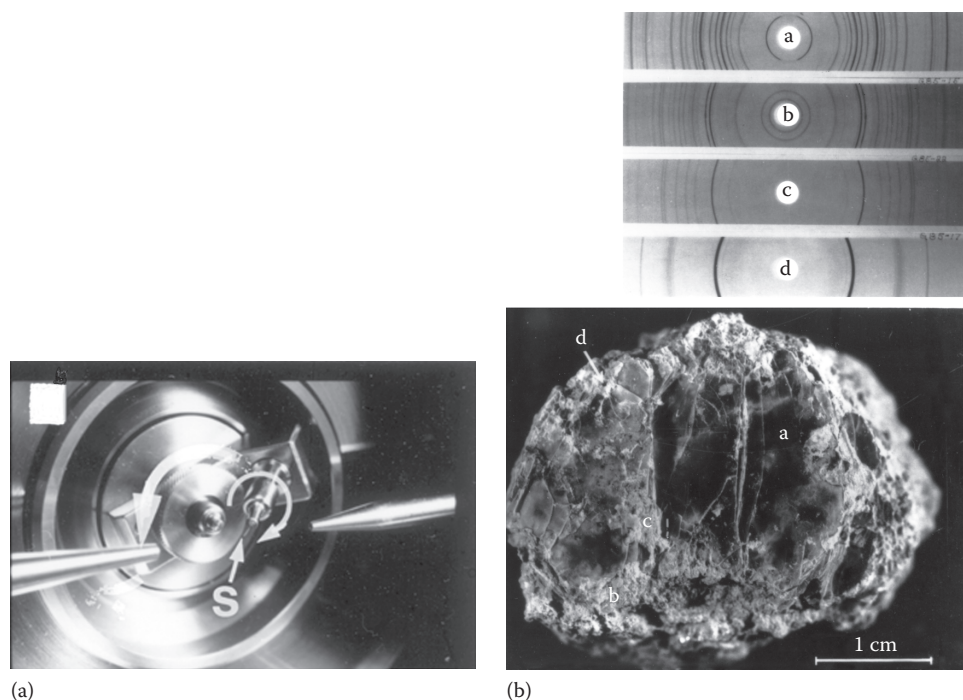


FIGURE 21.37 An application of Gandolfi diffraction camera method to a small grain of mineral for collecting data without pulverizing the sample. (a) Shows the mounted sample rotating around two axes. (b) XRD patterns obtained. A, Phlogopite; B, corrensite; C, calcite; and D, graphite. A, B, C, and D correspond to those locations in the weathered phlogopite crystal piece where samples were taken. (Modified after De Kimpe, C.R., N. Miles, H. Kodama, and J. Dejou. 1987. Alteration of phlogopite to corrensite at Sharbot Lake, Ontario. *Clays Clay Miner.* 35:150–158.)

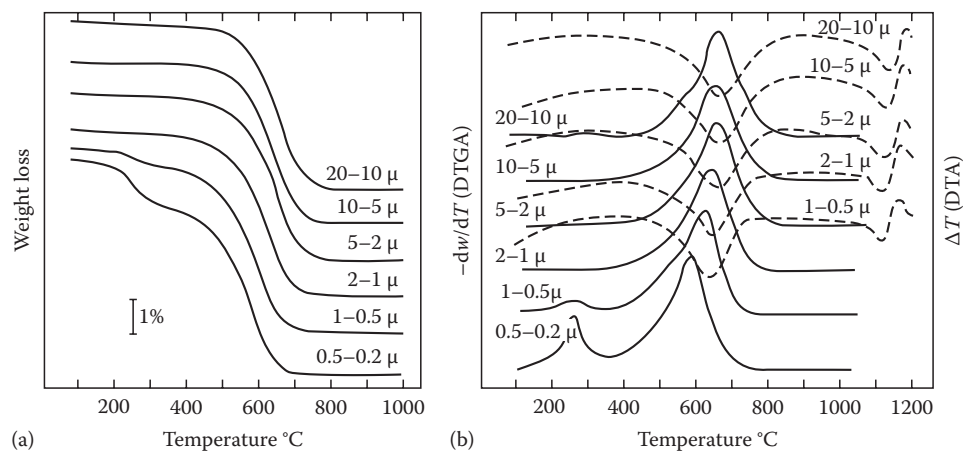


FIGURE 21.38 (a) TGA curves and (b) DTGA (solid lines) and DTA (dashed lines) curves of the fractionated samples of a naturally occurring micro-crystalline muscovite. (From Kodama, H., and J.E. Brydon. 1968b. Dehydroxylation of micro-crystalline muscovite. *Trans. Faraday Soc.* 64:3112–3119.)

21.5.3.2 Methods for Specific Characterization

As discussed in the section on crystal structures, the 1:1 type structures possess hydroxyls in two different octahedral environments, that is, one locates inside at the interface between the octahedral and tetrahedral sheets, and another is exposed to the outside of the octahedral sheet. This is one of the unique characteristics of the 1:1 layer silicates, which may be used for their identification. Infrared absorption spectroscopy can provide details of the OH-stretching bonds in the region of 4000–3000 cm^{-1} in terms of its orientation against the basal plane and its bond distance (O–H...O) as affected by octahedral environments, including elemental compositions (Tuddenham and Lyon, 1959; Nakamoto, 1963). The orientation is known to depend on octahedral cation vacancies; therefore, a similar view can be extended to the difference in dioctahedral and trioctahedral 2:1 type structures as well (Serratos and Bradley, 1958). A number of papers have been published along these lines (only selected ones: Vedder and McDonald, 1963; Vedder, 1964; Farmer, 1974; Robert and Kodama, 1988).

Dealing with iron-bearing phyllosilicates, the actual amount of iron incorporated structurally; the $\text{Fe}^{2+}:\text{Fe}^{3+}$ ratio as oxidation state; structural configuration, like distribution of these cations between *cis*- and *trans*-octahedral sites; the amount of Fe^{3+} in tetrahedral sites; and occasionally their role in the magnetic nature of the minerals are sought. In the presence of organic matter, the determination of Fe^{2+} is impossible by wet-chemical methods. Application of the Mössbauer effect under these situations is very appropriate. The ^{57}Fe Mössbauer spectroscopy provides parameters such as isomer shift, IS (mm s^{-1}), quadrupole splitting, ΔE_Q (mm s^{-1}), and internal magnetic hyperfine field, H (in $k\text{Oe}$), if magnetic ordering is present. Most key information is foiled in the quadrupole doublets. Spectra are recorded at temperatures ranging from 4 to 298 K (liquid He to room temperature) to identify the oxidation state, coordination environment, and magnetic exchange interactions occurring in the constituent minerals. The parameters allow the identification of Fe in various (oxyhydr)oxide and phyllosilicate phases in mixed mineral systems. Analysis of Mössbauer spectra is carried out by computer using a least-squares minimization fitting routine for obtaining the best peak profile. Spectral parameters obtained after refinement may give answers to the questions above (Stucki et al., 1988; Coey, 1988; Murad, 1988; Murad and Cashion, 2004). Among minerals having a chlorite structure, the distinction between iron atoms in the octahedral sheet and iron atoms in the hydroxide sheet has yet to succeed. Murad and Wagner (1991, 1994) succeeded in obtaining detailed characterization of kaolinite minerals and illite by the application of Mössbauer spectroscopy.

The distribution of aluminum atoms that substitute for silicon atoms in the tetrahedral sheet is an interesting subject from a crystallographic point of view (Loewenstein, 1954). Investigations by x-ray methods were performed as done for muscovite by Gatineau (1964). Because the data needed for this purpose require tedious recording and collection of non-Bragg reflections, only specialized laboratories can afford such experiments. Besides the x-ray

method, the application of ^{29}Si (and ^{27}Al) magic-angle spinning, solid-state nuclear magnetic resonance spectroscopy was introduced into the research in this line (Herrero et al., 1985). The spectra are obtained as chemical isomer (in this case ^{29}Si) shift (ppm), which is influenced by the chemical environment of the nucleus. The range where resonance spectra appear as a function of polymerization (if true mica, denoted as Q^3 for Si_3Al_1) and analysis of spectra provides information about Si and Al ordering in the tetrahedral sheet, including the number of next-neighbor Si in layer silicates. Conversely, using the ^{27}Al nucleus, spectra acquired supply information regarding Al and Si ordering and the number of next-neighbor Al in layer silicates (Sans and Serratos, 1984). Data can be used to compliment each other.

The origin of the total layer charge in phyllosilicates is due to ionic substitutions by atoms of lower valence for those of higher valence like $\text{Al}^{3+} \rightarrow \text{Si}^{4+}$, $\text{Fe}^{2+} \rightarrow \text{Fe}^{3+}$, $\text{Mg}^{2+} \rightarrow \text{Al}^{3+}$. The way in which layer charge is distributed in the structure of a specific phyllosilicate appears to closely relate to the course of weathering or alteration, which the mineral might take in nature. We often believe that phyllosilicates behave erratically, but this is because we normally treat them as if they were totally “structurally homogenous.” For instance, when smectite is suspended in water containing Na^+ and Ca^{2+} , a demixing phenomenon is observed (Glaeser and Méring, 1954; Glaeser, 1958). Certain phyllosilicates behave as if the distribution of their layer charge is not symmetrical, in other words, the layer charge distribution in the structure has a polarity. In this connection, the *n*-alkylammonium exchange method developed by Lagaly and Wiess (1969) is useful for estimating interlayer charge and characterizing expandable layer silicates by making complexes with the surface of the expandable layer silicates, then the d_{001} -spacings of the complexes are measured. The magnitude of the spacing is related to the size and tilt angle (α) of the *n*-alkylammonium intercalated between the expandable silicate layers. The tilt angle (α), that is, the angle between the alkyl chain and the basal plane of the clay, is related to the layer charge. To evaluate layer charge irregularity, peak positions and profiles of higher order basal reflections may need to be inspected in detail (Lagaly, 1979, 1982; Ghabru et al., 1989) Vali and Koster (1986) developed a method that allows us to make the alkylammonium ion treatment of clay minerals in ultrathin sections for high-resolution transmission electron microscope (HRTEM) observations. The method proved promising and awaits further applications, especially studies on microenvironments.

The task of distinguishing and quantifying the various types of water, that is, physically adsorbed, zeolitic, interlayer, and structural, is not easy. Thermoanalytical methods including thermogravimetric analysis (TGA), differential TGA (DTGA), and differential thermal analysis (DTA) are often applied for this purpose. Although TGA is indispensable for obtaining weight loss, DTGA is helpful to evaluate a critical temperature for distinguishing between water of two different types. The features in a TGA curve are generally too broad to pinpoint precisely the temperatures over which a dehydration reaction occurs (see Figure 21.38).

Water retention is one of the key properties of clay mineral surfaces, as already mentioned. This is due in part to the small particle size and large surface area of the clay minerals, as illustrated by the fact that a handful of clay provides enough surface area to cover an area the size of a football field. Among clay minerals, expandable minerals possess greater surface area than nonexpandable minerals, because in the former surfaces both internal and external to the particles contribute to the total surface area. Surface area measurements by N₂ gas adsorption, notably using the Brunauer, Emmett, and Teller (BET, method (Brunauer et al., 1938), are often applied for evaluating external surface area.

For total surface area (=external + internal) measurements, glycol retention method (Diamond and Kinter, 1958), ethylene glycol monoethyl ether (EGME) method (Carter et al., 1965), a modified EGME method (Eltantawy and Arnold, 1973), and methylene blue method (Hang and Brindley, 1970) are often applied.

Recent developments in analytical instrumentation enable us to explore objects in much smaller domains as they exist without separation, that is, almost in situ observations (e.g., Tessier, 1990). Perhaps, studies of clay minerals in soil aggregates and in the rhizosphere are certainly interesting. Ideas and concepts regarding mineral alteration mechanisms have long been speculated since Keller and Frederickson (1952) followed by Mortland et al. (1956). This appears recently to revive and improve with modern technologies (Robert and Berthelin, 1984; April and Keller, 1990; Hinsinger et al., 1992; Hinsinger and Jaillard, 1993). Approaches from different perspectives were attempted by Kodama et al. (1994) for the role of clay minerals in the rhizosphere and by Monreal and Kodama (1997) for the role of clay minerals as soil aggregates in microbial activity.

Interactions with microbes have received a great deal of attention. Huang and Schnitzer (1986) summarized an achievement of the workshop organized for interactions of soil minerals with natural organics and microbes. Reviews until 1997 can be seen in *Geomicrobiology* (Banfield and Nealson, 1997). Tazaki and Asada (2007) provided transmission electron micrographs showing intimate association where clay particles attached to a thick wall covering the bacteria. They explained that clay particles and the thick wall, a kind of cellular polymeric substance, are able to protect bacteria from toxic elements such as Hg. The research was performed by an appropriate application of energy-filtering transmission electron microscopy, scanning transmission microscopy equipped with energy dispersive x-ray spectroscopy, optical and fluorescence microscopy, XRD, and atomic absorption spectrometry.

21.5.4 Quantification

21.5.4.1 Basic Theory

Alexander and Klug (1948) showed that the XRD intensity (I_i) from the i th component in a multicomponent mixture can be related to the weight fraction of the component (x_i) by the equation,

$$I_i = \frac{K_i(x_i/\rho_i)}{(\sum \mu_i^* x_i)} \quad (21.5)$$

where

ρ_i and μ_i^* are the density and mass absorption coefficient of the component i , respectively

K_i depends upon the nature of component i and the geometry of the apparatus employed

By regarding the mixture of n components as if it consisted of just two components, component 1 to be analyzed and the sum of the other components designated as matrix, Equation 21.5 may be extended to a very useful form:

$$I_1 = \frac{K_1 x_1}{\{\rho_1 [x_1(\mu_1^* - \mu_M^*) + \mu_M^*]\}} \quad (21.6)$$

where μ_M^* is the mass absorption coefficient of the matrix. Equation 21.6 is the basic relationship underlying quantitative analysis of multicomponent mixtures with the x-ray diffractometer (Alexander and Klug, 1948; Klug and Alexander, 1954). The diffraction intensity of component 1 is thus related to its concentration in the mixture and to relative mass absorption coefficients of the component and matrix. Because of this relationship, except for the case where $\mu_1^* = \mu_M^*$, that is, the case of a mixture consisting of only polymorphic substances, the intensity-concentration relation is generally not linear. Since mass absorption coefficients are functions of the chemical composition of the absorber and of the wavelength of x-rays irradiated, it is readily understood that the choice of radiation to be employed is important. Practical solutions to Equations 21.5 and 21.6 are discussed in the following section.

21.5.4.2 Intensity-Concentration Calibration Curve

For general analytical purposes, one possible solution of Equation 21.6 is to establish intensity-concentration working curves from multicomponent standard synthetic mixtures that simulate a natural system in question. This approach has been attempted for the quantitative estimation of clay minerals by Talvenheimo and White (1952) among others. However, numerous combinations of mineral associations occur in nature, so to cover all possible cases by preparing synthetic standard mixtures is not practical. Thus, this approach is necessarily restricted to simple systems. One of the more practical solutions to the analysis of complicated multicomponent systems may be to compare intensities of two components in a multicomponent mixture and to relate them to their weight proportions. By introducing the average mass absorption coefficient, μ^* , for the mixture, we can simplify Equation 21.5 to

$$I_i = K_i' \left[\frac{x_i}{(\rho_i \mu^*)} \right] \quad (21.7)$$

Then a comparison between intensities of the i th and j th components produces the relation independent of μ^* (Brindley, 1961) as follows:

$$\frac{I_i}{I_j} = \frac{K_i' x_i \rho_j}{(K_j' x_j \rho_i)} = K'' \left(\frac{x_i}{x_j} \right) \quad (21.8)$$

where K'' includes all constants, K_i^+ , K_i^- , ρ_i , and ρ_j , for two mineral components i and j . Equation 21.8 suggests a linear relationship between the intensity ratio ($I_i:I_j$) and the ratio of weight fractions ($x_i:x_j$) for the two mineral components. Therefore, if the K'' is evaluated experimentally by synthetic mixtures, the relative weight fractions in unknowns can be determined from measurements of intensity ratios. In a multicomponent system, the weight fraction of each mineral component can be estimated by integration of the results on mineral pairs, which cover all mineral species in the sample. This method was applied to clay minerals by Theisen and Bellis (1964).

21.5.4.3 Internal Standard Method

The use of an internal standard also permits quantitative analysis without any direct knowledge of the mass absorption coefficients of components (μ_i^*), since the method is based on a relation similar to Equation 21.8. Suppose that a known and constant amount of an internal standard, which will be designated by the subscript "s" is added to an unknown mixture. Then the weight fraction of component 1 (x_1) in the original mixture is changed to x_1' , which is expressed by the relation, $x_1 = x_1'/(1 - x_s)$. This relation can be derived as follows: since $w_s/x_s = (w + w_s)$, where w and w_s are the total sample weight before the addition of the standard and the weight of the standard added, respectively; thus, $1 - x_s = w/(w + w_s)$. On the other hand, $x_1' = w_1/(w + w_s)$ and $x_1 = w_1/w$, therefore $x_1 = x_1'/(1 - x_s)$. Taking the intensity ratio of I_1 to I_s in a manner similar to Equation 21.8, we obtain the relation

$$\frac{I_1}{I_s} = \frac{K_1 x_1' \rho_s}{K_s x_s \rho_1} = \frac{[K_1' x_1 (1 - x_s) \rho_s]}{K_s x_s \rho_1} \quad (21.9)$$

All components but x_1 in the right-hand term of Equation 21.9 are regarded as constant; Equation 21.9 can, therefore, be arranged to

$$x_1 = k \left(\frac{I_1}{I_s} \right) \quad (21.10)$$

Thus, the concentration of component 1 is proportional to the intensity ratio $I_1:I_s$ alone and independent of mass absorption coefficients of a specific mineral and matrix. This method has been applied to clays and related minerals using internal standards such as fluorite (CaF_2) (Alexander and Klug, 1948), boehmite (AlOOH) (Brindley and Kurtossy, 1961), Zn(OH)_2 (Mossman et al., 1967), and pyrophyllite (Mossman et al., 1967).

21.5.4.4 Standard Additional Method (Spike Method)

As described by Brindley and Udagawa (1960), this method involves an addition of a known amount of a pure mineral component to a sample in which the mineral component is to be analyzed. The method is useful if the characteristics of the mineral component in the sample closely resemble those of the pure mineral component to be added. If the change in the average

μ^* of Equation 21.7 by this addition can be neglected, then the ratio (I_1/I_1') of intensities of component 1 being analyzed before (I_1) and after (I_1') should be directly proportional to the ratio of weight fractions as follows (Brindley and Udagawa, 1960):

$$\frac{I_1'}{I_1} = \frac{(x_1 + x_1')}{[x_1(1 + x_1')]} \quad (21.11)$$

where the right-hand term is the weight fraction of the component after the addition of the component to the sample. It should be borne in mind that the optimum amount of the pure mineral added depends upon the initial amount of the mineral component in the sample. As a general guide, 25%–100% of the initial amount may be recommended.

21.5.4.5 External Standard Method (Direct Method)

This method requires mass absorption coefficient measurements and has been applied by Williams (1959), Norrish and Taylor (1962), and others. Such measurements are, however, rather time-consuming and the method has only limited application to complicated mineral mixtures in soils.

21.5.4.6 Estimation Based on Intensity Factor Ratios

The diffraction intensity, I_{hkl} , of the hkl reflection is proportional to the square of the structure factor, F_{hkl} , thus, $I_{hkl} \sim KIF_{hkl}^2$, where K depends upon experimental conditions and the value of F is related to the numbers and kinds of atoms involved in the reflection plane hkl of a mineral structure. Consider a mixture consisting of two minerals A and B with equal amounts and let I_A and I_B be the diffraction intensities from any reflection planes of minerals A and B , respectively. The ratio $I_B:I_A$ should be constant regardless of the absolute amounts of both minerals, and this constant factor, k , may be expressed by IF_B^2/IF_A^2 , where F_A and F_B are the structure factors for the corresponding reflections of minerals A and B , respectively. The I_A is, therefore, equal to I_B/k . If the amounts of minerals A and B are not the same, they would be proportional to $I_A/1$ and I_B/k , respectively. This is the basic concept for the quantification method based on the intensity factor ratios. The concept can be extended easily to multicomponent systems.

The preferred orientation method is widely applied to identify clay minerals. It is, therefore, very convenient and practical that the basal reflections are used for quantification. The basal intensity factor ratios may be obtained (a) directly from structure factor calculations or (b) by graphical approximation from squared moduli of layer structure factors prepared by Bradley (1953), MacEwan et al. (1961), and Cole and Lancucki (1966) for various types. By these approaches, Johns et al. (1954) first attempted the quantification of clay minerals and many investigators followed (e.g., Weaver, 1958; Schultz, 1960, 1964; Dell, 1973). Another way to evaluate the factors is by an experimental determination based upon synthetic standard mixtures. The advantage of the latter is that the factors evaluated can include all necessary correction factors due to experimental conditions

as well as the intensity factor. Therefore, the factors can be applied immediately to estimate quantities of clay minerals, as long as the experimental conditions are the same as those for the synthetic standard mixtures from which the factors were evaluated. In general practice for the quantification of clay minerals, intensity factors are determined using a series of binary mineral systems, like minerals *A* and *B*, with equal amounts at several different levels. Similar experiments should be extended to other binary systems like minerals *A* and *C*, or *A* and *D*, and so on. Obviously, the intensity factors of mineral *A* are expected for normalization for the whole. The mineral illite is often chosen for this purpose due to various merits. This approach was chosen by Oinuma et al. (1961). Most clay minerals vary in crystallinity and composition, which greatly affect their basal reflection intensities. Because of this, quantitative estimations made from these intensity factor methods are crude in comparison with those done by methods described in previous sections. In view of difficulties due to variations in clay minerals, however, such an approach is believed to be the best compromise.

21.5.4.7 General Outline for Soil Mineral Quantification

Since soils are complex mixtures of substances of varying degrees of crystallinity ranging from amorphous to strongly crystalline, achieving quantitative analysis with a comparable precision for all mineral components at the same time is almost impossible. Although a major emphasis should be put on clay minerals that usually constitute a large portion of crystalline substances in the clay-size fraction of soils, depending upon the type of minerals involved, a more precise estimation may be made by choosing a suitable method for a specific case. Thus, the general outline adapted in our laboratory for the soil mineral quantification is a combination of methods as follows (Kodama et al., 1977):

1. The method using intensity factor ratios for clay minerals (phyllosilicates) in general
2. The intensity–concentration calibration method for quartz
3. The internal standard method for hematite and goethite
4. A combination of the intensity–concentration and internal standard methods for feldspars and amphiboles
5. The standard addition method for minerals such as calcite, dolomite, gypsum, serpentine minerals, talc, pyrophyllite, and jarosite, which occur less frequently in soils and whose crystallinities do not vary much so that a standard representing the mineral to be analyzed in a sample is easily available

Addendum

After the preparation of this chapter, the author received a copy of the following manuscript: The Mica Group, *In Kluwer Encyclopaedia of Mineralogy* by A.E. Lalonde, 90 pp with nine figures. This appears to be available online.

Appendix

Glossary of Phyllosilicates

Notes:

1. Every valid mineral species names are listed in bold face.
2. Mineral group names are in italic.
3. Majority of interstratified minerals listed here are given in a form of binary system expressed by mineral group names (mica–smectite, vermiculite–smectite, etc.).

A

Aliettite 1:1 regular interlayering of talc–trioctahedral smectite-group mineral, *Interstratified Layer Silicate Group*

Allevardite = **Rectorite**

Alurgite = magnesian manganiferous **Muscovite**

Amesite $Mg_2Al(Si,Al)O_5(OH)_4$, *Serpentine–Kaolin Group*

Amesite-2H

Amesite-6R

Anandite $Ba,K(Fe^{2+},Mg)_3(Si,Al,Fe^{3+})_4O_{10}(O,OH)_2$, *Brittle Mica Group*

Anandite-2M₁

Anandite-2Or

Anauxite = mixture of kaolinite and amorphous silica

Annite $K(Fe^{2+})_3(AlSi_3)O_{10}(OH,F)_2$, *True Mica Group*

Antigorite $(Mg,Fe)_3Si_2O_5(OH)_4$, *Serpentine–Kaolin Group*

Aphrosiderite = ferroan **Clinochlore**

Aspidolite = sodium **Phlogopite**

Attapulgitite = **Palygorskite**

B

Baileychlore $(Zn,Fe^{2+},Al,Mg)_6(Si,Al)_4O_{10}(OH)_8$, *Chlorite Group*

Bannisterite $KCa(Fe,Mn,Zn,Mg)_{20}(Si,Al)_{32}O_{76}(OH)_{16} \cdot 4-12H_2O$, *Modulated Layer Silicate Group*

Baumite = zirconian Caryophilite, zirconian **Greenalite**

Bementite $Mn_7Si_6O_{15}(OH)_8$, *Modulated Layer Silicate Group*

Beidellite $(Na,Ca)_{0.3}(Al)_2(Si,Al)O_{10}(OH)_2 \cdot nH_2O$, *Smectite Group*

Bentonite = (a) impure **Montmorillonite**, (b) **Beidellite**

Berthierine $(Fe^{2+},Fe^{3+},Mg)_{2-3}(Si,Al)_2O_5(OH)_4$, *Serpentine–Kaolin Group*

Berthierine-1M

Biotite $K(Mg,Fe^{2+})_3(Al,Fe^{3+})Si_3O_{10}(OH,F)_2$, *True Mica Group*

Bityite $CaLiAl_2(AlBeSi_2)O_{10}(OH)_2$, *Brittle Mica Group*

Bowingite = **Saponite**

Bramallite = sodian **Muscovite** (**Illite**)

Brandisite = **Clintonite**

Brindleyite $(Ni,Mg,Fe^{2+})_2Al(Si,Al)O_5(OH)_4$, *Serpentine–Kaolin Group*

Brunsvigite = **Chamosite**

C

Cardenite = ferrian **Saponite**

Carlosturanite $(Mg,Fe^{2+},Ti)_{21}(Si,Al)_{12}O_{28}(OH)_{34}$, *Modulated Layer Silicate Group*

Caryopilite $(\text{Mn}^{2+}, \text{Mg})_3\text{Si}_2\text{O}_5(\text{OH})_4$, *Modulated Layer Silicate Group*

Celadonite $\text{K}(\text{Mg}, \text{Fe}^{2+})_3(\text{Fe}^{3+}, \text{Al})\text{Si}_4\text{O}_{10}(\text{OH})_2$, *True Mica Group*

Cerolite = (a) talc; (b) mixture of *serpentine* and **Stevensite**

Chamosite $(\text{Fe}^{2+}, \text{Mg}, \text{Fe}^{3+}, \text{Al})_5\text{Al}(\text{Si}_3\text{Al})\text{O}_{10}(\text{OH}, \text{O})_8$, *Chlorite Group*
Chamosite-7Å

Chernykhite $(\text{Ba}, \text{Na})(\text{V}^{3+}, \text{Al})_2(\text{Si}, \text{Al})_4\text{O}_{10}(\text{OH})_2$, *True Mica Group*

Chlorite A mineral group, with general structural formula, $(\text{Mg}, \text{Fe}^{2+}, \text{Fe}^{3+}, \text{Li}, \text{Al}, \text{Mn}, \text{Ni}, \text{Zn})_{4-6}(\text{Si}, \text{Al}, \text{B}, \text{Fe}^{3+})_4\text{O}_{10}(\text{OH}, \text{O})_8$

Chlorite-mica See Mica-chlorite

Chlorite-smectite Interlayering of chlorite and smectite minerals with various mixing ratio and layer-stacking sequence of the two components, *Interstratified Layer Silicate Group*

Chlorite-talc See Talc-chlorite

Chlorite-vermiculite Interlayering of chlorite and vermiculite minerals with various mixing ratio and layer-stacking sequence of the two components, *Interstratified Layer Silicate Group*

Chloropal = **Nontronite**

Chrysocolla $(\text{Cu}^{2+}, \text{Al})_2\text{H}_2\text{Si}_2\text{O}_5(\text{OH})_4 \cdot n\text{H}_2\text{O}$, *Serpentine-Kaolin Group*

Chrysolite $\text{Mg}_3\text{Si}_2\text{O}_5(\text{OH})_4$, *Serpentine-Kaolin Group*

Chrysolite-1 M_{cl}

Chrysolite-2 M_{cl}

Chrysolite-2 Or_{cl}

Clinochlore $(\text{Mg}, \text{Fe}^{2+})_5\text{Al}(\text{Si}_3\text{Al})\text{O}_{10}(\text{OH}, \text{O})_8$, forms a series with Chamosite, *Chlorite Group*

Clinochrysotile = **Chrysolite-1 M_{cl}**

Clintonite $\text{Ca}(\text{Mg}, \text{Al})_3(\text{Al}_3\text{Si})\text{O}_{10}(\text{OH})_2$, *Brittle Mica Group*

Clintonite-1 M

Clintonite-2 M

Cookeite $\text{Li}, \text{Al}_4(\text{Si}_3\text{Al})\text{O}_{10}(\text{OH})_8$, *Chlorite Group*

Corrensite 1:1 Regular interlayering of trioctahedral chlorite-smectite or vermiculite-group mineral, with approximate structural formula $(\text{Mg}, \text{Fe}, \text{Al})_9(\text{Si}, \text{Al})_8\text{O}_{20}(\text{OH}, \text{O})_{10} \cdot n\text{H}_2\text{O}$, *Interstratified Layer Silicate Group*

Corundphilite = ferroan **Clinochlore**

Cronstedtite $\text{Fe}_3^{2+}\text{Fe}^{3+}(\text{Si}, \text{Fe}^{3+})_2\text{O}_5(\text{OH})_4$, *Serpentine-Kaolin Group*

Cronstedtite-1 H

D

Daphnite = manganoan **Chamosite**

Delessite = magnesian **Chamosite** or ferrous **Clinochlore**

Deweylite = mixture of **Chrysotile** or **Lizardite** and **Stevensite**

Diabantite = ferroan **Clinochlore**, **Chamosite**

Dickite $\text{Al}_2\text{Si}_2\text{O}_5(\text{OH})_4$, polymorphic relationship with kaolinite and nacrite,

Donbassite $\text{Al}_{4-5}(\text{Si}_3\text{Al})\text{O}_{10}(\text{OH})_8$, *Chlorite Group*

E

Eastonite = (a) **Biotite**, (b) **Vermiculite**, (c) **Phlogopite**

Endellite = (a) Hydrated halloysite, (b) **Halloysite**

Ephesite $\text{NaLiAl}_2(\text{Al}_2\text{Si}_2)\text{O}_{10}(\text{OH})_2$, *Brittle Mica Group*

F

Falcondoite $(\text{Ni}, \text{Mg})_4\text{Si}_6\text{O}_{15}(\text{OH})_2 \cdot 6\text{H}_2\text{O}$, a nickeloan variety of **Sepiolite**, *Sepiolite-Palygorskite Group*

Ferriannite (Ferri-annite) $\text{K}(\text{Fe}^{2+}, \text{Mg})_3(\text{Fe}^{3+}, \text{Al})\text{Si}_3\text{O}_{10}(\text{OH}, \text{F})_2$, *True Mica Group*

Ferriphlogopite = ferrian **Phlogopite**

Ferripyrophyllite $\text{Fe}_2^{3+}\text{Si}_4\text{O}_{10}(\text{OH})_2$, compare **Pyrophyllite**

Fraipontite $(\text{Zn}, \text{Al})_3(\text{Si}, \text{Al})_2\text{O}_5(\text{OH})_4$, *Serpentine-Kaolin Group*

G

Ganophyllite $(\text{K}, \text{Na})_2(\text{Mn}, \text{Al}, \text{Mg})_8(\text{Si}, \text{Al})_{12}\text{O}_{29}(\text{OH})_7 \cdot 8-9\text{H}_2\text{O}$, *Modulated Layer Silicate Group*

Garnierites = general term for hydrous nickel silicates, mainly **Népouite**, **Falcondoite**

Ghassoulite = **Hectorite**

Glaucosite $(\text{K}, \text{Na})(\text{Fe}^{3+}, \text{Al}, \text{Mg})_2(\text{Si}, \text{Al})_4\text{O}_{10}(\text{OH})_2$, *True Mica Group*

Gonyerite $(\text{Mn}^{2+}, \text{Mg})_5\text{Fe}^{3+}(\text{Si}_3\text{Fe}^{3+})\text{O}_{10}(\text{OH})_8$, *Modulated Layer Silicate Group*

Greenalite $(\text{Fe}^{2+}, \text{Fe}^{3+})_{2-3}\text{Si}_2\text{O}_5(\text{OH})_4$, *Modulated Layer Silicate Group*

Griffithite = ferroan **Saponite**

Grovesite = **Pennantite**

H

Halloysite $\text{Al}_2\text{Si}_2\text{O}_5(\text{OH})_4$, *Serpentine-Kaolin Group*

Halloysite-7 Å $\text{Al}_2\text{Si}_2\text{O}_5(\text{OH})_4$

Halloysite-10 Å $\text{Al}_2\text{Si}_2\text{O}_5(\text{OH})_4 \cdot 2\text{H}_2\text{O}$

Halloysite—hydrated halloysite Interlayering of halloysite-7 Å and halloysite-10 Å, with various mixing ratio and stacking sequence of the two components, *Interstratified Layer Silicate Group*

Hectorite $\text{Na}_{0.3}(\text{Mg}, \text{Li})_3\text{Si}_4\text{O}_{10}(\text{F}, \text{OH})_2$, *Smectite Group*

Hendricksite $\text{K}(\text{Zn}, \text{Mg}, \text{Mn}^{2+})_3(\text{Si}_3\text{Al})\text{O}_{10}(\text{OH})_2$, *True Mica Group*

Hydrated halloysite = Halloysite-10 Å

Hydrobiotite 1:1 Regular interlayering of biotite and vermiculite, *Interstratified Layer Silicate Group*

Hydromicas K-poor and H_2O -rich **Muscovite** (illite); altered **Muscovite**

Hydromuscovite = Hydromicas

I

Illite $(\text{K}, \text{H}_3\text{O})(\text{Al}, \text{Mg}, \text{Fe})_2(\text{Si}, \text{Al})_4\text{O}_{10}[(\text{OH})_2, \text{H}_2\text{O}]$, *True Mica Group*

Illite-chlorite Compare Mica-chlorite, *Interstratified Layer Silicate Group*

Illite-smectite Compare Mica-smectite, *Interstratified Layer Silicate Group*

Illite-vermiculite Compare Mica-vermiculite, *Interstratified Layer Silicate Group*

K

Kämmererite = chromian **Clinochlore**

Kaolin A general term for kaolin minerals, with Serpentine forms *Serpentine-Kaolin Group*

Kaolin-smectite Interlayering of kaolin and smectite minerals with various mixing ratio and various stacking sequence of the two components, *Interstratified Layer Silicate Group*

Kaolinite $\text{Al}_2\text{Si}_2\text{O}_5(\text{OH})_4$, *Serpentine-Kaolin Group*

Kellyite $(\text{Mn}^{2+}, \text{Mg}, \text{Al})_3(\text{Si}, \text{Al})_2\text{O}_5(\text{OH})_4$, *Serpentine-Kaolin Group*

Kerolite (a) Mixture of serpentine and stevensite; (b) talc

Kinoshitalite $(\text{Ba}, \text{K})(\text{Mg}, \text{Mn}, \text{Al})_3(\text{Si}, \text{Al})_4\text{O}_{10}(\text{OH}, \text{F})_2$, *Brittle Mica Group*

Kotschubeite = ferroan **Clinochlore**

Kulkeite $(\text{Na}_{0.4}\text{Mg}_8\text{Al}(\text{Al}, \text{Si}_7)\text{O}_{20}(\text{OH})_{10})$, a 1:1 interlayering of talc and trioctahedral chlorite, *Interstratified Layer Silicate Group*

L

Lepidolite $\text{K}(\text{Li}, \text{Al})_3(\text{Si}, \text{Al})_4\text{O}_{10}(\text{F}, \text{OH})_2$, *True Mica Group*

Lepidolite-1M

Lepidolite-2M₁

Lepidolite-2M₂

Lepidolite-3T

Leptochlorite = iron-rich *Chlorite*, mainly **Chamosite**

Leuchtenbergite = iron-deficient **Clinochlore**

Lizardite $\text{Mg}_3\text{Si}_2\text{O}_5(\text{OH})_4$, *Serpentine-Kaolin Group*

Lizardite-1T

Lizardite-2H

Lizardite-6T

M

Manganopyrosmalite *Modulated Layer Silicate Group*

Margarite $\text{CaAl}_2(\text{Al}_2\text{Si}_2)_4\text{O}_{10}(\text{OH})_2$, *Brittle Mica Group*

Margarite-2M

Masutomilite $\text{K}(\text{Li}, \text{Al}, \text{Mn}^{2+})_3(\text{Si}, \text{Al})_4\text{O}_{10}(\text{F}, \text{OH})_2$, *True Mica Group*

Medomontite = mixture of **Chrysocolla** and mica or hydromica

Metahalloysite = Halloysite-7 Å, dehydrated halloysite

Mica A mineral group, with general structural formula, $(\text{Ba}, \text{Ca}, \text{Cs}, \text{H}_3\text{O}^+, \text{K}, \text{Na}, \text{NH}_4)(\text{Al}, \text{Cr}, \text{Fe}^{2+}, \text{Fe}^{3+}, \text{Li}, \text{Mg}, \text{Mn}^{2+}, \text{Mn}^{3+}, \text{V}, \text{Zn})_{2-3}(\text{Al}, \text{Be}, \text{Fe}^{3+}, \text{Si})_4\text{O}_{10}(\text{OH}, \text{F})_2$

Mica-chlorite Interlayering mica and chlorite minerals with various mixing ratio and layer-stacking sequence of the two components, *Interstratified Layer Silicate Group*

Mica-smectite Interlayering of mica and smectite minerals with various mixing ratio and layer-stacking sequence of the two components, *Interstratified Layer Silicate Group*

Mica-vermiculite Interlayering of mica and vermiculite minerals with various mixing ratio and layer-stacking sequence of the two components, *Interstratified Layer Silicate Group*

Minnesotaite $(\text{Fe}^{2+}, \text{Mg})_3\text{Si}_4\text{O}_{10}(\text{OH})_2$, *Modulated Layer Silicate Group*

Montdorite = aluminum-deficient **Biotite**

Montmorillonite $(\text{Na}, \text{Ca})_{0.3}(\text{Al}, \text{Mg})_2\text{Si}_4\text{O}_{10}(\text{OH})_2 \cdot n\text{H}_2\text{O}$, *Smectite Group*

Muscovite $\text{KAl}_2(\text{Si}_3\text{Al})\text{O}_{10}(\text{OH}, \text{F})_2$, *True Mica Group*

Muscovite-1M

Muscovite-2M₁

Muscovite-2M₂

Muscovite-3T

N

Nacrite $\text{Al}_2\text{Si}_2\text{O}_5(\text{OH})_4$ polymorphic relationship with **Dickite**, **Halloysite**, and **Kaolinite**, *Serpentine-Kaolin Group*

Nanpiningite $\text{Cs}(\text{Al}, \text{Mg}, \text{Fe}^{2+}, \text{Li})_2(\text{Si}_3\text{Al})\text{O}_{10}(\text{OH}, \text{F})_2$, *True Mica Group*

Népouite $\text{Ni}_3\text{Si}_2\text{O}_5(\text{OH})_4$, *Serpentine-Kaolin Group*

Nimite $(\text{Ni}, \text{Mg}, \text{Fe}^{2+})_5\text{Al}(\text{Si}_3\text{Al})\text{O}_{10}(\text{OH})_8$, *Chlorite Group*

Nontronite $\text{Na}_{0.3}\text{Fe}_2^{3+}(\text{Si}, \text{Al})_4\text{O}_{10}(\text{OH})_2 \cdot n\text{H}_2\text{O}$, *Smectite Group*

Norrishite $\text{KLiMn}_2^{3+}\text{Si}_4\text{O}_{12}$, *True Mica Group*

O

Odinite $(\text{Fe}^{3+}, \text{Mg}, \text{Al}, \text{Fe}^{2+})_{2.5}(\text{Si}, \text{Al})_2\text{O}_5(\text{OH})_4$, *Serpentine-Kaolin Group*

Odinite-1M

P

Palygorskite $(\text{Mg}, \text{Al})_2\text{Si}_4\text{O}_{10}(\text{OH})_4 \cdot 4\text{H}_2\text{O}$, *Sepiolite-Palygorskite Group*

Paragonite $\text{NaAl}_2(\text{Si}_3\text{Al})\text{O}_{10}(\text{OH})_2$, *True Mica Group*

Parsettensite $(\text{K}, \text{Na}, \text{Ca})(\text{Mn}, \text{Al})_7\text{Si}_8\text{O}_{20}(\text{OH})_8 \cdot 2\text{H}_2\text{O}$, *Modulated Layer Silicate Group*

Pecoraite $\text{Ni}_3\text{Si}_2\text{O}_5(\text{OH})_4$, dimorphic relationship with népouite, *Serpentine-Kaolin Group*

Pennantite $\text{Mn}_5^{2+}\text{Al}(\text{Si}_3\text{Al})\text{O}_{10}(\text{OH})_8$, *Chlorite Group*

Penninite = **Clinochlore**

Phengite $\text{KAl}_{1.5}(\text{Mg}, \text{Fe}^{2+})_{0.5}(\text{Si}_{3.5}\text{Al}_{0.5})\text{O}_{10}(\text{OH}, \text{F})_2$, *True Mica Group*

Phlogopite $\text{K}(\text{Mg}, \text{Fe}^{2+})_3\text{Si}_3\text{AlO}_{10}(\text{F}, \text{OH})_2$, *True Mica Group*

Polythionite $\text{KLi}_2\text{AlSi}_4\text{AlO}_{10}(\text{F}, \text{OH})_2$, *True Mica Group*

Preiswerkite $\text{Na}(\text{Mg}_2\text{Al})(\text{Si}_2\text{Al}_2)\text{O}_{10}(\text{OH})_2$, *True Mica Group*

Prochlorite = ferroan **Clinochlore**

Pseudophite = **Clinochlore**

Pyrophyllite $\text{Al}_2\text{Si}_4\text{O}_{10}(\text{OH})_2$, *Talc-Pyrophyllite Group*

Pyrophyllite-2M

Pyrophyllite-smectite Interlayering of pyrophyllite and smectite minerals with various mixing ratio and layer-stacking sequence of the two components, *Interstratified Layer Silicate Group*

R

Rectorite $(\text{Na}, \text{Ca})\text{Al}_4(\text{Si}, \text{Al})_8\text{O}_{20}(\text{OH})_4 \cdot 2\text{H}_2\text{O}$, a 1:1 interlayering of dioctahedral mica and dioctahedral smectite and rectorite may further be distinguished into the following:

Ca-Rectorite = the mica-like layer whose composition is similar to that of margarite

Na-Rectorite = rectorite in which its nonexpandable layer is similar to paragonite

K-Rectorite = the mica-like layer whose composition is similar to that of muscovite

Ripidolite = ferroan **Clinochlore**, magnesian **Chamosite**

Roscoelite $\text{K}(\text{V}^{3+}, \text{Al}, \text{Mg})_2(\text{Si}, \text{Al})_4\text{O}_{10}(\text{OH})_2$, *True Mica Group*

S

Saponite $(\text{Ca}, \text{Na})_{0.3}(\text{Mg}, \text{Fe}^{2+})_3(\text{Si}, \text{Al})_4\text{O}_{10}(\text{OH})_2 \cdot 4\text{H}_2\text{O}$, *Smectite Group*

Iron saponite = saponite with $\text{Fe} > \text{Mg}$ in its octahedral sheet

Sauconite $\text{Na}_{0.3}\text{Zn}_3(\text{Si}, \text{Al})_4\text{O}_{10}(\text{OH})_2 \cdot 4\text{H}_2\text{O}$, *Smectite Group*

Sepiolite $\text{Mg}_4\text{Si}_6\text{O}_{15}(\text{OH})_2 \cdot 6\text{H}_2\text{O}$, *Sepiolite–Palygorskite Group*

Septechlorite = amesite, antigorite, berthierine, chrysotile, cronstedtite, lizardite, etc., trioctahedral kaolinite–serpentine minerals

Sericite = (a) **Muscovite (illite)**; (b) fine-grained mica-like minerals

Serpentine = a group name for minerals with the general formula, $(\text{Mg}, \text{Fe}, \text{Ni})_3\text{Si}_2\text{O}_5(\text{OH})_4$

Seybertite = **Clintonite**

Sheridanite = aluminum **Clinochlore**, ferroan **Clinochlore**

Shirozulite $\text{KMn}_3^{2+}(\text{Si}, \text{Al})_4\text{O}_{10}(\text{OH})_2$, *True Mica Group*

Siderophyllite $\text{KFe}_2^{2+}\text{Al}(\text{Al}_2\text{Si}_2)_4\text{O}_{10}(\text{F}, \text{OH})_2$, *True Mica Group*

Smectite represent the smectite-group minerals, with general formula $X_{0.3}Y_{2-3}Z_4\text{O}_{10}(\text{OH})_2 \cdot n\text{H}_2\text{O}$ where $X = \text{Ca}, \text{Li}, \text{Na}$; $Y = \text{Al}, \text{Cr}, \text{Cu}, \text{Fe}^{2+}, \text{Fe}^{3+}, \text{Li}, \text{Mg}, \text{Ni}, \text{Zn}$; $Z = \text{Al}, \text{Si}$, *Smectite Group*

Smectite–chlorite See Chlorite–smectite

Smectite–illite Compare Mica–smectite

Smectite–kaolin See Kaolin–smectite

Smectite–mica See Mica–smectite

Smectite–pyrophyllite See Pyrophyllite–smectite

Smectite–talc See Talc–smectite

Smectite–vermiculite See Vermiculite–smectite

Stevensite $\text{Ca}_{0.15}\text{Mg}_3\text{Si}_4\text{O}_{10}(\text{OH})_2$, *Smectite Group*

Stilpnomelane $\text{K}(\text{Fe}^{2+}, \text{Mg}, \text{Fe}^{3+})_8(\text{Si}, \text{Al})_{12}\text{O}_{10}(\text{O}, \text{OH})_{27}$, *Modulated Layer Silicate Group*

Sudoite $\text{Mg}_2(\text{Al}, \text{Fe}^{3+})_3\text{Si}_3\text{AlO}_{10}(\text{OH})_8$, *Chlorite Group*

Swinefordite $(\text{Ca}, \text{Na})_{0.3}(\text{Li}, \text{Mg})_2(\text{Si}, \text{Al})_4\text{O}_{10}(\text{OH}, \text{F})_2 \cdot 2\text{H}_2\text{O}$, *Smectite Group*

T

Taeniolite $\text{K}(\text{LiMg}_2)\text{Si}_4\text{O}_{10}(\text{F}, \text{OH})_2$

Talc $\text{Mg}_3\text{Si}_4\text{O}_{10}(\text{OH})_2$, *Talc–Pyrophyllite Group*

Talc–chlorite Interlayering of talc and chlorite minerals with various mixing ratio and layer-stacking sequence of the two components, *Interstratified Layer Silicate Group*

Talc–saponite Compare Talc–smectite

Talc–smectite Interlayering of talc and smectite minerals with various mixing ratio and layer-stacking sequence of the two components, *Interstratified Layer Silicate Group*

Tarasovite A regular interstratified mineral of illite (I) and smectite (S) with nearly IIS sequence. The ratio = 0.75:0.25, *Interstratified Layer Silicate Group*

Thuringite = ferrian **Chamosite**

Tobelite $(\text{NH}_4, \text{K})\text{Al}_2(\text{Si}_3\text{Al})\text{O}_{10}(\text{OH})_2$, *True Mica Group*

Tosudite A 1:1 interlayering of chlorite and a smectite-group phase, with composition, $\text{Na}_{0.5}(\text{Al}, \text{Mg})_6(\text{Si}, \text{Al})_8\text{O}_{18}(\text{OH}, \text{F})_{12} \cdot 5\text{H}_2\text{O}$, *Interstratified Layer Silicate Group*

Trilithionite $\text{K}(\text{Li}_{1.5}\text{Al}_{1.5})(\text{Si}_3\text{Al})_4\text{O}_{10}(\text{F}, \text{OH})_2$, *True Mica Group*

V

Vermiculite A majority of this mineral are trioctahedral and with a sample composition, $(\text{Mg}, \text{Ca})_{0.3}(\text{Mg}_{2.5}\text{Fe}_{0.5})(\text{Al}_{1.2}\text{Si}_{2.8})\text{O}_{10}(\text{OH})_2 \cdot 4\text{H}_2\text{O}$, *Vermiculite Group*

Vermiculite A group name for minerals with the general formula, $(\text{Mg}, \text{Ca})_{0.35}(\text{Mg}, \text{Fe}, \text{Al})_3(\text{Al}, \text{Si})_4\text{O}_{10}(\text{OH})_2 \cdot 4\text{H}_2\text{O}$

Vermiculite–mica See Mica–vermiculite

Vermiculite–chlorite See Chlorite–vermiculite

Vermiculite–smectite Interlayering of vermiculite and smectite minerals with various mixing ratio and layer-stacking sequence of the two components, *Interstratified Layer Silicate Group*

Volkonskoite $\text{Ca}_{0.3}(\text{Cr}^{3+}, \text{Mg})_2(\text{Si}, \text{Al})_4\text{O}_{10}(\text{OH})_2 \cdot 4\text{H}_2\text{O}$, *Smectite Group*

W

Wonesite $(\text{Na}, \text{K})(\text{Mg}, \text{Fe}, \text{Al})_6(\text{Si}, \text{Al})_8\text{O}_{20}(\text{OH}, \text{F})_4$, *True Mica Group*

X

Xanthophyllite = **Clintonite**

Z

Zinnwaldite $\text{KLiFe}^{2+}\text{Al}(\text{AlSi}_3)\text{O}_{10}(\text{F}, \text{OH})_2$, *True Mica Group*

Zussmanite $\text{K}(\text{Fe}^{2+}, \text{Mg}, \text{Mn}^{2+})_{13}(\text{Si}, \text{Al})_{18}\text{O}_{42}(\text{OH})_{14}$, *Modulated Layer Silicate Group*

References

- Alexander, L., and H.P. Klug. 1948. Basic aspects of X-ray absorption in quantitative diffraction analysis of powder mixtures. *Anal. Chem.* 20:886–889.
- Anthony, J.W., R.A. Bideaux, K.W. Bladh, and M.C. Nichols. 1995. *Handbook of mineralogy. Vol. II. Silica, silicates. Parts I and II.* Mineral Data Publishing, Tucson, AZ.
- April, R., and D. Keller. 1990. Mineralogy of the rhizosphere in forest soils of the eastern United States. *Mineralogical studies of the rhizosphere. Biogeochemistry* 9:1–18.
- Bailey, S.W. 1969. Polytypism of trioctahedral 1:1 layer silicates. *Clays Clay Miner.* 17:355–371.
- Bailey, S.W. 1972. Determination of chlorite compositions by X-ray spacings and intensities. *Clays Clay Miner.* 20:381–388.
- Bailey, S.W. (ed.). 1984. *Micas: Reviews in mineralogy. Vol. 13.* Mineralogical Society of America, Chelsea, MI.
- Bailey, S.W. (ed.). 1988. *Hydrous phyllosilicates (exclusive of micas). Reviews in mineralogy. Vol. 19.* Mineralogical Society of America, Chelsea, MI.
- Bailey, S.W., G.W. Brindley, D.S. Fanning, H. Kodama, and R.T. Martin. 1984. Report of the CMS Nomenclature Committee for 1982 and 1983. *Clays Clay Miner.* 32:239.
- Bailey, S.W., G.W. Brindley, H. Kodama, and R.T. Martin. 1982. Nomenclature for regular interstratifications. Report of the CMS Nomenclature Committee for 1980–1981. *Clays Clay Miner.* 30:76–78.

- Ball, D.F., and P. Beaumont. 1972. Vertical distribution of extractable iron and aluminum in soil profiles from a brown earth-peaty podzol association. *J. Soil Sci.* 23:298–308.
- Banfield, J.F., and K.H. Nealson (eds.). 1997. *Geomicrobiology: Interactions between microbes and minerals. Reviews in mineralogy.* Vol. 35. Mineralogical Society of America, Washington, DC.
- Barnhisel, R.I., and P.M. Bertsch. 1989. Chlorites and hydroxyl-interlayered vermiculite and smectite, p. 729–788. *In* J.B. Dixon and S.B. Weed (eds.) *Minerals in soil environments.* 2nd edn. SSSA Book Series No. 1. SSSA, Madison, WI.
- Basset, W.A. 1960. Role of hydroxyl orientation in mica alteration. *Bull. Geol. Soc. Am.* 71:449–456.
- Bear, F.E. (ed.). 1964. *Chemistry of the soil.* 2nd edn. Reinhold Publishing Corporation, New York.
- Biermans, V., and L. Baert. 1977. Selective extraction of the amorphous Al, Fe and Si oxides using an alkaline tiron solution. *Clay Miner.* 12:127–135.
- Blackburn, W.H., and W.H. Dennen. 1997. *Encyclopedia of mineral names.* The Canadian Mineralogist Special Publication 1. Mineralogical Association of Canada.
- Bloss, F.D. 1971. *Crystallography and crystal chemistry.* Holt, Rinehart and Winston, Inc., New York.
- Bradley, W.F. 1945. Diagnostic criteria for clay minerals. *Am. Mineral.* 30:704–713.
- Bradley, W.F. 1953. Analysis of mixed-layer clay minerals. *Anal. Chem.* 25:727–730.
- Bradley, W.F., and R.E. Grim. 1948. Colloid properties of layer silicates. *J. Phys. Chem.* 52:1404–1413.
- Bragg, W.L. 1950. *Atomic structure of minerals* (2nd print). Cornell University Press, New York.
- Brindley, G.W. (ed.). 1951. *The X-ray identification and crystal structures of clay minerals.* The Mineralogical Society (Clay Minerals Group), London, U.K.
- Brindley, G.W. 1961. Quantitative analysis of clay mixtures, p. 489–516. *In* G. Brown (ed.) *The X-ray identification and crystal structures of clay minerals.* Mineralogical Society, London, U.K.
- Brindley, G.W., and G. Brown (eds.). 1980. *Crystal structures of clay minerals and their X-ray identification.* Mineralogical Society, London, U.K.
- Brindley, G.W., and S.S. Kurtossy. 1961. Quantitative determination of kaolinite by X-ray diffraction. *Am. Mineral.* 46:1205–1215.
- Brindley, G.W., and S. Udagawa. 1960. High temperature reactions of clay minerals mixtures and their ceramic properties. *I. J. Am. Ceram. Soc.* 43:59–65.
- Brown, G. 1953. Dioctahedral analogue of vermiculite. *Clay Miner. Bull.* 2:64–69.
- Brown, G. (ed.). 1961. *The X-ray identification and crystal structures of clay minerals.* Mineralogical Society, London, U.K.
- Brunauer, S., P.H. Emmett, and E. Teller. 1938. Adsorption of gases in multi-molecular layers. *J. Am. Chem. Soc.* 60:309–319.
- Burst, J.F. 1969. Diagenesis of Gulf coast clayey sediments and its possible relationship to petroleum migration. *AAPG Bull.* 53:73–93.
- Camazano, M.S., and S.G. Garcia. 1966. Complejos interlaminares de caolinita y hallosita con líquidos polares. *An. Edafol. Agrobiol.* 25:9–25.
- Carter, M.R. (ed.). 1993. *Soil sampling and methods of analysis.* Canadian Society of Soil Science, Lewis Publishers, Boca Raton, FL.
- Carter, D.L., M.D. Heilman, and C.L. Gonzalez. 1965. Ethylene glycol monoethyl ether for determination surface area of silicate minerals. *Soil Sci.* 100:356–360.
- Chao, T.T., and L. Zhou. 1983. Extraction techniques for selective dissolution of amorphous iron oxides from soils and sediments. *Soil Sci. Soc. Am. J.* 47:225–232.
- Chester, R., and M.J. Hughes. 1967. A chemical technique for the separation of ferro-manganese minerals, carbonate minerals and adsorbed trace elements from pelagic sediments. *Chem. Geol.* 2:249–262.
- Coe, J.M.D. 1988. Magnetic properties of iron in soil iron oxides and clay minerals, p. 397–466. *In* J.W. Stucki, B.A. Goodman, and U. Schwertmann (eds.) *Iron in soils and clay minerals.* D. Reidel, Dordrecht, the Netherlands.
- Cole, W.F., and C.J. Lancucki. 1966. Tabular data of layer structure factors for clay minerals. *Acta Crystallogr.* 21:836–838.
- De Kimpe, C.R., N. Miles, H. Kodama, and J. Dejou. 1987. Alteration of phlogopite to corrensite at Sharbot Lake, Ontario. *Clays Clay Miner.* 35:150–158.
- Deb, B.C. 1950. The estimation of free iron oxides in soils and clays and their removal. *J. Soil Sci.* 1:212–220.
- Deer, W.A., R.A. Howie, and J. Zussman. 1962. *Rock-forming minerals.* Vol. 3. Sheet silicates. John Wiley & Sons, New York.
- Dell, C.I. 1973. A quantitative mineralogical examination of the clay-size fraction of Lake Superior sediments, p. 413–420. *Proc. 16th Conf. Great Lakes Res, International Association of Great Lake Research.*
- Diamond, S., and E.B. Kinter. 1958. Surface areas of clay minerals as derived from measurements of glycerol retention. *Clays Clay Miner.* 5:334–347.
- Dixon, J.M., and S.B. Weed (eds.). 1989. *Minerals in soil environments.* 2nd edn. SSSA Book Series No. 1. SSSA, Madison, WI.
- Duchaufour, P., and B. Souchier. 1966. Note sur une méthode d'extraction combinée de l'aluminium et fer libre dans sols. *Sci. Sol.* 1:17–29.
- Dunoyer de Segonzac, G. 1970. The transformation of clay minerals during diagenesis and low-grade metamorphism: A review. *Sedimentology* 15:281–346.
- Eltantawy, I.M., and P.W. Arnold. 1973. Reappraisal of ethylene glycol mono-ether (EGME) method for surface area estimations of clays. *J. Soil Sci.* 24:232–238.
- Fanning, D.S., V.Z. Keramidas, and M.A. El-Desoky. 1989. Micas, p. 551–634. *In* J.M. Dixon and S.B. Weed (eds.) *Minerals in soil environments.* SSSA, Madison, WI.
- Farmer, V.C. (ed.). 1974. *The infrared spectra of minerals.* Monograph No. 4. Mineralogical Society, London, U.K.

- Fleet, M.E. 2003. Sheet silicates: Micas. *In* W.A. Deer, R.A. Howie, and J. Zussman (eds.) *Rock-forming minerals*. 2nd edn. The Geological Society, London, U.K.
- Follett, E.A.C., W.J. McHardy, B.D. Michell, and B.F.L. Smith. 1965. Chemical dissolution techniques in the study of soil clays: Part I. *Clay Miner.* 6:23–34.
- Foster, M.D. 1953. Geochemical study of clay minerals. III. The determination of free silica and free alumina in montmorillonites. *Geochim. Cosmochim. Acta* 3:143–154.
- Gard, J.A. (ed.). 1971. *The electron-optical investigation of clays*. Monograph No. 3. Mineralogical Society, London, U.K.
- Gatineau, L. 1964. Structure réelle de la muscovite: Repartition des substitution isomorphes. *Bull. Soc. Fr. Miner. Crystallogr.* 87:321–355.
- Ghabru, S.K., A.R. Mermut, and R.J. St. Arnaud. 1989. Layer-charge and cation-exchange characteristics of vermiculite (weathered biotite) isolated from gray luvisols in northeastern Saskatchewan. *Clays Clay Miner.* 37:164–172.
- Glaeser, R. 1958. Détection de la démixion des cations Na, Ca dans une hectorite bi-Ioniques. *C.R. Acad. Sci., Paris.* 246:2909–2912.
- Glaeser, R., and J. Méring. 1954. Isothermes d'hydratation des montmorillonites bi-ioniques (Na, Ca). *Clay Miner. Bull.* 2:188–193.
- Graf von Reichenbach, H., and C.I. Rich. 1975. Fine-grained micas in soils, p. 59–95. *In* J.E. Gieseking (ed.) *Soil components*. Springer-Verlag, Berlin, Germany.
- Greene-Kelly, R. 1953. The identification of montmorillonoids in clays. *J. Soil Sci.* 4:233–237.
- Greene-Kelly, R. 1955. Sorption of aromatic organic compounds by montmorillonite. *Trans. Faraday Soc.* 51:425–430.
- Greenland, D.J., and M.H.B. Hayes (eds.) 1978. *The chemistry of soil constituents*. John Wiley & Sons, New York.
- Grim, R.E. 1968. *Clay mineralogy*. McGraw-Hill Book Co. Inc., New York.
- Grim, R.E., and H. Kodama. 1997. Clay minerals, p. 207–215. *In* *Minerals and rocks*. Encyclopaedia Britannica. Vol. 24.
- Guggenheim, S., and S.W. Bailey. 1982. The superlattice of minnesotaite. *Can. Mineral.* 20:579–584.
- Guggenheim, S., S.W. Bailey, R.A. Eggleton, and P. Wilkes. 1982. Structural aspects of greenalite and related minerals. *Can. Mineral.* 20:1–18.
- Guggenheim, S., and R.A. Eggleton. 1988. Crystal chemistry, classification, and identification of modulated layer silicates, p. 675–725. *In* S.W. Bailey (ed.) *Hydrous phyllosilicates (exclusive of micas)*. Reviews in mineralogy. Vol. 19. Mineralogical Society of America, Chelsea, MI.
- Hang, P.T., and G.W. Brindley. 1970. Methylene blue absorption by clay minerals. Determination of surface areas and cation exchange capacities (clay-organic study XVIII). *Clays Clay Miner.* 18:203–212.
- Hashimoto, I., and M.L. Jackson. 1960. Rapid dissolution of allophane and kaolinite-halloysite after dehydration. *Clays Clay Miner.* 7:102–113.
- Herrero, C.P., J. Sanz, and J.M. Serratosa. 1985. Si, Al distribution in micas: Analysis by high-resolution ^{29}Si NMR spectroscopy. *J. Phys. C: Solid State Phys.* 53:151–154.
- Higashi, S. 1982. Tobelite, a new ammonium dioctahedral mica. *Mineral. J.* 11:138–146.
- Hinsinger, P., and B. Jaillard. 1993. Root-induced release of inter-layer potassium and vermiculization of phlogopite as related potassium depletion in the rhizosphere of ryegrass. *J. Soil Sci.* 44:525–534.
- Hinsinger, P., B. Jaillard, and J.E. Dufey. 1992. Rapid weathering of a trioctahedral mica by the roots of ryegrass. *Soil Sci. Soc. Am. J.* 56:977–982.
- Hofmann, U., and R. Klemen. 1950. Verlust der Austauschfähigkeit von Lithiumionen An Bentonit durch Erhizung. *Z. Anorg. Allg. Chem.* 262:95–99.
- Huang, P.M., and M. Schnitzer (eds.). 1986. *Interactions of soil minerals with natural organics and microbes*. SSSA Special Publication No. 17. SSSA, Madison, WI.
- Jackson, M.L. 1967. *Soil chemical analysis*. Prentice-Hall, Inc., Englewood Cliffs, NJ.
- Jeffries, C.D. 1946. A rapid method for removal of free iron oxides in soils prior to petrographic analysis. *Soil Sci. Soc. Am. Proc.* 11:211–212.
- Johns, W.D., R.E. Grim., and W.F. Bradley. 1954. Quantitative estimations of clay minerals by diffraction methods. *J. Sediment. Petrol.* 24:242–251.
- Kakinoki, J., and Y. Komura. 1952. Intensity of X-ray diffraction by an one-dimensionally disordered crystal. (1) General derivation in cases of the “Reichweite” $s = 0$ and 1. *J. Phys. Soc. Jpn.* 7:30–35.
- Kakinoki, J., and Y. Komura. 1954. Intensity of X-ray diffraction by an one-dimensionally disordered crystal. II: General derivation in the case of the correlation range $s \geq 2$. *J. Phys. Soc. Jpn.* 9:169–183.
- Keller, W.D., and A.F. Frederickson. 1952. Role of plants and colloidal acids in the mechanism of weathering. *Am. J. Sci.* 250:594–608.
- Kittrick, J.A. (ed.). 1985. *Mineral classification of soils*. SSSA Special Publication No. 16. SSSA, Madison, WI.
- Klein, C., and C.S. Hurlbut, Jr., 1985. *Manual of mineralogy*. John Wiley & Sons, Inc., New York.
- Klug, H.P., and L.E. Alexander. 1954. *X-ray diffraction procedures for polycrystalline and amorphous materials*. John Wiley & Sons, Inc., New York.
- Klute, A. (ed.) 1986. *Methods of soil analysis*. Part I. Physical and mineralogical methods. 2nd edn. SSSA Book Series No. 5. ASA-SSSA, Madison, WI.
- Kodama, H. 1990. Use of color-coded transparencies for visualizing layer silicate structures, p. 169–175. *In* V.C. Farmer and Y. Tardy (eds.) *Proc. 9th Int. Clay Conf.* 1989. Strasbourg, Sci. Géol., Mém. Strasbourg, France.
- Kodama, H., and J.E. Brydon. 1968a. A study of clay minerals in podzol soils in New Brunswick, eastern Canada. *Clay Miner.* 7:295–309.
- Kodama, H., and J.E. Brydon. 1968b. Dehydroxylation of microcrystalline muscovite. *Trans. Faraday Soc.* 64:3112–3119.

- Kodama, H., and R.S. Dean. 1980. Illite from Eldorado, Saskatchewan. *Can. Mineral.* 18:109–118.
- Kodama, H., L. Gatiéneau, and J. Méring. 1971. An analysis of X-ray diffraction line profiles of microcrystalline muscovites. *Clays Clay Miner.* 19:405–413.
- Kodama, H., S. Nelson, A.-F. Yang, and N. Kohyama. 1994. Mineralogy of rhizospheric and non-rhizospheric soils in corn fields. *Clays Clay Miner.* 42:755–763.
- Kodama, H., and G.J. Ross. 1991. Tiron dissolution method to remove and characterize inorganic components in soils. *Soil Sci. Soc. Am. J.* 55:1180–1187.
- Kodama, H., G.C. Scott, and N.M. Miles. 1977. X-ray quantitative analysis of minerals in soils. Soil Research Institute. Tech. Bull. Agriculture Canada, Ottawa, Canada.
- Kubler, B. 1966. La cristallinité de l'illite et les zones tout à fait supérieures du métamorphisme, p. 105–122. *Etages tectoniques Colloque de Neuchâtel 1966*. Institut de Géologie de l'Université de Neuchâtel.
- Kunze, G. 1956. Die gewellte Struktur des Antigorits. I. *Zeit. Krist.* 108:82–107.
- Lagaly, G. 1979. The layer charge of regular interstratified 2:1 clay minerals. *Clays Clay Miner.* 27:1–10.
- Lagaly, G. 1982. Layer charge heterogeneity in vermiculites. *Clays Clay Miner.* 30:215–222.
- Lagaly, G., and A. Weiss. 1969. Determination of the layer charge in mica-type layer silicates, p. 61–80. *Proc. 3rd Int. Clay Conf. Vol. 1*. Tokyo, Japan, September 5–9, 1969.
- Liebau, F. 1985. Structural chemistry of silicates: Structure, bonding, and classification. Springer-Verlag, New York.
- Loewenstein, W. 1954. The distribution of aluminum in the tetrahedral of silicates and aluminates. *Am. Mineral.* 39:92–96.
- MacEwan, D.M.C., A. Ruiz Amil, and G. Brown. 1961. Interstratified clay minerals, p. 393–445. *In* G. Brown (ed.) *The X-ray identification and crystal structures of clay minerals*. Mineralogical Society (Clay Minerals Group), London, U.K.
- MacEwan, D.M.C., and M.J. Wilson. 1980. Interlayer and intercalation complexes of clay minerals, p. 197–248. *In* G.W. Brindley and G. Brown (eds.) *Crystal structures of clay minerals and their X-ray identification*. Mineralogical Society, London, U.K.
- Mathieson, A.McL., and G.F. Walker. 1954. Crystal structure of magnesium-vermiculite. *Am. Mineral.* 39:231–255.
- Matsuda, T., H. Kodama, and A.-F. Yang. 1997. Ca-rectorite from Sano mine, Nagano prefecture, Japan. *Clays Clay Miner.* 45:773–780.
- McKeague, J.A. 1967. An evaluation of 0.1 M pyrophosphate and pyrophosphate-dithionite in comparison with oxalate as extractants of the accumulation products in podzols and some other soils. *Can. J. Soil Sci.* 47:95–99.
- McKeague, J.A. (ed.). 1976. *Manual on soil sampling and methods of analysis*. Soil Research Institute, Agriculture Canada, Ottawa, Canada.
- Mehra, Q.P., and M.L. Jackson. 1960. Iron oxide removal from soils and clays by a dithionite-citrate system with sodium bicarbonate buffer. *Clays Clay Miner.* 7:317–327.
- Méring, J. 1949. L'interférence des rayons X dans les systèmes à stratification désordonnée. *Acta Crystallogr.* 2:371–377.
- Méring, J. 1975. Smectites, p. 98–120. *In* J.E. Gieseking (ed.) *Soil components. Vol. II. Inorganic components*. Springer-Verlag, New York.
- Méring, J., and G.W. Brindley. 1967. X-ray diffraction band profiles of montmorillonite—Influence of hydration and exchangeable cations. *Clays Clay Miner.* 15:51–60.
- Méring, J., and A. Oberlin. 1967. Electron-optical study of smectites. *Clays Clay Miner.* 15:3–34.
- Méring, J., and A. Oberlin. 1971. The smectites, p. 193–229. *In* J.A. Gard (ed.) *Electron-optical investigation of clays*. Mineralogical Society, London, U.K.
- Mitchell, B.D., and V.C. Farmer. 1962. Amorphous clay minerals in some Scottish soil profiles. *Clay Miner. Bull.* 5:128–144.
- Monreal, C.M., and H. Kodama. 1997. Influence of aggregate architecture and minerals on living habitats. *Can. J. Soil Sci.* 77:367–377.
- Mooney, R.W., A.G. Keenan, and L.A. Wood. 1952. Adsorption of water vapour by montmorillonite II. Effect of exchange ions and lattice swelling as measured by X-ray diffraction. *J. Am. Chem. Soc.* 74:1371–1374.
- Moore, D.M., and R.C. Reynolds, Jr. 1989. *X-ray diffraction and the identification and analysis of clay minerals*. Oxford University Press, New York.
- Mortland, M.M., K. Lawton, and G. Uehara. 1956. Alteration of biotite to vermiculite by plant growth. *Soil Sci.* 82:477–481.
- Mossman, M.H., D.H. Freas, and S.W. Bailey. 1967. Orienting internal standard method for clay mineral X-ray analysis. *Clays Clay Miner.* 15:441–453.
- Murad, E. 1988. Properties and behavior of iron oxides as determined by Mössbauer spectroscopy, p. 309–350. *In* J.W. Stucki, B.A. Goodman, and U. Schwertmann (eds.) *Iron in soils and clay minerals*. D. Reidel, Dordrecht, the Netherlands.
- Murad, E., and J. Cashion. 2004. *Mössbauer spectroscopy of environmental materials and their industrial utilization*. Kluwer Academic Publishers, Dordrecht, the Netherlands.
- Murad, E., and U. Wagner. 1991. Mössbauer spectra of kaolinite, halloysite and the firing products of kaolinite: New results and a reappraisal of published work. *Neues Jahrb. Mineral. Abh.* 162:281–309.
- Murad, E., and U. Wagner. 1994. The Mössbauer spectrum of illite. *Clay Miner.* 29:1–10.
- Nadeau, P.H. 1985. The physical dimension of fundamental clay particles. *Clay Miner.* 20:499–514.
- Nadeau, P.H., M.J. Wilson, W.J. McHardy, and J.M. Tait. 1984a. Interstratified clays as fundamental particles. *Science* 225:923–925.
- Nadeau, P.H., M.J. Wilson, W.J. McHardy, and J.M. Tait. 1984b. Interparticle diffraction: A new concept for interstratified clays. *Clay Miner.* 19:757–769.
- Nakamoto, K. 1963. *Infrared spectra of inorganic and coordination compounds*. John Wiley & Sons, Inc., New York.
- Newman, A.C.D. (ed.). 1987. *Chemistry of clays and clay minerals*. Mineralogical Society, London, U.K.

- Norrish, K., and R.M. Taylor. 1962. Quantitative analysis by X-ray diffraction. *Clay Miner. Bull.* 5:98–109.
- Oberlin, A., and J. Méring. 1962. Observations en microscopie et microdiffraction électronique sur la montmorillonite Na. *J. Microscopie.* 1:107–120.
- Oinuma, K., K. Kobayashi, and T. Sudo. 1961. Procedure of clay mineral analysis. *Clay Sci.* 3:179–193.
- Pauling, L. 1929. The principles determining the structure of complex ionic crystals. *J. Am. Chem. Soc.* 51:1010–1026.
- Petruck, W. 1964. Determination of the heavy atom content in chlorite by means of the X-ray diffractometer. *Am. Mineral.* 49:61–71.
- Reynolds, R.C., Jr., 1980. Interstratified clay minerals, p. 249–303. *In* G.W. Brindley and G. Brown (eds.) *Crystal structures of clay minerals and their X-ray identification.* Mineralogical Society, London, U.K.
- Robert, M., and J. Berthelin. 1984. Role of biological and biochemical factors in soil mineral weathering, p. 453–495. *In* P.M. Huang and M. Schnitzer (eds.) *Interactions of soil minerals with natural organics and microbes.* SSSA Special Publication No. 17. SSSA, Madison, WI.
- Robert, J.-L., and H. Kodama. 1988. Generalization of the correlations between hydroxyl stretching wave numbers and composition of mica in the system K_2O – MgO – Al_2O_3 – SiO_2 – H_2O : A single model for trioctahedral and dioctahedral micas. *Am. J. Sci.* 288:196–212.
- Ross, G.J. 1978. Relationships of specific surface area and clay content to shrink-swell potential of soils having different clay mineralogical compositions. *Can J. Soil Sci.* 58:159–166.
- Ross, G.J., H. Kodama, C. Wang, J.T. Gray, and L.B. Lafreniere. 1983. Halloysite from a strongly weathered soil at Mont Jacques Cartier, Quebec. *Soil Sci. Soc. Am. J.* 47:327–332.
- Ross, G.J., C. Wang, and P.A. Schuppli. 1985. Hydroxylamine and ammonium oxalate solution as extractants for iron and aluminum from soils. *Soil Sci. Soc. Am. J.* 49:783–785.
- Sans, J., and J.M. Serratosa. 1984. ^{29}Si and ^{27}Al high-resolution MAS–NMR spectra of phyllosilicates. *J. Am. Chem. Soc.* 106:4790–4793.
- Sato, M. 1965. Structure of interstratified (mixed-layer) minerals. *Nature* 208:70–71.
- Sato, M. 1973. X-ray analysis of interstratified structure. *J. Clay Sci. Soc. Jpn.* 13:39–47.
- Schultz, L.G. 1960. Quantitative X-ray determination of some aluminous clay minerals in rocks. *Clays Clay Miner.* 7: 216–224.
- Schultz, L.G. 1964. Quantitative interpretation of mineralogical composition from X-ray and chemical data for the Pierre shale. U.S. Geological Survey Professional Paper 391-C.
- Schwertmann, U. 1959. Die fraktionierte Extraktion der freien Eisenoxide in Boden, ihre Mineralogischen Formen und ihre Entstehungsweisen. *Z. Pflanzenernähr. Dung. Bodenkd.* 84:194–204.
- Segalen, P. 1968. Note sur une méthode de détermination des produits minéraux amorphes dans certains sols a hydroxides tropicaux. *Cah. ORSTOM Ser. Pedol.* 6:105–126.
- Serratosa, J.M., and W.F. Bradley. 1958. Determination of the orientation of the OH bond axes in layer silicates by infrared absorption. *J. Phys. Chem.* 62:1164–1167.
- Shirozu, H., and S.W. Bailey. 1965. Chlorite polytypism: III. Crystal structure of an ortho-hexagonal iron chlorite. *Am. Mineral.* 50:868–885.
- Smith, J.V., and H.S. Yoder. 1956. Experimental and theoretical studies of mica polymorphs. *Mineral. Mag.* 31:209–235.
- Stucki, J.W., B.A. Goodman, and U. Schwertmann. 1988. Iron in soils and clay minerals. NATO ASI series. Series C: Mathematical and physical sciences. Vol. 217. D. Reidel, Dordrecht, the Netherlands.
- Sudo, T. 1959. Mineralogical study on clays of Japan. Maruzen Co. Ltd., Tokyo, Japan.
- Sudo, T., S. Shimoda, H. Yotsumoto, and S. Aita. 1981. Electron micrographs of clay minerals. *Developments in sedimentology.* Vol. 31. Elsevier Scientific Publishing Co., New York.
- Talvenheimo, G., and J.L. White. 1952. Quantitative analysis of clay minerals with the X-ray spectrometer. *Anal. Chem.* 24:1784–1789.
- Tamm, O. 1922. Um bestamning av de oorganiska komponenterna i markens gelkomplex. *Medd. Statens Skogsfoersoeksansalt.* 19:385–404.
- Tazaki, K., and R. Asada. 2007. Transmission electron microscopic observation of mercury-bearing bacterial clay minerals in a small-scale gold mine in Tanzania. *Geomicrobiol. J.* 24:477–489.
- Tessier, D. 1990. Behaviour and microstructure of clay mineral, p. 387–415. *In* M. De Boodt, M. Hayes, and A. Herbillon (eds.) *Soil colloids and their association in aggregates.* Plenum Publishing Corporation, New York.
- Theisen, A.A., and E. Bellis. 1964. Quantitative analysis of clay mineral mixtures by X-ray diffraction. *Nature* 204:1228–1230.
- Thorez, J. 1975. Phyllosilicates and clay minerals: A laboratory handbook for their X-ray diffraction analysis. G. Lelotte, Belgique, Belgium.
- Tuddenham, W.M., and R.J.P. Lyon. 1959. Relation of infrared spectra and chemical analysis for some chlorites and related minerals. *Anal. Chem.* 31:377–380.
- Vali, H., and H.M. Koster. 1986. Expanding behaviour, structural disorder, regular and random irregular interstratifications of 2:1 layer-silicates studied by high-resolution images of transmission electron microscopy. *Clay Miner.* 21:827–859.
- Vanders, I., and P. Kerr. 1967. Mineral recognition. John Wiley & Sons, Inc., New York.
- Vedder, W. 1964. Correlations between infrared spectrum and chemical composition of mica. *Am. Mineral.* 49:736–768.
- Vedder, W., and R.S. McDonald. 1963. Vibrations of the OH ions in muscovite. *J. Chem. Phys.* 38:1583–1590.
- Velde, B. 1992. Introduction to clay minerals. Chapman and Hall, London, U.K.
- Wada, K. 1959. Oriented penetration of ionic compounds between the silicate layers of halloysite. *Am. Mineral.* 44:153–165.
- Wada, K. 1961. Lattice expansion of kaolin minerals by treatment with potassium acetate. *Am. Mineral.* 44:1237–1247.

- Wada, K., and D.J. Greenland. 1970. Selective dissolution and differential infrared spectroscopy for characterization of 'amorphous' constituents in soil clays. *Clay Miner.* 8:241-254.
- Wada, K., and C. Mizota. 1982. Iron-rich halloysite (10Å) with crumpled lamellar morphology from Hokkaido, Japan. *Clays Clay Miner.* 30:315-317.
- Walker, G.F. 1949. Distinction of vermiculite, chlorite and montmorillonite in clays. *Nature* 164:577-578.
- Wang, C., H. Kodama, and N.M. Miles. 1981. Effect of various pretreatments on X-ray diffraction patterns of clay fractions of podzolic B horizons. *Can. J. Soil Sci.* 61:311-316.
- Weaver, C.E. 1958. Geologic interpretation of argillaceous sediments. Part I. Origin and significance of clay minerals in sedimentary rocks. *Am. Assoc. Pet. Geol. Bull.* 42:254-271.
- Weaver, C.E. 1989. Clays, muds and shales. *Developments in sedimentology*. Vol. 44. Elsevier Scientific Publishing Co., New York.
- Weiss, A., W. Thielepape, G. Goring, W. Ritter, and H. Schafer. 1963. Kaolinite intercalation compounds, p. 287-305. *Proc. Int. Clay Conf.* Vol. 1. Stockholm, Sweden.
- Wicks, F.J., and E.J.W. Whittaker. 1975. A reappraisal of the structure of the serpentine minerals. *Can Mineral.* 13:227-243.
- Wicks, F.J., and J. Zussman. 1975. Microbeam X-ray diffraction patterns of the serpentine minerals. *Can Mineral.* 13:244-258.
- Williams, P.P. 1959. Direct quantitative diffractometric analysis. *Anal. Chem.* 31:1842-1844.
- Wilson, M.J. (ed.). 1992. *Clay mineralogy: Spectroscopic and chemical determinative methods*, 367 pp. Chapman and Hall, London, U.K.
- Wilson, M.J., and D.R. Clark. 1978. X-ray identification of clay minerals in thin sections. *J. Sediment. Petrol.* 48:656-660.
- Yada, K. 1967. Study of chrysotile asbestos by a high resolution electron microscope. *Acta Crystallogr.* 23:704-707.
- Yong, R.N., and B.P. Warkentin. 1975. Soil properties and behaviour. *Developments in geotechnical engineering* 5. Elsevier Scientific Publishing Co., Amsterdam, the Netherlands.
- Yuan, H., and D.L. Bish. 2010. NEWMOD⁺, a new version of the NEWMOD program for interpreting X-ray powder diffraction patterns from interstratified clay minerals. *Clays Clay Miner.* 58:318-326.

Nestor Kämpf

Universidade Federal do
Rio Grande do Sul

Andreas C. Scheinost

Institute of Radiochemistry

Darrell G. Schulze

Purdue University

22.1	Introduction	22-1
22.2	Iron Oxides	22-1
	Mineral Phases • Occurrence and Formation • Influence on Soil Properties • Identification	
22.3	Manganese Oxides.....	22-9
	Mineral Phases • Occurrence and Formation • Influence on Soil Properties • Identification	
22.4	Aluminum Oxides.....	22-16
	Mineral Phases • Occurrence and Formation • Influence on Soil Properties • Identification	
22.5	Silicon Oxides.....	22-19
	Mineral Phases • Occurrence and Formation • Influence on Soil Properties • Identification	
22.6	Titanium and Zirconium Minerals	22-23
	Mineral Phases • Occurrence and Formation • Influence on Soil Properties • Identification	
	References.....	22-25

22.1 Introduction

Oxide minerals or oxides comprise the oxides, hydroxides, oxyhydroxides, and hydrated oxides of Fe, Mn, Al, Si, and Ti. They commonly occur in soils, particularly those in advanced stages of weathering where they can sometimes account for as much as 50% of the total soil mass. In the discussion to follow, a polyhedral approach will be used to introduce the mineral species and highlight their major differences and similarities (Figure 22.1). For additional structural details, the reader is referred to the literature cited. Thereafter, their occurrence and formation in soils and their influence on soil properties will be discussed, concluding with the major techniques for identifying these minerals in soils.

22.2 Iron Oxides

Iron oxide minerals are ubiquitous in soils and sediments. All of the Fe oxide minerals are strongly colored and, when finely dispersed throughout the matrix, even small amounts impart bright colors to soils. Iron oxides often cement other soil minerals into stable aggregates, and when they reach massive proportions, such cementations are called laterite or ferricrete. Because iron oxide surfaces have a strong affinity for the oxyanions of phosphorus and some transition metals, they play a significant role in the environmental cycling of these elements. A list of the Fe oxides is given in Table 22.1. Recent comprehensive reviews include Schwertmann and Taylor (1989), Cornell and Schwertmann (1996, 2003), and Bigham et al. (2002).

22.2.1 Mineral Phases

The structures of most Fe oxides can be described in terms of close-packed arrays of O and OH ions, with Fe occupying interstitial octahedral sites. Structures based on hexagonal close packing (hcp) of the anions are called α -phase, and those with cubic close packing (ccp), γ -phase (note that this convention is not necessarily followed for oxides of other elements). Both hcp and ccp structures also contain tetrahedral interstices. In two minerals, magnetite and maghemite, Fe is present in some of these tetrahedral sites as well. The basic structural unit for most of the Fe oxides, however, is an octahedron in which each Fe atom is surrounded either by six O or by both O and OH ions. The various Fe oxides differ mainly in the arrangement of these octahedra and in how they are linked.

22.2.1.1 Oxyhydroxides

Goethite (α -FeOOH) consists of double chains of edge-shared octahedra that are joined to other double chains by sharing corners and by hydrogen bonds (Figure 22.1; Cornell and Schwertmann, 1996). *Lepidocrocite* (γ -FeOOH) also contains double chains of octahedra, but they are joined by shared edges, resulting in corrugated sheets of octahedra. These corrugated sheets are stacked one on top of the other and are held together by hydrogen bonds (Figure 22.1; Ewing, 1935a, 1935b; Fasiska, 1967). *Akaganéite* (β -FeOOH) consists of double chains that share corners with adjacent chains to give a 3D structure containing tunnels 0.5 nm in cross section (Figure 22.1). These tunnels contain Cl^- ions that stabilize the structure (Post and Buchwald, 1991). *Schwertmannite* ($\text{Fe}_8\text{O}_8(\text{OH})_6(\text{SO}_4)$) is

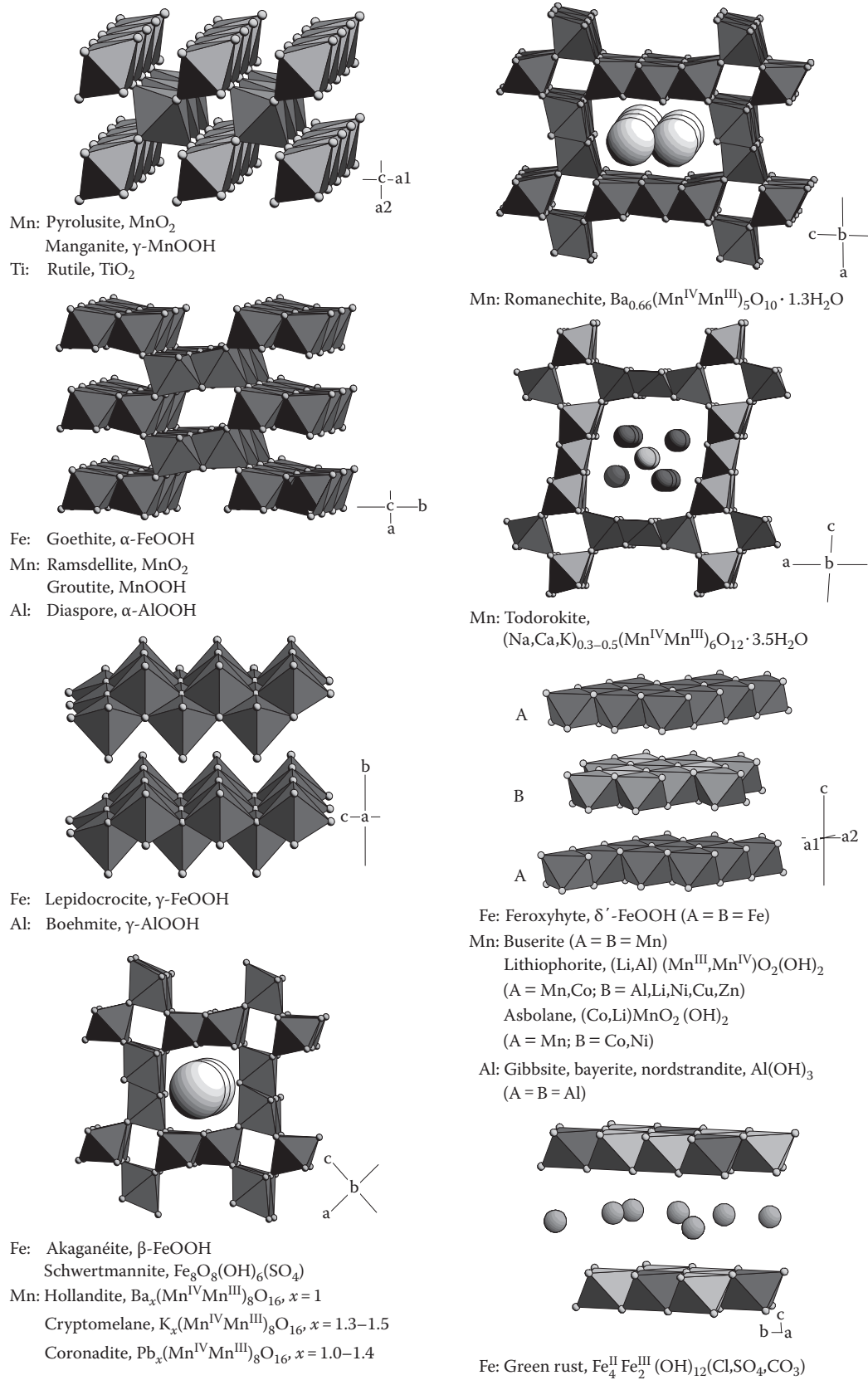


FIGURE 22.1 (See color insert.) Structural schemes for oxide minerals in soils.

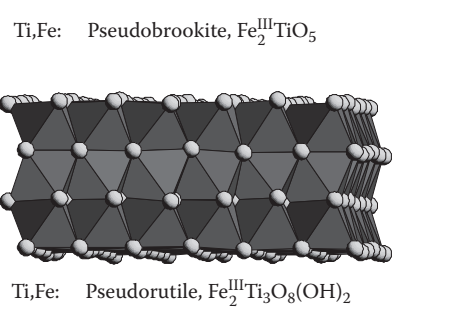
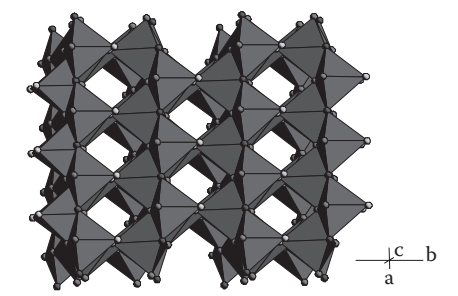
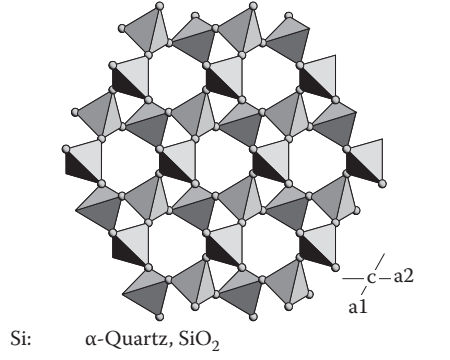
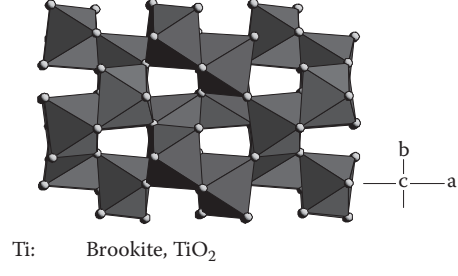
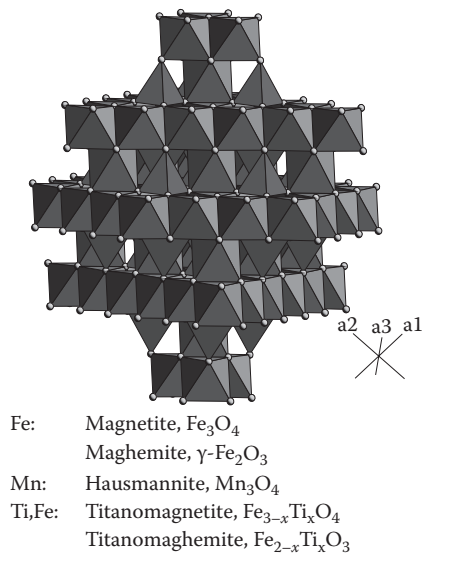
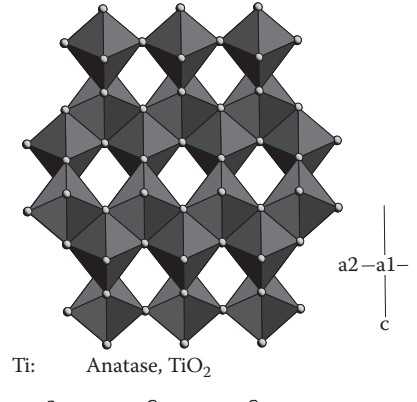
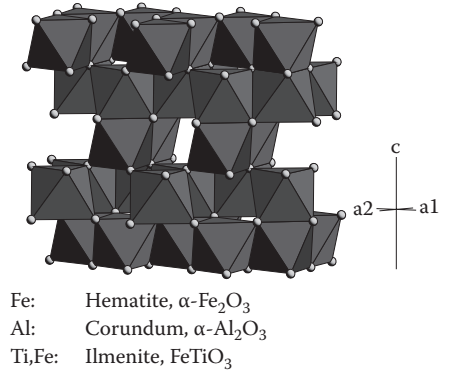
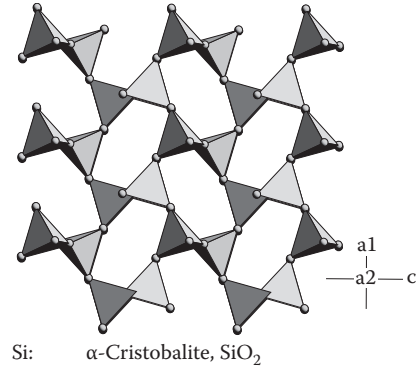
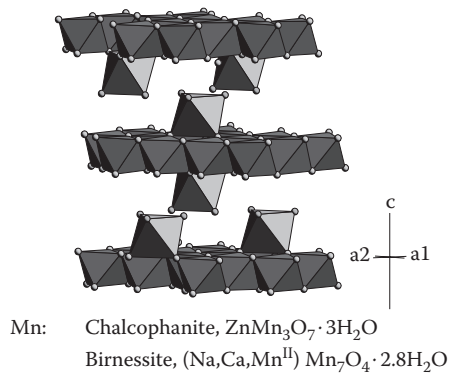


FIGURE 22.1 (continued)

TABLE 22.1 Iron Oxide Minerals: Crystallographic Properties and d Values for the Six Most Intense Diffraction Lines

Mineral	Chemical Formula	Crystal System, Space Group	Unit-Cell Dimensions (Å)	Six Most Intense Diffraction Lines d Value (Å), Relative Intensity						References ^a
Goethite	α -FeOOH	Orthorhombic, <i>Pbnm</i>	a = 4.608 b = 9.956 c = 3.021	4.183 100	2.450 50	2.693 35	1.719 20	2.190 18	2.253 14	29-0713
Lepidocrocite	γ -FeOOH	Orthorhombic, <i>Cmcm</i>	a = 3.07 b = 12.53 c = 3.88	6.260 100	3.290 90	2.470 80	1.937 70	1.732 40	1.524 40	Cornell and Schwertmann (2003); 08-0098
Akaganéite	β -FeOOH	Monoclinic, <i>I2/m</i>	a = 10.56 b = 3.031 c = 10.483 $\beta = 90^\circ 63'$	3.333 100	2.550 5	7.467 40	2.295 35	1.643 35	5.276 30	Post and Buchwald (1991); 34-1266
Schwertmannite	$\text{Fe}_8\text{O}_8(\text{OH})_6\text{SO}_4$	Tetragonal, <i>P4/m</i>	a = 10.66 c = 6.04	2.55 100	3.39 46	4.86 37	1.51 24	2.28 23	1.66 21	Bigham et al. (1994)
Feroxyhite	δ' -FeOOH	Hexagonal, <i>P3ml</i>	a = 2.93 c = 4.56	2.545 100	2.255 100	1.685 100	1.471 100	4.610 20	1.271 20	Cornell and Schwertmann (1996); 13-0087
Ferrihydrite	$\text{Fe}_5\text{HO}_8 \cdot 4\text{H}_2\text{O}$	Hexagonal	a = 5.08 c = 9.4	2.50 100	2.21 80	1.96 80	1.48 80	1.51 70	1.72 50	Towe and Bradley (1967); 29-0712
Hematite	α - Fe_2O_3	Hexagonal, <i>R3c</i>	a = 5.034 c = 13.752	2.700 100	2.519 70	1.694 45	1.840 40	3.684 30	1.486 30	33-0664
Magnetite	Fe_3O_4	Cubic, <i>Fd3m</i>	a = 8.3967	2.532 100	1.484 40	2.967 30	1.616 30	2.099 20	1.093 12	19-0629
Maghemite	γ - Fe_2O_3	Cubic, <i>Fd3m</i>	a = 8.35	2.518 100	2.953 40	1.476 30	1.607 20	2.088 15	1.704 10	Goss (1988); 39-1346
Bernalite	$\text{Fe}(\text{OH})_3$	Orthorhombic, <i>Immm</i>	a = 7.544 b = 7.560 c = 7.558	3.784 100	1.692 17	2.393 16	2.676 15	1.892 10	1.545 9	Birch et al. (1993)
Fougerite	$(\text{Fe}^{2+}, \text{Mg})_6$ $\text{Fe}_2^{3+}(\text{OH})_{18} \cdot 4\text{H}_2\text{O}$	Trigonal- hexagonal, <i>R3m</i>	a = 3.125 c = 22.5	7.97 100	2.692 34	3.97 32	2.027 19	1.563 10	1.595 9	http://webmineral.com
$\text{Fe}(\text{OH})_2$	$\text{Fe}(\text{OH})_2$	Hexagonal, <i>P3ml</i>	a = 3.262 c = 4.596	4.597 vs ^b	2.403 vs	2.817 s	1.782 s	1.629 s	1.535 w	Miyamoto (1976)
Green rust I	$\text{Fe}(\text{OH})_2\text{Fe}(\text{OH})_3\text{Cl}$ (variable)	Rhombohedral	a = 3.198 c = 24.21	8.02 vs	4.01 s	2.701 m	2.408 m	2.037 w	1.487 w	Bernal et al. (1959)
Green rust II	$\text{Fe}(\text{OH})_2\text{Fe}(\text{OH})_3\text{SO}_4$ (variable)	Hexagonal, <i>R3/m</i>	a = 3.174 b = 10.94	10.92 vs	5.48 s	3.65 s	2.747 m	2.660 ms	2.459 ms	Bernal et al. (1959)

^a Numbers of the format XX-XXXX indicate ICDD file number (ICDD, 1994).

^b vs, very strong; s, strong; ms, moderately strong; m, moderate; w, weak.

isostructural with akaganéite, but instead of Cl^- , SO_4^{2-} occupies the tunnels (Figure 22.1; Bigham et al., 1990, 1994). *Feroxyhite* (δ' -FeOOH) consists of sheets of edge-sharing octahedra (Figure 22.1), with the presence of face-sharing octahedra (Manceau and Combes, 1988; Drits et al., 1993a; Manceau and Drits, 1993). In naturally occurring feroxyhite, Fe^{3+} ions are randomly distributed over the octahedral sites, while in synthetic δ -FeOOH, the Fe^{3+} ions are orderly distributed over half of the octahedral sites (Waychunas, 1991). *Ferrihydrite* ($\text{Fe}_5\text{HO}_8 \cdot 4\text{H}_2\text{O}$) is a poorly ordered Fe oxide, with a variable degree of ordering. The structure is still being investigated (Drits et al., 1993b; Manceau and Drits, 1993; Manceau and Gates, 1997) but can be visualized as a defective hematite structure containing both edge- and face-sharing octahedra (Towe and Bradley, 1967). The Fe^{3+} ions are randomly distributed over the octahedral interstices, with

many sites vacant and more OH^- and H_2O and less Fe^{3+} than in hematite (Cornell and Schwertmann, 1996).

22.2.1.2 Hydroxides

Green rusts are a group of Fe^{2+} - Fe^{3+} hydroxy salts with a structure consisting of sheets of edge-shared $\text{Fe}^{2+}(\text{OH})_6$ octahedra in which some of the Fe^{2+} is replaced by Fe^{3+} , creating a positive layer charge. The charge is balanced by anions such as Cl^- , SO_4^{2-} , and CO_3^{2-} located between the octahedral sheets (Figure 22.1; Brindley and Bish, 1976; Taylor and McKenzie, 1980). *Bernalite*, $\text{Fe}(\text{OH})_3 \cdot n\text{H}_2\text{O}$ (Birch et al., 1993), is a rare Fe hydroxide and has not been found in soils. *Fougerite*, $(\text{Fe}^{2+}\text{Mg})_6 \text{Fe}_2^{3+}(\text{OH})_{18} \cdot 4\text{H}_2\text{O}$, has recently been identified as a green rust mineral in soils (Trolard et al., 2007), whereas the $\text{Fe}(\text{OH})_2$ compound has not been found as a mineral (Cornell and Schwertmann, 1996).

22.2.1.3 Oxides

Hematite (α -Fe₂O₃) consists of sheets of edge-shared octahedra with two-thirds of the available octahedral sites filled with Fe³⁺ ions. The unoccupied sites are regularly arranged to form sixfold rings of occupied octahedra analogous to dioctahedral phyllosilicate sheets (Chapter 21) and are stacked along the c-axis. Each plane of O is shared by two adjacent dioctahedral sheets. Each octahedron shares three edges with three neighboring octahedra in the same sheet and a face and six corners with nine octahedra in adjacent sheets (Figure 22.1; Blake et al., 1966; Maslen et al., 1994). *Magnetite* (Fe₃O₄), which differs from most other Fe oxides in that it contains both Fe²⁺ and Fe³⁺ ions, has an inverse spinel structure consisting of octahedral and mixed tetrahedral/octahedral layers stacked along the [111] plane, with Fe³⁺ occupying tetrahedral sites and both Fe²⁺ and Fe³⁺ in octahedral sites (Figure 22.1). *Titanomagnetites* (Fe_{3-x}Ti_xO₄) are solid solutions of magnetite with ulvöspinel (Fe₂TiO₄), with Ti⁴⁺ occupying only octahedral sites (Wechsler et al., 1984). *Maghemite* (γ -Fe₂O₃) has the chemical composition of hematite but has a structure analogous to magnetite (Figure 22.1). Most or all of the Fe occurs as Fe³⁺ and cation vacancies preserve charge balance caused by the oxidation of Fe²⁺ to Fe³⁺. The cations are randomly distributed over the tetrahedral and octahedral sites. The vacancies are also randomly distributed but are confined to the octahedral sites. *Titanomaghemites* are oxidation products of titanomagnetites, but their structure needs clarification (Waychunas, 1991). Maghemite–magnetite solid solutions are formed by varying degrees of oxidation of magnetite.

Other metallic cations with an ionic diameter similar to Fe³⁺ (Al, Ni, Ti, Mn, Co, Cr, Cu, Zn, V) may replace the Fe ion in the structure of various Fe oxides. Isomorphous substitution of Al³⁺ for Fe³⁺ occurs most frequently and to the greatest extent (Schwertmann and Carlson, 1994). In addition to M³⁺ cations, M²⁺ and M⁴⁺ cations may also enter Fe³⁺ oxide structures, but the uptake is usually less than 0.1 mol⁻¹ (Cornell and Schwertmann, 1996).

The typical shapes of well-crystallized Fe oxide samples are listed in Table 22.2. These shapes, usually observed in samples from synthetic preparations, rocks, ferricretes, and bauxites, are frequently less well expressed by soil Fe oxides. Soil hematites usually have a granular texture, and goethites show almost no acicularity (Figure 22.2), particularly in highly weathered soils (Schwertmann and Kämpf, 1985; de Brito Galvão and Schulze, 1996). Thus, morphology alone is unreliable for distinguishing these minerals by transmission electron microscopy (TEM) (Anand and Gilkes, 1987a; Singh and Gilkes, 1992), although soil lepidocrocites often appear as thin laths, very similar to synthetic lepidocrocites (Cornell and Schwertmann, 1996). Soil Fe oxides may range from a few to several hundred nanometers in length, but data are scarce because of their tendency to occur as microaggregates (Schwertmann, 1988).

22.2.2 Occurrence and Formation

The concentration of Fe oxides in soil ranges between <1 and >500 g kg⁻¹ and is related to parent material, degree of weathering, and pedogenic accumulation or depletion processes. Iron oxides

TABLE 22.2 Diagnostic Criteria for Iron Oxide Minerals

Mineral	Color and Munsell Hues Range	Typical Crystal Shape	DTA Events (°C)	IR Bands (cm ⁻¹)	Magnetic Hyperfine Field (kOe)		
					295 K	77 K	4 K
Goethite	Strong brown to yellowish brown, 7.5YR–2.5Y	Needles, laths	Endotherm, 280–400	890, 797	382	503	506
Lepidocrocite	Reddish yellow (“orange”), 5YR–7.5YR	Laths	Endotherm, 300–350 Exotherm, 370–500	1026, 1161, 753			458
Akaganéite	Strong brown to reddish yellow, 2.5YR–7.5YR	Spindle-shaped rods					489/478/473
Schwertmannite	Reddish yellow to yellow, 5YR–10YR	Fibers	Endotherm, 100–300, 650–710 Exotherm, 540–580	3300, 1634, 1186, 1124, 1038, 976, 608			456
Ferrihydrite	Dark red to strong brown, 2.5YR–7.5YR	Spherical	Endotherm, 150				470/500
Feroxyhite	Dark red to dark reddish brown, 1.5YR–5YR	Fibers, needles	Endotherm, 250	1110, 920, 790, 670	420	530	535
Hematite	Dusky red to dark red, 5R–2.5YR	Hexagonal plates	Nil	345, 470, 540	518	542/535 ^a	542/535 ^a
Maghemite	Dark reddish brown, 2.5YR–5YR	Cubes	Exotherm, 600–800	400, 450, 570, 590, 630	500		526
Magnetite	Black	Cubes	^b	400, 590	491/460 ^c		

^a With and without Morin transition, respectively.

^b Magnetite converts via maghemite or directly to hematite, depending on particle size.

^c For tetrahedral and octahedral Fe, respectively.

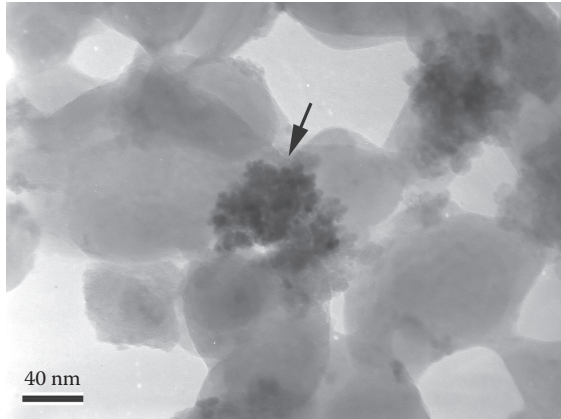


FIGURE 22.2 Transmission electron micrograph of the $<0.2\mu\text{m}$ fraction of a Rhodic Hapludox showing a goethite or hematite particle (arrow) surrounded by clean kaolinite particles. (Modified from de Brito Galvão, T.C., and D.G. Schulze. 1996. Mineralogical properties of a collapsible lateritic soil from Minas Gerais, Brazil. *Soil Sci. Soc. Am. J.* 60:1969–1978.)

may occur evenly distributed in the matrix or concentrated as ferriretes, layers, bands, horizons, nodules, mottles, plinthite, etc.

Iron, present as Fe^{2+} in primary minerals (mainly silicates) of most rocks, is released during weathering through protolysis and oxidation processes, hydrolyzes in contact with water, and then forms Fe^{3+} oxides. In most aerobic environments, the Fe oxides are evenly distributed resulting in homogeneous soil color. Under anaerobic conditions, however, Fe oxides may be reduced and dissolved, thus leading to a heterogeneous distribution of Fe oxides and color (redoximorphic features; Schwertmann, 1993). The formation of each of the Fe oxide minerals requires specific conditions that have been established for soils by laboratory and field observations (Schwertmann and Taylor, 1989).

In aerobic environments, goethite and hematite are the most common Fe oxides due to their high thermodynamic stability. Their formation pathway starts with Fe^{2+} released by weathering and its immediate oxidation to Fe^{3+} or by any other source of Fe^{3+} (e.g., dissolution of Fe oxides), which precipitates as ferrihydrite or goethite, depending on which of the solubility products is exceeded first (ferrihydrite, $K_{\text{sp}} \sim 10^{-39}$ or goethite, $10^{-44} < K_{\text{sp}} < 10^{-41}$). Hematite forms from its necessary precursor, ferrihydrite, through a solid-state reaction in which individual hematite crystals nucleate and grow within individual ferrihydrite aggregates by a dehydration and rearrangement process. All of the iron in each individual hematite crystal is derived from a single-ferrihydrite aggregate (Cornell and Schwertmann, 1996). The transformation of ferrihydrite to goethite, however, proceeds via a dissolution–precipitation process. The presence of face-sharing $\text{Fe}(\text{O},\text{OH})_6$ octahedra in ferrihydrite, as in hematite, prevents the direct solid-state transformation of ferrihydrite into goethite, which consists only of edge- and corner-sharing octahedra. Thus, the transformation of ferrihydrite to goethite requires the breakdown of the oxo-bridges of face-sharing octahedra (Combes et al., 1989). Goethite forms from Fe^{3+} ions in solution via a nucleation–crystal growth process. Hence, any Fe source (minerals, biological

exudates, organic compounds) able to keep a low Fe^{3+} activity in solution will favor goethite. Thus, the formation pathways of hematite and goethite are different but competitive.

Environmental conditions that favor the formation of ferrihydrite and its subsequent transformation to hematite are high Fe content in the parent rock (resulting in higher Fe release rate), near neutral pH (pH of minimum solubility of ferrihydrite), higher temperature or lower water activity (favoring the dehydration step) (Torrent et al., 1982), and rapid turnover of biomass (low Fe complexation) (Schwertmann, 1988). Such environmental conditions are usually related to climate (Kämpf and Schwertmann, 1983), landscape (Curi and Franzmeier, 1984; Schwertmann and Latham, 1986), landscape associated with drainage (Macedo and Bryant, 1987; da Motta and Kämpf, 1991; Peterschmitt et al., 1996; Fritsch et al., 2007), and soil depth (Biggam et al., 1978; Kämpf and Schwertmann, 1983).

In soils, the transformation rate of ferrihydrite to hematite is probably very rapid, whereas that of ferrihydrite to goethite, which proceeds through dissolution–recrystallization, is slower. This explains the widespread association of ferrihydrite–goethite, while that of ferrihydrite–hematite has been rarely found (Parfitt et al., 1988). There is no pedogenic indication for a solid-state transformation of goethite to hematite by simple dehydration, nor the inverse by simple hydration. However, high temperatures caused by forest or bush fires may transform goethite into hematite and lepidocrocite into maghemite (Stanjek, 1987; see maghemite below).

Both hematite and goethite have a similarly low solubility (Lindsay, 1979). Under moderately reducing conditions, however, a transformation of red into yellow soils (yellowing or xanthization) may take place due to a preferential dissolution of hematite over goethite (Macedo and Bryant, 1989; Jeanroy et al., 1991; Peterschmitt et al., 1996; Fritsch et al., 2005). The increased resistance of goethite to dissolution is explained by a higher Al for Fe substitution (Torrent et al., 1987; Trolard and Tardy, 1987). The solubility and dissolution of Fe oxides is reviewed by Schwertmann (1991). When Fe oxides are reduced in higher landscape positions, the soluble Fe^{2+} may be transported to lower landscape positions and reprecipitate as Fe oxides (Schwarz, 1994). In aquatic environments with prolonged waterlogging, the complete removal of Fe oxides may take place, resulting in soil bleaching (chroma < 2) (da Motta and Kämpf, 1991; Peterschmitt et al., 1996). The bleached color is due to the matrix minerals (phyllosilicates, quartz, etc.) in the absence of Fe oxides.

Many species of microorganisms, mainly anaerobic bacteria, are capable of reducing Fe oxides (Lovley, 1995). As heterotrophic organisms, they depend on available biomass for metabolic oxidation so that reduction in soils is most intense in the upper horizons. The process usually involves enzymatic transfer of electrons by microorganisms from the decomposing biomass to Fe^{3+} (Ghiorse and Ehrlich, 1992; Lovley, 1992, 1995).

Some Fe and Mn oxides may be formed by microorganisms in a biologically induced form outside the cell, or matrix mediated, by internal cellular precipitation (Ghiorse and Ehrlich, 1992). The most common occurrence of biotic formation of

Fe oxides is Fe ochre in field drains (Houot and Berthelin, 1992), the Fe plaque in the root zone of wetland plants (Weiss et al., 2003), and the Fe precipitate, yellow boy, in acid mine drainages (Bigham et al., 1992). Aspects of biomineralization of Fe and Mn in soils are reviewed in Skinner and Fitzpatrick (1992).

The typical Fe oxides of seasonally reduced soil environments are goethite, lepidocrocite, and ferrihydrite, formed by abiotic or biotic processes. Therefore, goethite and lepidocrocite are widely associated in reductomorphic soils, whereas hematite is restricted to mottles and nodules (Schwertmann and Kämpf, 1983; Fitzpatrick et al., 1985; Wang et al., 1993; dos Anjos et al., 1995). While goethite can form from either Fe^{2+} or Fe^{3+} ions in solution, lepidocrocite in soils seems to require the presence of Fe^{2+} ions (Schwertmann and Taylor, 1989). Thus, lepidocrocite, recognized by its bright orange color, indicates prevailing reductomorphic conditions in a soil profile leading to the formation of Fe^{2+} . Factors that favor the formation of goethite over lepidocrocite, however, are a higher partial pressure of CO_2 , normally found closer to roots, the presence of HCO_3^- or CO_3^{2-} , an increasing rate of oxidation, and the presence of Al in the system (Schwertmann and Taylor, 1989; Carlson and Schwertmann, 1990).

Ferrihydrite has been reported in ochreous precipitates from the oxidation of emerging, Fe^{2+} -containing waters (Schwertmann and Fischer, 1973; Carlson and Schwertmann, 1981; Schwertmann and Kämpf, 1983), in bog and lake Fe ores (Schwertmann et al., 1982), in podzol B horizons (Adams and Kassim, 1984), in placic horizons (Campbell and Schwertmann, 1984), in Andepts (Parfitt et al., 1988), in soil iron pans (Childs et al., 1990), and in constructed wetlands for acid drainage treatment (Karathanasis and Thompson, 1995). These occurrences reflect an environment where Fe^{2+} is rapidly oxidized (abiotically or biotically) in the presence of high concentrations of organic matter and/or Si. These compounds and possibly others hinder the immediate formation of FeOOH phases and the subsequent transformation of ferrihydrite to more stable Fe oxides (Schwertmann, 1966; Cornell, 1987). In contrast, in tropical soils, the concentration of ferrihydrite is very low because of low interference of Si and organics. The presence of ferrihydrite together with FeOOH phases may indicate that environmental conditions are not favorable for crystal development or that the formations are relatively young, as in paddy soils (Wang et al., 1993) and constructed wetlands (Karathanasis and Thompson, 1995).

Reductomorphic soils often display greenish-blue colors that change rapidly to yellowish brown on exposure to the air. These colors are indicative of the presence of green rusts, recently identified as fougérite (Trolard et al., 2007). Iron-reducing bacteria appear as the main factor involved in green rust formation (Berthelin et al., 2006). Green rusts occur under reducing and weakly acid to weakly alkaline conditions as intermediate phases in the abiotic formation of goethite, lepidocrocite, and magnetite (Schwertmann and Fechter, 1994).

Schwertmannite has been found in strongly acid, sulfate-rich waters associated with mining activities (Bigham et al., 1990, 1992, 1994, 1996b; Fanning et al., 1993), a Histosol that received runoff from lead smelting activities (Gao and Schulze,

2010a, 2010b), and in an acid alpine stream draining a pyritic schist (Schwertmann et al., 1995a). Most of these occurrences reflect acid environments where bacteria catalyze the oxidation of FeS_2 , releasing Fe^{3+} and SO_4^{2-} that, in the pH range 2.8–4.0, precipitate as schwertmannite (Bigham et al., 1992, 1996b). At lower pH, jarosite is favored, while at higher pH values, goethite and ferrihydrite form (Bigham et al., 1996a). Schwertmannite is metastable and converts to goethite over time. Bigham et al. (1992) proposed a biogeochemical model for the precipitation of jarosite, schwertmannite, and ferrihydrite, and their conversion to goethite. The model considers the oxidation of Fe^{2+} by *Thiobacillus ferrooxidans* or oxygen, the concentration of SO_4^{2-} , the pH, and the presence of other cations (K, Na) in the system.

Magnetite in soils is usually inherited from the parent rock (lithogenic), but both biologically (Fassbinder et al., 1990) and abiotically formed magnetite (Maher and Taylor, 1988) has been reported. The alteration of magnetite to hematite via solid-state transformation, with no evidence for maghemite development, is described by Gilkes and Suddhiprakarn (1979) and Anand and Gilkes (1984a). In laboratory studies, particle size determines whether hematite or maghemite forms when magnetite is oxidized below 220°C (Egger and Feitknecht, 1962; Gallagher et al., 1968). Particles less than 300 nm in diameter transform to maghemite, while larger particles oxidize to hematite. This may explain why soil maghemites typically occur in the clay fraction.

Maghemite is common in many different soils, especially in the tropics and subtropics, occurring dispersed or concentrated in concretions (Taylor and Schwertmann, 1974; Curi and Franzmeier, 1984; Anand and Gilkes, 1987a; Fontes and Weed, 1991). The two major possible pathways for maghemite formation in soils are the aerial oxidation of lithogenic magnetite (Fontes and Weed, 1991) and the transformation of other pedogenic Fe oxides by heating (between 300°C and 425°C) in the presence of organic compounds (Schwertmann and Fechter, 1984; Anand and Gilkes, 1987b; Stanjek, 1987).

Akaganéite and feroxyhite are both rare minerals. Akaganéite has been found in environments with high chloride concentrations (e.g., 0.1 M), low pH (e.g., 3–4), and high temperature (e.g., 60°C), as found in some hot springs and volcanic deposits (Schwertmann and Fitzpatrick, 1992) and has only recently been reported in soils (Fitzpatrick et al., 2008; Gao and Schulze, 2010a, 2010b). Laboratory synthesis showed that chloride is essential for the crystallization of akaganéite (Shah Singh and Kodama, 1994). The mechanism of feroxyhite formation in nature is unknown. It has been observed in rusty precipitates, formed in the interstices of sand grains from rapidly flowing Fe^{2+} -containing water, which was quickly oxidized (Carlson and Schwertmann, 1980). A possible association with dominant ferrihydrite in some typical Hydrandepts of Hawaii is reported by Parfitt et al. (1988). The similarity of the x-ray diffraction (XRD) patterns of feroxyhite and ferrihydrite makes it extremely difficult, however, to distinguish these minerals in natural samples (Carlson and Schwertmann, 1981).

The different types of Fe oxides may show a partial replacement of Fe by other cations. This substitution is conditioned

by the availability of cations that, in turn, makes it representative of specific environments of the Fe oxide formation, like a mineralogical–pedochemical signature. So far, such relationships have been established for Al substitution in goethites and for V^{3+} in goethite and hematite (Schwertmann and Pfab, 1994, 1996). Medium to high Al substitution (0.15–0.33 mol fraction) is usually observed in goethites from environments with low Si and high Al activity, found in highly weathered tropical and subtropical soils, bauxites, and saprolites (Fitzpatrick and Schwertmann, 1982; Curi and Franzmeier, 1984; Schwertmann and Kämpf, 1985; Anand and Gilkes, 1987a; Fontes et al., 1991; Singh and Gilkes, 1992; Muggler, 1998), whereas goethite with low substitution (0–0.15 mol fraction) prevails in slightly acidic, eutrophic soils and in redoximorphic soils (Fitzpatrick and Schwertmann, 1982). The occurrence of goethites with highly contrasting Al substitution indicates changes in the weathering rate or soil redox conditions (da Motta and Kämpf, 1991; Muggler, 1998). The presence of V^{3+} in goethite and hematite may be used as an indicator for former anoxic environments (Schwertmann and Pfab, 1996).

22.2.3 Influence on Soil Properties

Crystals of Fe oxides in soils are often extremely small, sometimes as small as 5 nm in diameter for poorly crystalline minerals like ferrihydrite or as small as 150 nm in diameter for better crystalline minerals like goethite and hematite. Structural disorder is common. Fe oxides, therefore, exhibit a large specific surface area (70–250 m² g⁻¹). They usually occur in higher amounts in comparison to Mn and Al oxides, they have a high point of zero charge (PZC; pH 7–9) and a pH-dependent surface charge. All these factors explain the substantial influence of Fe oxides on the physical and chemical properties of soils.

Significant correlations have been found between the sorption of heavy metals (Cu, Pb, Zn, Cd, Co, Ni, Mn), anions (PO_4 , SO_3 , MoO_4 , AsO_4 , Se_4O , S_4O , and organic anions), and the content and mineralogy of Fe oxides (Chapter 17).

The Munsell color ranges for the various Fe oxides are listed in Table 22.2. Detailed aspects of that subject are reviewed by Schwertmann (1993) and Cornell and Schwertmann (1996). The iron oxides may show a variation of color with their crystal size and the isomorphous substitution of Fe by foreign ions (Schwertmann, 1993). Basically, reddish soil color (Munsell hues 5YR and redder) is due to the presence of hematite (and maghemite in some tropical soils), masking the presence of goethite. Thus, the hematite content determines the redness of a soil (Torrent et al., 1983), while the yellow color due to goethite (Munsell hue between 7.5YR and 2.5Y) is expressed only in the absence of hematite. The presence of lepidocrocite is indicated by an orange color, normally restricted to mottles or localized spots in aquic environments. In surface soils, the colors due to Fe oxides may be masked by black organic compounds. Information about aeration and soil drainage can be inferred from the distribution or absence of different Fe oxide minerals in soils, according to their specific formation conditions described above.

Landscape sequences of red soils (hematite and goethite) on well-drained hilltops, through yellow soils (goethite) on moderately drained midslopes, to mottled and gray soils in poorly drained valleys are examples of Fe oxides acting as indicators of aerobic and anaerobic environments (Peterschmitt et al., 1996). Localized accumulations of Fe oxides (mottling, plinthite) and bleached matrix colors (chroma < 2), indicative of seasonal to permanent waterlogged soil environments, are used as diagnostic criteria for redoximorphic features and aquic regimes (Chapter 2).

The aggregating effect of Fe oxides in soils is indicated by significant correlations between the fraction of water-stable aggregates or related structural properties, and the content of Fe oxides (see Schwertmann and Taylor, 1989; Barthès et al., 2008), by electron microscopy (EM) observations of Fe oxide deposits on kaolinite platelets (Fordham and Norrish, 1979), and by the dispersion of aggregated soils after removal of their Fe oxides with a reducing agent (McNeal et al., 1968). Although an aggregating effect of the Fe oxides in soils is generally accepted, the exact mechanism remains obscure. Thin sections and scanning electron microscopy (SEM) observations of nodules, concretions, and ferricretes suggest that cementation develops through the growth of Fe oxide crystals in place between matrix particles, leading to a very stable, nondispersible association of matrix particles (Shafdan et al., 1985). Aggregates, on the other hand, seem to form through an attraction between positively charged Fe oxide particles and negatively charged matrix particles, mainly clay-sized phyllosilicates. A typical example of aggregation is the highly stable microaggregates (coffee powder structure) found in Oxisols. Because these aggregates are not dispersible in water, they have a significant influence on the water-holding capacity and the hydraulic conductivity of these soils (van Wambeke, 1992). On the other hand, these aggregates can be dispersed by organic ligands (oxalate, citrate) without solubilizing much iron (Pinheiro-Dick and Schwertmann, 1996).

22.2.4 Identification

22.2.4.1 Field Techniques

Fe oxides show striking colors, ranging between yellow and red. Particular colors are typical of the various forms and are helpful for their identification in the field (Table 22.2). Correlations have been established between Munsell hue and a redness or yellowness index based on hematite/goethite ratios and hematite content in soils (Torrent et al., 1983). Color alone is, however, not sufficient to unequivocally identify specific Fe oxide minerals. The presence of the magnetic Fe oxides, magnetite, and maghemite, can be easily detected in soils with a hand magnet (Schulze, 1988).

22.2.4.2 Chemical Dissolution Techniques

Chemical dissolution procedures for Fe oxides, initially proposed to eliminate their interference in the examination of phyllosilicates, were later developed to dissolve, and thus

to quantify, specific phases (see reviews by Borggaard, 1988; Parfitt and Childs, 1988). However, the identity of the dissolved phases must be determined by noninvasive techniques, such as XRD and Mössbauer spectroscopy. Potassium or Na pyrophosphate solutions have been used for estimating Fe (and Al) organic complexes (McKeague, 1967; Bascomb, 1968). The soil is usually shaken for 16 h with 0.1 M pyrophosphate at pH 10, but the extraction and clarification procedures are highly technique dependent (Schuppli et al., 1983; Loveland and Digby, 1984). For the extraction of short-range order Fe oxides (predominantly ferrihydrite), a 2 (Schwertmann, 1964) or 4 h (McKeague and Day, 1966) extraction with 0.2 M ammonium oxalate at pH 3 in the dark is widely used. This technique also extracts Fe from organic complexes and poorly crystalline lepidocrocite (Ohta et al., 1993), whereas some magnetites are partly dissolved. Ferrihydrite is more resistant to the 2 h oxalate treatment than ferrihydrite (Carlson and Schwertmann, 1980), and for schwertmannite, a 15 min treatment is used (Murad et al., 1994; Bigham et al., 1996b). According to Wang et al. (1993), a shorter oxalate treatment (~10–30 min) is more appropriate to measure ferrihydrite in <2 μm reductomorphic soil fractions than the much longer treatments commonly used for soils. For the complete dissolution of the pedogenic Fe oxide minerals, without dissolution of other minerals, a treatment with sodium dithionite–citrate–bicarbonate (DCB) is used. The extraction is carried out for 15 min at 75°C (Mehra and Jackson, 1960) or by shaking for 16 h with a dithionite–citrate solution at room temperature (Holmgren, 1967). However, as dissolution is affected by particle size, crystallinity (particularly for lithogenic magnetite and hematite) and high Al substitution (goethite and hematite), several DCB treatments may be required.

The ratio of oxalate-extractable Fe (Fe_o) to DCB-extractable Fe (Fe_d) quantifies the proportion of the more and less active fractions, respectively. A high Fe_o/Fe_d ratio and a loss in redness after oxalate treatment give first indication of ferrihydrite in a sample. Additionally, it is a useful parameter for characterizing soil properties (e.g., P sorption) and pedogenic processes (McKeague and Day, 1966; Blume and Schwertmann, 1969). The ratio of Fe_d to Fe_t (total Fe content by HCl or HF digestion) quantifies the proportion of Fe in primary silicate minerals, which has been released by weathering and precipitated as Fe^{3+} oxides, hence estimating Fe sources for potential Fe oxide formation and/or soil weathering stage. Advanced soil weathering stages, indicated by Fe_d/Fe_t ratios > 0.8, are usually shown by Oxisols and Ultisols.

A field test for the presence of Fe^{2+} ions and ferric-organic complexes in reductomorphic soils can be performed with a solution of α, α' -dipyridil (Childs, 1981; Kennedy et al., 1982) or with a solution of 1:10-phenanthroline (Richardson and Hole, 1979). Lovley and Phillips (1987) proposed the use of hydroxylamine hydrochloride to determine whether Fe^{3+} is available for microbial reduction. The amount of reducible Fe in natural wetlands and rice paddies is highly correlated to the labile and stable Fe^{3+} oxides (van Bodegom et al., 2003).

22.2.4.3 X-Ray Diffraction and Other Spectroscopic Techniques

The identification of the various Fe oxides requires physical methods, like XRD, differential thermal analysis (DTA), infrared spectroscopy (IR) (Cambier, 1986), Mössbauer spectroscopy (Murad, 1988, 1996), electron microscopy (EM) (Boudeulle and Muller, 1988; Eggleton, 1988), or magnetic measurements (Coe, 1988). A review of characterization methods for Fe oxides is given by Cornell and Schwertmann (1996) and Schwertmann and Taylor (1989). The most important diagnostic criteria are summarized in Tables 22.1 and 22.2. XRD patterns for the major soil Fe oxides are shown in Figure 22.3.

For powder XRD, unless one uses a monochromator, $CoK\alpha$ or $FeK\alpha$ radiation should be employed to avoid the high-fluorescence background that results when Fe-rich samples are irradiated with $CuK\alpha$ radiation. The sensitivity of XRD is improved by using a differential XRD method (Schulze, 1981) and selective dissolution treatments (Wang et al., 1993). Due to the low concentration of Fe oxides in soils, concentration techniques may be necessary (Schulze, 1988), like particle-size separation, magnetic separation (Schulze and Dixon, 1979), and, for goethite and hematite in kaolinitic soils, a 5 M NaOH treatment (Norrish and Taylor, 1961; Kämpf and Schwertmann, 1982a). A quantitative determination of Fe oxide minerals in soils is generally possible using the intensities of selected x-ray lines, DTA peaks, or Mössbauer hyperfine sextets. Suitable standards with the same characteristics may be isolated from soils or can be synthesized. The accuracy of the quantification can be controlled by comparison with the chemically determined total amount of Fe oxides (Fe_d) (Kämpf and Schwertmann, 1982b).

The Al substitution in goethite can be calculated from the unit-cell *c*-dimension by Al (mole fraction) = $17.30-57.20c$ (nm) (Schulze, 1984). The *c* value is obtained from the XRD positions $d(110)$ and $d(111)$ by $c = [1/d(111)^2 - 1/d(110)^2]^{-1/2}$, with all goethite data based on space group *Pbnm* (Table 22.1). In hematite, Al substitution is given by Al (mole fraction) = $31.09-61.71a$ (nm), where $a = d(110)2$, or, preferably, $a = d(300)2\sqrt{3}$ (Schwertmann et al., 1979).

22.3 Manganese Oxides

Manganese oxides are usually minor components in soils but with a significant influence on the soil chemical properties. While Mn is a micronutrient essential for plants and animals, it is the only plant essential element that also frequently occurs in toxic concentration in acid soils. The mineralogy of Mn oxides is complicated by the large number of minerals and the lack of precise knowledge of some of their structures, leading to uncertainties as to whether certain forms should be regarded as distinct mineral species, or merely as variants, or mixtures of other mineral forms (McKenzie, 1989; Post, 1992). The poor crystallinity and low concentration of these minerals in most soils is a further challenge for their characterization. A list of Mn oxides is given in Table 22.3. More information can be found in McKenzie (1989), Graham et al. (1988), and Dixon and White (2002).

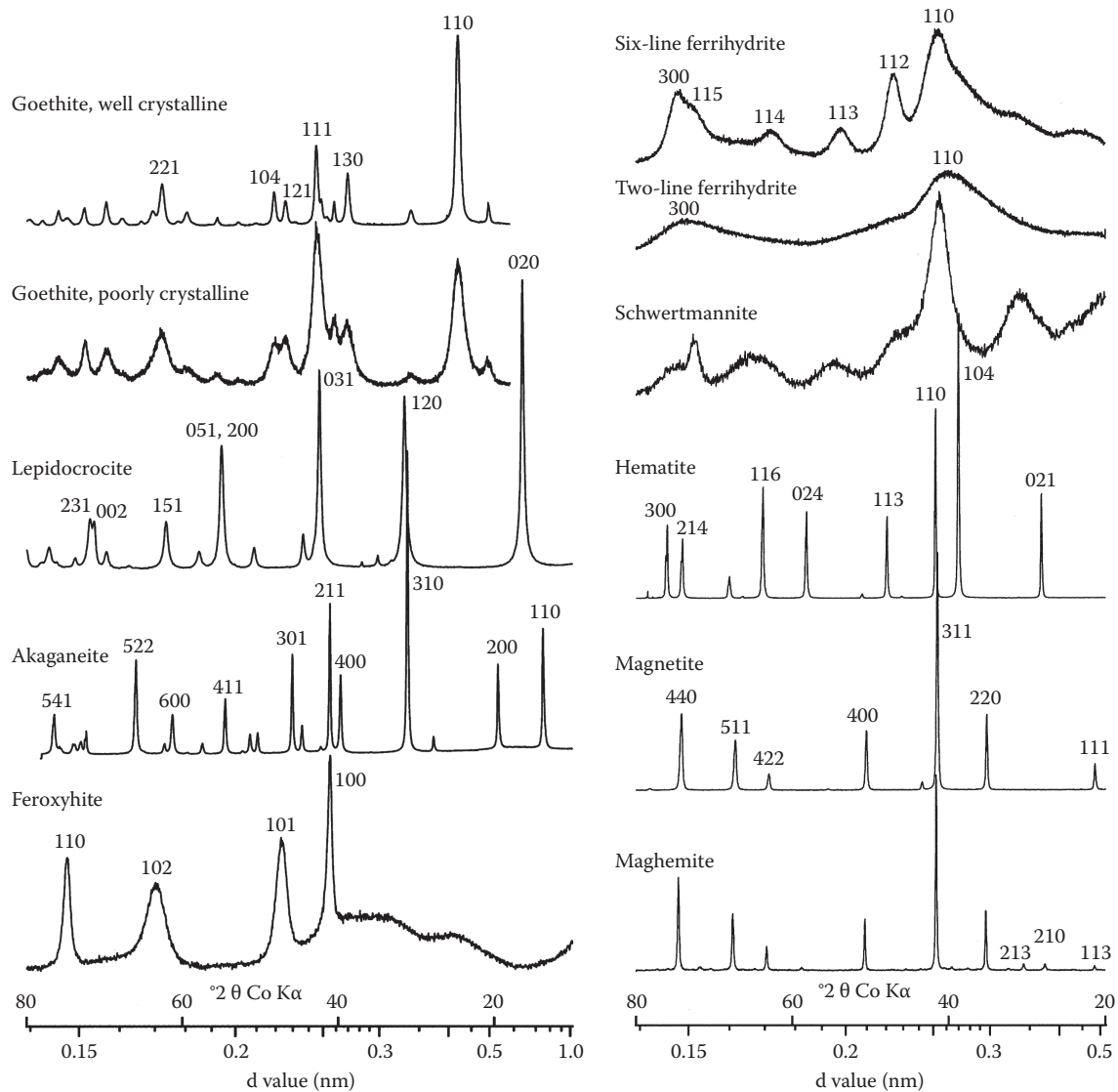


FIGURE 22.3 XRD patterns for the major soil iron oxide minerals (Co K α , peaks are labeled with their Miller indices). (From Cornell, R.M., and U. Schwertmann. 1996. *The iron oxides*. Wiley-VCH Verlag, Weinheim, Germany.)

22.3.1 Mineral Phases

Manganese oxides consist mainly of Mn in octahedral coordination. The various minerals differ in the arrangement and linkage of the octahedra. The Mn oxides may be placed into three groups: (1) Tectomanganates or tunnel structures, (2) phyllo-manganates or layer structures, both groups with mainly tetravalent Mn, and (3) the trivalent oxides or lower oxides.

22.3.1.1 Tectomanganates (Tunnel Structures)

Tectomanganates are formed from single, double, or wider chains of MnO₆ octahedra that are linked into a framework, thus forming tunnels (or channels) through the structures. These tunnels are occupied by large foreign cations and water molecules. Pyrolusite, ramsdellite, and nsutite are also referred

as chain structures because they do not contain tunnels but are included in the group of tectomanganates because of their structural similarity to the channel or tunnel structure members.

Pyrolusite, MnO₂, consists of single chains of edge-sharing MnO₆ octahedra linked by sharing corners to form 1 × 1 pseudotunnels (Figure 22.1; Baur, 1976). The single rows of unoccupied octahedral sites are not wide enough to accommodate foreign ions or water molecules. High-resolution transmission electron microscopy (HRTEM) of pyrolusite crystals showed lamellae with the structure of ramsdellite (Yamada et al., 1986). *Ramsdellite*, MnO₂, consists of double chains of MnO₆ octahedra forming 1 × 2 tunnels (Figure 22.1; Post, 1992), that possibly contain water molecules (Potter and Rossman, 1979). *Nsutite* has a structure formed by the intergrowth of pyrolusite-like single chains and ramsdellite-like double chains of octahedra

TABLE 22.3 Manganese Oxide Minerals: Crystallographic Properties and d Values for the Six Most Intense Diffraction Lines

Mineral (Synthetic Equivalent) ^a	Chemical Formula	Crystal System, Space Group	Unit-Cell Dimensions (Å)	Six Most Intense Diffraction Lines d Value (Å), Relative Intensity						References ^b
Pyrolusite; (β-MnO ₂)	MnO ₂	Tetragonal, <i>P4₂/mnm</i>	a = 4.398 c = 2.873	3.11 100	2.407 55	1.623 55	1.306 20	1.304 20	2.110 16	Baur (1976); 24-0735
Ramsdellite	MnO ₂	Orthorhombic, <i>Pnma</i>	a = 9.27 b = 2.866 c = 4.533	4.06 100	1.647 57	2.438 49	2.344 46	1.660 34	1.906 31	39-0375
Nsutite (γ-MnO ₂)	Mn ⁴⁺ Mn ³⁺ (O,OH) ₂	Hexagonal, <i>P</i>	a = 9.65 c = 4.43	1.635 100	4.00 95	2.33 70	2.42 65	2.13 45	1.60 45	Zwicker et al. (1962); 17-0510
Hollandite (α-MnO ₂)	Ba _x (Mn ⁴⁺ Mn ³⁺) ₈ O ₁₆ (x=1)	Monoclinic, <i>I2/m</i>	a = 10.026 b = 2.8782 c = 9.729 β = 91°03′	3.10 100	3.14 88	3.172 40	2.412 37	3.069 32	3.459 23	Post et al. (1982); 38-0476
Cryptomelane	K _x (Mn ⁴⁺ Mn ³⁺) ₈ O ₁₆ (x=1.3–1.5)	Monoclinic, <i>I2/m</i>	a = 9.956 b = 2.8705 c = 9.706 β = 90°95′	2.40 100	3.122 51	3.09 45	2.41 40	4.852 32	7.01 30	Post et al. (1982); 44-1386
Coronadite	Pb _x (Mn ⁴⁺ Mn ³⁺) ₈ O ₁₆ (x=1–1.4)	Monoclinic, <i>I2/m</i>	a = 9.938 b = 2.8678 c = 9.834 β = 90°39′	3.124 100	3.491 30	2.209 18	2.409 17	6.98 7	1.548 6	Post and Bish (1989); 41-0596
Romanèchite	Ba _{0.66} (Mn ⁴⁺ Mn ³⁺) ₅ O ₁₀ · 1.34H ₂ O	Monoclinic, <i>C2/m</i>	a = 13.919 b = 2.8459 c = 9.678 β = 92°39′	2.408 100	2.188 85	3.481 60	6.96 55	2.366 50	2.882 40	Turner and Post (1988); 14-0627
Todorokite	(Na,Ca,K) _{0.3–0.5} (Mn ⁴⁺ Mn ³⁺) ₆ O ₁₂ · 3.5H ₂ O	Monoclinic, <i>P2/m</i>	a = 9.764 b = 2.8416 c = 9.551 β = 94°06′	9.55 100	2.399 36	2.388 25	2.355 24	4.77 24	2.345 25	Post and Bish (1988); 38-0475
Chalcophanite	ZnMn ₃ O ₇ · 3H ₂ O	Trigonal, <i>R3</i>	a = 7.533 c = 20.794	6.93 100	2.228 40	4.07 29	1.590 23	3.507 19	2.550 17	Post and Appleman (1988); 45-1320

(continued)

TABLE 22.3 (continued) Manganese Oxide Minerals: Crystallographic Properties and d Values for the Six Most Intense Diffraction Lines

Mineral (Synthetic Equivalent) ^a	Chemical Formula	Crystal System, Space Group	Unit-Cell Dimensions (Å)	Six Most Intense Diffraction Lines d Value (Å), Relative Intensity						References ^b
Birnessite	(Na,Ca,Mn ²⁺)Mn ₇ O ₄ ·2.8 H ₂ O	Monoclinic, <i>C2/m</i>	Na: a = 5.175 b = 2.850 c = 7.337 β = 103°18'	7.14 100	3.57 27	2.519 14	2.429 13	2.154 7	2.222 5	Post and Veblen (1990); 43-1456
Vernadite (δ-MnO ₂)	MnO ₂ ·nH ₂ O	(Pseudo) tetragonal <i>I4/m</i>	a = 9.866 c = 2.844	2.39 100	3.11 60	2.15 60	1.827 40	1.537 40	1.422 40	Chukhrov et al. (1980); 15-0604
Rancieite	(Ca,Mn)Mn ₄ O ₉ ·nH ₂ O	Hexagonal, <i>P</i>	a = 8.68 c = 9.00	7.49 100	3.74 14	2.463 10	2.342 6	1.425 4	2.064 2	22-0718
Buserite	Na ₄ Mn ₁₄ O ₂₇ ·21H ₂ O	Orthorhombic	a = 17.5 b = 30.7 c = 10.2	10.1 100	5.01 70	3.34 50	1.46 50	2.56 30	2.47 30	32-1128
Lithiophorite	LiAl ₂ Mn ₂ ⁴⁺ Mn ³⁺ O ₆ (OH) ₆	Trigonal, <i>R3m</i>	a = 2.924 c = 28.169	4.71 100	9.43 68	2.371 24	1.880 14	3.143 7	1.453 4	Post and Appleman (1994); 41-1378
Groutite (α-MnOOH)	MnOOH	Orthorhombic, <i>Pbnm</i>	a = 4.560 b = 10.70 c = 2.870	4.20 100	2.81 70	2.67 70	2.30 60	1.695 50	2.38 40	Glasser and Ingram (1968); 12-0733
Manganite (γ-MnOOH)	MnOOH	Monoclinic, pseudoorthorhombic, <i>B2₁m</i>	a = 8.88 b = 5.25 c = 5.71 β = ~90°	3.40 100	2.64 24	1.782 21	2.417 17	1.672 17	2.414 16	Dachs (1963); in Bricker (1965); 41-1379
Feitknechtite (β-MnOOH)	MnOOH	Tetragonal, <i>P</i>	a = 8.6 c = 9.30	4.62 100	2.635 50	2.36 20	1.96 10	1.55 1	1.50 1	Bricker (1965); 18-0804
Hausmannite	Mn ₃ O ₄	Tetragonal, <i>I4₁/amd</i>	a = 5.7621 c = 9.4696	2.847 100	2.768 85	1.544 50	3.089 40	4.924 30	1.799 25	Bricker (1965); 24-0734
Manganosite	Mn ²⁺ O	Cubic, <i>Fm3m</i>	a = 4.4448	2.223 100	2.568 60	1.571 60	1.34 20	0.994 18	0.907 16	Sasaki et al. (1980); 7-0230
Bixbyite (α-Mn ₂ O ₃)	(Fe,Mn) ₂ O ₃	Cubic, <i>Ia3</i>	a = 9.4091	2.716 100	1.663 28	3.842 16	2.352 14	1.418 13	1.845 9	Geller (1971); 41-1442

^a Designation commonly used in the literature for a synthetic compound with the same crystal structure as the natural mineral are given in parentheses.

^b Numbers of the format XX-XXXX indicate ICDD file number (ICDD, 1994).

in random fashion (Zwicker et al., 1962; Potter and Rossman, 1979; Turner and Buseck, 1983). Inclusions of todorokite have also been found in nsutite (Turner and Buseck, 1983). *Hollandite*, *cryptomelane*, and *coronadite*, sometimes grouped as α - MnO_2 , consist of double chains of edge-sharing MnO_6 octahedra linked to form 2×2 tunnels (Figure 22.1; Post et al., 1982; Post and Burnham, 1986; Post and Bish, 1989). These minerals have the general formula $\text{A}_{0-2}(\text{Mn}^{4+}, \text{Mn}^{3+})_8(\text{O}, \text{OH})_{16}$. The tunnels contain water molecules along with the A cation, which is primarily Ba^{2+} in hollandite, K^+ in cryptomelane, and Pb^{2+} in coronadite. Natural samples usually contain a variety of cations in the tunnels. These large cations are located at specific tunnel sites, and their presence is necessary to prevent the structure from collapsing (Giovanoli, 1985a). The charges of the tunnel cations are balanced by the substitution of Mn^{4+} by Mn^{3+} ions. *Romanèchite* consists of double and triple chains of edge-sharing octahedra that share corners to form a framework containing 2×3 tunnels. The tunnels contain Ba^{2+} (and a variety of other large cations, such as Na, K, Sr) and water molecules (Figure 22.1; Turner and Post, 1988). The charges of the tunnel cations are balanced by the substitution of Mn^{4+} by Mn^{3+} ions. HRTEM images show that intergrowths of romanèchite and hollandite are common and are produced by the sharing of the double chains common to both minerals with double or triple chains occurring at random (Turner and Buseck, 1979). While romanèchite has also been called psilomelane, McKenzie (1989) used psilomelane for a structural type and Waychunas (1991) for mixtures of Mn oxide minerals. *Todorokite*, which had its structure and existence as a single mineral questioned until recently (Burns et al., 1985; Giovanoli, 1985b), consists of triple chains of edge-sharing MnO_6 octahedra linked to form large 3×3 tunnels (Post and Bish, 1988) containing Na, Ca, K, Ba, Sr, and water molecules (Figure 22.1). The octahedra at the edges of the triple chains are larger than those in the middle and, therefore, probably accommodate the larger, lower-valence cations (Mg^{2+} , Mn^{3+} , Cu^{2+} , Ni^{2+} , etc.) found in todorokite samples (Post and Bish, 1988). The occurrence of variable tunnel widths (3×2 , 3×3 , 3×4 , and 3×5) observed in HRTEM images suggests that todorokite represents a family rather than a single mineral (Turner and Buseck, 1981).

22.3.1.2 Phylломanganates (Layer Structures)

Chalcophanite has a layer structure composed of sheets of edge-sharing MnO_6 octahedra alternating with planes of Zn cations (but also Mn^{2+} , Ba, Ca, Mg, K, Pb, Cu, etc.) and water molecules (Figure 22.1; Ostwald, 1985; Post and Appleman, 1988). One of every seven octahedral sites in the Mn–O sheet is vacant, and the Zn cations are situated above and below the vacancies. The other phylломanganates are structurally analogous to chalcophanite, with Na^+ , Ca^{2+} , K^+ , and Mn^{2+} as interlayer cations. *Birnessite*, consists of a layer structure analogous to chalcophanite but with fewer vacancies in the octahedral sheets and with Na, K, or Mg replacing the Zn cations (Figure 22.1; Post and Veblen, 1990). The interlayer region contains water molecules as in chalcophanite. *Rancieite* has a layer

structure similar to birnessite, with Ca^{2+} as the main interlayer cation and interlayer water molecules (Bardossy and Brindley, 1978; Potter and Rossman, 1979; Chukhrov et al., 1980). The structure and existence in nature of *buserite*, also known as 10 Å manganite, are still unresolved. Buserite appears to have a layer structure similar to birnessite, with the larger, 10 Å layer spacing probably due to interlayer water (Waychunas, 1991). *Lithiophorite* has a layer structure comprising sheets of edge and corner-sharing MnO_6 octahedra alternating with sheets of $(\text{Al}, \text{Li})(\text{OH})_6$ octahedra (Figure 22.1; Post and Appleman, 1994). The cation sites in the Mn–O octahedral sheet are fully occupied, 2/3 with Mn^{4+} and 1/3 with Mn^{3+} . In the $(\text{Al}, \text{Li})\text{—OH}$ octahedral sheet, 2/3 of the sites are occupied by Al and 1/3 by Li cations. Lithiophorites with only traces of Li and others with wide variations in Ni, Co, Cu, and Zn concentrations inversely related to the Al content have been found (Ostwald, 1984a). According to Manceau et al. (1987, 1990), Co can occur within the octahedral Mn sheets, while Ni and Cu are located in the $(\text{Al}, \text{Li})\text{—OH}$ octahedral sheet, probably replacing Li, whereas in asbolane, Ni builds partial $\text{Ni}(\text{OH})_2$ sheets. Manceau et al. (1987) also found evidence for mixed layering between lithiophorite and asbolane, as observed by Ostwald (1984a). *Asbolane* has a layer structure with alternating sheets of $\text{Mn}^{4+}\text{—O}$ octahedra and Co–Ni–OH octahedra (Figure 22.1; Chukhrov and Gorshkov, 1981). The Co–Ni sheet may be discontinuous (island-like). The positive charge of the Mn^{4+} sheets is balanced by the negative charge of the Co–Ni sheets. Hydrogen bonding occurs between the oxygen atoms of the Mn sheets and the hydroxyl groups of the Co–Ni sheets. Most asbolanes are fine-grained, poorly crystalline minerals. *Vernadite* has been considered a disordered birnessite, lacking regular stacking in the c-axis. However, according to Chukhrov et al. (1980) and Chukhrov and Gorshkov (1981), it is a distinct mineral species with a disordered structure that has some similarity to that of birnessite, represented by layers of hexagonal close-packed O and water molecules in which less than half of the octahedra are occupied by Mn ions. Diffraction patterns of vernadite have only two d-spacings at ~ 2.4 and ~ 1.4 Å, whereas birnessite yields additional reflections at 7.0–7.2, 3.5–3.6 Å, and other spacings (Chukhrov et al., 1980).

22.3.1.3 Trivalent Manganese Oxides and Oxyhydroxides

Groutite (α - MnOOH) is isostructural with goethite and ramsdellite (Figure 22.1; Glasser and Ingram, 1968). *Feitknechtite* (β - MnOOH) has a structure similar to lepidocrocite (Figure 22.1), but its structure has not been refined (Waychunas, 1991). *Manganite* (γ - MnOOH) is similar to pyrolusite and rutile (Figure 22.1; Huebner, 1976). *Hausmannite* (Mn_3O_4) has a disordered spinel structure analogous to magnetite (Figure 22.1; Huebner, 1976). *Manganosite* has the NaCl structure and is of limited occurrence in nature (Huebner, 1976). *Bixbyite* (α - $(\text{Fe}, \text{Mn})_2\text{O}_3$) has an anion-deficient fluorite structure (Geller, 1971), while pure (synthetic) α - Mn_2O_3 is orthorhombic (Huebner, 1976; Waychunas, 1991).

22.3.2 Occurrence and Formation

Many studies have been made on the synthesis of Mn oxides (McKenzie, 1971; Hem and Lind, 1983; Giovanoli, 1985a) and the transformation of one form to another (Faulring et al., 1960; Bricker, 1965; Glasser and Smith, 1968; Rask and Buseck, 1986). Some of these studies, even if more applicable to diagenetic and hydrothermal conditions and to the formation of ore deposits, may be extrapolated to soil environments. Of the variety of Mn oxides found in terrestrial environments, only a few have been positively identified in soils. For example, nsutite and pyrolusite are common in Mn ore deposits (Zwicker et al., 1962; Varentsov, 1982) but have not been found in soils. Synthesis studies show that large amounts of foreign ions prevent the formation of nsutite, while even small amounts of foreign ions prevent the formation of pyrolusite. In soils, the foreign ions released by mineral weathering probably limit the formation of these Mn oxides, whereas in ore deposits, the abundance of Mn would aid in the removal of foreign ions, thus allowing the formation of nsutite and pyrolusite (McKenzie, 1989). According to Ostwald (1984b), the mineral associations birnessite–montmorillonite, chalcophanite–kaolinite, and lithiophorite–gibbsite observed in Australian Mn ore deposits may represent special cases of metasomatic replacements of clay minerals by phylломanganate minerals, whereas the occurrence of vernadite in a wide range of substrates is explained by its formation as a product of rapid microbial oxidation of Mn^{2+} (Chukhrov and Gorshkov, 1981).

Laboratory experiments show that Mn_3O_4 (hausmannite) is the initial product of the chemical oxidation of aqueous Mn^{2+} at 25°C in moderately alkaline solutions (pH 8.5–9.5). It converts to β - $MnOOH$ (feitknechtite) and then to γ - $MnOOH$ (manganite) by aging in solution (Hem and Lind, 1983; Murray et al., 1985). At 0°C, the initial product is feitknechtite, which converts to MnO_2 , identified as ramsdellite or birnessite (Hem and Lind, 1983). The formation and transformation of Mn oxides through successively increasing oxidation states are compatible with the common distribution of Mn oxides observed in supergene Mn ores (Bricker, 1965) and in lateritic weathering sequences (Parc et al., 1989). Minor inversions of that Mn oxidation sequence occur, however, due to the presence of foreign ions, thus promoting the formation of cryptomelane and lithiophorite instead of pyrolusite (Parc et al., 1989). The influence of microorganisms and organic compounds additionally increases the complexity of Mn oxide formation in soil environments.

Manganese is one of the first elements released during weathering of primary minerals, which explains its common accumulation in saprolites. Mobile in solution as Mn^{2+} , its oxidation to Mn^{3+} and Mn^{4+} and its subsequent precipitation is often accelerated by microorganisms (Ghiorse, 1988). Most of the Mn oxides found in surface environments are compounds of Mn^{4+} with some Mn^{3+} . The typical fine-grain size and poor crystallinity of the Mn oxides in soils are probably related to seasonal moisture changes, the presence of interfering organic and inorganic components in the soil solution, and the presence of multiple Mn oxidation states.

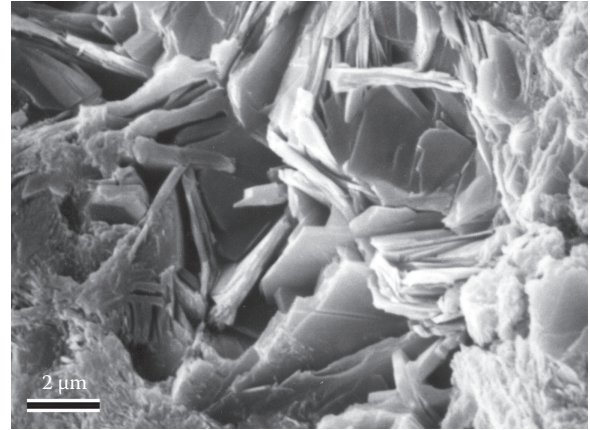


FIGURE 22.4 Scanning electron micrograph of the fractured surface of a nodule from a Tropeptic Eutrustox showing crystals of the Mn oxide mineral lithiophorite. (From Golden, D.C., J.B. Dixon, and Y. Kanehiro. 1993. The manganese oxide mineral, lithiophorite, in an Oxisol from Hawaii. *Aust. J. Soil Res.* 31:51–66.)

Manganese oxides are commonly of authigenic origin in soils, formed by direct chemical or biochemical precipitation from solution and by crystallization of poorly organized colloidal sols. However, little is known about the processes involved in their pedogenic formation. In most soils, Mn oxides occur as finely dispersed particles but may also be found as discontinuous black–brown coatings of ped surfaces (mangans), as pore fillings, and as concretions and nodules (Figure 22.4). Their presence and concentration are more likely in soil environments with alternate reducing and oxidizing conditions, which affect the mobility and the precipitation of Mn (White and Dixon, 1996). Thus, higher accumulations of Mn oxides are more frequent in soils with restricted drainage such as the aquic suborders (Aqualfs, Aquolls, Aquults, etc.), and intergrades (Aquic Hapludalfs, Aquic Dystrochrepts, etc.), and are also commonly found in saprolites. However, Mn accumulations in a soil are not necessarily an indication of a present redox environment but may reflect former wetter conditions (Allen and Hajek, 1989).

Mn and Fe oxides are usually associated in nodules with dominant silicates (quartz, clay minerals) that probably act as primary templates for the Mn and Fe oxidation and precipitation (Schwertmann and Fanning, 1976). Golden et al. (1986) demonstrated experimentally that Mn^{4+} oxide minerals can also act as oxidizing agents of Fe^{2+} ions in solution, causing the precipitation of Fe^{3+} oxides in association with Mn oxides. The crystal growth and progressive cementation of the nodules can be explained by an autocatalytic oxidation of Mn^{2+} adsorbed onto the formed Mn (and Fe) oxides (McBride, 1994). Thus, abiotic oxidation accelerates in response to the increased surface available for selective adsorption of Mn^{2+} . The overall process, of Mn oxidation and nodule formation, may also be promoted by Mn-oxidizing bacteria (Robbins et al., 1992; Ehrlich, 1996; Leinemann et al., 1997) and fungi (Thompson et al., 2005, 2006). Furthermore, microorganisms may indirectly control local environments, through elevation of pH and Eh, which favor

oxidation of Fe and Mn (Ghiorse and Ehrlich, 1992). Models of biotic oxidation of Mn (and Fe) are described by Ghiorse and Ehrlich (1992), Ehrlich (1990), and Tebo et al. (2004).

In soil samples from Australia, the abundance of Mn oxides decreased from birnessite and lithiophorite, over hollandite, to only one occurrence of each of pyrolusite and todorokite (Taylor et al., 1964). A high frequency of birnessite was also found in soils of other regions (Taylor, 1968; Ross et al., 1976). Todorokite formation from Mn released by the weathering of Mn-substituted siderite in lignite overburden was reported by Senkayi et al. (1986). Birnessite, lithiophorite, and lattice fringes attributed to todorokite were observed in nodules of a Vertic Argiustoll, while lithiophorite only was found in a Rhodic Paleudult (Uzochukwu and Dixon, 1986). Romanèchite was identified in nodules of a Typic Ochraqult (Robbins et al., 1992), and vernadite associated with feroxyhite was identified in a Scottish Gleyic Cambisol (Birnie and Paterson, 1991). Chukhrov and Gorshkov (1981), as cited by McKenzie (1989), reported that the most common Mn oxide in soils was vernadite, followed by birnessite, cryptomelane, todorokite, and hausmannite. Chukhrov and Gorshkov (1981) reported the presence of hausmannite in unspecified soils with pH ~ 8.2.

22.3.3 Influence on Soil Properties

The wide range of PZC values reported for synthetic samples of Mn oxides (Healy et al., 1966; Crowther and Dillard, 1983; Oscarson et al., 1983), from 1.5–3.5 for birnessite to 2.8–4.6 for the hollandite group and 6.4–7.3 for pyrolusite, is probably related to the synthesis conditions. In general, most Mn oxides have a PZC at a pH < 4.0, a high negative charge, a large range of surface area (5–360 m² g⁻¹), and show a strong specific adsorption of cations.

A high sorption capacity of Mn oxides for metal ions has been found by many authors (see Murray, 1975; McKenzie, 1989). In general, metal ions are sorbed in the increasing order Mg < Ca < Sr < Ba < Ni < Zn < Co < Mn < Cu < Pb (Murray, 1975), leading to the accumulation of relatively high concentrations of heavy metals (Childs, 1975; Sidhu et al., 1977) and actinides in the Mn oxides (Means et al., 1978; Cerling and Turner, 1982).

Manganese oxides are strong inorganic oxidants, thus affecting the availability or the hazard of particular metals. In the case of Co adsorption onto the birnessite surface at pH < 7, Co²⁺ is oxidized to Co³⁺ by Mn⁴⁺, with formation of Mn²⁺ in the process (Crowther and Dillard, 1983). The strong adsorption mechanism has a significant influence on the availability of Co to plants (Adams et al., 1969; McKenzie, 1978).

The Mn oxides have a major influence on the toxicity and bioavailability of As and Cr in terrestrial and aquatic environments. The reduced species As³⁺, which is more toxic, more soluble, and more mobile than the oxidized As⁵⁺ species, is effectively adsorbed and oxidized by Mn⁴⁺ oxides at pH < 6 (Oscarson et al., 1983; Thanabalasingam and Pickering, 1986; Scott and Morgan, 1995). However, the ability to deplete the concentration of As³⁺ in solution varies between different types of Mn oxides and is

related to the crystallinity, specific surface areas, and the PZC of the oxides. In contrast to other transition elements, Cr toxicity and mobility increase with its oxidation state. Thus, the presence of Mn oxides, as oxidizing agents for Cr³⁺ in soil systems, should be considered in disposal studies (Fendorf et al., 1992).

Manganese and Fe oxides also act as final electron acceptors oxidizing organic compounds and are conversely dissolved in the process. Organic compounds that form inner-sphere complexes with the oxide surface (e.g., catechol) dissolve the Mn oxide more quickly than those compounds that form outer-sphere complexes (e.g., hydroquinone) (Stone and Morgan, 1984a, 1984b; McBride, 1987). Lovley and Phillips (1988) found evidence that microorganisms can obtain energy for growth by coupling the oxidation of organic matter to the dissimilatory reduction of Fe³⁺ and Mn⁴⁺. They proposed a microbial food-chain model, in which fermentative organisms initially metabolize complex organic matter, and in the next stage, a separate group of bacteria oxidizes the fermentation products to CO₂ while reducing Fe³⁺ and Mn⁴⁺. The overall process may be an important degradative pathway for organic compounds and the formation of humic material, while the reduction and dissolution of Mn oxides increases the Mn mobility and bioavailability to organisms. Hui et al. (2003), for example, showed that aromatic amines are oxidized by soil Mn oxides resulting in the release of Mn²⁺ to solution.

22.3.4 Identification

Accumulations of Mn oxides in soils are readily identified by their characteristic black-brown coloration. The effervescence observed with the addition of H₂O₂ is a usual field criterion that helps to confirm the presence of these minerals. The small amount of Mn oxides in soils, the diffuse nature of the x-ray patterns of some of the minerals, and the coincidence of diagnostic lines with those of associated matrix minerals can make their identification by XRD difficult. Thus, XRD, preferably with Fe K α radiation, can be used only where natural segregations of the minerals occur, such as nodules, veins, or coatings. Even then, a concentration pretreatment may be necessary. Powder XRD patterns for some of the more important Mn oxide minerals are shown by Post (1992) and the most intense XRD lines of the major minerals are listed in Table 22.3. Because of the lower crystallinity, soil Mn oxides may, however, show some deviation from these patterns. A selective dissolution of Mn oxides with acidified hydroxylamine hydrochloride was proposed by Chao (1972), whereas Tokashiki et al. (1986) characterized Mn oxides by using successive sodium hydroxide, hydroxylamine hydrochloride, and DCB treatments. Concentration procedures for Mn oxides, selective chemical treatments, and identification by XRD and thermal methods are also reported by Uzochukwu and Dixon (1986). A comprehensive compilation of IR powder-absorption spectra of synthetic and naturally occurring Mn oxides is given by Potter and Rossman (1979).

Crystal structure and crystal chemistry refinements have been performed with HRTEM, electron-microprobe analysis, electron diffraction, powder XRD with Rietveld analysis

(Post and Appleman, 1988; Post and Bish, 1988; Post and Veblen, 1990), and x-ray absorption spectroscopy (Manceau et al., 1987, 1992a, 1992b; Manceau and Combes, 1988). HRTEM has led to the discovery of complex intergrowths of variable lattice periodicities in some Mn oxides (Turner and Buseck, 1979, 1981, 1983; Yamada et al., 1986).

22.4 Aluminum Oxides

Of six different Al oxide minerals, gibbsite and, less commonly, boehmite form under soil conditions. Nordstrandite and bayerite have only been identified in restricted geologic environments. Diaspore and corundum are occasionally found in bauxite deposits but are rare in soils. The relative rarity of Al oxide minerals in soils, which is in contrast to their structural Fe analogs, may be explained by the competitive formation of aluminosilicates and by the difficulty of identifying small amounts of these minerals by XRD (Taylor, 1987). More information on Al oxides is given by Hsu (1989) and Huang et al. (2002).

22.4.1 Mineral Phases

Crystallographic properties for the Al oxide minerals likely to occur in soils are listed in Table 22.4. Aluminum occurs exclusively in octahedral coordination in the Al oxides, and the

structures can be described in terms of the arrangement and linkage of Al-containing octahedra.

22.4.1.1 Hydroxides

Gibbsite (γ -Al(OH)₃) consists of sheets of edge-shared octahedra with two-thirds of the available octahedral sites filled with Al³⁺ ions. The occupied octahedral sites form sixfold rings, analogous to the dioctahedral sheet of phyllosilicates. The octahedral sheets are stacked along the c-axis, and the OH groups in one sheet reside directly above those in the next, rather than in the position of closest packing. The interlayer attractions are weak and are dominated by hydrogen bonding (Figure 22.1; Hsu, 1989). *Bayerite*, a second polymorphic form of Al(OH)₃, is analogous to gibbsite except that the OH groups of one sheet reside in the depressions between the O atoms of the next sheet and are in the close-packing position (Figure 22.1; Hsu, 1989). *Nordstrandite*, a third polymorphic form of Al(OH)₃, has a structure in which the stacking of the octahedral sheets alternate between the gibbsite and bayerite arrangements (Hsu, 1989). In addition to these crystalline phases, amorphous Al(OH)₃ may occur in soils (Süsser and Schwertmann, 1991). *Doyleite*, a fourth polymorphic form of Al(OH)₃, has a structure of sheets of edge-sharing octahedra (Chao et al., 1985) and is a rare hydrothermal mineral not found in soils.

TABLE 22.4 Aluminum Oxide Minerals: Crystallographic Properties and d Values for the Six Most Intense Diffraction Lines

Mineral	Chemical Formula	Crystal System, Space Group	Unit-Cell Dimensions (Å)	Six Most Intense Diffraction Lines d Value (Å), Relative Intensity						References ^a
Gibbsite	γ -Al(OH) ₃	Monoclinic, <i>P2₁/n</i>	a = 8.6552 b = 5.0722 c = 9.7161 $\beta = 94^{\circ}607'$	4.85 100	4.371 70	2.385 55	4.32 50	2.45 40	2.05 40	33-0018
Nordstrandite	Al(OH) ₃	Triclinic, <i>P1</i>	a = 5.082 b = 5.127 c = 4.980 $\alpha = 93^{\circ}40'$ $\beta = 118^{\circ}55'$ $\gamma = 70^{\circ}16'$	4.79 100	2.27 30	4.32 25	2.393 25	2.016 25	1.902 20	24-0006
Bayerite	Al(OH) ₃	Monoclinic, <i>P21/a</i>	a = 5.062 b = 8.671 c = 4.713 $\beta = 90^{\circ}27'$	2.222 100	4.71 90	4.35 70	1.723 40	3.20 30	1.333 18	20-0011
Doyleite	Al(OH) ₃	Triclinic, <i>P1</i> or <i>P1</i>	a = 5.00 b = 5.17 c = 4.98 $\alpha = 97.5^{\circ}$ $\beta = 118.6^{\circ}$ $\gamma = 104.74^{\circ}$	4.794 100	2.36 40	1.972 30	1.857 30	1.842 30	4.29 20	Chao et al. (1985)
Diaspore	α -AlOOH	Orthorhombic, <i>Pbnn</i>	a = 4.396 b = 9.426 c = 2.844	3.99 100	2.317 56	2.131 52	2.077 49	1.633 43	2.558 30	05-0355
Boehmite	γ -AlOOH	Orthorhombic, <i>Amam</i>	a = 3.70 b = 12.227 c = 2.868	6.11 100	3.164 65	2.346 55	1.86 30	1.85 25	1.453 16	21-1307
Corundum	α -Al ₂ O ₃	Rhombohedral, <i>R3c</i>	a = 4.7592 c = 12.992	2.086 100	2.551 98	1.60 96	3.48 72	1.374 57	1.74 48	43-1484

^a Numbers of the format XX-XXXX indicate ICDD file number (ICDD, 1994).

22.4.1.2 Oxyhydroxides

Diaspore (α -AlOOH) is isostructural with goethite (Figure 22.1; Ewing, 1935a, 1935b; Busing and Levy, 1958). *Boehmite* (γ -AlOOH) has the same structure as lepidocrocite (Figure 22.1). Poorly crystalline boehmite, formerly also called pseudo-boehmite, has a restricted number of unit cells along the b-axis (Tettenhorst and Hofmann, 1980).

22.4.1.3 Oxides

Corundum (α -Al₂O₃) is isostructural with hematite (Figure 22.1; Maslen et al., 1993).

22.4.2 Occurrence and Formation

Aluminum is a common element in primary silicate minerals, from which it may be released by weathering. Depending on the environmental conditions, the free Al hydrolyzes and precipitates as Al hydroxide or oxyhydroxide, and then crystallizes. The reason this fails to occur in many soils is because aluminum usually binds to silicon to form aluminosilicate clay minerals. Only in the most intense leaching environments is the Si concentration low enough that gibbsite may form. However, the detailed chemistry of Al oxide formation in soils remains obscure, mainly because of the uncertainties in the formation and the type of hydroxy polymers involved.

Synthesis studies have, so far, given an approximate outline of the probable processes of Al-hydroxide formation. The development of Al-hydroxide polymorphs appears to be related to the rate of precipitation, pH of the system, clay mineral surfaces, and the nature and concentration of inorganic and organic anions (Huang, 1988; Hsu, 1989). Only synthesis experiments related to pedogenic environments are summarized here. At room temperature, gibbsite forms in acid solutions (pH < 6) under slow hydrolysis, nordstrandite in neutral to alkaline solutions (pH > 7), and bayerite in alkaline solutions under fast hydrolysis (Hsu, 1966; Schoen and Roberson, 1970). These conditions agree with the natural occurrence of gibbsite in highly weathered acidic soils, whereas nordstrandite and bayerite have been found in association with limestone materials. Thermodynamically, gibbsite is the most stable of the three Al(OH)₃ polymorphs (Hemingway et al., 1991).

Anions that have strong affinity for Al³⁺, such as SO₄²⁻, CO₃²⁻, PO₄⁴⁻, and SiO₃²⁻, may interfere with the crystallization of Al(OH)₃ (Huang, 1988; Hsu, 1989). Organic ligands like citric, malic, tannic, aspartic, and fulvic acids block the coordination sites of polynuclear Al ions and restrain the hydrolysis, inhibiting the crystallization of Al(OH)₃ and influencing the nature of the precipitated compound (Kodama and Schnitzer, 1980; Violante and Violante, 1980; Violante and Huang, 1985; Singer and Huang, 1990). This explains why little or no gibbsite is found in the A horizon of acidic soils high in organic matter and exchangeable Al, while it is found in greater quantities in deeper horizons.

The pathway for gibbsite formation by direct desilication of primary Al silicates or through clay mineral intermediates (Jackson, 1964) is conditioned by the intensity of leaching, which,

in turn, is affected by rainfall, temperature, parent rock, topography, groundwater table, vegetation, and time. Environments with warm temperatures, high rainfall, and free drainage favor desilication and leaching of ions, as well as mineralization of organic matter. Oxisols and laterites found in these environments may have significant amounts of gibbsite associated with kaolinite and Fe oxides (Curi and Franzmeier, 1984; Macedo and Bryant, 1987). Gibbsite is frequently a minor component in ultisols, which are widespread in humid tropical, subtropical, and temperate regions (Allen and Hajek, 1989). High amounts of gibbsite may be found under temperate climates in deeper parts of soil profiles submitted to higher leaching rates (Norfleet et al., 1993; Ogg and Baker, 1999). The porosity of the soil parent material is important in determining whether or not gibbsite forms. In Kenya, for example, soils formed in porous volcanic ash on the slopes of Mt. Kenya contain considerably more gibbsite than soils from western Kenya formed from hard igneous and metamorphic rocks (Obura, 2008).

Nordstrandite has been found in nature as crystals radiating into solution cavities in limestone from Guam (Hathaway and Schlanger, 1965) and as small pellets in a limestone soil from Borneo (Wall et al., 1962). Bayerite found in calcareous material in Israel probably formed under hydrothermal conditions (Gross and Heller, 1963). The apparent rarity of bayerite and nordstrandite in soils may reflect identification difficulties, due to their low concentration and/or masking by the presence of gibbsite.

The same factors may be responsible for the rare reports of boehmite in soils (Taylor, 1987). Boehmite has been identified in lateritic materials (Gilkes et al., 1973) and together with diaspore in bauxites (Vgenopoulos, 1984). Boehmite often occurs in bauxite deposits in association with gibbsite, from which it is considered to form through partial dehydration by diagenesis or hydrothermal alteration. Hughes et al. (1994) identified boehmite in native American artifacts from an Ordovician-age paleosol in northwestern Illinois. The formation of poorly crystalline boehmite has been attributed to the presence of foreign ions during crystallization (Hsu, 1967). Since poorly crystalline boehmite alters to crystalline Al(OH)₃ polymorphs on removal of the foreign ions from the environment, the occurrence of crystalline boehmite in soils, other than those derived from bauxite, may be less common than believed (Taylor, 1987).

Diaspore in association with minor amounts of goethite has been identified as a surface weathering product formed by the desilication of a kaolinitic clay in Missouri (Keller, 1978). The possible influence of Fe in diaspore formation is supported by synthesis experiments and natural rock weathering and bauxite occurrences (Taylor, 1987). The formation of Fe-substituted diaspore is, however, unlikely because the large Fe³⁺ does not fit into the diaspore structure, in contrast to the substitution of the smaller Al³⁺ in the larger goethite structure (Davies and Navrotsky, 1983). In confirmation, Fe in a diaspore crystal has been identified as a hematite-like cluster (Hazemann et al., 1992).

Corundum occurs in pegmatites and other rocks associated with nepheline syenites, in high-grade aluminous metamorphic rocks, in aluminous xenoliths in igneous rocks, in

metamorphosed bauxitic deposits, and as a detrital mineral in sediments (Deer et al., 1992). Reports of corundum in soils are scarce, but because of its high resistance to weathering, it can be found as a residual mineral of igneous or thermally metamorphosed rocks, like in lateritic bauxites of Australia (Taylor et al., 1983) and in Brazilian Oxisols (Macedo and Bryant, 1987). In some Australian soils derived from corundum-free rocks, the presence of corundum is attributed to the heating of the soil by bush fires (Wells et al., 1989). The corundum may have formed in association with hematite by the dehydroxylation of Al-goethite. The associated crystallization of isostructural hematite may have acted as a template for the nucleation of corundum, thereby reducing the activation energy and enabling its formation at relatively low temperature via the epitaxial growth on hematite.

22.4.3 Influence on Soil Properties

Because of the high surface area ($100\text{--}220\text{ m}^2\text{ g}^{-1}$), high PZC (pH 5–9), and a variable surface charge, Al oxides favorably chemisorb heavy metals (Cu, Pb, Zn, Ni, Co, Cd) and anions (PO_4^{4-} , SiO_3^{2-} , MoO_4^{2-} , SO_4^{2-} , catechols) (Hingston et al., 1974; McBride and Wesselink, 1988; McBride, 1989). The adsorption is related to the reactive (singly coordinated OH^- groups at crystallite edges) rather than the total surface area. The high P retention in Oxisols and Ultisols is usually related to the content of gibbsite, in addition to that of Fe oxides (Juo, 1981; van Wambeke, 1992). Synthesis studies have shown the effectiveness of $\text{Al}(\text{OH})_3$ precipitates in improving the physical properties of soils and clay minerals (see Hsu, 1989). Aluminum oxides, mainly gibbsite, in addition to Fe oxides, are strongly associated with the aggregation of Oxisols and Ultisols, but the mechanism of aggregation is unclear.

22.4.4 Identification

Crystalline Al oxides can be identified and quantified by XRD, thermal analysis, IR, and EM with a combination of several methods being necessary. Currently, no selective dissolution methods are known for the specific dissolution of crystalline and noncrystalline Al forms in soil samples, but acid NH_4^+ oxalate treatment (Schwertmann, 1964) is frequently used to estimate the content of undefined, poorly crystalline Al forms in soils. The problems inherent in the identification of poorly crystalline Al oxides in the presence of clay minerals are illustrated by Violante and Huang (1994). By XRD analysis, the detection limit of poorly crystalline boehmite in samples containing kaolinite or montmorillonite was approximately 30%–40%. When both kaolinite and montmorillonite were present, however, the identification by DTA, IR, or TEM often failed even for concentrations of boehmite as high as 50%–80%.

Under the electron microscope, well-crystallized gibbsite occurs as hexagonal plates (Hsu, 1989) or as elongated hexagonal rods in synthetic crystals (Tait et al., 1983). Euhedral gibbsite crystals from a bauxite zone in a deep lateritic weathering profile are shown in Figure 22.5. Bayerite frequently occurs as a triangular pyramid, with its long direction perpendicular to the basal

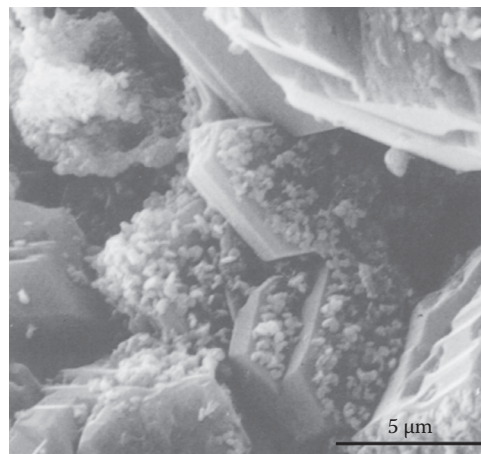


FIGURE 22.5 Scanning electron micrograph from a bauxitic zone in a deep lateritic profile from the Jos plateau, Nigeria, showing hematite crystal aggregates on large euhedral gibbsite crystals. (From Zeese, R., U. Schwertmann, G.F. Tietz, and U. Jux. 1994. Mineralogy and stratigraphy of three deep lateritic profiles of the Jos plateau (central Nigeria). *Catena* 21:195–214.)

plane (Schoen and Roberson, 1970; Violante and Jackson, 1981; Hsu, 1989). Synthetic nordstrandite shows rectangular plates, elongated parallelograms, ill-defined ovoidal particles, or clusters of acicular crystals (Shoen and Roberson, 1970; Violante and Jackson, 1979, 1981; Violante et al., 1982; Tait et al., 1983). With the exception of gibbsite, many of these crystal shapes seem to occur only in synthetic Al oxides.

22.4.4.1 X-Ray Diffraction

The main XRD peaks of the Al oxides are listed in Table 22.4. For specimens with poor crystallinity, these diffraction peaks may not be completely resolved. Gibbsite in soils can be quantified by XRD, but it will not be detected if its content is below about 50 g kg^{-1} (Jackson, 1969). The strongest peak for boehmite is the $d(020)$ at 6.11 \AA , while very fine boehmite particles show a broadening and an apparent line shift of the $d(020)$ peak to larger d -spacings due to a diffraction effect (Tettenhorst and Hoffman, 1980).

22.4.4.2 Thermal Analysis

DTA is frequently used for the identification of Al hydroxides and oxyhydroxides (Mackenzie, 1970, 1972; Karathanasis and Harris, 1994). The presence of 10 g kg^{-1} gibbsite can be detected by DTA, and its amount can be estimated by comparing the 300°C – 330°C endothermic peak with those of standards. The peak temperature for bayerite is only slightly lower than that for gibbsite, so that their differentiation in natural samples is impossible (Karathanasis and Harris, 1994). In soil samples, the 300°C – 330°C peak may overlap with that of goethite, requiring an additional DTA curve after the removal of goethite with sodium dithionite (Jackson, 1969). Diaspore yields an endothermic peak at 540°C , whereas boehmite has a peak that occurs in the range of 450°C – 580°C depending on crystallinity and particle size. The overlap with the kaolinite peak at 550°C limits the identification of these oxyhydroxides.

22.4.4.3 Infrared Absorption Analysis

Characteristic OH-stretching absorption spectra have been used to identify $\text{Al}(\text{OH})_3$ and AlOOH polymorphs in monomineralic samples. Gibbsite shows three absorption bands and another doublet, with reported bands for well-crystallized natural gibbsite at 3622, 3627, 3460, 3396, and 3384 cm^{-1} . Each of the absorption bands may shift slightly to lower wave numbers with decreasing crystallinity (Elderfield and Hem, 1973). The 3622 cm^{-1} absorption band is coincident with that of kaolinite and micaceous clays (Farmer and Russel, 1967), thus precluding its use for the identification of gibbsite. Boehmite and diaspore each show two OH-stretching bands, boehmite at 3087 and 3283 cm^{-1} and diaspore at 2922 and 2990 cm^{-1} (Ryskin, 1974). Raman microprobe spectroscopy offers an alternative procedure in characterizing $\text{Al}(\text{OH})_3$ polymorphs in soils (Rodgers, 1993).

22.5 Silicon Oxides

The Si oxides occurring in soils are given in Table 22.5. In nature, the SiO_2 polymorphs (quartz, tridymite, and cristobalite) occur as both higher temperature or β -phases and lower temperature or α -phases. In soils, however, only the α -phases are usually found. Opal is a hydrated form of Si of both biogenic and inorganic origin. Microcrystalline quartz, or microquartz, occurs in the form of chalcedony and chert (Heaney, 1994). Microcrystalline fibrous α -quartz, in the form of chalcedony, usually occurs as a secondary infilling of seams and cavities within rocks, sometimes creating concentrically banded agates or geodes. An intergrowth of authigenic microcrystalline α -quartz grains, which range in size from <1 to 50 μm , occurs in highly silicified sedimentary rocks in the form of chert (Knauth, 1994). More information about Si

oxides can be found in Drees et al. (1989), Heaney et al. (1994), and Monger and Kelly (2002).

22.5.1 Mineral Phases

The Si oxides are tectosilicates. The repeating unit is a SiO_4 tetrahedron in which each O is linked to Si atoms of adjacent tetrahedra, forming a 3D framework structure. This contrasts with the Fe, Al, Mn, and Ti oxides in which the basic unit is a cation in octahedral coordination. The pattern of the tetrahedral linkage is different for each Si oxide polymorph, and this difference is reflected in their structural, physical, and chemical properties. The structures of the α -phases are closely related to those of their high-temperature β -phase equivalents. Quartz consists of paired helical chains of corner sharing SiO_4 tetrahedra that spiral along the Z-axis (Heaney, 1994). The intertwined chains produce open channels parallel to c (Z) that appear hexagonal in projection (Figure 22.1). In *tridymite* and *cristobalite*, the idealized fundamental module consists of a sheet containing six-member rings of SiO_4 tetrahedra, with the tetrahedra alternately pointing above and below the plane defined by the basal oxygen atoms (Heaney and Banfield, 1993). Tridymite and cristobalite are differentiated by a different stacking arrangement of this tetrahedral sheet. In tridymite, the sheets are stacked such that the hexagonal rings (ditrigonal and oval rings in α -tridymite structures) lie directly over one another, creating continuous tunnels normal to the sheets (Figure 22.1). These tunnels account for the lower density of tridymite (2.26 g cm^{-3}) as compared to quartz (2.65 g cm^{-3}). In cristobalite, the stacking involves three sheets that are translated relative to one another such that the hexagonal rings

TABLE 22.5 Silicon Oxide Minerals: Crystallographic Properties and d Values for the Six Most Intense Diffraction Lines

Mineral	Chemical Formula	Crystal System, Space Group	Unit-Cell Dimensions (Å)	Six Most Intense Diffraction Lines ^a						References ^b
				d Value (Å)	Relative Intensity					
α -Quartz	SiO_2	Trigonal, $P3_121$	a = 4.912 c = 5.403	3.342 100	4.257 22	1.818 14	1.542 9	2.457 8	2.282 8	Will et al. (1988, in Heaney, 1994); 33-1161
α -Tridymite	SiO_2	Monoclinic, $C222_1$	a = 10.04 b = 17.28 c = 8.20 $\beta = 91^\circ 50'$	4.08 100	4.28 93	3.80 68	3.24 48	2.48 35	2.382 21	Heaney (1994); 42-1401
α -Cristobalite	SiO_2	Tetragonal $P4_12_12$	a = 4.969 c = 6.925	4.04 100	2.487 13	2.841 9	3.136 8	2.467 4	1.929 4	Schmahl et al. (1992, in Heaney, 1994); 39-1425
Opal (natural)				4.08 100	2.51 30	2.86 10	3.14 9	1.937 5	1.878 5	38-0448
Opal-C					~ α -Cristobalite + 4.3					Drees et al. (1989)
Opal-CT				4.10	4.29	2.50	3.34	3.18	2.85	Drees et al. (1989)
				vs	s	s	w	w	w	
Opal-A				4.1	2.0	1.5	1.2			Drees et al. (1989)
				sb	wd	wd	wd			

^a vs, Very strong; s, strong; w, weak; sb, strong broad; wd, weak diffuse.

^b Numbers of the format XX-XXXX indicate ICDD file number (ICDD, 1994).

(oval rings in α -cristobalite) do not superimpose (Figure 22.1). Thus, cristobalite lacks the continuous tunnels normal to the layers as in tridymite, but tunnel structures are formed parallel to the layers. Thus, the density of cristobalite is only slightly higher than that of tridymite (2.32 g cm^{-3}).

Opal is classified into three structural groups based on XRD powder patterns: Opal-C (well-ordered α -cristobalite), opal-CT (disordered α -cristobalite, α -tridymite), and opal-A (highly disordered, nearly amorphous) (Jones and Segnit, 1971; Deer et al., 1992), in a sequence of decreasing structural order. In opal-C, the stacking is predominantly cristobalitic, which is revealed by weak superstructure XRD reflections characteristic of α -cristobalite. Opal-CT consists of random stackings of α -cristobalite- and α -tridymite-like arrangements, yielding a disordered crystal structure. The microstructure of opal-CT is composed of small spheres less than $5 \mu\text{m}$ in diameter, called lepispheres, which consist of an interpenetrative growth of tiny cristobalite and tridymite blades (Hesse, 1988; Graetsch, 1994). Opal-A is a noncrystalline hydrous Si polymorph ($\text{SiO}_2 \cdot n\text{H}_2\text{O}$) differing from the crystalline polymorphs in that it lacks long-range atomic order. The microstructure of opal-A shows the closest packing of spheres of Si with diameters ranging from 10 to 50 nm (Greer, 1969) with water filling the interstices (Graetsch, 1994). The specific gravity of biogenic opal from soils and plants varies continuously over the range 1.5–2.3, with modal values from 2.10 to 2.15 g cm^{-3} (Drees et al., 1989). The broad range is a function of the submicron opal structure, H_2O content, occluded organic matter, and microscopic voids.

Quartz is one of the purest minerals known, and due to its more closed structure, it is purer than the other Si oxide polymorphs (Drees et al., 1989). Nevertheless, common trace elements in quartz, either interstitial or as substitutions, occur and include Al, Ti, Fe, Na, Li, K, Mg, Ca, OH. Both cristobalite and tridymite, which are also the major structural constituents of opal-CT, may accommodate more impurities than quartz because of their more open framework structure. The predominant impurity is Al, with lesser amounts of Fe, Ti, K, Na, Ca, and Mg. Opal-A contains $850\text{--}950 \text{ g kg}^{-1}$ of SiO_2 , $40\text{--}90 \text{ g kg}^{-1}$ of bound H_2O , and significant amounts of occluded, chemisorbed, or solid-solution impurities of Al, Fe, Ti, Mn, P, Cu, N, C, alkalis, and alkaline earths (Drees et al., 1989).

22.5.2 Occurrence and Formation

Quartz is a common constituent in many igneous, sedimentary, and metamorphic rocks, and also occurs as a secondary mineral, forming cementing materials in sediments. Tridymite is a typical mineral of acid volcanic rocks together with cristobalite that also occurs in basaltic rocks. Tridymite is also a common constituent of highly metamorphosed impure limestones and arkoses adjacent to basic igneous intrusions, while cristobalite occurs in metamorphosed sandstones and sandstone xenoliths in basic rocks. Opal is found in sedimentary, volcanic, and marine environments (Deer et al., 1992). Thus, quartz is the most abundant Si oxide in soil environments, cristobalite occurs

in soils developed from volcanic materials, opal may be a significant component of soils, but tridymite occurs only rarely.

Quartz in soils is mainly a primary mineral, inherited from the parent material. The higher stability of quartz compared to other silicate minerals is explained by its crystallization from magma closer to present earth-surface conditions. The higher stability of quartz relative to the other Si oxide polymorphs is due to a denser packing of the crystal structure and a higher energy required to break the Si–O–Si bond. Quartz in chert forms through a diagenetic transformation from opal-A via opal-CT and opal-C (Hesse, 1988). As demonstrated experimentally, quartz may also precipitate directly (Mackenzie and Gees, 1971). Authigenic quartz in the form of chemical precipitations and grain overgrowths frequently occurs in sediments (carbonates, sandstones) and is believed to form in soils, too (Drees et al., 1989).

Quartz is generally concentrated in the sand and silt fractions of soils, with a lower frequency in the coarse-clay fraction ($0.2\text{--}2 \mu\text{m}$). The depth distribution of quartz is a function of parent material and degree of weathering (Drees et al., 1989). In relatively undifferentiated soils (Entisols and Inceptisols), distributions of quartz reflect mainly variations in parent material. Quartz may comprise $>90\%$ of the inorganic fraction of Quartzipsamments. In Aridisols, quartz is generally abundant due to restricted weathering, while in moderately weathered soils (Spodosols, Alfisols, Mollisols, and Ultisols), the eluvial horizons are enriched in quartz relative to the parent material due to the weathering and removal of less resistant minerals. Conversely, illuvial horizons have lower quartz contents than eluvial horizons or parent materials due to the dilution by silicate clays, carbonates, or oxides. Highly weathered and leached Oxisols have only very low amounts of quartz left in the clay fraction.

Opal-CT, opal-C, and α -cristobalite are usually limited to specific geographic regions and rock-stratigraphic units. Opal-C and α -cristobalite have been reported in Andepts and other soils derived from volcanic material in South America, New Zealand, Central America, and Japan. Opal-CT has been identified in bentonites, siliceous shales, and indurated silicates. As a consequence, soils developed in these materials commonly contain opal-CT. It is also a primary constituent of many cherts, porcelanites, fossil wood, silcretes, and some duripans (Drees et al., 1989). According to synthesis experiments and evidence from diagenetic environments, opal-A transforms to opal-CT and quartz by a series of dissolution–precipitation reactions (Kastner et al., 1977; Williams and Crerar, 1985; Williams et al., 1985; Cady et al., 1996). The conversion is dependent on temperature, pressure, pH, pore solution chemistry, and specific surface area. As the transformation is mediated by clays, oxides, and carbonates, it is assumed to occur in soils (Drees et al., 1989).

Opal-A may form by both organic and inorganic processes in pedogenic environments. Biogenic opal-A originates from Si accumulated by plants and aquatic organisms, and thus occurs under a wide range of environmental conditions (Jones and Beavers, 1964; Wilding and Drees, 1971).

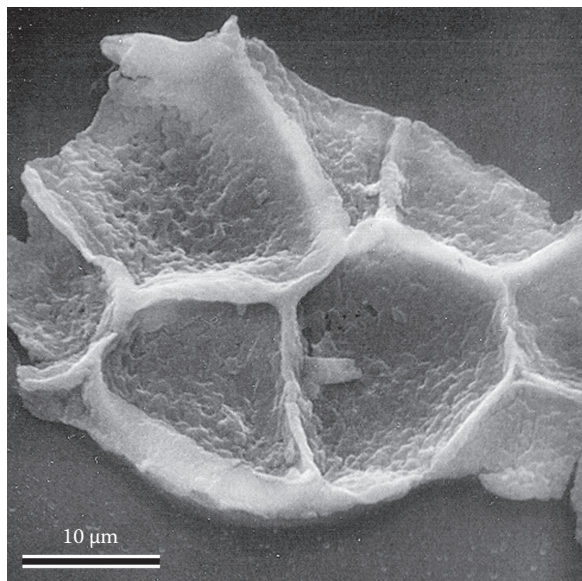


FIGURE 22.6 Scanning electron micrograph of an opal phytolith isolated from a forest soil. (From Drees, L.R., L.P. Wilding, N.E. Smeeck, and A.L. Senkayi. 1989. Silica in soils: Quartz and disordered silica polymorphs, p. 913–974. In J.B. Dixon and S.B. Weed (eds.) *Minerals in soil environments*. 2nd edn. SSSA, Madison, WI.)

Biogenic opal is a minor but nearly ubiquitous constituent of soils, with opal phytoliths (Figure 22.6) representing the major form in nonaquatic environments, while sponge spicules, diatoms, and radiolaria are the main opal form in aquatic environments and limestone residuum (Jones and Beavers, 1964; Wilding and Drees, 1971). Amounts of opal phytoliths in soils commonly range from <1 to 30 g kg^{-1} , usually occurring in the 5–20 and 20–50 μm size fractions and decreasing with soil depth (Drees et al., 1989). Phytoliths are recognized as the principal sink and source of Si in soil solutions (Lucas, 2001; Farmer et al., 2005).

Opal-A, which forms when the conditions favor supersaturation of Si in soil solution (Jones and Handreck, 1967), occurs as nodules and as a primary cement for indurated soil horizons (duripans) and silcretes. Such soils usually have pH and moisture regimes favoring solubilization and translocation of Si to lower positions in the soil profile. Geographically, duripans are restricted to materials that provide soluble Si, such as pyroclastics and intermediate and basic igneous rocks (Flach et al., 1969; Soil Survey Staff, 1975). According to Flach et al. (1969), pedogenic transformation of opal to quartz is believed to occur in duripans and in Si-cemented soils. Silica released by weathering of silicate minerals may precipitate as amorphous SiO_2 on soil particles, forming bridges between mineral grains, leading to the hardness and brittleness of fragipans (Franzmeier et al., 1989; Karathanasis, 1989).

At ambient temperature and neutral pH, the solubility of amorphous Si in soils is approximately $50\text{--}60 \text{ mg Si L}^{-1}$ and that of quartz is commonly $3\text{--}7 \text{ mg Si L}^{-1}$. The solubility of Si oxides is a function of temperature, pH, particle size, chemical

composition, and the presence of a disrupted surface layer. For both crystalline and amorphous Si polymorphs, it is essentially constant between the pH limits of 2 and 8.5, increasing rapidly above pH 9 due to the ionization of monosilicic acid.

The presence of organic molecules greatly enhances the dissolution rates of Si oxides. The dissolution of biogenic opal and quartz increases as particle size decreases due to the increase in surface area (Drees et al., 1989). Chemisorption of metallic ions such as Al, Fe, Mg, Ca, Cu, Pb, and Hg to Si surfaces reduces the dissolution rates of Si due to the formation of relatively insoluble Si coatings (Drees et al., 1989), thus increasing the stability of Si oxides. Oxides of Fe and Al, by acting as a soluble Si sink, greatly increase the dissolution rates of amorphous Si oxides and reactive uncoated quartz surfaces. Dissolution (weathering) of Si oxides is induced by the reduction of Si levels in soil solution by leaching and plant uptake. Dissolution of quartz initiates below approximately $3 \text{ mg of Si L}^{-1}$ (Kittrick, 1969).

22.5.3 Influence on Soil Properties

Noncemented soils comprised dominantly of quartz are non-plastic due to the weak cohesion (van der Waals forces) that develops between Si particles and show low water-retention capacity and high hydraulic conductivity. Duripans, cemented by even small amounts of Si, are hard to extremely hard when dry, have high unconfined compressive strength, and resist dispersion in Na hexametaphosphate (Flach et al., 1974).

Due to their essentially uncharged, poorly hydrated surface, crystalline Si oxides have relatively small effects on the physicochemical activity affecting the soil–plant relationship and act as a diluent to the much more reactive clay minerals and oxides of Fe, Al, and Mn. Silica is not essential for the growth of most plants, but orthosilicic acid, H_4SiO_4 , has a beneficial effect on the growth of some plants (Jones and Handreck, 1967). Rice and sugarcane, for example, often respond to fertilization with very soluble Si sources such as Si slag.

Due to its ubiquity, abundance, resistance to weathering, and immobility, quartz has been often used as an index mineral for weathering and soil formation (Barshad, 1964; Sudom and St. Arnaud, 1971). Extensive leaching may, however, drastically increase the solubility of primary quartz (Little et al., 1978; Asumadu et al., 1988; Pye and Mazzullo, 1994), and authigenic (Breese, 1960) as well as biogenic quartz may form in soils (Wilding and Drees, 1974), thus restricting the use of quartz as an index mineral.

The isotopic composition of quartz (^{18}O), which depends on the temperature of formation, has been used to identify eolian additions to soils (Clayton et al., 1972; Mizota and Matsuhisa, 1995) and the formation of authigenic opaline Si in volcanic ash soils (Mizota et al., 1991).

Opal phytoliths have been used to trace the origin of colluvial sediments (Lutwick and Johnston, 1969) and to identify surface horizons of paleosols (Dormaer and Lutwick, 1969). Depth distributions of sponge spicules may be useful to identify lithological discontinuities, and opal of aquatic organisms (diatoms,

sponge spicules, and siliceous shells) provides direct evidence that the parent material of the soil is of marine or lacustrine origin (Jones and Beavers, 1963, 1964; Wilding and Drees, 1968, 1971). Biogenic opal has been extensively used to reconstruct the vegetative history of soils (Drees et al., 1989; Fisher et al., 1995; Staller, 2002). The $^{13}\text{C}/^{12}\text{C}$ isotope ratio of C occluded in opal phytoliths was used to establish the succession of C3 and C4 grasses, providing a quantitative method for monitoring climatic changes (Kelly et al., 1991).

22.5.4 Identification

Silica oxides can be identified by XRD, SEM, microprobe analysis, IR, and light microscopy. Opal-CT and opal-A may need to be concentrated by particle-size fractionation, specific gravity, and/or differential dissolution. Counting particle size separates under the light microscope is the simplest method of quantifying Si oxides but is limited in resolution (5–10 μm) (Drees et al., 1989). A review of methodologies for extraction of amorphous Si from soils and aquatic sediments is given by Sauer et al. (2006) and Sacconne et al. (2007).

22.5.4.1 Crystal Form, Habit, and Color

In soils, quartz generally occurs as anhedral grains, rarely exhibiting the characteristic prismatic habit of macrocrystals. Angular grains are generally the result of mechanical fracturing, while rounding is a result of physical attrition during both transport and solution. Overgrowths on quartz grains may suggest long-term stable environments. Particles $<100\mu\text{m}$ are commonly shaped like flat plates due to cleavage (Drees et al., 1989). Thus, quartz grain surface morphology may be used to elucidate mineral origin and past and/or present chemical and physical environment.

Opal-CT is commonly observed in sediments as small ($<10\mu\text{m}$) lepispheres. The morphology of opal-A of biogenic origin is closely related to the biological cell or structure in which it originates: opal of forest origin consisting of cellular incrustations with numerous thin-sheet structures (Figure 22.6); opal of grass consisting of solid polyhedral structures resulting from the silicification of the entire cell; and opaline microfossils of sponge spicules, diatoms, and shells (Drees et al., 1989).

Pure Si oxides are colorless but chemical impurities may impart various colors. Quartz is usually colorless and transparent, or white, with a vitreous luster. Cristobalite is white to milky white and ranges from translucent to opaque. The color and degree of translucency of opal-CT seem to depend on the aggregation of lepispheres. For opal-A, color is not a diagnostic criterion because it is strongly affected by occluded chemical impurities and light interference and scattering. In transmitted light, biogenic opal isolated from soils ranges from colorless or light tan to various shades of brown or black (Drees et al., 1989).

22.5.4.2 X-Ray Diffraction

The diagnostic parameters for Si oxides are presented in Figure 22.7 and Table 22.5. Quartz is easily identified by its most intense reflections at 4.26 and 3.34 \AA , even in mixed mineral

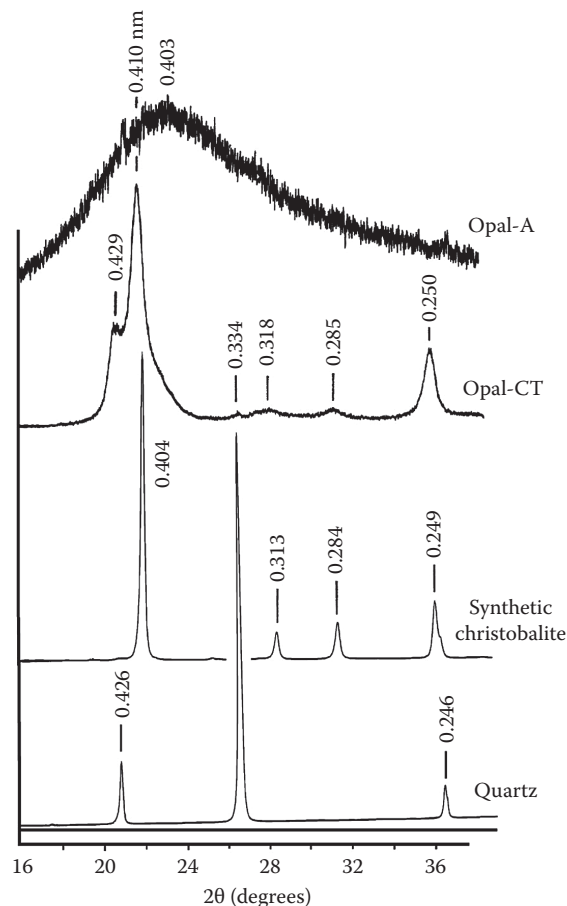


FIGURE 22.7 XRD patterns for quartz, synthetic cristobalite, opal-CT, and opal-A (Cu $K\alpha$ radiation, peak position in nanometers). (Modified from Drees, L.R., L.P. Wilding, N.E. Smeck, and A.L. Senkayi, 1989. Silica in soils: Quartz and disordered silica polymorphs, p. 913–974. In J.B. Dixon and S.B. Weed (eds.) *Minerals in soil environments*. 2nd edn. SSSA, Madison, WI.)

assemblages. The accuracy of the quantitative determination of quartz depends on sample preparation and the diffraction peak used (Rowse and Jepson, 1972). For well-ordered or α -cristobalite, the 4.04 \AA peak is the main clue in mixed samples provided that no feldspars are present. Opal-C gives a pattern resembling that of α -cristobalite, except for slight line broadening and minor evidence of tridymite stacking. Opal-CT usually exhibits broad cristobalite peaks at about 4.1 and 2.5 \AA and a peak at 4.3 \AA , which is attributed to tridymite. The wide variations in the intensity and line profiles make its quantification by XRD difficult. The short-range order in opal-A produces a diffuse, broad x-ray hump centered at about 4.0 \AA .

22.5.4.3 Thermal Properties

Quartz exhibits a sharp endothermic DTA peak at about 570°C (Drees et al., 1989), which may not be evident for microcrystalline quartz ($<0.05\mu\text{m}$). Well-ordered synthetic cristobalite has a characteristic endothermic peak at about 260°C, whereas opal-CT and opal-A do not yield a characteristic endotherm below 600°C.

According to Rowse and Jepson (1972), DTA is better than either XRD or chemical techniques for detecting small quantities of quartz in clay materials.

22.5.4.4 Infrared Spectroscopy

All tectosilicates are characterized by Si–O–Si stretching vibrations between 950 and 1200 cm^{-1} and by O–Si–O bending vibrations between 400 and 550 cm^{-1} . Quartz is distinguished from the other Si polymorphs by a distinctive absorption band at 692 cm^{-1} and two strong doublets, one at 395 and 370 cm^{-1} and the other at 800 and 780 cm^{-1} (Drees et al., 1989). The latter doublet has been used also for the quantification of quartz (Chester and Green, 1968). This method is, however, restricted to samples <1 μm in particle size and free of other Si polymorphs.

The disordered Si polymorphs, opal-C, opal-CT, and opal-A, have a single band around 800 cm^{-1} in common. Well-ordered cristobalite and opal-C show additional bands at 620 and 380 cm^{-1} . Opal-A of biogenic origin is characterized by much weaker and broader absorption bands at 460 and 1100 cm^{-1} as compared to the better crystallized polymorphs and an additional weak band at 965 cm^{-1} (Drees et al., 1989).

22.6 Titanium and Zirconium Minerals

Of all Ti and Zr compounds in soil and weathered materials, the Ti oxides (rutile, anatase, and ilmenite) and the Zr silicate (zircon) are the most ubiquitous. The principal Ti and Zr minerals are listed in Table 22.6. Additional information about Ti and Zr minerals can be found in Milnes and Fitzpatrick (1989), Lindsley (1976, 1991), and Fitzpatrick and Chittleborough (2002). Titanomagnetite and titanomaghemite are described in Section 22.2.

22.6.1 Mineral Phases

Titanium occurs primarily in octahedral coordination, and like the Fe and Mn oxides, the structures of the various Ti oxide minerals can be described in terms of the different arrangement of the Ti-containing octahedra (Lindsley, 1976; Waychunas, 1991; Heaney and Banfield, 1993).

Rutile (TiO_2) is isostructural with pyrolusite and manganese, consisting of single chains of edge-sharing TiO_6 octahedra (Figure 22.1; Heaney and Banfield, 1993). *Anatase* consists of TiO_6 octahedra that share four O–O edges, two at the top and two at right angles at the bottom. The octahedra outline a 3D framework, rather than distinct chains (Figure 22.1; Waychunas, 1991). Schwertmann et al. (1995b) reported the substitution of Ti^{4+} by Fe^{3+} up to 0.1 mol fraction in pedogenic and synthetic anatase. Charge compensation is achieved by the incorporation of structural OH. *Brookite* has a more complex structure than rutile or anatase, consisting of deformed TiO_6 octahedra sharing three O–O edges to form staggered, cross-linked chains that are oriented along the c-axis (Figure 22.1; Lindsley, 1976). *Ilmenite* (FeTiO_3) is almost isostructural with hematite, with one-half of the Fe atoms replaced by Ti, so that the Fe^{3+} – O_3 – Fe^{3+} units in hematite become Fe^{2+} – O_3 – Ti^{4+} units in ilmenite (Figure 22.1; Lindsley, 1976). *Pseudobrookite* (ideally Fe_2TiO_5) has strongly distorted octahedra but can be described in terms of an ideal cubic close packing anion arrangement (Figure 22.1; Waychunas, 1991). The two types of octahedral sites are M1 and M2 in the ratio 1:2, ideally occupied by Fe^{3+} and Ti^{4+} , respectively. *Pseudorutile* ($\text{Fe}_2\text{O}_3 \cdot n\text{TiO}_2 \cdot m\text{H}_2\text{O}$; $3 < n < 5$ and $1 < m < 2$) is a structurally disordered and poorly characterized mineral formed by the alteration of ilmenite. Its structure is based on a hexagonal closest packing of O^{2-} anions and has been described as an intergrowth of a rutile-type structure with a goethite-type

TABLE 22.6 Titanium and Zr Oxide Minerals: Crystallographic Properties and d Values for the Six Most Intense Diffraction Lines

Mineral	Chemical Formula	Crystal System, Space Group	Unit-Cell Dimensions (Å)	Six Most Intense Diffraction Lines						References ^a
				d Value (Å)	Relative Intensity					
Rutile	TiO_2	Tetragonal, $P4_2/mnm$	a = 4.5933 c = 2.9592	3.247 100	1.687 60	2.487 50	2.188 25	1.624 20	1.36 20	21-1276
Anatase	TiO_2	Tetragonal, $I4_1/amd$	a = 3.7853 c = 9.5139	3.52 100	1.892 35	2.378 20	1.70 20	1.666 20	1.481 14	21-1272
Brookite	TiO_2	Orthorhombic, $Pbca$	a = 5.4558 b = 9.1819 c = 5.1429	3.152 100	2.90 90	3.465 80	1.893 30	1.66 30	2.476 25	29-1360
Ilmenite	$\text{Fe}^{2+}\text{TiO}_3$	Hexagonal, $R3$	a = 5.0884 c = 14.093	2.754 100	2.544 70	1.726 55	1.868 40	1.468 35	3.737 30	29-0733
Pseudobrookite	$\text{Fe}_2^{3+}\text{TiO}_5$	Orthorhombic, $Bbmm$	a = 9.7965 b = 9.9805 c = 3.7301	3.486 100	2.752 77	4.90 42	2.458 23	1.865 23	2.407 22	41-1432
Pseudorutile	$\text{FeIII}_2\text{Ti}_3\text{O}_8(\text{OH})_2$	Hexagonal, $P6_322$	a = 14.486 c = 4.467	3.50 100	2.66 90	2.51 80	1.687 70	3.67 40	3.23 30	Waychunas (1991)
Ulvöspinel	Fe_2TiO_4	Cubic, $Fd3m$	a = 8.393–8.536	2.573 100	1.509 39	3.018 33	1.642 33	2.134 19	1.742 10	34-0177
Zircon	ZrSiO_4	Tetragonal, $I4_1/amd$	a = 6.604 c = 5.979	3.30 100	4.434 45	2.518 45	1.712 40	2.066 20	1.908 14	6-266

^a Numbers of the format XX-XXXX indicate ICDD file number (ICDD, 1994).

structure (Figure 22.1; Grey et al., 1983). Zircon ($ZrSiO_4$) is an orthosilicate with a structure consisting of chains of alternating edge-sharing SiO_4 tetrahedra and $[ZrO_8]$ triangular dodecahedra. The chains are joined laterally by dodecahedra-sharing edges in an arrangement that produces unoccupied octahedral voids (Speer, 1982).

22.6.2 Occurrence and Formation

Rutile, anatase, ilmenite, and less frequently brookite are found as accessory minerals in many igneous and metamorphic rocks and as detrital minerals in sediments, although anatase is often also of authigenic origin (Deer et al., 1992). The Ti and Zr minerals in soils may be residual minerals inherited from the parent material, formed through weathering of Ti- and Zr-bearing minerals, or authigenic (Milnes and Fitzpatrick, 1989). Rutile, anatase, ilmenite, and zircon are commonly residual minerals occurring in the sand and silt fractions of a variety of soils. Ilmenite may weather to pseudorutile and mixtures of rutile, anatase, and Fe oxides. Some evidence indicates that anatase and ilmenite weathering occurs by organic acids in A horizons of Scottish podzols (Berrow et al., 1978), and weathering features were observed on the surface of zircon and rutile grains of Australian Spodic Quartzipsamments (Tejan-Kella et al., 1991).

Many examples of secondary Ti oxides formed through weathering of primary minerals are found in saprolites and in soils. The data on the secondary or authigenic formation of Zr minerals are, however, controversial (Milnes and Fitzpatrick, 1989). The alteration of ilmenite under oxidizing conditions leads to the formation of pseudorutile (Grey and Reid, 1975; Anand and Gilkes, 1984b) but, at this stage, there is no clear evidence that it also takes place under pedogenic conditions (Berrow et al., 1978). Authigenic formation of poorly crystalline anatase as an alteration product of sphene was observed in peaty podzols from Scotland (Berrow et al., 1978). In conclusion, basic aspects of the Ti and Zr minerals, such as whether the minerals are relict or pedogenic, and the conditions responsible for their weathering and formation in soils, are still unresolved (Taylor, 1987; Milnes and Fitzpatrick, 1989).

22.6.3 Influence on Soil Properties

Because of their generally low concentrations in soils, there is little evidence of the effect of Ti and Zr minerals on soil reactivity. Only in tropical soils where their concentrations are much higher some effects may be expected. The broken-edge bonds of anatase are hydroxylated and can exhibit variable charge characteristics (Fitzpatrick et al., 1978). The rutile and anatase surface has hydroxyl groups with different reactivities (Tanaka and White, 1982) that can adsorb and retain phosphate and arsenate (Cabrera et al., 1977; Fordham and Norrish, 1983).

Because ilmenite and zircon are generally very resistant in soils, they may be used as reference minerals in weathering and soil genesis studies (Bleeker, 1972; Mitchell, 1975; Claridge and Weatherhead, 1978; Tejan-Kella et al., 1991). The immobility of these minerals must, however, be previously assured (Colin et al., 1993; Anda et al., 2009).

22.6.4 Identification

As Ti and Zr minerals can occur in different particle-size fractions and exhibit variable crystallinity, a variety of techniques may be necessary to identify and characterize them. Optical microscopy is a useful technique for examining and identifying these minerals, both in undisturbed form in thin sections and as components separated by physical or chemical techniques (Mitchell, 1975). A combination of XRD, IR absorption, DTA, and electron microprobe techniques is useful for identifying the Ti and Zr minerals in the sand and silt fractions of soils but may be less satisfactory for the clay fractions due to the interference of layer silicates (Milnes and Fitzpatrick, 1989). TEM along with energy-dispersive x-ray analysis of individual particles can be used to identify Ti oxide crystals in soil clay fractions (Figure 22.8). Titanium oxides may be concentrated in kaolinitic soils by dissolution of clay minerals in boiling 5 M NaOH alone (Norrish and Taylor, 1961) or by a combination of boiling 5 M KOH and DCB treatments (Zeese et al., 1994). Amorphous Ti oxides can be separated from more crystalline forms by extraction in acid ammonium oxalate (Fitzpatrick et al., 1978). Minor amounts of anatase (>0.02%) can be identified by Raman spectroscopy (Murad, 1997). Tejan-Kella et al. (1991) described an SEM method to characterize microtextural features of zircon and rutile grains. In XRD of the clay fraction, the strong, sharp anatase peak at 3.52 Å (Table 22.6) is often clearly resolved after the interfering 3.59 Å kaolinite line has been eliminated by heating at 550°C.

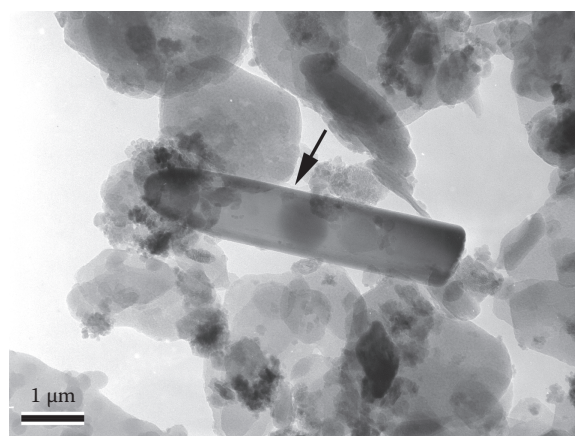


FIGURE 22.8 Transmission electron micrograph of the 2–0.2 μm fraction of a Rhodic Hapludox showing an anatase or rutile particle (arrow) surrounded by kaolinite and iron oxide particles. (Modified from de Brito Galvão, T.C., and D.G. Schulze. 1996. Mineralogical properties of a collapsible lateritic soil from Minas Gerais, Soil Sci. Soc. Am. J. 60:1969–1978.)

References

- Adams, S.N., J.L. Honeysett, K.G. Tiller, and K. Norrish. 1969. Factors controlling the increase of cobalt in plants following the addition of a cobalt fertilizer. *Aust. J. Soil Res.* 7:29–42.
- Adams, W.A., and J.K. Kassim. 1984. Iron oxyhydroxides in soils developed from lower palaeozoic sedimentary rocks in mid-Wales and implications for some pedogenetic processes. *J. Soil Sci.* 35:117–126.
- Allen, B.L., and B.F. Hajek. 1989. Mineral occurrence in soil environments, p. 199–278. *In* J.B. Dixon and S.B. Weed (eds.) *Minerals in soil environments*. SSSA, Madison, WI.
- Anand, R.R., and R.J. Gilkes. 1984a. Mineralogical and chemical properties of weathered magnetite grains from lateritic saprolite. *J. Soil Sci.* 35:559–567.
- Anand, R.R., and R.J. Gilkes. 1984b. Weathering of ilmenite in a lateritic pallid zone. *Clays Clay Miner.* 32:363–374.
- Anand, R.R., and R.J. Gilkes. 1987a. Variations in the properties of iron oxides within individual specimens of lateritic duricrust. *Aust. J. Soil Res.* 25:287–302.
- Anand, R.R., and R.J. Gilkes. 1987b. The association of maghemite and corundum in Darling Range laterites, Western Australia. *Aust. J. Soil Res.* 25:303–311.
- Anda, M., D.J. Chittleborough, and R.W. Fitzpatrick. 2009. Assessing parent material uniformity of a red and black soil complex in the landscapes. *Catena* 78:142–153.
- Asumadu, K., R.J. Gilkes, T.M. Armitage, and H.M. Churchward. 1988. The effects of chemical weathering on the morphology and strength of quartz grains—An example from S.W. Australia. *Eur. J. Soil Sci.* 39:375–383.
- Bardossy, G., and G.W. Brindley. 1978. Rancieite associated with a karstic bauxite deposit. *Am. Mineral.* 63:762–767.
- Barshad, I. 1964. Chemistry of soil development, p. 1–70. *In* F.E. Bear (ed.) *Chemistry of soil*. Reinhold Publishing Corporation, New York.
- Barthès, B.G., E. Kouakoua, M.-C. Larré-Larrouy, T.M. Razafimbelo, E.F. de Luca, A. Azontonde, C.S.V.J. Neves, P.L. de Freitas, and C.L. Feller. 2008. Texture and sesquioxide effects on water-stable aggregates and organic matter in some tropical soils. *Geoderma* 143:14–25.
- Bascomb, C.L. 1968. Distribution of pyrophosphate-extractable iron and organic carbon in soils. *J. Soil Sci.* 19:251–268.
- Baur, W.H. 1976. Rutile-type compounds. V. Refinement of MnO_2 and MgF_2 . *Acta Crystallogr. B* 32:2200–2204.
- Bernal, J.D., D.R. Dasgupta, and A.L. Mackay. 1959. The oxides and hydroxides of iron and their structural interrelationships. *Clay Miner. Bull.* 4:15–30.
- Berrow, M.L., M.J. Wilson, and G.A. Reaves. 1978. Origin of extractable titanium and vanadium in the A horizon of Scottish podzols. *Geoderma* 21:89–103.
- Berthelin, J., G. Ona-Nguema, S. Stemmler, C. Quantin, M. Abdelmoula, and F. Jorand. 2006. Bioreduction of iron species and biogenesis of green rusts in soils. *C.R. Geosci.* 338:447–455.
- Bigham, J.M., L. Carlson, and E. Murad. 1994. Schwertmannite, a new iron oxyhydroxy-sulfate from Pyhäsalmi, Finland and other localities. *Mineral. Mag.* 58:641–648.
- Bigham, J.M., R.W. Fitzpatrick, and D.G. Schulze. 2002. Iron oxides, p. 323–366. *In* J.B. Dixon and D.G. Schulze (eds.) *Soil mineralogy with environmental applications*. SSSA, Madison, WI.
- Bigham, J.M., D.C. Golden, L.H. Bowen, S.W. Buol, and S.B. Weed. 1978. Mössbauer and X-ray evidence for the pedogenic transformation of hematite to goethite. *Soil Sci. Soc. Am. J.* 42:979–981.
- Bigham, J.M., U. Schwertmann, and L. Carlson. 1992. Mineralogy of precipitates formed by biogeochemical oxidation of Fe(II) in mine drainage. *Catena Suppl.* 1:219–232.
- Bigham, J.M., U. Schwertmann, L. Carlson, and E. Murad. 1990. A poorly crystallized oxyhydroxide of iron formed by bacterial oxidation of Fe(II) in acid mine waters. *Geochim. Cosmochim. Acta* 54:2743–2758.
- Bigham, J.M., U. Schwertmann, and G. Pfab. 1996a. Influence of pH on mineral speciation in a bioreactor simulating acid mine drainage. *Appl. Geochem.* 11:845–849.
- Bigham, J.M., U. Schwertmann, S.J. Traina, R.L. Winland, and M. Wolf. 1996b. Schwertmannite and goethite solubilities and the chemical modelling of iron in acid sulfate waters. *Geochim. Cosmochim. Acta* 60:2111–2121.
- Birch, W.D., A. Pring, A. Reller, and H. Schmalle. 1993. Bernalite, $\text{Fe}(\text{OH})_3$, a new mineral from Broken Hill, New South Wales: Description and structure. *Am. Mineral.* 78:827–834.
- Birnie, A.C., and E. Paterson. 1991. The mineralogy and morphology of iron and manganese oxides in an imperfectly-drained Scottish soil. *Geoderma* 50:219–237.
- Blake, R.L., R.E. Hessevick, T. Zoltai, and L.W. Finger. 1966. Refinement of the hematite structure. *Am. Mineral.* 51:123–129.
- Bleeker, P. 1972. The mineralogy of eight latosolic and related soils from Papua-New Guinea. *Geoderma* 8:191–205.
- Blume, H.P., and U. Schwertmann. 1969. Genetic evaluation of the profile distribution of aluminum, iron and manganese oxides. *Soil Sci. Soc. Am. Proc.* 33:438–444.
- Borggaard, O.K. 1988. Phase identification by selective dissolution techniques, p. 83–98. *In* J.W. Stucki, B.A. Goodman, and U. Schwertmann (eds.) *Iron in soils and clay minerals*. D. Reidel Publishing Co., Dordrecht, the Netherlands.
- Boudeulle, M., and J.-P. Muller. 1988. Structural characteristics of hematite and goethite and their relationship with kaolinite in a laterite from Cameroon. A TEM study. *Bull. Minér.* 111:149–166.
- Breese, G.F. 1960. Quartz overgrowths as evidence of silica deposition in soils. *Aust. J. Sci.* 23:18–20.
- Bricker, O. 1965. Some stability relations in the system $\text{Mn-O}_2\text{-H}_2\text{O}$ at 25°C and one atmosphere total pressure. *Am. Mineral.* 50:1296–1354.
- Brindley, G.W., and D.L. Bish. 1976. Green rust: A pyroaurite type structure. *Nature* 263:353.

- Burns, R.G., V.M. Burns, and H.W. Stockman. 1985. The todorokite-buserite problem: Further considerations. *Am. Mineral.* 70:205–208.
- Busing, W.R., and H.A. Levy. 1958. A single crystal neutron diffraction study of diasporite, $\text{AlO}(\text{OH})$. *Acta Crystallogr.* 11:798–803.
- Cabrera, F., L. Madrid, and P. de-Armbarri. 1977. Adsorption of phosphate by various oxides: Theoretical treatment of the adsorption envelope. *J. Soil Sci.* 28:306–313.
- Cady, S.L., H.-R. Wenk, and K.H. Downing. 1996. HRTEM of microcrystalline opal in chert and porcelanite from the Monterey Formation, California. *Am. Mineral.* 81:1380–1395.
- Cambier, P. 1986. Infrared studies of goethites of varying crystallinity and particle size: I. Interpretation of OH and lattice vibration frequencies. *Clay Miner.* 21:191–200.
- Campbell, A.S., and U. Schwertmann. 1984. Iron oxide mineralogy of placic horizons. *J. Soil Sci.* 35:569–582.
- Carlson, L., and U. Schwertmann. 1980. Natural occurrence of feroxyhite (δ' - FeOOH). *Clays Clay Miner.* 28:272–280.
- Carlson, L., and U. Schwertmann. 1981. Natural ferrihydrites in surface deposits from Finland and their association with silica. *Geochim. Cosmochim. Acta* 45:421–429.
- Carlson, L., and U. Schwertmann. 1990. The effect of CO_2 and oxidation rate on the formation of goethite versus lepidocrocite from an Fe(II) system at pH 6 and 7. *Clay Miner.* 25:65–71.
- Cerling, T.E., and R.R. Turner. 1982. Formation of freshwater Fe–Mn coatings on gravel and the behaviour of ^{60}Co , ^{90}Sr , and ^{137}Cs in a small watershed. *Geochim. Cosmochim. Acta* 46:1333–1343.
- Chao, T.T. 1972. Selective dissolution of manganese oxides from soils and sediments with acidified hydroxylamine hydrochloride. *Soil Sci. Soc. Am. J.* 36:764–768.
- Chao, G.Y., J. Baker, A.P. Sabina, and A.C. Green. 1985. Doyleite, a new polymorph of $\text{Al}(\text{OH})_3$, and its relationship to bayerite, gibbsite, and nordstrandite. *Can. Mineral.* 23:21–28.
- Chester, R., and R.N. Green. 1968. The infra-red determination of quartz in sediments and sedimentary rocks. *Chem. Geol.* 3:199–212.
- Childs, C.W. 1975. Composition of iron–manganese concretions from some New Zealand soils. *Geoderma* 13:141–152.
- Childs, C.W. 1981. Field tests for ferrous iron and ferric-organic complexes (on exchange sites or in water-soluble forms) in soils. *Aust. J. Soil Res.* 19:175–180.
- Childs, C.W., R.W.P. Palmer, and C.W. Ross. 1990. Thick iron oxide pans in soils of Taranaki, New Zealand. *Aust. J. Soil Res.* 28:245–257.
- Chukhrov, F.V., and A.I. Gorshkov. 1981. On the nature of some hypergene manganese minerals. *Chem. Erde* 40:207–216.
- Chukhrov, F.V., A.I. Gorshkov, E.S. Rudnitskaya, V.V. Beresovskaya, and A.V. Sivtsov. 1980. Manganese minerals in clays: A review. *Clays Clay Miner.* 28:346–354.
- Claridge, G.G.C., and A.V. Weatherhead. 1978. Mineralogy of silt fractions of New Zealand soils. *N.Z. J. Sci.* 21:413–423.
- Clayton, R.N., R.W. Rex, J.K. Syers, and M.L. Jackson. 1972. Oxygen isotope abundance in quartz from Pacific pelagic sediments. *J. Geophys. Res.* 77:3907–3915.
- Coe, J.M.D. 1988. Magnetic properties of iron in soil iron oxides and clay minerals, p. 397–466. *In* J.W. Stucki, B.A. Goodman, and U. Schwertmann (eds.) *Iron in soils and clay minerals*. D. Reidel Publishing Company, Dordrecht, the Netherlands.
- Colin, F., C. Alarçon, and P. Vieillard. 1993. Zircon: An immobile index in soils? *Chem. Geol.* 107:273–276.
- Combes, J.M., A. Manceau, G. Calas, and J.Y. Bottero. 1989. Formation of ferric oxides from aqueous solutions: A polyhedral approach by X-ray absorption spectroscopy: I. Hydrolysis and formation of ferric gels. *Geochim. Cosmochim. Acta* 53:583–594.
- Cornell, R.M. 1987. Comparison and classification of the effects of simple ions and molecules upon the transformation of ferrihydrite into more crystalline products. *Z. Pflanzenernähr. Bodenk.* 150:304–307.
- Cornell, R.M., and U. Schwertmann. 1996. *The iron oxides*. Wiley-VCH Verlag, Weinheim, Germany.
- Cornell, R.M., and U. Schwertmann. 2003. *The iron oxides*. 2nd edn. Wiley-VCH Verlag, Weinheim, Germany.
- Crowther, D.L., and J.G. Dillard. 1983. The mechanism of Co(II) oxidation on synthetic birnessite. *Geochim. Cosmochim. Acta* 47:1399–1403.
- Curi, N., and D.P. Franzmeier. 1984. Toposequence of Oxisols from the Central Plateau of Brazil. *Soil Sci. Soc. Am. J.* 48:341–346.
- Dachs, H. 1963. Neutronen- und Röntgenuntersuchungen an Manganit, MnOOH . *Z. Krist.* 118:303–326.
- da Motta, P.E.F., and N. Kämpf. 1991. Iron oxide properties as support to soil morphological features for prediction of moisture regimes in Oxisols of central Brazil. *Z. Pflanzenernähr. Bodenk.* 155:385–390.
- Davies, P.K., and A. Navrotsky. 1983. Quantitative correlations of deviations from ideality in binary and pseudobinary solid solutions. *J. Solid State Chem.* 46:1–22.
- de Brito Galvão, T.C., and D.G. Schulze. 1996. Mineralogical properties of a collapsible lateritic soil from Minas Gerais, Brazil. *Soil Sci. Soc. Am. J.* 60:1969–1978.
- Deer, W.A., R.A. Howie, and J. Zussman. 1992. *An introduction to the rock-forming minerals*. 2nd edn. Longman Scientific and Technical, Essex, UK.
- Dixon, J.B., and G.N. White. 2002. Manganese oxides, p. 367–388. *In* J.B. Dixon and D.G. Schulze (eds.) *Soil mineralogy with environmental applications*. SSSA, Madison, WI.
- Dormaer, J.F., and L.E. Lutwick. 1969. Infrared spectra of humic acids and opal phytoliths as indicators of paleosols. *Can. J. Soil Sci.* 49:29–37.
- dos Anjos, L.H.C., D.P. Franzmeier, and D.G. Schulze. 1995. Formation of soils with plinthite on a toposequence in Maranhão State, Brazil. *Geoderma* 64:257–279.
- Drees, L.R., L.P. Wilding, N.E. Smeck, and A.L. Senkayi. 1989. Silica in soils: Quartz and disordered silica polymorphs, p. 913–974. *In* J.B. Dixon and S.B. Weed (eds.) *Minerals in soil environments*. 2nd edn. SSSA, Madison, WI.

- Drits, V.A., B.A. Sakharov, and A. Manceau. 1993a. Structure of feroxyhite as determined by simulation of X-ray curves. *Clay Miner.* 28:209–221.
- Drits, V.A., B.A. Sakharov, A.L. Salyn, and A. Manceau. 1993b. Structural model for ferrihydrite. *Clay Miner.* 28:185–207.
- Egger, K., and W. Feitknecht. 1962. Über die Oxidation von Fe_3O_4 zu γ - und α - Fe_2O_3 . Die differenzthermoanalytische (DTA) und thermogravimetrische (TG) Verfolgung des Reaktionsablaufes an künstlichen Formen von Fe_3O_4 . *Helv. Chim. Acta* 45:2042–2057.
- Eggleton, R.A. 1988. The application of micro-beam methods to iron minerals in soils, p. 165–201. *In* J.W. Stucki, B.A. Goodman, and U. Schwertmann (eds.) *Iron in soils and clay minerals*. D. Reidel Publishing Company, Dordrecht, the Netherlands.
- Ehrlich, H.L. 1990. *Geomicrobiology*. 2nd edn. Marcel Dekker, New York.
- Ehrlich, H.L. 1996. How microbes influence mineral growth and dissolution. *Chem. Geol.* 132:5–9.
- Elderfield, H., and H.D. Hem. 1973. The development of crystalline structure in aluminum hydroxide polymorphs on aging. *Mineral. Mag.* 39:89–96.
- Ewing, F.J. 1935a. The crystal structure of lepidocrocite. *J. Chem. Phys.* 3:420–424.
- Ewing, F.J. 1935b. The crystal structure of diaspore. *J. Chem. Phys.* 3:203–207.
- Fanning, D.S., M.C. Rabenhorst, and J.M. Bigham. 1993. Colors of acid sulfate soils, p. 91–108. *In* J.M. Bigham and E.J. Ciolkosz (eds.) *Soil color*. SSSA Special Publication No. 31. SSSA, Madison, WI.
- Farmer, V.C., E. Delbos, and J.D. Miller. 2005. The role of phytolith formation and dissolution in controlling concentrations of silica in soil solution and streams. *Geoderma* 127:71–79.
- Farmer, V.C., and J.D. Russel. 1967. Infrared absorption spectrometry in clay studies. *Clays Clay Miner.* 15:121–141.
- Fasiska, E.J. 1967. Structural aspects of the oxides and oxidehydrates of iron. *Corros. Sci.* 7:833–839.
- Fassbinder, J.W.E., H. Stanjek, and H. Vali. 1990. Occurrence of magnetic bacteria in soil. *Nature* 343:161–163.
- Faulring, F.M., W.K. Zwicker, and W.D. Forgeng. 1960. Thermal transformations and properties of cryptomelane. *Am. Mineral.* 45:946–959.
- Fendorf, S.E., M. Fendorf, D.L. Sparks, and R. Gronsky. 1992. Inhibitory mechanisms of Cr(III) oxidation by γ - MnO_2 . *J. Colloid Interface Sci.* 153:37–54.
- Fisher, R.F., C.N. Bourn, and W.F. Fisher. 1995. Opal phytoliths as an indicator of the floristics of prehistoric grasslands. *Geoderma* 68:243–255.
- Fitzpatrick, R.W., and D.J. Chittleborough. 2002. Titanium and zirconium minerals, p. 667–690. *In* J.B. Dixon and D.G. Schulze (eds.) *Soil mineralogy with environmental applications*. SSSA, Madison, WI.
- Fitzpatrick, R., B. Degens, A. Baker, M. Raven, P. Shand, M. Smith, S. Rogers, and R. George. 2008. Avon Basin, WA Wheatbelt: Acid sulfate soils and salt efflorescences in open drains and receiving environments, p. 189–204. *In* R. Fitzpatrick and P. Shand (eds.) *Inland acid sulfate soil systems across Australia*. CRC LEME open file report No. 249 (thematic volume). CRC LEME, Perth, Australia.
- Fitzpatrick, R.W., J. LeRoux, and U. Schwertmann. 1978. Amorphous and crystalline iron–titanium oxides in synthetic preparation, at near ambient conditions, and in soil clays. *Clays Clay Miner.* 26:189–201.
- Fitzpatrick, R.W., and U. Schwertmann. 1982. Al-substituted goethite—An indicator of pedogenic and other weathering environments in South Africa. *Geoderma* 27:335–347.
- Fitzpatrick, R.W., R.M. Taylor, U. Schwertmann, and C.W. Childs. 1985. Occurrence and properties of lepidocrocite in some soils of New Zealand, South Africa and Australia. *Aust. J. Soil Res.* 23:543–567.
- Flach, K.W., W.D. Nettleton, L.H. Gile, and J.C. Cady. 1969. Pedocementation: Induration by silica, carbonates, and sesquioxides in the quaternary. *Soil Sci.* 107:442–453.
- Flach, K.W., W.D. Nettleton, and R.E. Nelson. 1974. The micro-morphology of silica-cemented soil horizons in western North America, p. 714–729. *In* G.K. Rutherford (ed.) *Soil microscopy*. The Limestone Press, Kingston, Canada.
- Fontes, M.P.F., L.H. Bowen, and S.B. Weed. 1991. Iron oxides in selected Brazilian Oxisols: II. Mössbauer studies. *Soil Sci. Soc. Am. J.* 55:1150–1155.
- Fontes, M.P.F., and S.B. Weed. 1991. Iron oxides in selected Brazilian Oxisols: I. Mineralogy. *Soil Sci. Soc. Am. J.* 55:1143–1149.
- Fordham, A.W., and K. Norrish. 1979. Electron microprobe and electron microscope studies of soil clay particles. *Aust. J. Soil Res.* 17:283–306.
- Fordham, A.W., and K. Norrish. 1983. The nature of soil particles particularly those reacting with arsenate in a series of chemically treated samples. *Aust. J. Soil Res.* 21:455–477.
- Franzmeier, D.P., L.D. Norton, and G.C. Steinhardt. 1989. Fragipan formation in loess of the midwestern United States, p. 69–97. *In* N.E. Smeck and E.J. Ciolkosz (eds.) *Fragipans: Their occurrence, classification, and genesis*. SSSA Special Publication No. 24. SSSA, Madison, WI.
- Fritsch, E., A.J. Herbillon, N.R. do Nascimento, M. Grimaldi, and A.J. Melfi. 2007. From plinthic acrisols to plinthosols and gleysols: Iron and groundwater dynamics in the tertiary sediments of the upper Amazon basin. *Eur. J. Soil Sci.* 58:989–1006.
- Fritsch, E., G. Morin, A. Bedidi, D. Bonnin, E. Balan, S. Caquineau, and G. Calas. 2005. Transformation of haematite and Al-poor goethite to Al-rich goethite and associated yellowing in a ferrallitic clay soil profile in the middle Amazon Basin (Manaus, Brazil). *Eur. J. Soil Sci.* 56:575–588.
- Gallagher, K.J., W. Feitknecht, and U. Mannweiler. 1968. Mechanism of oxidation of magnetite to γ - Fe_2O_3 . *Nature* 217:1118–1121.
- Gao, X., and D.G. Schulze. 2010a. Chemical and mineralogical characterization of arsenic, lead, chromium, and cadmium in a metal-contaminated Histosol. *Geoderma* 156:278–286.

- Gao, X., and D.G. Schulze. 2010b. Precipitation and transformation of secondary Fe oxyhydroxides in a Histosol impacted by runoff from a lead smelter. *Clays Clay Miner.* 58:377–387.
- Geller, S. 1971. Structures of $\alpha\text{-Mn}_2\text{O}_3$, $(\text{Mn}_{0.983}\text{Fe}_{0.017})_2\text{O}_3$ and $(\text{Mn}_{0.37}\text{Fe}_{0.63})_2\text{O}_3$ and relation to magnetic ordering. *Acta Crystallogr. B* 27:821–828.
- Ghiorse, W.C. 1988. The biology of manganese transforming microorganisms in soil, p. 75–85. *In* R.D. Graham, R.J. Hannam, and N.C. Uren (eds.) *Manganese in soils and plants*. Kluwer Academic Publishers, Boston, MA.
- Ghiorse, W.C., and H.L. Ehrlich. 1992. Microbial biomineralization of iron and manganese. *Catena Suppl.* 21:75–99.
- Gilkes, R.J., G. Scholz, and G.M. Dimmock. 1973. Lateritic deep weathering of granite. *J. Soil Sci.* 24:523–536.
- Gilkes, R.J., and A. Suddhiprakarn. 1979. Magnetite alteration in deeply weathered adamellite. *J. Soil Sci.* 30:357–361.
- Giovanoli, R. 1985a. Layer structures and tunnel structures in manganates. *Chem. Erde* 44:227–244.
- Giovanoli, R. 1985b. A review of the todorokite–buserite problem: Implications to the mineralogy of marine manganese nodules: Discussion. *Am. Mineral.* 70:202–204.
- Glasser, L.S.D., and L. Ingram. 1968. Refinement of the crystal structure of groutite, $\alpha\text{-MnOOH}$. *Acta Crystallogr. B* 24:1233–1236.
- Glasser, L.S.D., and I. Smith. 1968. Oriented transformations in the system $\text{MnO}-\text{O}-\text{H}_2\text{O}$. *Mineral. Mag.* 36:976–987.
- Golden, D.C., C.C. Chen, J.B. Dixon, and Y. Tokashiky. 1986. Pseudomorphic replacement of manganese oxides by iron oxide minerals. *Geoderma* 42:199–211.
- Golden, D.C., J.B. Dixon, and Y. Kanehiro. 1993. The manganese oxide mineral, lithiophorite, in an Oxisol from Hawaii. *Aust. J. Soil Res.* 31:51–66.
- Goss, C.J. 1988. Saturation magnetization, coercivity and lattice parameter changes in the system $\text{Fe}_3\text{O}_4-\gamma\text{Fe}_2\text{O}_3$, and their relationship to structure. *Phys. Chem. Miner.* 16:164–171.
- Graetsch, H. 1994. Structural characteristics of opaline and microcrystalline silica minerals. *Rev. Mineral. Geochem.* 29:209–232.
- Graham, R.D., R.J. Hannam, and N.C. Uren. 1988. *Manganese in soils and plants*. Kluwer Academic Publishers, Dordrecht, the Netherlands.
- Greer, R.T. 1969. Submicron structure of amorphous opal. *Nature* 224:1199–1200.
- Grey, I.E., C. Li, and J.A. Watts. 1983. Hydrothermal synthesis of goethite–rutile intergrowth structures and their relationship to pseudorutile. *Am. Mineral.* 68:981–988.
- Grey, I.E., and A.F. Reid. 1975. The structure of pseudorutile and its role in the natural alteration of ilmenite. *Am. Mineral.* 60:898–906.
- Gross, S., and L. Heller. 1963. A natural occurrence of bayerite. *Mineral. Mag.* 33:723–724.
- Hathaway, J.C., and S.O. Schlanger. 1965. Nordstrandite ($\text{Al}_2\text{O}_3 \cdot 3\text{H}_2\text{O}$) from Guam. *Am. Mineral.* 50:1029–1037.
- Hazemann, J.L., A. Manceau, P. Saintavit, and C. Malgrange. 1992. Structure of the $\alpha\text{Fe}_x\text{Al}_{1-x}\text{OOH}$ solid solution. I. Evidence by polarized EXAFS for an epitaxial growth of hematite-like clusters in diaspore. *Phys. Chem. Miner.* 19:25–38.
- Healy, T.W., A.P. Herring, and D.W. Fuerstenau. 1966. The effect of crystal structure on the surface properties of a series of manganese dioxides. *J. Colloid Interface Sci.* 21:435–444.
- Heaney, P.J. 1994. Structure and chemistry of the low-pressure silica polymorphs. *Rev. Mineral. Geochem.* 29:1–40.
- Heaney, P.J., and J.A. Banfield. 1993. Structure and chemistry of silica, metal oxides, and phosphates. *Rev. Mineral. Geochem.* 28:185–233.
- Heaney, P.J., C.T. Prewit, and G.V. Gibbs (eds.) 1994. *Silica. Physical behavior, geochemistry and materials applications*. *Rev. Mineral.* 29:375.
- Hem, J.D., and C.J. Lind. 1983. Nonequilibrium models for predicting forms of precipitated manganese oxides. *Geochim. Cosmochim. Acta* 47:2037–2046.
- Hemingway, B.S., R.A. Robie, and J.A. Apps. 1991. Revised values for the thermodynamic properties of boehmite, $\text{AlO}(\text{OH})$, and related species and phases in the system $\text{Al}-\text{H}-\text{O}$. *Am. Mineral.* 76:445–451.
- Hesse, R. 1988. Origin of chert: Diagenesis of biogenic siliceous sediments. *Geosci. Can.* 15:171–192.
- Hingston, F.J., A.M. Posner, and J.P. Quirk. 1974. Anion adsorption by goethite and gibbsite. I. The role of the proton in determining adsorption envelopes. *J. Soil Sci.* 23:177–192.
- Holmgren, G.G.S. 1967. A rapid citrate–dithionite extractable iron procedure. *Soil Sci. Soc. Am. Proc.* 31:210–211.
- Houot, S., and J. Berthelin. 1992. Submicroscopic studies of iron deposits occurring in field drains: Formation and evolution. *Geoderma* 52:209–222.
- Hsu, P.H. 1966. Formation of gibbsite from aging hydroxy-aluminum solutions. *Soil Sci. Soc. Am. Proc.* 30:173–176.
- Hsu, P.H. 1967. Effect of salts on the formation of bayerite versus pseudoboehmite. *Soil Sci.* 103:101–110.
- Hsu, P.H. 1989. Aluminum hydroxides and oxyhydroxides, p. 331–378. *In* J.B. Dixon and S.B. Weed (eds.) *Minerals in soil environments*. SSSA, Madison, WI.
- Huang, P.M. 1988. Ionic factors affecting aluminum transformations and the impact on soil and environmental sciences. *Adv. Agron.* 8:1–78.
- Huang, P.M., M.K. Wang, N. Kämpf, and D.G. Schulze. 2002. Aluminum hydroxides, p. 261–289. *In* J.B. Dixon and D.G. Schulze (eds.) *Soil mineralogy with environmental applications*. SSSA, Madison, WI.
- Huebner, J.S. 1976. The manganese oxides—A bibliographic commentary, p. SH1–SH17. *In* D. Rumble (ed.) *Oxide minerals*. Mineralogical Society of America Short Course Notes. Vol. 3. Mineralogical Society of America, Washington, DC.
- Hughes, R.E., D.M. Moore, and H.D. Glass. 1994. Qualitative and quantitative analysis of clay minerals in soils, p. 330–359. *In* J.E. Amonette and L.W. Zelazny (eds.) *Quantitative methods in soil mineralogy*. SSSA, Madison, WI.

- Hui, L., L.S. Lee, D.G. Schulze, and C.A. Guest. 2003. Role of soil manganese in the oxidation of aromatic amines. *Environ. Sci. Technol.* 37:2686–2693.
- ICDD. 1994. Powder diffraction file 1995. PDF-2 database sets 1–45, Minerals. International Centre for Diffraction Data, Newtown Square, PA.
- Jackson, M.L. 1964. Chemical composition of soils, p. 71–141. *In* F.E. Bear (ed.) *Chemistry of the soil*. Van Nostrand-Reinhold, New York.
- Jackson, M.L. 1969. *Soil chemical analysis. Advanced course*. Parallel Press, Madison, WI.
- Jeanroy, E., J.L. Rajot, P. Pillon, and A.J. Herbillon. 1991. Differential dissolution of hematite and goethite in dithionite and its implication on soil yellowing. *Geoderma* 50:79–94.
- Jones, R.L., and A.H. Beavers. 1963. Sponge spicules in Illinois soils. *Soil Sci. Soc. Am. Proc.* 27:438–440.
- Jones, R.L., and A.H. Beavers. 1964. Variation of opal phytolith content among some great soil groups of Illinois. *Soil Sci. Soc. Am. Proc.* 28:711–712.
- Jones, L.H.P., and K.A. Handreck. 1967. Silica in soils, plants and animals. *Adv. Agron.* 19:107–149.
- Jones, J.B., and E.R. Segnit. 1971. The nature of opal. I. Nomenclature and constituent phases. *J. Geol. Soc. Aust.* 18:57–68.
- Juo, A.S.R. 1981. Chemical characteristics, p. 51–79. *In* D.J. Greenland (ed.) *Characterization of soils*. Oxford University Press, New York.
- Kämpf, N., and U. Schwertmann. 1982a. The 5M NaOH concentration treatment for iron oxides in soils. *Clays Clay Miner.* 30:401–408.
- Kämpf, N., and U. Schwertmann. 1982b. Quantitative determination of goethite and hematite in kaolinitic soils by X-ray diffraction. *Clay Miner.* 17:359–363.
- Kämpf, N., and U. Schwertmann. 1983. Goethite and hematite in a climosequence in southern Brazil and their application in classification of kaolinitic soils. *Geoderma* 29:27–39.
- Karathanasis, A.D. 1989. Solution chemistry of fragipans: Thermodynamic approach to understanding fragipan formation, p. 113–139. *In* N.E. Smeck and E.J. Ciolkosz (eds.) *Fragipans: Their occurrence, classification, and genesis*. SSSA Special Publication No. 24. SSSA, Madison, WI.
- Karathanasis, A.D., and W.G. Harris. 1994. Quantitative thermal analysis of soil materials, p. 360–411. *In* J.E. Amonette and L.W. Zelazny (eds.) *Quantitative methods in soil mineralogy*. SSSA, Madison, WI.
- Karathanasis, A.D., and Y.L. Thompson. 1995. Mineralogy of iron precipitates in a constructed acid mine drainage wetland. *Soil Sci. Soc. Am. J.* 59:1773–1781.
- Kastner, M., J.B. Keene, and J.M. Gieskes. 1977. Diagenesis of siliceous oozes—1. Chemical controls on the rate of opal-A to opal-CT transformation—An experimental study. *Geochim. Cosmochim. Acta* 41:1041–1059.
- Keller, W.D. 1978. Diaspore recrystallization at low temperature. *Am. Mineral.* 63:326–329.
- Kelly, E.F., R.G. Amundson, B.D. Marino, and M.J. Deniro. 1991. Stable isotope ratios of carbon in phytoliths as a quantitative method of monitoring vegetation and climate change. *Quat. Res.* 35:222–233.
- Kennedy, J.A., H.K.J. Powell, and J.M. White. 1982. A modification of Child's field test for ferrous iron and ferric-organic complexes in soils. *Aust. J. Soil Res.* 20:261–263.
- Kittrick, J.A. 1969. Soil minerals in the $\text{Al}_2\text{O}_3\text{-SiO}_2\text{-H}_2\text{O}$ system and a theory of their formation. *Clays Clay Miner.* 17:157–167.
- Knauth, L.P. 1994. Petrogenesis of chert. *Rev. Mineral. Geochim.* 29:233–258.
- Kodama, H., and M. Schnitzer. 1980. Effect of fulvic acid on the crystallization of aluminum hydroxide. *Geoderma* 24:195–205.
- Leinemann, C.-P., M. Taillefert, D. Perret, and J.-F. Gaillard. 1997. Association of cobalt and manganese in aquatic systems: Chemical and microscopic evidence. *Geochim. Cosmochim. Acta* 61:1437–1466.
- Lindsay, W.L. 1979. *Chemical equilibria in soils*. Wiley Interscience, New York.
- Lindsay, D.H. 1976. The crystal chemistry and structure of oxide minerals as exemplified by the Fe–Ti oxides. *Rev. Mineral.* 3:L1–L60.
- Lindsay, D.H. 1991. *Oxide minerals: Petrologic and magnetic significance*. Mineralogical Society of America, Washington, DC.
- Little, I.P., T.M. Armitage, and R.J. Gilkes. 1978. Weathering of quartz in dune sands under subtropical conditions in Eastern Australia. *Geoderma* 20:225–237.
- Loveland, P.J., and P. Digby. 1984. The extraction of Fe and Al by 0.1 M pyrophosphate solutions: A comparison of some techniques. *J. Soil Sci.* 35:243–250.
- Lovley, D.R. 1992. Microbial oxidation of organic matter coupled to the reduction of Fe(III) and Mn(IV) oxides, p. 101–114. *In* H.C.W. Skinner and R.W. Fitzpatrick (eds.) *Biomining: Processes of iron and manganese—Modern and ancient environments*. Catena Suppl. 21. Catena Verlag, Cremlingen, Germany.
- Lovley, D.R. 1995. Microbial reduction of iron, manganese, and other metals. *Adv. Agron.* 54:175–231.
- Lovley, D.R., and E.J.P. Phillips. 1987. Rapid assay for microbially reducible ferric iron in aquatic sediments. *Appl. Environ. Microbiol.* 53:1536–1540.
- Lovley, D.R., and E.J.P. Phillips. 1988. Novel mode of microbial energy metabolism: Organic carbon oxidation coupled to dissimilatory reduction of iron or manganese. *Appl. Environ. Microbiol.* 54:1472–1480.
- Lucas, Y. 2001. The role of plants in controlling rates and products of weathering: Importance of biological pumping. *Annu. Rev. Earth Planet. Sci.* 29:135–163.
- Lutwick, L.E., and A. Johnston. 1969. Cumulic soils of the rough fescue prairie–poplar transition region. *Can. J. Soil Sci.* 49:199–203.
- Macedo, J., and R.B. Bryant. 1987. Morphology, mineralogy, and genesis of a hydrosquence of Oxisols in Brazil. *Soil Sci. Soc. Am. J.* 51:690–698.

- Macedo, J., and R.B. Bryant. 1989. Preferential microbial reduction of hematite over goethite in a Brazilian Oxisol. *Soil Sci. Soc. Am. J.* 53:1114–1118.
- Mackenzie, R.C. 1970. Oxides and hydroxides of higher valency elements, p. 271–302. *In* R.C. Mackenzie (ed.) *Differential thermal analysis*. Vol. 1. Academic Press Ltd., New York.
- Mackenzie, R.C. 1972. Soils, p. 267–297. *In* R.C. Mackenzie (ed.) *Differential thermal analysis*. Vol. 2. Academic Press Ltd., New York.
- Mackenzie, F.T., and R. Gees. 1971. Quartz: Synthesis at earth-surface conditions. *Science* 173:533–535.
- Maher, B.A., and R.M. Taylor. 1988. Formation of ultrafine-grained magnetite in soils. *Nature* 336:368–370.
- Manceau, A., P.R. Buseck, D. Miser, J. Rask, and D. Nahon. 1990. Characterization of Cu in lithiophorite from a banded Mn ore. *Am. Mineral.* 75:490–494.
- Manceau, A., and J.M. Combes. 1988. Structure of Mn and Fe oxides and oxyhydroxides: A topological approach by EXAFS. *Phys. Chem. Miner.* 15:283–295.
- Manceau, A., and V.A. Drits. 1993. Local structure of ferrihydrite and ferroxihite by EXAFS spectroscopy. *Clay Miner.* 28:165–184.
- Manceau, A., and W.P. Gates. 1997. Surface structural model for ferrihydrite. *Clays Clay Miner.* 45:448–460.
- Manceau, A., A.I. Gorshkov, and V.A. Drits. 1992a. Structural chemistry of Mn, Fe, Co, and Ni in manganese hydrous oxides: I. Information from XANES spectroscopy. *Am. Mineral.* 77:1133–1143.
- Manceau, A., A.I. Gorshkov, and V.A. Drits. 1992b. Structural chemistry of Mn, Fe, Co, and Ni in manganese hydrous oxides: II. Information from EXAFS spectroscopy and electron and X-ray diffraction. *Am. Mineral.* 77:1144–1157.
- Manceau, A., S. Llorca, and G. Calas. 1987. Crystal chemistry of cobalt and nickel in lithiophorite and asbolane from New Caledonia. *Geochim. Cosmochim. Acta* 51:105–113.
- Maslen, E.N., V.A. Streltsov, N.R. Streltsova, and N. Ishizawa. 1994. Synchrotron X-ray study of the electron density in α -Fe₂O₃. *Acta Crystallogr. B* 50:435–441.
- Maslen, E.N., V.A. Streltsov, N.R. Streltsova, N. Ishizawa, and Y. Satow. 1993. Synchrotron X-ray study of the electron density in α -Al₂O₃. *Acta Crystallogr. B* 49:973–980.
- McBride, M.B. 1987. Adsorption and oxidation of phenolic compounds by iron and manganese oxides. *Soil Sci. Soc. Am. J.* 51:1466–1472.
- McBride, M.B. 1989. Reactions controlling heavy metal solubility in soils. *Adv. Agron.* 10:1–56.
- McBride, M.B. 1994. *Environmental chemistry of soils*. Oxford University Press, New York.
- McBride, M.B., and L.G. Wesslink. 1988. Chemisorption of catechol on gibbsite, boehmite, and noncrystalline alumina surfaces. *Environ. Sci. Technol.* 22:703–708.
- McKeague, J.A. 1967. An evaluation of 0.1 M pyrophosphate and pyrophosphate-dithionite in comparison with oxalate as extractants of the accumulation products in podzols and some other soils. *Can. J. Soil Sci.* 47:95–99.
- McKeague, J.A., and J.H. Day. 1966. Dithionite- and oxalate-extractable Fe and Al as aids in differentiating various classes of soils. *Can. J. Soil Sci.* 46:13–22.
- McKenzie, R.M. 1971. The synthesis of cryptomelane and some other oxides and hydroxides of manganese. *Mineral. Mag.* 38:493–502.
- McKenzie, R.M. 1978. The effect of two manganese dioxides on the uptake of Pb, Co, Ni, Cu and Zn by subterranean clover. *Aust. J. Soil Res.* 16:209–214.
- McKenzie, R.M. 1989. Manganese oxides and hydroxides, p. 439–465. *In* J.B. Dixon and S.B. Weed (eds.) *Minerals in soil environments*. SSSA, Madison, WI.
- McNeal, B.L., D.A. Layfield, W.A. Norvell, and J.D. Rhoades. 1968. Factors influencing hydraulic conductivity of soils in the presence of mixed salt solution. *Soil Sci. Soc. Am. Proc.* 32:187–190.
- Means, J.L., D.A. Crerar, M.P. Borcsik, and J.O. Duguid. 1978. Adsorption of cobalt and selected actinides by Mn and Fe oxides in soils and sediments. *Geochim. Cosmochim. Acta* 42:1763–1773.
- Mehra, O.P., and M.L. Jackson. 1960. Iron oxide removal from soils and clays by a dithionite–citrate system buffered with sodium bicarbonate, p. 317–342. *In* A. Swineford (ed.) *Proc. 7th Clays Clay Miner. Conf.*, Pergamon Press, Elmsford, New York.
- Milnes, A.R., and R.W. Fitzpatrick. 1989. Titanium and zirconium minerals, p. 1131–1205. *In* J.B. Dixon and S.B. Weed (eds.) *Minerals in soil environments*. 2nd edn. SSSA, Madison, WI.
- Mitchell, W.A. 1975. Heavy minerals, p. 450–480. *In* J.E. Gieseking (ed.) *Soil components*. Vol. 2. Inorganic components. Springer-Verlag, Berlin, Germany.
- Miyamoto, H. 1976. The magnetic properties of Fe(OH)₂. *Mater. Res. Bull.* 11:329–336.
- Mizota, C., M. Itoh, M. Kusakabe, and M. Noto. 1991. Oxygen isotope ratios of opaline silica and plant opal in three recent volcanic ash soils. *Geoderma* 50:211–217.
- Mizota, C., and Y. Matsuhisa. 1995. Isotopic evidence for the eolian origin of quartz and mica in soils developed on volcanic materials in the Canary Archipelago. *Geoderma* 66:313–320.
- Monger, H.C., and E.F. Kelly. 2002. Silica minerals, p. 611–636. *In* J.B. Dixon and D.G. Schulze (eds.) *Soil mineralogy with environmental applications*. SSSA, Madison, WI.
- Muggler, C.C. 1998. Polygenetic Oxisols on tertiary surfaces, Minas Gerais, Brazil: Soil genesis and landscape development. Ph.D. Thesis. Wageningen, the Netherlands.
- Murad, E. 1988. Properties and behavior of iron oxides as determined by Mössbauer spectroscopy, p. 309–350. *In* J.W. Stucki, B.A. Goodman, and U. Schwertmann (eds.) *Iron in soils and clay minerals*. D. Reidel Publishing Company, Dordrecht, the Netherlands.
- Murad, E. 1996. Magnetic properties of microcrystalline iron(III) oxides and related materials as reflected in their Mössbauer spectra. *Phys. Chem. Miner.* 23:248–262.

- Murad, E. 1997. Identification of minor amounts of anatase in kaolins by Raman spectroscopy. *Am. Mineral.* 82:203–206.
- Murad, E., U. Schwertmann, J.M. Bigham, and L. Carlson. 1994. Mineralogical characteristics of poorly crystallized precipitates formed by oxidation of Fe^{2+} in acid sulfate waters. *ACS Symp. Ser.* 550:190–200.
- Murray, J.W. 1975. The interactions of metal ions at the manganese dioxide–solution interface. *Geochim. Cosmochim. Acta* 39:505–519.
- Murray, J.W., J.G. Dillard, R. Giovanoli, H. Moers, and W. Stumm. 1985. Oxidation of Mn(II): Initial mineralogy, oxidation state and aging. *Geochim. Cosmochim. Acta* 49:463–470.
- Norfleet, M.L., A.D. Karathanasis, and B.R. Smith. 1993. Soil solution composition relative to mineral distribution in Blue Ridge mountain soils. *Soil Sci. Soc. Am. J.* 57:1375–1380.
- Norrish, K., and R.M. Taylor. 1961. The isomorphous replacement of iron by aluminium in soil goethites. *J. Soil Sci.* 12:294–306.
- Obura, P.A. 2008. Effect of soil properties on bioavailability of aluminum and phosphorus in selected Kenyan and Brazilian acid soils. Ph.D. Thesis. Purdue University, West Lafayette, IN.
- Ogg, C.M., and J.C. Baker. 1999. Pedogenesis and origin of deeply weathered soils formed in alluvial fans of the Virginia Blue Ridge. *Soil Sci. Soc. Am. J.* 63:601–606.
- Ohta, S., S. Effendi, N. Tanaka, and S. Miura. 1993. Ultisols of lowland Dipterocarp forest in east Kalimantan, Indonesia. *Soil Sci. Plant Nutr.* 39:1–12.
- Oscarson, D.W., P.M. Huang, W.K. Liaw, and U.T. Hammer. 1983. Kinetics of oxidation of arsenite by various manganese oxides. *Soil Sci. Soc. Am. J.* 47:644–648.
- Ostwald, J. 1984a. Two varieties of lithiophorite in some Australian deposits. *Mineral. Mag.* 48:383–388.
- Ostwald, J. 1984b. The influence of clay mineralogy on the crystallization of the tetravalent manganese layer-lattice minerals. *Neues Jahrb. Mineral. Abh.* 1984:9–16.
- Ostwald, J. 1985. Some observations on the chemical composition of chalcophanite. *Mineral. Mag.* 49:752–755.
- Parc, S., D. Nahon, Y. Tardy, and P. Vieillard. 1989. Estimated solubility products and fields of stability for cryptomelane, nsutite, birnessite, and lithiophorite based on natural lateritic weathering sequences. *Am. Mineral.* 74:466–475.
- Parfitt, R.L., and C.W. Childs. 1988. Estimation of forms of Fe and Al: A review, and analysis of contrasting soils by dissolution and Moessbauer methods. *Aust. J. Soil Res.* 26:121–144.
- Parfitt, R.L., C.W. Childs, and D.N. Eden. 1988. Ferrihydrite and allophane in four Andepts from Hawaii and implications for their classifications. *Geoderma* 41:223–241.
- Peterschmitt, E., E. Fritsch, J.L. Rajot, and A.J. Herbillon. 1996. Yellowing, bleaching and ferritisation processes in soil mantle of the Western Ghats, South India. *Geoderma* 74:235–253.
- Pinheiro-Dick, D., and U. Schwertmann. 1996. Microaggregates from Oxisols and Inceptisols: Dispersion through selective dissolutions and physicochemical treatments. *Geoderma* 74:49–63.
- Post, J.E. 1992. Crystal structures of manganese oxide minerals, p. 51–73. *In* H.C.W. Skinner and R.W. Fitzpatrick (eds.) *Biom mineralization. Processes of iron and manganese—Modern and ancient environments.* Catena Suppl. 21. Catena Verlag, Cremlingen, Germany.
- Post, J.E., and D.E. Appleman. 1988. Chalcophanite, $\text{ZnMn}_3\text{O}_7 \cdot 3\text{H}_2\text{O}$: New crystal-structure determinations. *Am. Mineral.* 73:1401–1404.
- Post, J.E., and D.E. Appleman. 1994. Crystal structure refinement of lithiophorite. *Am. Mineral.* 79:370–374.
- Post, J.E., and D.L. Bish. 1988. Rietveld refinement of the todorokite structure. *Am. Mineral.* 73:861–869.
- Post, J.E., and D.L. Bish. 1989. Rietveld refinement of the coronadite structure. *Am. Mineral.* 74:913–917.
- Post, J.E., and V.F. Buchwald. 1991. Crystal structure refinement of akaganéite. *Am. Mineral.* 76:272–277.
- Post, J.E., and C.W. Burnham. 1986. Modelling tunnel-cation displacements in hollandites using structure-energy calculations. *Am. Mineral.* 71:1178–1185.
- Post, J.E., and D.R. Veblen. 1990. Crystal structure determinations of synthetic sodium, magnesium, and potassium birnessite using TEM and the Rietveld method. *Am. Mineral.* 75:477–489.
- Post, J.E., R.B. von Dreele, and P.R. Buseck. 1982. Symmetry and cation displacements in hollandites: Structure refinements of hollandite, cryptomelane and priderite. *Acta Crystallogr. B* 38:1056–1065.
- Potter, R.M., and G.R. Rossman. 1979. The tetravalent manganese oxides: Identification, hydration, and structural relationships by infrared spectroscopy. *Am. Mineral.* 64:1199–1218.
- Pye, K., and J. Mazzullo. 1994. Effects of tropical weathering on quartz grain shape. An example from northeastern Australia. *J. Sediment. Res. A* 64:500–507.
- Rask, J.H., and P.R. Buseck. 1986. Topotactic relations among pyrolusite, manganite, and Mn_5O_8 : A high-resolution transmission electron microscopy investigation. *Am. Mineral.* 71:805–814.
- Richardson, J.L., and F.D. Hole. 1979. Mottling and iron distribution in a Glossoboralf-Haplaquoll hydrosequence on a glacial moraine in northwestern Wisconsin. *Soil Sci. Soc. Am. J.* 43:552–558.
- Robbins, E.I., J.P. D'Agostino, J. Ostwald, D.S. Fanning, V. Carter, and R.L. Van Hoven. 1992. Manganese nodules and microbial oxidation of manganese in the Huntley Meadows wetland, Virginia, USA, p. 179–202. *In* H.C.W. Skinner and R.W. Fitzpatrick (eds.) *Biom mineralization. Processes of iron and manganese—Modern and ancient environments.* Catena Suppl. 21. Catena Verlag, Cremlingen, Germany.
- Rodgers, K.A. 1993. Routine identification of aluminum hydroxide polymorphs with the laser Raman microprobe. *Clay Miner.* 28:85–99.
- Ross, S.J., Jr., D.P. Franzmeier, and C.B. Roth. 1976. Mineralogy and chemistry of manganese oxides in some Indiana soils. *Soil Sci. Soc. Am. J.* 40:137–143.
- Rowse, J.B., and W.B. Jepson. 1972. The determination of quartz in clay minerals: A critical comparison of methods. *J. Therm. Anal.* 4:169–175.

- Ryskin, Y.I. 1974. The vibration of protons in minerals: Hydroxyl, water and ammonium, p. 137–181. *In* V.C. Farmer (ed.) *Infrared spectra of minerals*. Mineralogical Society, London, UK.
- Sacconne, L., D.J. Conley, E. Koning, D. Sauer, M. Sommer, D. Kaczorek, S.W. Blecker, and E.F. Keller. 2007. Assessing the extraction and quantification of amorphous silica in soils of forest and grassland ecosystems. *Eur. J. Soil Sci.* 58:1446–1459.
- Sasaki, S., K. Fukino, Y. Takéuchi, and R. Sadanaga. 1980. On the estimation of atomic charges by the x-ray method for some oxides and silicates. *Acta Crystallogr. A* 36:904–915.
- Sauer, D., L. Sacconne, D.J. Conley, L. Herrmann, and M. Sommer. 2006. Review of methodologies for extracting plant-available and amorphous Si from soils and aquatic sediments. *Biogeochemistry* 80:89–108.
- Schmahl, W.W., I.P. Swinson, M.T. Dove, and A. Graeme-Barber. 1992. Landau free energy and order parameter behavior of the α/β phase transition in cristobalite. *Z. Kristallogr.* 201:125–145.
- Schoen, R., and C.E. Roberson. 1970. Structures of aluminum hydroxide and geochemical implications. *Am. Mineral.* 55:43–77.
- Schulze, D.G. 1981. Identification of soil iron oxide minerals by differential x-ray diffraction. *Soil Sci. Soc. Am. J.* 45:437–440.
- Schulze, D.G. 1984. The influence of aluminum on iron oxides. VIII. Unit cell dimensions of Al substituted goethites and estimation of Al from them. *Clays Clay Miner.* 32:36–44.
- Schulze, D.G. 1988. Separation and concentration of iron-containing phases, p. 63–81. *In* J.W. Stucki, B.A. Goodman, and U. Schwertmann (eds.) *Iron in soils and clay minerals*. D. Reidel Publishing Company, Dordrecht, the Netherlands.
- Schulze, D.G., and J.B. Dixon. 1979. High gradient magnetic separation of iron oxides and magnetic minerals from soil clays. *Soil Sci. Soc. Am. J.* 43:793–799.
- Schuppli, P.A., G.J. Ross, and J. McKeague. 1983. The effective removal of suspended materials from pyrophosphate extracts of soils from tropical and temperate regions. *Soil Sci. Soc. Am. J.* 47:1026–1032.
- Schwarz, T. 1994. Ferricrete formation and relief inversion: An example from Central Sudan. *Catena* 21:257–268.
- Schwertmann, U. 1964. Differenzierung der Eisenoxide des Bodens durch photochemische Extraktion mit saurer Ammoniumoxalat-Lösung. *Z. Pflanzenernähr. Bodenk.* 105:194–202.
- Schwertmann, U. 1966. Inhibitory effect of soil organic matter on the crystallization of amorphous ferric hydroxide. *Nature (London)* 212:645–646.
- Schwertmann, U. 1988. Occurrence and formation of iron oxides in various pedoenvironments, p. 267–308. *In* J.W. Stucki, B.A. Goodman, and U. Schwertmann (eds.) *Iron in soils and clay minerals*. D. Reidel Publishing Company, Dordrecht, the Netherlands.
- Schwertmann, U. 1991. Solubility and dissolution of iron oxides. *Plant Soil* 130:1–25.
- Schwertmann, U. 1993. Relation between iron oxides, soil color, and soil formation, p. 51–69. *In* J.M. Bigham and E.J. Ciolkosz (eds.) *Soil color*. SSSA, Madison, WI.
- Schwertmann, U., J.M. Bigham, and E. Murad. 1995a. The first occurrence of schwertmannite in a natural stream environment. *Eur. J. Miner.* 7:547–552.
- Schwertmann, U., and L. Carlson. 1994. Aluminum influence on iron oxides. XVII. Unit-cell parameters and aluminum substitution of natural goethites. *Soil Sci. Soc. Am. J.* 58:256–261.
- Schwertmann, U., and D.S. Fanning. 1976. Iron–manganese concretions in hydrosquences of soils in loess in Bavaria. *Soil Sci. Soc. Am. J.* 40:731–738.
- Schwertmann, U., and H. Fechter. 1984. The influence of aluminium on iron oxides. XI. Aluminium substituted maghemite in soils and its formation. *Soil Sci. Soc. Am. J.* 48:1462–1463.
- Schwertmann, U., and H. Fechter. 1994. The formation of green rust and its transformation to lepidocrocite. *Clay Miner.* 29:87–92.
- Schwertmann, U., and W.R. Fischer. 1973. Natural “amorphous” ferric hydroxide. *Geoderma* 10:237–247.
- Schwertmann, U., and R.W. Fitzpatrick. 1992. Iron minerals in surface environments, p. 7–30. *In* H.C.W. Skinner and R.W. Fitzpatrick (eds.) *Biomineralization—Processes of iron and manganese*. Catena Verlag, Cremlingen, Germany.
- Schwertmann, U., R.W. Fitzpatrick, R.M. Taylor, and D.G. Lewis. 1979. The influence of aluminium on iron oxides. Part II. Preparation and properties of Al substituted hematites. *Clays Clay Miner.* 27:105–112.
- Schwertmann, U., J. Friedl, G. Pfab, and A.U. Gehring. 1995b. Iron substitution in soil and synthetic anatase. *Clays Clay Miner.* 43:599–606.
- Schwertmann, U., and N. Kämpf. 1983. Oxidos de ferro jovens em ambientes pedogeneticos brasileiros. *Rev. Bras. Cienc. Solo* 7:251–255.
- Schwertmann, U., and N. Kämpf. 1985. Properties of goethite and hematite in kaolinitic soils of southern and central Brazil. *Soil Sci.* 139:344–350.
- Schwertmann, U., and M. Latham. 1986. Properties of iron oxides in some New Caledonian Oxisols. *Geoderma* 39:105–123.
- Schwertmann, U., and G. Pfab. 1994. Structural vanadium in synthetic goethite. *Geochim. Cosmochim. Acta* 58:4349–4352.
- Schwertmann, U., and G. Pfab. 1996. Structural vanadium and chromium in lateritic iron oxides: Genetic implications. *Geochim. Cosmochim. Acta* 60:4279–4283.
- Schwertmann, U., D.G. Schulze, and E. Murad. 1982. Identification of ferrihydrite in soils by dissolution kinetics, differential x-ray diffraction and Mössbauer spectroscopy. *Soil Sci. Soc. Am. J.* 46:869–875.
- Schwertmann, U., and R.M. Taylor. 1989. Iron oxides, p. 379–438. *In* J.B. Dixon and S.B. Weed (eds.) *Minerals in soil environments*. SSSA, Madison, WI.
- Scott, M.J., and J.J. Morgan. 1995. Reactions at oxide surfaces. 1. Oxidation of As(III) by synthetic birnessite. *Environ. Sci. Technol.* 29:1898–1905.

- Senkayi, A.L., J.B. Dixon, and L.R. Hossner. 1986. Todorokite, goethite, and hematite: Alteration products of siderite in east Texas lignite overburden. *Soil Sci.* 142:36–42.
- Shafdan, H., J.B. Dixon, and F.G. Calhoun. 1985. Iron oxide properties versus strength of ferruginous crust and iron glaucohalite in soils. *Soil Sci.* 140:317–325.
- Shah Singh, S., and H. Kodama. 1994. Effect of the presence of aluminum ions in iron solutions on the formation of iron oxyhydroxides (FeOOH) at room temperature under acidic environment. *Clays Clay Miner.* 42:606–613.
- Sidhu, P.S., J.L. Sehgal, M.K. Sinha, and N.S. Randhawa. 1977. Composition and mineralogy of iron–manganese concretions from some soils of the Indo-Gangetic plain in north-west India. *Geoderma* 18:241–249.
- Singer, A., and P.M. Huang. 1990. Effects of humic acids on the crystallization of aluminum hydroxides. *Clays Clay Miner.* 38:47–52.
- Singh, B., and R.J. Gilkes. 1992. Properties and distribution of iron oxides and their association with minor elements in the soils of south-western Australia. *J. Soil Sci.* 43:77–98.
- Skinner, H.C.W., and R.W. Fitzpatrick (eds.). 1992. Biomineralization. Processes of iron and manganese. *Catena Suppl.* 21. Catena Verlag, Cremlingen, Germany.
- Soil Survey Staff. 1975. Soil taxonomy—A basic system of soil classification for making and interpreting soil surveys. *Agricultural Handbook No. 436*. U.S. Government Printing Office, Washington, DC.
- Speer, J.A. 1982. Zircon, p. 67–112. *In* P.H. Ribbe (ed.) *Reviews in mineralogy*. Vol. 5. Orthosilicates. Mineralogical Society of America, Washington, DC.
- Staller, J.E. 2002. A multidisciplinary approach to understanding the initial introduction of maize into coastal Ecuador. *J. Archaeol. Sci.* 29:33–50.
- Stanjek, H. 1987. The formation of maghemite and hematite from lepidocrocite and goethite in a Cambisol from Corsica, France. *Z. Pflanzenernähr. Bodenk.* 150:314–318.
- Stone, A.T., and J.J. Morgan. 1984a. Reduction and dissolution of manganese(III) and manganese(IV) oxides by organics. 1. Reaction with hydroquinone. *Environ. Sci. Technol.* 18:450–456.
- Stone, A.T., and J.J. Morgan. 1984b. Reduction and dissolution of manganese(III) and manganese(IV) oxides by organics. 2. Survey of the reactivity of organics. *Environ. Sci. Technol.* 18:617–624.
- Sudom, M.D., and R.J. St. Arnaud. 1971. Use of quartz, zirconium and titanium as indices in pedological studies. *Can. J. Soil Sci.* 51:385–396.
- Süsser, P., and U. Schwertmann. 1991. Proton buffering in mineral horizons of some acid forest soils. *Geoderma* 49:63–76.
- Tait, J.M., A. Violante, and P. Violante. 1983. Coprecipitation of gibbsite and bayerite with nordstrandite. *Clay Miner.* 18:95–99.
- Tanaka, K., and J. White. 1982. Characterization of species adsorbed on oxidized and reduced anatase. *J. Phys. Chem.* 86:4708–4714.
- Taylor, R.M. 1968. The association of manganese and cobalt in soils—Further observations. *J. Soil Sci.* 19:77–80.
- Taylor, R.M. 1987. Non-silicates oxides and hydroxides, p. 129–201. *In* A.C.D. Newman (ed.) *Chemistry of clays and clay minerals*. John Wiley & Sons, New York.
- Taylor, R.M., and R.M. McKenzie. 1980. The influence of aluminium on iron oxides. VI. The formation of Fe(II)–Al(III) hydroxy-chlorides, -sulphates, and -carbonates as new members of the pyroaurite group and their significance in soils. *Clays Clay Miner.* 28:179–187.
- Taylor, R.M., R.M. McKenzie, A.W. Fordham, and G.P. Gillman. 1983. Oxide minerals, p. 309–334. *In* *Soils: An Australian viewpoint*. Academic Press, London, UK.
- Taylor, R.M., R.M. McKenzie, and K. Norrish. 1964. The mineralogy and chemistry of manganese in some Australian soils. *Aust. J. Soil Res.* 2:235–248.
- Taylor, R.M., and U. Schwertmann. 1974. Maghemite in soils and its origin. I. Properties and observations on soil maghemites. *Clay Miner.* 10:289–298.
- Tebo, B.M., J.R. Bargar, B.G. Clement, G.J. Dick, K.J. Murray, D. Parker, R. Verity, and S.M. Webb. 2004. Biogenic manganese oxides: Properties and mechanisms of formation. *Annu. Rev. Earth Planet. Sci.* 32:287–328.
- Tejan-Kella, M.S., R.W. Fitzpatrick, and D.J. Chittleborough. 1991. Scanning electron microscope study of zircons and rutiles from a podzol chronosequence at Cooloola, Queensland, Australia. *Catena* 18:11–30.
- Tettenhorst, R., and D.A. Hofmann. 1980. Crystal chemistry of boehmite. *Clays Clay Miner.* 28:373–380.
- Thanabalasingam, P., and W.F. Pickering. 1986. Effect of pH on the interaction between As(III) or As(V) and manganese(IV) oxide. *Water Air Soil Pollut.* 29:205–216.
- Thompson, I.A., D.M. Huber, C.A. Guest, and D.G. Schulze. 2005. Fungal manganese oxidation in a reduced soil. *Environ. Microbiol.* 7:1480–1487.
- Thompson, I.A., D.M. Huber, and D.G. Schulze. 2006. Evidence of a multicopper oxidase in Mn oxidation by *Gaeumannomyces graminis* var. *tritici*. *Phytopathology* 96:130–136.
- Tokashiki, Y., J.B. Dixon, and D.C. Golden. 1986. Manganese oxide analysis in soils by combined x-ray diffraction and selective dissolution methods. *Soil Sci. Soc. Am. J.* 50:1079–1084.
- Torrent, J., R. Guzman, and M.A. Parra. 1982. Influence of relative humidity on the crystallization of Fe(III) oxides from ferrihydrite. *Clays Clay Miner.* 30:337–340.
- Torrent, J., U. Schwertmann, and V. Barrón. 1987. The reductive dissolution of synthetic goethite and hematite in dithionite. *Clay Miner.* 22:329–337.
- Torrent, J., U. Schwertmann, H. Fechter, and F. Alferez. 1983. Quantitative relationships between soil colour and hematite content. *Soil Sci.* 136:354–358.
- Towe, K.M., and W.F. Bradley. 1967. Mineralogical constitution of colloidal “hydrous ferric oxides”. *J. Colloid Interface Sci.* 24:384–392.

- Trolard F., G. Bourrié, M. Abdelmoula, P. Refait, and F. Feder. 2007. Fougérite, a new mineral of the pyroaurite-iowaite group: Description and crystal structure. *Clays Clay Miner.* 55:323–334.
- Trolard, F., and Y. Tardy. 1987. The stabilities of gibbsite, boehmite, aluminous goethites and aluminous hematites in bauxites, ferricretes, and laterites as a function of water activity, temperature, and particle size. *Geochim. Cosmochim. Acta* 51:945–957.
- Turner, S., and P.R. Buseck. 1979. Manganese oxide tunnel structures and their intergrowths. *Science* 203:456–458.
- Turner, S., and P.R. Buseck. 1981. Todorokites: A new family of naturally occurring manganese oxides. *Science* 212:1024–1027.
- Turner, S., and P.R. Buseck. 1983. Defects in nsutite (γ - MnO_2) and dry-cell battery efficiency. *Nature* 304:143–146.
- Turner, S., and J.E. Post. 1988. Refinement of the substructure and superstructure of romanèchite. *Am. Mineral.* 73:1155–1161.
- Uzochukwu, G.A., and J.B. Dixon. 1986. Manganese oxide minerals in nodules of two soils of Texas and Alabama. *Soil Sci. Soc. Am. J.* 50:1358–1363.
- van Bodegom, P.M., J. van Reeve, and H.A.C.D. van der Gon. 2003. Prediction of reducible soil iron content from iron extraction data. *Biogeochemistry* 64:231–245.
- van Wambeke, A. 1992. *Soils of the tropics*. McGraw-Hill, New York.
- Varentsov, I.M. 1982. Groote Eylandt manganese oxide deposits, Australia. *Chem. Erde* 41:157–173.
- Vgenopoulos, A.G. 1984. Genesis of boehmite resp. diaspore in bauxite in dependence of redox equilibrium. *Chem. Erde* 43:149–159.
- Violante, A., and P.M. Huang. 1985. Influence of inorganic and organic ligands on the formation of aluminum hydroxides and oxyhydroxides. *Clays Clay Miner.* 33:181–192.
- Violante, A., and P.M. Huang. 1994. Identification of pseudo-boehmite in mixtures with phyllosilicates. *Clay Miner.* 29:351–359.
- Violante, A., and M.L. Jackson. 1979. Crystallization of nordstrandite in citrate systems and in the presence of montmorillonite, p. 517–525. *In* M.M. Mortland and V.C. Farmer (eds.) *Proc. Intl. Clay Conf. 1978* (Oxford), Elsevier Scientific Publishing Company, Amsterdam, the Netherlands.
- Violante, A., and M.L. Jackson. 1981. Clay influence on the crystallization of aluminum hydroxide polymorphs in the presence of citrate, sulfate or chloride. *Geoderma* 25:199–214.
- Violante, A., and P. Violante. 1980. Influence of pH, concentration and chelating power of organic anions on the synthesis of aluminum hydroxides and oxyhydroxides. *Clays Clay Miner.* 28:425–434.
- Violante, P., A. Violante, and J.M. Tait. 1982. Morphology of nordstrandite. *Clays Clay Miner.* 30:431–437.
- Wall, J.R.D., E.B. Wolfenden, E.H. Beard, and T. Deans. 1962. Nordstrandite in soil from West Sarawak, Borneo. *Nature* 196:264–265.
- Wang, H.D., G.N. White, F.T. Turner, and J.B. Dixon. 1993. Ferrihydrite, lepidocrocite, and goethite in coatings from east Texas vertic soils. *Soil Sci. Soc. Am. J.* 57:1381–1386.
- Waychunas, G.A. 1991. Crystal chemistry of oxides and oxyhydroxides, p. 11–68. *In* D.H. Lindsley (ed.) *Reviews in mineralogy*. Vol. 25. Oxide minerals: petrologic and magnetic significance. Mineralogical Society of America, Washington, DC.
- Wechsler, B.A., D.H. Lindsley, and C.T. Prewitt. 1984. Crystal structure and cation distribution in titanomagnetite ($\text{Fe}_{3-x}\text{Ti}_x\text{O}_4$). *Am. Mineral.* 69:754–770.
- Weiss, J.V., D. Emerson, S.M. Backer, and J.P. Megonigal. 2003. Enumeration of Fe(II)-oxidizing and Fe(III)-reducing bacteria in the root zone of wetland plants: Implications for a rhizosphere iron cycle. *Biogeochemistry* 64:77–96.
- Wells, M.A., R.J. Gilkes, and R.R. Anand. 1989. The formation of corundum and aluminous hematite by thermal dehydroxylation of aluminous goethite. *Clay Miner.* 24:513–530.
- White, G.N., and J.B. Dixon. 1996. Iron and manganese distribution in nodules from a young Texas Vertisol. *Soil Sci. Soc. Am. J.* 60:1254–1262.
- Wilding, L.P., and L.R. Drees. 1968. Distribution and implications of sponge spicules in surficial deposits in Ohio. *Ohio J. Sci.* 68:92–99.
- Wilding, L.P., and L.R. Drees. 1971. Biogenic opal in Ohio soils. *Soil Sci. Soc. Am. Proc.* 35:1004–1010.
- Wilding, L.P., and L.R. Drees. 1974. Contributions of forest opal and associated crystalline phases to fine silt and clay fractions of soils. *Clays Clay Miner.* 22:295–306.
- Will, G., M. Bellotto, W. Parrish, and M. Hart. 1988. Crystal structures of quartz and magnesium germanate by profile analysis of synchrotron-radiation high-resolution powder data. *J. Appl. Cryst.* 21:182–191.
- Williams, L.A., and D.A. Crerar. 1985. Silica diagenesis, II. General mechanisms. *J. Sediment. Petrol.* 55:312–321.
- Williams, L.A., G.A. Parks, and D.A. Crerar. 1985. Silica diagenesis, I. Solubility controls. *J. Sediment. Petrol.* 55:301–311.
- Yamada, N., M. Ohmasa, and S. Horiuchi. 1986. Textures in natural pyrolusite, β - MnO_2 , examined by 1 MV HRTEM. *Acta Crystallogr. B* 42:58–61.
- Zeese, R., U. Schwertmann, G.F. Tietz, and U. Jux. 1994. Mineralogy and stratigraphy of three deep lateritic profiles of the Jos plateau (central Nigeria). *Catena* 21:195–214.
- Zwicker, W.K., W.O.J.G. Meijer, and H.W. Jaffe. 1962. Nsutite—A widespread manganese oxide mineral. *Am. Mineral.* 47:246–266.

Poorly Crystalline Aluminosilicate Clay Minerals

23.1	Structure of Poorly Crystalline Materials.....	23-1
	Definition of Short-Range Ordered Materials • Structure of Imogolite • Structure of Allophane	
23.2	Identification and Synthesis of Allophane and Imogolite.....	23-5
	Imogolite Identification and Synthesis • Allophane Identification and Synthesis	
23.3	Occurrence of Imogolite and Allophane in Natural Environments	23-5
23.4	Surface Charge Characteristics of Short-Range Ordered Aluminosilicates and Variable-Charge Soils.....	23-6
	Surface Charge Determination • Interaction with Anions and Cations	
23.5	Interaction of Allophane and Imogolite with Other Soil Constituents.....	23-8
	Organic Matter and Iron Oxides • Water	
	References.....	23-10

James Harsh

Washington State University

This chapter covers the poorly crystalline aluminosilicate materials, commonly known as allophane and imogolite. With dimensions generally less than 50 nm, allophane and imogolite are naturally occurring nanoparticles. Their solubility, high specific surface area, variable charge, and unique physical behavior impart special properties to soils that contain them. Although often associated with soils formed from volcanic material (Andisols), allophane and imogolite are found within a wide range of soil orders and derived from a variety of parent materials. Ferrihydrite, a poorly crystalline iron oxide that often occurs with allophane and imogolite, is covered elsewhere in this handbook. A timely review by Parfitt (2009) considered the role of allophane and imogolite in biogeochemical processes, Dahlgren et al. (2004) reviewed volcanic soils, and Floody et al. (2009) discussed industrial applications of allophane and other natural nanoclays.

23.1 Structure of Poorly Crystalline Materials

23.1.1 Definition of Short-Range Ordered Materials

Crystalline materials exhibit long-range order in their atomic structure. Structural features repeat over scales of at least micrometers in a single crystal or over several particles in a powder. Such minerals display narrow x-ray diffraction peaks and their crystal habit can be directly observed at the scale of an optical microscope or by the naked eye in the case of large crystals. Amorphous materials, on the other hand, exhibit no order, even in the local

environment of the atoms. The atoms are arranged in a variety of states and structures where bond lengths, coordination, and geometry vary from site to site. Poorly crystalline materials fall in between these two extremes, showing short-range, medium-range, or limited long-range order. Short-range order is observable by techniques that probe the local environment of each atom, such as nuclear magnetic resonance (NMR) or x-ray photoelectron spectroscopy. X-ray diffraction peaks are indicative of, at least, medium-range order, whereas long-range order is detectable by electron microscopy. Poorly crystalline materials lack medium-range repetition of structural units in at least one of the three spatial dimensions; that is, well defined electron or x-ray diffraction patterns (XRD) are not produced. Allophane and imogolite practically represent the range from amorphous to crystalline materials (Fyfe et al., 1987). In the interest of brevity, allophane, imogolite, and poorly crystalline iron hydrous oxides will be referred to collectively as short-range ordered (SRO) materials.

In spite of their wide occurrence as intermediates in soil formation, allophane and imogolite were, until the second-half of the Twentieth Century, missed or ignored because of their virtual absence from XRD. When they were found to be important constituents of soils derived from volcanic ash (Taylor, 1933; Yoshinaga and Aomine, 1962; Abidin et al., 2007), researchers turned to a variety of methods more conducive to their identification, characterization, and quantification. These include selective dissolution by oxalic acid to quantify Si and Al, thermoanalytic methods to identify and quantify specific minerals, structural characterization by vibrational spectroscopy (IR and FTIR) (Farmer et al., 1977; Dahlgren, 1994), and electron microscopy

(Wilson, 1987). Short-range structural information has been obtained with solid-state NMR and x-ray absorption spectroscopy (XAS). Even the diffuse peaks in XRD patterns are useful to identify and quantify poorly crystalline materials (Cruz and Real, 1991). More recently, computer modeling has been employed to test proposed structures against spectroscopic data and to determine which structures give an energy minimum (Guimaraes et al., 2007; Creton et al., 2008; Zhao et al., 2009). The application of such methods to determine imogolite and allophane structure is discussed in the following sections.

23.1.2 Structure of Imogolite

Imogolite is a mineral with relatively constant chemical composition ($\text{SiAl}_2\text{O}_5 \cdot 2\text{H}_2\text{O}$), only six-fold coordination for Al, as many as seven x-ray diffraction peaks and two very broad “bands” (Table 23.1), and a distinctive tubular morphology observable under the electron microscope (Figure 23.1). Thus, imogolite has the major features of a crystalline mineral, but some consider it paracrystalline because each tube displays long-range order primarily in one dimension—along the length of the tube (Greenland, 1982). Diffraction patterns and electron micrographs, however, show that bundles of imogolite are aligned in an array with a repeat distance of around 2 nm, consistent with the diameter of the tubes (Figure 23.1; Cradwick et al., 1972). Thus, imogolite displays an added dimension of repeating units similar to layered aluminosilicates with regular stacking.

The Al in imogolite occurs in a gibbsite-like sheet and the Si is coordinated to three oxygen atoms and one hydroxyl group. The oxygen atoms are shared with the Al octahedra and the apical hydroxyls point toward the inside of the imogolite tube (Figure 23.2; Cradwick et al., 1972; Zhao et al., 2009). The separation distances between close-packed tubes are typically around 2.3 nm for natural and 2.7–3.2 nm for synthetic imogolite (Mukherjee et al., 2005) and the repeat distance along the gibbsite sheet (c-axis) is 0.84 nm (Wada and Yoshinaga, 1969).

TABLE 23.1 Powder X-Ray Diffraction Peaks for Proto-Imogolite Allophane and Imogolite

d (nm)	Proto-Imogolite Allophane		Imogolite	
	I		d (nm)	I
1.2vb ^a	70		1.6vb	100
0.43vb	10		0.79	70
0.34vb ^b	100		0.56	35
0.22vb ^b	50		0.44	10
0.19 ^a	10		0.41	10
0.17	10		0.37	20
0.14 ^b	20		0.33vb	65
			0.31	5
			0.26	5
			0.225vb	25

^a Also present in halloysite-like allophane.

^b Present in all three allophanes.

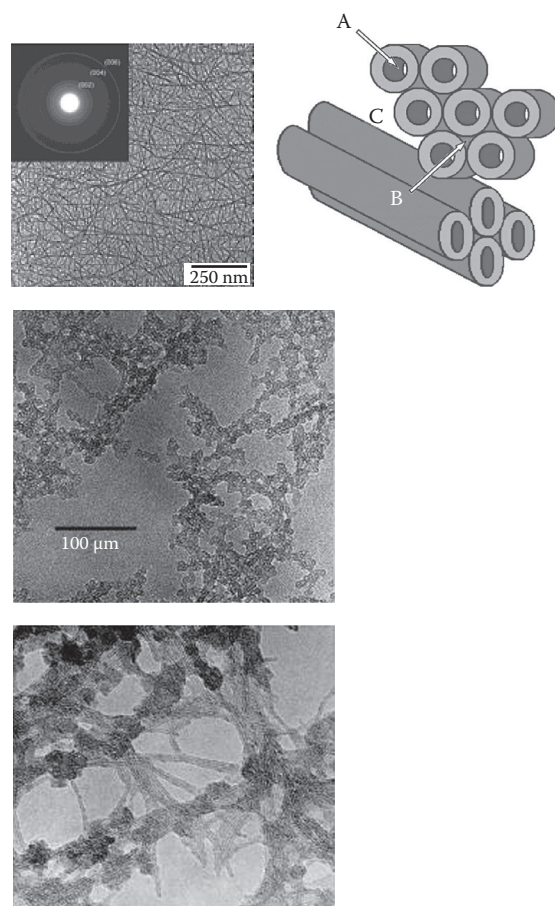


FIGURE 23.1 Electron micrographs of synthetic imogolite with selected area electron diffraction pattern (top left) (Yang et al., 2008), natural imogolite from pumice (bottom left), and allophane from pumice (center). (Reproduced from Parfitt, R.L. 2009. Allophane and imogolite: Role in soil biogeochemical processes. *Clay Miner.* 44:135–155. With the permission of the Mineralogical Society of Great Britain & Ireland.) The cartoon at the top right shows the orientation of imogolite nanotube bundles. (From Bonelli, B., I. Bottero, N. Ballarini, S. Passeri, F. Cavani, and E. Garrone. 2009. IR spectroscopic and catalytic characterization of the acidity of imogolite-based systems. *J. Catal.* 264:15–30.)

Unraveling the structure of imogolite relies on spectroscopy and modeling. Infrared spectra give absorption bands indicative of both the gibbsite-like sheet and the orthosilicate anion. The Si–O stretching vibration at 960 cm^{-1} is consistent with unpolymerized orthosilicate groups and the OH-stretching bands are consistent with Al–OH and Si–OH structures described by Cradwick et al. (1972). In addition, the band at 348 cm^{-1} indicates that one hydroxyl of the octahedral Al sheet is replaced by the silica oxyanion. This band distinguishes imogolite and proto-imogolite allophane from other SRO aluminosilicates (Farmer et al., 1977). Molecular dynamics simulations that generate XRD patterns and vibrational spectra based on the Cradwick model compared favorably with the experimental ones (Creton et al., 2008).

Solid-state NMR spectra also support the above model for imogolite (Goodman et al., 1985; Wilson et al., 1986; He et al., 1995).

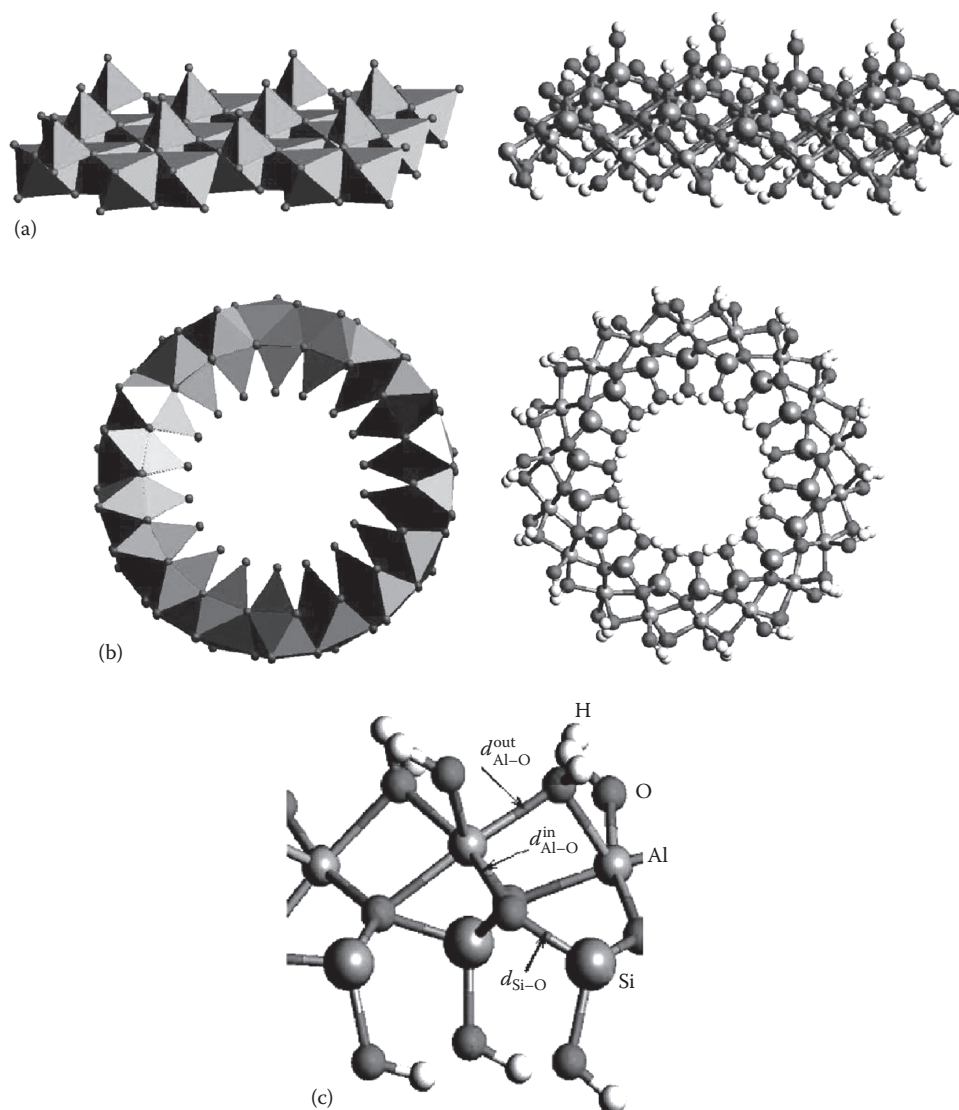


FIGURE 23.2 Polyhedral representations (left panel) and atomic structures (right panel) of (a) imogolite sheet and (b) imogolite nanotube with $N_{\mu} = 9$. (c) The local map of atomic structure. Si, Al, O, and H atoms and some representative bonds are indicated. (From Zhao, M., Y. Xia, and L. Mei. 2009. Energetic minimum structures of imogolite nanotubes: A first-principles prediction. *J. Phys. Chem. C* 113:14834–14837.)

The ^{27}Al -NMR spectra for various samples of synthetic and natural imogolite show little or no evidence of tetrahedrally coordinated Al (Figure 23.3). The ^{29}Si resonance line at -78 ppm of imogolite is consistent with Si bound to three Al–O and one OH group and serves to identify imogolite or proto-imogolite allophane in whole soils (Wilson et al., 1986).

The difference in size between natural and synthetic imogolite—2.3 vs. 2.7–3.2 nm—can be explained by density functional theory first-principle calculations that show two energy minima for the imogolite structure (Figure 23.4). The global minimum occurs with a gibbsite sheet consisting of 9 gibbsite units around the imogolite circumference and a local minimum with 12 gibbsite units (Zhao et al., 2009). These minima are consistent with the external diameters, circumferences, separation distances, and axial dimensions of imogolite determined experimentally by XRD and electron diffraction.

23.1.3 Structure of Allophane

Allophane refers to a group of SRO aluminosilicate clay minerals with no long-range order, only two diffuse XRD bands, and variable composition, generally ranging from 2:1 to 1:1 Al/Si molar ratio (Harsh et al., 2002). Endmember allophane would be completely disordered, but probably does not exist in nature (Fyfe et al., 1987). The further structural and chemical characterization of allophane found in natural environments has led to the identification of three major types of allophane. These have been tentatively named proto-imogolite allophane, halloysite-like (or defect kaolin) allophane, and hydrous feldspathoid allophane.

Proto-imogolite allophane (Al-rich allophane) has an Al/Si ratio close to 2, a gibbsite-like sheet of octahedrally coordinated Al, and orthosilicate groups sharing three oxygens with Al. Thus, proto-imogolite allophane has the same short-range order

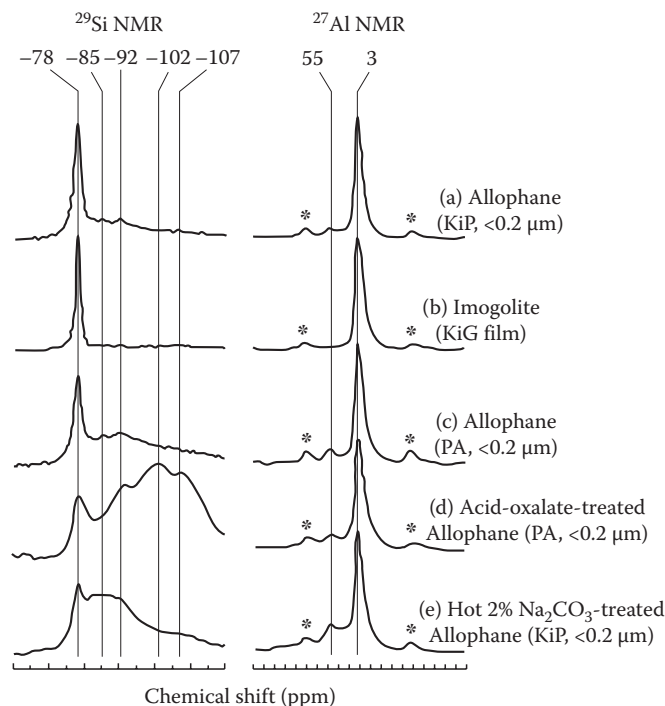


FIGURE 23.3 ^{29}Si and ^{27}Al MAS NMR spectra of (a) Al-rich KiP allophane ($<0.2\ \mu\text{m}$), (b) imogolite (KiG) film, (c) Si-rich PA allophane ($<0.2\ \mu\text{m}$), (d) acid-oxalate-treated Si-rich PA allophane, and (e) hot 2% Na_2CO_3 -treated Al-rich KiP allophane. *, Spinning side band (SSB). (From Hiradate, S., and S.-I. Wada. 2005. Weathering process of volcanic glass to allophane determined by ^{27}Al and ^{29}Si solid-state NMR. *Clays Clay Miner.* 53:401–408. Figure 3. Reproduced with kind permission of The Clay Minerals Society, publisher of *Clays and Clay Minerals*.)

as imogolite, but does not exhibit the tubular morphology. Instead, it first forms fragments of the imogolite structure, then, depending on solution conditions, forms imogolite or spherical allophane particles about 3.5 nm in diameter (Farmer and Russell, 1990). The NMR and FTIR spectra are nearly identical to those for imogolite (Figure 23.3). The XRD “peaks” are very broad and the pattern lacks several lines indicative of imogolite (Table 23.1).

According to one view, allophane with an Al/Si ratio near 1:1 probably has a structure that is closer to kaolinite or halloysite with defects in the tetrahedral sheet. Infrared spectra of Si-rich allophanes indicate the presence of polymerized silica tetrahedra and octahedrally coordinated Al (Parfitt et al., 1980; Farmer and Russell, 1990; Parfitt, 1990). Both IR and NMR spectra suggest that Si-rich allophanes often contain both the halloysite and imogolite structural units. The halloysite-like feature in the NMR spectrum is characterized by a broad ^{29}Si resonance around $-86\ \text{ppm}$. Varying amounts of the two types of allophane could account for a large variation in the Al/Si ratios (from 2.5 to 1) when found in weathered pumice. Recent solid-state NMR (MacKenzie et al., 1991) and x-ray photoelectron spectroscopy (He et al., 1995) studies of the silica-rich allophane support the presence of both imogolite-like and defect kaolin-like structures.

Recent Al-K edge x-ray absorption near edge structure (XANES) analysis of Al-rich allophanes and imogolite, raises

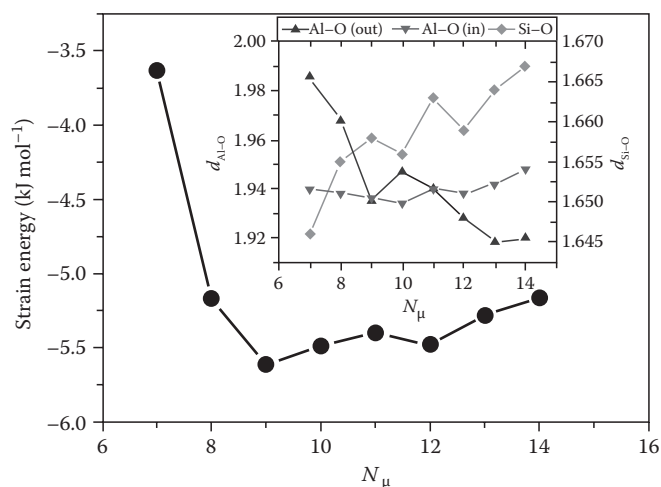
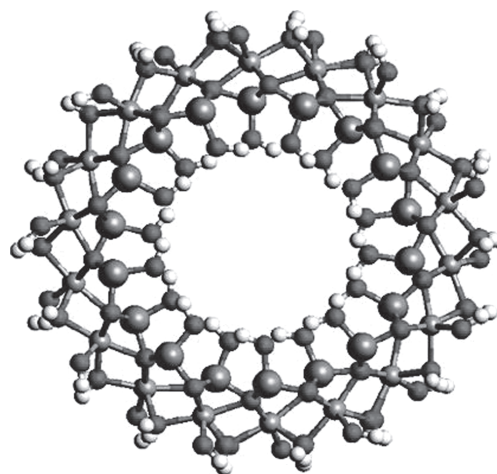


FIGURE 23.4 Variation of the strain energy of imogolite nanotubes (cross section shown above) relative to imogolite sheet as a function of N_μ (number of gibbsite units in the circumference). The error bars ($<0.003\ \text{kJ mol}^{-1}$) are smaller than symbols. The bond length evolution of Al–O and Si–O bonds is plotted in the inset of this figure. (From Zhao, M., Y. Xia, and L. Mei. 2009. Energetic minimum structures of imogolite nanotubes: A first-principles prediction. *J. Phys. Chem. C* 113:14834–14837.)

questions about the above models. Specifically, Al-K-XANES shows only one octahedral Al site in both imogolite and allophane, regardless of Al/Si ratio (Ildefonse et al., 1994). In contrast, gibbsite and 1:1 clay minerals have two octahedral Al sites, while 2:1 phyllosilicates have one. This implies allophane and imogolite have a dioctahedral sheet that resembles that of pyrophyllite or mica rather than kaolinite.

Another Si-rich allophane with a significant, if not dominant, amount of tetrahedrally coordinated Al resembles a hydrous feldspathoid and contains no imogolite units. The basic structure appears to be that of a framework silicate with 1:3 Al for Si substitution. Octahedral Al neutralizes some of the negative charge generated by the substitution and may be associated with the inner surfaces of spherical particles. Particles isolated from a stream deposit in New Zealand are less than 3 nm in diameter and form in CO_2 -charged water that increases in pH as it

degases (Wells et al., 1977; Childs et al., 1990). Similar particles can be synthesized in neutral to alkaline solutions and IR and NMR spectra are consistent with a hydrous feldspathoid structure (Farmer et al., 1979a; Wada and Wada, 1981). No -78 ppm resonance is observed in the ^{29}Si NMR spectra, as in imogolite, and the changes in NMR spectra with heating confirm that the hydrous feldspathoid allophane differs in structure from both proto-imogolite and kaolin defect allophane (MacKenzie et al., 1991; Ildefonse et al., 1994). Ildefonse et al. (1994) used ^{27}Al NMR and Al-K XANES to characterize Si-rich allophanes from soils and found them to be similar to those found in stream deposits, suggesting that Si activity in solution determines their formation.

23.2 Identification and Synthesis of Allophane and Imogolite

23.2.1 Imogolite Identification and Synthesis

Imogolite can be separated from soils and pumice deposits after removing material that strongly interacts with its surface. Pretreatment usually includes a dithionite–citrate–bicarbonate extraction to remove iron oxides and hydrogen peroxide to remove organic matter. Neither significantly dissolves nor alters imogolite or allophane. Following pretreatment, ultrasonic dispersion of the suspended pumice or soil at low pH (e.g., pH 4 HCl) separates imogolite from phyllosilicate clay minerals. As discussed in Section 23.4.1, imogolite surfaces are positively charged in acid solutions and form stable suspensions, while the 2:1 phyllosilicates flocculate at low pH. Further concentration of SRO materials is accomplished by separating the $<0.08\ \mu\text{m}$ fraction because average allophane and imogolite particle sizes are much less than those of the 1:1 phyllosilicates. Of course, no purification procedure is ideal; unwanted minerals and some alteration of the target material will always be present.

While spectroscopic methods elucidate imogolite structure and often aid in quantitative methods, electron microscopy is the most reliable indicator of its presence in soils or successful synthesis in the laboratory. Both synthetic imogolite and that isolated from a pumice bed show long, bundled tubes (Figure 23.1), whereas, imogolite isolated from a forest soil is somewhat more fragmented (Su and Harsh, 1996).

Refluxing an acidic solution with millimolar concentrations of aluminum perchlorate and tetraethyl orthosilicate for 5 days at 95°C produces imogolite nearly identical to the natural material isolated from soils or pumice except for the larger diameter mentioned above (Farmer et al., 1983). The larger diameter may be due, in part, to the high-temperature synthesis, because imogolite prepared at room temperature has a diameter of about $23\ \text{\AA}$ (Wada, 1987). Levard et al. (2009) synthesized imogolite from decimolar concentrations of Al and Si, perhaps opening the door to manufacture of large quantities of material.

23.2.2 Allophane Identification and Synthesis

Separation of allophane from natural deposits, including soils, is similar to that of imogolite. Allophane is positively charged in

a low pH solution and will form a stable suspension along with imogolite when ultrasonically dispersed. The same pretreatment to remove iron oxides and organic material applies. With allophane, however, separation from imogolite is possible in principle because it is negatively charged in alkaline solutions where imogolite flocculates.

After separation, one can discern allophane in electron micrographs, but it is far less distinctive than imogolite (Figure 23.4). It generally occurs as an amorphous mass of material coating other particles. Often the spheroidal morphology is evident in the Al-rich allophane. The spheroids of Al-rich allophane form aggregates that do not disperse easily. Damage from the electron beam is rapid and care must be taken to obtain good micrographs.

Like imogolite, allophane is synthesized from millimolar solutions of Al and monomeric $\text{Si}(\text{OH})_4$. Allophane can be precipitated rapidly from solutions at room temperature. Methods, including heated synthesis, have been developed to precipitate allophane from concentrated solutions—10–100 mM (Ohashi et al., 1998; Montarges-Pelletier et al., 2005). The Al/Si ratio and pH of the matrix solution determine the nature of the products. Al-rich allophane forms at room temperature from an acidic Al and orthosilicate solution with Al/Si ratio near 2:1. The presence of Ca and Mg ions favors allophane formation over imogolite, whereas Na and K do not (Abidin et al., 2007). Because the acidic environment keeps Al in octahedral coordination, decreasing the Al/Si ratio while keeping the pH below neutral probably favors the defect kaolinite structure. Between pH 6 and 7, the hydrous feldspathoid structure predominates with the proportion of tetrahedral Al increasing as the Al/Si ratio decreases (Farmer and Russell, 1990). This structure exists in natural alkaline environments, including the Silica Springs deposit in New Zealand (Wells et al., 1977) and many soils (Childs et al., 1990; Ildefonse et al., 1994). Farmer and Russell (1990) reviewed the synthesis and occurrence of imogolite and the three types of allophane described here.

23.3 Occurrence of Imogolite and Allophane in Natural Environments

Allophane and imogolite tend to be associated with volcanic ash deposits and soils derived from volcanic debris, because the rapid release of Al and Si from materials such as volcanic glass results in the precipitation of SRO aluminosilicates. The Kitakami pumice beds in Japan have long been a source of relatively pure separates of both allophane and imogolite and are among the most studied of the naturally occurring SRO materials, including the KiG imogolite in Figure 23.3 (Miyachi and Aomine, 1966; Wada and Matsubara, 1968; Yoshinaga, 1968; Yoshinaga et al., 1973). Imogolite was first identified in Ando (dark-colored) soils of Japan (Yoshinaga and Aomine, 1962) and allophane was found to give them many of their unique properties. Since then, SRO aluminosilicates have been identified in soils derived from many parent materials, including sandstone, gneiss, granite, and basalt (Harsh et al., 2002). In basalt, ferrihydrite, a poorly crystalline

iron oxide, often occurs in addition to allophane and imogolite. Nevertheless, the largest concentrations of SRO aluminosilicates occur in deposits of volcanic tephra and soils developed therein. Soils derived from volcanic tephra occur all over the world with well studied examples from New Zealand (Taylor, 1933; Wells et al., 1977; Parfitt, 1990), Chile (Vicente and Besoain, 1961; Besoain, 1969; Nissen and Kuehne, 1976; Besoain and Gonzalez, 1977; Floody et al., 2009), and the Cascade Range of North America (Ugolini and Dahlgren, 1991). A large deposit of allophane—more than 4000 km² and 16 m thick—was recently discovered in Ecuador and may be a source for commercial allophane (Kaufhold et al., 2009, 2010). McDowell and Hamilton (2009) report that SRO aluminosilicates are probably present on Mars and interfere with quantification of phyllosilicates on the surface.

The key factor in the formation of allophane and imogolite in soil is sufficient Al and Si in solution. Thus, conditions that lead to rapid weathering of primary minerals, such as high rainfall and low pH, favor their formation. Both imogolite and Al-rich allophane tend to dominate at low pH where Al/Si is high, whereas halloysite and/or Si-rich allophanes form when soluble Si is high (>10^{-3.45}). As a result, low rainfall or xeric-moisture regimes, concentrating soluble silica, have been observed to favor halloysite formation at the expense of allophane and imogolite (Parfitt and Wilson, 1985; Singleton et al., 1989; Takahashi et al., 1993). Noncrystalline minerals are found in Andisols, Inceptisols, Entisols, Spodosols, and Ultisols. Generally, allophane and imogolite occur in horizons where organic matter is low so that Al exists in inorganic complexes. Al-humus complexes, which give soils many of the same properties attributed to allophanic soils, often dominate organic and A horizons, particularly in forested soils (Dahlgren et al., 2004). Complexation of Al by organic acids and humic materials inhibits SRO aluminosilicate formation indicating that free Al³⁺ or Al-hydroxy complexes may be required.

Short-range ordered materials are generally less stable than their crystalline counterparts, particularly kaolinite. Their rapid formation results because the interfacial energy difference between mineral surfaces and an aqueous solution slows nucleation. Poorly crystalline surfaces have lower surface tensions and nucleate more easily, that is, at a lower saturation index than a crystalline mineral of similar composition. As a result, allophane and imogolite are often found as precursors to kaolinite in weathering soil profiles and may serve as templates for its heterogeneous nucleation (Steeffel et al., 1990).

Quantification of SRO aluminosilicates in soils is achieved by selective chemical extraction and solution analysis of Al and Si (Dahlgren, 1994). Commonly, one extracts the soil first with Na-pyrophosphate, which effectively extracts Al and Fe from soil organic complexes, but dissolves little from the inorganic fraction. Then, an acid ammonium oxalate solution (0.2 M, pH 3) selectively dissolves allophane, imogolite, and poorly crystalline iron oxides such as ferrihydrite. Subtracting the organically complexed from the oxalate-extracted, gives the SRO-associated Al and Fe. Dividing this SRO Al value by the oxalate-extractable Si provides the average SRO Al/Si ratio (Parfitt and Wilson, 1985). A ratio near 2:1 suggests a soil dominated by imogolite

and proto-imogolite allophane whereas a smaller value indicates Si-rich allophane is present. Embryonic halloysite may also partially dissolve in the oxalate solution (Wada and Kakuto, 1985). Ratios greater than 2:1 may occur when other labile sources of Al are present, such as hydroxy-Al interlayers in clay minerals.

23.4 Surface Charge Characteristics of Short-Range Ordered Aluminosilicates and Variable-Charge Soils

23.4.1 Surface Charge Determination

23.4.1.1 Operational Definitions

Two major sources of surface charge on SRO aluminosilicates will be considered here, that is, permanent structural charge (σ_o) from isomorphic substitution of Al in Si tetrahedra and variable surface charge due to ion association at surface hydroxyl groups (Sposito, 2004). Ion associations with surface hydroxyls include complexed protons (σ_H), inner-sphere complexes with ions other than H⁺ (σ_{IS}), and outer-sphere complexes (σ_{OS}). A charge balance equation can be written as follows:

$$\sigma_p = \sigma_o + \sigma_H + \sigma_{IS} + \sigma_{OS} = -\sigma_D \quad (23.1)$$

where

σ_p represents the particle charge or total charge from all sources

σ_D is the diffuse layer charge that consists of the net charge from the swarm of hydrated ions around the particle

The proton charge on variable-charge surfaces is determined by potentiometric titration with H and OH, which adsorb to surface silanol ($\equiv\text{Si-OH}$) or aluminol ($\equiv\text{Al-OH}$) groups. Relative proton adsorption is easy to determine from the difference between added and remaining protons in solution, but the absolute proton charge on the surface is not evident because the initial charge, before titration, is not known. The point of zero net proton charge (PZNPC) is often estimated by the point of zero salt effect (PZSE)—the pH at the crossover point of three or more titrations at different background salt concentrations. If the background salt does not form inner-sphere complexes, only the proton charge is determined in the titration. The proton charge is more reliably determined by plotting the net adsorbed ion charge ($\sigma_{IS} + \sigma_{OS} + \sigma_D$) against proton charge (σ_H) (Chorover and Sposito, 1995). The slope should be -1 and the x- and y-intercepts equal to σ_o . The PZNPC is then the pH where $(\sigma_{IS} + \sigma_{OS} + \sigma_D) = -\sigma_o$.

Inner-sphere, outer-sphere, and diffuse layer cations and anions balance the total negative and positive charge on the surface. Thus, the point of zero net charge (PZNC) can be determined by ion adsorption across a range of pH in an electrolyte, such as NaCl, whose ions do not form inner-sphere complexes with the aluminol or silanol groups. Finally, electrophoretic mobility provides information about the tendency for ions to

form outer-sphere complexes with allophane and imogolite. Their mobility when suspended in an aqueous solution subjected to an electric field depends on the ionic strength of the solution and the nature of the surface complexes. The isoelectric point is the pH where the particles are stationary in the field and is an estimate of the PZC—the point where $\sigma_D = 0$.

With all Al in imogolite and proto-imogolite allophane in octahedral coordination, no structural charge arises from isomorphous substitution. Gustafsson (2001), however, proposed that structural charge could arise from differences in Al–O bond valences leading to a weak positive charge on outer tube walls and negative charge in tubular pores. This hypothesis was later

supported by quantum mechanical calculations of charge distribution in imogolite (Guimaraes et al., 2007). The Si-rich allophane, on the other hand, has structural charge arising from Al for Si substitution. However, Su et al. (1992) found in synthetic allophanes of this type that structural charge from tetrahedral Al was not completely balanced by exchangeable cations. In this case, it was hypothesized that Al present as hydroxy complexes or polymers balanced much of the negative σ_o .

The charge characteristics of imogolite and some synthetic allophanes as determined by these methods are summarized in Figure 23.5 and Table 23.2. Because the PZNC and PZSE values of imogolite and Al-rich allophane are all greater than 6, these

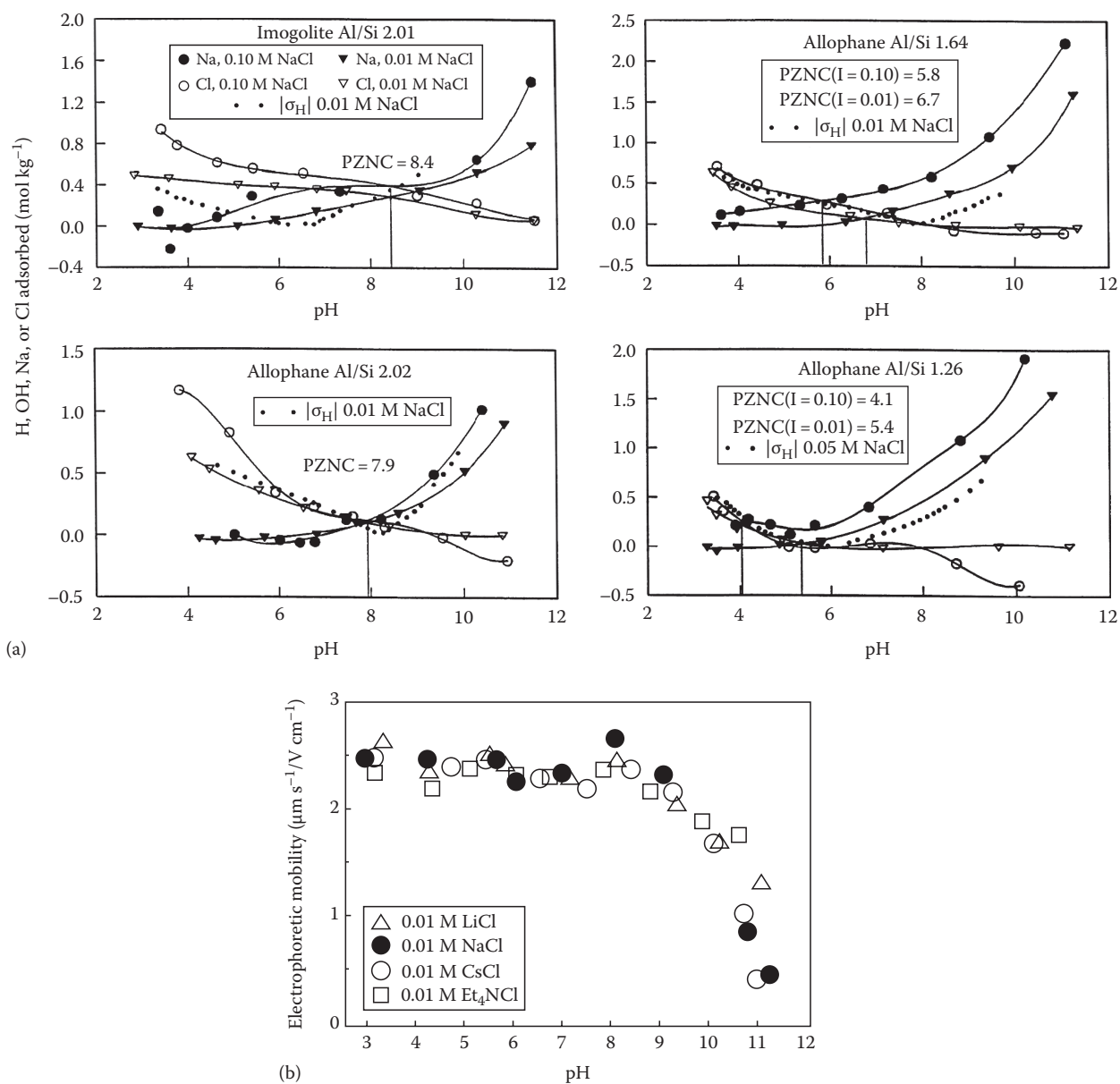


FIGURE 23.5 Charge properties of synthetic imogolite and allophane determined by (a) potentiometric titration and ion adsorption (From Su, C.M. et al., *Clays Clay Miner.*, 40, 280, 1992, Figure 1. Reproduced with kind permission of The Clay Minerals Society, publisher of *Clays and Clay Minerals*.) (b) electrophoretic mobility (From Harsh, J.B., S.J. Traina, J. Boyle, and Y. Yang. 1992. Adsorption of cations on imogolite and their effect on surface-charge characteristics. *Clays Clay Miner.* 40:700–706, Figure 4. Reproduced with kind permission of The Clay Minerals Society, publisher of *Clays and Clay Minerals*.)

TABLE 23.2 PZCs of Synthetic Imogolite and Allophanes

Material	Al/Si	PZNC in NaCl		PZSE	PZC
		0.10 M	0.01 M		
Imogolite	2.0	8.4	8.4	6.5	>10
Allophane	2.0	7.9	7.9	8.3	10
Allophane	1.6	5.8	6.7	7.7	9
Allophane	1.2	4.1	5.4	5.9	7.6

Source: Su, C.M., J.B. Harsh, and P.M. Bertsch. 1992. Sodium and chloride sorption by imogolite and allophanes. *Clays Clay Miner.* 40:280–286.

materials impart positive charge in acid soils. The Si-rich allophanes may be either positively or negatively charged depending on soil pH. The Si-rich allophanes also have a PZSE greater than the PZNC, another indicator that permanent negative charge exists in these materials as a result of Al for Si substitution. Imogolite has a PZSE greater than its PZNC, constant adsorption of Cl over a large pH range, and an isoelectric point above pH 10 (Harsh et al., 1992; Tsuchida et al., 2005), all of which might be due in part to cation distribution inside imogolite tubes as well as structural charge distribution from bond valence differences as discussed above (Gustafsson, 2001).

23.4.2 Interaction with Anions and Cations

Inner-sphere complexation of anions on allophane and imogolite is common. Phosphate, fluoride, citrate, borate, arsenate, and selenite are known to form inner-sphere complexes with SRO aluminosilicates. This reaction contributes to σ_{IS} and can shift the points of zero charge (PZCs) of the material. As a result, more negative charge is likely in the presence of these anions, particularly in acid soils. Caution should be used in interpreting any strong sorption as surface complexation. Veith and Sposito (1977) and Su and Harsh (1993) showed that phosphate and fluoride, respectively, may react with SRO aluminosilicates to form new solid phases. Boron may substitute into tetrahedral sites in coprecipitation with allophane (Su and Suarez, 1997).

In soils containing allophane and imogolite, strong interaction with phosphate can lead to deficiency of this macronutrient in crops. Calcium silicate can be added to such soils to compete for sorption sites and enhance phosphate availability. The ability of SRO materials and allophanic soils to adsorb anions by ligand or anion exchange has led to suggestions that they be used to remove contaminants such as phosphate, selenium, technetium, glyphosate, chromium, arsenic, and iodine from wastewaters (Wells and Parfitt, 1987; Gu and Schulze, 1991; Babel and Opiso, 2007; Gimsing et al., 2007; Hopp et al., 2008; Opiso et al., 2009; Ballantine and Tanner, 2010).

Many trace metals and metalloids form surface complexes with aluminol and silanol groups as evidenced by extensive studies on silica and aluminum oxides; however, fewer studies have been performed on SRO aluminosilicates or soils containing them. One study of metal adsorption to a soil dominated

by allophane and imogolite in the clay fraction showed the following order of decreasing affinity, which is quite similar to the selectivity of aluminol groups for divalent metals (Abd-Elfattah and Wada, 1981):



As on Al oxides, Pb, Cu, Zn, and Co appear to form inner-sphere surface complexes, whereas Cd, Ca, and Mg are held by electrostatic forces (Clark and McBride, 1984; Yuan et al., 2002). Alkaline earth and alkali metals, halide anions, NO_3^- , SO_4^{2-} , and ClO_4^- will generally exist as outer-sphere complexes or in the diffuse layer of allophane and imogolite. Adsorption of exchangeable cations on allophanic soils appears to be similar to that on soils dominated by smectites (Nakahara and Wada, 1994). Highly selective K exchange on Andisols has been reported (Espino-Mesa and Hernández-Moreno, 1994), but this could result from trace amounts of illitic minerals or alunite formation in addition to reactions with allophane or imogolite. Allophanic soils do seem capable of adsorbing large amounts of nitrate below the root zone, presumably through interaction with SRO aluminosilicates (Maeda et al., 2008). Circumstantial evidence exists for specific adsorption of Cl on imogolite, as discussed above, but this issue has not been resolved and is not consistent with electrophoretic measurements (Figure 23.5).

The interaction of allophane and allophanic soils with organic matter (discussed in the following section) also affects the surface charge and sorption properties of the materials. Organic matter can be expected to increase the negative charge on minerals dominated by aluminol surface groups because of the carboxylate groups of humic materials. Treatment of allophanic materials and soils with hydrogen peroxide to remove organic matter increases the PZC (Escudéy et al., 1986) and decreases phosphate sorption (Mora and Canales, 1995), respectively. Conversely, adding iron oxides increases the PZC of allophane, rendering the surface more positively charged (Escudéy and Galindo, 1983). Iron oxides may react selectively with silanol groups, which have an acid PZNPC. The PZNPCs of Fe and Al oxides, on the other hand, are greater than 6.

23.5 Interaction of Allophane and Imogolite with Other Soil Constituents

23.5.1 Organic Matter and Iron Oxides

The term “Andisol” comes from the Japanese words *ando* and *sol*, meaning dark-colored soil. The dark color comes from the fact that soils formed from volcanic debris are often high in organic matter, especially in surface horizons. Noncrystalline materials may play a role in organic matter retention through one or more mechanisms. First, humic substances adsorb strongly to imogolite and allophane (Parfitt et al., 1977; Parfitt, 2009) and sorption is possibly responsible for inhibiting degradation (Basile-Doelsch et al., 2005; Schneider et al., 2010). Second, reactive Al released

from SRO materials complexes with humic and fulvic acids and leads to precipitation and/or inhibition of degradation (Boudot, 1992; Wada, 1995; Matus et al., 2008). Finally, SRO materials may enhance the “humification” of soil organic carbon by facilitating bonding reactions or molecular assemblages (Gonzalez-Perez et al., 2007; Fukushima et al., 2009). In the presence of hydrogen peroxide, allophane associated with Fe may catalyze the degradation of organic materials, including xenobiotics, by Fenton reactions (Garrido-Ramirez et al., 2010).

Reaction with organic matter may give soils containing SRO aluminosilicates an important role in carbon sequestration. If these materials are instrumental in increasing the residence time of organic matter in soils, then preserving the soils containing them may be beneficial in order to reduce emission of

greenhouse gases such as CO₂. Dahlgren et al. (2004) stated that 0.8% of the world’s soils are allophanic and that they contain 5% of the global soil carbon. In his excellent review of the biogeochemistry of allophane and imogolite, Parfitt (2009) points out that the stabilization of organic matter is partially maintained as forests are converted to pasture, but does not apply to fresh organic matter or plant-derived material. The recalcitrant carbon originates from microbial byproducts, is stabilized slowly, and persists for thousands of years.

23.5.2 Water

Both a high specific surface area and a high value of the relative microporosity characterize allophane. The latter probably

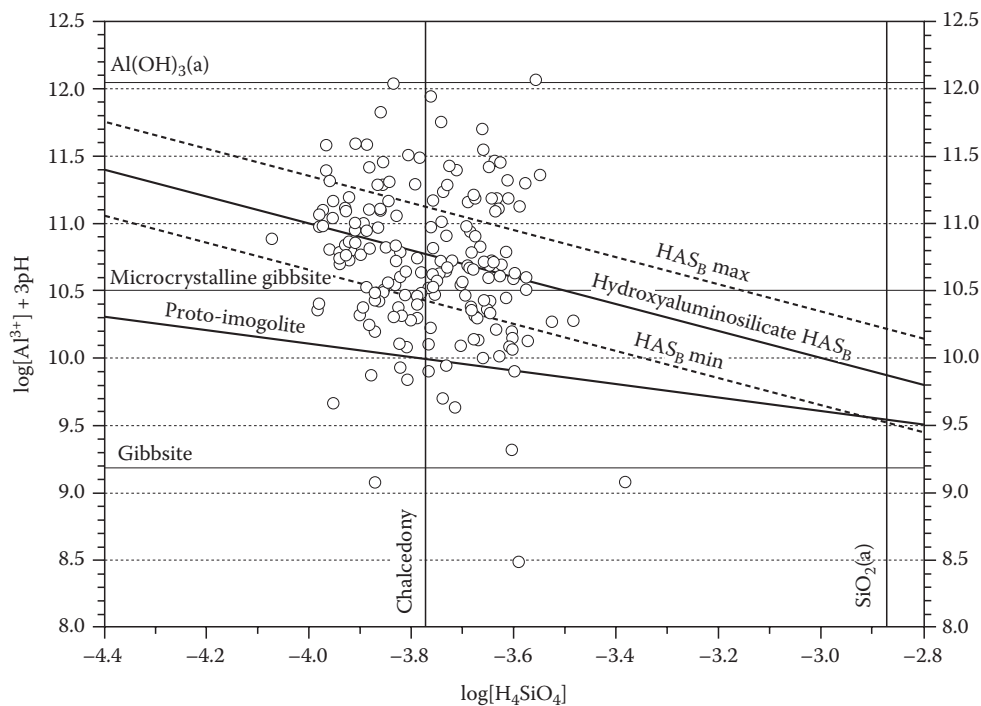
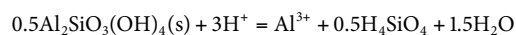


FIGURE 23.6 Stability relations for proto-imogolite (Lumsdon and Farmer, 1995), Si-rich allophane (HAS_B), gibbsite, and microcrystalline gibbsite. (From Dobrzynski, D. 2007. Chemistry of neutral and alkaline waters with low Al³⁺ activity against hydroxyaluminosilicate HASB solubility. The evidence from ground and surface waters of the Sudetes Mts. (SW Poland). *Aquat. Geochem.* 13:197–210.)

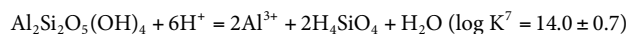
(Two-ion parameter log[Al³⁺] + 3pH versus log[H₄SiO₄] in waters with log[Al³⁺] < -10 (size—188 samples). Solubility lines for amorphous Al(OH)₃ and SiO₂ forms plotted at 7°C, after solubility constant for gibbsite (log K²⁵ = 8.11), microcrystalline gibbsite (log K²⁵ = 9.35), and Al(OH)₃(a) (log K²⁵ = 10.8) calculated using the van’t Hoff equation. Solubility constant log K⁷ for chalcodony and amorphous SiO₂ calculated using the analytical expression after Nordstrom et al. (1990).

Proto-imogolite solubility line at 7°C plotted for the reaction:



(log K²⁵ = 7.02, ΔH = -96.8 kJ mol⁻¹) after Lumsdon and Farmer (1995).

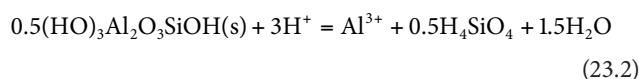
HASB solubility line for the reaction:



with uncertainty of solubility plotted.)

results largely from micropores formed from aggregates of particles because the porosity decreases with the shrinkage observed on drying. As a result, water retention in allophanic soils is very high at a given water potential compared to soils dominated by crystalline clays. This, in part, accounts for the high productivity often seen in forested soils high in SRO materials (Martini and Luzuriaga, 1989; Nizeyimana, 1997). Macroporosity is also high in most allophanic soils resulting in good infiltration and hydraulic conductivity. The latter parameter has been found to decrease significantly in soils at pH values where allophane is known to disperse easily (pH = 3 and 11) (Nakagawa and Ishiguro, 1994).

The aqueous solubility of imogolite and proto-imogolite allophane shows them to be less stable than kaolinite at soluble silica activities expected in natural soils (Farmer et al., 1979b; Percival, 1991; Su and Harsh, 1994; Gustafsson et al., 1998; Su and Harsh, 1998; Wada and Kakuto, 1999). However, imogolite and proto-imogolite allophane are more stable than halloysite at low Si activity (Su and Harsh, 1994). Thermodynamically, halloysite is stable relative to imogolite at a log Si(OH)₄ activity greater than about -3.5. Halloysite is more stable than allophane at a lower Si activity, but allophane formation in preference to halloysite is commonly observed in soils at log (H₄SiO₄) > -3.45 (Singleton et al., 1989). This incongruity may indicate that soil solution analyses performed at a later date may not be relevant to the time of mineral formation. Kinetic considerations may favor the SRO materials relative to halloysite; this certainly is true relative to kaolinite. The solubility constants determined for imogolite and allophane may be incorrect or the solid phases controlling the solubility of Al, such as gibbsite or Al complexed with organic matter, may not be well understood (Gustafsson et al., 2001). Current solubility data seem to support different solubility constants for synthetic and soil imogolite—log K_{syn} = 6.05 and log K_{soil} = 6.60 at 25°C for the reaction:



The solubility of minerals in soils is complicated by nonequilibrium conditions, difficulty in speciating soluble ions, particularly Al, and determination of controlling phases (Gustafsson et al., 2001). Nevertheless, the chemistry of soil solutions and natural waters may often be determined by these rapidly formed, but persistent, poorly crystalline materials (Dobrzynski, 2007) (Figure 23.6).

References

- Abd-Elfattah, A., and Wada, K. (1981). Adsorption of lead, copper, zinc, cobalt, and cadmium by soils that differ in cation-exchange materials. *J. Soil Sci.* 32:271–283.
- Abidin, Z., N. Matsue, and T. Henmi. 2007. Differential formation of allophane and imogolite: Experimental and molecular orbital study. *J. Comput. Aided Mater. Des.* 14:5–18.
- Babel, S., and E.M. Opiso. 2007. Removal of Cr from synthetic wastewater by sorption into volcanic ash soil. *Int. J. Environ. Sci. Technol.* 4:99–107.
- Ballantine, D.J., and C.C. Tanner. 2010. Substrate and filter materials to enhance phosphorus removal in constructed wetlands treating diffuse farm runoff: A review. *N.Z. J. Agric. Res.* 53:71–95.
- Basile-Doelsch, I., R. Amundson, W.E.E. Stone, C.A. Masiello, J.Y. Bottero, F. Colin, F. Masin, D. Borschneck, and J.D. Meunier. 2005. Mineralogical control of organic carbon dynamics in a volcanic ash soil on La Reunion. *Eur. J. Soil Sci.* 56:689–703.
- Besoain, E. 1969. Imogolite [allophane] in volcanic soils in Chile. *Geoderma* 2:151–169.
- Besoain, M.E., and M.S.P. Gonzalez. 1977. Mineralogy, genesis and classification of volcanic ash soil derivatives of the central-south region of Chile. *Cienc. Invest. Agrar.* 4:109–130.
- Bonelli, B., I. Bottero, N. Ballarini, S. Passeri, F. Cavani, and E. Garrone. 2009. IR spectroscopic and catalytic characterization of the acidity of imogolite-based systems. *J. Catal.* 264:15–30.
- Boudot, J.P. 1992. Relative efficiency of complexed aluminum, noncrystalline Al hydroxide, allophane and imogolite in retarding the biodegradation of citric acid. *Geoderma* 52:29–39.
- Childs, C.W., R.L. Parfitt, and R.H. Newman. 1990. Structural studies of Silica Springs allophane. *Clay Miner.* 25:329–341.
- Chorover, J., and G. Sposito. 1995. Surface-charge characteristics of kaolinitic tropical soils. *Geochim. Cosmochim. Acta* 59:875–884.
- Clark, C.J., and McBride, M.B. (1984). Chemisorption of Cu(II) and Co(II) on allophane and imogolite. *Clays Clay Miner.* 32:300–310.
- Cradwick, P.D.G., V.C. Farmer, J.D. Russell, C.R. Masson, K. Wada, and N. Yoshinaga. 1972. Imogolite, a hydrated aluminum silicate of tubular structure. *Nat. Phys. Sci.* 240:187–189.
- Creton, B., D. Bougeard, K.S. Smirnov, J. Guilment, and O. Poncelet. 2008. Molecular dynamics study of hydrated imogolite. 1. Vibrational dynamics of the nanotube. *J. Phys. Chem. C* 112:10013–10020.
- Cruz, M.D.R., and L.M. Real. 1991. Practical determination of allophane and synthetic alumina and iron-oxide gels by x-ray-diffraction. *Clay Miner.* 26:377–387.
- Dahlgren, R.A. 1994. Quantification of allophane and imogolite, p. 430–451. *In* J. Amonette and L.W. Zelazny (eds.) *Quantitative methods in soil mineralogy*. SSSA, Madison, WI.
- Dahlgren, R.A., M. Saigusa, and F.C. Ugolini. 2004. The nature, properties and management of volcanic soils. *Adv. Agron.* 82:113–182.
- Dobrzynski, D. 2007. Chemistry of neutral and alkaline waters with low Al³⁺ activity against hydroxyaluminosilicate HASB solubility. The evidence from ground and surface waters of the Sudetes Mts. (SW Poland). *Aquat. Geochem.* 13:197–210.

- Escudéy, M., and G. Galindo. 1983. Effect of iron-oxide coatings on electrophoretic mobility and dispersion of allophane. *J. Colloid Interface Sci.* 93:78–83.
- Escudéy, M., G. Galindo, and J. Ervin. 1986. Effect of iron oxide dissolution treatment on the isoelectric point of allophanic soils. *Clays Clay Miner.* 34:108–110.
- Espino-Mesa, M., and J.M. Hernández-Moreno. 1994. Potassium selectivity in Andic soils in relation to induced acidity, sulphate status and layer silicates. *Geoderma* 61:191–201.
- Farmer, V.C., M.J. Adams, A.R. Fraser, and F. Palmieri. 1983. Synthetic imogolite: Properties, synthesis, and possible applications. *Clay Miner.* 18:459–472.
- Farmer, V.C., A.R. Fraser, J.D. Russell, and N. Yoshinaga. 1977. Recognition of imogolite structures in allophanic clays by infrared spectroscopy. *Clay Miner.* 12:55–57.
- Farmer, V.C., and J.D. Russell. 1990. Structures and genesis of allophanes and imogolite and their distribution in non-volcanic soils, p. 165–178. *In* M.F. De Boodt, M.H.B. Hayes and A. Herbillon (eds.) *Soil colloids and their associations in aggregates*. Plenum Press, New York.
- Farmer, V.C., J.D. Russell, and M.L. Berrow. 1979a. Characterization of the chemical structure of natural and synthetic aluminosilicate gels and sols by infrared spectroscopy. *Geochim. Cosmochim. Acta* 43:1417–1420.
- Farmer, V.C., B.F.L. Smith, and J.M. Tait. 1979b. The stability, free energy and the heat of formation of imogolite. *Clay Miner.* 14:103–107.
- Floody, M.C., B.K.G. Theng, P. Reyes, and M.L. Mora. 2009. Natural nanoclays: Applications and future trends—A Chilean perspective. *Clay Miner.* 44:161–176.
- Fukushima, M., A. Miura, M. Sasaki, and K. Izumo. 2009. Effect of an allophanic soil on humification reactions between catechol and glycine: Spectroscopic investigations of reaction products. *J. Mol. Struct.* 917:142–147.
- Fyfe, C., L. Evans, W. Chesworth, J. Graham, and M. McBride. 1987. Operation definition of imogolite/allophane phases by multitechnique analysis, p. 829–836. *In* C.R. Rodriguez and Y. Tardy (eds.) *Geochemistry and mineral formation in the earth surface*. Cons. Super. Invest. Cient, Spain. CNRS, France.
- Garrido-Ramirez, E.G., B.K.G. Theng, and M.L. Mora. 2010. Clays and oxide minerals as catalysts and nanocatalysts in Fenton-like reactions—A review. *Appl. Clay Sci.* 47:182–192.
- Gimsing, A.L., C. Szilas, and O.K. Borggaard. 2007. Sorption of glyphosate and phosphate by variable-charge tropical soils from Tanzania. *Geoderma* 138:127–132.
- Gonzalez-Perez, J.A., C.D. Arbelo, F.J. Gonzalez-Vila, A.R. Rodriguez, G. Almendros, C.M. Armas, and O. Polvillo. 2007. Molecular features of organic matter in diagnostic horizons from andosols as seen by analytical pyrolysis. *J. Anal. Appl. Pyrol.* 80:369–382.
- Goodman, B.A., J.D. Russell, B. Montez, E. Oldfield, and R.J. Kirkpatrick. 1985. Structural studies of imogolite and allophanes by aluminum-27 and silicon-29 nuclear magnetic resonance spectroscopy. *Phys. Chem. Miner.* 12:342–346.
- Greenland, D.H. 1982. Chemistry and the soil environment—Surfaces and sorption processes, p. 99–110. *In* K.J. Laidler (ed.) *IUPAC frontiers in chemistry*. IIRRI, Manila, Philippines.
- Gu, B., and R.K. Schulze. 1991. Anion retention in soil: Possible application to reduce migration of buried technetium and iodine. NUREG/CR-5464. U.S. Nuclear Regulatory Commission, Washington, DC.
- Guimaraes, L., A.N. Enyashin, J. Frenzel, T. Heine, H.A. Duarte, and G. Seifert. 2007. Imogolite nanotubes: Stability, electronic, and mechanical properties. *ACS Nano* 1:362–368.
- Gustafsson, J.P. 2001. The surface chemistry of imogolite. *Clays Clay Miner.* 49:73–80.
- Gustafsson, J.P., D. Berggren, M. Simonsson, M. Zysset, and J. Mulder. 2001. Aluminium solubility mechanisms in moderately acid Bs horizons of podzolized soils. *Eur. J. Soil Sci.* 52:655–665.
- Gustafsson, J.P., D.G. Lumsdon, and M. Simonsson. 1998. Aluminium solubility characteristics of spodic B horizons containing imogolite-type materials. *Clay Miner.* 33:77–86.
- Harsh, J.B., J. Chorover, and E. Nizeyimana. 2002. Allophane and imogolite, p. 291–322. *In* J.B. Dixon and D.G. Schulze (eds.) *Soil mineralogy with environmental applications*. SSSA Book Series No. 7. SSSA, Madison, WI.
- Harsh, J.B., S.J. Traina, J. Boyle, and Y. Yang. 1992. Adsorption of cations on imogolite and their effect on surface-charge characteristics. *Clays Clay Miner.* 40:700–706.
- He, H., T.L. Barr, and J. Klinowski. 1995. ESCA and solid-state NMR studies of allophane. *Clay Miner.* 30:201–209.
- Hiradate, S., and S.-I. Wada. 2005. Weathering process of volcanic glass to allophane determined by ²⁷Al and ²⁹Si solid-state NMR. *Clays Clay Miner.* 53:401–408.
- Hopp, L., P.S. Nico, M.A. Marcus, and S. Peiffer. 2008. Arsenic and chromium partitioning in a podzolic soil contaminated by chromated copper arsenate. *Environ. Sci. Technol.* 42:6481–6486.
- Ildefonse, P., R.J. Kirkpatrick, B. Montez, G. Calas, A.M. Flank, and P. Lagarde. 1994. ²⁷Al MAS NMR aluminum x-ray absorption near edge structure study of imogolite and allophanes. *Clays Clay Miner.* 42:276–287.
- Kaufhold, S., A. Kaufhold, R. Jahn, S. Brito, R. Dohrmann, R. Hoffmann, H. Gliemann, P. Weidler, and M. Frechen. 2009. A new massive deposit of allophane raw material in Ecuador. *Clays Clay Miner.* 57:72–81.
- Kaufhold, S., K. Ufer, A. Kaufhold, J.W. Stucki, A.S. Anastácio, R. Jahn, and R. Dohrmann. in press. Quantification of allophane clay from Ecuador. *Clays Clay Miner.* 58:707–716.
- Levard, C., A. Masion, J. Rose, E. Doelsch, D. Borschneck, C. Dominici, F. Ziarelli, and J.-Y. Bottero. 2009. Synthesis of imogolite fibers from decimolar concentration at low temperature and ambient pressure: A promising route for inexpensive nanotubes. *J. Am. Chem. Soc.* 131:17080–17081.
- Lumsdon, D.G., and V.C. Farmer. 1995. Solubility characteristics of proto-imogolite sols—How silicic-acid can de-toxify aluminum solutions. *Eur. J. Soil Sci.* 46:179–186.

- MacKenzie, K.J.D., M.E. Bowden, and R.H. Meinhold. 1991. The structure and thermal transformations of allophanes studied by silicon-29 and aluminum-27 high-resolution solid-state NMR. *Clays Clay Miner.* 39:337–346.
- Maeda, M., H. Ihara, and T. Ota. 2008. Deep-soil adsorption of nitrate in a Japanese andisol in response to different nitrogen sources. *Soil Sci. Soc. Am. J.* 72:702–710.
- Martini, J.A., and C. Luzuriaga. 1989. Classification and productivity of six Costa Rican andepts. *Soil Sci.* 147:326–338.
- Matus, F., E. Garrido, N. Sepulveda, I. Carcamo, M. Panichini, and E. Zagal. 2008. Relationship between extractable Al and organic C in volcanic soils of Chile. *Geoderma* 148:180–188.
- McDowell, M.L., and V.E. Hamilton. 2009. Seeking phyllosilicates in thermal infrared data: A laboratory and Martian data case study. *J. Geophys. Res.* 114:E06007/1–E06007/21.
- Miyauchi, N., and S. Aomine. 1966. Mineralogy of gel-like substance in the pumice bed in Kanuma and Kitakami districts. *Soil Sci. Plant Nutr. (Tokyo)* 12:187–190.
- Montarges-Pelletier, E., S. Bogenez, M. Pelletier, A. Razafitianamaharavo, J. Ghanbaja, B. Lartiges, and L. Michot. 2005. Synthetic allophane-like particles: Textural properties. *Colloids Surf., A* 255:1–10.
- Mora, M.L., and J. Canales. 1995. Humic-clay interactions on surface reactivity in Chilean Andisols. *Commun. Soil Sci. Plant Anal.* 26:2819–2828.
- Mukherjee, S., V.A. Bartlow, and S. Nair. 2005. Phenomenology of the growth of single-walled aluminosilicate and aluminogermanate nanotubes of precise dimensions. *Chem. Mater.* 17:4900–4909.
- Nakagawa, T., and M. Ishiguro. 1994. Hydraulic conductivity of an allophanic andisol as affected by solution pH. *J. Environ. Qual.* 23:208–210.
- Nakahara, O., and S.I. Wada. 1994. Ca²⁺ and Mg²⁺ adsorption by an allophanic and a humic andisol. *Geoderma* 61:203–212.
- Nissen M.J., and A.G. Kuehne. 1976. Mineralogical study of three forest soils from Valdivia Province, Chile. *Agro Sur* 4:1–11.
- Nizeyimana, E. 1997. A toposequence of soils derived from volcanic materials in Rwanda: Morphological, chemical, and physical properties. *Soil Sci.* 162:350–360.
- Nordstrom, D.K., Plummer, L.N., Langmuir, D., Busenberg, E., May, H.M., Jones, B.F., and Parkhurst, D.L. (1990). Revised chemical-equilibrium data for major water-mineral reactions and their limitations. *ACS Symposium Series* 416:398–413.
- Ohashi, F., M. Maeda, M. Suzuki, S. Tomura, S. Wada, and Y. Kakuto. 1998. Synthesis of spherical hollow amorphous aluminosilicate using rapid mixing method. *Natl Ind. Res. Inst. Nagoya* 46:397–404.
- Opiso, E., T. Sato, and T. Yoneda. 2009. Adsorption and coprecipitation behavior of arsenate, chromate, selenate and boric acid with synthetic allophane-like materials. *J. Hazard. Mater.* 170:79–86.
- Parfitt, R.L. 1990. Allophane in New Zealand—A review. *Aust. J. Soil Res.* 28:343–360.
- Parfitt, R.L. 2009. Allophane and imogolite: Role in soil biogeochemical processes. *Clay Miner.* 44:135–155.
- Parfitt, R.L., A.R. Fraser, and V.C. Farmer. 1977. Adsorption on hydrous oxides 3. Fulvic-acid and humic-acid on goethite, gibbsite and imogolite. *J. Soil Sci.* 28:289–296.
- Parfitt, R.L., R.J. Furkert, and T. Henmi. 1980. Identification and structure of two types of allophane from volcanic ash soils and tephra. *Clays Clay Miner.* 28:328–334.
- Parfitt, R.L., and A.D. Wilson. 1985. Estimation of allophane and halloysite in three sequences of volcanic soils, New Zealand, p. 1–8. *In* E.F. Caldas and D.H. Yaalon (eds.) *Volcanic soils: Weathering and landscape relationships of soils on Tephra and Basalt*. *Catena Suppl.* 7. Catena-Verlag, Cremling-Destedt, Germany.
- Percival, H. 1991. Soil water chemistry and mineral stability in soils. A physical chemistry approach. *Chem. N.Z.* 55: 66–70, 74.
- Schneider, M.P.W., T. Scheel, R. Mikutta, P. van Hees, K. Kaiser, and K. Kalbitz. 2010. Sorptive stabilization of organic matter by amorphous Al hydroxide. *Geochim. Cosmochim. Acta* 74:1606–1619.
- Singleton, P.L., M. McLeod, and H.J. Percival. 1989. Allophane and halloysite content and soil solution silicon in soils from rhyolitic volcanic material. *N.Z. Aust. J. Soil Res.* 27:67–77.
- Sposito, G. 2004. *The surface chemistry of natural particles*. Oxford University Press, New York.
- Steeffel, C.I., P. van Capellen, K.L. Nagy, and A.C. Lasaga. 1990. Modeling water-rock interaction in the surficial environment: The role of precursors, nucleation, and Ostwald ripening, p. 322–325. *In* *Geochemistry of the earth's surface and of mineral formation*. 2nd Int. Symp. Aix-en-Provence, France.
- Su, C.M., and J.B. Harsh. 1993. The electrophoretic mobility of imogolite and allophane in the presence of inorganic anions and citrate. *Clays Clay Miner.* 41:461–471.
- Su, C.M., and J.B. Harsh. 1994. Gibbs free energies of formation at 298 K for imogolite and gibbsite from solubility measurements. *Geochim. Cosmochim. Acta* 58:1667–1677.
- Su, C.M., and J.B. Harsh. 1996. Alteration of imogolite, allophane, and acidic soil clays by chemical extractants. *Soil Sci. Soc. Am. J.* 60:77–85.
- Su, C.M., and J.B. Harsh. 1998. Dissolution of allophane as a thermodynamically unstable solid in the presence of boehmite at elevated temperatures and equilibrium vapor pressures. *Soil Sci.* 163:299–312.
- Su, C.M., J.B. Harsh, and P.M. Bertsch. 1992. Sodium and chloride sorption by imogolite and allophanes. *Clays Clay Miner.* 40:280–286.
- Su, C.M., and D.L. Suarez. 1997. Boron sorption and release by allophane. *Soil Sci. Soc. Am. J.* 61:69–77.
- Takahashi, T., R. Dahlgren, and P. Vansusteren. 1993. Clay mineralogy and chemistry of soils formed in volcanic materials in xeric moisture regime of northern California. *Geoderma* 59:131–150.

- Taylor, N.H. 1933. Soil processes in volcanic ash-beds. *N.Z. J. Sci. Technol.* 14:338–352.
- Tsuchida, H., S. Ooi, K. Nakaishi, and Y. Adachi. 2005. Effects of pH and ionic strength on electrokinetic properties of imogolite. *Colloids Surf., A* 265:131–134.
- Ugolini, F.C., and R.A. Dahlgren. 1991. Weathering environments and occurrence of imogolite allophane in selected Andisols and spodosols. *Soil Sci. Soc. Am. J.* 55:1166–1171.
- Veith, J.A., and G. Sposito. 1977. Reactions of aluminosilicates, aluminum hydrous oxides, and aluminum oxide with o-phosphate: The formation of x-ray amorphous analogs of variscite and montebasite. *Soil Sci. Soc. Am. J.* 41:870–876.
- Vicente, J.G., and E. Besoain. 1961. Mineralogy of clays from some volcanic soils of Chile. *An. Edafol. Agrobiol.* 20:497–550.
- Wada, S. 1987. Imogolite synthesis at 25-degrees-C. *Clays Clay Miner.* 35:379–384.
- Wada, K. 1995. Role of aluminum and iron in the accumulation of organic matter in soils with variable charge, p. 47–58. *In* P.M. Huang et al. (eds.) *Environmental impact of soil component interactions*. CRC Press, Boca Raton, FL.
- Wada, K., and Y. Kakuto. 1985. Embryonic halloysites in Ecuadorian soils derived from volcanic ash. *Soil Sci. Soc. Am. J.* 49:1309–1318.
- Wada, S., and Y. Kakuto. 1999. Solubility and standard gibbs free energy of formation of natural imogolite at 25degrees C and 1 atm. *Soil Sci. Plant Nutr.* 45:947–953.
- Wada, K., and I. Matsubara. 1968. Differential formation of allophane, imogolite, and gibbsite in the Kitakami pumice bed. *Trans. 9th Int. Congr. Soil Sci.* 3:123–131.
- Wada, S.I., and K. Wada. 1981. Reactions between aluminate ions and orthosilicic acid in dilute, alkaline to neutral solutions. *Soil Sci.* 132:267–273.
- Wada, K., and N. Yoshinaga. 1969. Structure of imogolite. *Am. Mineral.* 54:50–71.
- Wan, G., Peraval, H.J., Theng, B.K.G., and Parfitt, R.L. (2002). Sorption of copper and cadmium by allophane-humic complexes. *Dev. Soil Sci.* 28A:37–47.
- Wells, N., C.W. Childs, and C.J. Downes. 1977. Silica Springs, Tongariro National Park, New Zealand—Analyses of the spring water and characterization of the aluminosilicate deposit. *Geochim. Cosmochim. Acta* 41:1497–1506.
- Wells, N., and R.L. Parfitt. 1987. Occurrences of short-range order clays and their use in pollution control. *Proc. Pacific Rim Congress* 87:469–473.
- Wilson, M.J. 1987. *A handbook of determinative methods in clay mineralogy*. Blackie and Son, Ltd., Glasgow, U.K.
- Wilson, M.A., S.A. McCarthy, and P.M. Fredericks. 1986. Structure of poorly-ordered aluminosilicates. *Clay Miner.* 21:879–897.
- Yang, H., C. Wang, and Z. Su. 2008. Growth mechanism of synthetic imogolite nanotubes. *Chem. Mater.* 20:4484–4488.
- Yoshinaga, N. 1968. Identification of imogolite in the filmy gel materials in the Imaichi and Shichihonzakura pumice beds. *Soil Sci. Plant Nutr. (Tokyo)* 14:238–246.
- Yoshinaga, N., and S. Aomine. 1962. Imogolite in some Ando soils. *Soil Sci. Plant Nutr. (Tokyo)* 8:114–121.
- Yoshinaga, N., M. Nakai, and M. Yamaguchi. 1973. Unusual accumulation of gibbsite and halloysite in the Kitakami pumice bed, with a note on their genesis. *Clay Sci.* 4: 155–165.
- Yuan, G., Percival, H.J. Theng, B.K.G., and Parfitt, R.L. (2002). Sorption of Copper and Cadmium by allophane-humic complexes. *Dev. Soil Sci.* 28A:37–47.
- Zhao, M., Y. Xia, and L. Mei. 2009. Energetic minimum structures of imogolite nanotubes: A first-principles prediction. *J. Phys. Chem. C* 113:14834–14837.

